Green chemistry

Edited by Luigi Vaccaro

Imprint

Green chemistry

Luigi Vaccaro[§]

Editorial

Since their initial appearance in the scientific literature, the terms "green" and "sustainable" have been increasingly used and are nowadays ubiquitously present in the terminology of several research areas. The seminal origin of what is considered "green chemistry" today might be ascribed to the launch of the Responsible Care® initiative by the American Chemistry Council (ACC) [1] and to the Brundtland report [2]. The concept was then further refined and completed with the Pollution Prevention Act (approved by the American Congress [3]) and the definition of the Anastas and Warner's 12 principles of green chemistry [4,5]. Very generally, green chemistry may be considered as the scientific and economical context in which academia, industry and government are attempting to converge their efforts for the development of a sustainable civilization.

The first goal of green chemistry is to provide a solid solution to the need for an ex novo design of the existing and necessary chemical processes by primarily considering safety, pollution prevention, waste minimization and energy optimization. To achieve such goals, the necessity of chemists from different areas is evident. Also important is how this novel approach to scientific research has led to a different and hopefully more effective paradigm in the collaboration between industry and academia.

It is obvious that the chemical yield represents just one of the many features that a process must possess to be considered efficient. It is of extreme importance nowadays to consider not only the safety of a chemical procedure, but also the proper selection of solvents, starting materials, and technologies used to generate and control reactive intermediates. In addition, the need for minimizing toxic waste and the respective disposal cost highlights how crucial it is to consider the recovery and reuse of the materials needed for a synthetic process. It is also very important to promote the use of biomass-derived chemicals that feature an intrinsically lower CO_2 consumption.

Additionally, the pivotal role of catalysis is indisputable. Significant efforts are being directed towards the development of effective catalytic methodologies with safer and cheaper substrates where reactivity is achieved through catalysis that can replace the classically used, highly reactive species. While for immediate economical reasons the use of well-established methodologies based on homogeneous catalysis may be initially preferred, many efforts are directed toward the development of

heterogeneous catalytic approaches, aiming at an easier recovery and better reuse of the catalyst.

Another key aspect of green chemistry, closely related to the chemical efficiency and efficiency of a protocol, is the technology behind the process. In fact, energy and time optimization are important factors. Increasing interest is being directed towards the development of innovative mixing and heating technologies that, individually or in combination, may furnish an innovative solution for controlling the safety and the reactivity of a chemical process and may facilitate the recovery and reuse of the materials used, which contribute to minimizing the energy consumption and increasing the overall efficiency of a process. Flow chemistry, microwave or ultrasonic irradiation, and mechano-chemistry are just a few representative examples of research platforms being independently developed, but all offer innovative tools for realizing chemically and environmentally efficient processes. Representative examples of these directions have been the subject of other excellent Thematic Series in the *Beilstein Journal of Organic Chemistry*, including "Strategies in asymmetric catalysis" by Tehshik P. Yoon [6], "Organometallic chemistry" by Bernd F. Straub and Lutz H. Gade [7], "C–H functionalization/activation in organic synthesis" by Richmond Sarpong [8], "Bifunctional catalysis" by Darren J. Dixon [9], "Sustainable catalysis" by Nicholas J. Turner [10], and "Organic synthesis using photoredox catalysis" by Axel G. Griesbeck [11], proving that green chemistry and sustainability can be approached from many different perspectives.

The breadth of chemical and technological innovations makes the definition of novel metrics for the evaluation of the quality of a new process in the field of green chemistry necessary. A key aspect of green chemistry is in fact the comparison of the different strategies available by considering as many experimental aspects as possible. Of course the most important feature to be evaluated is the correct measure of the waste generated, which is derived from both the synthetic strategy and the technology used. The fundamental role of green metrics is to evaluate the modern classification of chemical transformations in relation to the potential or actual pollution produced. In some cases, such as calculating the waste associated with the mass of the material used, this is easily evaluated. However, it may be more difficult to compare energy, time, labor costs, and other variables of a process. Certainly, innovation is the most important goal of green chemistry, but it is also the most difficult feature to measure and evaluate. Novel chemistry and innovative technologies are needed for the development of future, sustainable, chemical production. To reach this goal, both fundamental research, as well as the ability to translate the innovation into real world applications, should be combined.

Organic chemistry, with its kaleidoscope of interests and applications, offers the arena where countless opportunities exist to effectively contribute to the development of green chemistry. Journals dedicated to the field of organic chemistry, such as the *Beilstein Journal of Organic Chemistry*, represent an ideal medium for disseminating scientific efforts in this context. This Thematic Series, "Green chemistry", collects original research and review articles, where an obviously limited but highly exemplificative portion of the broad field of green chemistry is described.

Luigi Vaccaro

Perugia, November 2016

References

1. Formerly "Chemical Manufacturers' Association (CMA)". http://responsiblecare.americanchemistry.com/Home-Page-Content/Responsible-Care-Timeline.pdf.
2. *Bruntland's report the World Commission on Environmental and Development: World Commission on Environment and Development, Our Common Future,* 27 April 1987 ed.; Oxford University Press: Oxford, UK, 1987.
3. *Pollution Prevention Act of 1990;* US Government Printing Office: Washington, 1995; p 617.
4. Anastas, P. T.; Warner, J. C. *Green Chemistry: Theory and Practice;* Oxford University Press: New York, 1998.
5. Linthorst, J. A. *Found. Chem.* **2010,** *12,* 55–68. doi:10.1007/s10698-009-9079-4 See for a very interesting overview on the origin of green chemistry.
6. Thematic Series "Strategies in asymmetric catalysis". http://www.beilstein-journals.org/bjoc/browse/singleSeries.htm?sn=62 (accessed Dec 12, 2016).
7. Straub, B. F.; Gleiter, R.; Meier, C.; Gade, L. H. *Beilstein J. Org. Chem.* **2016,** *12,* 2216–2221. doi:10.3762/bjoc.12.213
8. Sarpong, R. *Beilstein J. Org. Chem.* **2016,** *12,* 2315–2316. doi:10.3762/bjoc.12.224
9. Dixon, D. J. *Beilstein J. Org. Chem.* **2016,** *12,* 1079–1080. doi:10.3762/bjoc.12.102
10. Turner, N. J. *Beilstein J. Org. Chem.* **2016,** *12,* 1778–1779. doi:10.3762/bjoc.12.167
11. Griesbeck, A. G. *Beilstein J. Org. Chem.* **2014,** *10,* 1097–1098. doi:10.3762/bjoc.10.107

Ionic liquids as transesterification catalysts: applications for the synthesis of linear and cyclic organic carbonates

Maurizio Selva[*], Alvise Perosa, Sandro Guidi and Lisa Cattelan

Abstract

The use of ionic liquids (ILs) as organocatalysts is reviewed for transesterification reactions, specifically for the conversion of nontoxic compounds such as dialkyl carbonates to both linear mono-transesterification products or alkylene carbonates. An introductory survey compares pros and cons of classic catalysts based on both acidic and basic systems, to ionic liquids. Then, innovative green syntheses of task-specific ILs and their representative applications are introduced to detail the efficiency and highly selective outcome of ILs-catalyzed transesterification reactions. A mechanistic hypothesis is discussed by the concept of cooperative catalysis based on the dual (electrophilic/nucleophilic) activation of reactants.

Review
Introduction
Transesterification catalysts

The transesterification is one of the classical organic reactions that has found numerous applications in laboratory practice as well as in the synthesis of a variety of intermediates in the pharmaceutical, cosmetic, fragrance, fuel and polymers industries [1]. Transesterification reactions are catalyzed under acidic, basic or even neutral conditions [2]. An excellent review by Otera et al. has detailed many applications of the most popular catalytic systems [3]. These include both acids such as sulfuric, sulfonic, phosphoric, and hydrochloric, and bases such as metal

alkoxides, acetates, oxides, and carbonates. It is worth mentioning, that transesterification reactions are frequently carried out over solid (heterogeneous) catalysts to facilitate work-up, recycling, and purification of products, especially for large-scale preparations. These heterogeneous systems include supported metal oxides and binary oxide mixtures. For example, MoO_3/SiO_2 and sol–gel MoO_3/TiO_2 is used for the preparation of diphenyl oxalate monomer (DPO, Scheme 1) in polycarbonate chemistry [4,5], and TiO_2/SiO_2 and similar binary combina-
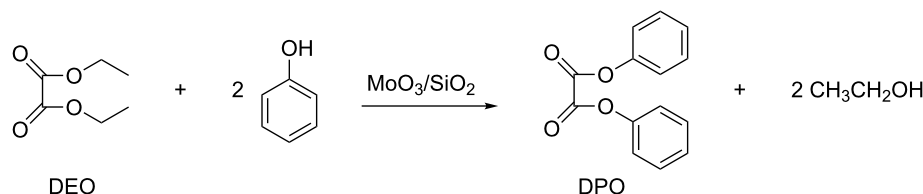
Scheme 1: The transesterification of diethyl oxalate (DEO) with phenol catalyzed by MoO_3/SiO_2.

tions are applied in the transesterification of β-ketoesters [6], and in the synthesis of unsymmetrical carbonates $R^1OC(O)OR^2$ [7].

Superacidic solids have also been described as transesterification catalysts and a remarkable example is the recently patented synthesis of sucrose-6-ester – a food sweetener – carried out over a mixture of sulfated oxides of various metals [8]. In addition, acidic ion exchange resins are worth mentioning in this context. Van de Steene et al. have proved the performance of such systems in an elegant investigation on the model transesterification of ethyl acetate with methanol [9].

The production of biodiesel blends is another sector in which the catalytic transesterification is extensively used. In particular, heterogeneous catalysts including calcium, manganese and zinc oxides as such or as mixtures are widely used to convert natural triglycerides into FAMEs or FAEEs (fatty acid methyl or ethyl esters) with methanol or ethanol, respectively [10]. The most commonly used system is CaO, which is obtained by calcination of readily available and cheap resources including waste products such as shells and even livestock bones [11-14]. However, traditional catalysts such as alkali hydroxides or alkaline methoxides are still encountered even for novel syntheses of biofuels. An example is the transesterification of oils by dimethyl carbonate (DMC) in the presence of KOH (Scheme 2) [15,16].

The reaction allows obtaining FAMEs and fatty acid glycerol carbonate monoesters (FAGCs), without the concurrent

formation of glycerol, a frequently formed highly undesirable byproduct.

Enzyme catalysts: A major driving force for the choice of enzymes is their high efficiency, which allows reactions to be performed under very mild conditions and with a variety of raw materials. However, the high cost and relatively short lifetime of enzymes partly offset their advantages and an implementation of biocatalytic processes makes sense almost exclusively for the preparation of high added-value chemicals. This holds true also for enzyme-catalyzed transesterification reactions. To cite a few examples, the literature claims the use of lipase as a biocatalyst for i) the reaction of glycerol with DMC for the synthesis of glycerol carbonate (GlyC) under solvent-free conditions. A 60% yield was achieved along with an effective recycle of the catalyst [17], ii) the formation of six-membered cyclic carbonates by the transesterification of dialkyl carbonates with trimethylolpropane. The products were achieved in high yields (85%) and used as monomers for polyurethanes and polycarbonates [18], and iii) the conversion of oils for which lipase was identified as the most suitable enzyme for an innovative and green production of biodiesel [19].

Other catalytic systems: In addition to the above-described catalysts, amines and organometallic derivatives also find applications in the field of homogeneous catalytic systems for transesterification reactions. Remarkable examples are those of triethylamine (TEA) and Fe–Zn double-metal cyanide complexes [20,21]. Among other applications, these compounds successfully catalyzed the reaction of DMC and other organic carbon-
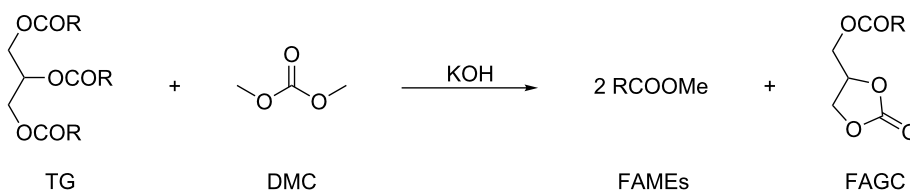
Scheme 2: Transesterification of a triglyceride (TG) with DMC for biodiesel production using KOH as the base catalyst.

ates with polyols (e.g., glycerol) to produce the expected transesterification products with total conversion and selectivity.

Ionic liquid-based organocatalysts

Conventional acid or base liquid catalysts for transesterification processes often entail several synthetic and environmental concerns including equipment corrosion, separation and purification drawbacks, and production of waste. As already mentioned in the previous paragraph, practical solutions to such problems are offered by using solid acids, although these systems may suffer from mass-transfer limitations causing low activity, and consequently, extended reaction times and deactivation from coking [22,23]. Valuable alternatives are biocatalysts, which are very active but costly. Economic issues usually restrict the use of enzymes to highly specialized productions rather than to large commercial applications [24].

In this scenario, the implementation of transesterification procedures based on innovative and possibly green catalysts remains still a highly desirable target. A strategy can be conceived by the use of task-specific ionic liquids (ILs). These compounds have shown to catalyze a number of different reactions. Only to cite a few: nitrations, Michael reactions, Friedel–Crafts alkylations and acylations are successfully promoted by ILs [25,26]. The key to such a flourishing research lies in the unique physical properties (negligible vapor pressure, wide liquid range, and non-flammability) of ILs, but mostly on the virtually infinite number of different chemical structures for liquid organic salts. These properties are often referred to as "tunable catalysts", "task-specific ionic liquids", and "designer solvents", which involve the concept of optimizing the use of ILs by tailoring their chemical features for a specific transformation or for classes of similar processes [27,28]. Notably, the screening of the reaction variables includes not only the required reaction steps, but also the associated operations including separation and purification of products, recycling of solvents and catalysts, and waste treatments as well. All these additional steps contribute to the impact of the chemical process as the whole from an environmental and sustainability standpoint. For example, the isolation and purification of the desired product and reuse of the

IL-based catalyst may require additional solvents for extraction and/or complex and energy-intensive separation and purification technologies. Therefore, when designing a catalytic IL-based process, one should factor-in all the reagents and solvents as well as all the downstream operations, in order to evaluate the advantages of the proposed process correctly. In this context, green metrics can provide a screening guide.

IL-based catalysts for transesterification reactions

Synthesis of IL-catalysts: IL-based catalysts for transesterification reactions mostly comprise imidazolium, phosphonium, ammonium, sulfonium and pyridinium salts. The conventional syntheses of such compounds usually start from the protonation or quaternization of neutral precursors (imidazoles, amines, phosphines, pyridine or sulfides) with Brønsted acids or haloalkanes/dialkylsulfates, respectively. In the next step, a variety of ionic liquids are obtainable by anion exchange, either through direct treatments with Lewis acids or by anion metathesis [29]. There are several reviews detailing these synthetic procedures [30,31].

More sustainable methods that avoid the use of noxious and undesirable halogens have also been recently designed [32,33]. An example is the preparation of methyl carbonate onium salts ($[Q_{1nnn}][MeOCO_2]$; Q = N, P; n = 4, 6, 8, Ph), obtained by the methylation of trialkylphosphines or -amines with nontoxic DMC (Scheme 3, top) [34,35]. Such methyl carbonate onium salts are versatile platforms as they allow access to a number of ionic liquids via anion-metathesis reactions, which produce only CH_3OH and CO_2 as byproducts (Scheme 3, bottom).

Seedon et al. reported another green protocol for the preparation of ILs. The authors described the synthesis of aqueous hydroxide solutions of organic cations, subsequently neutralized by simple acid–base reactions, giving access to ionic liquids that are difficult to prepare by any other route. This protocol avoids the use of halides, and generates water as the only byproduct [33].
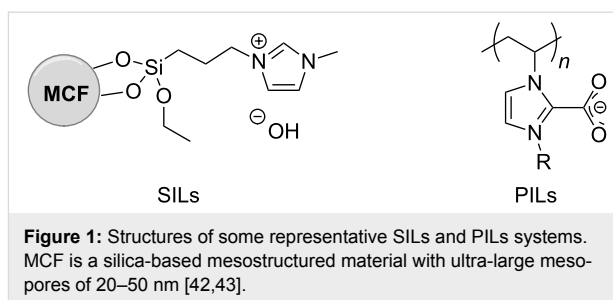
Synthesis of supported ionic liquids (SILs): Ionic liquids are far more expensive than classical solvents, with costs higher by
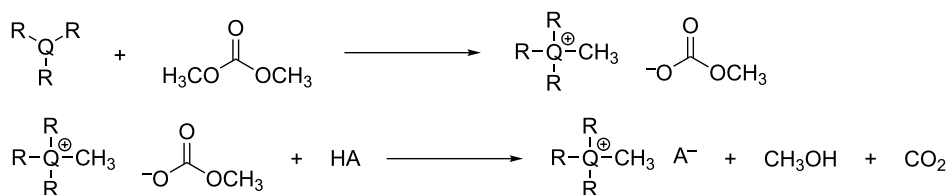
Scheme 3: Top: Green methylation of phosphines and amines by dimethyl carbonate (Q = N, P). Bottom: anion metathesis of methyl carbonate onium salts.

a factor of 10-to-50. The recycling of the ILs is therefore imperative not only to limit their release to the environment, but also for economic reasons. One strategy to cope with the recycling issue is based on the immobilization of ionic liquids onto solid supports. In the specific field of transesterification reactions, supported ionic liquid (SILs) catalysts are achieved by the dispersion of liquid organic salts on highly porous materials, amongst which montmorillonite clays, modified silica, and polystyrene-based solids are the most frequently used [36,37]. Some very recent examples described the production of biodiesel via the transesterification of glycerol trioleate with methanol: both, acidic ionic liquids (e.g., 1-allyl-3-(butyl-4-sulfonyl)imidazolium trifluoromethanesulfonate [BsAIm][OTf]) supported onto sulfhydryl-group-modified SiO$_2$ (MPS-SiO$_2$) [38], and imidazolium salts (e.g., 1-allyl-dodecylimidazolium hydroxide ([ADIm][OH]) dispersed on magnetic mesoporous SiO$_2$/CoFe$_2$O$_4$ and CoFe$_2$O$_4$ nanoparticles [39,40] have been reported as catalysts. In addition, the reaction of ethylene carbonate with methanol for the synthesis of DMC was described in the presence of a mesocellular silica foam (MCF) material [41]. These catalysts are easy to recover and recycled by physical separation, washing and drying.
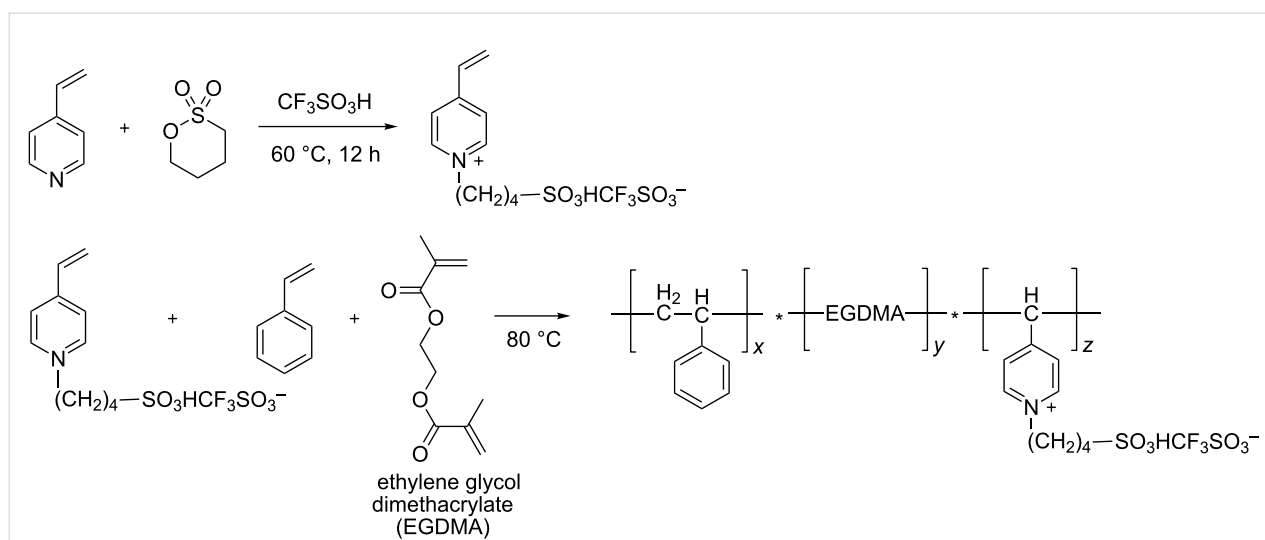
A similar approach has been implemented through the design of polymeric ionic liquid (PILs) based systems, such as poly(*N*-heterocyclic carbene)s and ordered mesoporous resol (OMR) polymers (OMR based on hexamethylenetetramine, [C$_4$HMTA][SO$_4$H]). They have been employed to catalyze different transesterification reactions, including also the conversion of brown grease into biodiesel [42,43]. Recycling tests of polymeric ionic liquids proved their robustness for prolonged use (Figure 1).

Figure 1: Structures of some representative SILs and PILs systems. MCF is a silica-based mesostructured material with ultra-large mesopores of 20–50 nm [42,43].

Recently, Zhan et al. synthesized a new acidic polyionic liquid by the copolymerization of a zwitterionic liquid based on vinyl-pyridinium, styrene and ethyleneglycol dimethacrylate (Scheme 4) [44]. The resulting PIL with particle sizes of about 0.5–3 mm, was an efficient catalyst for a series of esterification reactions of different acids including acetic, succinic, benzoic, and methacrylic acid and alcohols such as linear, branched and cyclic C$_1$–C$_6$ compounds. The PIL could be reused up to five times without any loss of catalytic activity and yields of various esters were always nearly quantitative.

Applications of ILs: Organocatalysts find uses in place of the common homogeneous or heterogeneous catalysts for the transesterification of natural triglycerides in the production of biodiesel. A recent example has reported that a methylimidazolium salt with an alkyl chain mimicking the glycerol structure, promotes the almost quantitative conversion of rapeseed oils into FAMEs products [45].

A series of Brønsted acidic imidazolium ILs has been investigated for the catalytic synthesis of *sec*-butanol by transesterification of *sec*-butyl acetate with methanol (Scheme 5) [46].

Scheme 4: Synthesis of the acid polymeric IL. EGDMA: ethylene glycol dimethacrylate.

Scheme 5: The transesterification of sec-butyl acetate with MeOH catalyzed by some acidic imidazolium ILs.
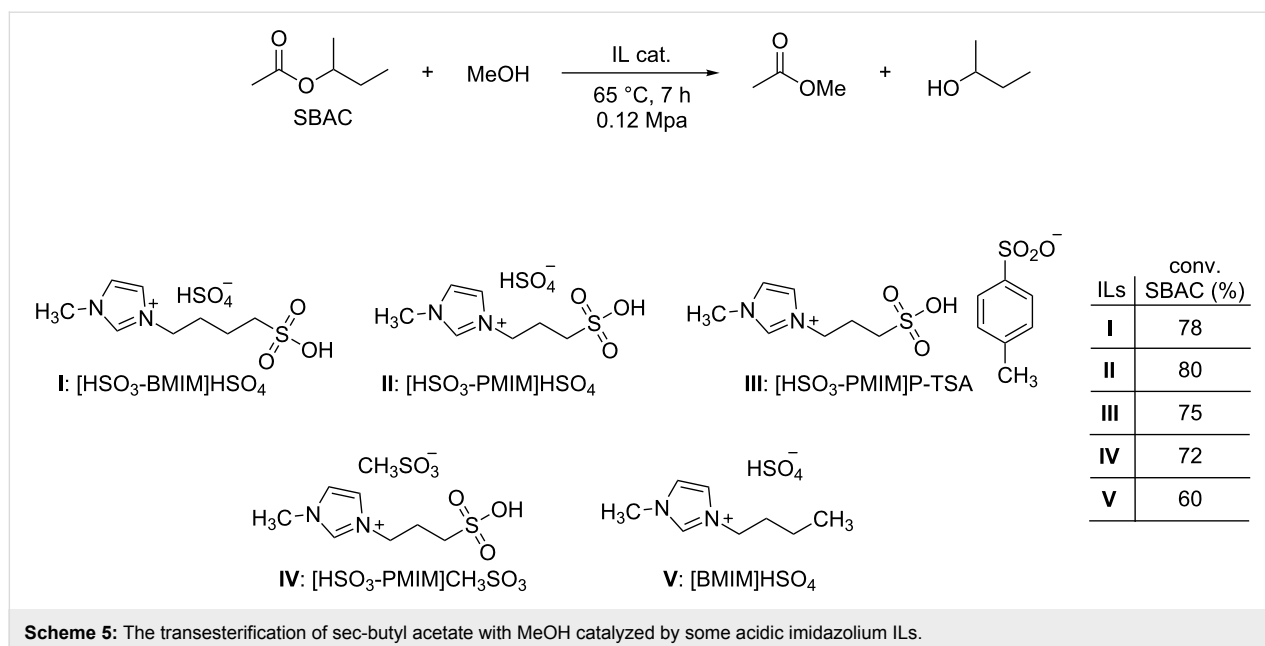
The reaction is of interest for the preparation of less toxic oxygenated derivatives, such as *sec*-butanol, in place of compounds like MTBE (methyl *tert*-butyl ether) for the formulation of gasoline blends. Tests with the imidazolium salts collected in Scheme 5 have demonstrated that they are not only competitive with conventional acid catalysts, but that they also can be recovered and reused to allow quantitative conversions even after several recycles. Moreover, the study highlighted that the catalytic activity increased with increasing acidity of the ILs and particularly with cations bearing SO_3H anions (Scheme 5: ILs **I**, **II**, **III**, and **IV**). The same imidazolium salts (**I** and **II**, respectively) have been used also by Cui et al. for the transesterification of methyl acetate and *n*-butanol [47]. The authors observed that the presence of two acidic sites in both the cation and the anion of ILs improved the performance of the catalyst, in analogy to previously reported results for the synthesis of esters from the reaction of nitriles and alcohols [48].

4-(3-Methyl-1-imidazolium)-1-butanesulfonic acid triflate ([HSO_3-BMIM][CF_3SO_3]) has been chosen as a model organocatalyst to explore the kinetics of the transesterification of methyl acetate with ethanol [49,50]. Again, in this case, the investigation proved that the activity of the organic salt was higher than that of sulfuric acid.

The use of ionic liquids for the catalytic production of biodiesel was recently reviewed by Fauzi and Amin [51], who focused on the improvements made possible by organocatalysts with respect to traditional homogenous systems in terms of milder reaction conditions and easier separation and recycle workups. Two representative examples of ionic liquids employed for the

synthesis of FAMEs are the pyridinium and oxazolidinone-based compounds shown in Figure 2 [52,53].

Figure 2: Representative examples of ionic liquids for biodiesel production.
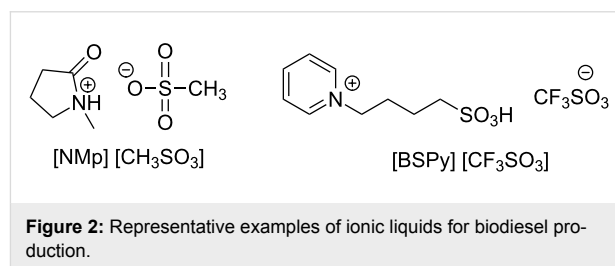
It should be noted that for such reactions, acidic IL-based catalysts are preferred over basic ones due to the presence of significant amounts of free fatty acids in the bio-oils used as feedstocks for biodiesel. Li et al. for example designed an innovative combination of imidazolium ILs and metal sulfates acting as Brønsted and Lewis acids, respectively [54]. A model case is [HSO_3-BMIM]HSO_4–$Fe_2(SO_4)_3$ that offered an excellent catalytic performance in the transesterification of *Camptotheca acuminata* seed oil with methanol, with substantially quantitative conversions achieved in only 60 minutes at 60 °C.

The transesterification reaction for the synthesis of organic carbonates

Organic carbonates (OCs) are promising candidates as *green* replacements of conventional noxious solvents and fuel additives as well as for the development of innovative intermediates in the pharma, lubricant and polymer industries [55,56]. Before the 1980's, the industrial synthesis of the simplest representative of the series, dimethyl carbonate (DMC), was based on the

phosgenation of methanol, which used a lethal chemical reagent such as phosgene (Scheme 6, top). Since then, the processes for the production of DMC have progressively evolved in terms of environmental impact, safety and economics.

Thus, by the end of the 1990's, two main phosgene-free large-capacity processes were operative, both based on the incorporation of carbon monoxide (CO) and methanol by transition metal catalysis: one developed by EniChem [57,58], and the other by Ube Industries [59]. The EniChem process involved an oxidative carbonylation of methanol, i.e., the reaction of methanol with carbon monoxide and oxygen catalyzed by cuprous chloride, while the Ube process used an oxidative carbonylation of methanol via methyl nitrite using NOx as oxidant, instead of oxygen and a palladium catalyst (Scheme 6, middle). Though safer than the phosgenation of methanol, these synthetic routes still involved poisonous carbon monoxide and methyl nitrite, and chlorine-based catalysts.
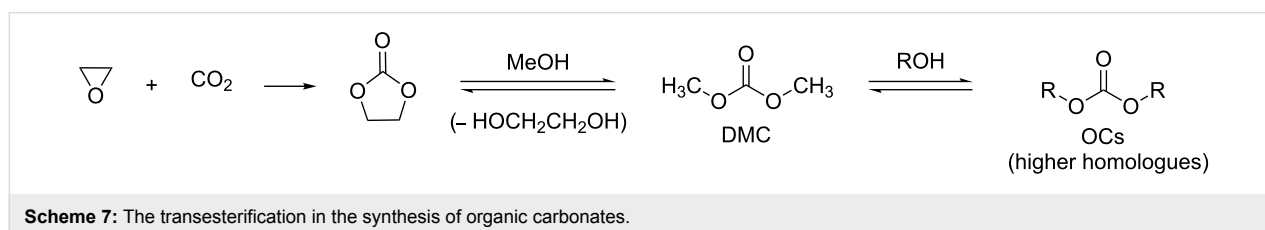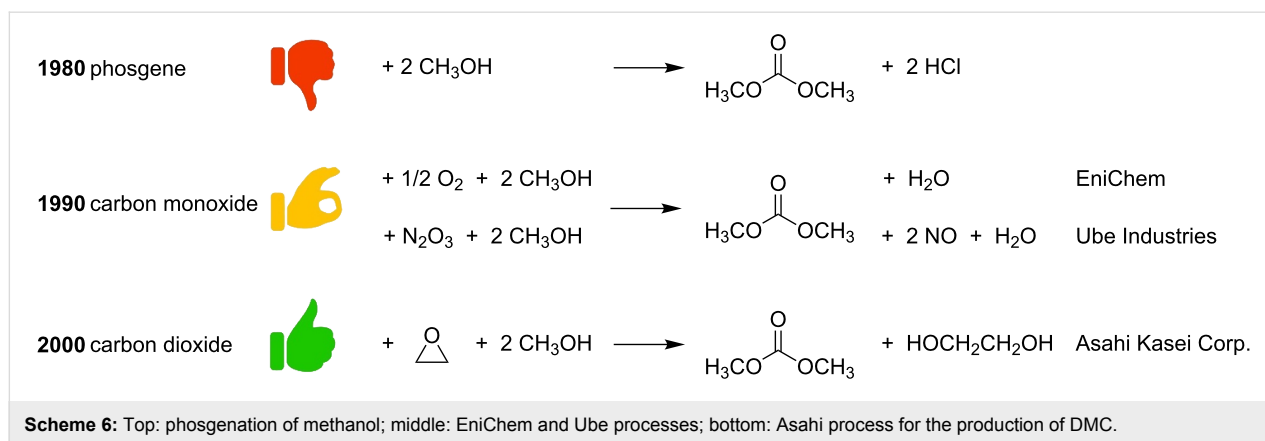
Carbon dioxide is the natural green alternative carbonyl source to these undesirable feedstocks, in particular to CO, except that its thermodynamic stability poses severe challenges. This potential limitation was overcome by the Asahi Kasei Corp. that recently industrialized a catalytic polycarbonate production process based on the use of carbon dioxide (CO_2) for the synthesis of DMC as an intermediate towards the diphenyl carbonate monomer. The first step is the insertion of CO_2 into ethylene oxide to give ethylene carbonate, which is catalyzed by onium salts. The second step involves the transesterification of ethylene carbonate with methanol. The reaction is carried out in a continuous distillation reactor loaded with quaternary ammonium strongly basic anion exchange resin and alkali hydroxides: dimethyl carbonate (DMC) is achieved in practically quantitative yields (Scheme 6, bottom). The third and final step is the transesterification of DMC with phenol by a catalytic reactive distillation in the presence of a homogeneous Ti, Bu–Sn, or Pb catalyst. This reaction provides the desired diphenyl carbonate (yield up to 99%) in a high purity [60].

The catalytic transesterification appears therefore as a crucial reaction, not only for the preparation of the simplest homologue, dimethyl carbonate (DMC), but also for the synthesis of higher organic carbonates as well (Scheme 7).

Notwithstanding the excellent results with respect to previous methods, it should be pointed out, that ethylene oxide still represents a concern for its carcinogenic and mutagenic properties. Future procedures should therefore implement greener reactions, such as the direct carboxylation of diols by CO_2, for which however, effective catalysts are currently not available.

The Asahi Kasei process also highlights that the synthesis of DMC by transesterification of ethylene carbonate with methanol does not necessarily require transition metal catalysis as did the EniChem and Ube processes. Instead, the reaction can be effectively catalyzed by a combination of supported basic ammonium resins and homogeneous alkaline bases [60], thereby

Scheme 6: Top: phosgenation of methanol; middle: EniChem and Ube processes; bottom: Asahi process for the production of DMC.

Scheme 7: The transesterification in the synthesis of organic carbonates.

demonstrating the potential of transition metal-free catalytic systems for the synthesis and the further transformation of organic carbonates. These transesterification catalysts can include both acidic and basic ionic liquids, which will be a topic of the further discussion.

Applications of ionic liquids for the synthesis of organic carbonates

The commonly used method to synthesize organic carbonates consists in the acid or base-catalyzed transesterification of dimethyl carbonate (DMC), the simplest organic carbonate, with alcohols R–OH or diols to yield either acyclic organic carbonates or cyclic carbonates, respectively (Scheme 8).
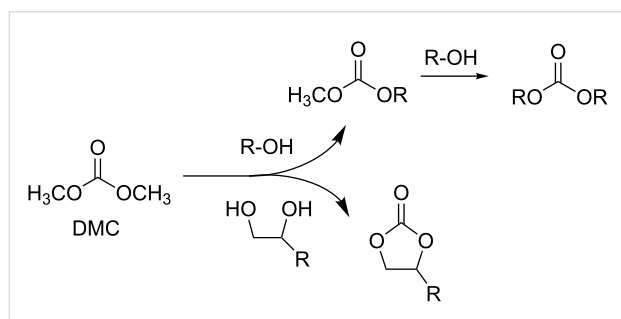
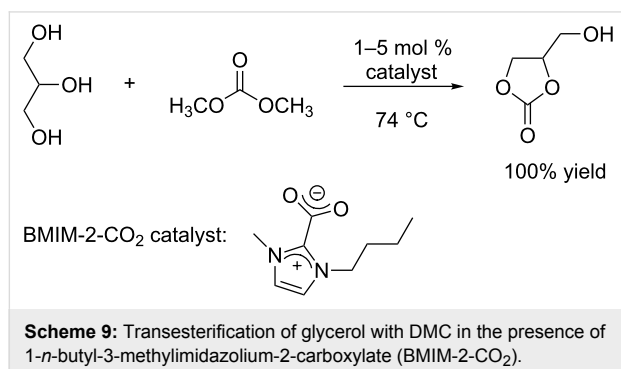**Scheme 8:** The transesterification of DMC with alcohols and diols.

A literature survey on the synthesis of organic carbonates by ionic-liquid catalysis goes back approximately five years. Both acidic and basic ionic liquids were employed as catalysts for the pursuit of this scope. The following section is divided into two topics: the first focuses on basic catalysis, and the second on acid catalysis.

Basic catalysis: In a communication published in 2009, Naik P. U. et al. reported an expeditious protocol towards the formation of glycerol carbonate through the transesterification of glycerol with DMC (Scheme 9) [61]. They employed the ionic liquid 1-*n*-butyl-3-methylimidazolium-2-carboxylate (BMIM-2-CO$_2$) in a concentration of only 1–5 mol %, and the

Scheme 9: Transesterification of glycerol with DMC in the presence of 1-*n*-butyl-3-methylimidazolium-2-carboxylate (BMIM-2-CO$_2$).

target molecule was quantitatively obtained in 30 min at 74 °C, by using 3.2 equivalents of DMC with respect to glycerol.

As the BMIM-2-CO$_2$ catalyst is synthesized starting from butylimidazole and DMC (Scheme 10), the authors also attempted to combine the in situ formation of the catalyst with the transesterification of glycerol. The process however, became much slower due to an induction time required to obtain BMIM-2-CO$_2$.
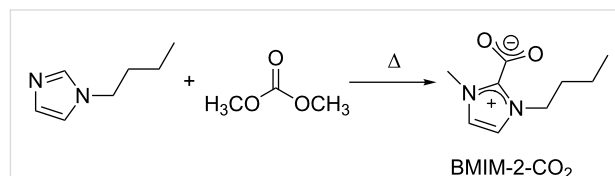

Scheme 10: Synthesis of the BMIM-2-CO$_2$ catalyst from butylimidazole and DMC.

The study proved that even starting from crude glycerol (which contained 41 mol % water and alkaline salts) and 5 mol % BMIM-2-CO$_2$, glycerol carbonate was achieved with a 93% yield after 5 h.

More recently, Yuxuan Yi et al. described the transesterification of glycerol with DMC in the presence of four catalytic ionic liquids such as 1-methyl-3-butylimidazolium imidazolium ([BMIM]Im), 1-methyl-3-allylimidazolium imidazolium ([AMIM]Im), 1-methyl-3-butylimidazolium hydroxide ([BMIM]OH), and 1-methyl-3-allylimidazolium hydroxide ([AMIM]OH) [62]. The highest activity was achieved with [BMIM][Im]: after screening of reaction conditions, using 10 mol % of catalyst, 98.4% glycerol conversion and up to 100% selectivity towards glycerol carbonate were reached at 70 °C and ambient pressure. An easy recovery of the catalyst allowed the reuse of the IL up to three times without significant reduction of its activity.

According to the authors, the result was due to a higher basicity of the imidazolium anion with respect to the hydroxy group, and to the poorer steric hindrance of the AMIM cation with respect to the BMIM cation, the latter exerting less effective interactions with the corresponding (imidazolium) anion. Regardless of its nature, the cation might also activate DMC towards nucleophilic addition: a cooperative nucleophilic–electrophilic mechanism could therefore operate (Scheme 11) [63].

Munshi et al. also recently investigated the reaction of glycerol and DMC by proposing a novel ionic liquid catalyst based on the reaction of diazabicyclo[5.4.0]undec-7-ene (DBU) with an alcohol ROH and CO$_2$ (Scheme 12) [64].
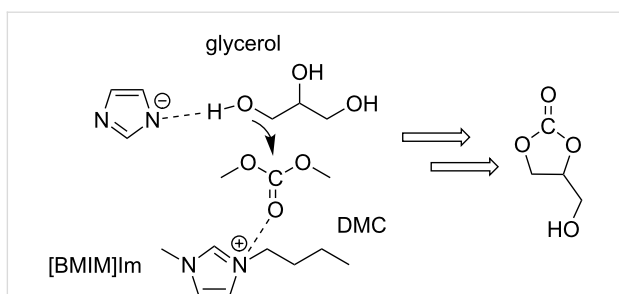
Scheme 11: Plausible cooperative (nucleophilic–electrophilic) mechanism for the transesterification of glycerol with DMC in the presence of [BMIM]Im.
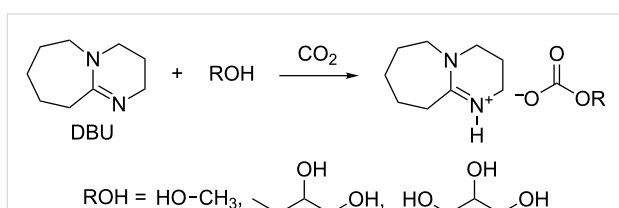
Scheme 12: Synthesis of diazabicyclo[5.4.0]undec-7-ene-based ionic liquids.

As best found reaction conditions (only 0.22 mol % IL loading, glycerol to DMC molar ratio 1:3, 100 °C), conversion and selectivity (towards glycerol carbonate) were 96% and 82%, respectively, after 30 min reaction time. Glycidol (GD, 18%) was the major byproduct. In a further study by the same group, the formation of glycidol from glycerol carbonate was examined in the presence of the ionic liquid DABCO–DMC obtained in situ by reacting DABCO and DMC (Scheme 13) [65].

DABCO by itself is more basic than the DABCO–DMC IL as indicated by its pH in aqueous solution. Nonetheless the DABCO–DMC IL promoted higher glycerol conversion (77% vs 19% after 10 minutes), and, most importantly, higher GD selectivity (63% compared to 45% after 30 minutes) under the same reaction conditions. In order to explain such a behavior, a cooperative mechanism for the ionic liquid catalysis was invoked, whereby the electrophilic nitrogen atom aids in activating the carbonyl moiety (Scheme 14).

It must be noted that in these two examples the selectivity of the reaction could be tuned just by changing the catalyst precursor: by switching from the DBU-based IL to the DABCO–DMC IL, the selectivity changed from 82% for glycerol carbonate, to 83% for glycidol.

In another publication, Gade et al. also achieved a high selectivity toward GD in a one-pot reaction starting from glycerol and DMC [66]. Using tetramethylammonium hydroxide ([TMA][OH]) as basic catalyst, a high selectivity (78%) for GD was reached under mild operating conditions (80 °C, 90 min). The results suggested that the decarboxylation of glycerol carbonate increased with increasing catalyst concentration in solution and thus, the high basicity of the catalyst was not the sole reason for the high activity.

This implied that both, the presence of a basic (anionic) center and an electrophilic (cationic) center in the ionic liquid were involved in the reaction. It was therefore proposed that an interaction of the quaternary ammonium center with the carbonyl oxygen of glycerol carbonate (GlyC) could weaken the C=O bond (Scheme 15).

It is worth mentioning that glycidol was previously obtained at much higher temperatures (170–200 °C).

An acyclic organic carbonate that has recently received attention from the synthetic lubricant market is dipentyl carbonate (DPC). An environmentally friendly process for its synthesis has been recently proposed by the transesterification of DMC with 1-pentanol in the presence of 2 mol % of 1-butyl-3-methylimidazolium hydroxide ([BMIM]OH) as a basic ionic liquid catalyst [67]. At the best found reaction conditions (110 °C, DMC:1-pentanol in 1:4 ratio), DPC was obtained in 76% yield after 4 h reaction time. The catalyst proved to be very stable and active even after five reaction cycles where the DPC yield still exceeded 70%. The proposed reaction mechanism consisted in the activation of the carbonyl group of DMC by the hydrogen-bond interaction with the cation of the IL catalyst followed by a nucleophilic attack of 1-pentanol (Scheme 16).
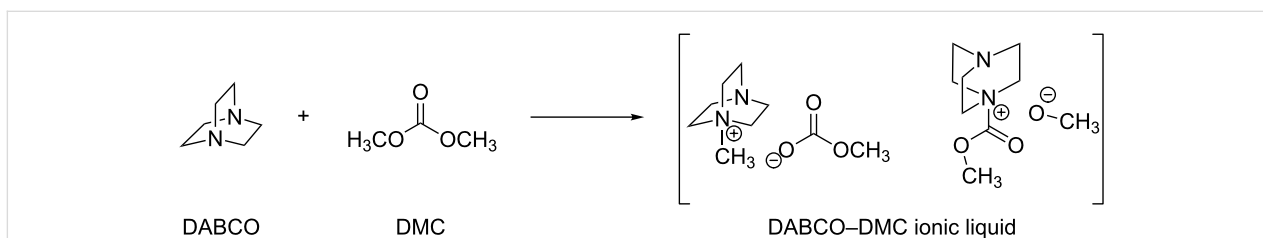
Scheme 13: Synthesis of the DABCO–DMC ionic liquid.
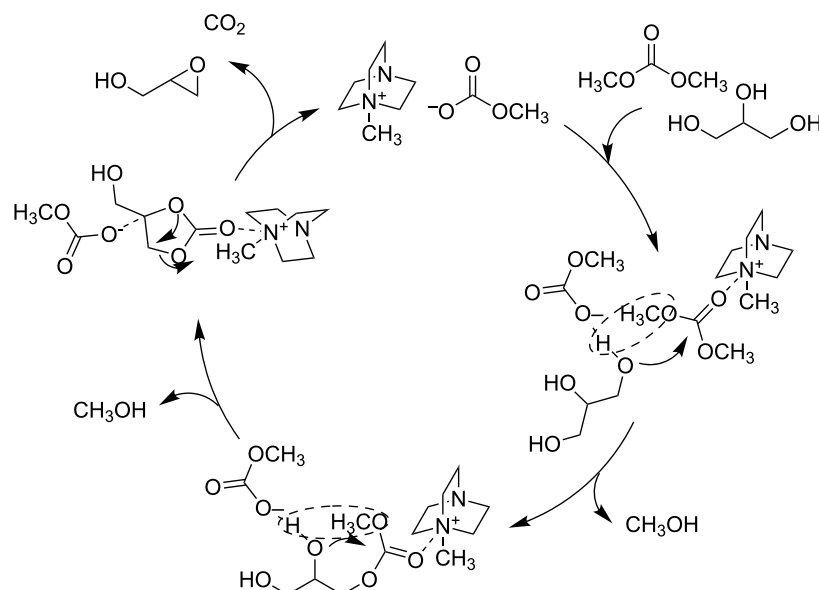
Scheme 14: Cooperative mechanism of ionic liquid-catalyzed glycidol production.
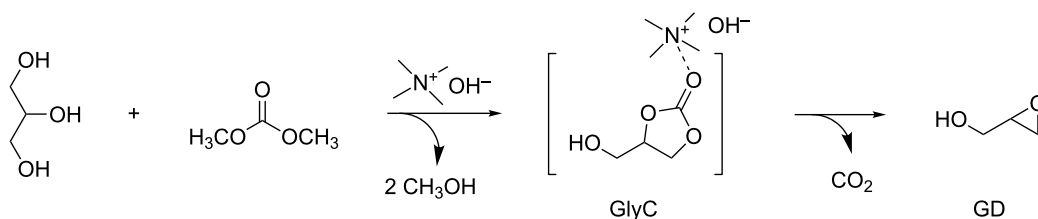
Scheme 15: [TMA][OH]-catalyzed synthesis of glycidol (GD) from glycerol and dimethyl carbonate [46].
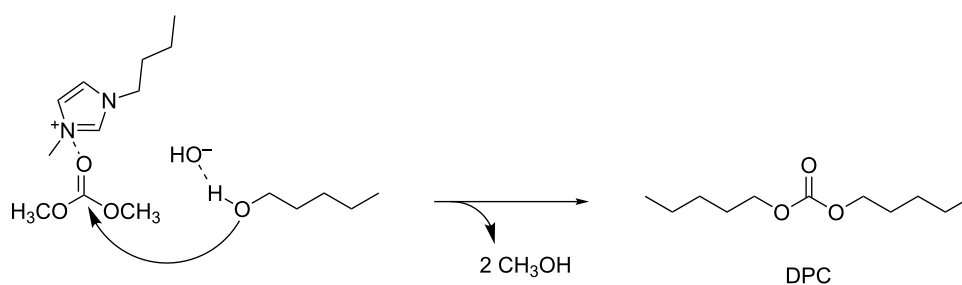
Scheme 16: [BMIM]OH-catalyzed synthesis of DPC from DMC and 1-pentanol.

A similar transesterification reaction of dimethyl carbonate with *n*-butanol has been accomplished using tetraethylammonium-based amino acid ionic liquids ([N_{2222}][AA]) as homogeneous catalysts (Figure 3) [68]. [N_{2222}][Pro] exhibited the best catalytic activity yielding an overall 72% yield of the dibutyl carbonate (DBC) product. Quantum-mechanical calculations indicated that the catalyst synergistically activated both BuOH and DMC.

A wide variety of acyclic non-symmetrical organic carbonates of general formula $ROC(O)OCH_3$ were prepared by Kumar et al. through the transesterification of DMC using the ionic liquid 1-(trimethoxysilyl)propyl-3-methylimidazolium chloride as the catalyst (Figure 4). With a 10 mol % ionic liquid loading, the transesterification reaction of DMC with eighteen different alcohols ROH yielded the desired unsymmetrical carbonates

Figure 3: Representative examples of ionic liquids for biodiesel production.
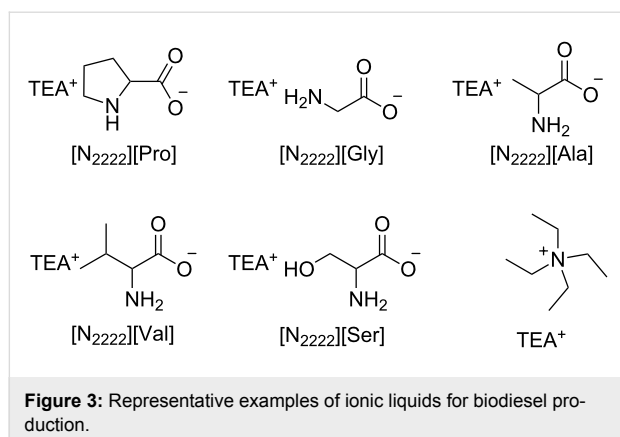
(Figure 4) under mild reaction conditions (80 °C, DMC:ROH in 1:1 ratio) [69].

Acid catalysis: In the transesterification reaction of dimethyl carbonate with phenol to methyl phenyl carbonate (MPC) and diphenyl carbonate (DPhC), Deshmukh et al. studied dibutyltin oxide as a catalyst in conjunction with Brønsted and Lewis acidic ionic liquids [70]. The authors investigated the relative Lewis and Brønsted acidity of the ionic liquids by monitoring the IR bands in the presence of pyridine as a probe molecule. The highest conversions (30–39%) of phenol and the best selectivity toward DPhC were achieved using *N*-methyl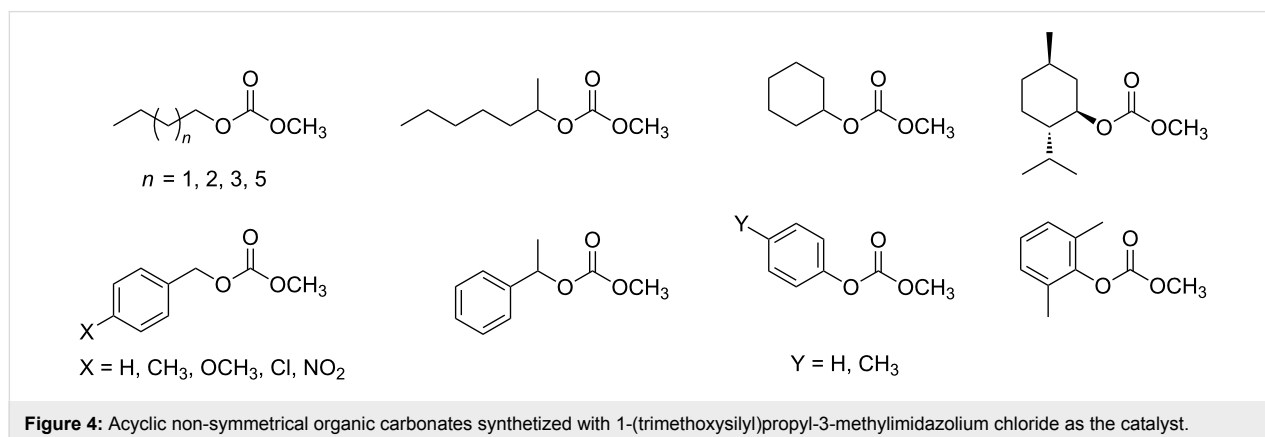-2-pyrrolidone hydrogen sulfate [NMP][HSO$_4$] and choline chloride zinc chloride ([ChCl][ZnCl$_2$]). The ionic liquid increases the catalytic activity of dibutyltin oxide fourfold probably by forming a highly active tin species where the anion of the ionic liquid acts as a ligand. The developed protocol was further studied for various substituted phenols, proving that electron-donating groups (EDG) at the para position enhance the substrate conversion, while electron-withdrawing groups (EWG) provide the aryl methyl carbonate with a very low conversion. Any substituents in the ortho position led to lower conversions due to an increase of the steric hindrance.

Ionic liquid catalyzed transesterification for dimethyl carbonate production: Ionic liquid-based catalysts brought about a number of improvements for the synthesis of DMC. As mentioned above, the synthesis of DMC through CO$_2$ insertion into an epoxide and the subsequent transesterification of the formed cyclic carbonate with methanol represent a valid alternative for the industrial production of DMC [59]. Although ionic liquids can catalyze both reactions, this review will only briefly discuss the second transesterification step. Yang et al. tested many basic ILs derived from DABCO for the synthesis of DMC starting from ethylene carbonate (EC) and methanol [71]. In their study, the best performing one was 1-butyl-4-azo-1-azoniabicyclo[2.2.2]octane hydroxide ([C$_4$DABCO]OH), that achieved 90% conversion, 81% DMC yield and 82% EC yield under optimized conditions (EC:methanol in a 1:10 molar ratio, 1 mol % catalyst loading with respect to EC; 4 h, 70 °C). The catalyst reusability was tested in four successive runs, in which the conversion decreased from 90 to 88% and the DMC yield from 81 to 79%, thereby proving the high stability of the investigated IL and the greenness of the process.

A one-step synthesis of DMC from ethylene oxide (EO), CO$_2$ and methanol was proposed by Li et al., using a series of quaternary ammonium ILs in reactions carried out in an autoclave at 150 °C, and under CO$_2$ pressure (2 MPa) [72]. Even though conversions were good after 8 h, the selectivity toward the desired product was still subject to improvement. Up to 99% EO conversion and 74% DMC selectivity were the best performances, obtained using 6-(*N',N'*-dimethylamino)-1-(*N,N,N*-trimethylammonium)hexane iodide [N$_{111,6}$N$_{11}$]I as the catalyst. The reusability of the catalyst was further studied in eight subsequent reactions. Wang et al. investigated the dependence of the catalytic activity on the structure of IL cations and anions for the synthesis of DMC through the transesterification of EC with methanol [73]. They achieved the best results using a halogen and metal-free IL such as 1,3-dimethylimidazolium-2-carboxylate (DMIM-2-CO$_2$), which was easily prepared by the

Figure 4: Acyclic non-symmetrical organic carbonates synthetized with 1-(trimethoxysilyl)propyl-3-methylimidazolium chloride as the catalyst.

reaction methylimidazole and DMC. Under the best found reaction conditions (1 mol % catalyst loading with respect to EC, EC:MeOH in 1:10 molar ratio, 110 °C, 80 min) the IL catalyst demonstrated high activity, as it gave 82% and 99% yield and selectivity, respectively, on DMC. Scheme 17 summarizes the reaction mechanism proposed for the synthesis of DMC. The same paper described also the results obtained by supporting the imidazolium salt onto a polystyrene resin (PS). This catalytic system proved to be highly stable and no loss of activity was detected after 200 h of reaction performed in a fixed bed reactor at 110 °C. The authors indicated the perspective of full industrial application for such a system.

**Scheme 17:** A simplified reaction mechanism for DMC production.
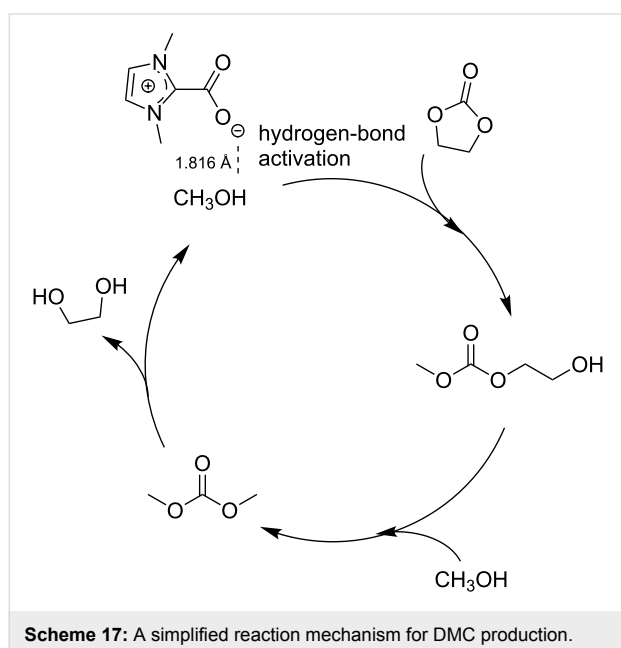
Phosphonium salts as catalysts for the selective transesterification of carbonates

As mentioned above, the transesterification reaction between organic carbonates and alcohols or diols can be carried out in the presence of basic (e.g., tertiary phosphines and amines, alkali metal hydroxides, alkoxides, halides, carbonates, alkali metal exchanged faujasites and hydrotalcites) or acidic catalysts o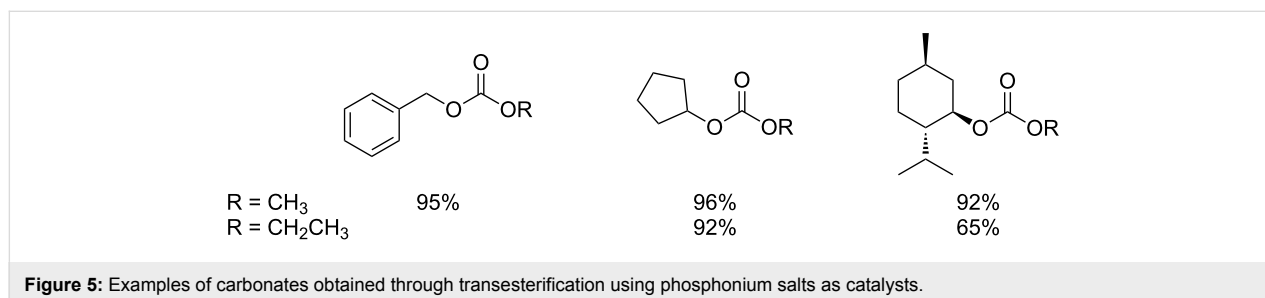r co-catalysts, and under thermal (non-catalytic) conditions. All applicable catalysts show common issues: the reactions (i) often proceed beyond the mono-transesterification products to yield the symmetrical higher organic carbonate, (ii) with polyols, primary and secondary OH groups are not discriminated leading to mixtures of different carbonates.

An effective strategy to improve the mono-transesterification selectivity of such reactions is through the design of new ionic liquid catalysts, such as the recently developed methyl trioctylphosphonium methyl carbonate ($[P_{8881}][MeOCO_2]$) and its anion metathesis analogues (Scheme 3) [34]. Of note, the preparation of these organocatalysts offers several practical advantages: (i) the synthesis of $[P_{8881}][CH_3OCO_2]$ involves a halide-free methylation of a trialkyl phosphine with nontoxic DMC, (ii) acetate and phenolate salt derivatives could be obtained from $[P_{8881}][CH_3OCO_2]$ through a chlorine-free metathesis with acetic acid and phenol (Scheme 18), and (iii) all the ILs are produced in very high purity, they are stable for months and usable straight from the reaction vessel.

Scheme 18: $[P_{8881}][MeOCO_2]$ metathesis with acetic acid and phenol.
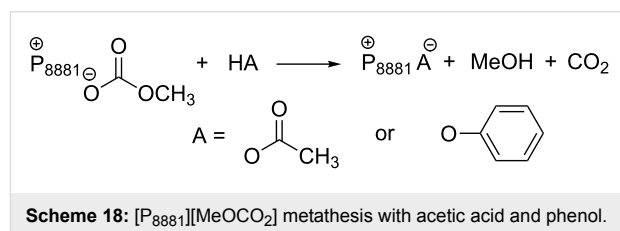
Carbonate, acetate and phenolate phosphonium catalysts were shown to be effective for the mono-transesterification reaction of DMC and DEC with a number of alcohols such as benzyl alcohol, cyclopentanol and menthol [74]. Figure 5 shows some examples of the carbonates obtained in the study. The desired products were achieved at temperatures between 90 and 220 °C.

These results highlight the excellent activity and selectivity of these catalytic systems (conversion >99% and yield >90%) with respect to conventional organic and inorganic bases. In addition, the reactions proceed without decarboxylation even at high temperatures ($T > 150$ °C), as opposed to the outcome using both solid bases and zeolites, that generate large amounts of CO_2.

| R = CH$_3$ | 95% | 96% | 92% |
| R = CH$_2$CH$_3$ | | 92% | 65% |

Figure 5: Examples of carbonates obtained through transesterification using phosphonium salts as catalysts.

The transesterification activity of $[P_{8881}][CH_3OCO_2]$-based ionic liquids was also tested on bio-based diols possessing primary and secondary hydroxy groups. Although a number of different products is expectable, the organocatalysts allowed highly selective reactions. For example, 1,2-diols afforded exclusively the corresponding cyclic carbonates, while 1,3-diols, depending on their structures, could yield both, cyclic or acyclic carbonates, such as the ones shown in Scheme 19 [75].

Scheme 19: Examples of carbonates obtained from different bio-based diols using $[P_{8881}][CH_3OCO_2]$ as catalyst.
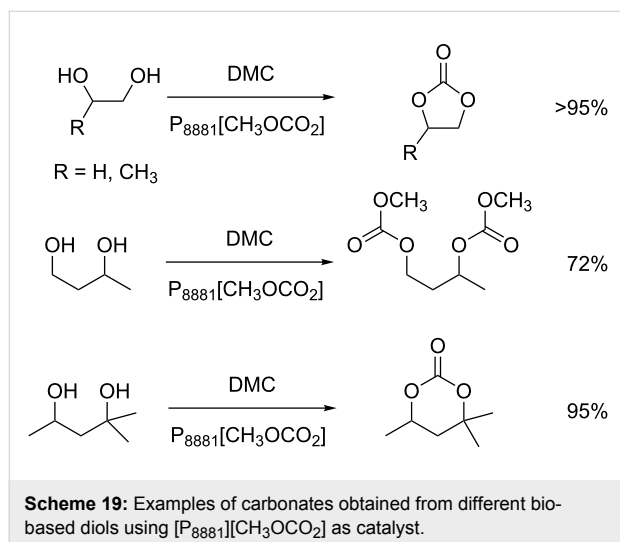
There is no direct relation of the performance of these IL-catalysts to their basicity. Curiously, it should be noted that the activity of such systems was found to be higher than that of strong bases including DBU or DABCO. This phenomenon was observed by several authors [64,76] and explained by a cooperative ambiphilic (nucleophilic–electrophilic) activation effect in which the IL anion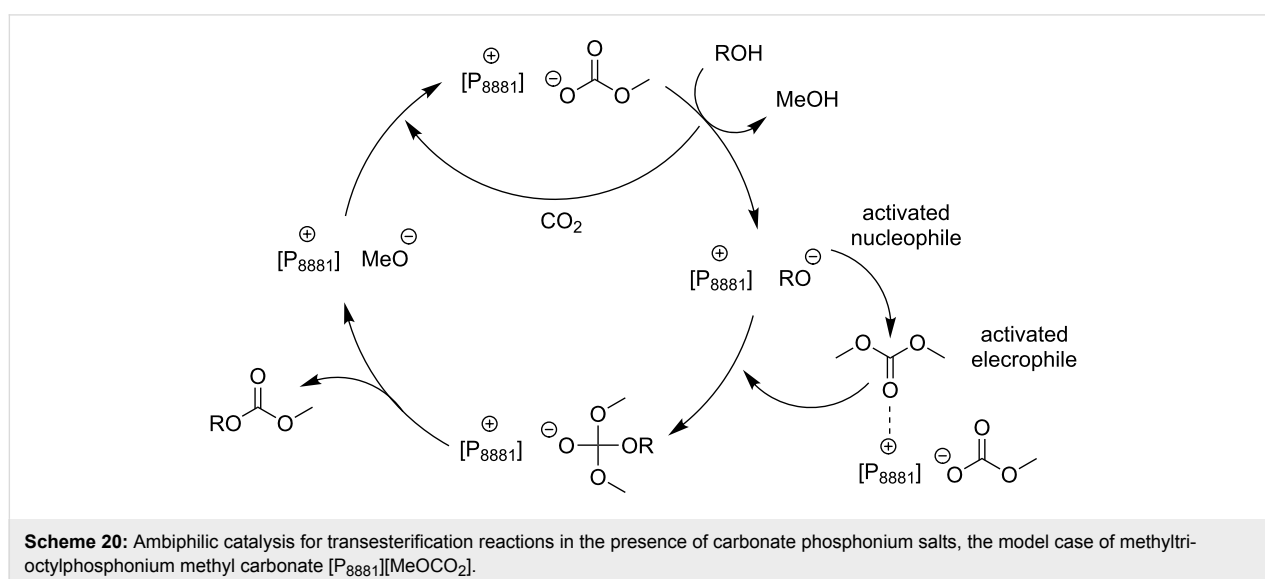 and cation may activate respectively the nucleophile and the electrophile. Scheme 20 shows the proposed mechanisms for the exemplar transesterification of a generic alcohol ROH with DMC using $[P_{8881}][MeOCO_2]$ as catalyst.

The catalytic cooperative activation also explains the selective formation of cyclic or linear products of Scheme 20, without the concurrent production of polycarbonate byproducts. In fact, the selectivity is plausibly due to the steric hindrance of the products, which are much less prone to electrophilic activation (by the catalyst) than the starting DMC or DEC.

Recently, phosphonium salts have been reported as transesterification catalysts of light organic carbonates (dimethyl and diethyl carbonate) with complex polyalcohols, such as cellulose. In particular, trioctylphosphonium acetate ($[P_{8881}][OAc]$) was active for the synthesis of cellulose dialkyl carbonates which find applications as intermediates, supports for the delivery of therapeutics, imaging agents and packaging films and coatings [77].

Conclusion

The literature survey illustrated in this review highlights three main facts. Firstly, organocatalysis by ionic liquids can be an efficient tool for base and even acid-catalyzed transesterification reactions in place of traditional inorganic or solid acids and bases. Advantages in this case are mainly the recovery and recyclability of the catalyst system and the improved selectivity that is often achievable. Secondly, the here presented reactions have a common mechanistic feature based on the cooperative nucleophilic–electrophilic catalysis by the ionic liquid. This type of ambiphilic catalysis is characterized by the nucleophile and the electrophile both being activated respectively by the

Scheme 20: Ambiphilic catalysis for transesterification reactions in the presence of carbonate phosphonium salts, the model case of methyltri-octylphosphonium methyl carbonate $[P_{8881}][MeOCO_2]$.

anion and by the cation of the ionic liquid. Thirdly, organic carbonates – used as feedstocks or produced by transesterification – are valuable synthetic targets in view of the development of new greener solvents, additives, reagents, and in general of chemical products with improved safety and chemical properties.

References

1. Riemenschneider, W.; Bolt, H. M. *Esters, Organic;* Wiley-VCH Verlag GmbH & Co. KGaA: Weinheim, Germany, 2000.
2. Smith, M. B.; March, J. Addition to Carbon–Hetero Multiple Bonds. *March's Advanced Organic Chemistry: Reactions, Mechanisms, and Structure,* 6th ed.; John Wiley & Sons: Hoboken, NJ, U.S.A., 2006. doi:10.1002/9780470084960.ch16
3. Otera, J. *Chem. Rev.* **1993,** *93,* 1449–1470. doi:10.1021/cr00020a004
4. Biradar, A. V.; Umbarkar, S. B.; Dongare, M. K. *Appl. Catal., A* **2005,** *285,* 190–195. doi:10.1016/j.apcata.2005.02.028
5. Kotbagi, T.; Nguyen, D. L.; Lancelot, C.; Lamonier, C.; Thavornprasert, K.-A.; Wenli, Z.; Capron, M.; Jalowiecki-Duhamel, L.; Umbarkar, S.; Dongare, M.; Dumeignil, F. *ChemSusChem* **2012,** *5,* 1467–1473. doi:10.1002/cssc.201100802
6. Srinivas, D.; Srivastava, R.; Ratnasamy, P. *Catal. Today* **2004,** *96,* 127–133. doi:10.1016/j.cattod.2004.06.113
7. Yanmin, D.; Xingquan, C.; Chunxiang, Z.; Tiansheng, Z. *J. Mol. Catal. A: Chem.* **2010,** *331,* 125–129. doi:10.1016/j.molcata.2010.08.015
8. Ho, D. L.; Zhenghao, W. Process for the preparation of sucrose-6-ester by esterification in the presence of solid superacid catalyst. U.S. Patent 0,103,295 A1, May 1, 2008.
9. Van de Steene, E.; De Clercq, J.; Thybaut, J. W. *Chem. Eng. J.* **2014,** *242,* 170–179. doi:10.1016/j.cej.2013.12.025
10. Limmanee, S.; Naree, T.; Bunyakiat, K.; Ngamcharussrivichai, C. *Chem. Eng. J.* **2013,** *225,* 616–624. doi:10.1016/j.cej.2013.03.093
11. Boro, J.; Deka, D.; Thakur, A. J. *Renewable Sustainable Energy Rev.* **2012,** *16,* 904–910. doi:10.1016/j.rser.2011.09.011
12. Suryaputra, W.; Winata, I.; Indraswati, N.; Ismadji, S. *Renewable Energy* **2013,** *50,* 795–799. doi:10.1016/j.renene.2012.08.060
13. Smith, S. M.; Oopathum, C.; Weeramongkhonlert, V.; Smith, C. B.; Chaveanghong, S.; Ketwong, P.; Boonyuen, S. *Bioresour. Technol.* **2013,** *143,* 686–690. doi:10.1016/j.biortech.2013.06.087
14. Rezaei, R.; Mohadesi, M.; Moradi, G. R. *Fuel* **2013,** *109,* 534–541. doi:10.1016/j.fuel.2013.03.004
15. Kai, T.; Mak, G. L.; Wada, S.; Nakazato, T.; Takanashi, H.; Uemura, Y. *Bioresour. Technol.* **2014,** *163,* 360–363. doi:10.1016/j.biortech.2014.04.030
16. Zhang, L.; Sheng, B.; Xin, Z.; Liu, Q.; Sun, S. *Bioresour. Technol.* **2010,** *101,* 8144–8150. doi:10.1016/j.biortech.2010.05.069
17. Tudorache, M.; Protesescu, L.; Coman, S.; Parvulescu, V. I. *Green Chem.* **2012,** *14,* 478–482. doi:10.1039/c2gc16294f
18. Pyo, S.-H.; Persson, P.; Lundmark, S.; Hatti-Kaul, R. *Green Chem.* **2011,** *13,* 976–982. doi:10.1039/c0gc00783h
19. Guldhe, A.; Singh, B.; Mutanda, T.; Permaul, K.; Bux, F. *Renewable Sustainable Energy Rev.* **2015,** *41,* 1447–1464. doi:10.1016/j.rser.2014.09.035
20. Ochoa-Gómez, J. R.; Gómez-Jiménez-Aberasturi, O.; Ramírez-López, C.; Maestro-Madurga, B. *Green Chem.* **2012,** *14,* 3368–3376. doi:10.1039/c2gc35992h
21. Srivastava, R.; Srinivas, D.; Ratnasamy, P. *J. Catal.* **2006,** *241,* 34–44. doi:10.1016/j.jcat.2006.04.002
22. Tanabe, K.; Hölderich, W. F. *Appl. Catal., A* **1999,** *181,* 399–434. doi:10.1016/S0926-860X(98)00397-4
23. Clark, J. H. *Green Chem.* **1999,** *1,* 1–8. doi:10.1039/a807961g
24. Parawira, W. *Crit. Rev. Biotechnol.* **2009,** *29,* 82–93. doi:10.1080/07388550902823674
25. Olivier-Bourbigou, H.; Magna, L.; Morvan, D. *Appl. Catal., A* **2010,** *373,* 1–56. doi:10.1016/j.apcata.2009.10.008
26. Zhang, Q.; Zhang, S.; Deng, Y. *Green Chem.* **2011,** *13,* 2619–2637. doi:10.1039/c1gc15334j
27. Giernoth, R. *Angew. Chem., Int. Ed.* **2010,** *49,* 2834–2839. doi:10.1002/anie.200905981
28. Chatel, G.; Pereira, J. F. B.; Debbeti, V.; Wang, H.; Rogers, R. D. *Green Chem.* **2014,** *16,* 2051–2083. doi:10.1039/c3gc41389f
29. Wasserscheid, P.; Welton, T. *Ionic Liquids In Synthesis;* Wiley-VCH: Weinheim, Germany, 2002.
30. Weber, C. C.; Masters, A. F.; Maschmeyer, T. *Green Chem.* **2013,** *15,* 2655–2679. doi:10.1039/c3gc41313f
31. Hallett, J. P.; Welton, T. *Chem. Rev.* **2011,** *111,* 3508–3576. doi:10.1021/cr1003248
32. Holbrey, J. D.; Reichert, W. M.; Swatloski, R. P.; Broker, G. A.; Pitner, W. R.; Seddon, K. R.; Rogers, R. D. *Green Chem.* **2002,** *4,* 407–413. doi:10.1039/b204469b
33. Ferguson, J. L.; Holbrey, J. D.; Ng, S.; Plechkova, N. V.; Seddon, K. R.; Tomaszowska, A. A.; Wassell, D. F. *Pure Appl. Chem.* **2012,** *84,* 723–744. doi:10.1351/PAC-CON-11-07-21
34. Fabris, M.; Lucchini, V.; Noè, M.; Perosa, A.; Selva, M. *Chem. – Eur. J.* **2009,** *15,* 12273–12282. doi:10.1002/chem.200901891
35. Cattelan, L.; Noè, M.; Demitri, N.; Selva, M.; Perosa, A. *ChemSusChem* **2015,** *8,* 3963–3966. doi:10.1002/cssc.201500935
36. Selvam, T.; Machoke, A.; Schwieger, W. *Appl. Catal., A* **2012,** *445–446,* 92–101. doi:10.1016/j.apcata.2012.08.007
37. Ratti, R.; Kaur, S.; Vaultier, M.; Singh, V. *Catal. Commun.* **2010,** *11,* 503–507. doi:10.1016/j.catcom.2009.11.015
38. Zhen, B.; Jiao, Q.; Wu, Q.; Li, H. *J. Energy Chem.* **2014,** *23,* 97–104. doi:10.1016/S2095-4956(14)60122-4
39. Zhang, Y.; Jiao, Q.; Zhen, B.; Wu, Q.; Li, H. *Appl. Catal., A* **2013,** *453,* 327–333. doi:10.1016/j.apcata.2012.12.029
40. Mrówczyński, R.; Nan, A.; Liebscher, J. *RSC Adv.* **2014,** *4,* 5927–5952. doi:10.1039/c3ra46984k
41. Xu, J.; Wu, H.-T.; Ma, C.-M.; Xue, B.; Li, Y.-X.; Cao, Y. *Appl. Catal., A* **2013,** *464–465,* 357–363. doi:10.1016/j.apcata.2013.06.016
42. Pinaud, J.; Vignolle, J.; Gnanou, Y.; Taton, D. *Macromolecules* **2011,** *44,* 1900–1908. doi:10.1021/ma1024285
43. Coupillaud, P.; Pinaud, J.; Guidolin, N.; Vignolle, J.; Fèvre, M.; Veaudecrenne, E.; Mecerreyes, D.; Taton, D. *J. Polym. Sci., Part A: Polym. Chem.* **2013,** *51,* 4530–4540. doi:10.1002/pola.26869
44. Zhang, J.; Zhang, S.; Han, J.; Hu, Y.; Yan, R. *Chem. Eng. J.* **2015,** *271,* 269–275. doi:10.1016/j.cej.2015.02.093
45. Nowicki, J.; Nosal, H.; Muszyński, M. *ChemPlusChem* **2015,** *80,* 648–651. doi:10.1002/cplu.201402366
46. Wang, H.; Wu, C.; Bu, X.; Tang, W.; Li, L.; Qiu, T. *Chem. Eng. J.* **2014,** *246,* 366–372. doi:10.1016/j.cej.2014.02.081
47. Cui, X.; Cai, J.; Zhang, Y.; Li, R.; Feng, T. *Ind. Eng. Chem. Res.* **2011,** *50,* 11521–11527. doi:10.1021/ie2000715
48. Jiang, D.; Wang, Y. Y.; Tu, M.; Dai, L. Y. *React. Kinet. Catal. Lett.* **2008,** *95,* 265–271. doi:10.1007/s11144-008-5345-8

49. Peng, Y.; Cui, X.; Zhang, Y.; Feng, T.; Tian, Z.; Xue, L. *Appl. Catal., A* **2013,** *466,* 131–136. doi:10.1016/j.apcata.2013.06.048

50. Peng, Y.; Cui, X.; Zhang, Y.; Feng, T.; Tian, Z.; Xue, L. *Int. J. Chem. Kinet.* **2014,** *46,* 116–125. doi:10.1002/kin.20835

51. Fauzi, A. H. M.; Amin, N. A. S. *Renewable Sustainable Energy Rev.* **2012,** *16,* 5770–5786. doi:10.1016/j.rser.2012.06.022

52. Li, K.-X.; Chen, L.; Yan, Z.-C.; Wang, H.-L. *Catal. Lett.* **2010,** *139,* 151–156. doi:10.1007/s10562-010-0409-x

53. Zhang, L.; Xian, M.; He, Y.; Li, L.; Yang, J.; Yu, S.; Xu, X. *Bioresour. Technol.* **2009,** *100,* 4368–4373. doi:10.1016/j.biortech.2009.04.012

54. Li, J.; Peng, X.; Luo, M.; Zhao, C.-J.; Gu, C.-B.; Zu, Y.-G.; Fu, Y.-J. *Appl. Energy* **2014,** *115,* 438–444. doi:10.1016/j.apenergy.2013.10.025

55. Santos, B. A. V.; Silva, V. M. T. M.; Loureiro, J. M.; Rodrigues, A. E. *ChemBioEng Rev.* **2014,** *1,* 214–229. doi:10.1002/cben.201400020

56. Martín, C.; Fiorani, G.; Kleij, A. W. *ACS Catal.* **2015,** *5,* 1353–1370. doi:10.1021/cs5018997

57. Romano, U.; Tesei, R.; Cipriani, G.; Micucci, L. Method for the preparation of esters of carbonic acid. U.S. Patent 4,218,391, Aug 19, 1980.

58. Romano, U.; Tesel, R.; Mauri, M. M.; Rebora, P. *Ind. Eng. Chem. Prod. Res. Dev.* **1980,** *19,* 396–403. doi:10.1021/i360075a021

59. Nishihira, K.; Yoshida, S.; Tanaka, S. Process for purifying dimethyl carbonate. U.S. Patent 5,292,917, March 8, 1994.

60. Fukuoka, S.; Fukawa, I.; Tojo, M.; Oonishi, K.; Hachiya, H.; Aminaka, M.; Hasegawa, K.; Komiya, K. *Catal. Surv. Asia* **2010,** *14,* 146–163. doi:10.1007/s10563-010-9093-5

61. Naik, P. U.; Petitjean, L.; Refes, K.; Picquet, M.; Plasseraud, L. *Adv. Synth. Catal.* **2009,** *351,* 1753–1756. doi:10.1002/adsc.200900280

62. Yi, Y.; Shen, Y.; Sun, J.; Wang, B.; Xu, F.; Sun, R. *Chin. J. Catal.* **2014,** *35,* 757–762. doi:10.1016/S1872-2067(14)60036-X

63. Lucchini, V.; Noè, M.; Selva, M.; Fabris, M.; Perosa, A. *Chem. Commun.* **2012,** *48,* 5178–5180. doi:10.1039/c2cc31099f

64. Munshi, M. K.; Biradar, P. S.; Gade, S. M.; Rane, V. H.; Kelkar, A. A. *RSC Adv.* **2014,** *4,* 17124–17128. doi:10.1039/c3ra47433j

65. Munshi, M. K.; Gade, S. M.; Rane, V. H.; Kelkar, A. A. *RSC Adv.* **2014,** *4,* 32127–32133. doi:10.1039/C4RA04290E

66. Gade, S. M.; Munshi, M. K.; Chherawalla, B. M.; Rane, V. H.; Kelkar, A. A. *Catal. Commun.* **2012,** *27,* 184–188. doi:10.1016/j.catcom.2012.07.003

67. Han, S.; Luo, M.; Zhou, X.; He, Z.; Xiong, L. *Ind. Eng. Chem. Res.* **2012,** *51,* 5433–5437. doi:10.1021/ie202628m

68. Ouyang, F.; Wang, Z.-Z.; Zhou, Y.; Cheng, Z.; Lu, Z.-H.; Yang, Z.; Tao, D.-J. *Appl. Catal., A* **2015,** *492,* 177–183. doi:10.1016/j.apcata.2014.12.037

69. Kumar, S.; Jain, S. L. *New J. Chem.* **2013,** *37,* 3057–3061. doi:10.1039/c3nj00640a

70. Deshmukh, K. M.; Qureshi, Z. S.; Dhake, K. P.; Bhanage, B. M. *Catal. Commun.* **2010,** *12,* 207–211. doi:10.1016/j.catcom.2010.09.017

71. Yang, Z.-Z.; He, L.-N.; Dou, X.-Y.; Chanfreau, S. *Tetrahedron Lett.* **2010,** *51,* 2931–2934. doi:10.1016/j.tetlet.2010.03.114

72. Li, J.; Wang, L.; Shi, F.; Liu, S.; He, Y.; Lu, L.; Ma, X.; Deng, Y. *Catal. Lett.* **2011,** *141,* 339–346. doi:10.1007/s10562-010-0498-6

73. Wang, J.-Q.; Sun, J.; Cheng, W.-G.; Shi, C.-Y.; Dong, K.; Zhang, X.-P.; Zhang, S.-J. *Catal. Sci. Technol.* **2012,** *2,* 600–605. doi:10.1039/C1CY00342A

74. Selva, M.; Noè, M.; Perosa, A.; Gottardo, M. *Org. Biomol. Chem.* **2012,** *10,* 6569–6578. doi:10.1039/c2ob25447f

75. Selva, M.; Caretto, A.; Noè, M.; Perosa, A. *Org. Biomol. Chem.* **2014,** *12,* 4143–4155. doi:10.1039/c4ob00655k

76. Chakraborti, A. K.; Roy, S. R. *J. Am. Chem. Soc.* **2009,** *131,* 6902–6903. doi:10.1021/ja900076a

77. Labafzadeh, S. R.; Helminen, K. J.; Kilpeläinen, I.; King, A. W. T. *ChemSusChem* **2015,** *8,* 77–81. doi:10.1002/cssc.201402794

Scope and limitations of a DMF bio-alternative within Sonogashira cross-coupling and Cacchi-type annulation

Kirsty L. Wilson[1], Alan R. Kennedy[1], Jane Murray[2], Ben Greatrex[3], Craig Jamieson[1] and Allan J. B. Watson[*1]
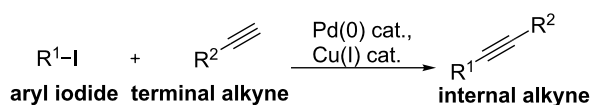
Abstract

Pd-catalysed C–C bond formation is an essential tool within the pharmaceutical and agrochemical industries. Many of these reactions rely heavily on polar aprotic solvents; however, despite their utility, these solvents are incompatible with the drive towards more sustainable chemical synthesis. Herein, we describe the scope and limitations of an alternative to DMF derived from renewable sources (Cyrene[TM]) in Sonogashira cross-coupling and Cacchi-type annulations.

Introduction

The Sonogashira reaction [1,2] (Scheme 1) is a robust and broadly applicable Pd-catalysed bond-forming process that, alongside the Suzuki–Miyaura reaction [3], has steadily become an indispensible tool for C–C bond formation in the pharmaceutical industry [4]. While the Sonogashira reaction can be effec-

tively carried out in a variety of media [1,2], in the general sense this process clearly relies upon the use of dipolar aprotic solvents, in particular DMF. Indeed, some 41% of all Sonogashira reactions reported using aryl iodides can be linked to the use of DMF as a solvent [5].

In this context, the sustainability movement within pharmaceutical research and development strives to substitute solvents that have regulatory and environmental issues for those with a lower perceived risk. Indeed, solvent replacement has been designated a key research area with numerous pharmaceutical companies detailing their efforts towards a more sustain-

Scheme 1: The Sonogashira reaction.

able solvent selection as part of their overall sustainability programmes [6-23].

Based on its associated regulatory issues [24], it is perhaps no surprise that DMF continues to be a priority solvent for replacement. With legislation surrounding the use of DMF becoming increasingly stringent [24], numerous efforts have been made towards the use of alternative media in the Sonogashira reaction [25-30]. However, notwithstanding its issues, DMF is an excellent solvent for the Sonogashira reaction and its replacement frequently occurs at the expense of increased temperature (and therefore potentially substrate compatibility), reaction time, catalyst loading or the requirement for non-commercial/ expensive catalysts, and yield [25-30]. Consequently, poor choice of solvent replacement can result in one of industry's workhorse reactions becoming rather less predictable and robust.

In this regard, dihydrolevoglucosenone (Cyrene, Figure 1), accessed in two steps from cellulose [31,32], has been shown to possess similar physical properties to those of DMF and other dipolar aprotic solvents [31,32]. In addition to its renewability, Cyrene, as yet, has no associated pernicious effects and could potentially represent a direct and functional replacement in many of the fundamental reactions that typically employ DMF [31,32]. The replacement of solvents with regulatory issues with bio-derived alternatives has provided a series of advances within the cross-coupling arena [33], allowing efficient C–C bond formation via cornerstone Pd-based methods including Suzuki–Miyaura [34,35], Mizoroki–Heck [36,37], Sonogashira [38], Stille [39], Hiyama reactions [40], and hydroformylation reactions [41].
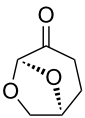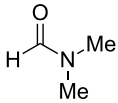

Figure 1: Cyrene vs. DMF – selected physical properties [31,32].

In the current study, we present the use of Cyrene as an alternative solvent (direct DMF replacement) for the Sonogashira reaction, as well as related Cacchi-type annulations [42,43], with an emphasis on scope and limitations of its application.

Results and Discussion

To explore the use of Cyrene in the context of the Sonogashira cross-coupling, we established a simple benchmark reaction

using iodobenzene (**1a**) and phenylacetylene (**2a**) (Table 1). A typical literature-derived catalyst system was employed (Pd(PPh$_3$)$_2$Cl$_2$ with CuI additive [44,45]) and conversion to diphenylacetylene (**3a**) was monitored.

Table 1: Reaction optimisation and comparison with existing solvents.[a]

Entry	Reaction conditions	3a (%)[b]
1	0.1 M, Et$_3$N (3 equiv), 20 °C, 5 h	94
2	0.3 M, Et$_3$N (3 equiv), 20 °C, 5 h	98
3	0.5 M, Et$_3$N (3 equiv), 20 °C, 5 h	100
4	0.5 M, K$_3$PO$_4$ (3 equiv), 20 °C, 5 h	–[c]
5	0.5 M, Cs$_2$CO$_3$ (3 equiv), 20 °C, 5 h	–[c]
7	0.5 M, Et$_3$N (1.1 equiv), 20 °C, 5 h	98
8	0.5 M, Et$_3$N (1.1 equiv), 30 °C, 1 h	96
9[d]	0.5 M, Et$_3$N (1.1 equiv), 30 °C, 1 h	81
10[e]	0.5 M, Et$_3$N (1.1 equiv), 30 °C, 1 h	87

[a]**1** (1 equiv, 0.25 mmol), **2** (1.05 equiv, 0.26 mmol), Pd(PPh$_3$)$_2$Cl$_2$ (2 mol %), CuI (4 mol %), base (see table), Cyrene, temperature (see table), time (see table), N$_2$. [b]Isolated yield. [c]Reaction mixture solidified, product was not isolated. [d]THF used as solvent. [e]DMF used as solvent.

Pleasingly, high conversion to product was immediately observed at room temperature in 5 h (94%, Table 1, entry 1). This high conversion was consistent across several reaction concentrations (Table 1, entries 2 and 3) allowing for a reduction in solvent volume, commensurate with the principles of green chemistry [46,47].

In attempts to further limit waste, we scanned a series of bases (see Supporting Information File 1); organic bases consistently performed more effectively and alternatives to Et$_3$N provided no significant advantages. However, during this process we identified some potential limitations of this emerging solvent. Specifically, inorganic bases such as K$_3$PO$_4$ and Cs$_2$CO$_3$ (Table 1, entries 4 and 5) resulted in the generation of a solid reaction mixture. Further analysis revealed that the aldol products **4a** and **4b** (Figure 2) were generated under specific reaction conditions.

The manufacturers note that when using Cyrene, materials to avoid are strong acids, and strong oxidising and reducing agents. Since sensitivity to base was not specified, we surveyed a range of bases at various temperatures to evaluate the limitations of Cyrene under such conditions (Table 2).
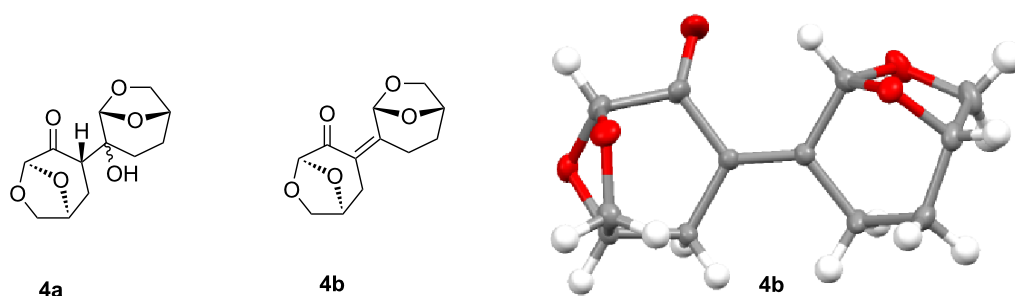
Figure 2: Aldol products **4a** and **4b** and single crystal X-ray structure of **4b**.

Table 2: Evaluation of the base sensitivity of Cyrene.[a]

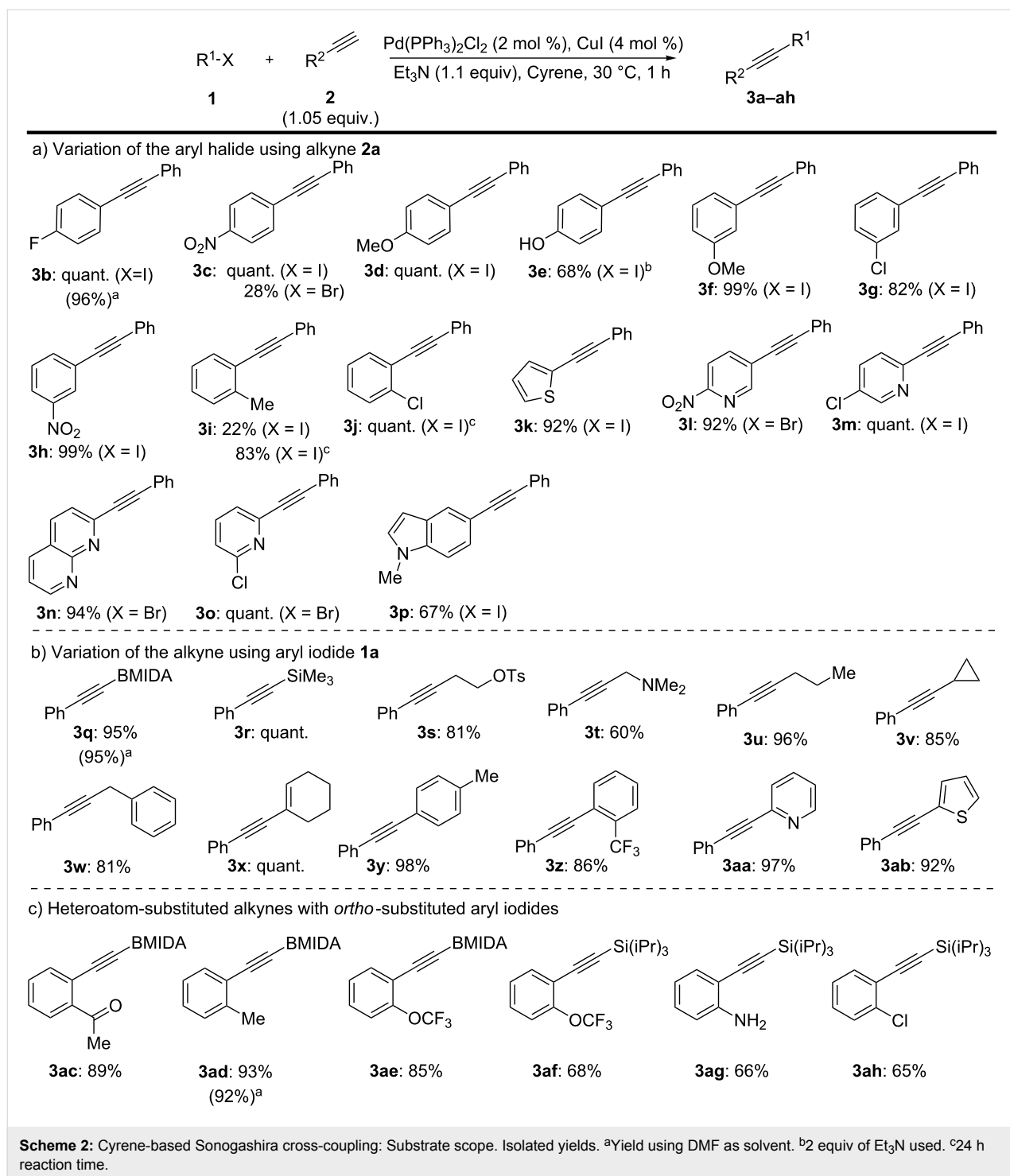| Entry	Base	Temp. (°C)	Reaction (Y/N)[b]
1	KOAc	25	N
		50	Y
		100	Y
2	Pyridine	25	N
		50	Y
		100	Y
3	K_2CO_3	25	Y
		50	Y
		100	Y
4	DIPEA	25	N
		50	N
		100	Y
5	Cs_2CO_3	25	Y
		50	Y
		100	Y
6	Et_3N	25	N
		50	N
		100	Y
7	K_3PO_4	25	Y
		50	Y
		100	Y
8	DBU	25	Y
		50	Y
		100	Y
9	KOH	25	Y
		50	Y
		100	Y
10	*t*-BuOK	25	Y
		50	Y
		100	Y
11	NaH	25	Y
		50	Y
		100	Y

[a]Reaction conditions: base (0.07 mmol) and Cyrene (0.5 mL) stirred at the indicated temeperature for 24 h before analysis by TLC and ^{1}H NMR . [b]Y = reaction occurs, N = no reaction. See Supporting Information File 1.

Under these specific reaction conditions, with the exception of Et_3N and DIPEA, there was a clear base sensitivity displayed by Cyrene in the presence of all bases when the temperature was elevated above 25 °C. Organic bases such as pyridine (Table 2, entry 2), DIPEA (Table 2, entry 4), and Et_3N (Table 2, entry 6) were tolerated at 25 °C with DIPEA and Et_3N also tolerated at 50 °C. DBU, however, was not tolerated at any temperature (Table 2, entry 8). With the exception of KOAc (Table 2, entry 1), all inorganic bases resulted in reaction with the solvent at room temperature (Table 2, entries 3, 5, 7, and 9–11). The extent of the reaction varied from the generation of additional components, such as **4a** and **4b**, to gelation or complete solidification of the reaction mixture. However, in a moderately basic reaction mixture (e.g., using Et_3N) at mild reaction temperatures this issue could be entirely avoided. As such, optimisation of the Sonogashira process allowed complete conversion and 96% isolated yield in 1 h at 30 °C (Table 1, entry 8). Importantly, the Cyrene-based system compared very favourably upon comparison with standard solvents (THF and DMF; Table 1, entries 9 and 10, respectively).

Continuing with the primary investigation and with an optimised set of reaction conditions, we sought to explore the generality of Cyrene in the Sonogashira cross-coupling (Scheme 2). Significantly, a broad range of functionalised aryl and heteroaryl iodides were tolerated (Scheme 2a).

In addition, electron-deficient aryl bromides were accommodated, although with some variation in yield (**3c**, **3l**, **3o**, **3n**). Functionality on the alkyne component was also typically well tolerated (Scheme 2b). While **3i** and **3j** required an extended reaction time, this was a substrate-specific problem for the use of **2a** with these *ortho*-substituted aryl iodides that was not apparent for other alkyne/*ortho*-substituted iodoarene combinations (Scheme 2c).

Judicious selection of reacting components also enabled the development of a useful Cacchi-type annulation (Scheme 3)

Scheme 2: Cyrene-based Sonogashira cross-coupling: Substrate scope. Isolated yields. [a]Yield using DMF as solvent. [b]2 equiv of Et₃N used. [c]24 h reaction time.

[42,43]. Specifically, employing *ortho*-amino (**5**) or *ortho*-hydroxyaryl iodides (**6**) in the Sonogashira process generated an alkyne intermediate that, upon increasing the reaction temperature from 30 °C to 60 °C, could undergo 5-*endo*-dig cyclisation to forge functionalised and pharmaceutically relevant indole, benzofuran, and aza-indole scaffolds in a single operation (**7a–f**) [48-52].

Finally, with the viewpoint of generality of DMF substitution by Cyrene, the base/temperature sensitivity issue may have potential implications for further applications of Cyrene within well-used organic transformations. For example, the majority of many other standard cross-coupling processes employ inorganic or organic bases and heat (e.g., Suzuki–Miyaura, Heck). Accordingly, Cyrene may be projected to be incompatible with
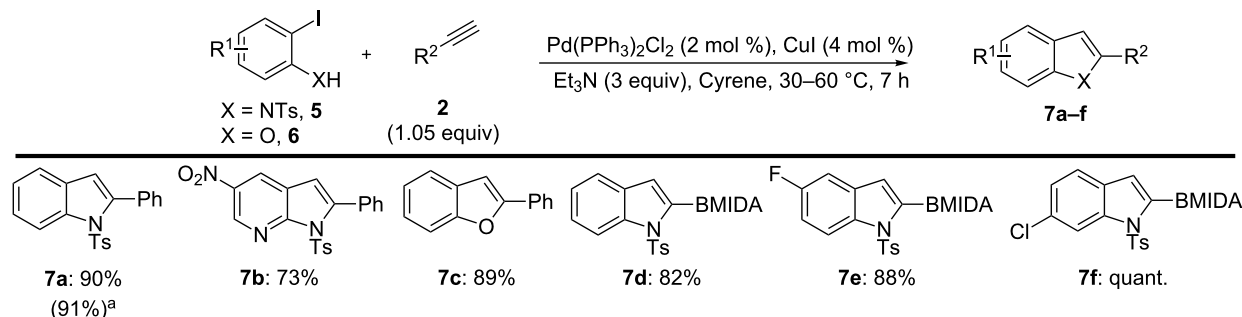
Scheme 3: Cacchi-type annulation of *o*-amino/hydroxy iodoarenes. Isolated yields. [a]Yield using DMF as solvent.

standard conditions for these reactions and its use would necessitate base-free or exceptionally mildly basic reaction conditions. In contrast, amide-bond formation is the most practiced reaction in the pharmaceutical industry [4] and these are routinely performed in DMF at room temperature in the presence of organic bases [53]. As such, Cyrene may offer considerable potential in this area. However, additional work will be required to validate the practicality of Cyrene as a viable DMF replacement in these applications.

Conclusion

In summary, we have developed a mild and robust method for the Sonogashira reaction, employing the bio-derived and sustainable alternative to DMF, Cyrene. In addition, we have shown the capacity for extension of the utility of this new solvent towards enabling the cascade synthesis of functionalised indoles and benzofurans via a Cacchi-type annulation. Perhaps more importantly, we have documented some of the limitations of the use of Cyrene as a solvent, providing guidance emerging in relation to the thermal and chemical (base) stabilities of this promising green solvent.

Supporting Information

Supporting Information File 1

Experimental procedures, analytical data, copies of NMR spectra, and single X-ray crystal diffraction data of **4b**. [http://www.beilstein-journals.org/bjoc/content/supplementary/1860-5397-12-187-S1.pdf]

Acknowledgements

References

1. Chinchilla, R.; Nájera, C. *Chem. Soc. Rev.* **2011,** *40,* 5084–5121. doi:10.1039/c1cs15071e
2. Chinchilla, R.; Nájera, C. *Chem. Rev.* **2007,** *107,* 874–922. doi:10.1021/cr050992x
3. Miyaura, N.; Suzuki, A. *Chem. Rev.* **1995,** *95,* 2457–2483. doi:10.1021/cr00039a007
4. Roughley, S. D.; Jordan, A. M. *J. Med. Chem.* **2011,** *54,* 3451–3479. doi:10.1021/jm200187y
5. A SciFinder search of Sonogashira reaction of aryl iodides revealed that of 341979 reactions, 140997 were performed in DMF. Search conducted 7th June 2016.
6. Breeden, S. W.; Clark, J. H.; Macquarrie, D. J.; Sherwood, J. Green solvents. In *Green Techniques for Organic Synthesis and Medicinal Chemistry;* Zhang, W.; Cue, B. W., Jr., Eds.; Wiley: Chichester, United Kingdom, 2012.
7. Prat, D.; Hayler, J.; Wells, A. *Green Chem.* **2014,** *16,* 4546–4551. doi:10.1039/C4GC01149J
8. Eastman, H. E.; Jamieson, C.; Watson, A. J. B. *Aldrichimica Acta* **2015,** *48,* 51–55.
9. Curzons, A. D.; Constable, D. C.; Cunningham, V. L. *Clean Prod. Process.* **1999,** *1,* 82–90.
10. Jiménez-González, C.; Curzons, A. D.; Constable, D. J. C.; Cunningham, V. L. *Clean Technol. Environ. Policy* **2004,** *7,* 42–50. doi:10.1007/s10098-004-0245-z
11. Constable, D. J. C.; Dunn, P. J.; Hayler, J. D.; Humphrey, G. R.; Leazer, J. L., Jr.; Linderman, R. J.; Lorenz, K.; Manley, J.; Pearlman, B. A.; Wells, A.; Zaks, A.; Zhang, T. Y. *Green Chem.* **2007,** *9,* 411–420. doi:10.1039/B703488C
12. Alfonsi, K.; Colberg, J.; Dunn, P. J.; Fevig, T.; Jennings, S.; Johnson, T. A.; Kleine, H. P.; Knight, C.; Nagy, M. A.; Perry, D. A.; Stefaniak, M. *Green Chem.* **2008,** *10,* 31–36. doi:10.1039/B711717E
13. http://www.acs.org/content/dam/acsorg/greenchemistry/industriainnovation/roundtable/solvent-selection-guide.pdf. AstraZeneca's guidance.
14. Henderson, R. K.; Jiménez-González, C.; Constable, D. J. C.; Alston, S. R.; Inglis, G. G. A.; Fisher, G.; Sherwood, J.; Binks, S. P.; Curzons, A. D. *Green Chem.* **2011,** *13,* 854–862. doi:10.1039/c0gc00918k
15. Prat, D.; Pardigon, O.; Flemming, H.-W.; Letestu, S.; Ducandas, V.; Isnard, P.; Guntrum, E.; Senac, T.; Ruisseau, S.; Cruciani, P.; Hosek, P. *Org. Process Res. Dev.* **2013,** *17,* 1517–1525. doi:10.1021/op4002565

16. Byrne, F. P.; Jin, S.; Paggiola, G.; Petchey, T. H. M.; Clark, J. H.; Farmer, T. J.; Hunt, A. J.; McElroy, C. R.; Sherwood, J. *Sustainable Chem. Processes* **2016,** *4,* 7. doi:10.1186/s40508-016-0051-z

17. Alder, C. M.; Hayler, J. D.; Henderson, R. K.; Redman, A. M.; Shukla, L.; Shuster, L. E.; Sneddon, H. F. *Green Chem.* **2016,** *18,* 3879–3890. doi:10.1039/C6GC00611F

18. Chandrasekhar, S.; Narsihmulu, C.; Shameem Sultana, S.; Ramakrishna Reddy, N. *Org. Lett.* **2002,** *4,* 4399–4401. doi:10.1021/ol0266976

19. MacMillan, D. S.; Murray, J.; Sneddon, H. F.; Jamieson, C.; Watson, A. J. B. *Green Chem.* **2012,** *14,* 3016–3019. doi:10.1039/c2gc36378j

20. Taygerly, J. P.; Miller, L. M.; Yee, A.; Peterson, E. A. *Green Chem.* **2012,** *14,* 3020–3025. doi:10.1039/c2gc36064k

21. MacMillan, D. S.; Murray, J.; Sneddon, H. F.; Jamieson, C.; Watson, A. J. B. *Green Chem.* **2013,** *15,* 596–600. doi:10.1039/c2gc36900a

22. McGonagle, F. I.; MacMillan, D. S.; Murray, J.; Sneddon, H. F.; Jamieson, C.; Watson, A. J. B. *Green Chem.* **2013,** *15,* 1159–1165. doi:10.1039/c3gc40359a

23. Skowerski, K.; Białecki, J.; Tracz, A.; Olszewski, T. K. *Green Chem.* **2014,** *16,* 1125–1130. doi:10.1039/C3GC41943F

24. European Chemicals Agency (ECHA), Candidate List of Substances of Very High Concern for Authorisation. http://echa.europa.eu/candidate-list-table (accessed May 23, 2016).

25. Fleckenstein, C. A.; Plenio, H. *Green Chem.* **2008,** *10,* 563–570. doi:10.1039/b800154e

26. Bakherad, M. *Appl. Organomet. Chem.* **2013,** *27,* 125–140. doi:10.1002/aoc.2931

27. Ibrahim, M. B.; Ali, B. E.; Malik, I.; Fettouhi, M. *Tetrahedron Lett.* **2016,** *57,* 554–558. doi:10.1016/j.tetlet.2015.12.086

28. Gonçalves, R. S. B.; de Oliveira, A. B. V.; Sindra, H. C.; Archanjo, B. S.; Mendoza, M. E.; Carneiro, L. S. A.; Buarque, C. D.; Esteves, P. M. *ChemCatChem* **2016,** *8,* 743–750. doi:10.1002/cctc.201500926

29. Camp, J. E.; Dunsford, J. J.; Dacosta, O. S. G.; Blundell, R. K.; Adams, J.; Britton, J.; Smith, R. J.; Bousfield, T. W.; Fay, M. W. *RSC Adv.* **2016,** *6,* 16115–16121. doi:10.1039/C5RA25712C

30. McAfee, S. M.; Cann, J. R.; Josse, P.; Blanchard, P.; Cabanetos, C.; Welch, G. C. *ACS Sustainable Chem. Eng.* **2016,** *4,* 3504–3517. doi:10.1021/acssuschemeng.6b00554

31. Sherwood, J.; De Bruyn, M.; Constantinou, A.; Moity, L.; McElroy, C. R.; Farmer, T. J.; Duncan, T.; Raverty, W.; Hunt, A. J.; Clark, J. H. *Chem. Commun.* **2014,** *50,* 9650–9652. doi:10.1039/C4CC04133J

32. Koseki, K.; Ebata, T.; Kawakami, H.; Matsushita, H.; Itoh, K.; Naoi, Y. Method of producing (*S*)-4-hydroxymethyl-γ-lactone. U.S. Patent 5112994, May 12, 1992.

33. Ilgen, F.; König, B. *Green Chem.* **2009,** *11,* 848–854. doi:10.1039/b816551c

34. Azua, A.; Mata, J. A.; Heymes, P.; Peris, E.; Lamaty, F.; Martinez, J.; Colacino, E. *Adv. Synth. Catal.* **2013,** *355,* 1107–1116. doi:10.1002/adsc.201201047

35. Wan, J.-P.; Wang, C.; Zhou, R.; Liu, Y. *RSC Adv.* **2012,** *2,* 8789–8792. doi:10.1039/c2ra21632a

36. Strappaveccia, G.; Ismalaj, E.; Petrucci, C.; Lanari, D.; Marrocchi, A.; Drees, M.; Facchetti, A.; Vaccaro, L. *Green Chem.* **2015,** *17,* 365–372. doi:10.1039/C4GC01677G

37. Rasina, D.; Kahler-Quesada, A.; Ziarelli, S.; Warratz, S.; Cao, H.; Santoro, S.; Ackermann, L.; Vaccaro, L. *Green Chem.*, in press. doi:10.1039/C6GC01393G

38. Strappaveccia, G.; Luciani, L.; Bartollini, E.; Marrocchi, A.; Pizzo, F.; Vaccaro, L. *Green Chem.* **2015,** *17,* 1071–1076. doi:10.1039/C4GC01728E

39. Imperato, G.; Vasold, R.; König, B. *Adv. Synth. Catal.* **2006,** *348,* 2243–2247. doi:10.1002/adsc.200600248

40. Ismalaj, E.; Strappaveccia, G.; Ballerini, E.; Elisei, F.; Piermatti, O.; Gelman, D.; Vaccaro, L. *ACS Sustainable Chem. Eng.* **2014,** *2,* 2461–2464. doi:10.1021/sc5004727

41. Pongrácz, P.; Kollár, L.; Mika, L. T. *Green Chem.* **2016,** *18,* 842–847. doi:10.1039/C5GC01778E

42. Cacchi, S.; Fabrizi, G. *Chem. Rev.* **2011,** *111,* PR215–PR283. doi:10.1021/cr100403z

43. Humphrey, G. R.; Kuethe, J. T. *Chem. Rev.* **2006,** *106,* 2875–2911. doi:10.1021/cr0505270

44. Stuart, D. R.; Bertrand-Laperle, M.; Burgess, K. M. N.; Fagnou, K. *J. Am. Chem. Soc.* **2008,** *130,* 16474–16475. doi:10.1021/ja806955s

45. Chen, X.; Wu, Y.; Xu, J.; Yao, H.; Lin, A.; Huang, Y. *Org. Biomol. Chem.* **2015,** *13,* 9186–9189. doi:10.1039/C5OB01338K

46. Anastas, P. T.; Warner, J. C. *Green Chemistry: Theory and Practice;* Oxford University Press: New York, NY, U.S.A., 1998; p 30.

47. Anastas, P.; Eghbali, N. *Chem. Soc. Rev.* **2010,** *39,* 301–312. doi:10.1039/B918763B

48. Heinrich, T.; Seenisamy, J.; Emmanuvel, L.; Kulkarni, S. S.; Bomke, J.; Rohdich, F.; Greiner, H.; Esdar, C.; Krier, M.; Grädler, U.; Musil, D. *J. Med. Chem.* **2013,** *56,* 1160–1170. doi:10.1021/jm3016014

49. Hong, S.; Kim, J.; Seo, J. H.; Jung, K. H.; Hong, S.-S.; Hong, S. *J. Med. Chem.* **2012,** *55,* 5337–5349. doi:10.1021/jm3002982

50. Hong, S.; Lee, S.; Kim, B.; Lee, H.; Hong, S.-S.; Hong, S. *Bioorg. Med. Chem. Lett.* **2010,** *20,* 7212–7215. doi:10.1016/j.bmcl.2010.10.108

51. Tang, J.; Hamajima, T.; Nakano, M.; Sato, H.; Dickerson, S. H.; Lackey, K. E. *Bioorg. Med. Chem. Lett.* **2008,** *18,* 4610–4614. doi:10.1016/j.bmcl.2008.07.019

52. Seath, C. P.; Wilson, K. L.; Campbell, A.; Mowat, J. M.; Watson, A. J. B. *Chem. Commun.* **2016,** *52,* 8703–8706. doi:10.1039/C6CC04554E

53. El-Faham, A.; Albericio, F. *Chem. Rev.* **2011,** *111,* 6557–6602. doi:10.1021/cr100048w

Solvent-free synthesis of novel *para*-menthane-3,8-diol ester derivatives from citronellal using a polymer-supported scandium triflate catalyst

Lubabalo Mafu, Ben Zeelie and Paul Watts[*]

Abstract

The use of natural resources as a chemical feedstock for the synthesis of added-value products is gaining interest; as such we report an environmentally friendly method for the synthesis of *para*-menthane-3,8-diol from natural citronellal oil in 96% yield, under solvent free aqueous conditions. The acylation of *para*-menthane-3,8-diol with various acid anhydrides over polymer-supported scandium triflate (PS-Sc(OTf)$_3$) catalyst was subsequently developed, where both hydroxy groups of *para*-menthane-3,8-diol could be simultaneous acylated under mild reaction conditions to form the corresponding diesters in good yields. The advantages of this method include a simple procedure from natural resources, using solvent-free reaction conditions.

Introduction

Although South Africa has a substantial petrochemical industry, the fine chemical industry is very small and most chemicals are imported. As such there is significant interest in the use of natural resources for the manufacture of added value products; ideally enabling the economy to become more self-sufficient by manufacturing advanced materials within the country. Furthermore, in the long term it is hoped that this will result in job creation and stimulate economic growth. The use of natural resources is gaining interest from a sustainability perspective,

but clearly it is necessary to develop protocols that are as environmentally friendly and sustainable as possible.

The terpene, citronellal (3,7-dimethyl-6-octenal, **1**) is widely used as a feedstock material in the synthesis of fine chemicals such as menthol (**2**) and *para*-menthane-3,8-diol (**3**) [1,2]. These chemical derivatives have a wide range of uses in pharmaceuticals, cosmetics, toothpastes, insect repellents, cleaning agents and other products [3]. The synthesis of menthol

involves the acid-catalysed cyclisation of **1** to form isopulegol **4** as a stable intermediate. The latter is further hydrogenated over a metal-supported catalyst to yield the *cis* and *trans* isomers of menthol **2** (Scheme 1) [4].

Alternatively the acid-catalysed hydration of citronellal (**1**) results in the synthesis of the *cis* and *trans* isomers of *para*-menthane-3,8-diol (**3**, Scheme 2). This chemical derivative is well-known as an active insect repellent and can be found naturally as a minor component of citriodora oil [2]. Considering the chemical structure of **3**, two reactive hydroxy groups are present which can undergo an organic transformation, such as acylation, to yield natural bio-based compounds.

The acylation of alcohols, thiols and amines is a fundamental reaction in organic synthesis. It is mostly used to protect these functional groups in multi-step synthesis processes. The acylation reaction is typically carried-out with activated carboxylic acid derivatives such as acid anhydrides [5], acyl halides [6], acyl imidazoles or acyl ureas [7]. Acylation of alcohols in particular, provides a cheap and effective method for the synthesis of esters with potential applications in pharmaceutical products such as fragrances, flavours, surfactants or solvents [8,9]. Generally, these reactions are done in the presence of amines such as pyridine, triethyl amine or 4-(dimethylamino)pyridine [7] homogeneous Lewis acid catalysts (AlCl$_3$, BF$_3$, TaCl$_5$) [10] or inorganic acids are also used [11]. Recent publications have reported scandium triflate (Sc(OTf)$_3$) to be an effective catalyst in the acylation of alcohols with acid anhydrides and the reaction can be carried out under mild conditions [10,11].

As part of our research investigations, we report the synthesis of novel diester derivatives of *para*-menthane-3,8-diol (PMD, **3**). These diester derivatives are currently being studied within our group for a variety of applications. The synthesis method involves the acylation of **3** with various acid anhydrides. The synthesis method also employs a polymer-supported scandium triflate as a water resistant and environmentally friendly acid catalyst.

Scheme 2: Synthesis of *para*-menthane-3,8-diol.
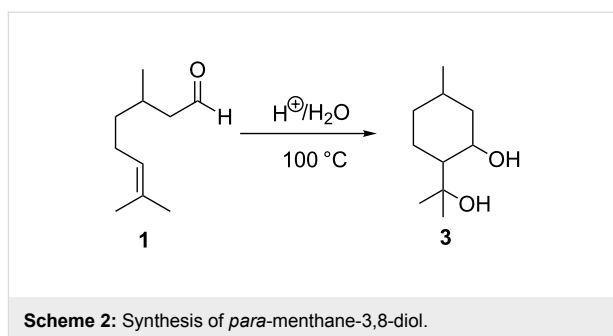
Results and Discussion
Synthesis *para*-menthane-3,8-diol from citronellal

para-Menthane-3,8-diol (**3**) was synthesised according to our earlier developed procedure, which has not been reported in open literature. The synthesis procedure involves the acid-catalysed cyclisation of **1** in aqueous sulfuric acid (Scheme 2) at 100 °C. After which the oil simply separates from the aqueous acid to furnish the product. After recrystallization, the final product **3** was obtained as white crystals in 96% isolated yield.

Synthesis of diester derivatives

Having successfully demonstrated the synthesis of **3**, the investigation was extended to the preparation of diester derivatives of **3** via the acylation reaction with acid anhydrides (Scheme 3). It needs to be clarified that earlier attempts to perform classic esterifications by reaction of the alcohols with a carboxylic acid were not particularly successful, as very complex reaction mixtures were produced as a result of dehydration of the starting material. During the study, various acid anhydrides such as acetic **5**, propionic **6**, pentanoic **7** and hexanoic anhydride **8** were used to prepare the corresponding diester derivatives **9–12**.

To afford an environmentally-friendly process, a polymer-bound scandium triflate (PS-Sc(OTf)$_3$) catalyst was used. Moreover, all the reactions were carried-out under solvent-free conditions. Reaction parameters such as temperature, reaction

Scheme 1: Synthesis of menthol.
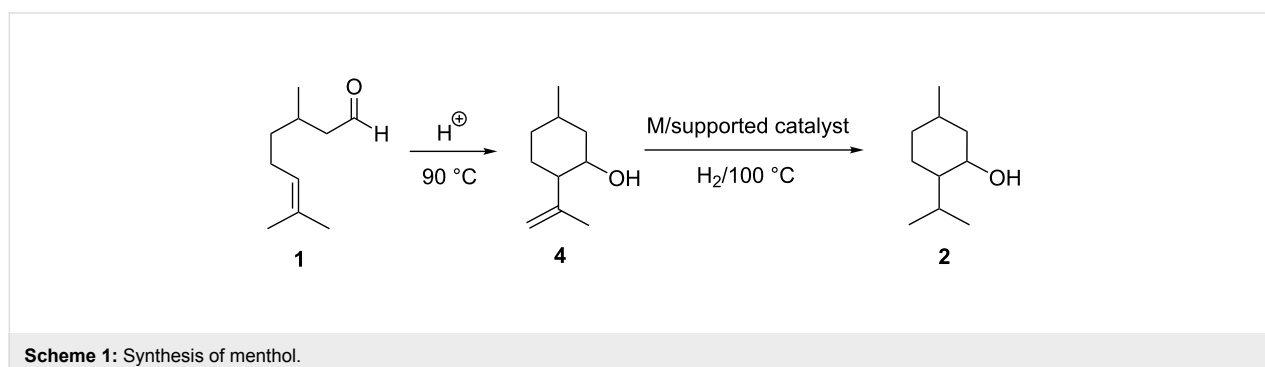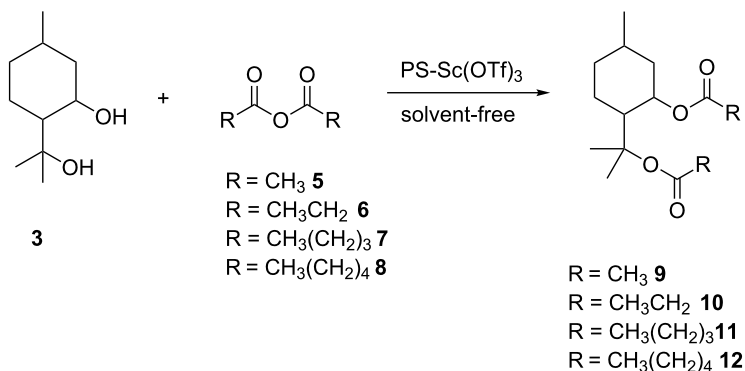
Scheme 3: Synthesis of *para*-menthane diester derivatives.

time and reagent molar ratio were studied towards the substrate conversion and product selectivity.

Effect of reaction temperature and reaction time

In order to determine the effect of temperature and reaction time towards the diester formation, the acylation reaction of *para*-menthane-3,8-diol (**3**) with acetic anhydride **5** was carried out using equimolar amounts of reagent (i.e. 2 equivalents of anhydride per mole of diol). The reaction was conducted at various temperatures ranging from 50 to 80 °C, while other parameters such as stoichiometric ratio, reaction time, catalyst loading and stirring rate were kept constant. The reactions were followed by taking samples at hourly time intervals and quanti-

fied by gas chromatography. Figure 1 shows the graphical presentation of PMD **3** conversion to the desired product at various temperatures.

It can be seen on the graph in Figure 1 that the PMD **3** conversion to diesters has its optimum at lower temperatures. When the reaction is operated at 70 °C and above, dehydration of the substrate starts to occur, leading to complex reaction mixtures.

When considering the diester selectivity (Figure 2), a rapid acetylation of the secondary hydroxy group is evident at short reaction times and lower reaction temperatures between 50 and 60 °C [12].
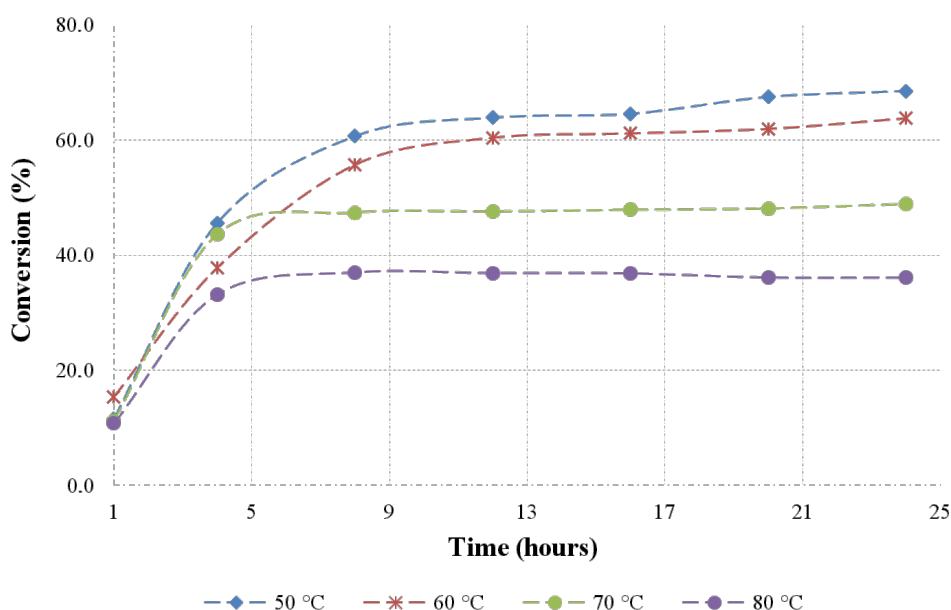
Figure 1: PMD conversion using stoichiometric quantities of acetic anhydride.
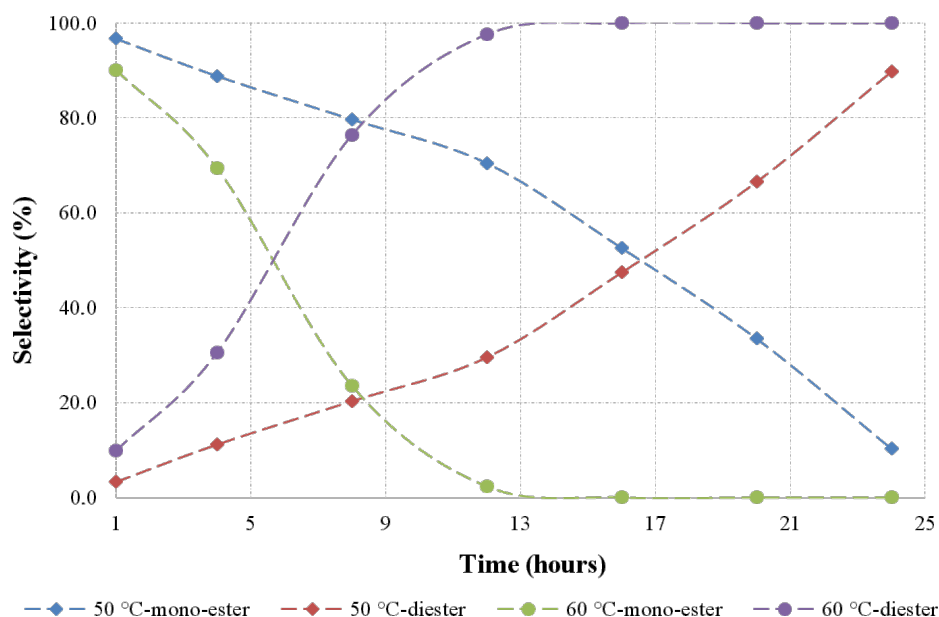
Figure 2: Product distribution as a function of time.

Further increase in the reaction time leads to the acetylation of the less reactive tertiary hydroxy group. Consequently, the diacetate **9** becomes the major product of the reaction. As demonstrated on the graph, the slow reaction rate is evident at lower temperature [12]. A slight increase in temperature improves the reaction rate, as well as the selectivity to diacetate **9**. On further increase in temperature to 70 °C (Figure 3), the decomposition of the starting material is observed and these conditions are clearly unfeasible. However, diacetate selectivity is achieved in shorter residence time. Above 80 °C, poor conversion of **3** and selectivity of **9** are evident. This clearly indicates that this reaction does not tolerate reaction temperatures higher as 70 °C.
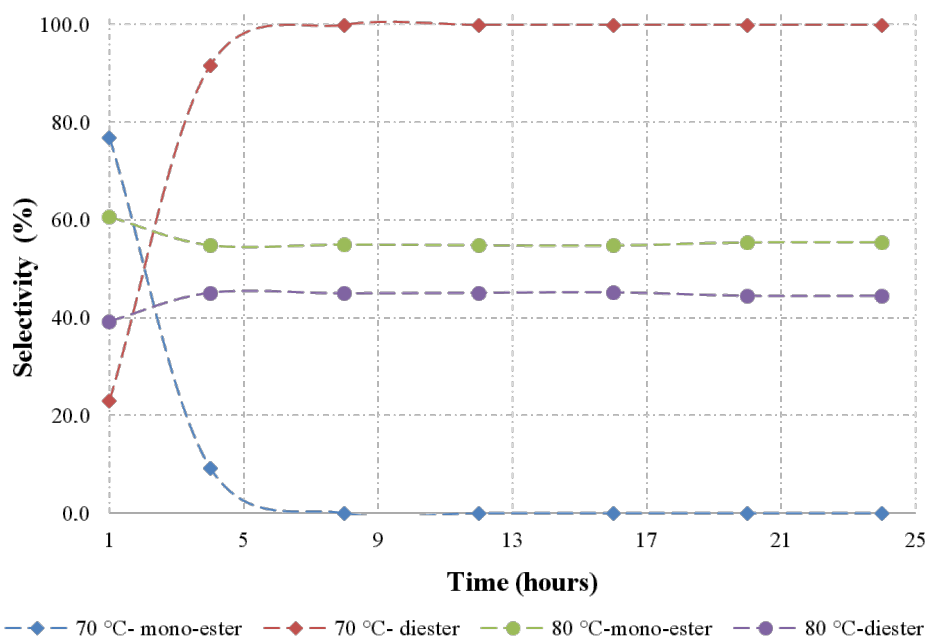
Figure 3: Product distribution as a function of time.

The optimum conditions for the reaction are found to be a temperature of 60 °C and a reaction time of 12 hours. At these conditions, the reaction gives a substrate conversion of 60% and 100% diacetate selectivity, without any dehydration or mono acetate **13** formation.

Effect of molar ratio

The effects of the molar ratio toward the conversion of **3** and the selectivity for **9** were further evaluated at the optimum conditions as highlighted above. The acetic anhydride to *para*-menthane-3,8-diol molar ratio ranging from 2 to 6 were used for the study and other reaction parameters were kept constant. Figure 4 shows the PMD **3** conversion and the selectivity for the formation of **9**, where the graph clearly shows that the use of excess anhydride **5** does not enhance the substrate conversion.

It is clearly shown that when performing an acetylation reaction with 2:1 molar ratio, the reaction affords the same results as when excess anhydride **5** is used. Moreover, the minimum use of the acetylating reagent helps to reduce the formation of carboxylic acid as the by-product. As a consequence, a more cost-effective and environmentally-friendly process is achieved. These results are found to be in agreement to those of Gagea et al., when they demonstrated the effect of molar ratio of acid anhydride-to-alcohol over the silica embedded-triflate catalysts [8]. All the experiments were conducted using the same catalyst and we observed no degradation in performance. However, we are conducting further studies to see how long the reaction could be conducted from a production perspective.

Synthesis of propyl, pentyl and hexyl diester derivatives

Having successfully synthesised the diacetate **9**, other acid anhydrides were evaluated in the process to yield diester derivatives. These include the propionic, pentanoic and hexanoic anhydrides, respectively. The following optimum conditions were used for the study; temperature of 60 °C, reaction time of 12 hours, catalyst loading of 0.3 g and molar ratio of 1:2. Table 1 below shows the acylation results obtained with various acid anhydrides.

It can be seen in Table 1, that the substrate conversion has remained unchanged under these conditions, with the remaining PMD being unreacted. On the other hand, the acid anhydrides with shorter carbon chain appear to be more reactive to yield the diester derivatives, with more monoester being formed as the length of the chain increased. In the case of propionic anhydride, its mono-ester derivative **14** is completely converted into its corresponding diester derivative **10** in 12 hours of reaction time (Scheme 4).

However, the change in the carbon chain length of acid anhydride to C_5 or C_6, leads to a significant decrease in the reactivity towards the tertiary hydroxy group. As a result, the monopentanoate **15** and monohexanoate **16** are found to be present in about 10% yield when the same procedure was used.

Conclusion

In conclusion, we have successfully demonstrated the synthesis of novel diester derivatives of *para*-menthane-3,8-diol. The
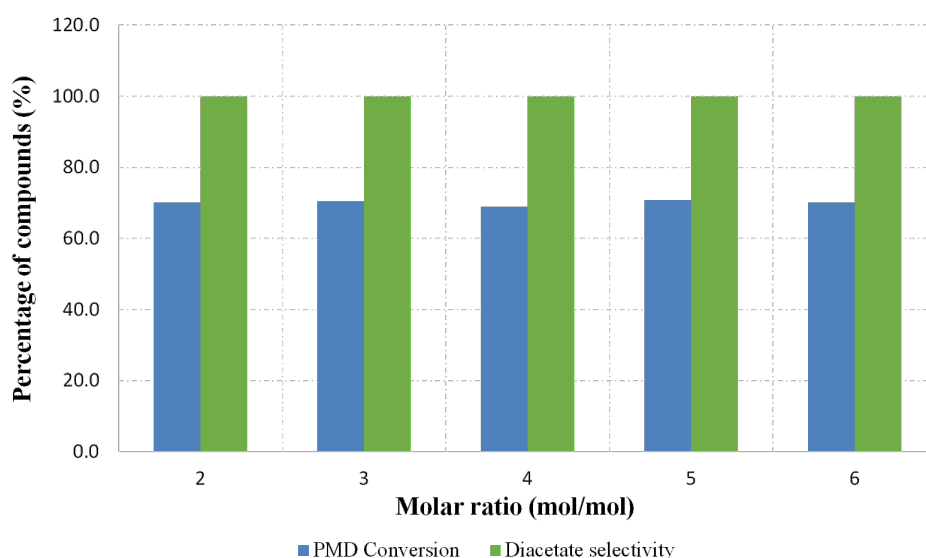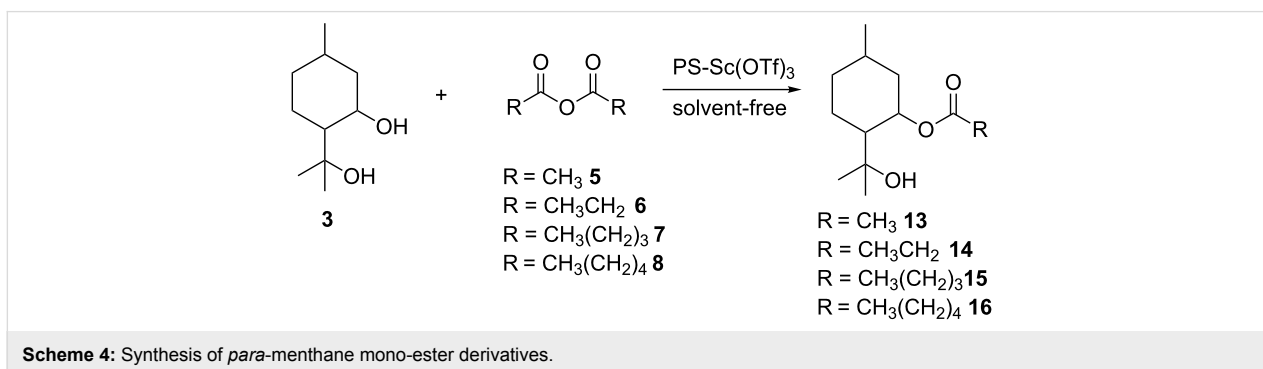

Figure 4: Effect of molar ratio in product distribution.

Table 1: Synthesis of propyl, pentyl and hexyl derivatives.

Reagent	PMD conv. (%)	Monoester sel. (%)	Diester sel. (%)
propionic anhydride	70.5	0	65.8
pentanoic anhydride	69.6	10	63.2
hexanoic anhydride	70.1	16	60.4

Scheme 4: Synthesis of *para*-menthane mono-ester derivatives.

process involves the use of a solvent-free system and the reaction occurs at mild conditions. In addition, the use of polymer-bound scandium triflate has been shown to be very efficient in the acylation reaction. Moreover, the catalyst was reusable in the process without significant change towards the substrate conversion and product selectivity. Using the methodology described herein, further studies are currently underway within our laboratory to optimise the developed method in a continuous flow process.

Experimental
Materials and methods
All the reagents (analytical grade) were purchased from Sigma-Aldrich and were used without purification. The citronellal feedstock material was purchased from Germany (Chemical point). The quantification of product mixtures were performed on an Agilent Gas chromatograph, equipped with a flame ionization detector, Econocap-5 column (film thickness 0.25 μm; internal diameter 0.25 mm; length 30 m) and ultra-high purity nitrogen (99.999%) carrier gas. The samples were analysed by using the following method; injector temperature 270 °C, nitrogen flow rate 0.5 mL·min^{-1}, oven temperature 70 °C for 5 min and then ramped to 270 °C at 10 °C min^{-1} an final hold-up time of 5 min. All NMR spectra were recorded as solutions in deuterochloroform (CDCl$_3$) using tetramethylsilane (TMS) as an internal standard. The spectra were recorded on a Bruker Ultrashield Plus spectrometer, which was operated at 400 MHz for proton and 100 MHz for carbon. The chemical shift values for all spectra are given in parts per million (ppm) with coupling constants in Hertz (Hz). The following observations are used to report NMR data; s = singlet,

d = doublet, t = triplet, br s = broad singlet, m = multiplet and C$_0$ = quaternary carbon. Gas chromatography (GC–MS) spectrometry was performed on a HP F5890 series LL plus gas chromatograph coupled to an HP 5972 series mass selective detector. The GC was equipped with a HP-5 MS capillary column (30 mm × 0.25 mm i.d.) and ultra-high purity helium (99.999%) carrier gas. The samples were analysed by using the following method; injector temperature 250 °C, helium flow rate 0.1 mL·min^{-1}, oven temperature 70 °C for 5 min and then ramped to 280 °C at 10 °C min^{-1} with split flow ratio of 60 mL·min^{-1}. The FTIR characteristic peaks were recorded on a Bruker Platinum Tensor 27 spectrophotometer with an ATR fitting. The analyses of samples were recorded in the range 4000–600 cm^{-1} and the peaks are reported in wavenumbers (cm^{-1}). The solid and liquid samples were analysed without any modification. The boiling points of the compounds were measured using a simulated distillation (Agilent SimDis FAST2887) instrument fitted with a CAP. EXT. 2887/AC column (film thickness 0.88 μm; internal diameter 0.53 mm; length 10 m).

Experimental procedures
Synthesis of *para*-menthane-3,8-diol from citronellal
Citronellal (30.08 g, 0.193 mol) was added into stirred dilute sulphuric acid (140 g, 0.0076 mol of a 0.3% (v/v)) solution at a temperature of 100 °C. After 4 hour of stirring the aqueous phase was separated from the organic oil phase. The organic phase was neutralised with 50 mL of 2.5% (v/v) sodium hydrogen carbonate (NaHCO$_3$) solution to remove the remains of sulphuric acid catalyst and dried (MgSO$_4$). The product was recrystallized from *n*-hexane at −18 °C for 24 hours. *p*-Menthane-

3,8-diol (**3**) was obtained as white crystals (96%). ^{1}H NMR (400 MHz, CDCl₃, ppm) δ 0.80–0.96 (m, 3H), 0.89–0.90 (m, 1H), 0.99–1.03 (m, 2H), 1.11–1.19 (m, 3H), 1.33 (s, 3H), 1.66–1.68 (m, 2H), 1.72–1.82 (m, 3H), 3.40 (s, 2H) and 4.38 (br s, 1H); ^{13}C NMR (100 MHz, CDCl₃, ppm) δ 20.2, 22.1, 25.5, 28.6, 29.9, 34.8, 42.4, 49.2, 67.7 and 73.2; FTIR (cm⁻¹): 3220, 2941, 2911, 1158 and 931; *m/z* (CI) 172 (M⁺, 1), 157 (9), 139 (20), 96 (50), 81 (100) and 59 (90); GC *t*R = 15.0 min.

General procedure for the synthesis of diester derivatives

para-Methane-3,8-diol (**3**, 5.0 g, 0.029 mol) and an appropriate molar equivalent of acid anhydride were transferred into the reactor concurrently. Both reagents were stirred and heated at 60 °C for 10 minutes. The homogeneous mixture was achieved and 0.3 g of polymer-bound scandium triflate (PS-Sc(OTf)₃) catalyst was added into the reaction mixture. The reaction was heated at the appropriate temperature for 24 hours, while followed by sampling at an hourly interval. Upon the completion of the reaction, the catalyst was separated from the product mixture by filtration and the acid byproduct was removed by vacuum distillation. The obtained crude sample was subsequently purified by column chromatography hexane/EtOAc (98:2).

Diacetate 9: The reaction was carried out in accordance with the general procedure using *para*-menthane-3,8-diol (**3**, 5.0 g, 0.029 mol) and acetic anhydride (**5**, 7.4 g, 0.073 mol) to give the title compound **9** as viscous colourless oily liquid, bp 288 °C, (6.8 g, 91%); ^{1}H NMR (400 MHz, CDCl₃, ppm) δ 0.78–0.79 (m, 3H), 0.89–1.04 (m, 2H), 1.35 (br d, *J* = 12 Hz, 6H), 1.53–1.60 (m, 3H), 1.72 (d, *J* = 16 Hz, 1H), 1.82 (d, *J* = 12 Hz, 1H), 1.88 (s, 3H), 1.96 (s, 3H), 2.02–2.08 (m, 1H) and 5.17 (br s, 1H); ^{13}C NMR (100 MHz, CDCl₃, ppm) δ 21.4, 21.9, 22.2, 22.3, 24.0, 25.1, 26.6, 34.6, 39.4, 47.3, 69.8, 84.2, 169.9 and 170.3; FTIR (cm⁻¹): 2949, 1728, 1180 and 1144; *m/z* (CI) 256 (M⁺, 1), 197 (78), 137 (71), 95 (62) and 81 (100); GC *t*R = 17.8 min.

Dipropionate 10: The reaction was carried out in accordance with the general procedure using *para*-menthane-3,8-diol (**3**, 5.0 g, 0.029 mol) and propionic anhydride (**6**, 9.4 g, 0.073 mol) to give the title compound **10** as viscous colourless oily liquid, bp 319 °C, (8.04 g, 97%); ^{1}H NMR (400 MHz, CDCl₃, ppm) δ 0.78–0.86 (m, 3H), 0.89–0.92 (m, 1H), 0.95–0.99 (m, 4H), 1.01–1.07 (m, 3H), 1.34 (br d, *J* = 12 Hz, 6H), 1.50–1.60 (m, 3H), 1.72 (br d, *J* =12 Hz, 1H), 1.83 (d, *J* = 12 Hz, 1H), 2.04 (d, *J* = 12 Hz, 1H), 2.03–2.27(m, 4H), and 5.18 (br s, 1H); ^{13}C NMR (100 MHz, CDCl3, ppm) δ 9.2, 22.0, 22.1, 24.1, 25.2, 26.7, 28.1, 28.8, 34.7, 39.5, 47.6, 50.0, 69.7, 84.1, 173.4 and 173.9; FTIR (cm⁻¹): 2946, 1728, 1169 and 1143; *m/z* (CI)

284 (M⁺, 1), 211.4 (10), 136 (22), 81 (23) and 57 (100); GC *t*R = 19.8 min.

Dipentanoate 11: The reaction was carried out in accordance with the general procedure using *para*-menthane-3,8-diol (**3**, 5.0 g, 0.029 mol) and pentanoic anhydride (**7**, 13.5 g, 0.073 mol) to give the title compound **11** as viscous colourless oily liquid, bp 363 °C, (10.2 g, 95%); ^{1}H NMR (400 MHz, CDCl₃, ppm) δ 0.78–0.84 (m, 9H), 0.92–1.04 (m, 1H), 1.25–1.28 (m, 5H), 1.32 (br d, *J* = 16 Hz, 6H), 1.48–1.56 (m, 7H), 1.72 (br d, *J* = 12 Hz, 1H), 1.84 (d, *J* = 16 Hz, 1H), 2.04 (d, *J* = 8 Hz, 1H), 2.12–2.22 (m, 4H), and 5.18 (br s, 1H); ^{13}C NMR (100 MHz, CDCl₃, ppm) δ 13.6, 13.7, 14.05, 22.2, 22.2, 22.3, 24.1, 24.6, 24.6, 25.1, 26.7, 27.0, 27.1, 47.4, 47.6, 69.7, 84.1, 84.3, 172.9 and 173.2; FTIR (cm⁻¹): 2954, 1727, 1169 and 1143; *m/z* (CI) 341 (M⁺, 8), 281 (27), 207 (30), 93 (18), 85 (47) and 73 (100); GC *t*R = 22.5 min.

Dihexanoate 12: The reaction was carried out in accordance with the general procedure using *para*-menthane-3,8-diol (**3**, 5.0 g, 0.029 mol) and hexanoic anhydride (**8**, 15.6 g, 0.073 mol) to give the title compound **12** as viscous colourless oily liquid, bp 395 °C, (10.4 g, 97%); ^{1}H NMR (400 MHz, CDCl3, ppm) δ 0.76–0.85 (m, 10H), 0.94–1.98 (m, 2H), 1.08–1.26 (m, 6H), 1.38 (d, *J* = 4 Hz, 1H), 1.54–157 (m, 5H), 1.62–1.77 (m, 6H), 1.86–1.94 (m, 3H), 2.19–2.23 (m, 3H), 4.64–4.73 (m, 2H) and 5.24 (br s, 1H); ^{13}C NMR (100 MHz, CDCl₃, ppm) δ 13.8, 13.8, 21.9, 22.2, 22.3, 24.1, 24.6, 24.6, 25.1, 26.7, 31.2, 31.3, 34.7, 34.8, 35.5, 39.5, 47.5, 69.6, 77.4, 84.0, 172.6 and 173.1; FTIR (cm⁻¹): 2952, 1728, 1128 and 1107; *m/z* (C.I) 369 (M⁺, 1), 253 (27), 136 (34) and 99 (100); GC *t*R = 26.4 min.

General procedure for the synthesis of monoester derivatives

para-Methane-3,8-diol (**3**, 5.0 g, 0.029 mol) and an appropriate molar equivalence of acid anhydride were transferred into the reactor concurrently. Both reagents were stirred and heated at 60 °C for 10 minutes. The homogeneous mixture was achieved and 0.3 g of polymer-bound scandium triflate (PS-Sc(OTf)₃) catalyst was added into the reaction mixture. The reaction was stirred 60 °C for 24 hours, while followed by sampling at an hourly interval. Upon the completion of the reaction, the catalyst was separated from the product mixture by filtration and the acid was removed by distillation. The obtained crude sample was purified by column chromatography hexane/EtOAc (98:2). The colourless oily products were analysed.

Monoacetate 13: The reaction was carried out in accordance with the general procedure using *para*-menthane-3,8-diol (**3**, 5.0 g, 0.029 mol) and acetic anhydride (**5**, 4.4 g, 0.044 mol) to give the title compound **13** as viscous colourless oily liquid,

bp 275 °C, (5.3 g, 85%); ^{1}H NMR (400 MHz, CDCl$_3$, ppm) δ 0.79–0.99 (m, 5H), 1.09 (br d, *J* = 12 Hz, 6H), 1.32 (d, *J* = 12 Hz, 1H), 1.54–1.67 (m, 3H), 1.74 (br d, *J* = 4 Hz, 1H), 1.88 (d, *J* = 16 Hz, 1H), 1.98 (br s, 3H), 2.29 (br s, 1H) and 5.29 (br s, 1H); ^{13}C NMR (100 MHz, CDCl$_3$, ppm) δ 21.5 21.9, 22.0, 26.5, 27.5, 28.5, 34.7, 39,4. 50.0, 71.1, 71.8 and 170.5; FTIR (cm^{-1}): 3435, 2948, 1734, 1455, 1241 and 1080; *m/z* (CI) 214 (M$^+$, 1), 197 (100), 137 (70), 95 (65), 81 (100) and 59 (48); GC t_R = 16.2 min.

Monopropionate 14: The reaction was carried out in accordance with the general procedure using *para*-menthane-3,8-diol (**3**, 5.0 g, 0.029 mol) and propionic anhydride (**6**, 5.7 g, 0.044 mol) to give the title compound **14** as viscous colourless oily liquid, bp 282 °C, (5.8 g, 87.6%); ^{1}H NMR (400 MHz, CDCl$_3$, ppm) δ 0.79 (d, *J* = 8 Hz, 3H), 0.6–1.11 (m, 10H), 1.33 (d, *J* = 16 Hz, 1H), 1.54–1.64 (m, 3H), 1.74 (d, *J* = 12 Hz, 1H), 1.87 (d, *J* = 12 Hz, 1H), 2.23–2.29 (m, 3H), 3.77 (br s, 1H) and 5.30 (br s, 1H); ^{13}C NMR (100 MHz, CDCl$_3$, ppm) δ 9.0, 21.9, 22.1, 26.6, 27.5, 28.2, 28.5, 34.7, 39.5 49.9, 71.0, 72.1, and 173.9; FTIR (cm^{-1}): 3425, 2947, 2870, 2847, 1730, 1375, 1279 and 1191; *m/z* (CI) 228 (M$^+$, 1), 211 (10), 136 (20), 81 (25) and 57 (100); GC t_R = 17.3 min.

Monopentanoate 15: The reaction was carried out in accordance with the general procedure using *para*-menthane-3,8-diol (**3**, 5.0 g, 0.029 mol) and pentanoic anhydride (**7**, 8.1 g, 0.044 mol) to give the titled compound **15** as viscous colourless oily liquid, bp 290 °C, (6.7 g, 90.1%); ^{1}H NMR (400 MHz, CDCl$_3$, ppm); δ 0.78–0.85 (m, 7H), 1.00 (d, *J* = 12 Hz, 6H), 1.04–1.11 (m, 3H), 1.12–1.33 (m, 5H), 1.68 (d, *J* = 12 Hz, 1H), 1.74 (d, *J* = 12 Hz, 1H), 1.86–2.08 (m, 2H), 2.09–2.23 (m, 2H) and 5.29 (br s, 1H); ^{13}C NMR (100 MHz, CDCl$_3$, ppm) δ 13.6, 22.0, 22.1, 22.2, 22.6, 26.9, 27.6, 28.6, 34.6, 34.7, 39.5, 49.8, 71.0, 71.9 and 173.3; FTIR (cm^{-1}): 3436, 2954, 2929, 2870, 1730, 1181, 1145 and 996; *m/z* (CI) 256 (M$^+$, 1), 136 (60), 86 (100), 57 (80), 29 (10); GC t_R = 18.1 min.

Monohexanoate 16 The reaction was carried out in accordance with the general procedure using *para*-menthane-3,8-diol (**3**, 5.0 g, 0.029 mol) and hexanoic anhydride (**8**, 9.3 g, 0.044 mol) to give the titled compound **16** as viscous colourless oily liquid, bp 297 °C, (6.9 g, 88.1%); ^{1}H NMR (400 MHz, CDCl3, ppm) δ 0.82–1.05 (m, 9H), 1.13 (br d, *J* = 16 Hz, 6H), 1.28–1.37 (m, 3H), 1.55–1.71 (m, 5H), 1.78 (br d, *J* = 16 Hz, 1H), 1.91 (d, *J* = 16 Hz, 1H), 2.26–2.31 (m, 4H) and 5.32 (br s, 1H); ^{13}C NMR (100 MHz, CDCl3, ppm) δ 13.6, 21.9, 22.1, 22.2, 26.6, 27.6, 28.6, 34.6, 34.7, 39.5, 49.9, 70.9, 71.9 and 173.3; FTIR (cm^{-1}): 3436, 2952, 2931, 2870, 1729, 1181 and 1146; *m/z* (CI) 270 (M$^+$, 1), 253 (10), 136 (20) and 99 (100); GC t_R = 19.2 min.

Supporting Information

Supporting Information File 1

NMR, IR and GC–MS spectra of synthesized compounds.
[http://www.beilstein-journals.org/bjoc/content/supplementary/1860-5397-12-193-S1.pdf]

Acknowledgements

References

1. da Silva, K. A.; Robles-Dutenhefner, P. A.; Sousa, E. M. B.; Kozhevnikova, E. F.; Kozhevnikov, I. V.; Gusevskaya, E. V. *Catal. Commun.* **2004,** *5,* 425–429. doi:10.1016/j.catcom.2004.05.001
2. Drapeau, J.; Rossano, M.; Touraud, D.; Obermayr, U.; Geier, M.; Rose, A.; Kunz, W. *C. R. Chim.* **2011,** *14,* 629–635. doi:10.1016/j.crci.2011.02.008
3. Imachi, S.; Owada, K.; Onaka, M. *J. Mol. Catal. A: Chem.* **2007,** *272,* 174–181. doi:10.1016/j.molcata.2007.03.032
4. Nie, Y.; Niah, W.; Jaenicke, S.; Chuah, G.-K. *J. Catal.* **2007,** *248,* 1–10. doi:10.1016/j.jcat.2007.02.018
5. Heravi, M. M.; Behbahani, F. K.; Bamoharram, F. F. *ARKIVOC* **2007,** *2007* (xvi), 123–131. doi:10.3998/ark.5550190.0008.g13
6. Sharma, R. K.; Gulati, S. *J. Mol. Catal. A: Chem.* **2012,** *363-364,* 291–303. doi:10.1016/j.molcata.2012.07.004
7. Chandra, K. L.; Saravanan, P.; Singh, R. K.; Singh, V. K. *Tetrahedron* **2002,** *58,* 1369–1374. doi:10.1016/S0040-4020(01)01229-7
8. Pârvulescu, A. N.; Gagea, B. C.; Poncelet, G.; Pârvulescu, V. I. *Appl. Catal., A* **2006,** *301,* 133–137. doi:10.1016/j.apcata.2005.10.025
9. Tashiro, D.; Kawasaki, Y.; Sakaguchi, S.; Ishii, Y. *J. Org. Chem.* **1997,** *62,* 8141–8144. doi:10.1021/jo971204+
10. Dumeunier, R.; Markó, I. E. *Tetrahedron Lett.* **2004,** *45,* 825–829. doi:10.1016/j.tetlet.2003.11.034
11. Mpuhlu, B. Synthesis of *p*-menthane-3,8-diol. Ph.D. Thesis, Nelson Mandela Metropolitan University, 2007.
12. Firouzabadi, H.; Iranpoor, N.; Farahi, S. *J. Mol. Catal. A: Chem.* **2008,** *289,* 61–68. doi:10.1016/j.molcata.2008.04.010

Superelectrophilic activation of 5-hydroxymethylfurfural and 2,5-diformylfuran: organic synthesis based on biomass-derived products

Dmitry S. Ryabukhin[1,2], Dmitry N. Zakusilo[1,3], Mikhail O. Kompanets[4], Anton A.Tarakanov[1], Irina A. Boyarskaya[2], Tatiana O. Artamonova[5], Mikhail A. Khohodorkovskiy[5], Iosyp O. Opeida[6] and Aleksander V. Vasilyev[*1,2]

Abstract

The reaction of 5-hydroxymethylfurfural (5-HMF) with arenes in superacidic trifluoromethanesulfonic acid (triflic acid, TfOH) as the solvent at room temperature for 1–24 h gives rise to 5-arylmethylfurfurals (yields of 17–91%) and 2-arylmethyl-5-(diaryl-methyl)furans (yields of 10–37%). The formation of these two types of reaction products depends on the nucleophilicity of the arene. The same reactions under the action of acidic zeolites H-USY in high pressure tubes at 130 °C for 1 h result in the formation of only 5-arylmethylfurfurals (yields of 45–79%). 2,5-Diformylfuran (2,5-DFF) in the reaction with arenes under the action of AlBr$_3$ at room temperature for 1 h leads to 5-(diarylmethyl)furfurals (yields of 51–90%). The reactive protonated species of 5-HMF and 2,5-DFF were characterized by NMR spectroscopy in TfOH and studied by DFT calculations. These reactions show possibilities of organic synthesis based on biomass-derived 5-HMF and 2,5-DFF.

Introduction

Nowadays great attention is paid to the use of renewable resources for obtaining fine chemicals and fuels (see numerous reviews [1-16]). The biorefinery of renewable lignin-carbo-hydrate materials affords various low-molecular weight organic molecules, such as alcohols, carboxylic acids, (hetero)aromatic ketones and aldehydes, phenols, etc. These biomass-derived platform chemicals are considered as an alternative and dis-placement to petroleum chemistry [17,18]. Among all these compounds, the preparation and reaction of 5-hydroxymethyl-furfural (5-HMF) attracts special attention (see fundamental review from 2013 [19] and recent papers [20-25]). The high functionality and reactivity of 5-HMF, due to the presence of oxymethyl and aldehyde substituents, along with the furan moiety, allows many transformations and therefore the produc-tion of new useful organic substances [26-30].

Based on our recent study on the synthesis of 5-HMF and its oxidation to 2,5-diformylfuran (2,5-DFF) [31] (Figure 1), this work is focused on developing methods of organic synthesis on the basis of electrophilic activation of these biomass-derived products.

Superelectrophilic activation is the generation of highly reac-tive di-, tri- (or even higher) cationic species by protonation and protosolvation of organic molecules with low nucleophilic Brønsted superacids, such as CF_3SO_3H (TfOH) or FSO_3H [32]. The same activation may be achieved with strong Lewis acids (AlX_3, X = Cl, Br) by their coordination with basic centers of organic compounds, or with acidic zeolites, possessing both Brønsted and Lewis acidity [33].

The main goal of this work was a study of reactions of 5-HMF and 2,5-DFF with arenes under electrophilic activation with Brønsted and Lewis superacids. Previously superelectrophilic activation of aldehyde groups was achieved for heteroaromatic aldehydes [34-37], substituted benzaldehydes and *o*-phthalic dicarboxaldehyde [38]. Based on these findings, one would expect the activation of an aldehyde group of 5-HMF and 2,5-DFF, and its participation in the hydroxyalkylation of arenes. However, furan carboxaldehydes in such reactions were studied in this work for the first time.

It should be noted, that reactions of arenes with hydroxymethyl and aldehyde groups of 5-HMF and 2,5-DFF may lead to various arylmethyl- and diarylmethyl-substituted furans, which are otherwise hardly available molecules [39-46] and used for the synthesis of bioactive compounds [47]. Thus, the superelec-trophilic activation of 5-HMF and 2,5-DFF could be of great value for organic synthesis.

Results and Discussion

The protonation of the carbonyl oxygen and hydroxy group of 5-HMF (**1a**) in strong acids gives rise to cationic species **A**, the dehydration of the latter may result in the formation of heteroaromatic benzyl-type dication **B** (Scheme 1). Protonation of the aldehyde groups in 2,5-DFF (**2**) leads to cation **C** and dication **D** (Scheme 1). All species **A**, **B**, **C**, and **D** may play a role as reactive intermediates derived from **1a** and **2** in superacids. To estimate the electrophilic properties of cations **A**, **B**, **C**, and **D** we performed quantum chemical calculations by the DFT method (Table 1). HOMO and LUMO energies, global
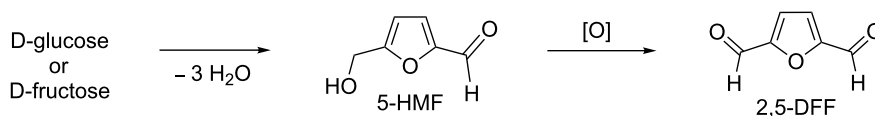
Figure 1: Formation of 5-HMF from D-glucose or D-fructose followed by oxidation to 2,5-DFF.
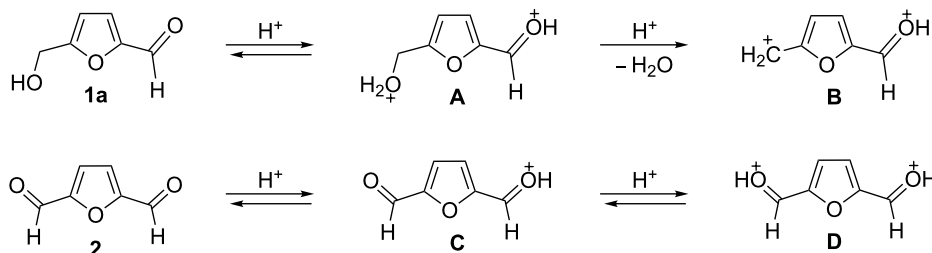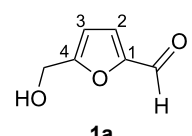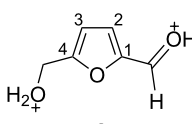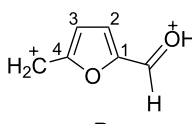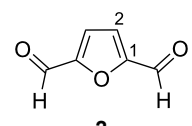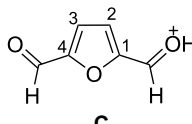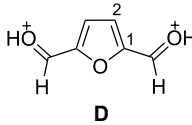
Scheme 1: Protonation of 5-HMF (**1a**) and 2,5-DFF (**2**) leading to cationic species **A**, **B**, **C**, **D**.

electrophilicity index ω [48,49], charge distribution, and contribution of atomic orbitals into the LUMO were calculated. The dications **B** and **D** having high ω values of 9.6 and 8 eV, respectively, should be very reactive electrophiles. The carbon atom of the protonated aldehyde group in species **A**, **B**, **C**, and **D** bears a large positive charge and shows a great contribution in the LUMO. This indicates that this carbon atom may be an electrophilic reactive center from both charge and orbital point of view. Apart from that, the increase of positive charge on heteroaromatic carbons C1, C4 and the decrease of negative charge on atoms C2, C3, and O$_{furan}$ upon protonation of furans **1a** and **2** reveal a significant positive charge delocalization into

Table 1: Selected electronic characteristics (DFT calculations) of starting furans **1a**, **2** and cationic species **A**, **B**, **C**, and **D**.

Species	E_{HOMO}, eV	E_{LUMO}, eV	ω,[a] eV	q(CH$_2$),[b] e	q(C=O),[b] e	k(CH$_2$)$_{LUMO}$,[c] %	k(C=O)$_{LUMO}$,[c] %
1a	−6.82	−2.20	2.2	−0.066	0.379	0.6	27.8
A	−8.93	−4.59	5.3	−0.060	0.428 (COH$^+$)	6.9	26.3 (COH$^+$)
B	−10.43	−6.65	9.6	0.054	0.528 (COH$^+$)	26.1	24.0 (COH$^+$)
2	−7.43	−3.06	3.1	–	0.391	–	15.4
C	−8.57	−4.60	5.5	–	0.400 0.417 (COH$^+$)	–	5.7 31.2 (COH$^+$)
D	−9.78	−5.91	8.0	–	0.488 (COH$^+$)	–	22.9 (COH$^+$)
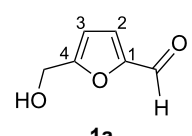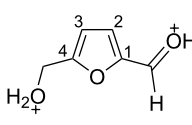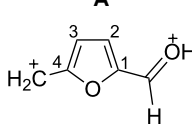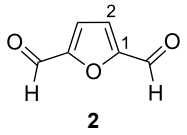
Species	q(C^1),[b] e	q(C^2),[b] e	q(C^3),[b] e	q(C^4),[b] e	q(O$_{furan}$),[b] e
1a	0.152	−0.192	−0.302	0.352	−0.464
A	0.158	−0.097	−0.220	0.371	−0.406
B	0.313	−0.162	−0.010	0.209	−0.374

Table 1: Selected electronic characteristics (DFT calculations) of starting furans **1a**, **2** and cationic species **A**, **B**, **C**, and **D**. (continued)

2	0.210	−0.209	−0.209	0.210	−0.568
C	0.161	−0.106	−0.217	0.330	−0.404
D	0.228	−0.119	−0.119	0.228	−0.376
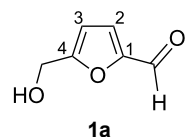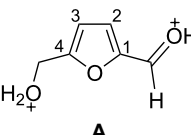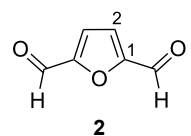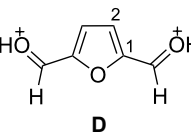
[a]Global electrophilicity index ω = (E_{HOMO} + E_{LUMO})^2/8(E_{LUMO} − E_{HOMO}). [b]Natural charges. [c]Contribution of atomic orbitals into the molecular orbital.

the furan ring in species **A**, **B**, **C**, and **D**. However, from these calculations no unambiguous answer could be obtained that reveals what cations in pairs **A** or **B**, and **C** or **D** may take part in electrophilic reactions.

To investigate this issue in more detail we studied the protonation of furans **1a** and **2** in the superacid TfOH by NMR spectroscopy. Upon dissolving **1a** and **2** in TfOH in the NMR tube the formation of deep-red solutions was observed. ^{1}H and ^{13}C NMR data of the generated cationic species are collected in Table 2 (see spectral figures in Supporting Information File 1).

The spectral data clearly prove that protonation of **1a** in TfOH gives rise to dication **A** (Scheme 1). Thus, in the ^{13}C NMR spectrum the signal at δ 67.5 ppm belongs to the protonated hydroxymethyl group $CH_2O^+H_2$. This means that dehydration of this group does not occur in TfOH and cation **B** is not formed. For comparison, chemical shifts of carbocationic centers in various benzyl cations (R_2)ArC$^+$ lie in a much more down-field range of ~182–270 ppm [50-57]. Comparison of ^{1}H and ^{13}C NMR spectra shows that signals of protons and carbons in the furan ring of **A** are substantially down-field shifted in comparison with the corresponding signals of its neutral precur-

Table 2: ^{1}H and ^{13}C NMR data of furans **1a, 2** in CDCl$_3$ and species **A, D** in TfOH at room temperature.

Species	Solvent	NMR data	
		[1]H	[13]C
1a	CDCl$_3$	2.84 (s, 1H, OH), 4.71 (s, 2H, CH$_2$), 6.51 (d,(J = 3.5 Hz, 1H, H2), 7.21 (d, J = 3.5 Hz, 1H, H3), 9.57 (s, 1H, CHO)	57.6 (CH$_2$), 109.9 (C2), 122.8 (C3), 152.4 (C4), 160.7 (C1), 177.7 (CHO)
A	TfOH	5.85 (s, 2H, CH$_2$), 7.44 (d, J = 4.2 Hz, 1H, H2), 8.79 (d, J = 4.2 Hz, 1H, H3), 9.04 (s, C=OH$^+$)	67.5 (CH$_2$), 121.0 (C2), 148.5 (C3), 152.8 (C4), 171.9 (C1), 175.9 (C=OH$^+$)
2	CDCl$_3$	7.33 (s, 2H, H2), 9.86 (s, CHO)	119.1 (C2), 154.2 (C1), 179.2 (CHO)
D	TfOH	8.48 (s, 2H), 9.84 (s, C=OH$^+$)	136.8 (C2), 156.0 (C1), 186.6 (C=OH$^+$)

sor **1a**. This reveals a significant positive charge delocalization in the furan ring in **A** that is in good agreement with the DFT calculations (vide supra).

According to the NMR data (Table 2 and Supporting Information File 1) protonation of **2** in TfOH leads to the *O,O*-diprotonated species **D**. Analogous to dication **A**, a down-field shift of signals of protons and carbons of the furan ring in ^{1}H and ^{13}C NMR spectra of **D** compared to the signals for **2** was observed, pointing out a charge delocalization in the furan moiety. Also, the down-field shift of the ^{13}C signal of the protonated aldehyde group in species **D** indicates that this carbon should be a reactive electrophilic center. Contrary to that, the signal of the carbon of the protonated aldehyde group in **A** is even slightly up-field shifted compared to the same signal in **1a**. This indicates weak electrophilic properties of the protonated aldehyde group in **A**. Signals of protons bonded to aldehyde and oxymethyl groups in species **A** and **D** were not registered in ^{1}H NMR due to the fast proton exchange with the superacidic medium at room temperature.

Thus, the NMR data revealed that protonation of furans **1a** and **2** in superacid TfOH resulted in the formation of dications **A** and **D**, respectively, although DFT calculations (Table 1) did not manifest that clearly.

Next, 5-HMF (**1a**), 5-(chloromethyl)furfural (**1b**) and 5-(bromomethyl)furfural (**1c**), both of which are also promising biomass-derived products [58,59], were reacted with benzene under the action of various acids (Table 3). In all cases 5-(phenylmethyl)furfural (**3a**) as Friedel–Crafts reaction product was obtained. Thus, only the hydroxymethyl or halogenomethyl group in furans **1a–c** were involved in the reactions. The aldehyde group remained intact despite the DFT calculations predicted a high electrophilicity for the carbon of the protonated aldehyde group (Table 1). The best results (the highest yield of **3a**) were achieved with TfOH at room temperature for 1 h (Table 3, entries 1, 7, and 9). Other acids were less efficient, leading to **3a** in lower yields or harsher conditions (130 °C) were required for acidic zeolites H-USY, CBV-720 and CBV-500 (Table 3, entries 3, 4, 8). Since the NMR data showed the generation of dication **A** from **1a** (Table 2), this reaction, most probably, proceeds through an S_N2 pathway, where "pure" heteroaromatic cation **B** is not formed. At least the reaction may go through late transition state, in which the C–O bond in the $CH_2O^+H_2$ group is rather elongated, resulting in a larger positive charge on this carbon than it has been predicted by calculations (see Table 1). It should be noted, that the yields of reaction products in Tables 3–5 are isolated yields after column chromatographic separation. The remaining materials are some oligomeric compounds.

Using these conditions (TfOH, rt, 1 h), we carried out reactions of 5-HMF (**1a**) with various arenes in TfOH. Additionally we investigated the reactions under the action of zeolite CBV-720, since zeolites are considered as "green" catalysts in organic synthesis [60-66] and the data are collected in Table 4. Similarly to the reaction with benzene (Table 3), **1a** with other

Table 3: Reactions of furans **1a–c** with benzene under the action of various acids.

X = OH (**a**), Cl (**b**), Br (**c**)
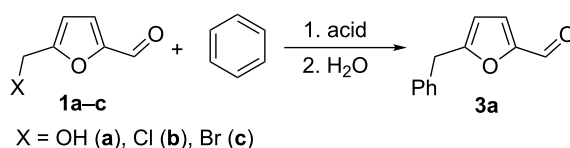
Entry	Reaction conditions				Yield of **3a**,[a] %
	Furan	Acid	*T*, °C	*t*, h	
1	**1a**	TfOH (20 equiv)	rt	1	91
2	**1a**	TfOH (20 equiv)	rt	1	–[b]
3	**1a**	zeolite CBV-500[c]	130	3	47
4	**1a**	zeolite CBV-720[c]	130	1	45
5	**1a**	H_2SO_4 (50 equiv)	rt	1	19
6	**1a**	$AlCl_3$ (5 equiv)	rt	1	oligomers
7	**1b**	TfOH (20 equiv)	rt	1	75
8	**1b**	zeolite CBV-500	130	3	25
9	**1c**	TfOH (20 equiv)	rt	1	68

[a]Isolated yields. [b]Reaction was carried out without benzene, and starting **1a** was quantitatively recovered. [c]The ratio of **1a–c**/zeolite Brønsted acidic sites was around 2:1.

Table 4: Reactions of 5-HMF (**1a**) with arenes under the action of TfOH or acidic zeolite CBV-720.
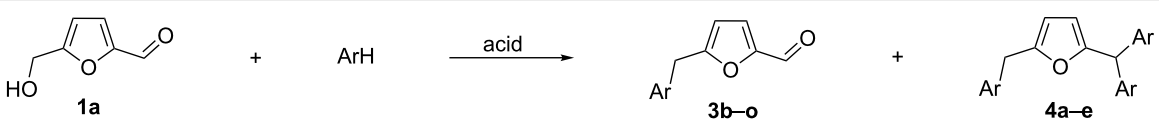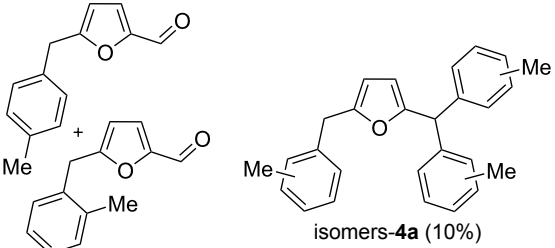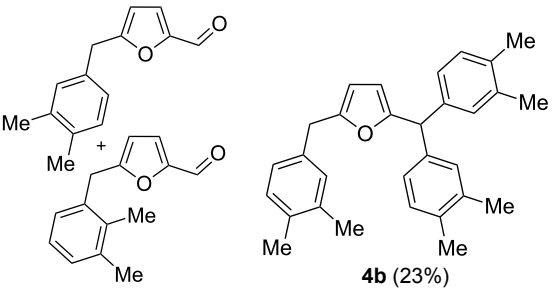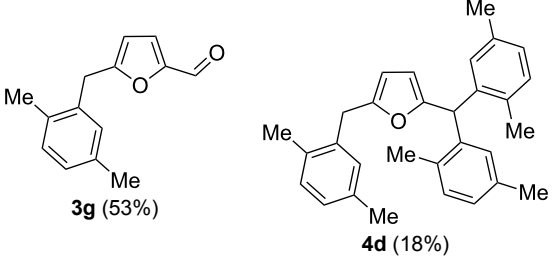
Entry	ArH	Reaction conditions				Reaction products[a]		Total yield[a], %
		ArH (equiv)	acid (equiv)	*T*, °C	*t*, h	**3**	**4**	
1	toluene	1.2	TfOH (20)	rt	1	**3b** (23%), **3c** (23%)	isomers-**4a** (10%)	56
2	toluene	4	TfOH (20)	rt	3	**3b** (44%), **3c** (44%)	isomers-**4a** (10%)	98
3	toluene	125	CBV-720[b]	130	1	**3b** (24%), **3c** (24%)	–	48
4	*o*-xylene	4	TfOH (20)	rt	1	**3d** (32%), **3e** (22%)	**4b** (23%)	77
5	*o*-xylene	4	TfOH (20)	rt	24	**3d** (37%), **3e** (22%)	**4b** (37%)	96
6	*m*-xylene	1.2	TfOH (20)	rt	1	**3f** (28%)	**4c** (6%)	34
7	*m*-xylene	4	TfOH (20)	rt	3	**3f** (75%)	**4c** (20%)	95
8	*m*-xylene	4	TfOH (20)	rt	24	**3f** (12%)	**4c** (32%)	44
9	*m*-xylene	4	TfOH (20)	rt	72	oligomers		–
10	*m*-xylene	2.5	CBV-720[b], CS₂	130	1	**3f** (79%)	–	79
11	*p*-xylene	1.2	TfOH (20)	rt	1	**3g** (53%)	**4d** (18%)	71

Table 4: Reactions of 5-HMF (**1a**) with arenes under the action of TfOH or acidic zeolite CBV-720. (continued)
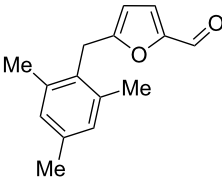
12	*p*-xylene	4	TfOH (20)	rt	3	**3g** (91%)	**4d** (5%)	96
13	*p*-xylene	4	TfOH (20)	rt	24	**3g** (21%)	**4d** (17%)	38
14	*p*-xylene	4	CBV-720[b], CS$_2$	130	1	**3g** (78%)	–	78
15	pseudo-cumene	4	TfOH (20)	rt	1	**3h** (28%), **3i** (12%)	**4e** (32%)	72
16	pseudo-cumene	10	TfOH (20)	rt	24	oligomers		–
17	pseudo-cumene	4	CBV-720[b], CS$_2$	130	1	**3h** (53%), **3i** (23%)	–	76
18	1,2-dichloro-benzene	4	TfOH (20)	rt	1	**3j** (36%), **3k** (17%)	–	53
19	1,2-dichloro-benzene	4	CBV-720[a], CS$_2$	130	1	**3j** (7%), **3k** (4%)	–	11
20	anisole	4	TfOH (20)	rt	1	**3l** (42%), **3m** (9%)	–	51
21	anisole	3	CBV-720[b], CS$_2$	130	1	**3l** (34%), **3m** (18%)	–	52
22	veratrole	4	TfOH (20)	rt	2	**3n** (62%)	–	62
23	veratrole	4	CBV-720[b], CS$_2$	130	1	**3n** (21%)	–	21

Table 4: Reactions of 5-HMF (**1a**) with arenes under the action of TfOH or acidic zeolite CBV-720. (continued)

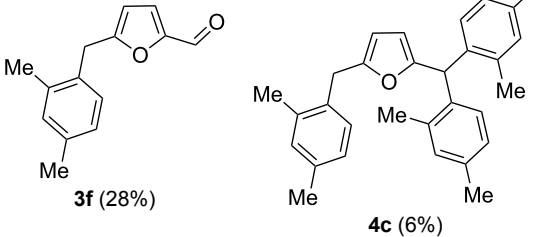| 24 | mesitylene | 5 | TfOH (20) | rt | 2 | | – | 17 |

3o (17%)

[a]Isolated yields. [b]The ratio of **1a**/zeolite Brønsted acidic sites was around 2:1.

arenes yielded 5-arylmethylfurfurals **3b–o** in TfOH or with zeolite CBV-720. However, the use of activated arenes, such as toluene, xylenes and pseudocumene, afforded additional Friedel–Crafts products, namely furans **4a–e** (Table 4, entries 1, 2, 4–8, 11–13, and 15). These compounds were formed by hydroxyalkylation due to the interaction of species **A** with arenes (see related reactions [34-38]). The polymethylated arenes possess a sufficient π-nucleophilicity for the reaction with the protonated aldehyde group of the intermediates generated from **1a** in TfOH. Whereas less nucleophilic arenes, such as benzene (Table 3) and 1,2-dichlorobenzene (Table 4, entries 18 and 19), did not give rise to the corresponding furans **4**. Also, the reactions with anisole and veratrole led only to furans **3l**, **m** and **3n**, respectively, and no formation of compounds **4** was observed (Table 4, entries 20–23). Under the superacidic conditions the substrates anisole and veratrole may be protonated at the oxygen atoms [33], thus leading to a decreased π-nucleophilicity of these arenes. It should be noted that in the case of zeolites we explored CS_2 as low coordinating solvent to avoid blocking zeolite acidic sites by π-donating arenes.

Individually isolated compounds **3f** and **3g** being dissolved in TfOH at room temperature for 24 h gave rise to mixtures containing furans **4c** and **4d** along with starting **3f** and **3g**, respectively. This may prove that compounds **4** are the secondary reaction products. It is interesting to note that compounds **4** were not observed in reactions with zeolite (Table 4, entries 3, 10, 14 and 17), most likely, due to lower acidity of the zeolite compared to TfOH and spatial restrictions in zeolite cages, diminishing the contact between protonated aldehyde groups and the substrate (arene) molecules.

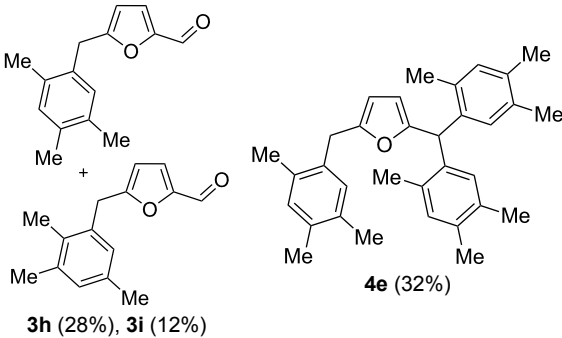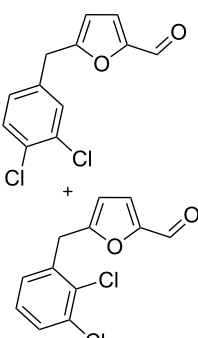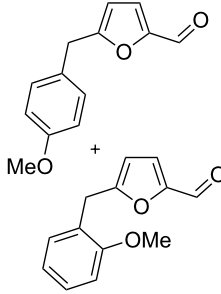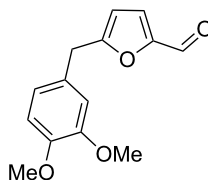We also varied reaction conditions (time, amount of arene) in TfOH to check yields of compounds **3** and **4**. In general, increasing the reaction time up to 3–24 h led to an increase in the yield of furans **4** and a decreased yield of compounds **3** (compare pairs of entries in Table 4: 4 and 5, 7 and 8, 12 and 13). But during long reaction times (24–72 h) compounds **3** and **4** were completely cleaved in TfOH (Table 4, entries 9 and 16),

showing complex behavior of these furans under superacidic conditions.

Concerning the reaction mechanism, according to NMR data (see Table 2) the reactive species, derived from **1a** in TfOH, is cation **A**. In zeolite cages the activation of the CH_2OH group of **1a** takes place due to the coordination of the basic centers of this molecule with Brønsted and Lewis acidic sites of zeolite.

2,5-DFF (**2**) reacted with arenes under electrophilic activation with formation of 5-diarylmethylfurfurals **5a–g** (Table 5, Figure 2). Contrary to compound **1a**, which was activated with the Brønsted superacid TfOH to achieve Friedel–Crafts products **3** and **4** (Table 3 and Table 4), compound **2** gave better results with strong Lewis acids AlX_3 (X = Cl, Br) (Table 5, entries 4, 5, 9, 11, 13, and 15). The coordination of aluminum halides with the aldehyde group results in the activation of one of the aldehyde groups, catalyzing the reaction subsequently with two arene molecules resulting in the 1,1-diarylated product. The second aldehyde group does not take part in the reaction (compare with data from ref. [38]). This is due to both, an insufficient electrophilic activation by these particular acids and the low nucleophilicity of benzene. Also the reaction of **2** with benzene was promoted by zeolite CBV-500, which is more acidic than CBV-720 (see Supporting Information File 1), and the latter was not be able to give rise to **5a** (Table 5, entries 6–8).

Electron-donating xylenes in the reaction with **2** showed a more complex behavior. The different isomeric xylenes led to compounds **5b–e** in the presence of $AlBr_3$ (Table 5, entries 9, 11, and 13). On the other hand, in the Brønsted superacid TfOH *o*- and *m*-xylenes gave rise to complex oligomeric mixtures (Table 5, entries 10 and 12) having masses up to 1400–1500 Da according to MALDI–MS (see Supporting Information File 1). These oligomers may have formed due to the participation of both aldehyde groups of species **D** (see Scheme 1 and Table 2) in the reaction with these electron-rich arenes. Under the action of $AlBr_3$ 2,5-DFF did not react with 1,2-dichlorobenzene, due

Table 5: Reactions of 2,5-DFF **2** with arenes under the action of various acids.

Entry	ArH	Reaction conditions			Reaction products, **5**	
		acid (equiv)	*T*, °C	*t*, h	substituents R in Ar	yield[a] (%)
1	benzene	TfOH (20)	rt	2	H	**5a** (90%)
2	benzene	H$_2$SO$_4$ (50)	rt	2	H	**5a** (74%)
3	benzene	FSO$_3$H (20), SO$_2$	−45	2	H	**5a** (84%)
4	benzene	AlCl$_3$ (5)	rt	1	H	**5a** (92%)
5	benzene	AlBr$_3$ (5)	rt	1	H	**5a** (98%)
6	benzene	CBV-500[b]	130	1	H	**5a** (13%)[c]
7	benzene	CBV-500[b]	130	10	H	**5a** (46%)
8	benzene	CBV-720[b]	130	10	H	—[d]
9	*o*-xylene	AlBr$_3$ (5)	rt	1	3,4-Me$_2$	**5b** (72%)
10	*o*-xylene	TfOH (20)	rt	1	oligomers	
11	*m*-xylene	AlBr$_3$ (5)	rt	1	3,5-Me$_2$	**5c** (36%)
					2,4-Me$_2$	**5d** (15%)
12	*m*-xylene	TfOH (20)	rt	1	oligomers	
13	*p*-xylene	AlBr$_3$ (5)	rt	1	2,5-Me$_2$	**5e** (78%)
14	*p*-xylene	TfOH (20)	rt	1	2,5-Me$_2$	**5e** (87%)
15	1,2-dichlorobenzene	TfOH (20)	rt	1	3,4-Cl$_2$	**5f** (82%)
					2,3-Cl$_2$	**5g** (16%)
16	1,2-dichlorobenzene	AlBr$_3$ (5)	rt	1	—[d]	

[a]Isolated yields. [b]The ratio of **2**/zeolite Brønsted acidic sites was around 2:1. [c]Incomplete conversion; 55% of starting **2** was recovered. [d]No reaction and quantitative recovery of starting **2**.
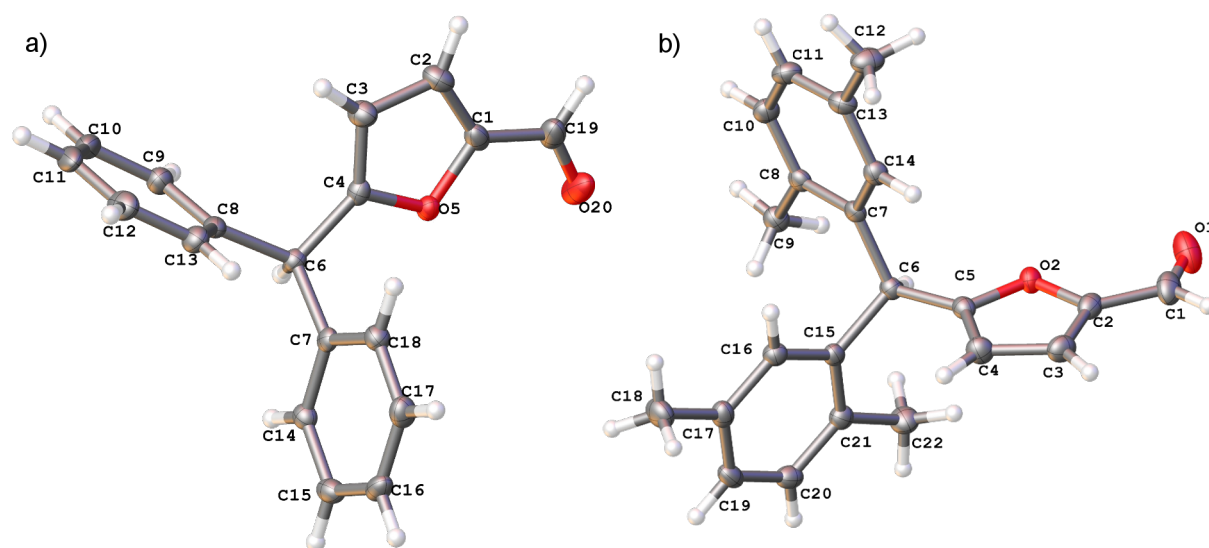
Figure 2: X-ray crystal structure of compounds **5a** (a), and **5c** (b) (ORTEP diagrams, ellipsoid contour of probability levels is 50%, CCDC reference numbers **5a**: 1483523, **5c**: 1483524).

to a too low nucleophilicity of the latter. However, this reaction took place in TfOH (Table 5, entries 15 and 16).

Conclusion

We have developed a simple and effective synthesis of various arylmethyl and diarylmethyl-substituted furans by reactions of 5-HMF and 2,5-DFF with arenes under electrophilic activation by Brønsted/Lewis (super)acids or acidic zeolites H-USY.

In these reactions 5-HMF in TfOH gives rise to 5-(aryl-methyl)furfurals and 2-(arylmethyl)-5-(diarylmethyl)furans. The latter compounds are formed in reactions with donating arenes. Reactions of 5-HMF with arenes under the action of acidic zeolites H-USY result in the selective formation of only 5-(arylmethyl)furfurals. 2,5-DFF in reactions with arenes under the action of AlBr$_3$ leads solely to 5-(diarylmethyl)furfurals.

The electrophilic intermediates derived from the protonation of 5-HMF and 2,5-DFF were investigated by means of DFT calculations and NMR in the superacid TfOH. These reactions are a contribution to organic syntheses based on biomass-derived products 5-HMF and 2,5-DFF.

Supporting Information

Supporting Information File 1

Experimental procedures, characterization of compounds, ^{1}H, ^{13}C, ^{19}F NMR spectra, and data on DFT calculations.
[http://www.beilstein-journals.org/bjoc/content/supplementary/1860-5397-12-202-S1.pdf]

Acknowledgements

References

1. Barta, K.; Ford, P. C. *Acc. Chem. Res.* **2014,** *47,* 1503–1512. doi:10.1021/ar4002894
2. Colmenares, J. C.; Luque, R. *Chem. Soc. Rev.* **2014,** *43,* 765–778. doi:10.1039/c3cs60262a
3. Straathof, A. J. J. *Chem. Rev.* **2014,** *114,* 1871–1908. doi:10.1021/cr400309c
4. Besson, M.; Gallezot, P.; Pinel, C. *Chem. Rev.* **2014,** *114,* 1827–1870. doi:10.1021/cr4002269
5. Moiseev, I. I. *Russ. Chem. Rev.* **2013,** *82,* 616–623. doi:10.1070/RC2013v082n07ABEH004393
6. Alonso, D. M.; Wettstein, S. G.; Dumesic, J. A. *Chem. Soc. Rev.* **2012,** *41,* 8075–8098. doi:10.1039/c2cs35188a
7. Gallezot, P. *Chem. Soc. Rev.* **2012,** *41,* 1538–1558. doi:10.1039/C1CS15147A
8. Ponomarev, A. V.; Ershov, B. G. *Russ. Chem. Rev.* **2012,** *81,* 918–935. doi:10.1070/RC2012v081n10ABEH004266
9. Sun, N.; Rodriguez, H.; Rahman, M.; Rogers, R. D. *Chem. Commun.* **2011,** *47,* 1405–1421. doi:10.1039/C0CC03990J
10. Varfolomeev, S. D.; Efremenko, E. N.; Krylova, L. P. *Russ. Chem. Rev.* **2010,** *79,* 491–510. doi:10.1070/RC2010v079n06ABEH004138
11. Marshall, A.-L.; Alaimo, P. *Chem. – Eur. J.* **2010,** *16,* 4970–4980. doi:10.1002/chem.200903028
12. Stöcker, M. *Angew. Chem., Int. Ed.* **2008,** *47,* 9200–9211. doi:10.1002/anie.200801476
13. Chheda, J. N.; Huber, G. W.; Dumesic, J. A. *Angew. Chem., Int. Ed.* **2007,** *46,* 7164–7183. doi:10.1002/anie.200604274
14. Huber, G. W.; Corma, A. *Angew. Chem., Int. Ed.* **2007,** *46,* 7184–7201. doi:10.1002/anie.200604504
15. Corma, A.; Iborra, S.; Velty, A. *Chem. Rev.* **2007,** *107,* 2411–2502. doi:10.1021/cr050989d
16. Huber, G. W.; Iborra, S.; Corma, A. *Chem. Rev.* **2006,** *106,* 4044–4098. doi:10.1021/cr068360d
17. Bozell, J. J.; Petersen, G. R. *Green Chem.* **2010,** *12,* 539–554. doi:10.1039/B922014C
18. Kamm, B. *Angew. Chem., Int. Ed.* **2007,** *46,* 5056–5058. doi:10.1002/anie.200604514
19. van Putten, R.-J.; van der Waal, J. C.; de Jong, E.; Rasrendra, C. B.; Heeres, H. J.; de Vries, J. G. *Chem. Rev.* **2013,** *113,* 1499–1597. doi:10.1021/cr300182k
20. Kashin, A. S.; Galkin, K. I.; Khokhlova, E. A.; Ananikov, V. P. *Angew. Chem., Int. Ed.* **2016,** *55,* 2161–2166. doi:10.1002/anie.201510090
21. Galkin, K. I.; Krivodaeva, E. A.; Romashov, L. V.; Zalesskiy, S. S.; Kachala, V. V.; Burykina, J. V.; Ananikov, V. P. *Angew. Chem., Int. Ed.* **2016,** *55,* 8338–8342. doi:10.1002/anie.201602883
22. Li, W.; Xu, Z.; Zhang, T.; Li, G.; Jameel, H.; Chang, H.; Ma, L. *BioResources* **2016,** *11,* 5839–5853. doi:10.15376/biores.11.3.5839-5853
23. Choudhary, V.; Mushrif, S. H.; Ho, C.; Anderko, A.; Nikolakis, V.; Marinkovic, N. S.; Frenkel, A. I.; Sandler, S. I.; Vlachos, D. G. *J. Am. Chem. Soc.* **2013,** *135,* 3997–4006. doi:10.1021/ja3122763
24. Hu, L.; Zhao, C.; Tang, X.; Wu, Z.; Xu, J.; Lin, L.; Liu, S. *Bioresour. Technol.* **2013,** *148,* 501–507. doi:10.1016/j.biortech.2013.09.016
25. Yang, J.; De OliveiraVigier, K.; Gu, Y.; Jérôme, F. *ChemSusChem* **2015,** *8,* 269–274. doi:10.1002/cssc.201402761
26. Iesce, M. R.; Sferruzza, R.; Cermola, F.; DellaGreca, M. *Helv. Chim. Acta* **2016,** *99,* 296–301. doi:10.1002/hlca.201500196
27. Palframan, M. J.; Pattenden, G. *Chem. Commun.* **2014,** *50,* 7223–7242. doi:10.1039/c4cc01196a
28. Dijkman, W. P.; Groothuis, D. E.; Fraaije, M. W. *Angew. Chem., Int. Ed.* **2014,** *53,* 6515–6518. doi:10.1002/anie.201402904
29. Ghezali, W.; De Oliveira Vigier, K.; Kessas, R.; Jérôme, F. *Green Chem.* **2015,** *17,* 4459–4464. doi:10.1039/C5GC01336D
30. Liu, F.; Audemar, M.; De Oliveira Vigier, K.; Clacens, J.-M.; De Campo, F.; Jérôme, F. *ChemSusChem* **2014,** *7,* 2089–2093. doi:10.1002/cssc.201402221
31. Kompanets, M. O.; Kushch, O. V.; Litvinov, Yu. E.; Pliekhov, O. L.; Novikova, K. V.; Novokhatko, A. O.; Shendrick, A. N.; Vasilyev, A. V.; Opeida, I. O. *Catal. Commun.* **2014,** *57,* 60–63. doi:10.1016/j.catcom.2014.08.005

32. Olah, G. A.; Klumpp, D. A. *Superelectrophiles and Their Chemistry;* Wiley: New York, 2008.

33. Olah, G. A.; Prakash, G. K. S.; Molnar, A.; Sommer, J. *Superacid Chemistry,* 2nd ed.; Wiley: New Jersey, 2009.

34. Prakash, G. K. S.; Paknia, F.; Chacko, S.; Mathew, T.; Olah, G. A. *Heterocycles* **2008,** *76,* 783–799. doi:10.3987/COM-08-S(N)90

35. Klumpp, D. A.; Jones, A.; Lau, S.; de Leon, S.; Garza, M. *Synthesis* **2000,** 1117–1120. doi:10.1055/s-2000-6322

36. Klumpp, D. A.; Kindelin, P. J.; Li, A. *Tetrahedron Lett.* **2005,** *46,* 2931–2935. doi:10.1016/j.tetlet.2005.02.152

37. Sheets, M. R.; Li, A.; Bower, E. A.; Weigel, A. R.; Abbot, M. P.; Gallo, R. M.; Mitton, A. M.; Klumpp, D. A. *J. Org. Chem.* **2009,** *74,* 2502–2507. doi:10.1021/jo802798x

38. Prakash, G. K. S.; Panja, C.; Shakhmin, A.; Shah, E.; Mathew, T.; Olah, G. A. *J. Org. Chem.* **2009,** *74,* 8659–8668. doi:10.1021/jo901668j

39. Cabares, J.; Mavoungou-Gomes, L. *Bull. Soc. Chim. Fr.* **1986,** 401–412.

40. Skrzyńska, A.; Przydacz, A.; Albrecht, Ł. *Org. Lett.* **2015,** *17,* 5682–5685. doi:10.1021/acs.orglett.5b02979

41. Onorato, A.; Pavlik, C.; Invernale, M. A.; Berghorn, I. D.; Sotzing, G. A.; Morton, M. D.; Smith, M. B. *Carbohydr. Res.* **2011,** *346,* 1662–1670. doi:10.1016/j.carres.2011.04.017

42. Ager, D. J. *Tetrahedron Lett.* **1983,** *24,* 5441–5444. doi:10.1016/S0040-4039(00)94107-8

43. Watanabe, N.; Matsugi, A.; Nakano, K.; Ichikawa, Y.; Kotsuki, H. *Synlett* **2014,** *25,* 438–442. doi:10.1055/s-0033-1340343

44. Gomes, R. F. A.; Coelho, J. A. S.; Frade, R. F. M.; Trindade, A. F.; Afonso, C. A. M. *J. Org. Chem.* **2015,** *80,* 10404–10411. doi:10.1021/acs.joc.5b01875

45. Pérez, M.; Mahdi, T.; Hounjet, L. J.; Stephan, D. W. *Chem. Commun.* **2015,** *51,* 11301–11304. doi:10.1039/C5CC03572D

46. Miao, M.; Luo, Y.; Li, H.; Xu, X.; Chen, Z.; Xu, J.; Ren, H. *J. Org. Chem.* **2016,** *81,* 5228–5235. doi:10.1021/acs.joc.6b00734

47. Villain-Guillot, P.; Gualtieri, M.; Bastide, L.; Roquet, F.; Martinez, J.; Amblard, M.; Pugniere, M.; Leonetti, J.-P. *J. Med. Chem.* **2007,** *50,* 4195–4204. doi:10.1021/jm0703183

48. Parr, R. G.; van Szentpály, L.; Liu, S. *J. Am. Chem. Soc.* **1999,** *121,* 1922–1924. doi:10.1021/ja983494x

49. Chattaraj, P. K.; Giri, S.; Duley, S. *Chem. Rev.* **2011,** *111,* PR43–PR75. doi:10.1021/cr100149p

50. Alkhafaji, H. M. H.; Ryabukhin, D. S.; Muzalevskiy, V. M.; Vasilyev, A. V.; Fukin, G. K.; Shastin, A. V.; Nenajdenko, V. G. *Eur. J. Org. Chem.* **2013,** 1132–1143. doi:10.1002/ejoc.201201375

51. Alkhafaji, H. M. H.; Ryabukhin, D. S.; Muzalevskiy, V. M.; Osetrova, L. V.; Vasilyev, A. V.; Nenajdenko, V. G. *Russ. J. Org. Chem.* **2013,** *49,* 327–341. doi:10.1134/S1070428013030032

52. Koltunov, K. Y.; Shakirov, M. M.; Repinskaya, I. B.; Koptug, V. A. *Zh. Org. Khim.* **1991,** *27,* 2622–2623.

53. Koltunov, K. Y.; Repinskaya, I. B. *Zh. Org. Khim.* **1993,** *30,* 90–93.

54. Walspurger, S.; Vasilyev, A. V.; Sommer, J.; Pale, P. *Tetrahedron* **2005,** *61,* 3559–3564. doi:10.1016/j.tet.2005.01.110

55. Rendy, R.; Zhang, Y.; McElrea, A.; Gomeez, A.; Klumpp, D. A. *J. Org. Chem.* **2004,** *69,* 2340–2347. doi:10.1021/jo030327t

56. Mühlthau, F.; Stadler, D.; Goeppert, A.; Olah, G. A.; Prakash, G. K. S.; Bach, T. *J. Am. Chem. Soc.* **2006,** *128,* 9668–9675. doi:10.1021/ja062102g

57. Olah, G. A.; Spear, R. J.; Forsyth, D. A. *J. Am. Chem. Soc.* **1977,** *99,* 2615–2621. doi:10.1021/ja00450a035

58. Mascal, M.; Nikitin, E. B. *Angew. Chem., Int. Ed.* **2008,** *47,* 7924–7926. doi:10.1002/anie.200801594

59. Kumari, N.; Olesen, J. K.; Pedersen, C. M.; Bols, M. *Eur. J. Org. Chem.* **2011,** 1266–1270. doi:10.1002/ejoc.201001539

60. Ennaert, T.; Van Aelst, J.; Dijkmans, J.; De Clercq, R.; Schutyser, W.; Dusselier, M.; Verboekend, D.; Sels, B. F. *Chem. Soc. Rev.* **2016,** *45,* 584–611. doi:10.1039/C5CS00859J

61. Sineva, L. V.; Asalieva, E. Yu.; Mordkovich, V. Z. *Russ. Chem. Rev.* **2015,** *84,* 1176–1189. doi:10.1070/RCR4464

62. Shi, J.; Wang, Y.; Yang, W.; Tang, Y.; Xie, Z. *Chem. Soc. Rev.* **2015,** *44,* 8877–8903. doi:10.1039/C5CS00626K

63. Dapsens, P. Y.; Mondelli, C.; Pérez-Ramírez, J. *Chem. Soc. Rev.* **2015,** *44,* 7025–7043. doi:10.1039/C5CS00028A

64. Van Speybroeck, V.; Hemelsoet, K.; Joos, L.; Waroquier, M.; Bell, R. G.; Catlow, C. R. A. *Chem. Soc. Rev.* **2015,** *44,* 7044–7111. doi:10.1039/C5CS00029G

65. Primo, A.; Garcia, H. *Chem. Soc. Rev.* **2014,** *43,* 7548–7561. doi:10.1039/C3CS60394F

66. Li, Y.; Yu, J. *Chem. Rev.* **2014,** *114,* 7268–7316. doi:10.1021/cr500010r

Silica-supported sulfonic acids as recyclable catalyst for esterification of levulinic acid with stoichiometric amounts of alcohols

Raimondo Maggi[*1], N. Raveendran Shiju[*2], Veronica Santacroce[1,2], Giovanni Maestri[1], Franca Bigi[1,3] and Gadi Rothenberg[2]

Address:
[1]Clean Synthetic Methodology Group, Dipartimento di Chimica, Università di Parma, Parco Area delle Scienze 17A, I-43124 Parma, Italy, [2]Van 't Hoff Institute for Molecular Sciences, University of Amsterdam, Science Park 904, 1098 XH, Amsterdam, The Netherlands. Tel: +31-20-5256515 and [3]Istituto IMEM-CNR, Parco Area delle Scienze 37/A, I-43124 Parma, Italy

Email:
Raimondo Maggi[*] - raimondo.maggi@unipr.it; N. Raveendran Shiju[*] - n.r.shiju@uva.nl

* Corresponding author

Keywords:
esterification; heterogeneous catalysis; renewable feedstocks; supported organic catalysts; sustainable chemistry

Abstract

Converting biomass into value-added chemicals holds the key to sustainable long-term carbon resource management. In this context, levulinic acid, which is easily obtained from cellulose, is valuable since it can be transformed into a variety of industrially relevant fine chemicals. Here we present a simple protocol for the selective esterification of levulinic acid using solid acid catalysts. Silica supported sulfonic acid catalysts operate under mild conditions and give good conversion and selectivity with stoichiometric amounts of alcohols. The sulfonic acid groups are tethered to the support using organic tethers. These tethers may help in preventing the deactivation of the active sites in the presence of water.

Introduction

Vegetal biomass is mankind's only source of renewable carbon on a human timescale. It is abundantly available, with the potential of replacing fossil-based carbon on a scale sufficient for covering the worldwide demand for non-fuel chemicals [1-4]. Currently, the main research thrust is directed at lignocellulose, the most abundant fraction of biomass. The mass com-

position of lignocellulose could be roughly represented by a 5/3/2 ratio of cellulose, hemicellulose and lignin, respectively. All of these polymers are the subject of many studies [5-11].

Levulinic acid (LA) is one of the most important platform chemicals as it is a versatile building block for a variety of value-added agrochemicals, fine chemicals and pharmaceutical intermediates [12,13] (Scheme 1, bottom). Moreover, it can be obtained from cellulose with relative ease and high selectivity (see Scheme 1, top) [14].

Scheme 1: Synthesis of levulinic acid from ligno-cellulosic feedstocks and its principal uses to access fine chemicals.

Levulinic acid esters are of particular interest for the chemical industry [12,13]. Their main current market is represented by the formulation of flavours and fragrances [15], although the scale of these preparations did not boosted demand yet. However, the seek to develop more eco-compatible solvents might

grant to levulinates a novel route of application. By tailoring their physicochemical properties they could become complementary to common esters and other solvents, which might be more harmful for both humans and the environment [16]. It should be also noted that ethyl levulinate could shrink the emission of nitrogen oxides from exhausts of diesel engines when used as additive [17,18].

Due to their importance, new strategies have been developed for the production of levulinic esters [19-22]. Homogeneous Brønsted acids could catalyse the esterification of levulinic acid in the presence of alcohols and reports on this reactivity date back to the nineties [23]. Although this route could ensure high chemical yields, it still presents a series of drawbacks. In particular, issues with catalyst recycling and product separation limits the environmental viability of this strategy. As a result, it remains of high interest to develop alternatives to trigger this reaction, which are more sustainable, for instance through the design of suitable and recyclable solid acid catalysts. In the literature, methods that use solid heteropolyacids, such as ammonium or mixed ammonium and silver-doped phosphotungstic acid, sulfated metal oxides (such as sulfated titania, sulfated zirconia), zeolites and hydrotalcites have been reported [24-30]. These solid catalysts share several advantages, including high activity and an easy recovery, which might provide a real basis for future application in commercial processes. Nevertheless, they require high temperatures (usually above 100 °C) and long reaction times [24-30]. Furthermore, they often share another common pitfall, namely the use of large molar excess of alcohol, either for practical convenience [31] or to minimise ester hydrolysis. As meaningful examples, it has been recently reported that acid ZSM-5 zeolites, with encapsulated maghemite particles to allow magnetic catalyst recover, could be used to directly convert furfuryl alchol into an alkyl levulinate upon warming at 130 °C for 8 hours in the presence of a large excess of alchol as solvent/reagent (100 equiv) [32]. Although the behaviour of many metal oxides has been investigated, reports featuring the activity of supported organic Brønsted acids are very few. In particular, Tejero reported that sulfonic acid supported on polymeric resins could catalyse the esterification of LA, providing conversions up to 94% upon warming at 80 °C for 8 hours in the presence of 3 equiv of *n*-butanol [33]. Melero described the synthesis of mesostructured silica frameworks featuring pending organosulfonic arms. The best catalyst provided quantitative conversion of LA upon warming of the reaction mixture at 130 °C for 2 hours in the presence of a five-fold molar excess of ethanol, used as solvent/reagent [34].

Here we present an alternative strategy in which a heterogeneous catalyst triggers the selective esterification of levulinic acid with a stoichiometric amount of alcohol.

In the last years, many methods have been developed for the transformation of homogeneous catalysts into recyclable heterogeneous ones. To prevent leaching, a common strategy is tethering the active species with the support via covalent bonds [35]. This approach increases the stability of the catalyst itself compared to impregnation (Figure 1). Furthermore, the activity of the catalyst can be tuned through adoption of a suitable linker.

Figure 1: Anchoring methodologies: a) impregnation; b) covalent binding.
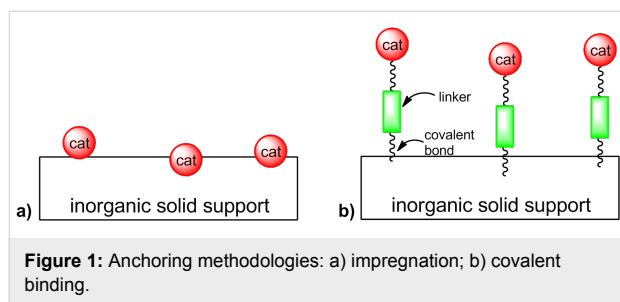
Results and Discussion

As part of our interest in acid catalysis [36-38], we prepared a set of solid materials for the esterification of levulinic acid. Upon preliminary screening, supported sulfonic acids seemed promising candidates. They were prepared following a reported procedure by the tethering method [39], which consists of the immobilisation of a functional moiety on an inorganic support via covalent bonds ensured by a suitable linker [35].

In preliminary experiments reactions were carried out with a five-fold molar excess of alcohol. We started from this ratio as

in the literature we did not retrieve any catalytic method for the esterification of biomass-derived acids that operates with a lower molar excess of alcohol [24-34]. 1-Pentanol was selected as model substrate in order to work over an ample range of operating temperatures. Thus, in a typical experiment, 10 mmol of levulinic acid were stirred at 100 °C in a sealed tube for 2 h under air in the presence of the amount of a solid catalyst necessary to have 1 mol % of acid sites. The results are reported in Table 1.

All of the prepared silica-supported sulfonic acids showed very good catalytic activity for the esterification of levulinic acid (Table 1, entries 1–4). Materials with an arylsulfonic moiety were initially investigated (Table 1, entries 1 and 2). They present a comparable loading of Brønsted sites (0.73 and 0.65 mmol/g respectively) and ensured conversion of **1** above 90% within two hours (94 and 92%). The catalyst without any alkyl tether was more selective, ultimately delivering the desired product **3a** in 90% yield. Silica-supported propyl sulfonic acid provided slightly better results (Table 1, entries 3 and 4). The material presented a lower density of Brønsted sites (0.51 mmol/g), but delivered almost complete conversion of **1** within 2 h (>95%), affording **3a** in 93% yield. We then repeated the experiment adding activated molecular sieve in the reaction flask (Table 1, entry 4) to check whether water coproduced by the reaction could cause any harm. The outcome paralleled the standard procedure, conversion and yield being 96% and 94%, respectively. This result shows that the presence of water is tolerated by the catalytic system, which in turn did not easily trigger the hydrolysis of levulinates under these conditions.

Table 1: Screening of different solid acids in the esterification reaction of levulinic acid with 1-pentanol.

Entry	Sulfonated catalyst	Catalyst acidity (mmol H^+/g)	Conversion of **1** (%)	Yield of **3a** (%)	Selectivity of **3a** (%)
1	SiO_2-$(CH_2)_3$-O-C_6H_4-SO_3H	0.73	94	84	89
2	SiO_2-C_6H_4-SO_3H	0.65	92	90	98
3	SiO_2-$(CH_2)_3$-SO_3H	0.51	95	93	98
4[a]	SiO_2-$(CH_2)_3$-SO_3H	0.51	96	94	98
5	Amberlyst 15	4.70	52	31	60
6	Nafion®	0.80	72	68	94
7	Aquivion®	0.12	84	80	95
8	H_2SO_4		57	55	96

[a]With the addition of 4 Å molecular sieves. Values by GC upon calculation of response factors for **1** and **3a** from pure samples over the concentration interval of the reaction; the selectivity has been calculated as the ration between yield of **3a** and conversion of **1**.

Remarkably, the presence of water on the catalyst surface can inhibit the catalytic sites of inorganic materials instead [40]. Acidic and/or hydrophilic metal oxides and sulfates easily adsorb water on their surface, which is the coproduct of the esterification. This can severely reduce the activity of the catalyst. Considering our supported sulfonic acids, we speculate that their organic tethers could smooth the hydrophilic character of their Brønsted sites and thus prevent the deactivation due to water.

We then tested a selection of commercial catalysts (Table 1, entries 5–7). Despite encouraging literature precedents [22,33], Amberlyst 15 gave only 52% conversion of **1** within 2 h (Table 1, entry 5, 31% yield). We then switched to perfluorinated resins. Nafion® and Aquivion® showed an interesting selectivity towards **3a**, but conversion of **1** proved once again below that observed with supported sulfonic acids (72% and 84%, respectively). Finally, a common homogeneous acid was used for comparison. The use of 1 mol % of H_2SO_4 (Table 1, entry 8) delivered **3a** in 55% yield only. Furthermore, conversion of **1** remained stuck at 57% even prolonging the reaction time for up to 24 h. This result shows that heterogeneous sulfonic acids outperform their homogeneous peer under these conditions.

Upon identification of silica-supported sulfonic acids as cheap and promising candidates for the selective esterification of LA, the reaction parameters were then optimized in order to maximise the environmental viability of the method. We thus tried to shelve the molar excess of the alcohol (Table 2).

Reactions were carried out at 100 °C and regularly monitored for 2 h. To our delight, varying the amount of alcohol did not hamper neither conversion nor selectivity. Indeed, **3a** was recovered in 93% yield using a two-fold molar excess of **2** (Table 2, entry 2). A comparable result was achieved with a stoichiometric amount of pentanol (Table 2, entry 3, 94% yield). It is remarkable that even in this case the amount of

water coproduced by the esterification did not cause any significant hydrolysis of the desired ester **3a**. Furthermore, the almost complete conversion of **1** with a stoichiometric amount of **2a** allows minimising the consumption of reagents and therefore the overall costs of the transformation. To the best of our knowledge, using stoichiometric amounts of alcohol has not been reported previously. In the present case, this can be possible as we could show that a relatively high concentration of water did not hinder the reaction. Catalysts more prone to deactivation might require a larger molar excess of alcohols to prevent water-poisoning.

The reaction conditions were further optimized studying the effect of the temperature. So, a series of experiments were carried out using the sulfonated catalyst (1%), an equimolecular amount of reagents under solvent free conditions, and varying the temperature between 50–100 °C. Results are reported in Table 3.

In all cases, the selectivity towards the esterification product **3a** remained complete. A comparable yield of **3a** was recovered reducing the temperature from 100 to 75 °C (Table 3, entry 2, 93%). By reducing the temperature to 50 °C (Table 3, entry 3), longer reaction times became necessary. At 50 °C, conversion peaked at 79% upon 7 h and no longer improved even by keeping the mixture for further 24 h. Reasoning on the practical viability of the method, we therefore continued our study fixing the temperature at 75 °C. We then evaluated the amount of catalyst (Table 4).

Surprisingly, an increase of the catalyst amount to 5 mol % resulted in lower selectivity towards **3a**, which has been retrieved in 85% yield together with traces of one unidentified byproduct (Table 4, entry 1). On the other hand, reduction of the catalyst loading to 0.1 mol % slows down the process, conversion being just 36% upon 2 h (Table 4, entry 3). Further reduction to 0.01 mol % confirmed this trend and delivered **3a** in 14% yield (Table 4, entry 4). Even by prolonging the reac-
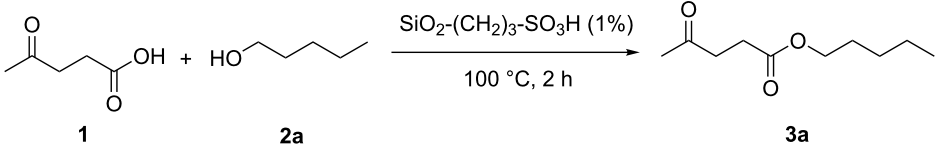
Table 2: Variation of the acid/alcohol ratio.

Entry	Acid:alcohol ratio	Conversion of **1** (%)	Yield of **3a** (%)	Selectivity of **3a** (%)
1	1:5	96	94	98
2	1:2	95	93	98
3	1:1	96	94	98

Table 3: Variation of the reaction temperature.

SiO$_2$-(CH$_2$)$_3$-SO$_3$H (1%)

acid:alcohol ratio = 1:1

1   **2a**   **3a**

Entry	Temperature (°C)	Conversion of 1 (%)	Yield of 3a (%)	Selectivity of 3a (%)	Time (h)
1	100	96	94	98	2
2	75	95	93	98	2
3	50	79	77	97	7

Table 4: Effect of the amount of catalyst.

SiO$_2$-(CH$_2$)$_3$-SO$_3$H

75 °C, 2 h
acid:alcohol ratio = 1:1

1   **2a**   **3a**

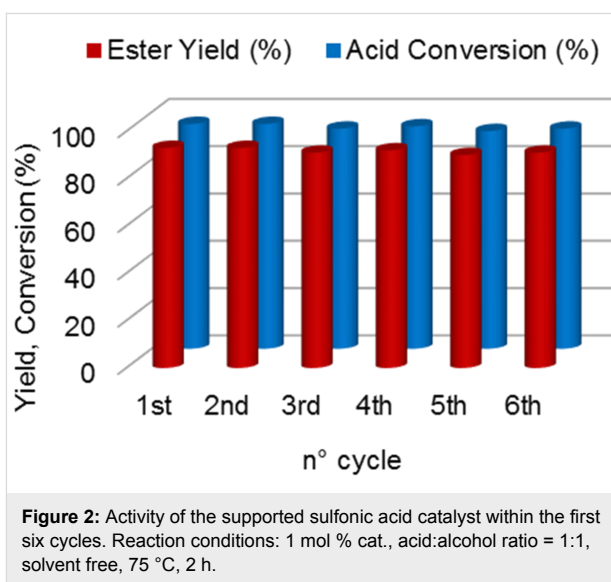| Entry	Catalyst amount (%)	Conversion of 1 (%)	Yield of 3a (%)	Selectivity of 3a (%)
1	5	95	85	89
2	1	95	93	98
3	0.1	36	35	97
4	0.01	15	14	93

tion time to 24 h, conversion did not reach completion and the ester was isolated in 58 and 38% yield with 0.1 and 0.01 mol % of catalyst, respectively. In any case, the selectivity remained almost complete (>98% by GC).

We then ensured that the catalyst acts as a heterogeneous species by performing a filtration test. In agreement with the hypothesis, we monitored no further conversion on the filtrate [41], proving that no leaching occurred. The recyclability of the catalyst was then evaluated. The catalyst was recovered by filtration, washed with ethyl acetate (10 mL), dried and reused for a further esterification. The results are shown in Figure 2.

The catalyst can be recovered and reused for 6 cycles at least, fully preserving its activity and selectivity. For instance, conversion of **1** and yield of **3a** were 94 and 92%, respectively, upon the fifth re-cycle.
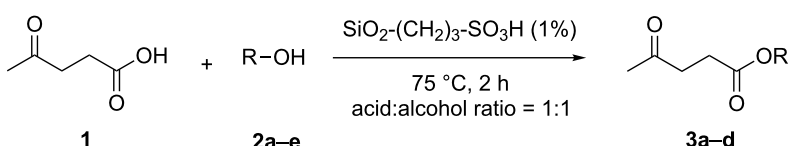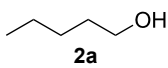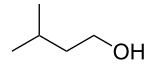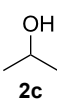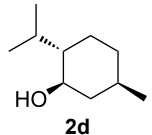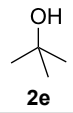
Finally, with optimized conditions in our hands, we checked the scope of this catalytic methodology (Table 5).

As expected, the best performances were obtained with primary alcohols (Table 5, entries 1 and 2), which afforded the desired ester in 93 and 79% yield, respectively. Gratifyingly, the

Figure 2: Activity of the supported sulfonic acid catalyst within the first six cycles. Reaction conditions: 1 mol % cat., acid:alcohol ratio = 1:1, solvent free, 75 °C, 2 h.

method could be extended to secondary alcohols as isopropanol and L-menthol. Despite their increased steric hindrance, very good results were obtained with a selectivity towards **3** >99% (Table 5; entries 3 and 4, 59 and 76% yield). In particular, it is important to underline that a single diastereomer of product **3d** was formed (Table 4, entry 4). This implies that the present

Table 5: Esterification of levulinic acid with different alcohols.

Entry	Alcohol	Conversion of **1** (%)	Yield of **3** (%)[a]	Selectivity of **3** (%)
1	**2a**	95	93	98
2[b]	**2b**	80	79	99
3	**2c**	60	59	98
4	**2d**	77	76	99
5[c]	**2e**	0	0	–

[a]Isolated yields upon chromatography; [b]by warming for 5 h; [c]by warming for 24 h.

method, likely thanks to its mild conditions, allows to preserve chiral information present on substrates and could thus efficiently transfer it on the products.

On the other hand, no conversion of **1** was observed using tertiary alcohols, as witnessed by entry 5. Probably, their steric hindrance quenches any reactivity.

Conclusion

Silica-supported sulfonic acids proved very active heterogeneous catalysts for the selective esterification of levulinic acid with stoichiometric amounts of primary alcohols. The esterification can be carried out under mild conditions (75 °C, 2 h) and provides good to excellent yields with various primary and secondary alcohols. The selectivity towards desired products remained complete in all cases. The coproduct of the reaction, namely water, did not hamper the efficiency of this solvent-free process.

The selected catalyst is cheap, can be easily prepared from commercial reagents and proved very robust. It is very active and selective, water-tolerant and recyclable. It represents therefore an interesting and complementary alternative to existing esterification catalysts. Together with the absence of solvents and of

any molar excess of reagents, these features highlight the practical and environmental viability of this catalytic method.

Experimental
Catalysts preparation

SiO$_2$-(CH$_2$)$_3$-SO$_3$H [35]: Amorphous silica (8.0 g) has been refluxed under stirring for 24 h with (3-mercaptopropyl)trimethoxysilane (MPTS) (1.15 mL; 6.1 mmol) in toluene (120 mL) and the resulting supported propylmercaptane has been oxidized to propanesulfonic acid by treatment with 30% aq H$_2$O$_2$ (100 mL; 1 mol) for 24 h under stirring at rt, adding a few drops of concentrated sulfuric acid after 12 h. Acidity has been measured via the titration method [35] (0.51 mmol H$^+$/g).

SiO$_2$-C$_6$H$_4$-SO$_3$H [35]: Amorphous silica (8.0 g) has been refluxed in toluene (120 mL) with phenyltriethoxysilane (2.0 mL, 8.3 mmol) under stirring for 24 hours. The resulting solid was then filtered off and washed with toluene (3 × 20 mL). The supported phenyl group was then sulfonated by refluxing in 1,2-dichloroethane (60 mL) the functionalized material with cholorosulfonic acid (10 mL, 150 mmol) under stirring for 4 hours. The solid was then recovered by filtration and washed with 1,2-dichloroethane (3 × 20 mL), acetone (3 × 20 mL) and water (3 × 50 mL) to deliver the title com-

pound. Acidity has been measured via the titration method [35] (0.65 mmol H$^+$/g).

SiO$_2$-(CH$_2$)$_3$-O-C$_6$H$_4$-SO$_3$H: A mixture of amorphous silica gel (2.0 g) and bromopropyltrimethoxysilane (0.76 mL, 4.0 mmol) was refluxed in toluene (80 mL) under stirring for 24 hours. The resulting silica supported 3-bromopropane was recovered by filtration and washed with toluene (3 × 50 mL). A mixture of this material (2.0 g) and sodium phenoxide (0.6 g, 6.0 mmol) in DMF (100 mL) was then heated at 100 °C under stirring for 24 hours. Afterwards, the material was filtered, washed with DMF (3 × 20 mL) and acetone (3 × 20 mL). The resulting solid material (2.0 g) and chlorosulfonic acid (4 mL, 60 mmol) were eventually stirred in refluxing 1,2-dichloro-ethane (60 mL) under stirring for 4 hours. The catalyst was then recovered by filtration and washed with 1,2-dichloroethane (3 × 20 mL), acetone (3 × 20 mL) and water (3 × 50 mL). Acidity has been measured via titration method [35] (0.73 mmol H$^+$/g).

Esterification reaction

Levulinic acid, pentanol and the heterogeneous catalyst were stirred for 24 hours in a batch reactor under air. The acid/alcohol ratio, the reaction temperature and the amount of the catalyst were modified as described in the previous section. In all cases, the solid catalyst was eventually recovered by filtration and the reaction mixture was analysed by high resolution capillary GC with a fused silica capillary column SE52 (5% phenyl, 95% methyl polysiloxane, 30 m × 25 mm). The products were isolated by flash chromatography on silica gel (eluent = hexane/ethyl acetate) and characterised by multinuclear NMR.

Supporting Information

Supporting Information File 1
Experimental part and NMR spectra of products.
[http://www.beilstein-journals.org/bjoc/content/supplementary/1860-5397-12-207-S1.pdf]

References

1. Gallezot, P. *Chem. Soc. Rev.* **2012,** *41,* 1538–1558. doi:10.1039/C1CS15147A
2. McKendry, P. *Bioresour. Technol.* **2002,** *83,* 37–46. doi:10.1016/S0960-8524(01)00118-3
3. Beerthuis, R.; Rothenberg, G.; Shiju, N. R. *Green Chem.* **2015,** *17,* 1341–1361. doi:10.1039/C4GC02076F
4. Climent, M. J.; Corma, A.; Iborra, S. *Green Chem.* **2014,** *16,* 516–547. doi:10.1039/c3gc41492b
5. Strassberger, Z.; Tanase, S.; Rothenberg, G. *Eur. J. Org. Chem.* **2011,** 5246–5249. doi:10.1002/ejoc.201101015
6. Van de Vyver, S.; Peng, L.; Geboers, J.; Schepers, H.; de Clippel, F.; Gommes, C. J.; Goderis, B.; Jacobs, P. A.; Sels, B. F. *Green Chem.* **2010,** *12,* 1560–1563. doi:10.1039/c0gc00235f
7. Fukuoka, A.; Dhepe, P. L. *Angew. Chem., Int. Ed.* **2006,** *45,* 5161–5163. doi:10.1002/anie.200601921
8. Demma Carà, P.; Pagliaro, M.; Elmekawy, A.; Brown, D. R.; Verschuren, P.; Shiju, N. R.; Rothenberg, G. *Catal. Sci. Technol.* **2013,** *3,* 2057–2061. doi:10.1039/c3cy20838a
9. Onda, A.; Ochi, T.; Yanagisawa, K. *Green Chem.* **2008,** *10,* 1033–1037. doi:10.1039/b808471h
10. Rinaldi, R.; Palkovits, R.; Schueth, F. *Angew. Chem., Int. Ed.* **2008,** *47,* 8047–8050. doi:10.1002/anie.200802879
11. Mäki-Arvela, P.; Salmi, T.; Holmbom, B.; Willför, S.; Murzin, D. Y. *Chem. Rev.* **2011,** *111,* 5638–5666. doi:10.1021/cr2000042
12. Corma, A.; Iborra, S.; Velty, A. *Chem. Rev.* **2007,** *107,* 2411–2502. doi:10.1021/cr050989d
13. Neves, P.; Antunes, M. M.; Russo, P. A.; Abrantes, J. P.; Lima, S.; Fernandes, A.; Pillinger, M.; Rocha, S. M.; Ribeiro, M. F.; Valente, A. A. *Green Chem.* **2013,** *15,* 3367–3376. doi:10.1039/c3gc41908h
14. de Souza, R. O. M. A.; Miranda, L. S. M.; Luque, R. *Green Chem.* **2014,** *16,* 2386–2405. doi:10.1039/c3gc41885e
15. Berger, R. G. *Flavours and Fragrances - Chemistry, Bioprocessing and Sustainability;* Springer, 2007. doi:10.1007/978-3-540-49339-6
16. Bozell, J. J.; Moens, L.; Elliott, D. C.; Wang, Y.; Neuenscwander, G. G.; Fitzpatrick, S. W.; Bilski, R. J.; Jarnefeld, J. L. *Resour., Conserv. Recycl.* **2000,** *28,* 227–239. doi:10.1016/S0921-3449(99)00047-6
17. Yan, K.; Jarvis, C.; Gu, J.; Yan, Y. *Renewable Sustainable Energy Rev.* **2015,** *51,* 986–997. doi:10.1016/j.rser.2015.07.021
18. Demma Carà, P.; Ciriminna, R.; Shiju, N. R.; Rothenberg, G.; Pagliaro, M. *ChemSusChem* **2014,** *7,* 835–840. doi:10.1002/cssc.201301027
19. Zhang, J.; Wu, S. B.; Li, B.; Zhang, H. D. *ChemCatChem* **2012,** *4,* 1230–1237. doi:10.1002/cctc.201200113
20. Patil, C. R.; Niphadkar, P. S.; Bokade, V. V.; Joshi, P. N. *Catal. Commun.* **2014,** *43,* 188–191. doi:10.1016/j.catcom.2013.10.006
21. Nandiwale, K. Y.; Bokade, V. V. *Chem. Eng. Technol.* **2015,** *38,* 246–252. doi:10.1002/ceat.201400326
22. Fernandes, D. R.; Rocha, A. S.; Mai, E. F.; Mota, C. J. A.; Teixeira da Silva, V. *Appl. Catal., A: Gen.* **2012,** *425-426,* 199–204. doi:10.1016/j.apcata.2012.03.020
23. Bart, H. J.; Reidetschlager, J.; Schatka, K.; Lehmann, A. *Ind. Eng. Chem. Res.* **1994,** *33,* 21–25. doi:10.1021/ie00025a004
24. An, S.; Song, D.; Lu, B.; Yang, X.; Guo, Y.-H. *Chem. – Eur. J.* **2015,** *21,* 10786–10798. doi:10.1002/chem.201501219
25. Su, F.; Ma, L.; Song, D.; Zhang, X.; Guo, Y. *Green Chem.* **2013,** *15,* 885–890. doi:10.1039/c3gc36912a
26. Pasquale, G.; Vázquez, P.; Romanelli, G.; Baronetti, G. *Catal. Commun.* **2012,** *18,* 115–120. doi:10.1016/j.catcom.2011.12.004
27. Peng, L.; Lin, L.; Zhang, J.; Shi, J.; Liu, S. *Appl. Catal., A* **2011,** *397,* 259–265. doi:10.1016/j.apcata.2011.03.008
28. Grecea, M. L.; Dimian, A. C.; Tanase, S.; Subbiah,, V.; Rothenberg, G. *Catal. Sci. Technol.* **2012,** *2,* 1500–1506. doi:10.1039/c2cy00432a
29. Subbiah, V.; van Zwol, P.; Dimian, A. C.; Gitis, V.; Rothenberg, G. *Top. Catal.* **2014,** *57,* 1545–1549. doi:10.1007/s11244-014-0337-x
30. Dimian, A. C.; Rothenberg, G. *Catal. Sci. Technol.* **2016,** *6,* 6097–6108. doi:10.1039/C6CY00426A

31. Zhou, X.; Li, Z. X.; Zhang, C.; Gao, X. P.; Dai, Y. Z.; Wang, G. Y.
J. Mol. Catal. A: Chem. **2016,** *417,* 71–75.
doi:10.1016/j.molcata.2016.03.006

32. Lima, T. M.; Lima, C. G. S.; Rathi, A. K.; Gawande, M. B.; Tucek, J.;
Urquieta-Gonzales, E. A.; Zbořil, L.; Paixão, M. W.; Varma, R. S.
Green Chem. **2016,** in press. doi:10.1039/C6GC01296E

33. Tejero, M. A.; Ramírez, E.; Fité, C.; Tejero, J.; Cunill, F. *Appl. Catal., A*
2016, *517,* 56–66. doi:10.1016/j.apcata.2016.02.032

34. Melero, J. A.; Morales, G.; Iglesias, J.; Paniagua, M.; Hernández, B.;
Penedo, S. *Appl. Catal., A* **2013,** *466,* 116–122.
doi:10.1016/j.apcata.2013.06.035

35. Corma, A.; Garcia, H. *Adv. Synth. Catal.* **2006,** *348,* 1391–1412.
doi:10.1002/adsc.200606192

36. Maggi, R.; Bosica, G.; Gherardi, S.; Oro, C.; Sartori, G. *Green Chem.*
2005, *7,* 182–184. doi:10.1039/B416665E

37. Maggi, R.; Chitsaz, S.; Loebbecke, S.; Piscopo, C. G.; Sartori, G.;
Schwarzer, M. *Green Chem.* **2011,** *13,* 1121–1123.
doi:10.1039/c0gc00887g

38. Cañeque, T.; Truscott, F. M.; Rodriguez, R.; Maestri, G.; Malacria, M.
Chem. Soc. Rev. **2014,** *43,* 2916–2926. doi:10.1039/c4cs00023d

39. Badley, R. D.; Ford, W. T. *J. Org. Chem.* **1989,** *54,* 5437–5443.
doi:10.1021/jo00284a014

40. Kiss, A. A.; Dimian, A. C.; Rothenberg, G. *Adv. Synth. Catal.* **2006,**
348, 75–81. doi:10.1002/adsc.200505160

41. Lempers, H. E. B.; Sheldon, R. A. *J. Catal.* **1998,** *175,* 62–69.
doi:10.1006/jcat.1998.1979

Diels–Alder reactions in confined spaces: the influence of catalyst structure and the nature of active sites for the retro-Diels–Alder reaction

Ángel Cantín[1], M. Victoria Gomez[*2] and Antonio de la Hoz[*2]

Full Research Paper

`Open Access`

Address:
[1]Instituto de Tecnología Química (UPV-CSIC), Universidad Politécnica de Valencia, Avda. Los Naranjos s/n, 46022 Valencia, Spain and [2]Área Química Orgánica, Facultad de Químicas, Universidad de Castilla-La Mancha, and Instituto Regional de Investigación Científica Aplicada (IRICA), Avda. Camilo José Cela s/n, E-13071-Ciudad Real, Spain

Email:
M. Victoria Gomez[*] - Mariavictoria.Gomez@uclm.es;
Antonio de la Hoz[*] - Antonio.Hoz@uclm.es

* Corresponding author

Abstract

Diels–Alder cycloaddition between cyclopentadiene and *p*-benzoquinone has been studied in the confined space of a pure silica zeolite Beta and the impact on reaction rate due to the concentration effect within the pore and diffusion limitations are discussed. Introduction of Lewis or Brønsted acid sites on the walls of the zeolite strongly increases the reaction rate. However, contrary to what occurs with mesoporous molecular sieves (MCM-41), Beta zeolite does not catalyse the retro-Diels–Alder reaction, resulting in a highly selective catalyst for the cycloaddition reaction.

Introduction

The Diels–Alder reaction (DAR) is one of the most useful reactions in organic synthesis. In order to improve the yield and to avoid the reversibility of the reaction, homogeneous Lewis acids [1-4], solid acids [5,6] as catalyst, high pressures [6-8] and/or water as a solvent [9,10] have been reported. In particular, and among the most interesting environmental-friendly reactions, the cycloaddition reaction occurs with high selectivity and atom economy. Moreover, Diels–Alder cycloadditions in combination with heterogeneous catalysts (i.e. doped-

microporous materials) represent an interesting approach for the conversion of biomass feedstock into stable chemicals such as furfural derivatives, platform molecules which can be converted into a variety of liquid hydrocarbon fuels and fuel additives [11,12]. Catalysis is considered as one of the foundational pillars of green chemistry. Catalysis often reduces the energy requirements, permits the use of renewable feedstocks and less toxic reagents. Moreover, in most cases yields are improved and selectivity is enhanced or modified [13]. In this regard, hetero-

geneous catalysis in general and zeolites in particular are remarkably efficient since they permit the replacement of toxic mineral acids and oxidants by easily recyclable catalysts [14].

One approach to improve yields and selectivity is the special confinement of the reactants and the presence of catalytic active sites, [15,16] by use of microporous materials doped with metals. While pore dimensions and topology of the microporous materials can affect the selectivity of the reaction, their activity can be strongly limited by a slow diffusion of reactants and products, unless microporous molecular sieves with the appropriated pore dimensions are used as catalyst. Thus, microporous molecular sieves with optimized pore diameters and topologies can be of interest to catalyze DAR [17-26] in where different stereoisomers could be obtained. Lewis-acid centers contained within the framework of zeolite beta (Zr-β, Sn-β) are useful catalysts in the Diels–Alder reaction for the production of bio-based terephthalic acid precursors, one of the monomers for the synthesis of polyethylene terephthalate that is used for the large-scale manufacture of plastic bottles among others. The authors do not find transport limitations within the zeolite framework to the rate of the reaction [27]. Interestingly, when Brønsted acid containing zeolites (Al-β) are used as catalyst, there is a decrease in the Diels–Alder reaction selectivity [28].

The DAR of cyclopentadiene with *p*-benzoquinone is a well-known example of cycloadditions, and some results can be found on the control of the selectivity to the different isomers. In homogeneous phase, equimolar amounts of diene and dienophile afford two isomers, the *endo* as the major and the *exo* as the minor product. The addition of a second equivalent of cyclopentadiene affords mainly the *endo-anti-endo* product as major isomer, and the *endo-anti-exo* product as the minor isomer. While CsY zeolite enhances the selectivity to the *endo-anti-exo* isomer [29], the mesoporous material MCM-41

enhances the conversion to the *endo-anti-endo* isomer as has been shown in a previous work [30]. However, MCM-41 in the form of aluminosilicate that contains Brønsted sites enhances the retro-Diels–Alder reaction increasing the selectivity to the *endo-anti-exo* isomer. Therefore, the framework and extra framework composition of mesoporous materials and zeolite could be used to control the selectivity of the DAR of cyclopentadiene and *p*-benzoquinone.

In the present work, a series of large pore, pure silica zeolites (in which rate enhancement can only occur by spatial confinement) and the same structures but containing framework Brønsted or Lewis acid sites have been studied for the DAR between cyclopentadiene and *p*-benzoquinone. The effects of pore dimensions and catalyst composition on diffusivity and selectivity with respect to the retro-Diels–Alder reaction (retro-DAR) are discussed.

Results and Discussion

As it was described previously [30], the Diels–Alder reaction (DAR) between cyclopentadiene and *p*-benzoquinone follows the reactions outlined in Scheme 1.

As expected, the Diels–Alder cycloaddition provides the kinetically controlled *endo* isomer that very rapidly reacts with a second molecule of the diene to give again the kinetic *endo-endo* isomer. It is remarkable that neither the thermodynamic *exo* isomer nor the secondary *exo-endo* and *exo-exo* products were detected under our reaction conditions. Thus, the observed products, *endo-endo* and *endo-exo* are obtained in different ratio according to the reaction conditions. This ratio can change with the time since the retro-Diels–Alder reaction appears as a competitive reaction. In this way, the final molecular product can revert to the initial *endo* isomer, which in turn can react again with a new cyclopentadiene molecule. This is
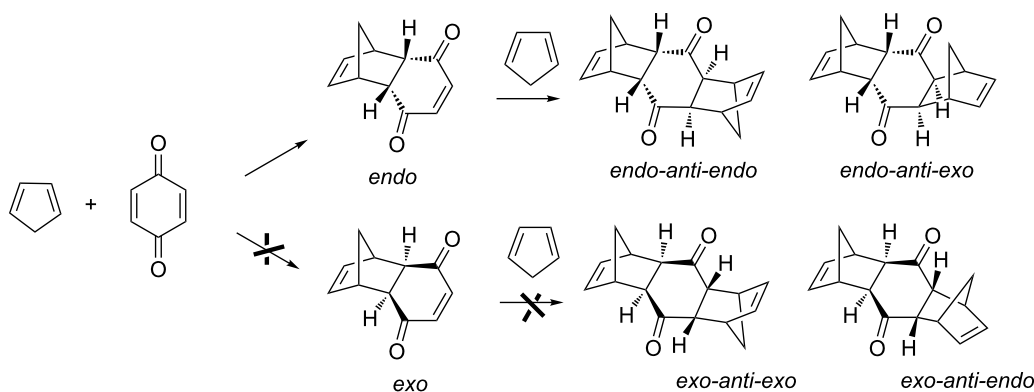
Scheme 1: Distribution of products in the Diels–Alder reaction between cyclopentadiene and *p*-benzoquinone.

reflected in the distribution products by a decrease of the *endo-endo* isomer (kinetic control product) jointed to an increase of the *endo-exo* (thermodynamic control product).

Influence of catalyst surface

We have seen that the DAR between cyclopentadiene and *p*-benzoquinone takes place thermally. The effect of confinement of the reactant within the pores of the catalyst can decrease the entropy of the activated complex [17-26,29,30] producing not only an increase of the reaction rate but also a modification of the selectivity. To study this effect, we have firstly carried out the reaction using a large pore Beta zeolite as catalyst. Thus, Figure 1 compares conversion results obtained for all silica Beta zeolite with that obtained during the thermal reaction or using Aerosil (amorphous non porous silica, BET surface area = 200 $m^2 g^{-1}$) as potential catalyst. Practically no differences were found on reaction rate nor on product distribution when the reaction occurs on nonporous silica, with Beta zeolite or even in absence of any solid. Considering that Aerosil is an amorphous solid, these results indicate that the catalytic reaction with pure silica Beta zeolite, if any, should only occur on the catalyst surface and the porous structure has not any effect on the reaction. Another hypothesis to explain these results is that diffusion of the products through the channels, if ever formed inside, is strongly restricted and the products remain adsorbed within the pores. To evaluate this second hypothesis, ^{13}C MAS NMR, elemental analysis and material balance were done, and the results obtained allow us to discard the accumulation of the reaction products inside the pores of the catalyst.

In order to check if the process is diffusion controlled within the pores of the zeolite and the reaction is mainly occurring on the external surface, the reaction was carried out with a pure silica nanocrystalline Beta (see Table 1). Table 1 shows differences between textural characteristics of all studied materials in this work. Figure 1 shows, an increase of the reaction rate when
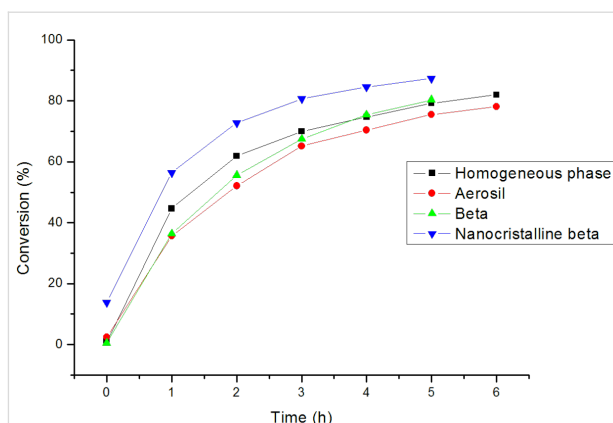

Figure 1: Conversion in the DAR catalysed by silica Beta zeolites and Aerosil.

reducing the crystallite size of the zeolite, indicating that there is a reactant diffusion control within the pores of Beta zeolite and consequently the reaction is mainly occurring in an outer shell of the crystals. If this is so, and since the reaction rate increases with the pure silica nanocrystalline Beta zeolite with an external surface area not too different from Aerosil silica, we can conclude that a concentration effect within the pore mouth of the zeolite may be responsible for the reaction rate enhancement observed with pure silica nanocristalline beta.

Introduction of Lewis and Brønsted acid sites in the solids

We have prepared Ti-Beta [31], Sn-Beta [32] and Al-Beta (Si/Al = 50) [33] considering that Lewis acid catalyzes the DAR [1]. This effect is known to occur by complexation of the carbonyl group of the dienophile with the Lewis acid that increases the electron deficiency of the dienophile, reducing the energy gap.

The results presented in Figure 2a, b clearly show an important increase in activity due to the presence of Brønsted and, espe-

Table 1: Textural characteristic of the studied materials.

Catalyst	Area ($m^2 g^{-1}$)[a]	Crystallite size (µm)[b]	Metal content (wt %)[c]	External surface ($m^2 g^{-1}$)[d]
Beta	457	0.5–1	–	24
Nanocrystalline Beta	595	0.015-0.02	–	100
Ti-Beta	454	1	1.2	25
Sn-Beta	470	1	1.6	30
Beta Si/Al = 13	518	0.1–0.2	2.8	34
Beta Si/Al = 50	484	0.2	0.9	50

[a]Area: Total area of the material per unit of mass. [b]Crystallite size: Size of the crystalline material (aggregate of a large number of single crystals). It can vary from a few nanometers to several millimeters. [c]Metal content: wt percentage of the metal content within the solid structure. [d]External surface: External area of the material per unit of mass.
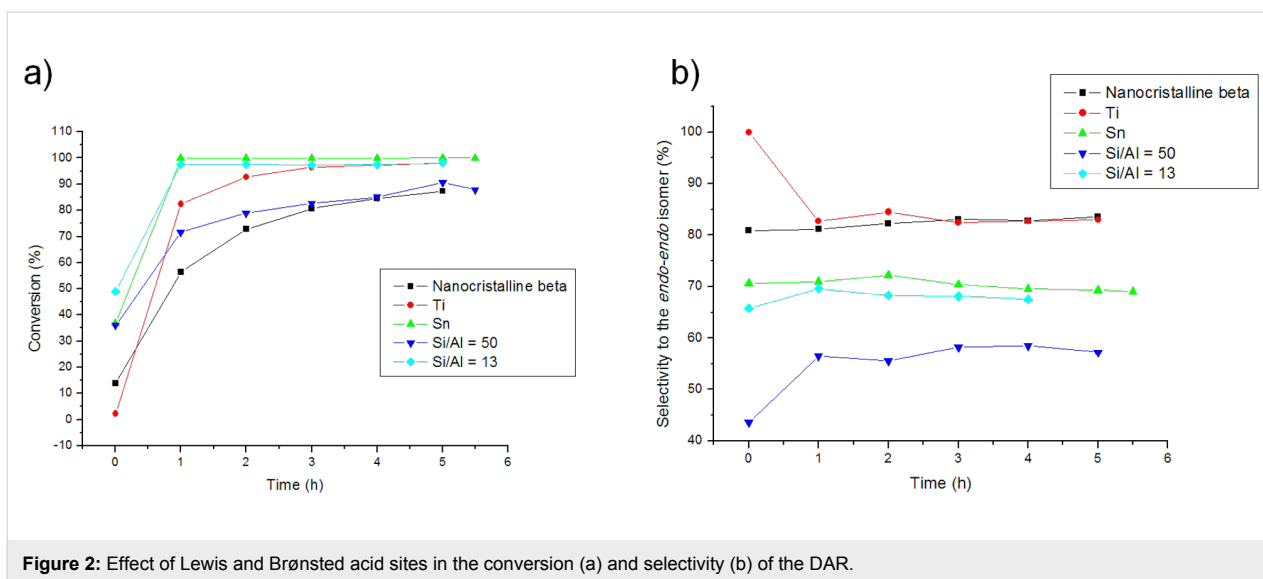
Figure 2: Effect of Lewis and Brønsted acid sites in the conversion (a) and selectivity (b) of the DAR.

cially, of Lewis acid sites. Indeed, despite the fact that the crystallite size of Ti- and Sn-Beta zeolites is much larger than Al-Beta (Table 1), the former give higher conversions.

Importantly, the catalytic effect on the selectivity of the competing retro-Diels–Alder reaction, which produces an enhancement of the *endo-exo* isomer from the *endo-endo* (see Scheme 1), is much lower for Ti-Beta and even for Al-Beta zeolites than for MCM-41 [30] (see Figure 2a, b) that owing to the retro-DA reaction the selectivity of the *endo-endo* isomer decreases from 85% to 65% as we previously reported. [30]

Considering the interesting application of beta zeolites as Lewis acid catalyst for Diels–Alder reactions in different fields, i.e., the formation of biofuels [34], it is important to get insight into

the lack of catalytic activity of Beta for the retro-DAR, and elucidate whether this is a general effect with zeolites. Due to the diffusion limitations with Beta we have selected two extra-large pore zeolites, SSZ-53 (BET surface area = 377 m^2/g) and SSZ-59 (BET surface area = 383 m^2/g), with 1D pore system and a Si/Al ratio of 49 and 53, respectively. The results given in Figure 3 clearly show that the extra-large pore zeolites with pore diameters of 8.7 Å and 8.5 Å for SSZ-53 and SSZ-59, respectively, give higher conversions than Beta zeolite, despite the smaller crystallite size of the last. Interestingly, the retro-DAR was neither observed with the two zeolites with extra-large pores. Similarly to that produced with the silica nanocrystalline Beta zeolite a concentration effect within the extra-large pore mouth may be responsible of the reaction rate enhancement observed with SSZ-53 and SSZ-59.
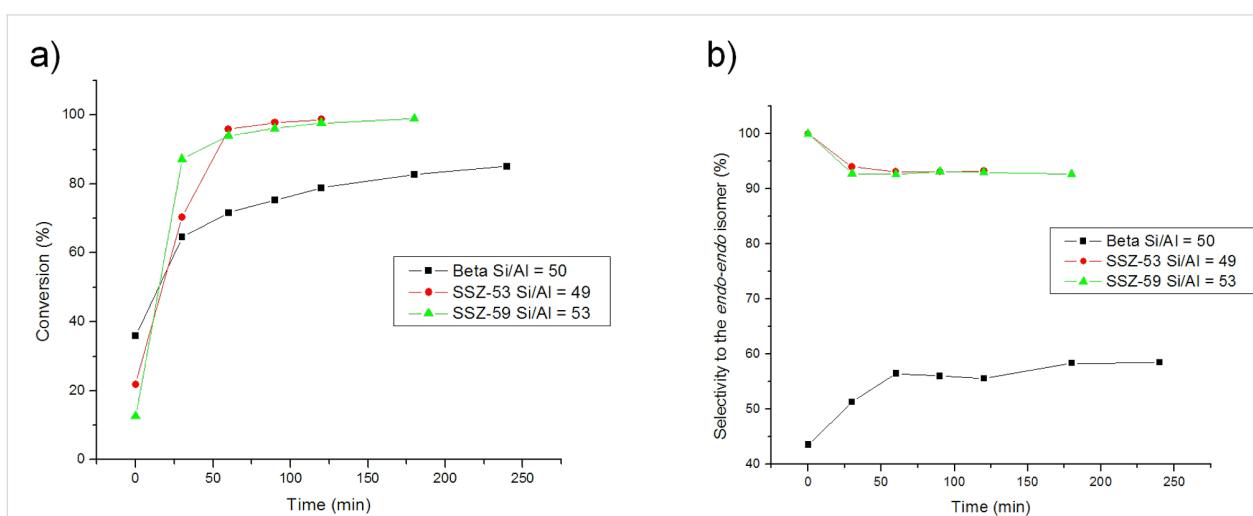

Figure 3: Effect of pore size in the conversion (a) and selectivity (b) of the DAR.

Therefore, the results seem to confirm that the occurrence of retro-DAR as a competitive reaction not only depends on the presence of Brønsted centers as previously reported for materials with lower amounts of Al centers [28], but the structure of the material can play a determinant role. This represents an interesting observation since it will imply that, in principle, it should be possible to change the relative selectivity for DAR and retro-DAR working with micro or mesoporous catalysts.

Thus, Figure 4a,b compares conversion and selectivity to the *endo-endo* isomer with Al-Beta zeolite and the mesoporous MCM-41 material previously studied [30] both with very close Si/Al ratios. It can be observed that both samples give the same conversion, but different selectivity behavior.

In the case of the microporous catalyst, Al-Beta zeolite, the selectivity to the *endo-endo* isomer remains constant with time, while with MCM-41 that is formed by larger channels, a continuous decrease of the *endo-endo* with time occurs and the thermodynamically controlled *endo-exo* product increases. The retro-Diels–Alder is a consecutive reaction that produces the thermodynamic product and it would occur if there is a certain confinement within the pores.

Thus, it was thought that if retro-DAR occurs in MCM-41 (40 Å), if the pore size is decreased, then this reaction should be enhanced because of a certain confinement effect through the reactants. As it can be observed in Figure 4a,b, when the reaction was carried out with a mesoporous material of ≈20 Å instead of 40 Å but with a similar Si/Al ratio, the retro-DAR was enhanced, illustrating a certain confinement effect within the pores.

Two extra-large pore 3D zeolites with pore diameters of 1.2 (ITQ-33) [35] and 1.9 nm (ITQ-37) [36] have also been tested.

These are aluminosilicogermanates that, as the previously tested Al-zeolites or the Al-MCM-41 material, present Brønsted acidity. Interestingly, the pore diameters of ITQ-33, and more so ITQ-37 are close to the pore of the mesoporous MCM-41 presented above with 2.0 nm. There is then a unique occasion to compare the catalytic behavior of an amorphous and a crystalline molecular sieve with practically the same pore diameter (Figure 5a,b).

As observed in Figure 5a,b, the crystalline structure of zeolites ITQ-33 and ITQ-37 do not favor neither the Diels–Alder cycloaddition between cyclopentadiene and *p*-benzoquinone, nor the retro-Diels–Alder reaction. This result suggests that the reaction takes place on the surface of the material and the pore structure does not have any influence on the reaction rate, neither for the DAR nor for the retro-DAR.

To further prove the effect of the structure, the reaction was carried out in presence of MCM-41 materials with different Si/Al ratios, and similar pore diameter. The results are collected in Figure 6a,b. As it could be expected no differences were found in the conversion. Meanwhile, in the case of the selectivity it is possible to observe that increasing the Al content and lowering the pore size produces an increase in the selectivity of the *endo-exo* isomer. However, this effect is much more marked when the pore size decreases.

Finally, to conclude the catalytic study of the reaction between cyclopentadiene and *p*-benzoquinone in presence of Beta zeolites, the ability of reuse of Beta Si/Al = 50 was examined. As shown in Figure 7a,b the activity of the catalyst decreases in some extension after repeated recycling. As expected for a less active catalyst, conversion falls partly while the selectivity to the kinetically controlled *endo-endo* isomer rises after recycling.
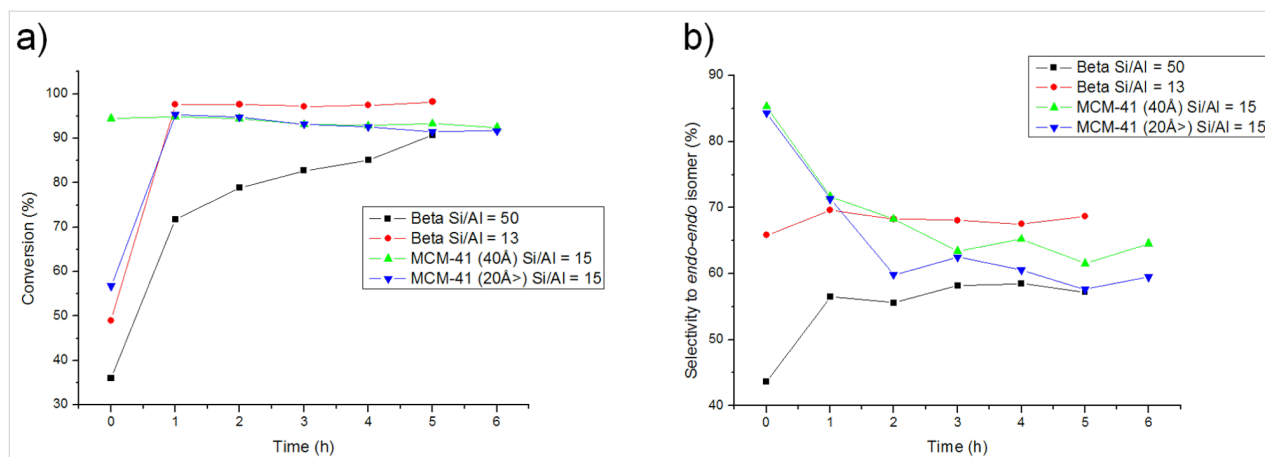

Figure 4: Comparison of conversion (a) and selectivity (b) of the DAR catalysed by Al-Beta zeolite and MCM-41.
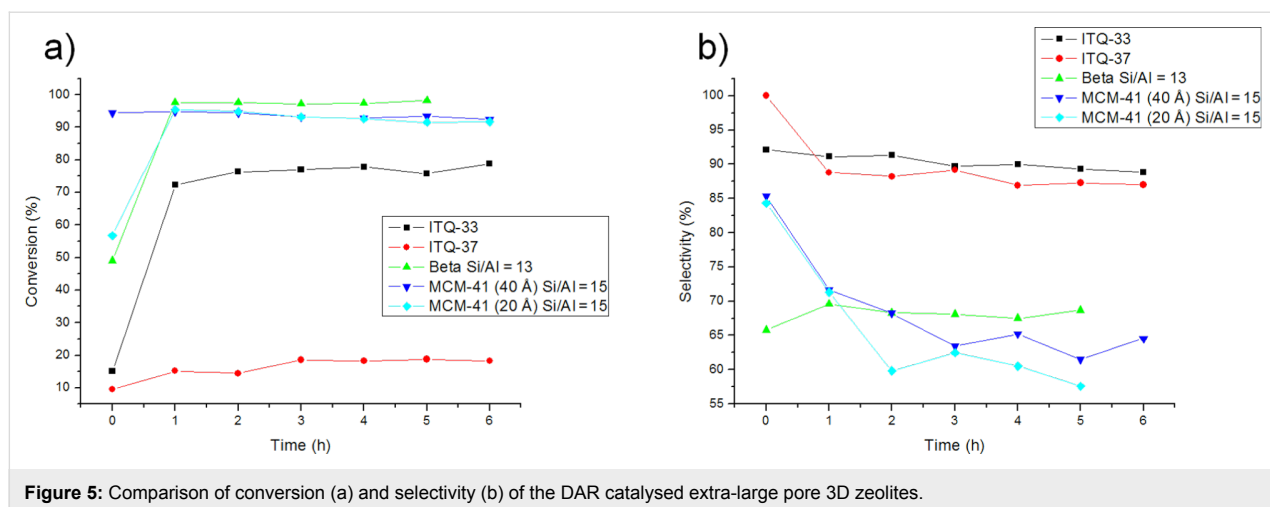
Figure 5: Comparison of conversion (a) and selectivity (b) of the DAR catalysed extra-large pore 3D zeolites.
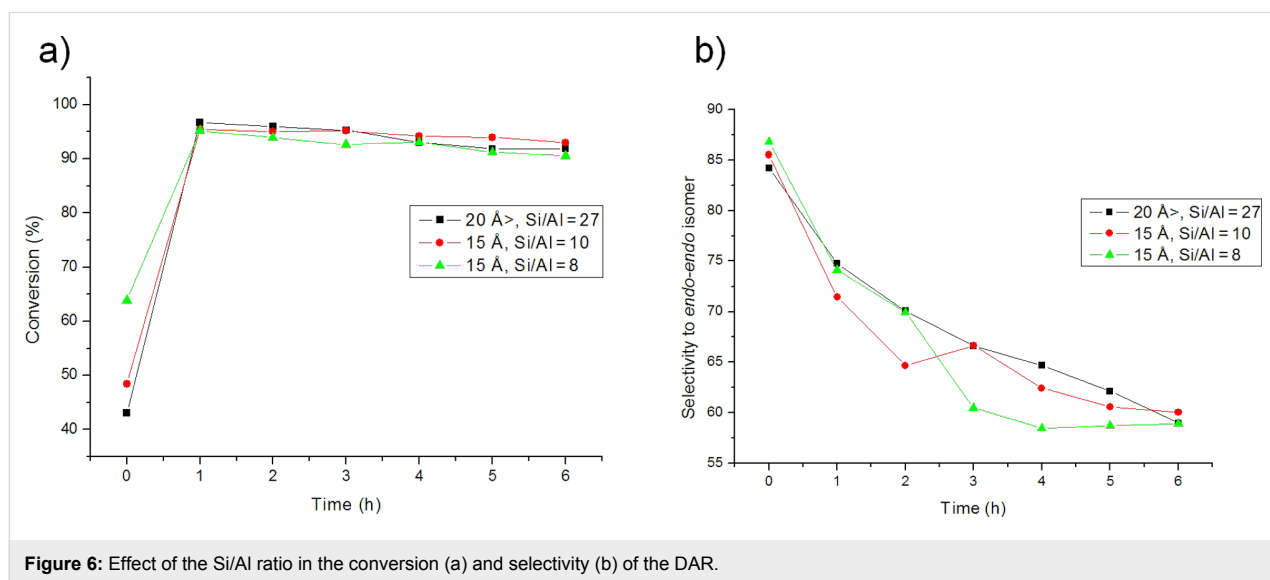

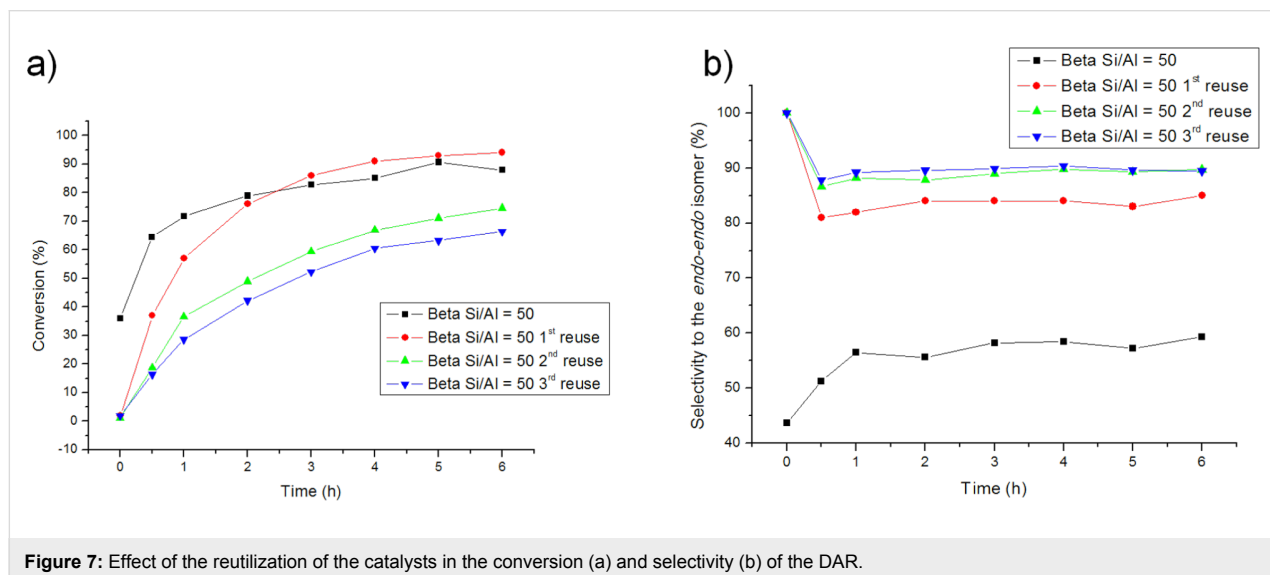**Figure 6:** Effect of the Si/Al ratio in the conversion (a) and selectivity (b) of the DAR.

Figure 7: Effect of the reutilization of the catalysts in the conversion (a) and selectivity (b) of the DAR.

Conclusion

In this work the DAR between cyclopentadiene and *p*-benzoquinone has been proved to take place on the catalyst surface when the reaction is carried out in presence of microporous materials, obtaining better results when a smaller crystal size catalyst is used.

When Lewis and Brønsted sites are inserted in the material structure, an improvement of the conversion degree is obtained as it occurs when MCM-41 and ITQ-2 were used [30]. However, a clear change in the selectivity behavior is observed. None of the used metals showed a retro-DAR enhancing reactivity, even Al, the best hydrogen-bond-donating agent. This result implies that the competitive retro-DAR takes place not only due to the capability to act as Brønsted sites of metallic centers, but also due to the structure of MCM-41 and ITQ-2. This effect can be used in order to obtain a selective product or the other isomer as a result of the chosen catalyst: The more Brønsted sites and the more confinement of the reactants, the more retro-DAR will be observed.

Experimental
Catalyst preparation

Beta zeolites [pure silica Beta, Beta (Ti), Beta (Sn) and Beta (Al)] were prepared according to [31-33], using tetraethylammonium hydroxide as template, tetraethyl orthosilicate (TEOS) as silica source and Ti(IV) ethoxide, $SnCl_4·5H_2O$ and metal Al as sources of heteroatoms. SSZ-53 and SSZ-59 were synthesized according to the procedures described in the literature [37-41]. The textural characteristics of the catalysts are given in Table 1.

Catalytic tests

In a similar manner as described in [30], after being activated at 250 °C under vacuum (10^{-2} mm Hg), 250 mg of the corresponding calcined material were introduced into a two necked bottom flask under N_2. Then, 108 mg of *p*-benzoquinone (1.0 mmol) and 10.0 mL of $CDCl_3$ were added. The mixture was stirred at room temperature for a few minutes and 0.2 mL of freshly distilled cyclopentadiene (3.0 mmol) were added with a syringe, being this moment considered $t = 0$ h. The system was heated at 60 °C and samples were taken every hour, being directly analyzed by ^{1}H NMR.

Reaction products were isolated by HPLC using mixtures of H_2O/MeOH/MeCN (45:50:5). Identification of these products was carried out by NMR techniques (^{1}H, ^{13}C, DEPT, COSY, HETCOR and NOE) being the spectral data fully coincident with those reported in the literature [42].

Conversion values for *endo-endo* and *endo-exo* products are always referred to conversion from the *endo* adduct. All compounds were previously described and fully characterized [30].

Acknowledgements

References

1. Yilmaz, Ö.; Kus, N. S.; Tunç, T.; Sahin, E. *J. Mol. Struct.* **2015,** *1098,* 72–75. doi:10.1016/j.molstruc.2015.06.012
2. Yamabe, S.; Dai, T.; Minato, T. *J. Am. Chem. Soc.* **1995,** *117,* 10994–10997. doi:10.1021/ja00149a023
3. Cativiela, C.; Fraile, J. M.; García, J. I.; Mayoral, J. A.; Pires, E.; Royo, A. J.; Figueras, F.; de Ménorval, L. C. *Tetrahedron* **1993,** *49,* 4073–4084. doi:10.1016/S0040-4020(01)89919-1
4. Song, S.; Wu, G.; Dai, W.; Guan, N.; Li, L. *J. Mol. Catal. A* **2016,** *420,* 134–141. doi:10.1016/j.molcata.2016.04.023
5. Cativiela, C.; Fraile, J. M.; García, J. I.; Mayoral, J. A.; Figueras, F.; de Menorval, L. C.; Alonso, P. J. *J. Catal.* **1992,** *137,* 394–407. doi:10.1016/0021-9517(92)90167-G
6. Figueras, F.; Cativiela, C.; Fraile, J. M.; García, J. I.; Mayoral, J. A.; de Ménorval, L. C.; Pires, E. *Stud. Surf. Sci. Catal.* **1994,** *83,* 391–398. doi:10.1016/S0167-2991(08)63280-2
7. Eckert, C. A.; Grieger, R. A. *J. Am. Chem. Soc.* **1970,** *92,* 7149–7153. doi:10.1021/ja00727a021
8. Mimoto, A.; Nakano, K.; Ichikawa, Y.; Kotsuki, H. *Heterocycles* **2010,** *80,* 799–804. doi:10.3987/COM-09-S(S)85
9. Rideout, D. C.; Breslow, R. *J. Am. Chem. Soc.* **1980,** *102,* 7816–7817. doi:10.1021/ja00546a048
10. Wijnen, J. W.; Engberts, J. B. F. N. *J. Org. Chem.* **1997,** *62,* 2039–2044. doi:10.1021/jo9623200
11. Moliner, M. *Dalton Trans.* **2014,** *43,* 4197–4208. doi:10.1039/C3DT52293H
12. Climent, M. J.; Corma, A.; Iborra, S. *Green Chem.* **2014,** *16,* 516–547. doi:10.1039/c3gc41492b
13. Anastas, P. T.; Kirchhoff, M. M. *Acc. Chem. Res.* **2002,** *35,* 686–694. doi:10.1021/ar010065m
14. Brown, S. H. Zeolites in Catalysis. In *Handbook of Green Chemistry; Green Catalysis, Heterogeneous Catalysis;* Crabtree, R. H.; Anastas, P. T., Eds.; Wiley-VCH: Weinheim, Germany, 2009; Vol. 2, pp 1–50.
15. Corma, A. *J. Catal.* **2003,** *216,* 298–312. doi:10.1016/S0021-9517(02)00132-X
16. Corma, A.; García, H. *Chem. Rev.* **2003,** *103,* 4307–4366. doi:10.1021/cr030680z
17. Koehle, M.; Lobo, R. F. *Catal. Sci. Technol.* **2016,** *6,* 3018–3026. doi:10.1039/C5CY01501D
18. Kang, J.; Rebeck, J., Jr. *Nature* **1997,** *385,* 50–52. doi:10.1038/385050a0
19. Orazov, M.; Davis, M. E. *Chem. Sci.* **2016,** *7,* 2264–2274. doi:10.1039/C5SC03889H

20. Chang, C.-C.; Cho, H. J.; Yu, J.; Gorte, R. J.; Gulbinski, J.; Dauenhauer, P.; Fan, W. *Green Chem.* **2016,** *18,* 1368–1376. doi:10.1039/C5GC02164B

21. Zendehdel, M.; Zamani, F.; Khanmohamadi, H. *Microporous Mesoporous Mater.* **2016,** *225,* 552–563. doi:10.1016/j.micromeso.2016.01.042

22. Onaka, M.; Yamasaki, R. *Chem. Lett.* **1998,** 259–260. doi:10.1246/cl.1998.259

23. Kugita, T.; Ezawa, M.; Owada, T.; Tomita, Y.; Namba, S.; Hashimoto, N.; Osaka, M. *Microporous Mesoporous Mater.* **2001,** *44–45,* 531–536. doi:10.1016/S1387-1811(01)00231-1

24. Mahmoud, E.; Yu, J.; Gorte, R. J.; Lobo, R. F. *ACS Catal.* **2015,** *5,* 6946–6955. doi:10.1021/acscatal.5b01892

25. Green, S. K.; Patet, R. E.; Nikbin, N.; Williams, C. L.; Chang, C.-C.; Yu, J. Y.; Gorte, R. J.; Caratzoulas, S.; Fan, W.; Vlachos, D. G.; Dauenhauer, P. J. *Appl. Catal., B* **2016,** *180,* 487–496. doi:10.1016/j.apcatb.2015.06.044

26. Corma, A. *Catal. Rev.: Sci. Eng.* **2004,** *46,* 369–417. doi:10.1081/CR-200036732

27. Pacheco, J. J.; Labinger, J. A.; Sessions, A. L.; Davis, M. E. *ACS Catal.* **2015,** *5,* 5904–5913. doi:10.1021/acscatal.5b01309

28. Pacheco, J. J.; Davis, M. E. *Proc. Natl. Acad. Sci. U. S. A.* **2014,** *111,* 8363–8367. doi:10.1073/pnas.1408345111

29. Mashayekhi, G.; Ghandi, M.; Farzaneh, F.; Shahidzadeh, M.; Najafi, H. M. *J. Mol. Catal. A: Chem.* **2007,** *264,* 220–226. doi:10.1016/j.molcata.2006.09.032

30. Gómez, M. V.; Cantín, A.; Corma, A.; de la Hoz, A. *J. Mol. Catal. A: Chem.* **2005,** *240,* 16–21. doi:10.1016/j.molcata.2005.06.030

31. Blasco, T.; Corma, A.; Esteve, P.; Guil, J. M.; Martinez, A.; Perdigon-Melon, J. A.; Valencia, S. *J. Phys. Chem. B* **1998,** *102,* 75–88. doi:10.1021/jp973288w

32. Corma, A.; Nemeth, L. T.; Renz, M.; Valencia, S. *Nature* **2001,** *412,* 423–425. doi:10.1038/35086546

33. Camblor, M. A.; Corma, A.; Valencia, S. *J. Mater. Chem.* **1998,** *8,* 2137–2145. doi:10.1039/a804457k

34. Dutta, S.; De, S.; Saha, B.; Alam, M. I. *Catal. Sci. Technol.* **2012,** *2,* 2025–2036. doi:10.1039/C2CY20235B

35. Corma, A.; Díaz-Cabañas, M. J.; Jordá, J. L.; Martínez, C.; Moliner, M. *Nature* **2006,** *443,* 842–845. doi:10.1038/nature05238

36. Sun, J.; Bonneau, C.; Cantín, Á.; Corma, A.; Díaz-Cabañas, M. J.; Moliner, M.; Zhang, D.; Li, M.; Zou, X. *Nature* **2009,** *458,* 1154–1157. doi:10.1038/nature07957

37. Elomari, S.; Zones, S. I. Zeolites and Mesoporous Materials at the Dawn of the 21st Century. In *Proceedings of the 13th International Zeolite Conference, Vol. 153,* Montpellier, France; Elsevier, 2001; pp 479–486.

38. Chen, C. Y.; Zones, S. I. Preparation of aluminum-, gallium-, and iron-exchanged borosilicate zeolites and their use as petroleum refining catalysts. U.S. Patent US 20030133870 A1, July 17, 2003.

39. Burton, A.; Elomari, S.; Chen, C.-Y.; Medrud, R. C.; Chan, I. Y.; Bull, L. M.; Kibby, C.; Harris, T. V.; Zones, S. I.; Vittoratos, E. S. *Chem. – Eur. J.* **2003,** *9,* 5737–5748. doi:10.1002/chem.200305238

40. Burton, A.; Elomari, S.; Chen, C. Y.; Harris, T. V.; Vittoratos, E. S., Eds. *Recent Advances in the Science and Technology of Zeolites and Related Materials, Proceedings of the 14th International Zeolite Conference, Vol. 154A, pp 126–132.,* Cape Town, South Africa; Elsevier, 2004.

41. Elomari, S. Zeolite SSZ-53 prepared by using templating agent to be catalyst. U.S. Patent US 20020104780 A1, Aug 8, 2002.

42. Yates, P.; Switlak, K. *Can. J. Chem.* **1990,** *68,* 1894–1900. doi:10.1139/v90-293

License and Terms

Regiocontroled Pd-catalysed C5-arylation of 3-substituted thiophene derivatives using a bromo-substituent as blocking group

Mariem Brahim[1,2], Hamed Ben Ammar[*2], Jean-François Soulé[*1] and Henri Doucet[*1]

Address:
[1]Institut des Sciences Chimiques de Rennes, UMR 6226 CNRS-Université de Rennes "Organométalliques: Matériaux et Catalyse", Campus de Beaulieu, 35042 Rennes, France. Tel.: 00-33-2-23-23-63-84 and [2]Laboratoire de Synthèse Organique Asymétrique et Catalyse Homogène, (UR 11ES56) Université de Monastir, Faculté des Sciences de Monastir, avenue de l'environnement, Monastir 5000, Tunisia

Email:
Hamed Ben Ammar[*] - hamed_benammar@yahoo.fr;
Jean-François Soulé[*] - jean-francois.soule@univ-rennes1.fr;
Henri Doucet[*] - henri.doucet@univ-rennes1.fr

* Corresponding author

Abstract

The use of a bromo-substituent as blocking group at the C2-position of 3-substituted thiophenes allows the regioselective introduction of aryl substituents at C5-position via Pd-catalysed direct arylation. With 1 mol % of a phosphine-free Pd catalyst, KOAc as the base and DMA as the solvent and various electron-deficient aryl bromides as aryl sources, C5-(hetero)arylated thiophenes were synthesized in moderate to high yields, without cleavage of the thienyl C–Br bond. Moreover, sequential direct thienyl C5-arylation followed by Pd-catalysed direct arylation or Suzuki coupling at the C2-position allows to prepare 2,5-di(hetero)arylated thiophenes bearing two different (hetero)aryl units in only two steps. This method provides a "green" access to arylated thiophene derivatives as it reduces the number of steps to prepare these compounds and also the formation of wastes.

Introduction

Thiophene derivatives bearing aryl substituents are important structures because of their biological and/or physical properties. Among them, 3-substituted 5-arylthiophenes are widely used as building blocks for the synthesis of semi-conductors [1-3].

Therefore, the discovery of more direct and selective procedures for access to 5-arylated 3-substituted thiophene derivatives is an important topic in sustainable chemistry [4]. Stille or Suzuki palladium-catalysed coupling reactions [5-10] are some

of the most efficient methods for the preparation of 5-arylated 3-substituted thiophenes [11-14]. However, before these coupling reactions can be performed, an organometallic compound must be synthesized. In 1990, Ohta and co-workers described the Pd-catalysed direct arylation of thiophene derivatives by coupling reaction with aryl halides [15,16]. This is a highly powerful method for a greener access to a very broad range of arylated thiophenes [17-25]. The method is very attractive in terms of green chemistry, because its major by-products are not metal salts but a base associated to HX, and synthesis of an organometallic derivative can be avoided. However, for C3-substituted thiophenes, arylation generally occurred at the C2-position or gave mixtures of C2- and C5-arylated products [26-33]. The introduction of blocking groups at C2-position on thiophene derivatives in order to arylate regiospecifically the C5-positions had been reported (Figure 1).

Figure 1: Regioselectivity of the arylation of 3-substituted thiophenes.
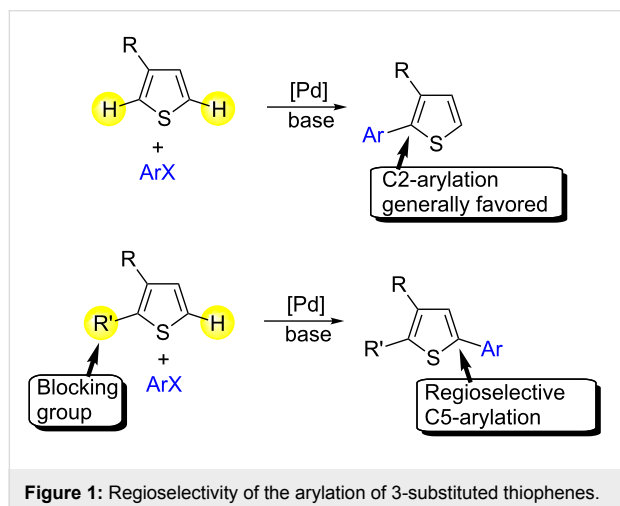
In 2010, Fagnou et al. attached a 2-chloro-substituent to the thiophene ring to selectively perform a Pd-catalysed direct arylation of 3-hexylthiophene at the C5-position (Scheme 1, top) [34]. An ester moiety as blocking group at the C2-position of 3-substituted thiophene could also direct regioselectivity of Pd-catalysed direct arylation to the C5-position (Scheme 1, middle) [35]. Mori et al. also reported two examples of C5-arylation of 2-bromo-3-methylthiophene with aryl iodides as aryl sources with 5 mol % PdCl$_2$(PPh$_3$)$_2$ catalyst and AgNO$_3$–KF as the base in DMSO (Scheme 1, bottom) [36].

Herein, we wish to report on green conditions in terms of number of steps, base nature, use of a phosphine-free catalyst at low loading and a quite "atom economic" aryl source promoting such a C5-arylation using C3-substituted 2-bromothiophenes. We report i) that only 1 mol % of air-stable Pd(OAc)$_2$ catalyst associated to KOAc promotes the regiospecific access to C5-arylated 2-bromothiophenes without cleavage of the thienyl

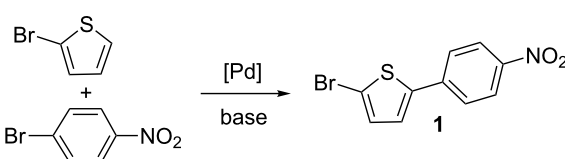**Scheme 1:** Blocking groups allowing regioselective C5-arylation of thiophenes.
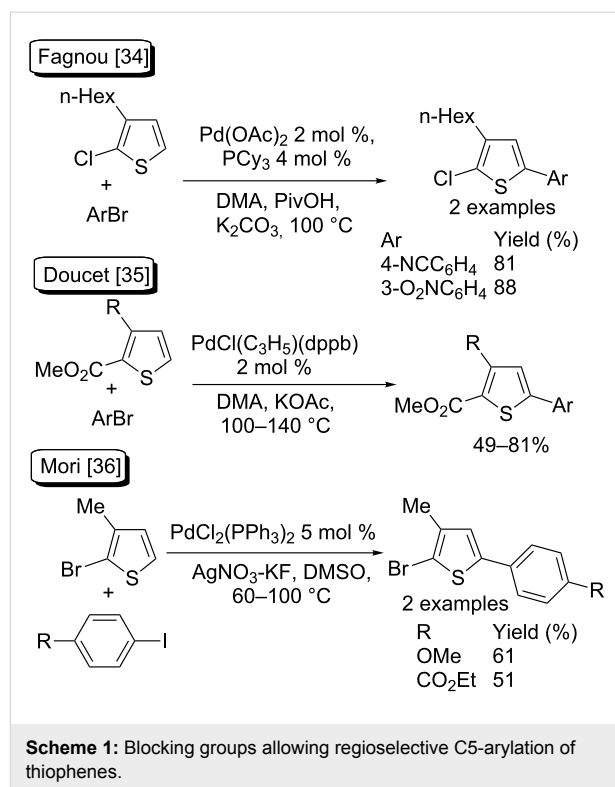
C–Br bond, ii) on the reaction scope using a set of aryl bromides and 2-bromo-3-substituted thiophenes, iii) conditions allowing either the sequential C5-arylation followed by C2-arylation or C2-heteroarylation followed by C5-arylation of C3-substituted thiophenes.

Results and Discussion
Based on some of our previous results on Pd-catalysed direct arylation, for this study, DMA and KOAc were selected as the solvent and base [35]. The reaction of 2 equiv of 2-bromothiophene with 1 equiv of 4-bromonitrobenzene using 1 mol % of phosphine-free Pd(OAc)$_2$ catalyst performed at 110 °C, only afforded the desired product **1** in a trace amount, but a complete conversion of 2-bromothiophene was observed, revealing the high reactivity of the thienyl C–Br bond under these conditions (Table 1, entry 1). Using a lower reaction temperature of 80 °C, and a reaction time of 15 h, the desired C5-arylated product **1** was formed in only 8% yield due again to the formation of several degradation products (Table 1, entry 2). Then, we examined the influence of the reaction time. After 2 or 4 h, higher yields of **1** (55% and 48%) were obtained, respectively; whereas, a very short reaction time of 0.5 h led to a lower yield of 27% due to the poor conversion of 4-bromonitrobenzene (Table 1, entries 3–6). The use of 0.5 mol % Pd(OAc)$_2$ catalyst at 80 °C during 2 h also afforded **1** in a lower yield of 35%. Again, a large amount of 4-bromonitrobenzene was recovered (Table 1, entry 7). When CsOAc, NaOAc or K$_2$CO$_3$ were em-

ployed as bases instead of KOAc, in the presence of 1 mol % Pd(OAc)$_2$ catalyst during 2 h, a partial conversion of 4-bromonitrobenzene was observed and **1** was isolated in 32–40% yield (Table 1, entries 8–10). It should be noted that in the presence of cyclopentyl methyl ether or diethyl carbonate as solvents, no formation of **1** was observed, and 4-bromonitrobenzene was recovered unreacted (Table 1, entries 11 and 12).

Table 1: Influence of the reaction conditions for the palladium-catalysed direct C5-arylation of 2-bromothiophene with 4-bromonitrobenzene.[a]


Entry	Pd(OAc)$_2$ (mol %)	Base	Temp (°C)	Time (h)	Yield in **1** (%)
1	1	KOAc	110	15	trace
2	1	KOAc	80	15	8
3	1	KOAc	80	4	48
4	1	KOAc	80	2	55
5	1	KOAc	80	1	42
6	1	KOAc	80	0.5	27
7	0.5	KOAc	80	2	35
8	1	CsOAc	80	2	35
9	1	NaOAc	80	2	32
10	1	K$_2$CO$_3$	80	2	40
11	1	KOAc	80	2	0[b]
12	1	KOAc	80	2	0[c]

[a]Conditions: Pd(OAc)$_2$, 2-bromothiophene (2 equiv), 4-bromonitrobenzene (1 equiv), base (2 equiv), DMA, isolated yields. [b]Cyclopentyl methyl ether as solvent. [c]Diethyl carbonate as solvent.

Then, we studied the scope of this reaction using a set of aryl bromides and 2-bromothiophene derivatives, employing the most effective reaction conditions for C5-arylation of 2-bromothiophene (Table 1, entry 4: 1 mol % Pd(OAc)$_2$, DMA,

KOAc, 80 °C, 2 h) (Schemes 2–4). First, we investigated the reaction of 2-bromothiophene with 4-bromobenzonitrile, 4-bromobenzaldehyde and 4-bromo-2-(trifluoromethyl)-nitrobenzene (Scheme 2). The expected coupling products **2–4** were obtained in moderate yields. On the other hand, with 4-bromoanisole as an electron-rich aryl bromide, the desired C5-arylated 2-bromothiophene could not be detected by GC–MS analysis of the crude mixture, and a large amount of unreacted 4-bromoanisole was recovered. Under these reaction conditions, the oxidative addition of 4-bromoanisole to palladium appears to be slower than the oxidative addition of 2-bromothiophene. Therefore, this procedure is limited to the use of electron-deficient aryl bromides. The reactivity of 2-bromofuran with 4-bromonitrobenzene was also investigated. Under the same reaction conditions, (1 mol % Pd(OAc)$_2$, DMA, KOAc, 80 °C, 2 h) no formation of the desired 2-bromo-5-aryl-furan derivative was observed.

The main interest to tolerate a C–Br bond at the C2-position on thiophene derivatives in the course of such couplings would be the regiospecific access to C5-arylated 3-substituted thiophenes, which cannot be obtained from 2-unsubstituted 3-substituted thiophenes such as 3-methylthiophene. Therefore, a set of aryl bromides was reacted with 2-bromo-3-methylthiophene, under these conditions (Scheme 3). Its reaction with aryl bromides *para*-substituted by nitro, cyano or formyl substituents gave the desired 5-arylated thiophenes **5–7** in 60–64% yields, without cleavage of the thienyl C–Br bond. Good yields of products **8** and **9** were also obtained from the *meta*-substituted aryl bromides, 3-bromobenzonitrile and 3-bromonitrobenzene. Again, a high yield of 85% of **10** was obtained with 4-bromo-2-(tri-fluoromethyl)nitrobenzene. Then, the reactivity of a set of *ortho*-substituted aryl bromides was examined. Bromobenzene containing nitro, nitrile or formyl *ortho*-substituents afforded the C5-arylated thiophenes **11–13** in 71–84% yields. Finally, 3-bromoquinoline and 3-bromopyrimidine were reacted with 2-bromo-3-methylthiophene affording **14** and **15** in 63% and 66% yields, respectively. The higher yields obtained for the arylation of 2-bromo-3-methylthiophene than with 2-bromo-
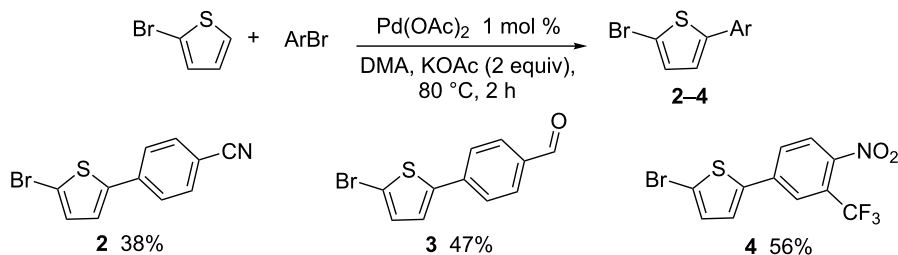
Scheme 2: Reactivity of 2-bromothiophene with aryl bromides.
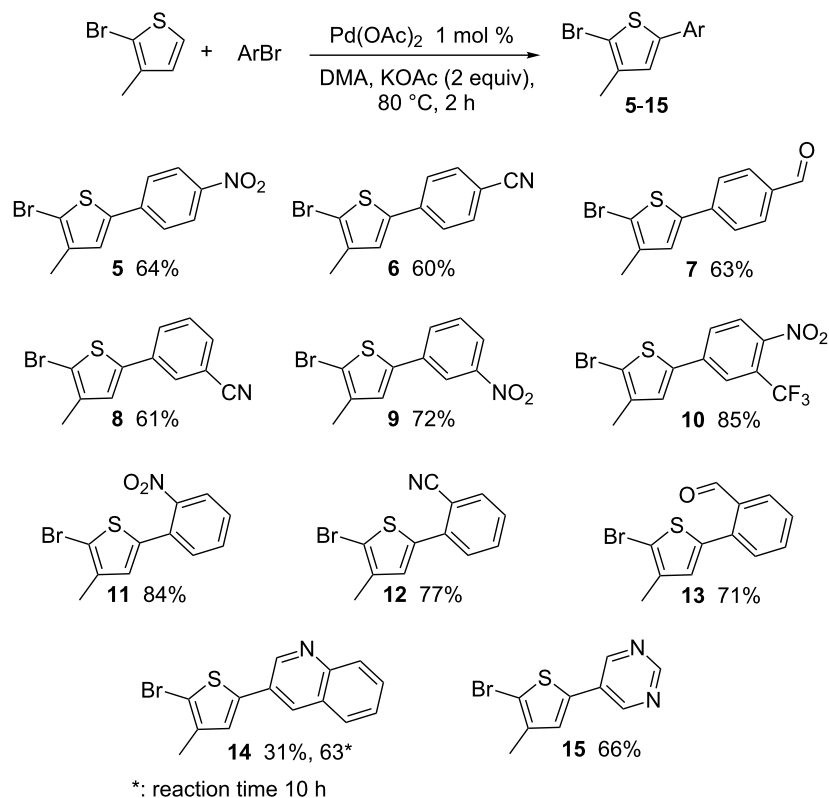
Scheme 3: Reactivity of 2-bromo-3-methylthiophene with (hetero)aryl bromides.
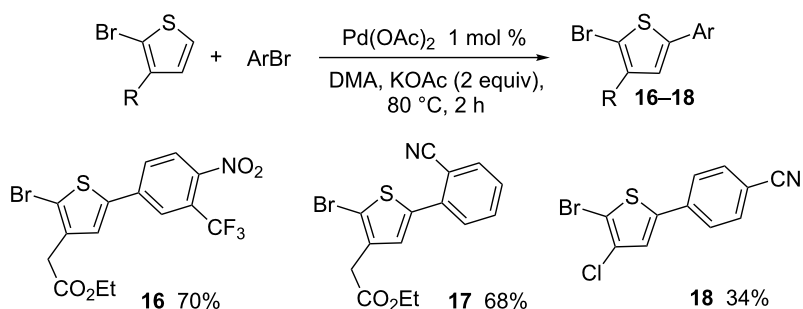

Scheme 4: Reactivity of 3-substituted 2-bromothiophenes with aryl bromides.

thiophene are probably due to a slower oxidative addition of 2-bromo-3-methylthiophene to palladium which reduces the formation of side-products.

The reaction is not limited to the use of 2-bromo-3-methylthiophene. A 2-bromothiophene derivative bearing a CH_2CO_2Et substituent at C3 also provides regioselectively the desired C5-arylated thiophenes **16** and **17** in good yields; whereas, a lower yield of **18** was obtained for the coupling of 2-bromo-3-chlorothiophene with 4-bromobenzonitrile (Scheme 4).

Then, to demonstrate the synthetic potential of the thienyl bromo-substituent, product **1** was coupled with 2-methylthiophene in the presence of 1 mol % $Pd(OAc)_2$ catalyst and KOAc as base (Scheme 5). The desired product **19** was obtained in 71% yield. Under the same conditions, a high yield of 91% in **20** was obtained from **2** and 2-methyl-4-ethylthiazole. These two reactions demonstrate that the sequential Pd-catalysed direct di-(hetero)arylation, using 2-bromothiophene as central unit, provides a powerful and simple access to non-symmetrically 2,5-di(hetero)arylated thiophene derivatives.
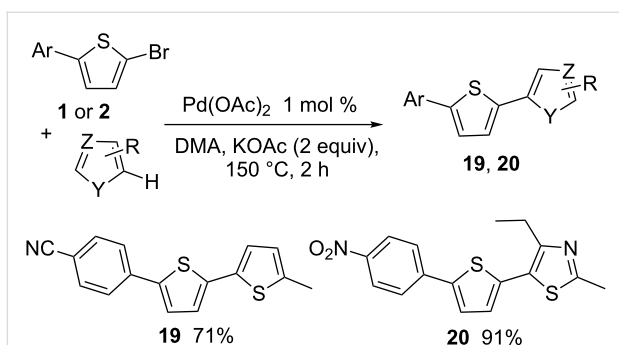
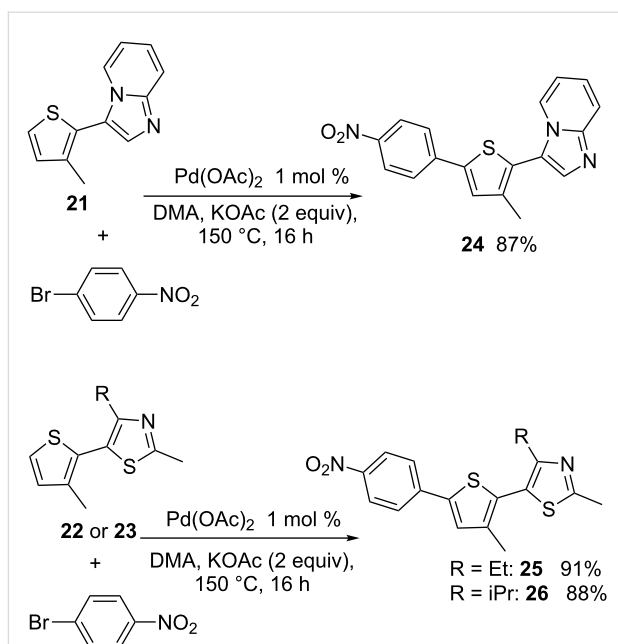**Scheme 5:** 5-Heteroarylation of 2-aryl-5-bromothiophenes.

3-Substituted thiophene derivatives containing a heteroaryl unit at the C2-position and an aryl at C5 can also be obtained by direct heteroarylation at the C2-position of the C3-substituted 2-bromothiophene, followed by direct arylation at C5 (Scheme 6 and Scheme 7). First, we introduced imidazopyridinyl or thiazolyl groups at C2-position of 2-bromo-3-methylthiophene. In the presence of 1 mol % Pd(OAc)$_2$ and KOAc as base at 150 °C the products **21**–**23** were obtained in 70–88% yields. In all cases, no C2-arylation of the 2-bromo-3-methylthiophene with itself to produce 5'-bromo-3,4'-dimethyl-2,2'-bithiophene was observed.
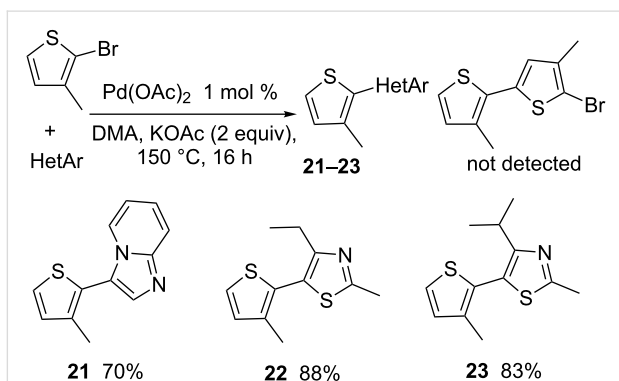

Scheme 6: 2-Heteroarylation of 2-bromo-3-methylthiophene.

Then, from the C2-heteroarylated 3-methylthiophenes **21**–**23**, a second direct arylation at position C5 allows to prepare the products **24**–**26** in 87–91% yields (Scheme 7).

The synthesis of 3-substituted thiophenes derivatives containing two different aryl groups at C2 and C5 positions via Suzuki coupling in the second step was also attempted (Scheme 8). The reaction of **5** with phenylboronic acid in the presence of only 1 mol % Pd(OAc)$_2$ catalyst and K$_2$CO$_3$ as base gave 3-methyl-5-(4-nitrophenyl)-2-phenylthiophene (**27**) in 60% yield. A higher yield of 80% in **28** was obtained for the coupling of **16** with phenylboronic acid.

Scheme 7: 5-Arylation of 2,3-disubstituted thiophenes.
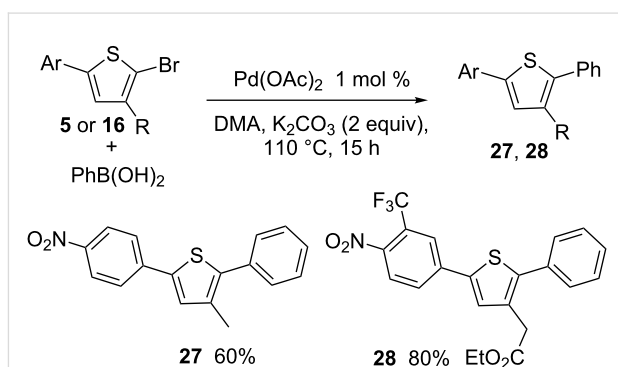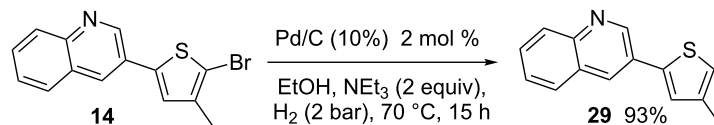

Scheme 8: 5-Arylation of 2-aryl-5-bromothiophenes.

In order to further demonstrate that a bromo-substituent at C2-position of the thiophenes can be considered as a protecting group, we removed it via palladium-catalysed hydrogenolysis (Scheme 9). Treatment of **14** with 2 mol % Pd/C (10%) and trimethylamine in ethanol under hydrogen pressure, gave the desired debrominated product **29** in almost quantitative yield.

Conclusion

In summary, we report here that the use of a 2-bromo-substituent on thiophenes acts as a blocking group, allowing their regioselective Pd-catalysed C5-arylation even in the presence of aryl bromides as aryl sources. Only 1 mol % of phosphine-free air stable Pd(OAc)$_2$ catalyst in the presence of KOAc as base promotes the C5-arylation of 2-bromothiophenes containing various C3-substituents with electron-deficient (hetero)aryl bro-

Scheme 9: Deprotection of 2-aryl-5-bromothiophene **14**.

mides. The sequential direct C5-arylation of 2-bromothiophenes followed either by a Suzuki coupling or a second direct arylation was found to allow the preparation of 2,5-di(hetero)arylated thiophenes bearing two different (hetero)aryl units. This method provides a convenient "greener" access to arylated thiophene derivatives as 1) it reduces the number of steps to prepare these compounds, 2) it employs the easily available Pd(OAc)$_2$ catalyst and aryl bromides as aryl sources, and the inexpensive base KOAc, 3) it reduces the formation of wastes.

Supporting Information

Supporting Information File 1
Procedures, ^{1}H and ^{13}C NMR data of all compounds.
[http://www.beilstein-journals.org/bjoc/content/supplementary/1860-5397-12-210-S1.pdf]

Acknowledgments

References

1. Crouch, D. J.; Skabara, P. J.; Lohr, J. E.; McDouall, J. J. W.; Heeney, M.; McCulloch, I.; Sparrowe, D.; Shkunov, M.; Coles, S. J.; Horton, P. N.; Hursthouse, M. B. *Chem. Mater.* **2005,** *17,* 6567–6578. doi:10.1021/cm051563i

2. Li, J.; Qiao, X.; Xiong, Y.; Li, H.; Zhu, D. *Chem. Mater.* **2014,** *26,* 5782–5788. doi:10.1021/cm502952u

3. Kim, H. G.; Kang, B.; Ko, H.; Lee, J.; Shin, J.; Cho, K. *Chem. Mater.* **2015,** *27,* 829–838. doi:10.1021/cm503864u

4. Li, C.-J.; Trost, B. M. *Proc. Natl. Acad. Sci. U. S. A.* **2008,** *105,* 13197–13202. doi:10.1073/pnas.0804348105

5. Li, J. J.; Gribble, G. W. *Palladium in Heterocyclic Chemistry;* Pergamon: Amsterdam, 2000.

6. *Handbook of Organopalladium Chemistry for Organic Synthesis;* Negishi, E., Ed.; Part III; Wiley-Interscience: New York, 2002; pp 213 ff.

7. Ackermann, L. In *Modern arylation methods;* Ackermann, L., Ed.; Wiley Online Library, 2009.

8. Brodnik, H.; Požgan, F.; Štefane, B. *Org. Biomol. Chem.* **2016,** *14,* 1969–1981. doi:10.1039/C5OB02364E

9. Tùng, Đ. T.; Tuân, Đ. T.; Rasool, N.; Villinger, A.; Reinke, H.; Fischer, C.; Langer, P. *Adv. Synth. Catal.* **2009,** *351,* 1595–1609. doi:10.1002/adsc.200900044

10. Toguem, S.-M. T.; Villinger, A.; Langer, P. *Synlett* **2010,** 909–912. doi:10.1055/s-0029-1219380

11. Hayashi, S.; Koizumi, T. *Angew. Chem., Int. Ed.* **2016,** *55,* 2701–2704. doi:10.1002/anie.201509319

12. Hung, W.-I.; Liao, Y.-Y.; Lee, T.-H.; Ting, Y.-C.; Ni, J.-S.; Kao, W.-S.; Lin, J. T.; Wei, T.-C.; Yen, Y.-S. *Chem. Commun.* **2015,** *51,* 2152–2155. doi:10.1039/C4CC09294E

13. Lincker, F.; Attias, A.-J.; Mathevet, F.; Heinrich, B.; Donnio, B.; Fave, J.-L.; Rannou, P.; Demadrille, R. *Chem. Commun.* **2012,** *48,* 3209–3211. doi:10.1039/c2cc17276c

14. Pei, J.; Ni, J.; Zhou, X.-H.; Cao, X.-Y.; Lai, Y.-H. *J. Org. Chem.* **2002,** *67,* 4924–4936. doi:10.1021/jo011146z

15. Ohta, A.; Akita, Y.; Ohkuwa, T.; Chiba, M.; Fukunaga, R.; Miyafuji, A.; Nakata, T.; Tani, N.; Aoyagi, Y. *Heterocycles* **1990,** *31,* 1951–1958. doi:10.3987/COM-90-5467

16. Aoyagi, Y.; Inoue, A.; Koizumi, I.; Hashimoto, R.; Tokunaga, K.; Gohma, K.; Komatsu, J.; Sekine, K.; Miyafuji, A.; Kunoh, J.; Honma, R.; Akita, Y.; Ohta, A. *Heterocycles* **1992,** *33,* 257–272. doi:10.3987/COM-91-S29

17. Li, B.-J.; Yang, S.-D.; Shi, Z.-J. *Synlett* **2008,** 949–957. doi:10.1055/s-2008-1042907

18. Roger, J.; Gottumukkala, A. L.; Doucet, H. *ChemCatChem* **2010,** *2,* 20–40. doi:10.1002/cctc.200900074

19. Ackermann, L.; Vincente, R.; Kapdi, A. R. *Angew. Chem., Int. Ed.* **2009,** *48,* 9792–9826. doi:10.1002/anie.200902996

20. Bellina, F.; Rossi, R. *Tetrahedron* **2009,** *65,* 10269–10310. doi:10.1016/j.tet.2009.10.015

21. Wencel-Delord, J.; Glorius, F. *Nat. Chem.* **2013,** *5,* 369–375. doi:10.1038/nchem.1607

22. Kuzhushkov, S. I.; Potukuchi, H. K.; Ackermann, L. *Catal. Sci. Technol.* **2013,** *3,* 562–571. doi:10.1039/C2CY20505J

23. Rossi, R.; Bellina, F.; Lessi, M.; Manzini, C. *Adv. Synth. Catal.* **2014,** *356,* 17–117. doi:10.1002/adsc.201300922

24. Yadav, M. R.; Rit, R. K.; Shankar, M.; Sahoo, A. K. *Asian J. Org. Chem.* **2015,** *4,* 846–864. doi:10.1002/ajoc.201500105

25. Bheeter, C. B.; Chen, L.; Soulé, J.-F.; Doucet, H. *Catal. Sci. Technol.* **2016,** *6,* 2005–2049. doi:10.1039/C5CY02095F

26. Lavenot, L.; Gozzi, C.; Ilg, K.; Orlova, I.; Penalva, V.; Lemaire, M. *J. Organomet. Chem.* **1998,** *567,* 49–55. doi:10.1016/S0022-328X(98)00667-6

27. Glover, B.; Harvey, K. A.; Liu, B.; Sharp, M. J.; Tymoschenko, M. F. *Org. Lett.* **2003,** *5,* 301–304. doi:10.1021/ol027266q

28. Dong, J. J.; Roy, D.; Jacob Roy, R.; Ionita, M.; Doucet, H. *Synthesis* **2011,** 3530–3546. doi:10.1055/s-0030-1260213

29. Chen, L.; Bruneau, C.; Dixneuf, P. H.; Doucet, H. *Tetrahedron* **2013,** *69,* 4381–4388. doi:10.1016/j.tet.2012.12.061

30. Rene, O.; Fagnou, K. *Org. Lett.* **2010,** *12,* 2116–2119.
doi:10.1021/ol1006136

31. Dong, J. J.; Doucet, H. *Eur. J. Org. Chem.* **2010,** 611–615.
doi:10.1002/ejoc.200901213

32. Forgione, P.; Brochu, M.-C.; St-Onge, M.; Thesen, K. H.; Bailey, M. D.;
Bilodeau, F. *J. Am. Chem. Soc.* **2006,** *128,* 11350–11351.
doi:10.1021/ja063511f

33. Borghese, A.; Geldhof, G.; Antoine, L. *Tetrahedron Lett.* **2006,** *47,*
9249–9252. doi:10.1016/j.tetlet.2006.10.130

34. Liégault, B.; Petrov, I.; Gorlesky, S. I.; Fagnou, K. *J. Org. Chem.* **2010,**
75, 1047–1060. doi:10.1021/jo902515z

35. Chen, L.; Bruneau, C.; Dixneuf, P. H.; Doucet, H. *Green Chem.* **2012,**
14, 1111–1124. doi:10.1039/c2gc16460d

36. Kobayashi, K.; Sugie, A.; Takahashi, M.; Masui, K.; Mori, A. *Org. Lett.*
2005, *7,* 5083–5085. doi:10.1021/ol052063y

Stereoselective synthesis of fused tetrahydroquinazolines through one-pot double [3 + 2] dipolar cycloadditions followed by [5 + 1] annulation

Xiaofeng Zhang[1], Kenny Pham[1], Shuai Liu[1], Marc Legris[1], Alex Muthengi[1], Jerry P. Jasinski[2] and Wei Zhang[*1]

Abstract

The one-pot [3 + 2] cycloaddition of an azomethine ylide with a maleimide followed by another [3 + 2] cycloaddition of an azide with the second maleimide gives a 1,5-diamino intermediate which is used for a sequential aminomethylation reaction with formaldehyde through [5 + 1] annulation to afford a novel polycyclic scaffold bearing tetrahydroquinazoline, pyrrolidine, pyrrolidinedione, and *N*-substituted maleimide in stereoselective fashion.

Introduction

The synthesis of new molecules with potential biological activity through pot, atom and step-economic (PASE) reactions is an attractive green organic technique [1-5]. By the combination of multicomponent reactions (MCR) [6-11] with stepwise one-pot reactions [12-17], our lab has introduced a series of synthetic methods for heterocyclic compounds **I–VI** bearing heterocyclic rings such as hydantoin, pyrrolidine, pyrrolidinedione, piperazinedione, and dihydrobenzodiazepinedione (Scheme 1) [4,18-21]. All these scaffolds were prepared using one-pot intermo-

lecular or intramolecular [3 + 2] azomethine ylide cycloadditions [22-27] as the initial step followed by cyclization or cycloaddition reactions to form polycyclic scaffolds with skeleton, substitution, and stereochemistry diversities. Introduced in this paper is a new sequence initiated with a three-component [3 + 2] cycloaddition for preparing polycyclic scaffold **1** bearing tetrahydroquinazoline, pyrrolidine, pyrrolidinedione, and *N*-substituted maleimide rings. Those heterocyclic fragments could be found in bioactive compounds such as bromodomain,

Scheme 1: Polycyclic scaffolds derived from [3 + 2] adducts **2**.
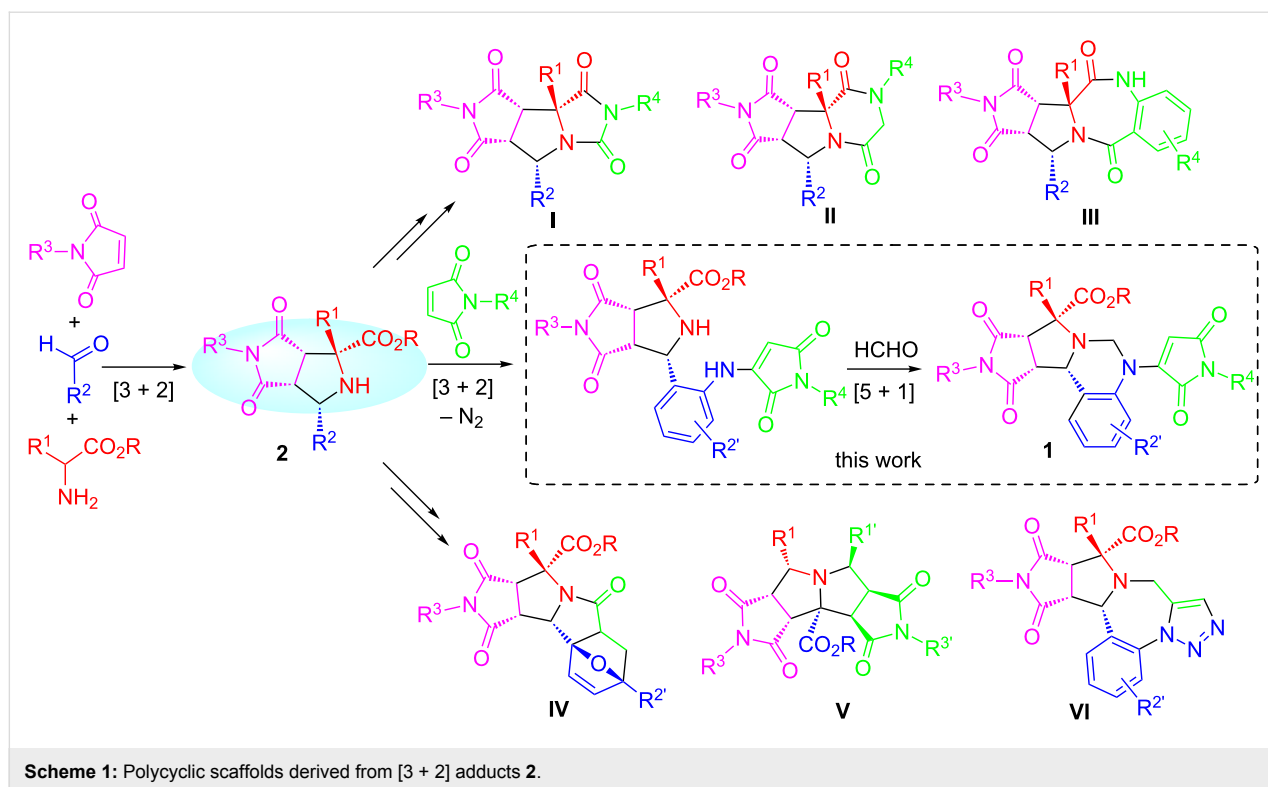
thrombin, potassium channel, mPGES-1, and tubulin inhibitors, as well as the immunomodulatory drug thalidomide [28-32] (Figure 1).

Results and Discussion

Our initial effort was focused on the development of reaction conditions for the one-pot double [3 + 2] cycloadditions. The first [3 + 2] cycloaddition of azomethine ylide was carried out using glycine methyl ester (**3a**), 2-azidobenzaldehyde (**4a**), and *N*-methylmaleimide (**5a**) as reactants [33]. After exploring the reactions with different temperatures, times, solvents, and bases, it was found that with a 1.2:1.1:1.0 ratio of **3a**:**4a**:**5a**, Et₃N as a base, and MeCN as a solvent, the three-component reaction for **2a** was completed under microwave heating at 115 °C for 25 min. Without work-up, the reaction mixture was directly reacted with 1.0 equiv of *N*-benzylmaleimide (**6a**)

Figure 1: Heterocyclic fragments in bioactive compounds.
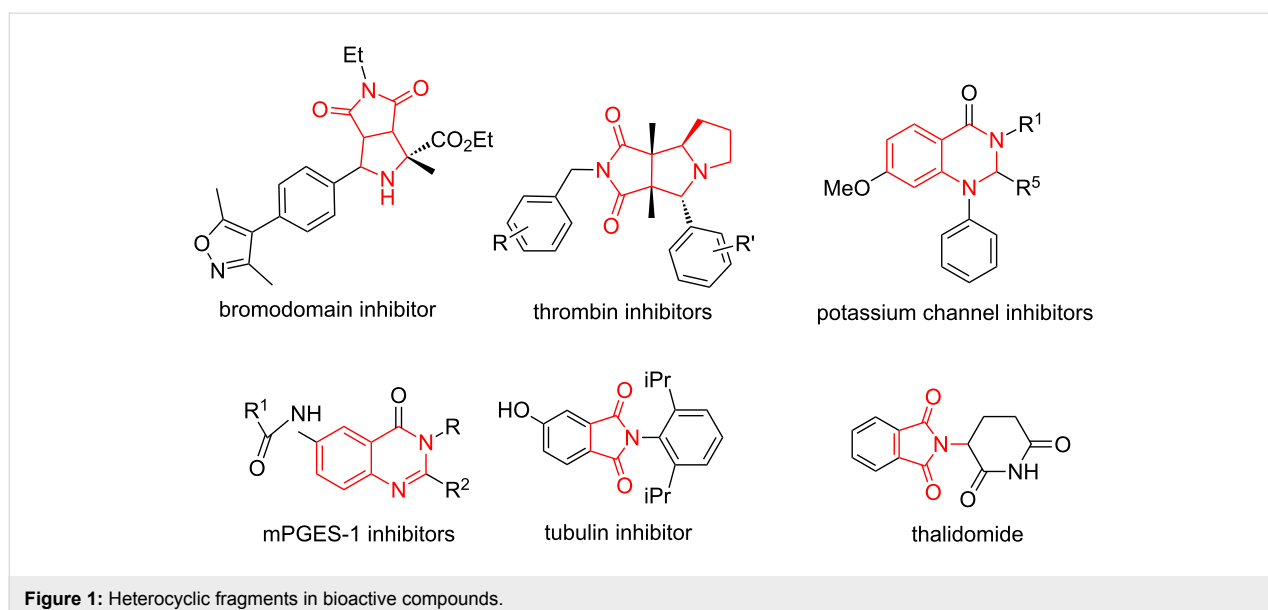
under microwave heating at 125 °C for 25 min to give **7a** as a major diastereomer of a denitrogenation compound in 74% LC yield with a 39:1 dr (Table 1, entry 5). The diastereomer **7a** was isolated in 65% yield by preparative chromatography. The stereochemistry of the final product was established during the first [3 + 2] cycloaddition of the azomethine ylide which has been well reported in literature [22-27].

We next explored the reaction scope of the one-pot double [3 + 2] reactions under the optimized conditions by using different sets of building blocks of **3**, **4**, **5**, and **6** to afford analogs **7a–p** in 21–73% isolated yields as single diastereomers (Figure 2). Compound **7b** was an exception, which was obtained in a trace amount. It was found that replacing maleimides **6** with other activated alkenes such as dimethyl maleate, benzoquinone, naphthalene-1,4-dione, and maleonitrile failed to afford products **7q–t,** probably due to unfavorable stereoelectronic effects associated with these substrates.

The stereochemistry of **7h** has been determined by X-ray single crystal structure analysis (Figure 3). As mentioned previously,

the stereoselectivity of the first [3 + 2] cycloaddition for compounds **2** has been well reported [22-27]. The mechanism for the second [3 + 2] cycloaddition of azide compounds **2** with maleimides and sequential denitrogenation to products **7** is proposed in Scheme 2.

1,5-Diamino compounds **7** generated by one-pot reactions are good substrates for [5 + 1] annulation with aldehydes to form tetrahydroquinazolines **1** [34,35]. After exploring the reaction conditions, it was found that the reaction of **7a** with formaldehyde in 1,4-dioxane at 110 °C afforded product **1a** in 93% isolated yield (Table 2, entry 3). Other reactants such as HC(OEt)$_3$, HCO$_2$H, and paraformaldehyde (PFA) were also employed for the [5 + 1] annulation reactions. But only formaldehyde afforded tetrahydroquinazoline **1a** in good yield under catalyst-free conditions. A number of [5 + 1] annulation reactions using selected compounds **7** were carried out to afford 10 analogs of tetrahydroquinazolines **1** in 88–95% isolated yields as single diastereomers (Figure 4). In addition to formaldehyde, other aldehydes could also be used for the [5 + 1] annulation according to literature [34,35].

Table 1: One-pot double [3 + 2] cycloaddition for **7a**[a].
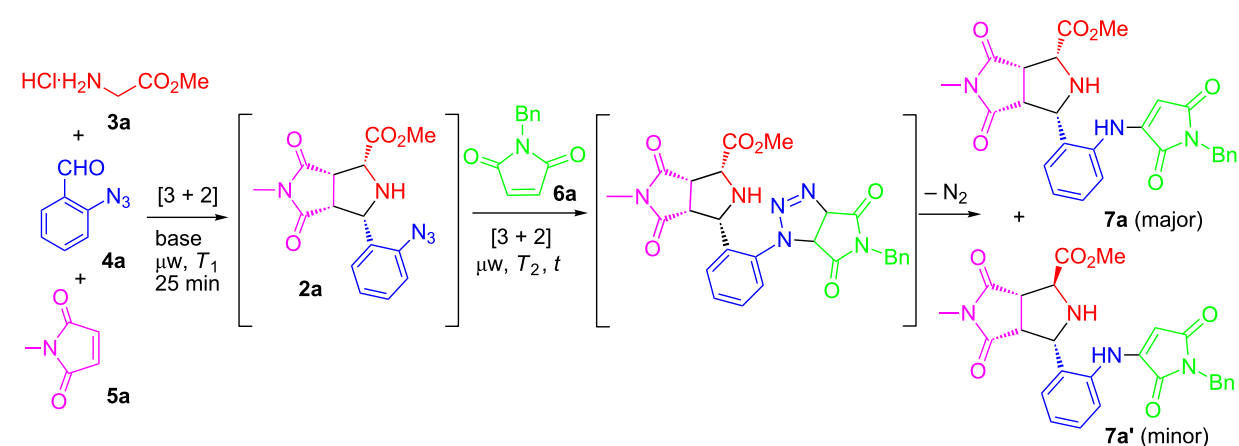
entry	T_1 (°C)	solvent	base (2 equiv)	T_2 (°C)	t (min)	7a (%)[b]	dr
1	150	toluene	Et$_3$N	150	25	65	40:1
2	125	dioxane	Et$_3$N	125	25	33	15:1
3	115	EtOH	Et$_3$N	115	25	45	21:1
4	115	CH$_3$CN	Et$_3$N	115	25	70	30:1
5	**115**	**CH$_3$CN**	**Et$_3$N**	**125**	**25**	**74 (65)[c]**	**39:1**
6	115	CH$_3$CN	K$_2$CO$_3$	125	25	51	9:1
7	115	CH$_3$CN	DBU	125	25	60	29:1
8	115	CH$_3$CN	DIPEA	125	25	72	38:1
9	115	CH$_3$CN	Et$_3$N	125	10	63	35:1
10	115	CH$_3$CN	Et$_3$N	125	50	72	39:1
11	115	CH$_3$CN	Et$_3$N	150	25	68	41:1

[a]1.2:1.1:1.0:1.0 of **3a:4a:5a:6a**; [b]detected by LC; [c]isolated yield.
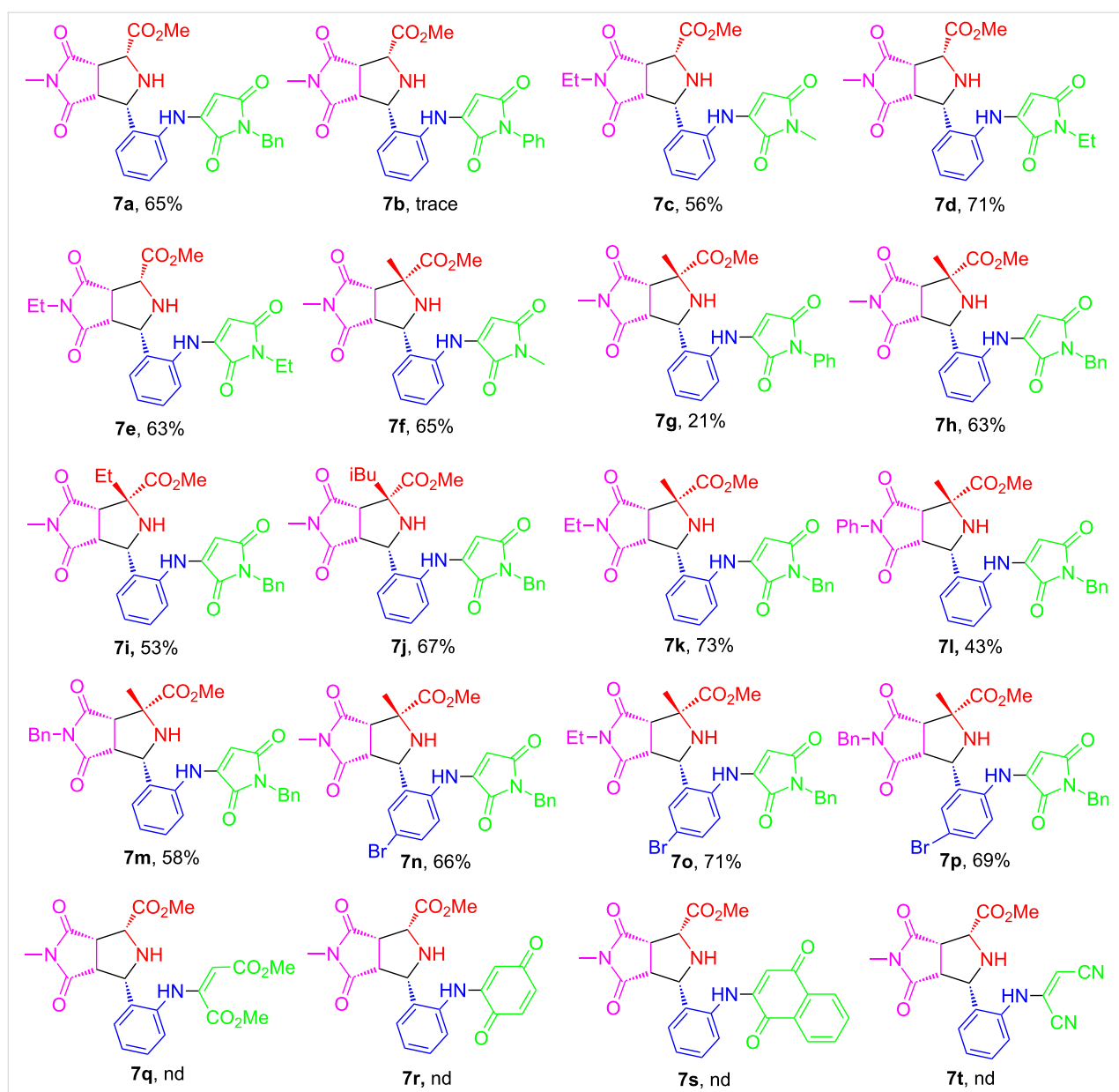
Figure 2: One-pot double [3 + 2] cycloadditions and denitrogenation for product **7** under the optimized reaction conditions, see Table 1, entry 5. nd = not detected.

Conclusion

A one-pot reaction sequence involving [3 + 2] cycloaddition of azomethine ylides, [3 + 2] cycloaddition of azides with alkenes, and denitrogenation followed by a [5 + 1] anulation has been developed for the synthesis of fused-tetrahydroquinazolines as single diastereomers. The formation of triazoles from the second [3 + 2] cycloaddition readily affords denitrogenated 1,5-diamino compounds which are good substrates for aminomethylation with formaldehyde through a [5 + 1] annulation. The final products have a unique polycyclic skeleton containing tetrahydroquinazoline, pyrrolidine, pyrrolidinedione, and *N*-substituted maleimide ring systems.

Experimental
General Information

Chemicals and solvents were purchased from commercial suppliers and used as received. ^{1}H NMR (300 or 400 MHz) and ^{13}C NMR spectra (75 or 101 MHz) were recorded on Agilent NMR spectrometers. Chemical shifts were reported in parts per million (ppm), and the residual solvent peak was used as an internal reference: proton (chloroform δ 7.26; dioxane δ 3.71; H$_2$O δ 1.56), carbon (chloroform δ 77.0). Multiplicity was indicated as follows: s (singlet), d (doublet), t (triplet), q (quartet), m (multiplet), dd (doublet of doublet), br s (broad singlet). Coupling constants were reported in hertz (Hz). LC–MS was per-
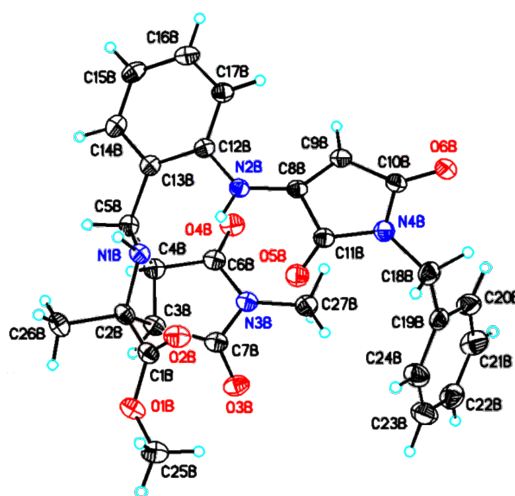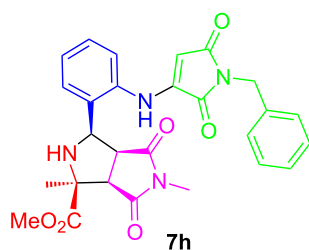
Figure 3: X-ray structure of **7h**.
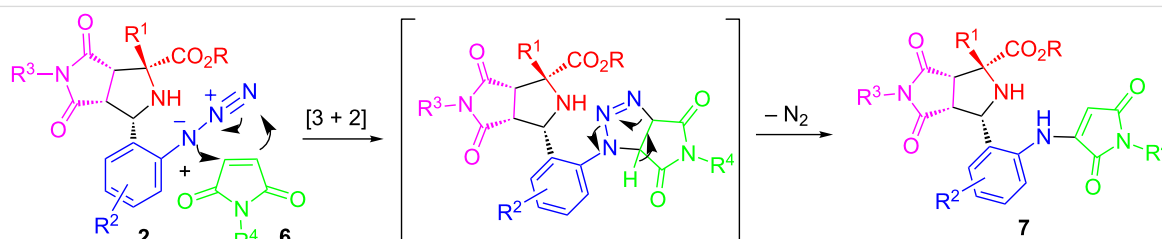
Scheme 2: Proposed mechanism for the 2nd [3 + 2] cycloaddition and denitrogenation.

Table 2: Optimization of [5 + 1] annulation for product **1a**[a].
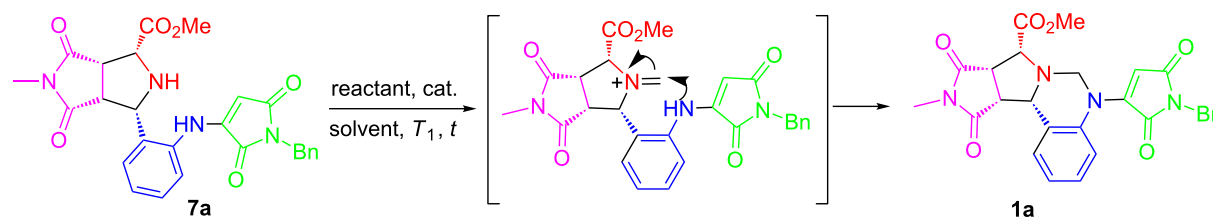
entry	reactant (equiv)	catalyst (equiv)	solvent	T_1 (°C)	t (h)	**1a** (%)[a]
1	HC(OEt)$_3$ (1.5)	NH$_4$Cl (2.0)	H$_2$O	100	3	51
2	HCO$_2$H (3.0)	–	H$_2$O	100	5	nd[b]
3	**HCHO (3.0)**	**–**	**1,4-dioxane**	**110**	**3**	**93**
4	PFA (2.0)	TFA (3.0)	1,4-dioxane	110	4	73

[a]Isolated yield; [b]nd = not detected.

formed on an Agilent 2100 LC with a 6130 quadrupole MS spectrometer. A C18 column (5.0 μm, 6.0 × 50 mm) was employed for the separation. The mobile phases were MeOH and H$_2$O both of which contained 0.05% CF$_3$CO$_2$H. A linear gradient from 25:75 (v/v) MeOH/water to 100% MeOH over 7.0 min at a flow rate of 0.7 mL/min was employed as a mobile phase. UV detections were conducted at 210 nm, 254 nm and 365 nm. Low resolution mass spectra were recorded with APCI (atmospheric pressure chemical ionization). The final products were purified on Angela HP-100 pre-LC system with a Venusil PrepG C18 column (10 μm, 120 Å, 21.2 mm × 250 mm).
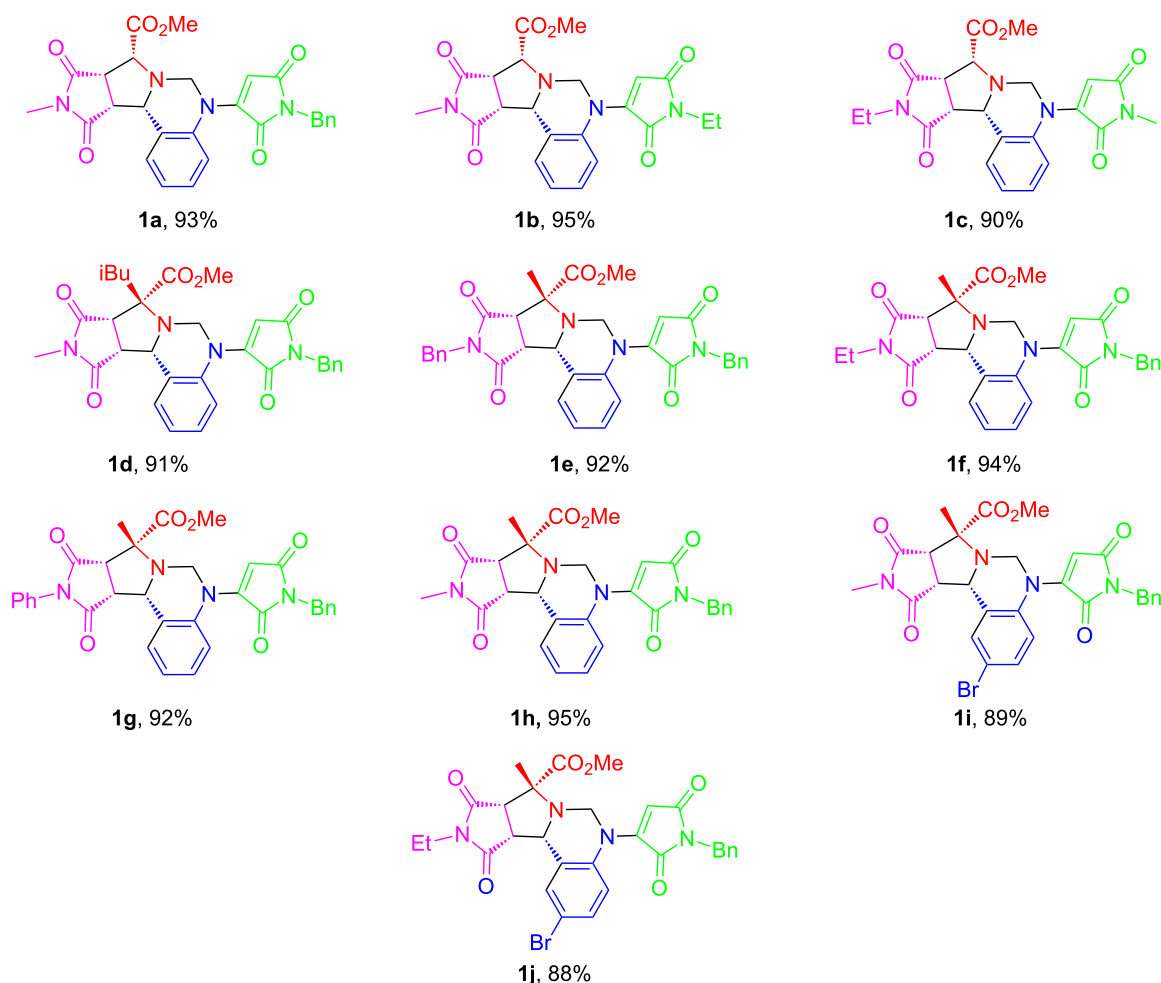
Figure 4: [5 + 1] Annulation for tetrahydroquinazolines **1**.

General procedure for the one-pot synthesis of compounds 7

The following procedure is analogous to one of our previous procedures [4]. To a solution of an amino ester **3** (1.2 mmol), 2-azidobenzaldehyde (**4**, 1.1 mmol), and maleimide **5** (1.0 mmol) in 2.0 mL of CH_3CN was added Et_3N (2.0 mmol). After being stirred at 25 °C for 5 min, the reaction mixture was heated by microwave irradiation at 115 °C for 25 min. Upon the completion of the reaction as monitored by LC–MS, maleimide **6** (1.0 mmol) was added to the reaction mixture and then heated by microwave irradiation at 125 °C for 25 min. The concentrated reaction mixture was isolated on a semi-preparative HPLC with a C18 column to afford purified product **7** as a single diastereomer.

General procedure for [5 + 1] annulation for the synthesis of products 1

To a solution of compound **7** (0.5 mmol), in 1.0 mL of 1,4-dioxane was added formaldehyde solution (16% in H_2O,

1.5 mmol). The reaction mixture was heated at 110 °C for 3 h. Upon the completion of the reaction as monitored by LC–MS, the reaction mixture was concentrated and then isolated on a semi-preparative HPLC with a C18 column to afford purified product **1**.

Supporting Information

Supporting Information File 1
Compound characterization data, X-ray report, and copies of NMR spectra.
[http://www.beilstein-journals.org/bjoc/content/supplementary/1860-5397-12-211-S1.pdf]

References

1. Clarke, P. A.; Santos, S.; Martin, W. H. C. *Green Chem.* **2007,** *9,* 438–440. doi:10.1039/B700923B

2. Bhuyan, D.; Sarma, R.; Dommaraju, Y.; Prajapati, D. *Green Chem.* **2014,** *16,* 1158–1162. doi:10.1039/C3GC42389A

3. Prasanna, P.; Perumal, S.; Menéndez, J. C. *Green Chem.* **2013,** *15,* 1292–1299. doi:10.1039/C3GC37128J

4. Zhang, X.; Zhi, S.; Wang, W.; Liu, S.; Jasinski, J. P.; Zhang, W. *Green Chem.* **2016,** *18,* 2642–2646. doi:10.1039/C6GC00497K

5. Weng, J.; Wang, S.; Huang, L.-J.; Luo, Z.-Y.; Lu, G. *Chem. Commun.* **2015,** *51,* 10170–10173. doi:10.1039/C5CC01077B

6. Cioc, R. C.; Ruijter, E.; Orru, R. V. A. *Green Chem.* **2014,** *16,* 2958–2975. doi:10.1039/C4GC00013G

7. Rotstein, B. H.; Zaretsky, S.; Rai, V.; Yudin, A. K. *Chem. Rev.* **2014,** *114,* 8323–8359. doi:10.1021/cr400615v

8. Estévez, V.; Villacampa, M.; Menéndez, J. C. *Chem. Soc. Rev.* **2014,** *43,* 4633–4657. doi:10.1039/C3CS60015G

9. Dömling, A.; Wang, W.; Wang, K. *Chem. Rev.* **2012,** *112,* 3083–3135. doi:10.1021/cr100233r

10. Brauch, S.; van Berkel, S. S.; Westermann, B. *Chem. Soc. Rev.* **2013,** *42,* 4948–4962. doi:10.1039/C3CS35505E

11. Gu, Y. *Green Chem.* **2012,** *14,* 2091–2128. doi:10.1039/C2GC35635J

12. Anastas, P.; Eghbali, N. *Chem. Soc. Rev.* **2010,** *39,* 301–312. doi:10.1039/B918763B

13. Nicolaou, K. C.; Chen, J. S. *Chem. Soc. Rev.* **2009,** *38,* 2993–3009. doi:10.1039/B903290H

14. Nicolaou, K. C.; Edmonds, D. J.; Bulger, P. G. *Angew. Chem., Int. Ed.* **2006,** *45,* 7134–7186. doi:10.1002/anie.200601872

15. Padwa, A.; Bur, S. K. *Tetrahedron* **2007,** *63,* 5341–5378. doi:10.1016/j.tet.2007.03.158

16. Enders, D.; Grondal, C.; Hüttl, M. R. M. *Angew. Chem., Int. Ed.* **2007,** *46,* 1570–1581. doi:10.1002/anie.200603129

17. Wasilke, J.-C.; Obrey, S. J.; Baker, R. T.; Bazan, G. C. *Chem. Rev.* **2005,** *105,* 1001–1020. doi:10.1021/cr020018n

18. Werner, S.; Nielsen, S. D.; Wipf, P.; Turner, D. M.; Chambers, P. G.; Geib, S. J.; Curran, D. P.; Zhang, W. *J. Comb. Chem.* **2009,** *11,* 452–459. doi:10.1021/cc900003q

19. Zhang, W.; Lu, Y.; Chen, C. H.-T.; Curran, D. P.; Geib, S. *Eur. J. Org. Chem.* **2006,** 2055–2059. doi:10.1002/ejoc.200600077

20. Lu, Q.; Huang, X.; Song, G.; Sun, C.-M.; Jasinski, J. P.; Keeley, A. C.; Zhang, W. *ACS Comb. Sci.* **2013,** *15,* 350–355. doi:10.1021/co400026s

21. Lu, Q.; Song, G.; Jasinski, J. P.; Keeley, A. C.; Zhang, W. *Green Chem.* **2012,** *14,* 3010–3012. doi:10.1039/C2GC36066G

22. Hashimoto, T.; Maruoka, K. *Chem. Rev.* **2015,** *115,* 5366–5412. doi:10.1021/cr5007182

23. Seidel, D. *Acc. Chem. Res.* **2015,** *48,* 317–328. doi:10.1021/ar5003768

24. Coldham, I.; Hufton, R. *Chem. Rev.* **2005,** *105,* 2765–2810. doi:10.1021/cr040004c

25. Pellissier, H. *Tetrahedron* **2007,** *63,* 3235–3285. doi:10.1016/j.tet.2007.01.009

26. Narayan, R.; Potowski, M.; Jia, Z.-J.; Antonchick, A. P.; Waldmann, H. *Acc. Chem. Res.* **2014,** *47,* 1296–1310. doi:10.1021/ar400286b

27. Zhang, W. *Chem. Lett.* **2013,** *42,* 676–681. doi:10.1246/cl.130504

28. Marineau, J. J.; Bradner, J. E.; Zhang, W.; Qi, J.; Mckeown, M. R.; Fu, H.; Liu, S. Inhibitors of transcription factors and uses thereof. WO Patent WO013635 A2, Jan 29, 2015.

29. Olsen, J.; Seiler, P.; Wagner, B.; Fischer, H.; Tschopp, T.; Obst-Sander, U.; Banner, D. W.; Kansy, M.; Müller, K.; Diederich, F. *Org. Biomol. Chem.* **2004,** *2,* 1339–1352. doi:10.1039/B402515F

30. Trotter, B. W.; Isaacs, R. Quinazoline potassium channel inhibitors. WO Patent WO030217 A1, April 7, 2015.

31. Rörsch, F.; la Buscató, E.; Deckmann, K.; Schneider, G.; Schubert-Zsilavecz, M.; Geisslinger, G.; Proschak, E.; Grösch, S. *J. Med. Chem.* **2012,** *55,* 3792–3803. doi:10.1021/jm201687d

32. Rashid, A.; Kuppa, A.; Kunwar, A.; Panda, D. *Biochemistry* **2015,** *54,* 2149–2159. doi:10.1021/bi501429j

33. Zhang, W.; Lu, Y.; Geib, S. *Org. Lett.* **2005,** *7,* 2269–2272. doi:10.1021/ol0507773

34. Korshin, E. E.; Sabirova, L. A.; Levinb, Y. A. *Synthesis* **2012,** *44,* 3512–3522. doi:10.1055/s-0032-1316802

35. Göblyös, A.; Lázár, L.; Fülöp, F. *Tetrahedron* **2002,** *58,* 1011–1016. doi:10.1016/S0040-4020(01)01196-6

License and Terms

Tunable microwave-assisted method for the solvent-free and catalyst-free peracetylation of natural products

Manuela Oliverio[*1,2], Paola Costanzo[1], Monica Nardi[3], Carla Calandruccio[1], Raffaele Salerno[2] and Antonio Procopio[1,2]

Full Research Paper

Address:
[1]Department of Health Science, University Magna Graecia of Catanzaro, Viale Europa, Loc. Germaneto, 88100 Catanzaro, Italy, [2]InterRegional Center for Food Safety and Health, University Magna Graecia of Catanzaro, Viale Europa, Loc. Germaneto, 88100 Catanzaro, Italy and [3]Department of Chemistry, Università della Calabria, Cubo 12C, 87036-Arcavacata di Rende (CS), Italy

Email:
Manuela Oliverio[*] - m.oliverio@unicz.it.

* Corresponding author

Abstract

Background: The peracetylation is a simple chemical modification that can be used to enhance the bioavailability of hydrophilic products and to obtain safe and stable pro-drugs.

Results: A totally green, solvent-free and catalyst-free microwave (MW)-assisted method for peracetylation of natural products such as oleuropein, alpha-hederin, quercetin and rutin is presented. By simply tuning the MW heating program, polyols with chemical diverse –OH groups or thermolabile functionalities can be peracetylated to improve the biological activity without degradation of the natural starting molecules. An evaluation of the process greenness was performed.

Conclusion: The method is potentially universally applicable for green acetylation of hydrophilic biological molecules, potentially easily scalable for industrial applications, including pharmaceutical, cosmetic and food industry.

Introduction

Peracetylation of alcohols, phenols and amino groups is a classical protection method in multistep syntheses as well as a transient chemical modification to improve the bioavailaibility and bioactivity of hydrophilic drugs and natural polyols [1-9].

Several in vitro and in vivo studies on peracetylated derivatives of natural products demonstrated that peracetylation increases the cell intake, the intragastric absorbance and the oral bioavailability in respect to the unprotected natural compound [2,3,8,9].

It has been hypothesized that peracetylated molecules can exploit the same pathway than unprotected molecules to pass the cell membrane [5] and, once inside the cells, acetyl groups can be removed by intracellular esterases thus resulting in an augmented dose of active principle [2,3]. Moreover, peracetylation affects the pharmacokinetics by prolonging the half-life of the unprotected molecules whose hydroxy groups are unstable in neutral, slight alkaline or oxidative environments [4]. Furthermore, acetylation is a chemical modification well accepted in a biological environment, being the N-acetylation, N,O-acyl transfer and the deacetylation some of the metabolic processes mediated by cytosolic and mitochondrial acetyl-CoA dependent enzymes, naturally addressed to lower the adverse biological effects or to ameliorate the biological response of several drugs [10]. Besides, well-known commercial drugs, such as acetylsalicylic acid (Aspirin), are acetylated molecules thus demonstrating that peracetylation has been approved by the FDA (Food and Drug Administration). Even the EFSA (European Food Safety Agency) accepted peracetylation as a method to improve the solubility of natural ingredients in fatty matrix (peracetylated starches are labeled as E1420 in the Union list of Food Additives) [11].

Classically peracetylation reactions have been performed by treatment of alcohols and phenols with acid anhydrides or acid chlorides in the presence of bases [12]. Recently, the urgency to find more environmental benign methods for standard transformations, led to the optimization of methods employing preferably acetic anhydride in solvent free conditions, in presence of non-toxic homogeneous catalysts such as environmental safe Lewis acids [13,14]. Moreover, the need to easily recover and reuse the catalyst, thus reducing the work-up procedure to a simple filtration, resulted in the growing use of heterogeneous or supported catalysts [15-17], solid nanopowders or nanoparticles [18,19], non-metal-based heterogeneous acetylation catalysts [20-22], as well as natural marine clays instead of homogeneous catalysts as reaction activators [23]. Even if these methods allow a complete peracetylation of several functionalities at room temperature in good to excellent yields, it is worth noting that some of them use metal-based catalysts needing long preparation procedures, or in the case of non-metal-based catalysts, inorganic acids are employed to activate acylation. On the other hand, the increasing attention to the final product safety, strictly connected to the consumers safety and health, push the pharmaceutical and food companies to prefer methods that allows to minimize the opportunity of the final product to get in touch with chemical additives. At the best of our knowledge, only few reports exist dealing with the acetylation of hydroxy groups under catalyst-free conditions. Most of them use alternative acetylating agents [24] or alternative energy sources [25], but none of them has been applied to complex

molecules or natural products. Between them a crucial report about the MW-assisted solvent-free and catalyst-free acetylation of anthranilic acid using acetic anhydride as acetylating agent, kept our attention [26]. According to this report, few minutes at maximum MW power (1000 Watt), without any temperature control, are needed to quantitative acetylate anthranilic acid. Obviously such uncontrolled conditions are not suitable for natural molecules, as they are often characterized by different moieties bonded each other by thermo or acid/base labile ester bonds; nevertheless such report furnished us the proof of principle that the rapid rise of temperature due to MW can catalyse acetylation using acetic anhydride. So, starting from this statement and trading on our experience in catalyst-free reactions [27,28] and MW-assisted chemistry [29-35], we propose here a universal MW-assisted method for peracetylation of multifunctional compounds. The method is totally green and safe as it employs food grade acetic anhydride as acetylating agent, solvent-free and catalyst-free conditions, an easy work-up procedure affording the peracetylated molecules without any chromatographic purification. The possibility to contemporary acetylate several chemically diverse –OH groups on thermolabile molecules simply tuning the heating program on the MW-oven is discussed.

Results and Discussion

Our work started from the results reported in literature for the MW-assisted acetylation of anthranilic acid. As the water content can be a limiting factor for the acetylation equilibrium, a pre-drying procedure is often required before the use of acetic anhydride [26]. In order to optimize a cheap, safe, green and easily scalable method for industrial application we decided to use food grade acetic anhydride (Eastman) as acetylating agent, after its anhydrification by simple passing it through a bed of activated molecular sieves under nitrogen steam. Such anhydrification technique was already proposed for several organic solvents as safer alternative to classical methods using reactive metals, metal hydrides or solvent distillation [36].

Moreover, in order to explore the versatility of the methodology we selected a set of representative molecules of different categories (Figure 1) such as pharmaceuticals (salicylic acid (**2**), paracetamol (**7**) and salbutamol (**9**)), cosmetic ingredients (cytronellol (**6**) and myrtenol (**10**)), biomolecules (cholesterol (**3**), N-Boc- tyrosine methyl ester (**8**), uridine (**12**) and methyl-α-D-glucopyranoside (**11**)) and natural antioxidant compounds in their simple (hydroxytyrosol (**4**), homovanillic alcohol (**5**), quercetin (**13**)) or glycosylated forms (oleuropein (**14**), rutin (**17**), alpha-hederin (**16**)). Because of their heterogeneity in terms of thermostability, number and reactivity of –OH groups, we decided to split the complete set in four subsets: molecules characterized by a good thermostability with up to three –OH
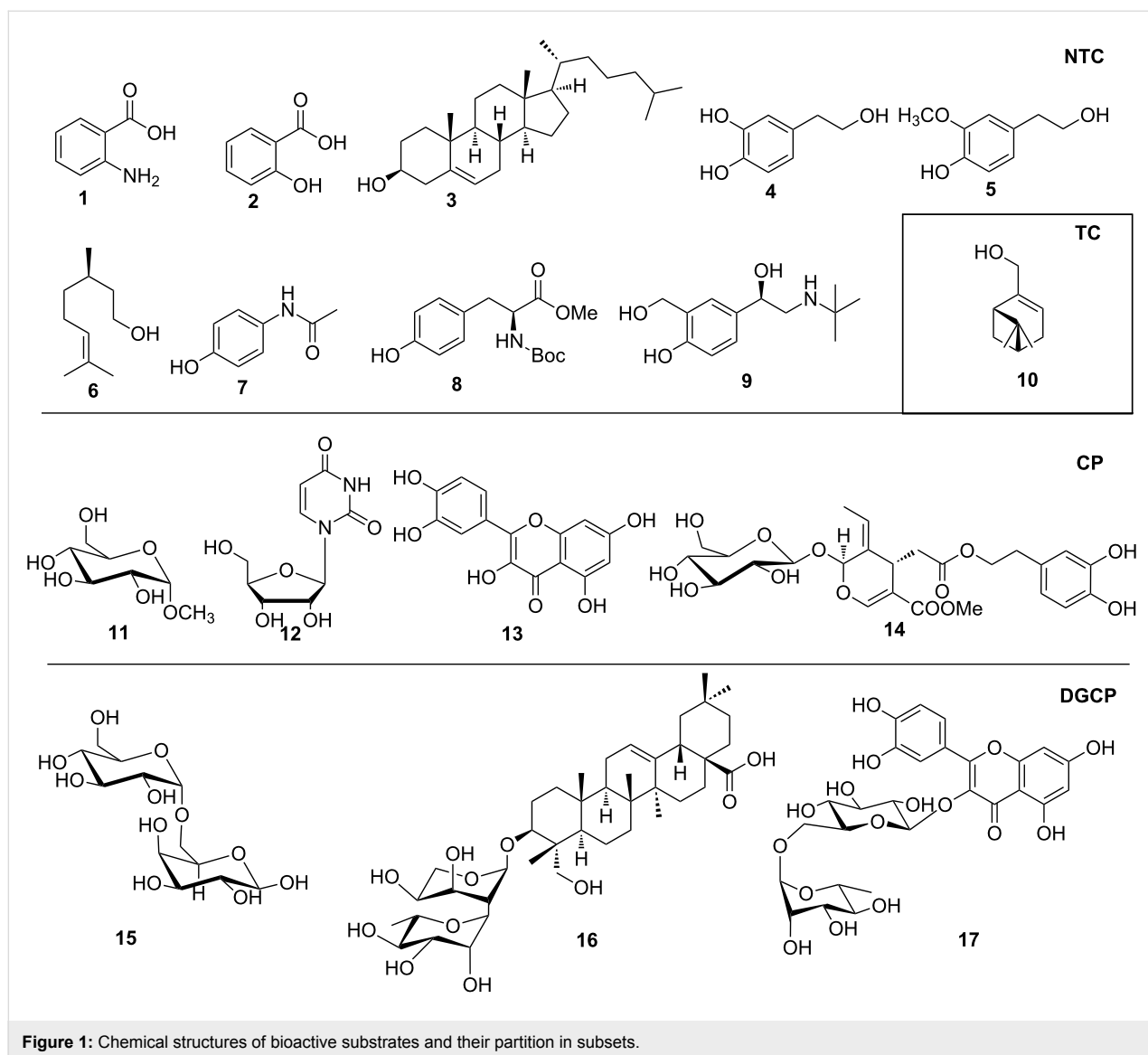
Figure 1: Chemical structures of bioactive substrates and their partition in subsets.
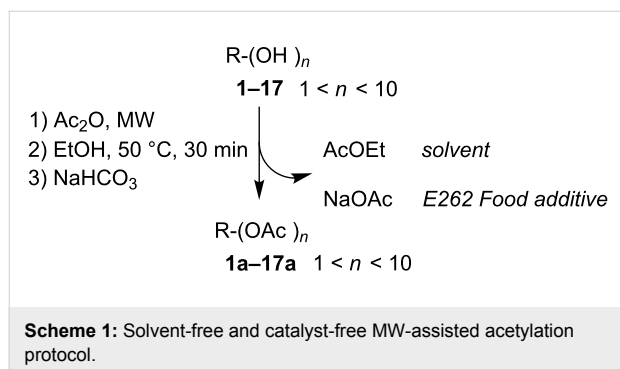
groups (non thermolabile compounds, NTC), molecules characterized by a strong thermolability (thermolabile compounds, TC), complex molecules characterized by at least two different chemical moieties and/or more than 3 –OH groups, (complex polyols, CP) and complex molecules with a disaccharide moiety, namely carrying a huge number of chemically different –OH groups (di-glycosylated complex polyols, DGCP). To set the reaction conditions we used the compounds belonging to the NTC group (**2**–**9**, Figure 1) comparing the obtained results to the literature reported for the anthranilic acid (**1**).

All the molecules were reacted in a Synthos 3000 (Anton-Paar) microwave oven equipped with an external IR sensor for the temperature control; they were solubilized in dry acetic anhydride in a concentration of 0.1 mmol/mL without any other solvent or catalyst, in presence of the 10% w/w of activated mo-

lecular sieves to preserve dryness. Moreover, it has been reported that molecular sieves can have a role in acetylation reaction, both under classical or alternative heating mode, thanks to their soft base character and MW absorbing power, respectively [37-40]. The reaction performed without molecular sieves gave rise to worse results (data not shown), even if a catalytic role could not be proved in our case, because the reactions were activated and gave rise to moderate yields as in a typical equilibrium system.

The reactions were monitored by TLC or GC–MS until the reagent disappeared and the work-up procedure was optimized in order to minimize the wastes of the process. Namely the reaction mixture was reacted with ethanol in order to eliminate the excess of acetic anhydride thus producing acetic acid and AcOEt, a common organic solvent with acceptable safety and

environmental characteristics [41], recoverable by simple evaporation under reduced pressure. After evaporation, the acetic acid was neutralized by adding a saturated solution of $NaHCO_3$ and the acetylated products were recovered by decantation without any other purification. The water solution of NaOAc obtained as byproduct can be reused as component for buffer solutions or as pickling agent for foods [11]. A complete scheme of the reaction protocol is depicted in Scheme 1.

R-(OH)$_n$
1–17   1 < n < 10

1) Ac$_2$O, MW
2) EtOH, 50 °C, 30 min   AcOEt   *solvent*
3) NaHCO$_3$
                                NaOAc   *E262 Food additive*

R-(OAc)$_n$
1a–17a   1 < n < 10

Scheme 1: Solvent-free and catalyst-free MW-assisted acetylation protocol.

Concerning the microwave settings we decided to extend the reaction time in respect to the reported acetylation of anthranilic acid [26] and to carefully monitor the microwave power, thus realizing a simple P-controlled program, corresponding to an internal temperature program, to softly reach the maximum power. An adjustment of the NCT P-program settings was performed for the other subsets, characterized by more instable or complex molecules, as it is described in Table 1.

The internal temperature profiles corresponding to each P-program are depicted in Figure 2.

The yields of the obtained peracetylated products (Table 2) are referred to isolated compounds, that have been fully characterized by HRMS, ^{1}H and ^{13}C NMR when unknown. The substrates giving rise to a mixture of inseparable acetylated derivatives were identified by LC/HRMS. In particular, UHPLC combined with an Orbitrap mass spectrometer at high resolving power, enabled the detection and the accurate mass measurement (<5 ppm error) of all the acetylated analytes in the mixture. The yields have been calculated on the peak intensities selecting the analytes having an ion current intensity value 10 fold lower than the main product. A little portion of the mixture was purified by flash chromatography for the structural characterization of the major product.

As it is reported in Table 2 we obtained good to excellent yields of acetylated products for all the substrates belonging to NTC group. More than one reaction cycle was needed when the reactant had a low solubility in acetic anhydride as in the case of cholesterol, *N*-Boc-tyrosine methyl ester and salbutamol (entries 3, 8 and 9, Table 2). Comparing to data reported in the literature [42,43], the modest yields of peracetylated product obtained in case of cholesterol **3** and salbutamol **9** were balanced by the absence of catalyst and by the reaction speed due to microwaves. The applied P-program was compatible with the *N*-Boc protecting group already present on the tyrosine methyl ester **8**. Concerning salbutamol (**9**) the reported yield

Table 1: P-controlled MW programs for peracetylation of compounds listed in Figure 1 (Synthos 3000, equipped with 64-MG5 rotor).

Entry	Method	Time (min)	Power (W)	$T_{internal}$ (°C)[a]	T_{IR} (°C)
1	NTC	0 → 5	0 → 300	25 → 100	85
		5 → 17	300	100	
		17 → 20	0	100 → 25	
2	TC	0 → 2	0 → 130	0 → 60	50
		2 → 7	130	60	50
		7 → 12	130 → 300	60 → 100	85
		12 → 22	300	100	85
		22 → 25	300 → 0	100 → 25	85
3	CP	0 → 5	0 → 300	0 → 100	85
		5 → 10	300	100	85
		10 → 12	300 → 400	100 → 120	105
		12 → 62	400	120	105
		62 → 65	0	120 → 25	105
4	DGCP	0 → 5	0 → 300	25 → 100	85
		5 → 10	300	100	85
		10 → 15	300 → 400	100 → 120	105
		15 → 45	400	120	105
		45 → 50	400 → 500	120 → 145	120
		50 → 90	500	145	120
		90 → 93	500 → 0	145 → 25	120

[a] Internal reaction temperature, related to IR limit temperature by the following equation: $T_{internal} = 1.214 \times T_{IR.}$ Maximum internal temperature for each category was established between many, by controlling the cleanness of the reaction profile.
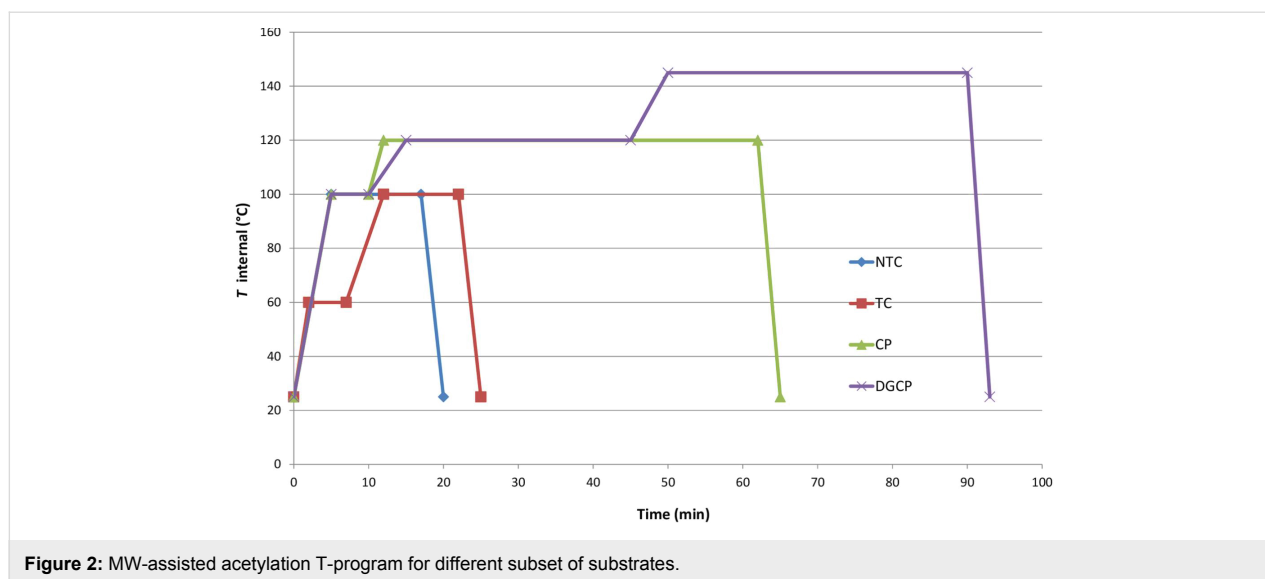
Figure 2: MW-assisted acetylation T-program for different subset of substrates.

was referred to the peracetylated product **9a** even if a quantitative conversion was registered and the obtained mixture of different acetylated derivatives was fully identified by GC–MS (see Supporting Information File 1). In this last case the change of the P-program was ineffective in increasing the yield of **9a** in respect to the other acetylated forms (data not shown).

As it can be argued by Figure 2 and Table 1, that the TC program (entry 2, Table 1) characterized by an intermediate step at lower temperature was necessary to avoid the degradation of TCs when exposed to the NTC program. In our case only a substrate, namely myrtenol (**10**), characterized by an allyl alcohol moiety, needed this softer program to be acetylated without degradation and/or polymerization (entry 10, Table 2).

Molecules bearing more than three –OH groups (CPs), besides *N*- or *O*- glycosidic bonds, needed a program composed of two steps with increasing temperature and power to complete (entry 3, Table 1). During the first step, where the MW conditions are very similar to NTC program, the more reactive –OH groups, such as primary or non-hindered phenolic groups, were acetylated, while a second step at higher power and temperature (Figure 2) was needed to realize the acetylation of all the –OH functionalities. The two-step temperature increase allowed to activate the reaction, limiting the exposure time of such compounds to the program higher temperature, thus preserving sensitive bonds.

All the polyols were peracetylated in good yields (entries 11–14, Table 2), even if in some cases more than one reaction cycle was necessary for complete conversion (entries 11, 12, 15, 16 and 17, Table 2). The only exception was the natural product quercetin (**13**) that, despite a quantitative conversion after

the first acetylation run, surprisingly gave a complex mixture of differently acetylated forms (Figure 3), among them the di-*O*-acetylated quercetin **13a** was the major product (60% of the total reaction products, entry 13, Table 2).

As the permeability and/or bioavailability of polyols is increased, no matter if the molecules are fully or partially acetylated, we decided to identify the full mixture by LC–MS analysis. We also provided a purification of the major product in order to carry out a structural characterization and to determine the yield of isolated product. Figure 3 shows the LC–HRMS of *O*-acetylated quercetin reaction mixture (for ^{1}H and ^{13}C NMR spectra of the mixture see Supporting Information File 1). Chemical structures of non-fully acetylated forms, i.e., tetra-*O*-acetylated-quercetin (8% of the mixture, entry B, Figure 3), di-*O*-acetylated quercetin (60% of the mixture, entry C, Figure 3), tri-*O*-acetylated quercetin (7% of the mixture, entry D, Figure 3), mono-*O*-acetylated-quercetin (25% of the mixture, entry E, Figure 3), could not be univocally assigned, except for the major product, characterized by ^{1}H NMR. The mixture of the acetylated forms can in principle work as bioactive component when used as crude reaction miture without purification.

Comparable results in terms of conversion to those collected for the CP group were obtained with the last group of molecules (DGCPs, entries 15–17, Table 2). Nevertheless, DGCP needed a MW three steps program, reaching the maximum power of 500 W (entry 4, Table 1), due to the increased number of chemical diverse –OH groups. In all cases a mixture of different acetylated forms were obtained and the prevalence of the peracetylated product was inversely proportional to the number of –OH groups within the molecule. So, good yields of peracetylated product **16a** were obtained from α-hederin (entry 16, Table 2),

Table 2: Solvent free and catalyst free peracetylation MW assisted of alcohols and polyols.
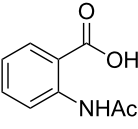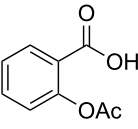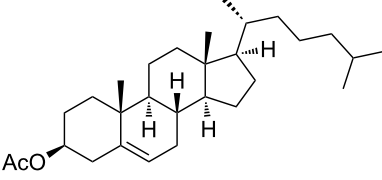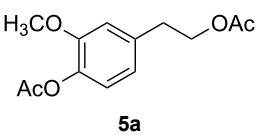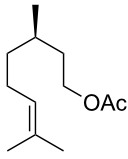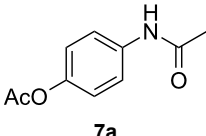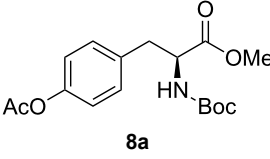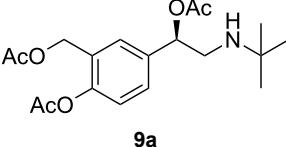
Entry	Path	Product	Conv. (%)[a]	Yield (%)[b]	N° Run
1	NTC	**1a**	100	100	1
2	NTC	**2a**	100	100	1
3	NTC	**3a**	70	62	3
4	NTC	**4a**	100	100	1
5	NTC	**5a**	100	100	1
6	NTC	**6a**	100	100[c]	1
7	NTC	**7a**	95	93	1
8	NTC	**8a**	100	95	2
9	NTC	**9a**	100	30[d]	3

Table 2: Solvent free and catalyst free peracetylation MW assisted of alcohols and polyols. (continued)
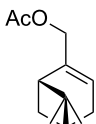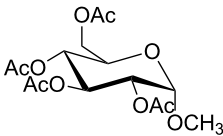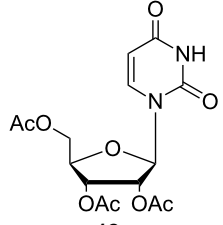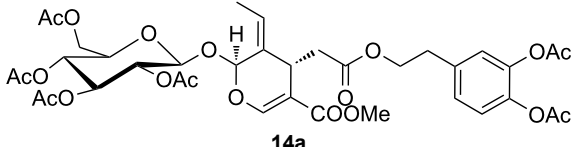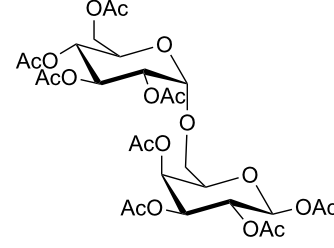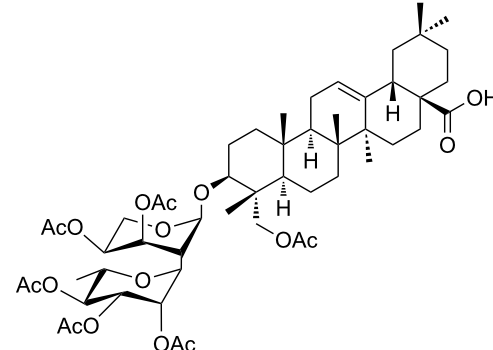
10	TC	**10a**	100	100	1
11	CP	**11a**	100	70[d,e]	2
12	CP	**12a**	100	92[d,e]	2
13	CP	**13a**[f]	94	60[d]	1
14	CP	**14a**	100	100	1
15	DGCP	**15a**	100	50[d,e]	2
16	DGCP	**16a**	100	85[d,e]	2

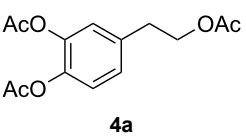**Table 2:** Solvent free and catalyst free peracetylation MW assisted of alcohols and polyols. (continued)

| 17 | DGCP | **17a** | 100 | 45[e] | 2 |
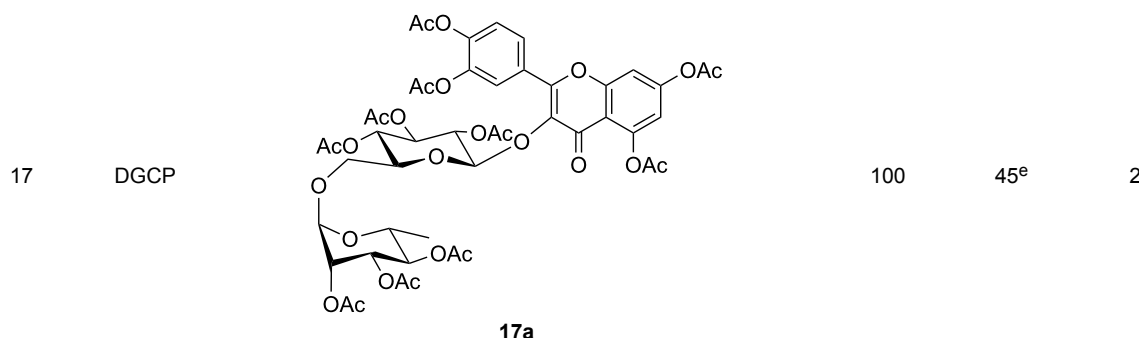
[a]Conversion determined by GC–MS or LC–MS and calculated as (100 − % area under the reagent peak). [b]Isolated products. [c]Volatile product. [d]A mix of acetylated forms has been obtained. The yield was determined on the major product after purification [e]Fresh Ac_2O added before each cycle. [f]Major isobar form from LC–MS. No attribution about the position of acetyl groups was made.

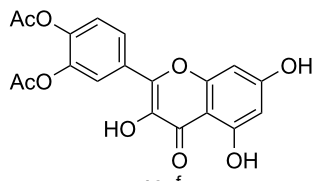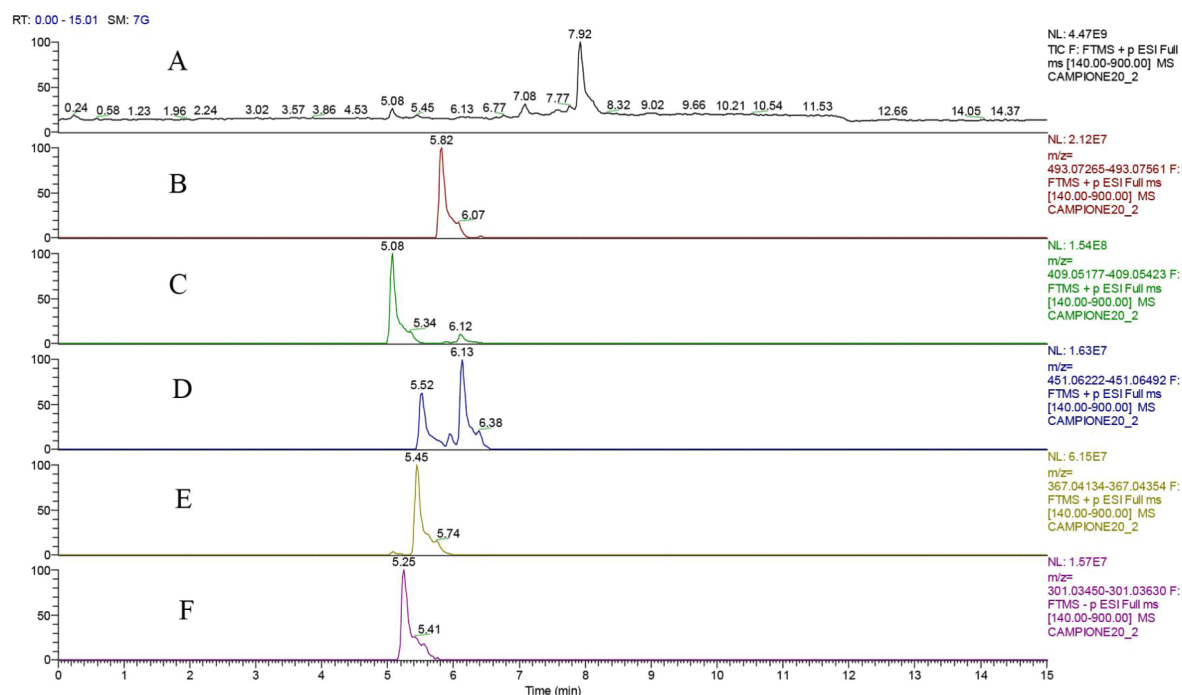**Figure 3:** LCHRMS (*m/z*, [M + Na]⁺ and [M − H]⁻ only for entry F) spectrum of *O*-acetylated quercetin (reaction mix) in total ion current (TIC, entry A) and extract ion Current (XIC, entries B–F) relative to main acetylated-forms: tetra-*O*-acetylated quercetin (8% of the mixture, entry B), di-*O*-acetylated quercetin (60% of the mixture, entry C), tri-*O*-acetylated quercetin (7% of the mixture, entry D), mono-*O*-acetylated-quercetin (25% of the mixture, entry E). The conversion was estimated around 96%, because of the presence of 6% of unreacted quercetin (entry F).

while medium yields were obtained for peracetylated-β-D-lactose **15a** (entry 15, Table 2) and peracetylated rutin **17a** (entry 17, Table 2) where the remaining 50% of product was constituted by a mixture of different non-fully acetylated forms, even after more than one acetylation run. Moreover, peracetylation of rutin (**17**), which is the di-glycosylated derivative of quercetin (**13**), demonstrated that an additional acetylation run could give rise also to a quercetin peracetylation.

An evaluation of the greenness of the process was performed by calculation of atom economy (AE), reaction mass efficiency (RME), mass intensity (MI) and mass productivity (MP), according to the definition summarized by Constable et al. [44] (see Supporting Information File 1). The values for all the previous parameters, calculated for the 17 performed reactions, are reported in Table 3. AE was referred to the peracetylated compound, as it was the reaction desired product.

Table 3: Process green chemistry metrics.

Entry	Yield (%)	AE (%)	RME (%)	MI	MP (%)
1	100	75	75	2	50
2	100	75	75	2	50
3	62	88	54	3	33
4	100	61	61	2	50
5	100	68	68	2	50
6	55	77	42	3	33
7	93	76	71	2	50
8	90	85	76	2	50
9	30	67	20	7	14
10	100	76	76	2	50
11	70	51	36	3	33
12	92	67	62	2	50
13	60	76	46	3	33
14	100	75	75	2	50
15	50	58	29	5	20
16	85	70	59	3	33
17	45	63	28	6	16

As expected, RME is a more realistic parameter than AE due to the influence of the reaction yield. Because MI and MP consider all the masses implied in the process and take into account yield, solvents and reaction auxiliaries, they are more useful parameters to evaluate the sustainability of the process from an industrial point of view [44]. For the calculation of MI and MP the reaction work-up was included as a reaction step (see Supporting Information File 1) because the products obtained by the hydrolysis of the excess of Ac_2O used, both as reaction reagent and solvent, are useful chemicals. The calculated values were good, thus demonstrating the versatility and sustainability of the process. Our prevision shows how the process remains reasonable in terms of mass productivity, ranging from 16% to 50%.

Finally a scaled protocol extended to the maximum oven capacity was tested using oleuropein (**14**) as test compound. 30 mL vials were reacted in the Synthos 3000 XF-100 rotor, after filling each vial with a ten-fold quantity of reactants, reaching a total processed oleuropein of 8 g/reaction cycle. Table S2 in Supporting Information File 1 shows the power-controlled MW protocol, adjusted in respect to the small-scale procedure. Figure S3 reports a comparison between the temperature profiles of the small and large scale peracetylations: the two curves are comparable, even if a better stability is registered for the experiment performed in small scale. Nevertheless, the large-scale process successfully produced 10 g of peracetylated oleuropein in 65 minutes (see Supporting Information File 1).

Conclusion

In conclusion, a solvent-free and catalyst-free MW-assisted method of peracetylation of natural polyols has been proposed. The method is high versatile such it can be applied to alcohols, phenols and polyols characterized by a huge chemical diversity and thermostability, simply tuning the MW settings. Such method is potentially universally applicable for green acetylation of hydrophilic biological molecules, thus improving their bioavailability and biological activity, no matter if they are simple polyphenols or glycosilated molecules. Thanks to the absolute absence of toxic reactants and byproducts the method is potentially easily scalable for industrial applications, including pharmaceutical, cosmetic and food industry, where the eco-compatibility of the reaction conditions, the easy waste management and the product safety are pivotal conditions for market.

Experimental
Materials and methods

MW-assisted reactions were performed in Synthos 3000 instrument from Anton Paar, equipped with a 64MG5 rotor and an IR probe as external control of the temperature. Using a temperature-controlled program the instrument is able to tune the power magnetron in order to reach and to maintain the fixed temperature throughout the experiment. For each run 16 positions of the rotor was occupied by 0.3–3 mL glass vials sealed with a dedicated PEEK screw-cup together with a reliable PTFE seal. Reactions were monitored by TLC using silica plates 60-F264 on alumina, commercially available from Merk. GC–MS spectra were recorded on a GC–MS Thermo Scientific workstation, formed by a Focus GC (30-m VARIAN-VF-5ms, 0.25 mm diameter capillary column, working on spitless mode, 1.2 mL/min He as carrier gas) and by an DSQ II mass detector. Chromatography was performed using a Thermo Scientific Dionex Ultimate 3000 RS, injecting directly onto a Thermo Scientific Hypersil Gold C18 column (50 × 2.1 mm, 1.9 μm particle size), equilibrated in 95% solvent A (0.1% aqueous solution of formic acid), 5% solvent B (methanol). The column and auto-sampler temperatures were maintained at 24 °C and 20 °C, respectively. The elution flow rate was 600 μL/min by linearly increasing the concentration of solvent B from 5 to 55% in 4 min, from 55% to 95% in 2 min and remaining for other 2 minutes in isocratic flow, then returning to 5% in 1 minute. At the end it was re-equilibrated for 3 minutes. The total run time, including column wash and equilibration was 15 min. A Thermo Scientific Q-ExactiveTM mass spectrometer was used for HRMS measurements using electrospray as ionization source with both negative and positive polarities, at a resolving power of 35.000 (defined as FWHM at *m/z* 200), IT = 100 ms, and ACG target = 500.000, by full scan analysis (mass range 140–900 amu for 2 samples and 200–1500 amu for other 2 samples). Source conditions were: spray voltage 2.9 kV, sheath gas:

30, arbitrary units, Auxiliary gas: 10, probe heater temperature: 280 °C; capillary temperature: 320 °C; S-Lens RF Level: 50. The instrument was calibrated by Thermo calibration solutions prior to the beginning the analysis. ^{1}H and ^{13}C spectra were recorded on a Bruker WM 300 instrument on samples dissolved in CDCl$_3$. Chemical shifts are given in parts per million (ppm) from tetramethylsilane as the internal standard (0.0 ppm). Coupling constants (*J*) are given in Hertz. All new compounds were characterized by HRMS, ^{1}H NMR and ^{13}C NMR, while known compounds were analysed by comparison with the data coming from literature [14,45-47]. All chemicals were used as commercially available.

A request for an Italian Patent concerning the present protocol was submitted by the authors of this article (request number n° 102016000052914, registration date 23/05/2016).

General procedure for Ac$_2$O purification

The acetic anhydride (food grade, Eastman) was dried prior to use through the following procedure: a glass column under N$_2$ was filled with 4 Å molecular sieves pre-activated at 350 °C overnight. The acetic anhydride was passed through the sieves 3 times and collected in a flask under N$_2$. The collected anhydride was gently stirred over 20% w/w of activated molecular sieves for 48 hours, before the use.

Optimized MW-assisted peracetylation

The substrate belonging to one of the subset reported in Table 1 (NTC, TC, CP, DGNP) (0.1 mmol) was left to react under MW heating (Synthos 3000, Anton Paar) with dry acetic anhydride (1 mL, 10 mmol) in a 3 mL vial (Rotor 64MG5), equipped with a magnetic stirrer in the presence of molecular sieves (10 % w/w). The microwave, equipped with IR sensor for external temperature control (IR limit calculated as follows: $T_{internal} = 1.214 \times T_{IR}$), has been set with the power programs provided for its subset as described in Table 1. At the end of the reaction, the mixture was filtered, diluted with ethanol (2 mL) and left under vigorous stirring for 30 minutes at 50 °C. The mixture was then evaporated under reduced pressure and a small amount of a saturated solution of sodium bicarbonate (3.8 mL, 10 mmol NaHCO$_3$) was added. After the evolution of CO$_2$, the precipitation of the peracetylated product was observed. The products were separated by simple decantation. For compounds which do not precipitate upon addition of NaHCO$_3$, an extraction with AcOEt was needed. The organic phase, after drying with Na$_2$SO$_4$, filtration and evaporation, gave the reaction crude.

Characterization of selected compounds

Peracetylated homovanillic alcohol (**5a**): Yellow oil; Yield 100%; MS (70 eV, IE) *m/z* (%): 252 [M$^+$] (1), 210 [M$^+$ −

CH$_2$=CH=O] (10), 192$^+$ [M − CH$_3$CO$_2$H] (1), 150 [C$_{11}$H$_{12}$O$_3^+$ − CH$_2$=CH=O] (100), 135 [C$_9$H$_9$O$^+$ − CH$_3$] (20); ^{1}H NMR (300 MHz, CDCl$_3$, 25 °C, TMS) δ 6.97 (d, J_{G-H} = 8 Hz, 1H, H$_H$), 6.81 (s, 1H, H$_F$), 6.80–6.78 (d, *J* = 8 Hz, 1H, H$_G$), 4.31–4.25 (t, J_{D-E} = 7 Hz, 1H, H$_D$), 3.82 (s, 3H, H$_B$), 2.95–2.89 (t, J_{D-E} = 7 Hz, 1H, H$_E$), 2.30 (s, 3H, H$_A$), 2.03 (s, 3H, H$_C$); ^{13}C NMR (75 MHz, CDCl$_3$, 25 °C, TMS) δ 171.3, 169.4, 151.3, 138.7, 137.0 123.0, 121.3, 113.4, 65.0 56.2, 35.3, 21.3, 21.0.

Acetyl salbutamol (**9a**): Yellow oil; inseparable mixture; pracetylated salbutamol (major product): Yield 30%; MS (70 eV, IE) *m/z* (%): 365 [M$^+$] (0.5), 249 [M$^+$ − CH$_3$COOCH$_3$-CH$_2$=C=O] (10), 188 [M$^+$ − 3 × CH$_3$COO] (10), 146 [C$_{13}$H$_{17}$NO$^+$ − *t*-Bu] (20), 86 [CH$_2$=NH*t*-Bu$^+$] (100); ^{1}H NMR (300 MHz, CDCl$_3$, 25 °C, TMS) δ 7.39 (d, J_{G-I} = 2 Hz, 1H, H$_G$), 7.33–7.30 (dd, J_{G-I} = 2 Hz, J_{H-I} = 8.3 Hz, 1H, H$_I$), 7.16–7.09 (d, J_{H-I} = 8.3 Hz, 1H, H$_I$), 5.96–5.88 (dd, J_{F-E} = 3.4 Hz, $J_{F-E'}$ = 10 Hz, 1H, H$_F$), 3.84–3.72 (dd, $J_{E-E'}$ = 16.3 Hz, $J_{F-E'}$ = 10 Hz, 1H, H$_{E'}$), 3.59–3.49 (dd, $J_{E-E'}$ = 16.3 J_{F-E} = 3.4 Hz, 1H, H$_E$), 2.34 (s, 3H, H$_B$), 2.23 (br s, 1H, NH), 2.11 (s, 3H, H$_C$), 2.08 (s, 3H, H$_A$), 1.49 (s, 9H, H$_D$); ^{13}C NMR (75 MHz, CDCl$_3$, 25 °C, TMS) δ 171.4, 170.9, 170.1, 169.5, 149.6, 136.3, 129.2, 129.1, 128.7, 127.8, 123.7, 61.5, 57.8, 51.2, 29.5, 25.8, 21.4, 21.2.

Acetylated Quercetin (**13a**): Yellow powder; inseparable mixture; di-*O*-acetylated quercetin (major product): Yield 60%; HRMS: [M + Na$^+$] *m/z*: 451.0635 (theoretical [M + Na$^+$] *m/z*: 451.0636); ^{1}H NMR (300 MHz, CDCl$_3$, 25 °C, TMS) δ 2.336 (s, 3H, Ac), 2.3381 (s, 3H, Ac), 2.3432 (s, 3H, Ac), 2.3483 (s, 3H, Ac), 6.86 (d, J_{meta}= 2.19 Hz, 1H, H$_E$), 7.34 (d, J_{meta}= 2.19 Hz, 1H, H$_A$), 7.37, (d, J_{ortho}= 8.6 Hz, 1H, H$_D$), 7.64 (d, J_{meta}= 2.19 Hz, 1H, H$_B$), 7.74 (dd, J_{ortho}= 8.6Hz, J_{meta}= 2.19 Hz, 1H, H$_C$); ^{13}C NMR (75 MHz, CDCl$_3$, 25 °C, TMS) δ 20.9, 21.0, 21.4, 21.5, 109.3, 114.2, 124.2, 124.3, 126.8, 128.14, 131.2, 142.6, 144.7, 150.8, 154.6, 157.2, 168.1, 168.2, 170.4.

Peracetylated α-hederine (**16a**) yellow oil: Yield 85%; HRMS: [M + Na$^+$] *m/z*: 1025.5045 (theoretical [M + Na$^+$] *m/z*: 1025.5080); ^{1}H NMR (300 MHz, CDCl$_3$, 25 °C, TMS) δ 0.73 (s, 3H, H$_A$), 0.79 (s, 3H, H$_B$), 0.90 (s, 3H, H$_H$), 0.92 (s, 3H, H$_L$), 0.95 (s, 3H, H$_Q$), 1.10 (s, 6H, H$_{G,J'}$), 1.23 (d, J_{O-N} = 6.6 Hz, 2H, H$_O$), 1.29–1.90 (m, 20H, H$_{C,D,E,F,I,J,P,S,V,K,R}$), 2.01 (s, 3H, Ac), 2.03 (s, 3H, Ac), 2.06 (s, 3H, Ac), 2.10 (s, 3H, Ac), 2.11 (s, 3H, Ac), 2.14 (s, 3H, Ac), 2.82 (m, 1H, H$_U$), 3.85–3.98 (m, 2H, H$_K$, H$_{E'}$), 4.07–4.17 (m, 4H, 1H$_{E'}$, H$_{B',F',L'}$), 4.43 (d, J_{N-O} = 6.6 Hz, 2H, H$_N$), 4.95–5.07 (m, 4H, H$_{C',D',G',J'}$), 5.22–5.30 (m, 3H, H$_{A',T,I'}$); ^{13}C NMR (75 MHz, CDCl$_3$, 25 °C, TMS) δ 182.8, 170.4, 170.3, 170.1, 170.0, 169.6, 143.6, 122.4, 103.5, 98.2, 81.9, 71.0, 69.5, 68.6, 67.8, 67.1, 62.6, 47.8, 46.4,

45.8, 41.9, 41.5, 41.0, 39.2, 38.3, 36.5, 33.7, 33.0, 32.4, 30.6, 27.5, 25.7, 25.4, 23.5, 23.4, 22.8, 20.9, 20.6, 17.9, 17.3, 16.9, 15.8, 12.6.

Peracetylated rutine (**17a**): Brown powder: Yield 45%; HRMS: [M + Na$^+$] m/z: 1053.2470 (theoretical [M + Na$^+$] m/z: 1053.2482); ^{1}H NMR (300 MHz, CDCl$_3$, 25 °C, TMS) δ 1.05 (d, $J_{L'K'}$ = 6.25 Hz, 3H, H$_{L'}$), 1.58 (s, 3H, Ac), 1.94 (s, 3H, Ac), 1.95 (s, 3H, Ac), 2.02 (s, 3H, Ac), 2.08 (s, 3H, Ac), 2.14 (s, 3H, Ac), 2.29 (s, 3H, PhOAc), 2.34 (s, 3H, PhOAc), 2.35 (s, 3H, PhOAc), 2.44 (s, 3H, PhOAc), 3.56–3.67 (m, 1H, H$_{E'}$), 3.50–3.54 (m, 2H, H$_{F'',J'}$), 4.91–4.97 (m, 2H, H$_{I',D'}$), 5.05–5.09 (m, 2H, H$_{B',H'}$), 5.14–5.20 (m, 1H, H$_{C'}$), 5.26 (d, $J_{F'F''}$ = 9.32 Hz, 1H, H$_{F'}$), 5.42, (d, $J_{G'H'}$ = 7.67 Hz, 1H, H$_{G'}$), 5.41 (d, $J_{A'B'}$ = 7.7 Hz, 1H, H$_{A'}$), 6.84 (d, J_{meta} = 2.19 Hz, 1H, H$_E$), 7.31 (d, J_{meta} = 2.19 Hz, 1H, H$_A$), 7.35, (d, J_{ortho} = 8.6 Hz, 1H, H$_D$), 7.90 (d, J_{meta}= 2.19 Hz, 1H, H$_B$), 7.95 (dd, J_{ortho} = 8.6 Hz, J_{meta} = 2.19 Hz, 1H, H$_C$); ^{13}C NMR (75 MHz, CDCl$_3$, 25 °C, TMS) δ 14.38, 17,52, 21.02 (×4), 21.42, 21.50, 23.33, 24.11, 29.27, 30.05, 30.72, 39.09, 66.68, 67.30, 68.51, 69.35, 69.72, 69.85, 71.24, 71.74, 72.90, 98.09, 99.94, 109.37, 113.77, 115.42, 123.80, 125.03, 127.57, 128.93, 137.28, 142.12, 144.44, 150.53, 154.30, 155.00, 156.96, 168.07, 168.21, 168.39, 169.59, 169.93, 170.07, 170.23, 170.41.

Supporting Information

Supporting Information File 1

Scaled oleuropein peracetylation procedure, GC–MS, LC–HRMS, ^{1}H and ^{13}C NMR spectra of new compounds, as well as calculation for green chemistry metrics.
[http://www.beilstein-journals.org/bjoc/content/supplementary/1860-5397-12-214-S1.pdf]

Acknowledgements

References

1. Green, T. W.; Wuts, P. G. M. *Protective Groups in Organic Synthesis,* 3rd ed.; Wiley: NewYork, 1999; pp. 150ff.
2. Lambert, J. D.; Sang, S.; Hong, J.; Kwon, S.-J.; Lee, M.-J.; Ho, C.-T.; Yang, C. S. *Drug Metab. Dispos.* **2006,** *34,* 2111–2116. doi:10.1124/dmd.106.011460
3. Lee, S.-C.; Chan, W.-K.; Lee, T.-W.; Lam, W.-H.; Wang, X.; Chan, T.-H.; Wong, Y.-C. *Nutr. Cancer* **2008,** *60,* 483–491. doi:10.1080/01635580801947674
4. Lam, W. H.; Kazi, A.; Kuhn, D. J.; Chow, L. M. C.; Chan, A. S. C.; Doub, Q. P.; Chana, T. H. *Bioorg. Med. Chem.* **2004,** *12,* 5587–5593. doi:10.1016/j.bmc.2004.08.002
5. Colin, D.; Lancon, A.; Delmas, D.; Lizard, G.; Abrossinow, J.; Kahn, E.; Jannin, B.; Latruffe, N. *Biochimie* **2008,** *90,* 1674–1684. doi:10.1016/j.biochi.2008.06.006
6. Higgs, G. A.; Salmon, J. A.; Henderson, B.; Vane, J. R. *Proc. Natl. Acad. Sci. U. S. A.* **1987,** *84,* 1417–1420. doi:10.1073/pnas.84.5.1417
7. Bulotta, S.; Corradino, R.; Celano, M.; Maiuolo, J.; D'Agostino, M.; Oliverio, M.; Procopio, A.; Filetti, S.; Russo, D. *J. Mol. Endocrinol.* **2013,** *51,* 181–189. doi:10.1530/JME-12-0241
8. Bulotta, S.; Corradino, R.; Celano, M.; D'Agostino, M.; Maiuolo, J.; Oliverio, M.; Procopio, A.; Iannone, M.; Rotiroti, D.; Russo, D. *Food Chem.* **2011,** *127,* 1609–1614. doi:10.1016/j.foodchem.2011.02.025
9. Lepore, S. M.; Morittu, V. M.; Celano, M.; Trimboli, F.; Oliverio, M.; Procopio, A.; Di Loreto, C.; Damante, G.; Britti, D.; Bulotta, S.; Russo, D. *Int. J. Endocrinol.* **2015,** No. 431453. doi:10.1155/2015/431453
10. King, C. M.; Glowinski, I. B. *Environ. Health Perspect.* **1983,** *49,* 43–50. doi:10.1289/ehp.834943
11. Annex III to Regulation (EC) No 1333/2008: *Union list of food additives approved for use in food additives, food enzymes, food flavourings and nutrients*.
12. Horton, D. In *Organic Synthesis Collective Volume 5;* Baumgarten, H. E., Ed.; John Wiley & Sons: NewYork, 1973; 1ff.
13. Dalpozzo, R.; De Nino, A.; Maiuolo, L.; Oliverio, M.; Procopio, A.; Russo, B.; Tocci, A. *Aust. J. Chem.* **2007,** *60,* 75–79. doi:10.1071/CH06346
14. Procopio, A.; Alcaro, S.; Nardi, M.; Oliverio, M.; Ortuso, F.; Sacchetta, P.; Pieragostino, D.; Sindona, G. *J. Agric. Food Chem.* **2009,** *57,* 11161–11167. doi:10.1021/jf9033305
15. Satam, J. R.; Jayaram, R. V. *Catal. Commun.* **2008,** *9,* 2365–2370. doi:10.1016/j.catcom.2008.05.033
16. Rajabi, F. *Tetrahedron Lett.* **2009,** *50,* 395–397. doi:10.1016/j.tetlet.2008.11.024
17. Zareyee, D.; Ghadikolaee, A. R.; Khalilzadeh, M. A. *Can. J. Chem.* **2012,** *90,* 464–468. doi:10.1139/v2012-018
18. Farhadi, S.; Zaidi, M. *J. Mol. Catal. A: Chem.* **2009,** *299,* 18–25. doi:10.1016/j.molcata.2008.10.013
19. Farhadi, S.; Panahandehjoo, S. *Appl. Catal., A* **2010,** *382,* 293–302. doi:10.1016/j.apcata.2010.05.005
20. Niknam, K.; Saberi, D. *Tetrahedron Lett.* **2009,** *50,* 5210–5214. doi:10.1016/j.tetlet.2009.06.140
21. Shimizu, K.-i.; Higuchi, T.; Takasugi, E.; Hatamachi, T.; Kodama, T.; Satsuma, A. *J. Mol. Catal. A: Chem.* **2008,** *284,* 89–96. doi:10.1016/j.molcata.2008.01.013
22. Das, B.; Thirupathi, P. *J. Mol. Catal. A: Chem.* **2007,** *269,* 12–16. doi:10.1016/j.molcata.2006.12.029
23. Sreedhar, B.; Arundhathi, R.; Amarnath Reddy, M.; Parthasarathy, G. *Appl. Clay Sci.* **2009,** *43,* 425–434. doi:10.1016/j.clay.2008.10.001
24. Pelagalli, R.; Chiarotto, I.; Ferocia, M.; Vecchio, S. *Green Chem.* **2012,** *14,* 2251–2255. doi:10.1039/c2gc35485c
25. Wang, X.-J.; Yang, Q.; Liu, F.; You, Q.-D. *Synth. Commun.* **2008,** *38,* 1028–1035. doi:10.1080/00397910701860372
26. Wilhite, D. M.; Baldwin, B. W. *J. Chem. Educ.* **2002,** *79,* 1344. doi:10.1021/ed079p1344
27. Cravotto, G.; Procopio, A.; Oliverio, M.; Orio, L.; Carnaroglio, D. *Green Chem.* **2011,** *13,* 2806–2809. doi:10.1039/c1gc15756f

28. Oliverio, M.; Costanzo, P.; Paonessa, R.; Nardi, M.; Procopio, A.
    RSC Adv. **2013,** *3,* 2548–2552. doi:10.1039/c2ra23067d
29. Procopio, A.; Gaspari, M.; Nardi, M.; Oliverio, M.; Tagarelli, A.;
    Sindona, G. *Tetrahedron Lett.* **2007,** *48,* 8623–8627.
    doi:10.1016/j.tetlet.2007.10.038
30. Procopio, A.; De Luca, G.; Nardi, M.; Oliverio, M.; Paonessa, R.
    Green Chem. **2009,** *11,* 770–773. doi:10.1039/b820417a
31. Procopio, A.; De Nino, A.; Nardi, M.; Oliverio, M.; Paonessa, R.;
    Pasceri, R. *Synlett* **2010,** *12,* 1849–1853. doi:10.1055/s-0030-1258126
32. Oliverio, M.; Procopio, A.; Glasnov, T. N.; Goessler, W.; Kappe, C. O.
    Aust. J. Chem. **2011,** *64,* 1522–1529. doi:10.1071/CH11125
33. Procopio, A.; Costanzo, P.; Curini, M.; Nardi, M.; Oliverio, M.;
    Sindona, G. *ACS Sustainable Chem. Eng.* **2013,** *1,* 541–544.
    doi:10.1021/sc4000219
34. Oliverio, M.; Nardi, M.; Costanzo, P.; Cariati, L.; Cravotto, G.;
    Giofrè, S. V.; Procopio, A. *Molecules* **2014,** *19,* 5599–5610.
    doi:10.3390/molecules19055599
35. Oliverio, M.; Nardi, M.; Cariati, L.; Vitale, E.; Bonacci, S.; Procopio, A.
    ACS Sustainable Chem. Eng. **2016,** *4,* 661–665.
    doi:10.1021/acssuschemeng.5b01201
36. Williams, D. B. G.; Lawton, M. *J. Org. Chem.* **2010,** *75,* 8351–8354.
    doi:10.1021/jo101589h
37. Adinolfi, M.; Barone, G.; Iadonisi, A.; Schiattarella, M. *Tetrahedron Lett.*
    2003, *44,* 4661–4663. doi:10.1016/S0040-4039(03)01072-4
38. Sá, M. M.; Meier, L. *Synlett* **2006,** *20,* 3474–3478.
    doi:10.1055/s-2006-958430
39. Cai, L.; Rufty, C.; Liquois, M. *Asian J. Chem.* **2014,** *26,* 4367–4369.
    doi:10.14233/ajchem.2014.16573
40. Cardozo, H. M.; Ribeiro, T. F.; Sá, M. M.; Sebrão, D.;
    Nascimento, M. G.; Silveira, G. P. *J. Braz. Chem. Soc.* **2015,** *26,*
    755–764. doi:10.5935/0103-5053.20150037
41. Henderson, R. K.; Jiménez-González, C.; Constable, D. J. C.;
    Alston, S. R.; Inglis, G. G. A.; Fisher, G.; Sherwood, J.; Binksa, S. P.;
    Curzons, A. D. *Green Chem.* **2011,** *13,* 854–862.
    doi:10.1039/c0gc00918k
42. Dalpozzo, R.; De Nino, A.; Maiuolo, L.; Procopio, A.; Nardi, M.;
    Bartoli, G.; Romeo, R. *Tetrahedron Lett.* **2003,** *44,* 5621–5624.
    doi:10.1016/S0040-4039(03)01358-3
43. Fenjan, A.-A. M.; Dhahir, S. A.; Al-Sahib, S. A.; Thanoon, S.
    J. Al Nahrain University - Science **2011,** *14,* 50–57.
44. Constable, D. J. C.; Curzons, A. D.; Cunningham, V. L. *Green Chem.*
    2002, *4,* 521–527. doi:10.1039/B206169B
45. *SDBS Web;* National Institute of Advanced Industrial Science and
    Technology, 2015, http://sdbs.db.aist.go.jp.
46. Horton, D.; Lauterback, J. H. *J. Org. Chem.* **1969,** *34,* 86–92.
    doi:10.1021/jo00838a021
47. Shull, B. K.; Wu, Z.; Koreeda, M. *J. Carbohydr. Chem.* **1996,** *15,*
    955–964. doi:10.1080/07328309608005701

Isosorbide and dimethyl carbonate: a green match

Fabio Aricò[*] and Pietro Tundo

Abstract

In this review the reactivity of the bio-based platform compounds D-sorbitol and isosorbide with green reagents and solvent dimethyl carbonate (DMC) is reported. Dehydration of D-sorbitol via DMC in the presence of catalytic amounts of base is an efficient and viable process for the preparation of the industrially relevant anhydro sugar isosorbide. This procedure is "chlorine-free", one-pot, environmental friendly and high yielding. The reactivity of isosorbide with DMC is equally interesting as it can lead to the formation of dicarboxymethyl isosorbide, a potential monomer for isosorbide-based polycarbonate, and dimethyl isosorbide, a high boiling green solvent. The peculiar reactivity of isosorbide and the non-toxic properties of DMC represent indeed a green match leading to several industrial appealing potential applications.

Review
Introduction

In the last twenty years biorefinery has gained exceptional attention in the scientific community. This interest has been prompted by the substitution of petroleum-based compounds with renewable substances with the aim of establishing a bio-based economically self-sustained industry [1].

In this prospect the US Department of Energy (DOE) has published a list of 15 target molecules [2], starting from 300 original candidates, that were considered of special interest for biorefinery development (Figure 1) [3]. These compounds have been selected by taking into consideration numerous factors such as available processes, economics, industrial viability, size

of markets and their possible employment as a platform for the production of derivatives.

Over the years, due to the considerable progress in biorefinery development, this list, as well as the criteria used to identify bio-based products have been revised (Table 1) [1]. Several new compounds substituted the ones that have not received a great research interest. However, among the original selected chemicals, D-sorbitol, together with ethanol and glycerol, still occupy top positions as they encompass all of the desired criteria for bio-based platform compounds.
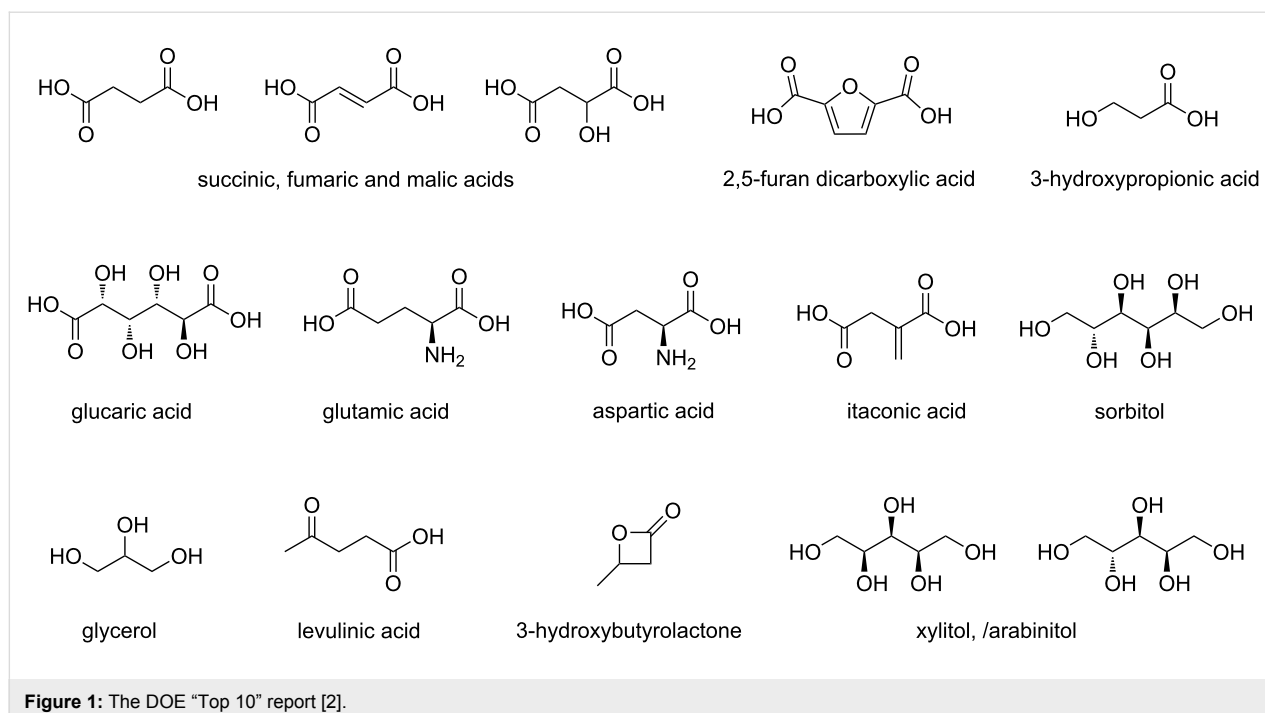
Figure 1: The DOE "Top 10" report [2].

Table 1: Top chemical opportunities from biorefinery carbohydrates and criteria of selection.[a]

| #	Bio-based compounds	Criteria
1	Ethanol	1, 2, 3, 4, 5, 6, 7, 8, 9
2	Furans	1, 2, 7, 8, 9
3	Glycerol and derivatives	1, 2, 3, 4, 5, 6, 7, 8, 9
4	Biohydrocarbons	Isoprene: 1, 2, 3, 4, 6, 7
5	Lactic acid	1, 2, 4, 7
6	Succinic acid	1, 2, 5, 6
7	Hydroxypropionic acid/aldehyde	1, 3, 4, 5
8	Levulinic acid	1, 2, 3, 5, 6, 8
9	D-sorbitol	1, 2, 3, 4, 5, 6, 7, 8, 9
10	Xylitol	1, 2, 5, 8, 9

[a]Criteria of selection:
1. The compound/technology has received significant attention in the literature.
2. The compound illustrates a broad technology applicable to multiple products.
3. The technology provides direct substitutes for existing petrochemicals.
4. The technology is applicable to high volume products.
5. A compound exhibits strong potential as a platform.
6. Scale-up of the product/technology to pilot, demo, or full scale is underway.
7. The bio-based compound is an existing commercial product, prepared at intermediate or commodity levels.
8. The compound may serve as a primary building block of the biorefinery.
9. Commercial production of the compound from renewable carbon is well established.

D-Sorbitol, namely 1,4:3,6-dianhydro-D-glucitol, is a sugar alcohol, found in nature as the sweet constituent of many berries and fruits from which it was isolated for the first time in 1872. Its large scale manufacture began in the 1950s, due to the growing applications as humectant in cosmetology and sugar substitute in confectionery. Nowadays the global market of D-sorbitol is estimated around 800 kt, half of which is produced in China with a demand currently growing at 2–3% rate annually.

The reason of such interest relies on the fact that D-sorbitol has all the characteristics of a typical bio-based platform chemical in terms of sustainability, applications and market value. In fact, dehydration of D-sorbitol (Scheme 1) produces anhydro sugar alcohols, including sorbitan (mono-anhydrosorbitol) and isosorbide (dianhydrosorbitol). Both these products have achieved commercial importance and can be used to synthesize numerous intermediates of industrial interest (Figure 2). Selected examples include isosorbide nitrate derivatives, well-known vasodilator drugs for treatment of heart-related deseases [4,5]; isosorbide alkyl esters, bio-based plasticizers [6-10] and short-chain aliphatic isosorbide ethers that have recently found application as coalescent for paints (Figure 2) [11-14].

The isosorbide moiety has also been incorporated in several bio-based polymers, i.e., poly(ethylene-*co*-isosorbide)terephthalate (PEIT), poly(isosorbide oxalate) and poly(isosorbide carbonate) [15-18] such as DURABIO® and PLANEXT®.
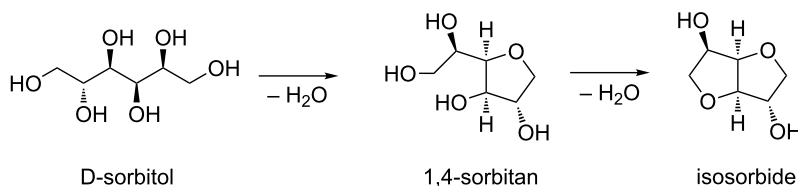
Scheme 1: Conversion of D-sorbitol to isosorbide via twofold dehydration reaction.
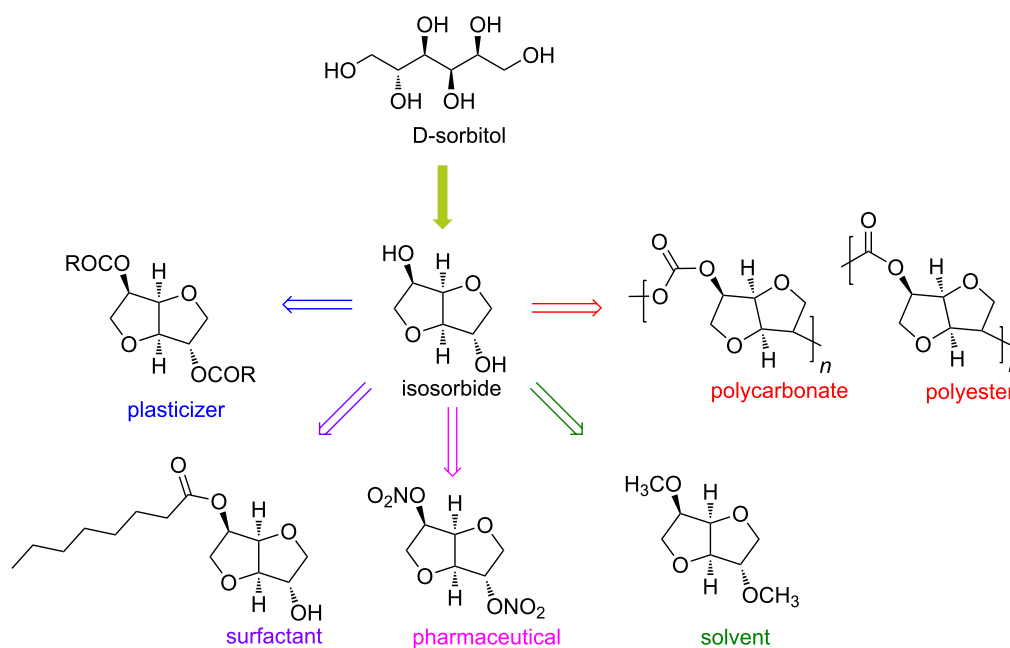
Figure 2: Chemical structure of isosorbide and its epimers isomannide and isoidide.

Furthermore dimethyl isosorbide (DMI; bp 235 °C) [19], has found applications as potential substitute of high-boiling solvents (DMSO, DMF) and long chain aliphatic ester derivatives of isosorbide (mono- and disubstituted) have been investigated as surfactants [20].

However, it should be pointed out that, despite D-sorbitol and isosorbide are renewable materials, their derivatizations do not always follow the green chemistry principles. In this prospect, the present work is focussed on the reactivity of D-sorbitol and isosorbide with the green reagent and solvent dimethyl carbonate (DMC).

Dimethyl carbonate, the simplest among the dialkyl carbonate (DAC) family, is nowadays produced by a clean and halogen-free process [21-23]. This compound has been extensively employed as green substitute of highly toxic phosgene in carboxymethylation reactions and methyl halides or other noxious methylating agents in methylation reactions [24-35].

The reactions between the bio-based chemicals D-sorbitol or isosorbide and DMC, are very appealing as they encompass the preparation, as well as the transformation of a renewable resource into industrially relevant products via a chlorine-free and green approach.

Synthesis of isosorbide via dimethyl carbonate

The current research on the preparation of D-sorbitol is mainly focussed on direct hydrolytic hydrogenation of cellulose [36-39] via a two-step reaction:

1. Conversion of cellulose into glucose by hydrolysis.
2. Hydrogenation of glucose to D-sorbitol.

An appropriate catalyst for this process should provide both acid sites (hydrolysis) and metallic sites (hydrogenation). Thus, several bifunctional catalytic systems have been investigated [40-44]. The use of ionic liquids as reaction media has been also

taken into consideration, although their use is limited by solubility problems and environmental concerns [45-48].

Despite the continuous research on its direct preparation from cellulose, D-sorbitol is nowadays synthesized on industrial scale by hydrogenation of glucose via biotechnological and chemocatalytic depolymerization of polysaccharides. The conversion of D-sorbitol into isosorbide via sorbitan is then usually performed by a twofold dehydration reaction using different types of catalysts (Scheme 1) [49-60].

In 1968 Fleche and co-workers reported the first synthesis of isosorbide from D-sorbitol using sulfuric acid as catalyst [61,62]. The reaction was performed at 400 K in a batch reactor. This process results in good yields (ca 70%), but it also poses some issues such as difficult separation of isosorbide from the reaction mixture and the use of a large amount of sulfuric acid. As a result current research on new synthetic approaches for the cyclic sugar isosorbide has been focussed on less toxic and easy to recover heterogeneous acidic catalysts. In particular, mixed oxides [49], phosphated or sulfated oxides [50-56], sulfonic resins [57-59] and bimetallic catalysts [60] have been investigated.

Extensive work has also been conducted on the use of zeolites, which compared to the above mentioned catalysts, have the advantage to be thermal stable and possess tuneable properties. However, zeolites are not very efficient catalysts for the dehydration of D-sorbitol as isosorbide yields usually range between 40 to 60% [57,63,64]. Furthermore they also require high temperature, i.e., 430–533 K.

Recently Fukuoka and co-workers reported a new efficent Hβ zeolite with a high Si/Al ratio (up to 75) that showed an improved activity and allowed dehydration of D-sorbitol into isosorbide in 76% yield at 400 K (127 °C) [65]. The Hβ zeolite

can also be reused up to five times before losing its activity as catalyst.

Despite this methodology being one of the most promising so far reported, it still requires the separation and purification of isosorbide from the reaction mixture. In this view, a different synthetic approach to isosorbide employs the versatile, green reagent and solvent dimethyl carbonate (DMC) as dehydrating agent.

The reaction between D-sorbitol and DMC performed in the presence of a base at reflux temperature (90 °C) leads to the high yielding formation of isosorbide (Table 2). The advantage of this synthesis is that the reagents are commercially available and isosorbide can be easily recovered by filtration of the excess of base and removal of the solvent which can be eventually reused.

A first set of experiments was conducted at 90 °C and atmospheric pressure using an excess of strong base, i.e., sodium methoxide (entries 1–3, Table 2). In particular, when the reaction was performed in the presence of 2 equiv of sodium methoxide, isosorbide was formed only in modest yield (entry 1, Table 2).

The main issue of this procedure was that isosorbide, once formed, can further react with DMC leading to the formation of its methoxycarbonyl and methyl derivatives [35]. However, when methanol was used as a solvent (entries 2–3, Table 2), the numerous equilibria that affect the formation of the product can be efficiently shifted towards isosorbide preventing any further reactions (Scheme 2). Best results were achieved when an excess of NaOMe was employed (entry 3, Table 2). The necessity of an excess of base might be ascribed to the complexity of this one-pot double cyclisation reaction that requires 2 equiv of base for each tetrahydrofuran formed.

Table 2: Synthesis of isosorbide by DMC chemistry.[a]

entry	Solvent	Cat./base (equiv)	DMC (equiv)	Time (h)	Isosorbide % (% isolated yield)
1	None	NaOMe (2.0)	20	8	16
2	MeOH	NaOMe (2.0)	4	8	80 (64)
3	MeOH	NaOMe (4.0)	8	8	98 (76)
4	MeOH	DBU (1.0)	8	7	100 (98)
5	MeOH	DBU (0.25)	8	7	100 (98)
6	MeOH	DBU (0.05)	8	24	100 (98)

[a]Reaction conditions: D-Sorbitol 2 g (1 equiv); reflux temperature; conversion of the starting material was in all cases quantitative.

Scheme 2: Possible reaction mechanism for the conversion of D-sorbitol to isosorbide.
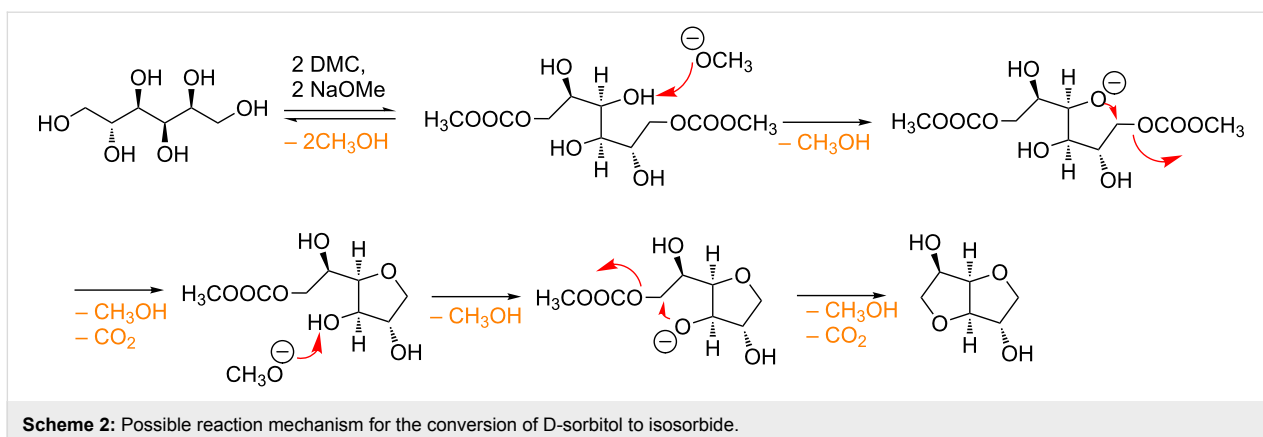
The reaction mechanism is quite complex (Scheme 2) since it encompasses two carboxymethylation reactions (via $B_{Ac}2$) followed by two intramolecular cyclisations (via $B_{Al}2$).

In order to avoid the use of excess base, several alternative catalysts and bases have been taken into consideration. Recently it has been reported that 1,5-diazabiciclo(5.4.0)undec-5-ene (DBU) can be used in stoichiometric amounts for the efficient synthesis of isosorbide via DMC chemistry (entry 4, Table 2) [66]. Under these reaction conditions, isosorbide was obtained in pure form by filtration on a silica pad and evaporation of the DMC. Even when the amount of DBU was reduced to 5 mol % (entries 4–6, Table 2) the cyclic sugar was still formed in quantitative yield. It is also noteworthy that, although the catalyst employed is homogenous, the amount of DBU used was, in the latter case (entry 6, Table 2) only 2.5 mol % for each tetrahydrofuranic cycle. The same synthetic approach can be also employed for the cyclisation of D-mannitol.

The synthesis of isosorbide via DMC chemistry takes advantage of the enhanced reactivity of DMC in the presence of the nitrogen bicyclic base DBU. It has been, in fact, reported that organic carbonates are activated by DBU via formation of an *N*-alkoxycarbonyl DBU derivative [67-71]. However, in this case study, DBU most probably promotes the formation of the methoxycarbonyl reaction intermediate, as well as the intramolecular cyclisation reaction ($B_{Al}2$ mechanism).

It is also noteworthy that in general alkylation reactions promoted by DMC chemistry are conducted at temperatures above 150 °C [24-35], but in this case study the intramolecular cyclisation step leading to isosorbide, which is an alkylation reaction (Scheme 2), takes place at the DMC refluxing temperature (90 °C).

To explain this result, computational investigations were conducted on a model compound. The collected results demonstrated that the cyclisation reaction leading to the 5-membered ring is a preferred pathway compared to other possible ones (7-membered ring closure, alcoholate attacks onto DMC) due to a big entropic effect [35].

Reactivity of isosorbide with dimethyl carbonate

One of the most investigated research fields for the sustainable platform chemical isosorbide is the synthesis of bio-based polymers (Figure 1). In fact, isosorbide has been extensively employed for the preparation of polyesters, polyurethanes and polycarbonates [72-81]. Isosorbide is also considered as a possible candidate to replace petroleum-derived and toxic bisphenol A in polycarbonate preparation. In this view, the main issue that limits the exploitation of this compound is its lower acidity. To overcome this problem, polycarbonates incorporating an isosorbide moiety have been synthesized via a chlorine-based approach, i.e., employing phosgene or its derivatives [82,83].

On another hand, a greener synthetic methodology to bio-based polymers is to first synthesize a more reactive derivative of isosorbide and then perform the polycondensation reaction (Scheme 4). In this prospect a good candidate is the dicarboxymethyl isosorbide (DCI). In fact, methoxycarbonylation of isosorbide via DMC chemistry is a relative simple reaction that has been extensively investigated ($B_{Ac}2$ mechanism according to Scheme 3).

Data reported in the literature show that carboxymethylation of isosorbide can be achieved by reacting isosorbide with an excess of DMC at refluxing temperature in the presence of potassium carbonate (Table 3) [84]. Under these conditions, due to the presence of four chiral centres in the isosorbide backbone, three products can be formed, the wanted dicarboxymethyl carbonate (DCI) and two monocarboxymethyl carbonates MCI-1 and MCI-2 (Scheme 3).
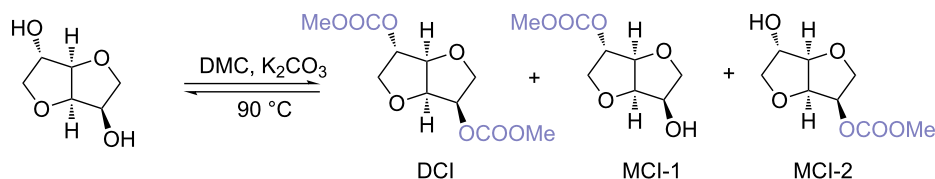
Scheme 3: Methoxycarbonylation of isosorbide via DMC chemistry.

Table 3: Synthesis of dicarboxymethyl isosorbide (DCI) by DMC chemistry.[a]

#	K$_2$CO$_3$	Selectivity (%)		
	(equiv)	MCI-1	MCI-2	DC
1[b]	1.00	37	9	54
2	1.00	10	5	85
3	0.50	11	4	85
4	0.10	8	2	90

[a]Reaction conditions: isosorbide DMC 1:30 equiv; temperature 90 °C; reaction time 6 h. All the reactions have been conducted under anhydrous conditions. Conversion was always quantitative. [b]The reaction has not been conducted under anhydrous conditions.

When isosorbide was reacted with an excess of DMC (30 equiv) in the presence of a stoichiometric amount of K$_2$CO$_3$ (1 equiv), a quantitative conversion of the substrate was observed, but the selectivity toward DCI was just moderate. Monocarboxymethyl derivatives MCI-1 and MCI-2 were still present in the reaction mixture (entry 1, Table 3).

However, repeating the reaction under anhydrous conditions, the selectivity towards DCI increased to 85% (entry 2, Table 3).

Most probably, even a small amount of water can affect the outcome of the reaction as it can hydrolyse the DMC molecule into CO$_2$ and methanol. The latter, once formed, shifts the reaction equilibrium towards the reagent and the monocarboxymethyl derivatives. When the reaction is performed under anhydrous conditions, the amount of potassium carbonate can be decreased up to 10 mol % (entries 3 and 4, Table 3) without affecting the reaction outcome.

Recently DCI has been also prepared via DMC chemistry in the presence of lithium acetylacetonate (Li(acac)) as catalyst [85]. Dicarboxymethyl isosorbide, once formed, has been directly converted into either homo- or co-polycarbonate via an easy straight-forward procedure (Scheme 4).

In the case of homopolymer preparation, DCI was synthesised by reacting isosorbide, DMC and Li(acac) at 98 °C. The polycondensation was then achieved employing an high vacuum and increasing the temperature to 240 °C. The so-formed poly(isosorbide carbonate) had a molecular weight (M_n) of 28,800 g/mol. The conversion of isosorbide was almost quantitative (95.2%).

Similarly poly(aliphaticdiol-*co*-isosorbide carbonate)s were prepared via melt polycondensation of DMC with isosorbide
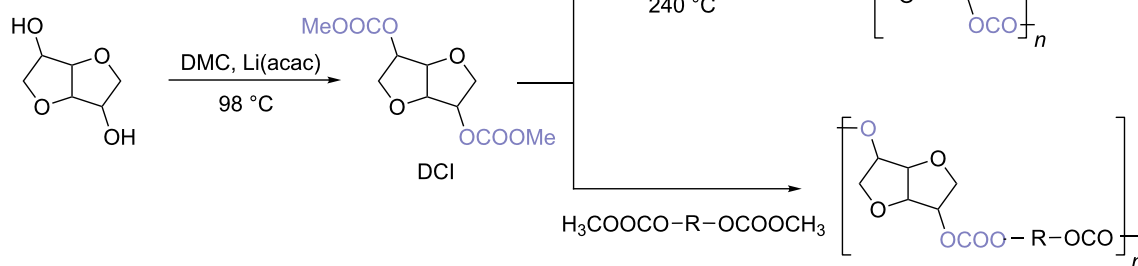
Scheme 4: Isosorbide homo- and co-polycarbonate via melt polycondensation.

and several aliphatic diols employing Li(acac) and the TiO$_2$/SiO$_2$-based catalyst (Scheme 4) [85].

High-molecular-weight (M_w = 32,600) and optically clear isosorbide-based polycarbonates were also reported by Shin and co-workers [86]. However, in this case, the polymerisation reaction was conducted using diphenyl carbonate in the presence of a catalytic amount of cesium carbonate.

Another interesting isosorbide derivative is dimethyl isosorbide (DMI) that has potential application as green solvent substitute of high boiling polar solvents. Recently DMI has also appeared as component in the formulation of deodorants [87].

Methylation of isosorbide has been investigated both at reflux and in autoclave conditions via DMC chemistry. It should be mentioned that generally methylation of secondary alcohols via DMC chemistry requires high temperatures (>150 °C) and was never obtained in high yield due to the formation of elimination products [88]. However, isosorbide, which incorporates in its backbone secondary hydroxy groups, was quantitatively methylated at the reflux temperature of DMC (90 °C) in the presence of a base (Table 3) [19]. This is particularly significant since the reaction of isosorbide with DMC (Scheme 5) can lead to the formation of numerous compounds such as: carboxymethyl derivates (MCI-1, MCI-2, DC), carboxymethyl methyl derivates (MCEI-1, MCEI-2) and methyl derivates (MMI-1, MMI-2 and DMI).

As reported in Table 4 performing the methylation reaction at the reflux temperature of DMC in the presence of a strong base (stoichiometric amount) resulted in a moderate yield of DMI (entries 1 and 2, Table 4). Quantitative conversion of isosorbide into DMI was obtained only using an excess of sodium methoxide (entry 3; Table 4).

In order to optimize the reaction conditions and reduce the amount of catalyst, the methylation of isosorbide was also conducted in an autoclave at higher temperature in the presence of a base. Using weak base K$_2$CO$_3$ in stoichiometric amount at 200 °C already resulted in a selectivity towards DMI of ca. 57%. Comparable results were achieved by using a stronger base, i.e., *t*-BuOK, (entry 5, Table 4).

However, when hydrotalcite KW2000 (Mg$_{0.7}$Al$_{0.3}$O$_{1.15}$), a catalyst that incorporates both acidic and basic sites, was used (1:1 w/w ratio) DMI formed in good yield (86%) (entries 6 and 7, Table 4). Hydrotalcite has the advantage to be heterogeneous, thus it can be eventually recycled. The reaction mechanism involving hydrotalcite is not yet fully understood, most probably the acidic sites activates the DMC molecule and at the same time the basic sites activate the substrate.

Interestingly, isosorbide peculiar backbone seems to play a very important role in the methylation reaction via DMC chemistry. In fact when the methylation via DMC reaction was performed on other secondary alcohols in the best found conditions at the reflux temperature of DMC, methyl derivatives were either not
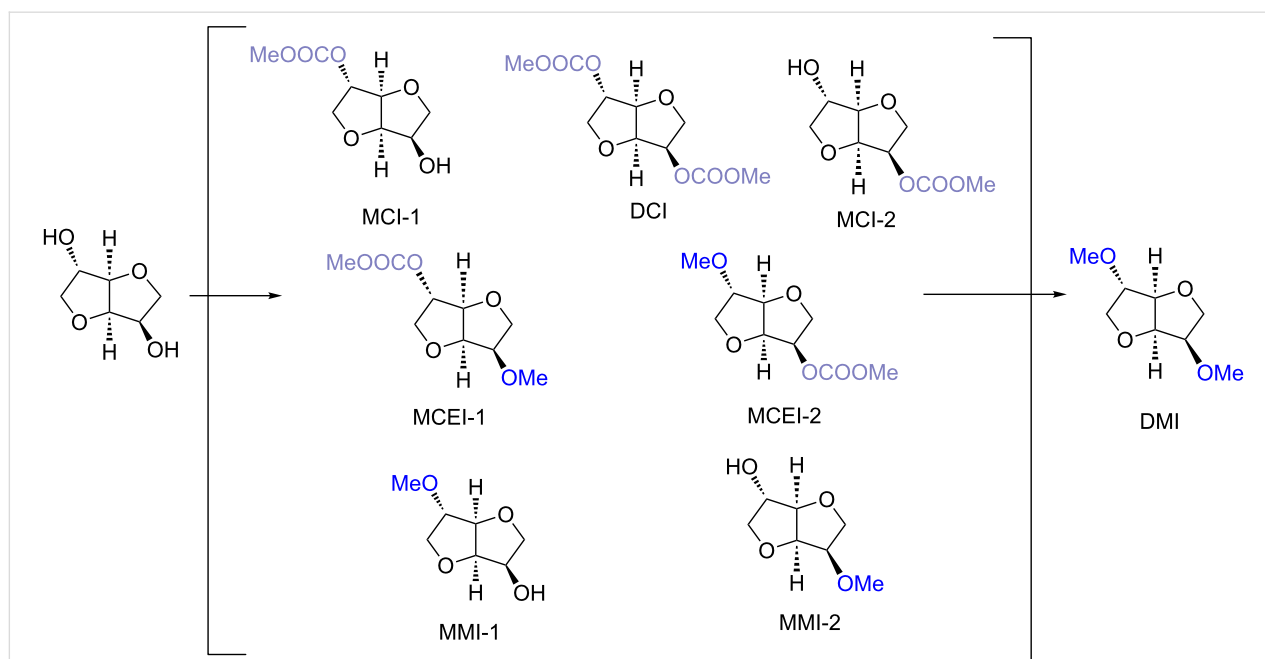
Scheme 5: Synthesis of DMI via DMC chemistry.

Table 4: Synthesis of dimethyl isosorbide (DMI) by DMC chemistry.[a]

| entry	Base	Temp	Selectivity (%)[b]				
	(equiv)	(°C)	DMI	MMI-1	MMI-2	MCEI-1	MCEI-2
1	*t*-BuOK (1.5)	90	40	2	2	37	18
2	NaOMe (1.5)	90	26	11	6	30	12
3	NaOMe (3.0)	90	100	0	0	0	0
4[c]	K_2CO_3 (1.0)	200	57	4	7	29	0
5[c]	*t*-BuOK (1.0)	200	55	5	6	34	0
6[c]	KW2000[d]	180	83	1	3	12	0
7[c]	KW2000[d]	200	86	0	2	12	0

[a]Reaction conditions: Isosorbide DMC 1:50 equiv; Reaction time 20 h; Conversion 100%. [b]Carboxymethyl derivatives MCI-1, MCI-2 and DC have been detected only in traces. [c]Reaction conducted in an autoclave under pressure. [d]Hydrotalcite was calcinated at 400 °C overnight prior its use.

observed or formed in small amount (Scheme 6). In particular, 2-octanol gave only the carboxymethyl derivative, meanwhile the methyl derivatives of propylene glycol propyl ether and 3-hydroxytetrahydrofuran formed only in scarce amount. Among the substrates investigated, isosorbide was the only one leading to almost quantitative methylation confirming the influence of its peculiar backbone on the reactivity of this compound.

In fact, the growing interest in isosorbide is justify not only by its bio-based nature and industrial applications, but also by its high reactivity and peculiar molecular structure [89]. Isosorbide has an open-book V-shaped configuration formed by two *cis*-connected tetrahydrofuran rings with an opening angle of 120°. The four oxygen atoms incorporated in the structure are in β-position to each other [61,62]. The secondary hydroxy moiety in the 2-position directed toward the V-shaped cavity is labelled as *endo*, meanwhile the one in the 5-position pointing outside of the sugar cavity is indicated as *exo* (Figure 3).

The configuration of the two hydroxy groups has been shown to influence the reactivity of isosorbide. In fact, its epimers,
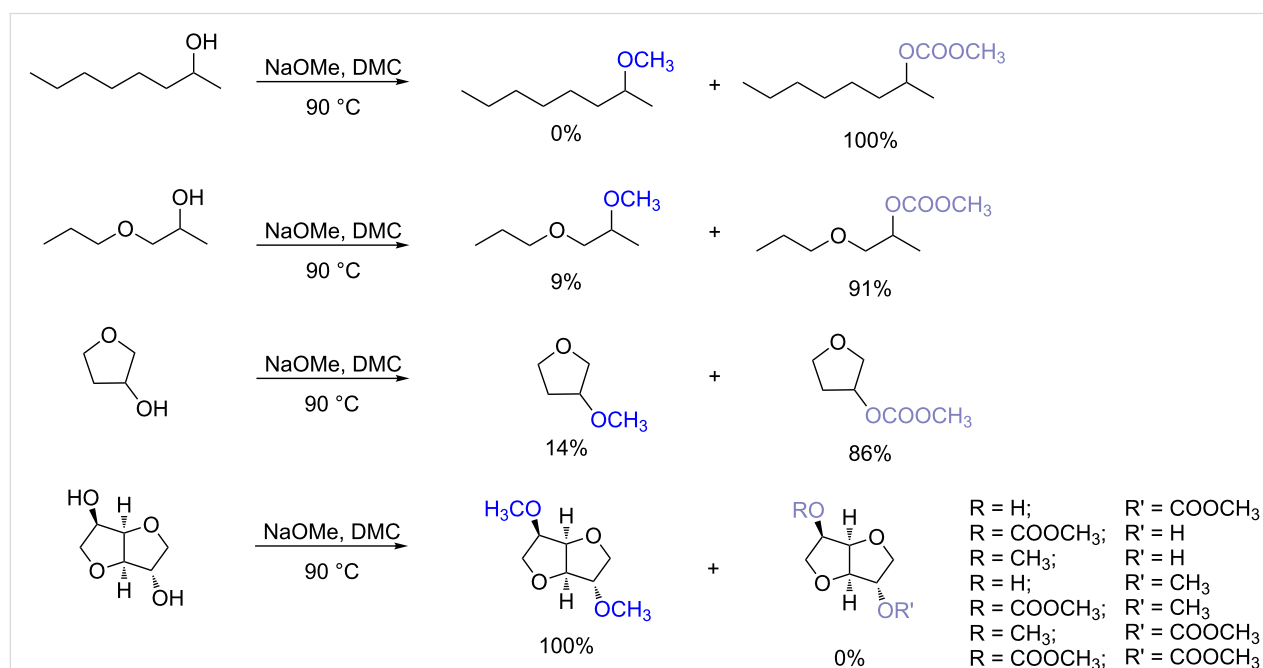
Scheme 6: Comparison of the reactivity of isosorbide with other secondary alcohols in methylation reaction. Reaction conditions: Isosorbide DMC 1:50 equiv; reaction time 20 h; 90 °C.

Figure 3: Chemical structure of isosorbide and its epimers isomannide and isoidide.
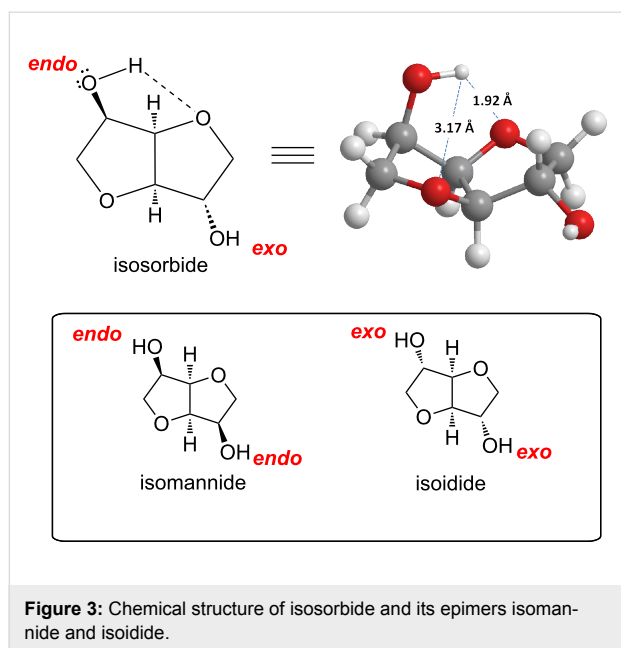
isoidide and isomannide, that incorporate only *exo* or *endo* hydroxy groups, have different physical/chemical properties, as well as diverse reactivity. Thus, the easy methylation of isosorbide is most probably due to the unique V-shaped structure of isosorbide in combination with the presence of four oxygen atoms all in β position to each other that enhance the nucleophilicity of the hydroxy groups.

Conclusion

Among the top chemical opportunities from biorefinery carbohydrates D-sorbitol is a platform chemical of considerable interest that has led to intensive research in the last years especially as the parent alcohol of isosorbide. The latter is also a platform chemical with applications in pharmaceuticals, detergents, fuel additives, monomers and building blocks for new polymers and functional materials and new high boiling organic solvents. Conversion of D-sorbitol into isosorbide and its consequent transformation into valuable derivatives is under intense investigation.

In this review, we have focussed on the reactivity of D-sorbitol and isosorbide with the green reagent and solvent DMC as a relevant example of green and halogen-free chemistry. It has been, in fact, reported that dehydration of D-sorbitol can be efficiently conducted using DMC used as dehydrating agent in the presence of a catalytic amount of the homogenous catalyst DBU under mild conditions. Compared to the other synthetic pathways reported in the literature, the DMC based synthetic approach is a "chlorine-free", one-pot and environmental friendly method that does not require any time consuming purification technique and allowed isolation of a very pure crystalline prod-

uct using commercially available reagents. To the best to our knowledge, this synthetic approach is the one resulting in the highest isolated yield.

Dicarboxymethyl isosorbide is also an intermediate of great interest in view of its application as monomer for homo- and co-polycarbonates incorporating the isosorbide subunit.

In this prospect, carboxymethylation of isosorbide can be efficiently carried out via DMC chemistry via a $B_{Ac}2$ mechanism employing a catalytic amount of K_2CO_3 at reflux conditions in anhydrous conditions.

Li(acac) has also been reported as efficient and selective catalyst that was efficiently used for carboxymethylation reaction of isosorbide and its consequent polymerization reaction to achieve bio-based polymers.

Another interesting derivate of isosorbide is dimethyl isosorbide that has potential in applications as green high boiling bio-based solvent. In this case, DMC was efficiently used as methylating agent of isosorbide at its reflux temperature (90 °C) in the presence of an excess of base. This result was ascribed to the neighbouring effect of the oxygen situated all in β-position to each other that most probably enhances the nucleophilicity of the corresponding hydroxy group.

Furthermore the amphoteric catalyst hydrotalcite was extremely efficient in the synthesis of DMI when tested in an autoclave at higher temperature and has the additional advantage that it can be recycled.

It is thus noteworthy that the reactions involving bio-based platform compounds D-sorbitol and isosorbide with green reagent and solvent DMC encompass free-halogen chemistry to achieve industrially relevant products that might substitute fossil-based compounds and that are a poignant example of innovation at molecular level that nicely combines green chemistry reactions with biorefinery of carbohydrates.

References

1. Bozell, J. J.; Petersen, G. R. *Green Chem.* **2010,** *12,* 539–554. doi:10.1039/b922014c
2. Despite being 15 this list is usually referred as DOE "Top 10" report.
3. Werpy, T.; Petersen, G. *Top Value Added Chemicals from Biomass. Results of Screening for Potential Candidates from Sugars and Synthesis Gas;* U.S. Department of Energy, 2004; Vol. I.
4. Parker, J. D.; Parker, J. O. *N. Engl. J. Med.* **1998,** *338,* 520–531. doi:10.1056/NEJM199802193380807
5. Obach, R. S.; Lombardo, F.; Waters, N. J. *Drug Metab. Dispos.* **2008,** *36,* 1385–1405. doi:10.1124/dmd.108.020479

6. Van Es, D. S.; Frissen, A. E.; Luitjes, H. Improved synthesis of anhydroglycitol esters of improved colour. WO Patent WO0183488A1, Nov 8, 2001.

7. Grass, M.; Scholz, N.; Kaizik, A.; Bueschken, W.; Lueken, H.-G. Mixture of diesters of dianhydrohexitol derivatives with carboxylic acids of the empirical formula $C_8H_{17}COOH$, process for preparing these diesters, and use of these mixtures. U.S. Patent U.S. 20090301348A1, Dec 10, 2009.

8. Grass, M.; Scholz, N.; Kaizik, A.; Büschken, W.; Lüken, H.-G. Mélanges de diesters de dérivés de dianhydrohexitol avec des acides carboxyliques de formule générale $C_8H_{17}COOH$, procédé de production de ces diesters, et utilisation de ces mélanges. WO Patent WO2008/095571A1, Aug 14, 2008.

9. Yang, Y.; Xiong, Z.; Zhang, L.; Tang, Z.; Zhang, R.; Zhu, J. *Mater. Des.* **2016,** *91,* 262–268. doi:10.1016/j.matdes.2015.11.065

10. Cui, C.; Zhen, Y.; Qu, J.; Chen, B.; Tan, T. *RSC Adv.* **2016,** *6,* 11959–11966. doi:10.1039/C5RA27537G

11. Durand, M.; Molinier, V.; Féron, T.; Aubry, J.-M. *Prog. Org. Coat.* **2010,** *69,* 344–351. doi:10.1016/j.porgcoat.2010.07.007

12. Durand, M.; Zhu, Y.; Molinier, V.; Féron, T.; Aubry, J.-M. *J. Surfactants Deterg.* **2009,** *12,* 371–378. doi:10.1007/s11743-009-1128-4

13. Zhu, Y.; Molinier, V.; Durand, M.; Lavergne, A.; Aubry, J.-M. *Langmuir* **2009,** *25,* 13419–13425. doi:10.1021/la902065q

14. Zhu, Y.; Durand, M.; Molinier, V.; Aubry, J.-M. *Green Chem.* **2008,** *10,* 532–540. doi:10.1039/b717203f

15. Fenouillot, F.; Rousseau, A.; Colomines, G.; Saint-Loup, R.; Pascault, J.-P. *Prog. Polym. Sci.* **2010,** *35,* 578–622. doi:10.1016/j.progpolymsci.2009.10.001

16. Charbonneau, L. F.; Johnson, R. E.; Witteler, H. B.; Khanarian, G. Isosorbide containing polyesters and methods for making same. U.S. Patent U.S. 6.063.464, May 16, 2000.

17. Ono, A.; Toyohara, K.; Minematsu, H.; Kageyama, Y. Polycarbonate and process for producing the same. U.S. Patent U.S. 7.365.148, April 29, 2008.

18. Fuertes, P.; Ibert, M.; Josien, E.; Tundo, P.; Aricò,, F. Procédé de préparation de di (alkylcarbonate) de dianhydrohexitol. WO Patent WO2011/039483A1, April 7, 2011.

19. Tundo, P.; Aricò, F.; Gauthier, G.; Rossi, L.; Rosamilia, A. E.; Bevinakatti, H. S.; Sievert, R. L.; Newman, C. P. *ChemSusChem* **2010,** *3,* 566–570. doi:10.1002/cssc.201000011

20. Lavergne, A.; Zhu, Y.; Molinier, V.; Aubry, J.-M. *Colloids Surf., A* **2012,** *404,* 56–62. doi:10.1016/j.colsurfa.2012.04.007

21. Fukuoka, S.; Miyaji, H.; Hachiya, H.; Matsuzaki, K. Process for industrially producing dialkyl carbonate and diol. U.S. Patent US8058465 B2, Nov 17, 2006.

22. Budavari, S., Ed. *The Merck Index,* 11th ed.; Merck and Co. Inc.: Ralway, NJ, 1989.

23. Wang, M.; Wang, H.; Zhao, N.; Wei, W.; Sun, Y. *Ind. Eng. Chem. Res.* **2007,** *46,* 2683–2687. doi:10.1021/ie061101u

24. Rosamilia, A. E.; Aricò, F.; Tundo, P. *J. Org. Chem.* **2008,** *73,* 1559–1562. doi:10.1021/jo701818d

25. Tundo, P.; McElroy, C. R.; Aricò, F. *Synlett* **2010,** *10,* 1567–1571. doi:10.1055/s-0029-1219927

26. Tundo, P.; Aricò, F.; Rosamilia, A. E.; Memoli, S. *Green Chem.* **2008,** *10,* 1182–1189. doi:10.1039/b809271k

27. Tundo, P.; Aricò, F.; Rosamilia, A. E.; Rigo, M.; Maranzana, A.; Tonachini, G. *Pure Appl. Chem.* **2009,** *81,* 1971–1979. doi:10.1351/PAC-CON-08-12-02

28. Grego, S.; Aricò, F.; Tundo, P. *Org. Process Res. Dev.* **2013,** *17,* 679–683. doi:10.1021/op4000048

29. Tundo, P.; Aricò, F.; Gauthier, G.; Baldacci, A. *C. R. Chim.* **2011,** *14,* 652–655. doi:10.1016/j.crci.2010.11.011

30. Aricò, F.; Tundo, P. *Russ. Chem. Rev.* **2010,** *79,* 479–489. doi:10.1070/RC2010v079n06ABEH004113

31. Rosamilia, A. E.; Aricò, F.; Tundo, P. *J. Phys. Chem. B* **2008,** *112,* 14525–14529. doi:10.1021/jp804814e

32. McElroy, C. R.; Aricò, F.; Benetollo, F.; Tundo, P. *Pure Appl. Chem.* **2011,** *84,* 707–719. doi:10.1351/PAC-CON-11-07-18

33. Aricò, F.; Chiurato, M.; Peltier, J.; Tundo, P. *Eur. J. Org. Chem.* **2012,** 3223–3228. doi:10.1002/ejoc.201200321

34. Aricò, F.; Evaristo, S.; Tundo, P. *ACS Sustainable Chem. Eng.* **2013,** *1,* 1319–1325. doi:10.1021/sc4001737

35. Aricò, F.; Tundo, P.; Maranzana, A.; Tonachini, G. *ChemSusChem* **2012,** *5,* 1578–1586. doi:10.1002/cssc.201100755

36. Van de Vyver, S.; Geboers, J.; Jacobs, P. A.; Sels, B. F. *ChemCatChem* **2011,** *3,* 82–94. doi:10.1002/cctc.201000302

37. Geboers, J.; Van de Vyver, S.; Carpentier, K.; de Blochouse, K.; Jacobs, P.; Sels, B. *Chem. Commun.* **2010,** *46,* 3577–3579. doi:10.1039/c001096k

38. Deng, W.; Liu, M.; Tan, X.; Zhang, Q.; Wang, Y. *J. Catal.* **2010,** *271,* 22–32. doi:10.1016/j.jcat.2010.01.024

39. Yamaguchi, A.; Sato, O.; Mimura, N.; Shirai, M. *Catal. Commun.* **2015,** *67,* 59–63. doi:10.1016/j.catcom.2015.04.009

40. Jollet, V.; Chambon, F.; Rataboul, F.; Cabiac, A.; Pinel, C.; Guillon, E.; Essayem, N. *Green Chem.* **2009,** *11,* 2052–2060. doi:10.1039/b915758a

41. Dhepe, P. L.; Fukuoka, A. *Catal. Surv. Asia* **2007,** *11,* 186–191. doi:10.1007/s10563-007-9033-1

42. Luo, C.; Wang, S.; Liu, H. *Angew. Chem., Int. Ed.* **2007,** *46,* 7636–7639. doi:10.1002/anie.200702661

43. Geboers, J.; Van de Vyver, S.; Carpentier, K.; Jacobs, P.; Sels, B. *Chem. Commun.* **2011,** *47,* 5590–5592. doi:10.1039/c1cc10422e

44. Op de Beeck, B.; Geboers, J.; Van de Vyver, S.; Van Lishout, J.; Snelders, J.; Huijgen, W. J. J.; Courtin, C. M.; Jacobs, P. A.; Sels, B. F. *ChemSusChem* **2013,** *6,* 199–208. doi:10.1002/cssc.201200610

45. Ignatyev, I. A.; Van Doorslaer, C.; Mertens, P. G. N.; Binnemans, K.; De Vos, D. E. *ChemSusChem* **2010,** *3,* 91–96. doi:10.1002/cssc.200900213

46. Van Doorslaer, C.; Wahlen, J.; Mertens, P. G. N.; Thijs, B.; Nockemann, P.; Binnemans, K.; De Vos, D. E. *ChemSusChem* **2008,** *1,* 997–1005. doi:10.1002/cssc.200800140

47. Berger, A.; de Souza, R. F.; Delgado, M. R.; Dupont, J. *Tetrahedron: Asymmetry* **2001,** *12,* 1825–1828. doi:10.1016/S0957-4166(01)00341-X

48. Zhu, Y.; Kong, Z. N.; Stubbs, L. P.; Lin, H.; Shen, S.; Anslyn, E. V.; Maguire, J. A. *ChemSusChem* **2010,** *3,* 67–70. doi:10.1002/cssc.200900235

49. Morita, Y.; Furusato, S.; Takagaki, A.; Hayashi, S.; Kikuchi, R.; Oyama, S. T. *ChemSusChem* **2014,** *7,* 748–752. doi:10.1002/cssc.201300946

50. Xi, J.; Zhang, Y.; Ding, D.; Xia, Q.; Wang, J.; Liu, X.; Lu, G.; Wang, Y. *Appl. Catal., A* **2014,** *469,* 108–115. doi:10.1016/j.apcata.2013.08.049

51. Gu, M.; Yu, D.; Zhang, H.; Sun, P.; Huang, H. *Catal. Lett.* **2009,** *133,* 214–220. doi:10.1007/s10562-009-0142-5

52. Xia, J.; Yu, D.; Hu, Y.; Zou, B.; Sun, P.; Li, H.; Huang, H. *Catal. Commun.* **2011,** *12,* 544–547. doi:10.1016/j.catcom.2010.12.002

53. Khan, N. A.; Mishra, D. K.; Ahmed, I.; Yoon, J. W.; Hwang, J.-S.; Jhung, S. H. *Appl. Catal., A* **2013,** *452,* 34–38. doi:10.1016/j.apcata.2012.11.022

54. Ahmed, I.; Khan, N. A.; Mishra, D. K.; Lee, J. S.; Hwang, J.-S.; Jhung, S. H. *Chem. Eng. Sci.* **2013,** *93,* 91–95. doi:10.1016/j.ces.2013.01.068

55. Shi, J.; Shan, Y.; Tian, Y.; Wan, Y.; Zheng, Y.; Feng, Y. *RSC Adv.* **2016,** *6,* 13514–13521. doi:10.1039/C5RA27510E

56. Rusu, O. A.; Hoelderich, W. H.; Wyart, H.; Ibert, M. *Appl. Catal., B: Environ.* **2015,** *176–177,* 139–149. doi:10.1016/j.apcatb.2015.03.033

57. Moore, K. M.; Sanborn, A. J.; Bloom, P. Process for the production of anhydrosugar alcohols. U.S. Patent U.S. 7.439.352, Oct 21, 2008.

58. Holladay, J. E.; Hu, J.; Zhang, X.; Wang, Y. Methods for dehydration of sugars and sugar alcohols. U.S. Patent U.S. 7.772.412, Aug 10, 2010.

59. Zhang, J.; Wang, L.; Liu, F.; Meng, X.; Mao, J.; Xiao, F.-S. *Catal. Today* **2015,** *242,* 249–254. doi:10.1016/j.cattod.2014.04.017

60. Montassier, C.; Ménézo, J. C.; Moukolo, J.; Naja, J.; Hoang, L. C.; Barbier, J.; Boitiaux, J. P. *J. Mol. Catal.* **1991,** *70,* 65–84. doi:10.1016/0304-5102(91)85006-N

61. Flèche, G.; Huchette, M. *Starch/Staerke* **1986,** *38,* 26–30. doi:10.1002/star.19860380107

62. Andrews, M. A.; Bhatia, K. K.; Fagan, P. J. Process for the manufacture of anhydro sugar alcohols with the assistance of a gas purge. U.S. Patent U.S. 6.689.892, Feb 10, 2004.

63. Kurszewska, M.; Skorupowa, E.; Madaj, J.; Konitz, A.; Wojnowski, W.; Wiśniewski, A. *Carbohydr. Res.* **2002,** *337,* 1261–1268. doi:10.1016/S0008-6215(02)00129-5

64. Li, N.; Huber, G. W. *J. Catal.* **2010,** *270,* 48–59. doi:10.1016/j.jcat.2009.12.006

65. Kobayashi, H.; Yokoyama, H.; Feng, B.; Fukuoka, A. *Green Chem.* **2015,** *17,* 2732–2735. doi:10.1039/C5GC00319A

66. Aricò, F.; Evaristo, S.; Tundo, P. *Green Chem.* **2015,** *17,* 1176–1185. doi:10.1039/C4GC01822B

67. Carafa, M.; Mesto, E.; Quaranta, E. *Eur. J. Org. Chem.* **2011,** 2458–2465. doi:10.1002/ejoc.201001725

68. Carafa, M.; Mele, V.; Quaranta, E. *Green Chem.* **2012,** *14,* 217–225. doi:10.1039/C1GC15984D

69. Heller, S. T.; Schultz, E. E.; Sarpong, R. *Angew. Chem., Int. Ed.* **2012,** *51,* 8304–8308. doi:10.1002/anie.201203976

70. Carafa, M.; Iannone, F.; Mele, V.; Quaranta, E. *Green Chem.* **2012,** *14,* 3377–3385. doi:10.1039/c2gc36103e

71. Quaranta, E.; Angelini, A.; Carafa, M.; Dibenedetto, A.; Mele, V. *ACS Catal.* **2014,** *4,* 195–202. doi:10.1021/cs400661q

72. Kricheldorf, H. R.; Chatti, S.; Schwarz, G.; Kruger, R.-P. *J. Polym. Sci., Part A: Polym. Chem.* **2003,** *41,* 3414–3424. doi:10.1002/pola.10933

73. Jasinska, L.; Koning, C. E. *J. Polym. Sci., Part A: Polym. Chem.* **2010,** *48,* 5907–5915. doi:10.1002/pola.24402

74. Quintana, R.; de Ilarduya, A. M.; Alla, A.; Muñoz-Guerra, S. *J. Polym. Sci., Part A: Polym. Chem.* **2011,** *49,* 2252–2260. doi:10.1002/pola.24657

75. Lee, C.-H.; Takagi, H.; Okamoto, H.; Kato, M.; Usuki, A. *J. Polym. Sci., Part A: Polym. Chem.* **2009,** *47,* 6025–6031. doi:10.1002/pola.23645

76. Beldi, M.; Medimagh, R.; Chatti, S.; Marque, S.; Prim, D.; Loupy, A.; Delolme, F. *Eur. Polym. J.* **2007,** *43,* 3415–3433. doi:10.1016/j.eurpolymj.2007.06.003

77. Marín, R.; Alla, A.; de Ilarduya, A. M.; Muñoz-Guerra, S. *J. Appl. Polym. Sci.* **2012,** *123,* 986–994. doi:10.1002/app.34545

78. Sun, S.-J.; Schwarz, G.; Kricheldorf, H. R.; Chang, T.-C. *J. Polym. Sci., Part A: Polym. Chem.* **1999,** *37,* 1125–1133. doi:10.1002/(SICI)1099-0518(19990415)37:8<1125::AID-POLA9>3.0.CO;2-J

79. Kricheldorf, H. R.; Sun, S.-J.; Gerken, A. *Macromolecules* **1996,** *29,* 8077–8082. doi:10.1021/ma960494d

80. Yokoe, M.; Aoi, K.; Okada, M. *J. Polym. Sci., Part A: Polym. Chem.* **2003,** *41,* 2312–2321. doi:10.1002/pola.10772

81. Chatti, S.; Schwarz, G.; Kricheldorf, H. R. *Macromolecules* **2006,** *39,* 9064–9070. doi:10.1021/ma0606051

82. Chatti, S.; Kricheldorf, H. R.; Schwarz, G. *J. Polym. Sci., Part A: Polym. Chem.* **2006,** *44,* 3616–3628. doi:10.1002/pola.21444

83. Noordover, B. A. J.; Haveman, D.; Duchateau, R.; van Benthem, R. A. T. M.; Koning, C. E. *J. Appl. Polym. Sci.* **2011,** *121,* 1450–1463. doi:10.1002/app.33660

84. Aricò, F.; Evaristo, S.; Tundo, P. *ScienceOpen Research* **2014.** doi:10.14293/S2199-1006.1.SORCHEM.AB3R7E.v1.

85. Li, Q.; Zhu, W.; Li, C.; Guan, G.; Zhang, D.; Xiao, Y.; Zheng, L. *J. Polym. Sci., Part A: Polym. Chem.* **2013,** *51,* 1387–1397. doi:10.1002/pola.26507

86. Seok Eo, Y.; Rhee, H.-W.; Shin, S. *J. Ind. Eng. Chem.* **2016,** *37,* 42–46. doi:10.1016/j.jiec.2016.03.007

87. Windisch, M.; Wieland, H. Deodorant comprising dimethyl isosorbide. Eur. Patent EP2574329, April 3, 2013.

88. Tundo, P.; Memoli, S.; Hérault, D.; Hill, K. *Green Chem.* **2004,** *6,* 609–612. doi:10.1039/B412722F

89. Rose, M.; Palkovits, R. *ChemSusChem* **2012,** *5,* 167–176. doi:10.1002/cssc.201100580

The weight of flash chromatography: A tool to predict its mass intensity from thin-layer chromatography

Freddy Pessel[1], Jacques Augé[2], Isabelle Billault[1] and Marie-Christine Scherrmann[*1]

Address:
[1]Université Paris Sud, ICMMO, UMR CNRS 8182, Bâtiment 420, 91405 Orsay Cedex, France and [2]Université de Cergy-Pontoise, LCB, EA 4505, 5 mail Gay-Lussac, Neuville sur Oise, 95031 Cergy-Pontoise, France

Email:
Marie-Christine Scherrmann[*] - marie-christine.scherrmann@u-psud.fr

* Corresponding author

Abstract

Purification by flash chromatography strongly impacts the greenness of a process. Unfortunately, due to the lack of the relevant literature data, very often this impact cannot be assessed thus preventing the comparison of the environmental factors affecting the syntheses. We developed a simple mathematical approach to evaluate the minimum mass intensity of flash chromatography from the retention factor values determined by thin-layer chromatography.

Introduction

As part of a more respectful environmental chemistry, many efforts have been made to reduce the impact of chemical transformations by developing high atom-economic reactions, alternative reaction media or high-performance catalysts. The formation of a pure chemical product not only requires reactants, solvents, promoters and catalysts used in the reaction, but also other materials used for the work-up and for the purification steps. The Sheldon *E* factor [1,2] and the mass intensity *MI* [3-5], which are defined according to Equation 1 and Equation 2, respectively, are classical metrics based on the economy of material for evaluating the greenness of a process.

It is worth noting that these mass-based metrics allowed to quantify the mass of waste but did not take into account their

potential for negative effects on the environment. These two metrics are related by Equation 3 [6].

$$E = \frac{\text{total mass of waste}}{\text{mass of product}} \quad (1)$$

$$MI = \frac{\text{total mass used in the process}}{\text{mass of product}} \quad (2)$$

$$MI = E + 1 \quad (3)$$

The amount of waste includes the amount of the byproducts, but also the amount of non-reacting starting materials, auxiliaries, catalysts or any additives such as acids, bases, salts, solvents of

the reaction or solvents required for the work-up and the purification. We demonstrated that the mass intensity could be easily calculated for linear and convergent sequences from the global material economy GME (Equation 4), which is related to the atom economy, the yields of each step, the excess of reactants and the mass of auxiliaries [6,7].

$$MI = \frac{1}{GME} \qquad (4)$$

It can be fractioned into three parts: reaction itself (MI_R), work-up (MI_W) and purification (MI_P) as shown by Equation 5 [8].

$$MI = MI_R + MI_W + MI_P \qquad (5)$$

Any value of the E factor which does not take into account the work-up and purification steps is nonsensical, since the values of MI_W and MI_P are often much higher than the value of MI_R.

In order to compare the greenness of different processes, each term of Equation 5 has to be known. From the literature data it is possible to retrieve information concerning the amount of reactants, solvents and catalysts allowing the calculation of MI_R. Moreover, since the work-up is usually well described, it is easy to gain access to MI_W. In contrast, the amount of auxiliaries and solvents used in the purification of products is very often omitted. For example, the mass of silica gel and eluents used are never mentioned, which prevents the reader from calculating MI_p, and thus having the actual value of the E factor. The impact of chromatography on sustainability was recently discussed [9] and we propose here a method to evaluate such an item. This tool can also allow the chemist to evaluate, from a thin-layer chromatography (TLC), the minimum

mass required to perform a flash chromatography. Our calculations are based on the preparative chromatographic technique largely used by chemists [10-12] and on our own experiments.

Results and Discussion

The publication of Still et al. [10] describing flash chromatography in 1978 greatly facilitated the post synthesis purifications which were, until then, often carried out by gravity column chromatography that was time consuming and did not always lead to effective separations. Since then, various automated systems equipped with pumps and eventually detectors and using disposable pre-packed silica cartridges were marketed offering great ease of use.

The mass intensity of purification by chromatography (MI_{Chr}) is the ratio between the total mass used to perform the chromatography (i.e., the sum of the mass of silica (m_{SiO_2}) and the mass of eluent (m_{eluent})) and m_p, the mass of the product (Equation 6).

$$MI_{Chr} = \frac{\text{total mass used for chromatography}}{\text{mass of product}} = \frac{m_{SiO_2} + m_{eluent}}{m_p} \qquad (6)$$

Mass of silica

The size of the column for chromatography and therefore the amount of silica and solvent depends on the mass of the sample and on the difficulty of separation of the products. This difficulty may be evaluated by ΔR_f that is the difference between the retention factor R_f of products in TLC (thin-layer chromatography). Based on their experimentations, Still et al. recommended typical column diameters (constant height) and sample loading for difficult separations ($0.2 > \Delta R_f \geq 0.1$) or more easier separations ($\Delta R_f \geq 0.2$) [10]. Using a column height of 5.9 inches (ca. 15 cm) and considering that the silica has a density of 0.5, correlations have been established between the mass of silica to be used and mass (m_s) of the sample to be purified (Table 1,

Table 1: Mass of silica (in grams) to be used depending on the mass of sample to be purified for manually packed columns and some commercial pre-packed cartridges.

Entry	Cartridge	Particles shape	Average particle size (µm)	$m_{SiO_2} = f(m_s)$		
				difficult separation	moderately difficult separation	easy separation
1	Silica gel[a]	irregular	40–63	151.2 m_s + 0.5	59.8 m_s	
2	RediSep[TM]	irregular	35–70	1000 m_s	25 m_s	14. m_s
3	EasyVario Flash[TM]	irregular	15–40		33.3 m_s	
4	SNAP[TM]	irregular	40–50	10 m_s	20 m_s	10 m_s
5	SNAP Ultra[TM]	spherical	25	50 m_s	10 m_s	5 m_s

[a]Manually packed glass column.

entry 1) [12]. For commercial pre-packed cartridge indications are also provided [13-15] and we have selected some data to obtain a general trend (Table 1).

The mass of silica required to purify m_s g of sample may therefore be estimated by Equation 7. Excluding the equation obtained for difficult separations with the RediSep[TM] cartridge leading to extremely high values of mass of silica (Table 1, entry 2), and partially the equations obtained with spherical silica (SNAP Ultra[TM], Table 1, entry 5), the values of A range from 10 to 152.

$$m_{SiO_2} = Am_s \quad 10 < A < 152 \tag{7}$$

Mass of eluent

The total amount of solvent required for carrying out a chromatography is composed of the part used to pack the column, of that needed to elute the sample, (i.e., the retention volume V_R and the half width of the chromatographic peak ω (Figure 1)), and the void volume V_0 that corresponds to the mobile phase volume in the packed column.
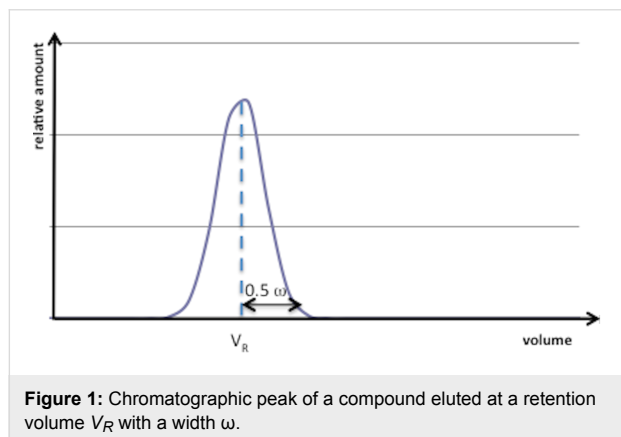

Figure 1: Chromatographic peak of a compound eluted at a retention volume V_R with a width ω.

Considering that the solvent used to pack the column is generally recycled, the volume of eluent required can then be expressed by Equation 8.

$$V_{eluent} = V_R + 0.5\omega + V_0 \tag{8}$$

Under ideal conditions, the retention volume V_R can be related to the R_f by Equation 9.

$$V_R^{ideal} = \frac{V_0}{R_f} \tag{9}$$

Some deviations of this equation were observed for silica gel column and a correction factor C was proposed [12], so that V_R

should be calculated using Equation 10. A value of 0.64 was found for manually packed columns, while for commercial cartridges, the value of C was 0.66.

$$V_R = C\frac{V_0}{R_f} \tag{10}$$

The half width of the chromatographic peak can be estimated by assuming that the peak is described by a Gaussian with a standard deviation σ (Equation 11).

$$\omega = 4\sigma = 4\frac{V_R}{\sqrt{N}} \tag{11}$$

In this equation, the term N represents the efficiency of the chromatographic column, i.e., the system's ability to elute the same compounds at identical rates in order to obtain thin peaks. N is defined as the number of theoretical plates of the column.

Using Equations 8,10 and 11, the mass of eluent can be expressed by:

$$m_{eluent} = \rho_{eluent}V_{eluent} = \rho_{eluent}V_0\left[\frac{C}{R_f}\left(1+\frac{2}{\sqrt{N}}\right)+1\right] \tag{12}$$

The void volume V_0 is connected to the column volume V_C by the porosity of the silica ε_{SiO_2} ($\varepsilon_{SiO_2} = 0.9$) and the volume of the column depends on the mass and density ($\rho_{SiO_2} = 0.5$) of the silica according to Equation 13 and Equation 14.

$$V_0 = \varepsilon_{SiO_2}V_C \tag{13}$$

$$V_C = \frac{m_{SiO_2}}{\rho_{SiO_2}} \tag{14}$$

We can then deduce the following equation for the mass of eluent:

$$m_{eluent} = 1.8\rho_{eluent}m_{SiO_2}\left[\frac{C}{R_f}\left(1+\frac{2}{\sqrt{N}}\right)+1\right] \tag{15}$$

Although N depends on various parameters such as the size of the column, the packing particles, the quality of the packing and the flow of the mobile phase, an average value of 35 was proposed for flash chromatography column [16]. Alternatively, in order to take into account broadening of the chromatographic peaks due to the amount of compounds in the sample, it was proposed [12] to evaluate N as a function of the mass fraction of the product in the sample ($m_P = xm_s$), for difficult

separation (Equation 16, B = 51.70) or more easier separation (Equation 16, B = 33.64).

$$N = B(x)^{-0.44} \qquad (16)$$

Mass intensity of a chromatography

As already stated above, the mass intensity of purification by chromatography is the ratio between the total mass m_T used to perform the chromatography and the mass m_P of the product (Equation 6). The total mass is the sum of the silica and eluent masses that can be expressed from Equation 7 and Equation 15.

$$m_T = Am_S + 1.8 Am_S \rho_{eluent} \left[\frac{C}{R_f} \left(1 + \frac{2}{\sqrt{N}} \right) + 1 \right] \qquad (17)$$

Considering x, the mass fraction of the product in the sample the theoretical expression of MI_{Chr} becomes:

$$MI_{Chr}^{th} = \frac{A}{x} + \frac{1.8 A \rho_{eluent}}{x} \left[\frac{C}{R_f} \left(1 + \frac{2}{\sqrt{N}} \right) + 1 \right] = A' + B' \rho_{eluent} \quad (18)$$

Application

We chose 4 syntheses whose crude reaction products were purified by flash chromatography to illustrate the calculations developed above (Scheme 1).

In all cases, C was set at 0.64 and MI_{Chr}^{th} was calculated using N_{calc} (Equation 16) or $N = 35$. The value of MI_{Chr}^{exp} was determined according to the experimental data.

Compound **1**, obtained by aldol condensation (Scheme 1, reaction a) in 80% yield [8], was chromatographed on a manually packed column using as eluent a 7:3 cyclohexane–acetone mixture (Table 2, entry 1). The mass fraction of product in the crude reaction mixture (79%) was calculated after chromatography taking into account the isolated mass of **1**. The values calculated using Equation 18 with $N = 35$ or N_{calc} (Equation 16, $B = 33.64$ or $B = 51.70$) deviated only from 6, 7 and 11% of the experimental value, respectively. Another experiment (a(bis), Table 2, entry 2) led to a crude reaction mixture containing 60% by weight of **1** which was purified using a disposable cartridge (PuriFlash SIHP 30 μm, Interchim) and cyclohexane–AcOEt (7:3) as the eluent. Also in this case, the calculated values were very close to the experimental ones (differences of 1, 3 or 6%).

The crude mixture of reaction b, a bromination in alpha position of a ketone leading to **2** [17,18] in 54% yield, was chromatographed using AcOEt–MeOH (9:1) as the eluent [8]. The mass fraction of compound **2** in the sample was only 38%, leading to high value of MI_{Chr}^{exp} (Table 2, entry 3). The calculations lead to MI_{Chr}^{exp} values having differences of 11, 14 and 17% compared to the experimental value. Obviously the lower is the
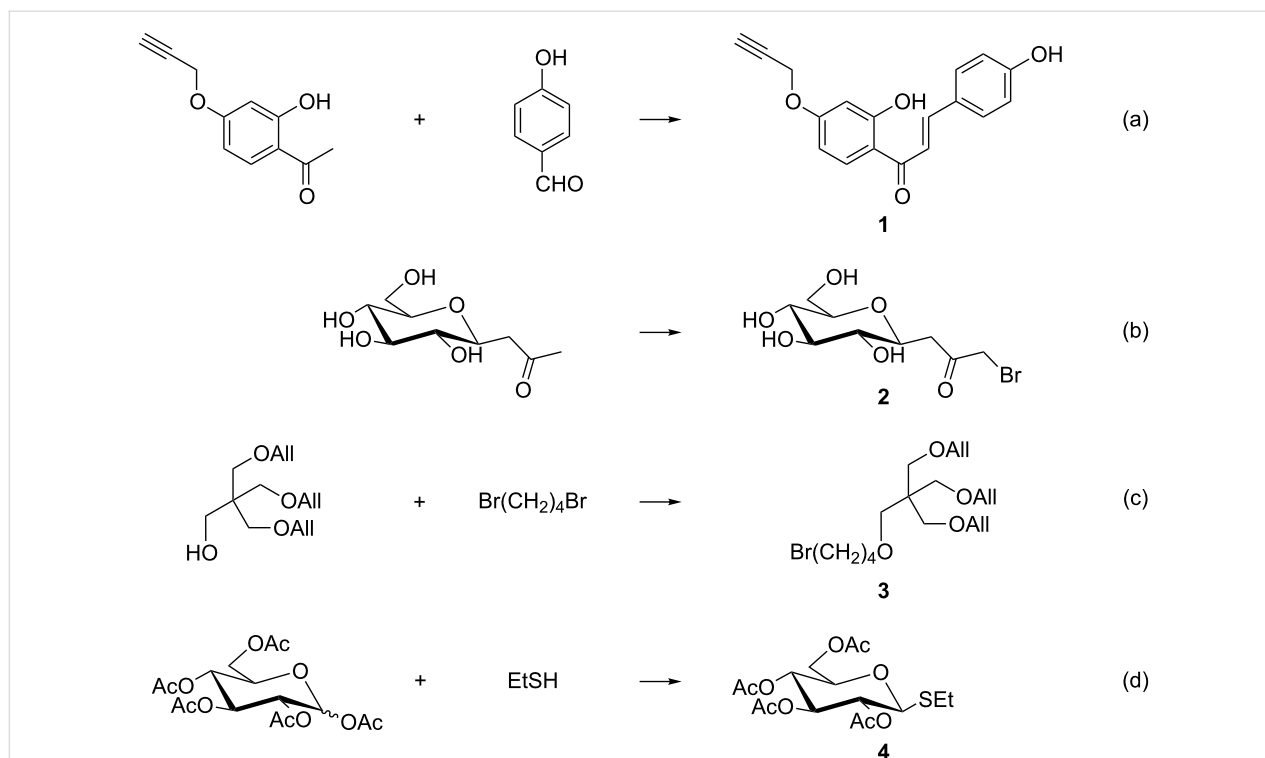
Scheme 1: Reactions used as examples. (Substrates and products, all the reagents are not shown).

Table 2: Comparison of the experimental values of the mass intensity of chromatography (MI_{Chr}^{exp}) with the theoretical estimated values (MI_{Chr}^{th}) for various reactions (Scheme 1).

| Entry	Reaction	R_f	A	x	A'	ρ_{eluent}	N	B'	$MI_{Chr}^{th\,a}$	MI_{Chr}^{exp}
1	a	0.1	49	0.79	62	0.78	35	1072	901	962
							37[b]	1065	896	
							57[c]	1019	860	
2	a(bis)[d]	0.15	47	0.60	78	0.81	35	946	843	857
							42[b]	928	829	
							65[c]	892	800	
3	b	0.13	30	0.38	79	0.89	35	1074	1031	1161
							51[b]	1033	994	
							79[c]	995	961	
4	c	0.30	20	0.42	47	0.65	35	324	258	250
							49[b]	314	252	
							76[c]	304	245	
5	d	0.20	30	0.61	49	0.81	35	468	427	458
							42[b]	459	421	
							64[c]	442	407	

[a]Calculated with the exact values and not with the rounded off numbers A' and B'. [b]Calculated using Equation 16 with B = 33.64; [c]Calculated using Equation 16 with B = 51.70. [d]Reaction a, other experimental conditions.

proportion by weight of the compound in the sample, the higher is the mass intensity for the chromatography. This variation in ($1/x$) was represented for reaction b in Figure 2. Therefore when this proportion is not precisely known, which is the most frequent case before performing the purification, it is possible to estimate a minimum value of MI_{Chr} setting $x = 1$, or, if the mass of the sample to be purified is higher than the theoretical mass of product, x can be calculated assuming a 100% yield (Equation 19).

$$x_{max} = \frac{M_W(\text{product})*\text{number of mole of substrate}}{m_s} \quad (19)$$

It is also clear that if a treatment (e.g. extraction) can reduce the mass of the sample to be purified, it would reduce the mass intensity related to chromatography. This should obviously not be to the detriment of the overall mass balance.

This can be illustrated by example c (Scheme 1). In fact, this alkylation reaction was carried out in the presence of a large excess (4 equiv) of dibromobutane to get compound **3** in a good yield (73%) [19]. Some of this excess was removed from the crude reaction product by distillation, reducing the mass of the sample by 53%. This allowed to recycle the reactant but also to greatly reduce the weight of silica to be used ($A = 20$) and, accordingly the mass of solvent (Table 2, entry 4). This purification with a particularly low MI_{Chr}, compared to the other examples, corresponded to a filtration on silica gel rather than to a flash chromatography.
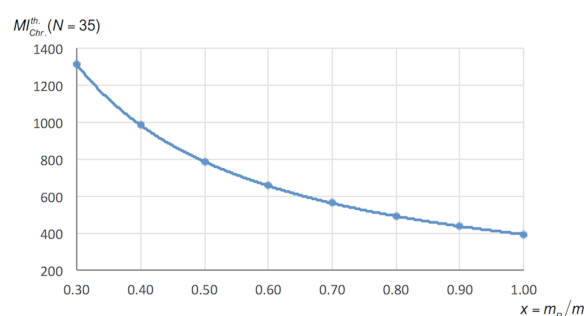

Figure 2: Variation of MI_{Chr}^{th} with x for reaction b (Scheme 1).

The last example (Scheme 1d) is a *S*-glycosylation (isolated yield = 62%) leading to compound **4** [20]. For this crude reaction mixture containing 61% of **4**, a correct separation was obtained on TLC with the mobile phase cyclohexane–EtOAc (75:25). Again, the values obtained by the calculation were close to the experimental ones, with differentials of 7, 8 and 11% depending on the value taken for N (Table 2, entry 5).

In each case, the calculation afforded values close (deviations <17%) to the experimental value (Figure 3). As already pointed out above, the calculation depends on the value of x that it is not always easy to estimate, but it is possible to estimate a minimum of the mass of intensity related to the chromatography by setting x closed to 1.

Figure 3: Comparison between calculated and experimental values of MI_{Chr} for the reactions of Scheme 1.
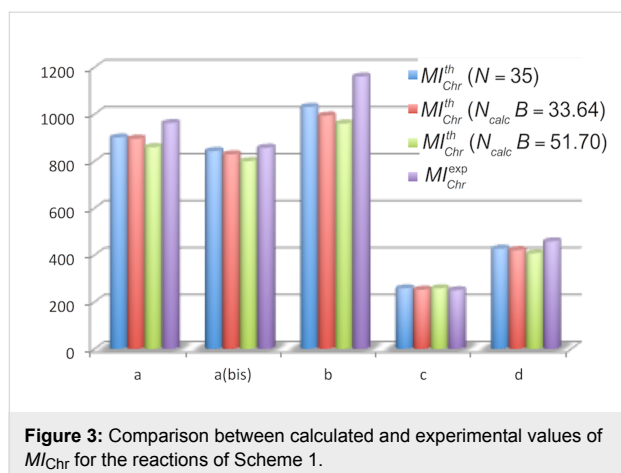
The value of MI_{Chr} also depends on the retention factor (R_f), especially when the latter is less than 0.2 (Figure 4). An estimation of the minimum is also possible by setting an R_f to a value close to 0.35, as recommended in the seminal paper of Still et al. [10].

Figure 4: Variation of MI_{Chr}^{th} (N = 35) with R_f for the reactions of Scheme 1.
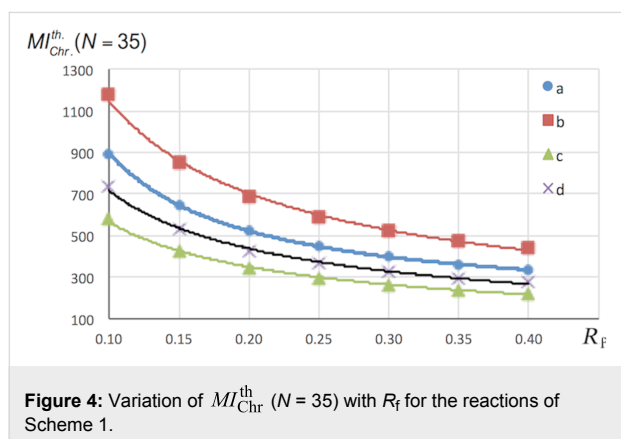
Conclusion

If the impact of chromatography on the environmental factor E of a process seems pretty obvious, we have developed here a tool to quantify it. In an extremely favourable case with a 95% pure sample (x = 0.95), a very easy separation achievable with a small mass of silica (A = 10) and R_f = 0.35, we find, for low density eluent (0.6), an MI_{Chr} value close to 50. By doubling the amount of silica, which is closer to reality, the MI_{Chr} value is about 100. In real cases chosen here as examples, we have shown that the values were fairly between about 200 and 1200.

Since it is clear that chromatography should be avoided wherever possible, works proposing alternative purification methods have been published [9,21,22]. When the purification by flash chromatography is necessary, solvents with low environmental impacts should be used [23-25]. In this context, super critical chromatography which allows to obtain very low retention volumes and easy recycling offers an interesting alternative [26] but requires a significant investment.

Acknowledgements

References

1. Sheldon, R. A. *CHEMTECH* **1994,** *24,* 38–47.
2. Sheldon, R. A. *Green Chem.* **2007,** *9,* 1273–1283. doi:10.1039/b713736m
3. Curzons, A. D.; Constable, D. J. C.; Mortimer, D. N.; Cunningham, V. L. *Green Chem.* **2001,** *3,* 1–6. doi:10.1039/b007871i
4. Constable, D. J. C.; Curzons, A. D.; Cunningham, V. L. *Green Chem.* **2002,** *4,* 521–527. doi:10.1039/B206169B
5. Eissen, M.; Metzger, J. O. *Chem. – Eur. J.* **2002,** *8,* 3580–3585. doi:10.1002/1521-3765(20020816)8:16<3580::AID-CHEM3580>3.0.CO;2-J
6. Augé, J. *Green Chem.* **2008,** *10,* 225–231. doi:10.1039/B711274B
7. Augé, J.; Scherrmann, M.-C. *New J. Chem.* **2012,** *36,* 1091–1098. doi:10.1039/c2nj20998e
8. Pessel, F.; Billault, I.; Scherrmann, M.-C. *Green Chem.* **2016,** *18,* 5558–5568. doi:10.1039/C6GC01647B
9. Peterson, E. A.; Dillon, B.; Raheem, I.; Richardson, P.; Richter, D.; Schmidt, R.; Sneddon, H. F. *Green Chem.* **2014,** *16,* 4060–4075. doi:10.1039/C4GC00615A
10. Still, W. C.; Kahn, M.; Mitra, A. *J. Org. Chem.* **1978,** *43,* 2923–2925. doi:10.1021/jo00408a041
11. Stevens, W. C., Jr.; Hill, D. C. *Mol. Diversity* **2009,** *13,* 247–252. doi:10.1007/s11030-008-9104-x
12. Fair, J. D.; Kormos, C. M. *J. Chromatogr. A* **2008,** *1211,* 49–54. doi:10.1016/j.chroma.2008.09.085
13. *Effective Organic Compound Purification - Guideline and tactics for Flash Chromatography,* 4th ed.; Teledyne Isco Inc, 2010. (www.isco.com).
14. New Generation of Ready to Connect Cartridges using MERCK silica. EasyVarioFlash® (Götec-Labortechnik GmbH), 2007; http://www.swisslabs.eu/uploads/files/Flash_Chromatography_New_Generation_ReadytoUse_Cartridges.pdf.
15. *Biotage Flash Cartridge User Guide* - The Definitive Guide to Flash Chromatography. Biotage, 2014; http://www.biotage.com/product-group/flash-cartridges.
16. Meyer, V. R. *Practical high-performance liquid chromatography;* Wiley, 2010. doi:10.1002/9780470688427
17. Howard, S.; Withers, S. G. *J. Am. Chem. Soc.* **1998,** *120,* 10326–10331. doi:10.1021/ja981580r
18. Billault, I.; Pessel, F.; Petit, A.; Turgis, R.; Scherrmann, M.-C. *New J. Chem.* **2015,** *39,* 1986–1995. doi:10.1039/C4NJ01784F
19. Turgis, R.; Billault, I.; Acherar, S.; Augé, J.; Scherrmann, M.-C. *Green Chem.* **2013,** *15,* 1016–1029. doi:10.1039/c3gc37097f
20. Ferrier, R. J.; Furneaux, R. H. *Carbohydr. Res.* **1976,** *52,* 63–68. doi:10.1016/S0008-6215(00)85946-7
21. Prosa, N.; Turgis, R.; Piccardi, R.; Scherrmann, M.-C. *Eur. J. Org. Chem.* **2012,** 2188–2200. doi:10.1002/ejoc.201101726
22. Weiß, M.; Brinkmann, T.; Gröger, H. *Green Chem.* **2010,** *12,* 1580–1588. doi:10.1039/c002721a

23. MacMillan, D. S.; Murray, J.; Sneddon, H. F.; Jamieson, C.; Watson, A. J. B. *Green Chem.* **2012,** *14,* 3016–3019. doi:10.1039/c2gc36378j

24. Taygerly, J. P.; Miller, L. M.; Yee, A.; Peterson, E. A. *Green Chem.* **2012,** *14,* 3020–3025. doi:10.1039/c2gc36064k

25. Pena-Pereira, F.; Kloskowski, A.; Namiesnik, J. *Green Chem.* **2015,** *17,* 3667–3705. doi:10.1039/C5GC00611B

26. Miller, L.; Mahoney, M. *J. Chromatogr. A* **2012,** *1250,* 264–273. doi:10.1016/j.chroma.2012.06.029

Efficient mechanochemical synthesis of regioselective persubstituted cyclodextrins

Laszlo Jicsinszky[*], Marina Caporaso, Katia Martina, Emanuela Calcio Gaudino and Giancarlo Cravotto[*]

Abstract

A number of per-6-substituted cyclodextrin derivative syntheses have been effectively carried out in a planetary ball mill under solvent-free conditions. The preparation of Bridion® and important per-6-amino/thiocyclodextrin intermediates without polar aprotic solvents, a source of byproducts and persistent impurities, could be performed. Isolation and purification processes could also be simplified. Considerably lower alkylthiol/halide ratio were necessary to reach the complete reaction in comparison with thiourea or azide reactions. While the presented mechanochemical syntheses were carried out on the millimolar scale, they are easily scalable.

Introduction

Cyclodextrins (CDs) are cyclic α(1→4)glucopyranosides and have been fully described in a number of publications [1-3]. They are most noted for their ability to form non-covalent associations called "inclusion complexes". Natural CDs exhibit many favourable properties, which advance their use in a wide range of applications. However, syntheses for many special applications, such as DNA sequencing [4,5], gene delivery [6], and drug targeting hosts [7,8], can be problematic as they require sophisticated, efficient and yet simple methods which lead to acceptable purity and impurity profiles. Furthermore, the special structural properties of selectively substituted CDs mean that their syntheses are not always environmentally friendly

procedures. Ball mill assisted syntheses are good alternatives to overcome solubility difficulties in syntheses or isolation of natural compounds from vegetables using CDs [9,10]. Environmentally benign synthetic methods of CD derivatives have been recently reviewed [11].

The key intermediate in the bulk preparation of selectively per-6 substituted CDs is the per-6-deoxy-6-halide derivative, which covers per-6-bromo [12] and per-6-iodo [13] compounds. Although per-6-chloro-CD derivatives can also be easily prepared [14] but the lower reactivity of chloro compounds restricts the use of per-6-chloro-CDs [15] in solution. The solubility of per-

6-halogeno-CDs is very limited in water and the majority of organic solvents, meaning that their preparation and purification is far from being environmentally friendly.

Per-6-*S*-(3-mercapto)propionyl-γ-CD (Sugammadex, Bridion®) is not only the biggest success that CD derivatization has had, but its use in the removal of muscle relaxants may revolutionize surgery. It has very high affinity with curare analogues, especially rucoronium ($K_{11} \approx 1.8 \times 10^7$ M^{-1}) [7], which are widely used in surgery [6]. Its everyday use has led to increasing demand and ever higher amounts being employed, meaning it will likely soon become a generic molecule in most hospitals. The solventless preparation technique can provide clear advantages over classic methods since its use in humans requires very high purity. The standard preparation of Sugammadex uses a harsh base, such as sodium hydride, to activate the thiol group of 3-mercaptopropionic acid (MPA) and *N,N*-dimethylformamide (DMF) [16]. In the reaction solution and particularly on larger scales (from 10 g to kilo lab scale), impurities that arise from incomplete conversions, product and byproduct decomposition as well as solvent impurities increase synthesis and purification costs and time.

Selectively per-6-thiolated CDs are also used in gold nanoparticle chemistry, particularly in electrochemical sensors [17]. Thiourea (TU) is one of the best precursors of those CDs because as the halogen is exchanged to the thiouronium salt of CDs thiols can readily be obtained under aqueous basic conditions. Thioureido-CDs are crystalline compounds that are readily soluble in water, easy to purify and convert to thiols [8]. These intermediates can be efficiently prepared via the reaction of a TU excess (2–3 mol TU/halogen) and per-6-halogenated CDs. The preparation is also carried out in a polar aprotic solvent, as in case of the azide exchange, while byproducts may also be similar despite the higher nucleophilicity of sulfur. The reaction under classic conditions usually requires large TU excess.
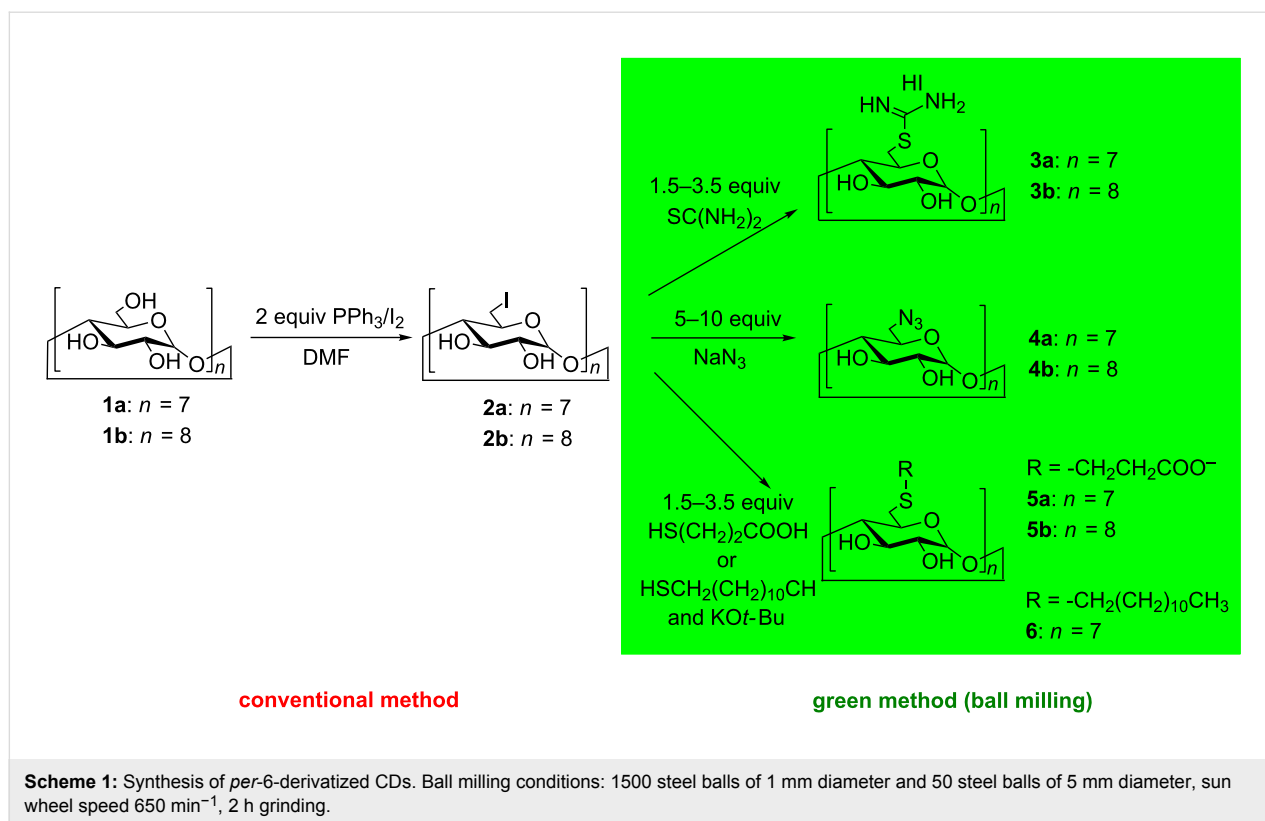
Various per-6-alkylthio-β-CD derivatives are used in siRNA delivery and gene therapy [6]. The alkyl chain, usually C_{10}–C_{16}, makes the product very amphiphilic, which means that it is difficult to purify not only from possible byproducts but also from the reagents. Additionally, sulfur-containing organic compounds can form very strong complexes with not only the native but with the substituted CDs, too. Although a solvent-free synthetic method does not solve the problem of complexation but the reduced amount of reagents can simplify the purification.

Heptakis(6-azido-6-deoxy)-β-CD is the precursor to per-6-amino-β-CD, which is an important component of DNA sequencing equipment [4]. *p*-Toluenesulfonyl (Ts) esters are still an irreplaceable leaving group for carbohydrates as well. The Ts → azide exchange in Ts-β-CD is effective in both solution and under high-energy ball milling (HEBM) conditions, whereas it is difficult in the per-halide analogues, because of sodium azide's poor solubility in DMF, *N,N*-dimethylacetamide, *N*-methylpyrrolidone and dimethyl sulfoxide. A solution to this problem might be found in the successive addition of sodium azide, considerably longer reaction times and/or higher temperatures (≈100 °C) for the complete reaction. Per-6-bromo- and per-6-iodo-CDs are inevitably able to react with dimethylamine, a common decomposition product of DMF. While the formation of dimethylamine-moiety-containing CDs is virtually negligible – thankfully, as it can cause serious problems in pharmaceutical or biological preparations – its physicochemical properties are very similar to those of the perazido derivatives, making separation impossible. The similarity is even higher after the azide's conversion to an amine. Solvent removal in the synthesis of per-6-azido-CDs is generally also challenging because of the high boiling polar aprotic solvents used; their complete removal is a difficult task under laboratory conditions, even at high vacuum.

Ball milling is an effective method for the preparation of inclusion complexes which has recently begun to be appreciated by organic chemists for its simplicity and flexibility [18-21]. While the mechanochemical manipulation of covalent bonds is hardly a brand new concept, its diffusion into carbohydrate chemistry, and particularly into CD derivatization, has been rather slow [22,23]. The ability of HEBM to favour the nucleophilic substitution reaction of 6^I-monotosyl-β-CD has been demonstrated in a previous article [22]. Most interestingly, the side reactions that appear to be unavoidable in the classical solution syntheses can be eliminated in the solvent-free method described for the preparation of various CD derivatives. HEBM was found to be particularly efficient when good nucleophiles, such as sulfur-containing reactants or inorganic azides, were used.

The aim of our study is to highlight the use of HEBM in the preparation of a number of practically important CD derivatives, as seen in Scheme 1. Although in our work neither the reaction conditions nor the purifications were optimized in any terms the presented results can serve as starting point to develop more environmentally benign synthetic methods of important CD derivatives. The well-established engineering of HEBM reactions makes them easy to scale-up, while simplified work-up procedures can further reduce the presence of unwanted byproducts which explains our interest in the preparation of compounds such as **3a**, **5b**, and **6** (Scheme 1).

Scheme 1: Synthesis of *per*-6-derivatized CDs. Ball milling conditions: 1500 steel balls of 1 mm diameter and 50 steel balls of 5 mm diameter, sun wheel speed 650 min⁻¹, 2 h grinding.

Results and Discussion

Per-6-iodinated and, in some cases, per-6-brominated CD derivatives are the most common activated per-6-CDs. Their synthesis can be performed on large scales under safe conditions. However, there can be some difficulties (compounds **3** and **4**, entries 2–4, 7–11 in Table 1) in reaction and during purification, meaning that we therefore also decided to test per-6-chloro-β-CD from which the more ionic TU salt can be formed and the chloride has less affinity to the macrocycle. It was not possible to reproduce the literature method [14] for per-6-chloro-β-CD synthesis, but a protocol using *p*-toluenesulfonyl chloride under reaction conditions that were analogous to the iodination/bromination reaction resulted in the targeted heptakis(6-chloro-6-deoxy)-β-CD being produced in good yields [20]. Not unexpectedly, per-6-chlorinated-β-CD showed very poor reactivity, not only under classic solvent reaction conditions (entry 14 in Table 1), but also under ball milling (entries 5 and 15 in Table 1).

Mechanochemical syntheses from 6ᴵ-O-monotosyl-β-CD usually require moderate reactant excesses and similar molar ratios to the solution method [24]. Despite the expectations, based on the monosubstituted case [24], the persubstitutions usually needed higher reagent/CD molar ratio. However, except the azide cases (**4a** and **4b**), the reagent/halogen molar ratios did not change such extent (Table 1). This can be explained

satisfactorily by the complexation of the leaving group which might have high affinity to the CD cavity [3,25,26] preventing its departure from the reaction centres resulting in steric blocking. While the halogen → azide exchange required considerably larger halogen/reagent ratios than the solution reactions, sulfur nucleophiles showed a more favourable tendency and the reagent/halogen ratio was either roughly equal or slightly lower than for the monosubstitution. In the solution synthesis [6] of β-CD-per-6-dodecane thioether (**6**) the residual DMF increases the product solubility in methylene chloride and precipitation with MeOH removes the unreacted 1-dodecanethiol (DDS), whereas the absence of DMF, together with the strong complex formed between DDS and the product, meant that the product isolation was more difficult. The resulting crude mixture was only partially soluble in methylene chloride and MeOH precipitation gave a difficult-to-filter product, which still contained at least one mole of complexed DDS. This complexation resulted in not only technical difficulties, but also confounded the removal of impurities. The strong complex between the reagent and product also resulted in an impure product of the β-CD version of Sugammadex (**5b**). The reagent/halogen ratio was practically identical to the one used in the solution method of the originator [16] when mercaptopropionic acid reacted with the halogenated CD (entries 22, 23, and 26–28 in Table 1) despite the use of the considerably milder and safer base, potassium *tert*-butoxide (KO*t*-Bu).

Table 1: Comparison of classic and green methods for the preparation of CD derivatives.

Entry	Compound	Reagent/solvent	Reagent/ halogen molar ratio	Method	Batch size [mmol]	Yield[a] [%]	Final temp. [°C]	React. time [h]
1	**3a**	thiourea/DMF	2	soln.	7.5	75	80	3 [27]
2		thiourea	1.5	BM	0.1	12	89	2
3		thiourea	3.5	BM	0.1	25	89	2
4		thiourea	3.5	BM	1	61	88	2
5		thiourea[b]	3.5	BM	0.1	traces[c]	92	2
6	**3b**	thiourea/DMF	2	soln.	5	90	80	16
7		thiourea	1.5	BM	0.1	14[c,d]	85	2
8		thiourea[e]	1.5	BM	0.1	9[c,d]	82	2
9		thiourea	3.5	BM	0.05	33[d]	85	2
10		thiourea[e]	3.5	BM	0.05	39[d]	82	2
11		thiourea[e]	3.5	BM	0.5	57[d]	86	2
12	**4a**	NaN$_3$/DMF	1.25	soln.	5	90	100–105	~4.5
13		NaN$_3$/DMF	1.25	soln.	0.5	76	100–105	5
14		NaN$_3$/DMF[b]	1.25	soln.	0.5	traces[c]	100–105	5 [24]
15		NaN$_3$[b]	5	BM	0.1	traces[c]	86	2
16		NaN$_3$	5	BM	0.1	69	88	2
17		NaN$_3$	5	BM	0.5	72	90	2
18	**4b**	NaN$_3$/DMF	1.25	soln.	5	84	100–105	≈4.5
19		NaN$_3$	10	BM	0.05	67	82	2
20		NaN$_3$	10	BM	0.5	71	84	2
21	**5a**	MPA/Cs$_2$CO$_3$/DMF	1.5	soln.	5	60	50	25 [28]
22		MPA/KOt-Bu[f]	1.43	BM	0.1	86	72	2
23		MPA/KOt-Bu	1.5	BM	1	71	75	2
24	**5b**	MPA/NaH/DMF	1.25	soln.	1.4	60	70	12 [16]
25		MPA/TEA/DMF[f]	3	soln.	2.5	60[c]	60	24
26		MPA/KOt-Bu	1.25	BM	0.05	81	73	2
27		MPA/KOt-Bu[e]	1.5	BM	0.05	86	71	2
28		MPA/KOt-Bu[e]	1.5	BM	0.5	72[d]	76	2
29	**6**	DDS/K t-Bu/DMF	no data	soln.	1	>90	80	96 [29]
30		DDS/KOt-Bu/DMF[g]	3	soln.	0.5	83	80	120
31		DDS/KOt-Bu[g]	1.6	BM	0.1	95	62	2

[a]Isolated yields but due to small batch-sizes and not optimized purifications the yields of BM reactions are informative only. [b]From per-6-chloro-β-CD. [c]Contains also incompletely substituted structures, further isolation/purification were not performed. [d]The mother liquor contained considerable amounts of product by TLC. [e]From per-6-bromo-γ-CD. [f]MPA: 3-mercaptopropionic acid; TEA: *N,N,N*-triethylamine; KOt-Bu: potassium *tert*-butoxide; KOt-Bu/MPA molar ratio ≈2.1:1.;[g]DDS: 1-dodecanethiol; DDS/KOt-Bu molar ratio 1:1.

Our first target was to investigate the reaction between a good nucleophile (sulfur) and per-halogenated CDs. The TU method is widely used in the synthesis of various thiols and thioester compounds [8,30] and the CD thiouronium salt intermediates are not isolated [8] despite their good crystallization properties, while the excess/residual TU and used solvents are removed upon the conversion to thiols only. However, the easy crystallization of these salts is a nice feature of these compounds as it can help to remove incompletely substituted compounds (defected structures) and unused reagent as the thiolate is less stable after their basic decomposition; thiols are easy to oxidize

to disulfide under basic conditions. The TU reactions (**3a** and **3b**) in the ball mill gave yields that were usually lower that those given by the monosubstitution reactions [22]. The very low aqueous solubility of the CD halides led to the intact starting materials being completely lost during the work-up. The low TU/halogen ratio (entries 2, 7 and 8 in Table 1) gave incomplete reactions. Incompletely substituted derivatives were in the majority in the product, as can be seen in the multiple anomeric proton peaks in the ^{1}H NMR spectra and the CH$_2$-halogen signals in the 2D NMR spectra. The larger excess of TU gave the complete substitution of the halogen (entries 3, 4,

9–11 in Table 1), but the TU removal also caused difficulties on the hundred-milligram scale despite the crude products only contained the targeted derivative. The higher yields of the 10-times larger scale (entries 4 and 11in Table 1) clearly demonstrate the technical difficulty of purification and the effect of batch sizes on yields. It was found that a considerable portion of TU-CD remained in the mother liquor because of the relatively high amounts of used solvents and the solubility of thiouronium-CDs in EtOH. Solubility difficulties led to chromatographic purification attempts failing even in RP-18 silicagel columns, too. The yield increased considerably when bromine derivatives (entries 10 and 11 in Table 1) were used instead of their iodine analogues (entries 7 and 9 in Table 1). An identical TU/Br to TU/I ratio was used in case of **3b** and further reduced the yield (entry 8 in Table 1), demonstrating that the similar halogen/tosyl ratio used in the monotosylated case is not sufficient to lead to complete substitution. Owing to the lower reactivity of bromo-CD a higher TU/per-6-bromo-γ-CD ratio had to be used. The more ionic character of formed thiouronium bromide was seen not only in the higher yields, but also in the lower product content of the ethanolic mother liquor. Chloride salts are even more ionic compounds whose character can reduce the organic solvent solubility of thiouronium chlorides. It, however, seemed reasonable to test a per-6-chlorinated CD. Unfortunately, practically no reaction was found to occur and the reaction mixture contained only traces of incompletely substituted TUβ-CD (entry 5 in Table 1). A further increase in the TU/chlorine ratio seemed to be unreasonable, as removing the higher amount of TU brings back the purification problems. The higher TU ratio somehow also increased the yield in the β-CD version. Ten-fold scaling up of the experiments showed increasing yields (entries 4 and 11 in Table 1) but the small scale still prevented to reach the solution reaction outcome but proved our concept. Gram-scale preparations easily overcome the technical difficulties of TU removal found in the small scale, as it becomes clear in the scale-up experiments (entries 4 and 11 in Table 1).

Although the preparation of 6^I-monoazido-6^I-monodeoxy-β-CD [22] was very effective, the analogue reactions with per-6-substituted CDs (**4a** and **4b**) were less efficient. Either the reaction did not proceed at all or only partial substitution was achieved at low NaN₃/halogen ratios, while only an increased NaN₃ ratio afforded the complete substitution of the CH$_2$–I groups, possibly because of the steric hindrance of the bulky sodium iodide. Iodine and metal iodides are preferred salts in various CD complexes [26,31]. Lack of solvents the diffusion/decomplexation of NaI from the cavity is slow. The higher amounts of sodium azide can exclude the formed NaI from the CD cavity in solid state. However, on a larger multigram scale the higher amount of used NaN₃ can be easily regenerated

because the products are very poorly soluble in water and NaI and NaN₃ can be readily separated. In order to accelerate the decomposition of the assumed NaI/CD complex first water then 50% aq EtOH was used as wetting substance. Usually 50% EtOH is able to decompose most of the CD complexes and owing to the hydrogen bonding destruction increases the solubility of poorly soluble CD derivatives. Wetting the solid dispersion with water and 50% EtOH resulted in not only lower temperature but practically no reaction was experienced as confirmed by the lack of azide in the IR spectrum of the isolated solid. As it is previously found [22] applying a wetting substance the grinding temperature is always lower than the dry milling. It was assumed that the very low solubility of both perhalogeno and per-azido-CDs in water or 50% EtOH and complete dissolution of the sodium azide the milling energy was not enough to warm the reaction mixture to an appropriate value. The very low solubility of the CD azides created an additional disadvantage and so we discarded the use of these wetting solvents. Alternatively, a wetting substance, which is an equally poor solvent for the CD derivatives and NaI, 1-pentanol [22] was also tested. In this case, the final grinding temperature was also found lower, approximately 20 °C lower, than the dry milling and no azido-CD was found by IR spectroscopy in the isolated solid.

In the TU reactions, we found that the isolated yields depend on batch-size and we studied the effect of downsizing a solution reaction for the preparation of compound **4a** (entry 13 in Table 1). In the downsized reaction due to the low solubility of the NaN₃ in DMF, an unreasonably high solvent/reagent ratio was necessary in the solution reaction and the yield was decreased due to the technical difficulties in the purification, e.g., relatively larger loss upon mass transfers or filtrations. No essential differences in reaction time were found despite all the necessary NaN₃ being dissolved at the beginning of the reaction and only a slightly longer reaction time was required to the complete reaction despite the higher dilution. Although in this case the crude contained relatively less residual DMF but its complete removal was still impossible. The scaled up ball mill azidations (entries 17 and 20 in Table 1) resulted in little higher yields but the relatively small amounts still caused technical difficulties which is shown in the yield-increasing ratios of the β- and γ-CDs.

Finally, the smaller solution reaction scale resulted in considerably reduced yields, which were however close to those of the scaled-up mechanochemical method. The mechanochemical syntheses of **4a** and **4b** were successfully scaled up 10-fold (entries 17 and 20 in Table 1) with acceptable yields which provide the proof of concept for the ball-mill-assisted synthesis of per-6-azido-CDs.

Chloride salts have considerably less affinity to the β-CD cavity (≈1/6 of iodide [26]). Per-6-chlorinated CD were also tested in this reaction despite the fact that only traces of incompletely substituted azido-CDs and decomposition products were found in solution and that the reaction mixture composition was similar to the solution composition (entries 14 and 15 in Table 1).

In conclusion, it appears that the advantage of mechanochemistry is restricted to the elimination of high boiling solvents in the azide cases (entries 16, 17, 19, and 20 in Table 1) which provides significant, if not dramatic, improvements in the synthesis. However, it is also true that the price of sodium azide is considerable lower than the costs of the utilization and regeneration of polar aprotic organic solvents, including environmental impact.

The TU reactions (compounds **3a** and **3b**) demonstrated that a good nucleophile, such as sulfur, could be effectively used in the preparation of useful per-6-thio-CD derivatives. While simple CD-6-thiols are still at the scientific stage, the sodium salt of octakis(6-deoxy-6-*S*-(3-mercapto)propionyl)-γ-CD has been slowly becoming an important surgical aid. The solution phase reaction is a dangerous process due to the use of sodium hydride. The relatively large number of possible side-reactions in solution brings further challenges to production. The efficient and green synthesis of Sugammadex is an exciting task. The comparable masses of reaction components meant that reaction assembly had less influence on the yields in the preparation of 3-mercaptopropionyl derivatives (**5a** and **5b**). While an inert wetting component (1-pentanol) was needed in the monosubstituted analogue [22], no such component was necessary in the per-6-substitution and the order in which the reagents were added had no effect on the yield. Purification and conversion to the pharmaceutically active form became very simple, as the protonated form is poorly soluble in water: the precipitate formed upon acidification by HCl, was filtered and the solid was re-dissolved in the equivalent amount of base. But, it is also true, that complex formation between the MPA and the product, particularly in case of the β-CD version, pointed out that pharmaceutical grade preparations need more fine tuning not only in the reaction but in the purification method, as well. Although, Bridion® is a sodium salt of the MPAγ-CD but in order to avoid the overdosing of base on the small preparation scale in our experiments aqueous ammonia was chosen as base and acetone was needed to get less deficit in the precipitates. Considerable losses during filtrations were found in the small-scale cases, which significantly reduced the yields because of the inevitably used diluted solutions.

The ten-fold scale up (entry 28 in Table 1) further simplified the product isolation because no acetone was necessary to precipi-

tate the product from the acidic solution, which could be isolated by filtration, and then it was immediately converted to the ammonium salt. Although, some cases the further simplified work-up resulted in somehow lower yields because of the redissolution of the protonated product during the filtration, the complete elimination of an organic solvent could be achieved. Yields can be improved further at even larger scales.

The encouraging results with MPA led us to an attempt to simplify the synthesis of an intermediate of a promising candidate for siRNA delivery. The solution phase synthesis of heptakis(6-deoxy-6-*S*-alkyl)-β-CDs is typical for the syntheses of intermediates of such compounds, however, their high lipophilicity means that isolation is not a technically trivial task.

Scale up of the 1-dodecanethiol mechanochemical reaction (synthesis of compound **6**, entry 31 in Table 1) was not performed because the batch size was in the range of our solution reaction. Mechanochemical synthesis was much more efficient than conventional solution methods. The final temperature was considerably lower (entry 31 vs 30 in Table 1) and the reaction time was dramatically shorter. The lack of residual DMF somehow changed the solubility behaviour of the product and affected the purification to some extent. This green approach resulted in better yields and purity despite the lower molar ratio of the reagent DDS.

The persubstituted species showed less variability in their susceptibility to the heat effect of the ball milling than their monosubstituted analogues. The temperatures inside the jar were considerably lower when one of the reactants was liquid or became liquid during the reaction (entries 22, 23, 26–28 and 31 in Table 1). In all cases, the temperature-time curves showed a saturation-like trend (see Supporting Information File 1 for details) and processes were generally in the 70–90 °C range at the end of the reaction, which is not essentially different from the monosubstituted case [18].

Although limits caused by the intrinsic complexation properties of CDs sometimes affected the reaction rate, a solvent-free synthetic method may simplify the purification of compounds **5** and **6**.

Conclusion

Syntheses of per-6-substituted CD derivatives can be effectively carried out in a ball mill under solvent-free conditions. In many cases, ball mill preparations display a positive balance in cost-benefit analyses. Wet grinding for the preparation of per-6-azido-CDs, using solubilizing and non-solubilizing solvents, showed practically no reaction in the planetary ball mill. Important intermediates and final products of per-6-amino- and per-6-

thio-CDs can be prepared without polar aprotic solvents, by which the byproduct formation and difficult-to-remove impurities can be eliminated. The lack of solvents in the examples described herein simplified the isolation and purification processes. Our basic aim was to proof the concept and although the purifications were not optimized the prepared compounds were enough pure to record correct NMR spectra to identify the substitution location and completeness.

Although in the monosubstituted case usually less reagent/ leaving group molar ratios were found [22], in the majority of per-substitutions higher reagent/CD molar ratio was needed but the reagent/halogen ratio not always changed dramatically. As may be expected, the sulfur nucleophiles resulted in considerably better or almost equal yields as compared to the conventional solution methods. A potential drawback of the method lies in the fact that the lack of highly solubilizing organic solvents can cause difficulties in the primary stage of purification.

Experimental
Full synthetic details and spectroscopic data are reported in Supporting Information File 1.

The syntheses of per-6-iodo-β- and -γ-CD, I$_7$β-CD (**2a**) and I$_8$γ-CD (**2b**), were performed using a small modification to the known method [13], from freshly dried CDs on a 0.01 mol scale with triphenylphosphine and iodine in DMF. Per-6-bromo-γ-CD (**2b'**) was prepared in *N*-methylpyrrolidone by the same method using bromine. Per-6-chloro-β-CD (**2a'**) was synthesized in a similar manner to per-6-iodo-CDs using *p*-toluenesulfonyl chloride.

General conditions for the solution reactions
Syntheses of compounds **3a**, **3b**, **4a**, **4b**, **5b** and **6** were carried out in DMF at 60–100 °C. For **5b**, triethylamine was used as base, while KO*t*-Bu was used for **6**.

General procedures for the high-energy ball milling reactions
Syntheses of compounds **3a**, **3b**, **4a**, **4b**, **5b** and **6** were carried out in a Retsch PM100 High Speed Planetary Ball Mill. 1500 steel balls of 1 mm diameter (44.94 g) and 50 steel balls of 5 mm diameter (25.54 g, total weight of balls = 70.5 g, V = 15 mL), were placed in a stainless steel jar of 50 mL, with a sun wheel speed of 650 min^{-1} for 120 min, weight = 780 g (jar, cap, and balls). Temperatures were measured using a Lafayette TRI-88 no-contact thermometer, built-in laser pointer, with ±2 °C reading accuracy, distance to spot size = 8:1, measuring distance 18–23 cm. The measurement matrix formed "a five on a die", two measurements were made at each point and the values were averaged.

Supporting Information

Supporting Information File 1
Details of synthetic procedures and characterization of prepared compounds.
[http://www.beilstein-journals.org/bjoc/content/supplementary/1860-5397-12-230-S1.pdf]

Acknowledgements

References
1. Bender, M. L.; Komiyama, M. *Cyclodextrin Chemistry. Reactivity and Structure: Concepts in Organic Chemistry;* Springer: Berlin-Heidelberg, 1978; Vol. 6. doi:10.1007/978-3-642-66842-5
2. Szejtli, J. *Cyclodextrins and Their Inclusion Complexes;* Akadémiai Kiadó: Budapest, 1982.
3. Szejtli, J.; Oda, T., Eds. *Cyclodextrins. Comprehensive Supramolecular Chemistry;* Pergamon: New York, 1996; Vol. 3.
4. Astier, Y.; Braha, O.; Bayley, H. *J. Am. Chem. Soc.* **2006,** *128,* 1705–1710. doi:10.1021/ja057123+
5. Sanderson, K. *Nature* **2008,** *456,* 23–25. doi:10.1038/456023a
6. Gooding, M.; Malhotra, M.; McCarthy, D. J.; Godinho, B. M. D. C.; Cryan, J. F.; Darcy, R.; O'Driscoll, C. M. *Eur. J. Pharm. Sci.* **2015,** *71,* 80–92. doi:10.1016/j.ejps.2015.02.007
7. Zhang, M.-Q. *Drug Discovery Today: Technol.* **2010,** *7,* e131–e137. doi:10.1016/j.ddtec.2010.07.002
8. Rojas, M. T.; Koeniger, R.; Stoddart, J. F.; Kaifer, A. E. *J. Am. Chem. Soc.* **1995,** *117,* 336–343. doi:10.1021/ja00106a036
9. Martina, K.; Rinaldi, L.; Baricco, F.; Boffa, L.; Cravotto, G. *Synlett* **2015,** *26,* 2789–2794. doi:10.1055/s-0035-1560173
10. Rinaldi, L.; Binello, A.; Stolle, A.; Curini, M.; Cravotto, G. *Steroids* **2015,** *98,* 58–62. doi:10.1016/j.steroids.2015.02.016
11. Cravotto, G.; Caporaso, M.; Jicsinszky, L.; Martina, K. *Beilstein J. Org. Chem.* **2016,** *12,* 278–294. doi:10.3762/bjoc.12.30
12. Vizitiu, D.; Walkinshaw, C. S.; Gorin, B. I.; Thatcher, G. R. J. *J. Org. Chem.* **1997,** *62,* 8760–8766. doi:10.1021/jo9711549
13. Gadelle, A.; Defaye, J. *Angew. Chem., Int. Ed. Engl.* **1991,** *30,* 78–80. doi:10.1002/anie.199100781
14. Khan, A. R.; D'Souza, V. T. *J. Org. Chem.* **1994,** *59,* 7492–7495. doi:10.1021/jo00103a051
15. No hits until 01/05/2016 in Science direct (http://www.sciencedirect.com), Scifinder® (http://scifinder.cas.org), and Web of Science™ (http://apps.webofknowledge.com).
16. Bom, A.; Bradley, M.; Cameron, K.; Clark, J. K.; van Egmond, J.; Feilden, H.; MacLean, E. J.; Muir, A. W.; Palin, R.; Rees, D. C.; Zhang, M.-Q. *Angew. Chem.* **2002,** *114,* 275–280. doi:10.1002/1521-3757(20020118)114:2<275::AID-ANGE275>3.0.CO; 2-A
17. Wu, T.; Liu, Z.; Guo, Y.; Dong, C. *J. Electroanal. Chem.* **2015,** *759,* 137–143. doi:10.1016/j.jelechem.2015.11.005
18. Stolle, A.; Szuppa, T.; Leonhardt, S. E. S.; Ondruschka, B. *Chem. Soc. Rev.* **2011,** *40,* 2317–2329. doi:10.1039/C0CS00195C

19. Beyer, M. K.; Clausen-Schaumann, H. *Chem. Rev.* **2005,** *105,* 2921–2948. doi:10.1021/cr030697h

20. Hernández, J. G.; Avila-Ortiz, C. G.; Juaristi, E. Useful Chemical Activation Alternatives in Solvent-Free Organic Reactions. In *Comprehensive Organic Synthesis,* 2nd ed.; Molander, G. A.; Knochel, P., Eds.; Elsevier BV, 2014; pp 287–314. doi:10.1016/B978-0-08-097742-3.00935-6

21. Ranu, B. C.; Chatterjee, T.; Mukherjee, N. Carbon–Heteroatom Bond Forming Reactions and Heterocycle Synthesis under Ball Milling. In *Ball Milling Towards Green Chemistry;* Stolle, A.; Ranu, B., Eds.; RSC Green Chemistry; Royal Society of Chemistry: Cambridge, U.K., 2014; pp 1–33. doi:10.1039/9781782621980-00001

22. Jicsinszky, L.; Caporaso, M.; Tuza, K.; Martina, K.; Calcio Gaudino, E.; Cravotto, G. *ACS Sustainable Chem. Eng.* **2016,** *4,* 919–929. doi:10.1021/acssuschemeng.5b01006

23. Menuel, S.; Doumert, B.; Saitzek, S.; Ponchel, A.; Delevoye, L.; Monflier, E.; Hapiot, F. *J. Org. Chem.* **2015,** *80,* 6259–6266. doi:10.1021/acs.joc.5b00697

24. Tuza, K. Synthesis of Cyclodextrin based C. Perfringens Antidotes. (Hungarian), Master's Thesis, Univ. L. Eötvös, Budapest, Hungary, 2011.

25. Matsui, Y.; Ono, M.; Tokunaga, S. *Bull. Chem. Soc. Jpn.* **1997,** *70,* 535–541. doi:10.1246/bcsj.70.535

26. Rohrbach, R. P.; Rodriguez, L. J.; Eyring, E. M.; Wojcik, J. F. *J. Phys. Chem.* **1977,** *81,* 944–948. doi:10.1021/j100525a003

27. Uccello-Barretta, G.; Evangelisti, C.; Balzano, F.; Vanni, L.; Aiello, F.; Jicsinszky, L. *Carbohydr. Res.* **2011,** *346,* 753–758. doi:10.1016/j.carres.2011.02.001

28. Adam, J. M.; Bennett, D. J.; Bom, A.; Clark, J. K.; Feilden, H.; Hutchinson, E. J.; Palin, R.; Prosser, A.; Rees, D. C.; Rosair, G. M.; Stevenson, D.; Tarver, G. J.; Zhang, M.-Q. *J. Med. Chem.* **2002,** *45,* 1806–1816. doi:10.1021/jm011107f

29. Mazzaglia, A.; Donohue, R.; Ravoo, B. J.; Darcy, R. *Eur. J. Org. Chem.* **2001,** 1715–1721. doi:10.1002/1099-0690(200105)2001:9<1715::AID-EJOC1715>3.0.CO;2-A

30. Eccles, K. S.; Elcoate, C. J.; Lawrence, S. E.; Maguire, A. R. *ARKIVOC* **2010,** No. ix, 216–228.

31. Mochida, K.; Kagita, A.; Matsui, Y.; Date, Y. *Bull. Chem. Soc. Jpn.* **1973,** *46,* 3703–3707. doi:10.1246/bcsj.46.3703

BEILSTEIN JOURNAL OF ORGANIC CHEMISTRY

Selective and eco-friendly procedures for the synthesis of benzimidazole derivatives. The role of the Er(OTf)₃ catalyst in the reaction selectivity

Natividad Herrera Cano[1], Jorge G. Uranga[1], Mónica Nardi[2], Antonio Procopio[3], Daniel A. Wunderlin[4] and Ana N. Santiago[*1,§]

Address:
[1]INFIQC-CONICET and Facultad de Ciencias Químicas, Departamento de Química Orgánica, Universidad Nacional de Córdoba, Ciudad Universitaria, Córdoba, 5000 Argentina, [2]Dipartimento di Chimica, Università della Calabria Cubo 12C, 87036-Arcavacata di Rende (CS), Italia, [3]Dipartimento di Scienze della Salute, Università Magna Graecia, Viale Europa, 88100-Germaneto (CZ), Italia and [4]ICYTAC-CONICET and Facultad de Ciencias Químicas, Departamento de Química Orgánica, Universidad Nacional de Córdoba, Ciudad Universitaria, Córdoba, 5000 Argentina

Email:
Ana N. Santiago[*] - santiago@fcq.unc.edu.ar

* Corresponding author
§ Tel: +54 351 5353867, extension 53314

Abstract

An improved and greener protocol for the synthesis of benzimidazole derivatives, starting from *o*-phenylenediamine, with different aldehydes is reported. Double-condensation products were selectively obtained when Er(OTf)₃ was used as the catalyst in the presence of electron-rich aldehydes. Conversely, the formation of mono-condensation products was the preferred path in absence of this catalyst. One of the major advantages of these reactions was the formation of a single product, avoiding extensive isolation and purification of products, which is frequently associated with these reactions.

Theoretical calculations helped to understand the different reactivity established for these reactions. Thus, we found that the charge density on the oxygen of the carbonyl group has a significant impact on the reaction pathway. For instance, electron-rich aldehydes better coordinate to the catalyst, which favours the addition of the amine group to the carbonyl group, therefore facilitating the formation of double-condensation products.

Reactions with aliphatic or aromatic aldehydes were possible, without using organic solvents and in a one-pot procedure with short reaction time (2–5 min), affording single products in excellent yields (75–99%). This convenient and eco-friendly methodology offers numerous benefits with respect to other protocols reported for similar compounds.

Introduction

The formation of heterocyclic compounds is a very important task in organic synthesis, mainly because they are present in numerous biologically active compounds and in several natural products [1]. Among them the presence of benzimidazole [2-7] or benzothiazole [8,9] rings in numerous compounds is an important structural element for their biological and medical applications. For example benzimidazoles are widely spread in antiulcer, antihypertensive, antiviral, antifungal, anticancer, and antihistaminic medicines, among others [10-12].

One frequently used protocol for the synthesis of benzimidazole derivatives is the coupling of *o*-phenylenediamines with carboxylic acids [13,14]. Another widely used procedure for the same synthesis represents the condensation of *o*-phenylenediamine with aldehydes. The latter approach has become more widely accepted, because of the easy access to a variety of substituted aldehydes. For instance, the reaction between *o*-phenylenediamine and benzaldehyde readily affords benzimidazole derivatives (Scheme 1). However, the reaction is not selective, affording both 2-substituted (**a**) and 1,2-disubstituted benzimidazoles (**b**).

Therefore, the main drawbacks of current protocols for the synthesis of benzimidazoles include the use of expensive reagents, difficulties in the preparation of the catalyst, long reaction times, a narrow scope of substrates, tedious work-up procedures, the use of hazardous organic solvents and lack of selectivity [15-21].

Rare earth metals are economical and readily available from commercial sources and represent useful catalysts in organic synthesis [22]. In particular, erbium(III) promotes environmentally friendly reactions [23-25], and has been successfully applied to the synthesis of natural products [26-28]. For instanc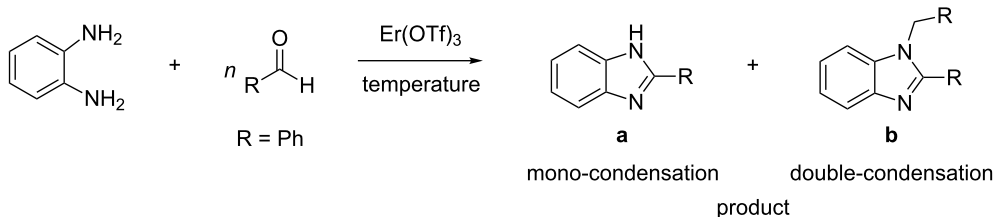e, an efficient method for the synthesis of a wide range of 3,3-dimethyl-11-alkyl, or aryl 2,3,4,5-tetrahydro-1*H*-dibenzo[*b*,*e*][1,4]diazepin-1-ones was reported using erbium(III) trifluoromethanesulfonate, Er(OTf)$_3$ as catalyst. The reaction comprises a one-pot condensation between *o*-phenylenediamine and 5,5-dimethylcyclohexane-1,3-dione, followed by a Er(OTf)$_3$-catalyzed cyclization with diverse alkyl- or arylcarbonyl chlorides [29,30].

In view of these previous applications, our main goal was the development of an environmentally friendly synthetic method, to obtain different derivatives containing the benzimidazole core by a one-pot reaction. Additionally, Er(OTf)$_3$ was selected as the catalyst to achieve the selective formation of products in order to avoid tedious work-up and product separation procedures. Moreover, differences in reactivity were investigated by by means of theoretical calculations.
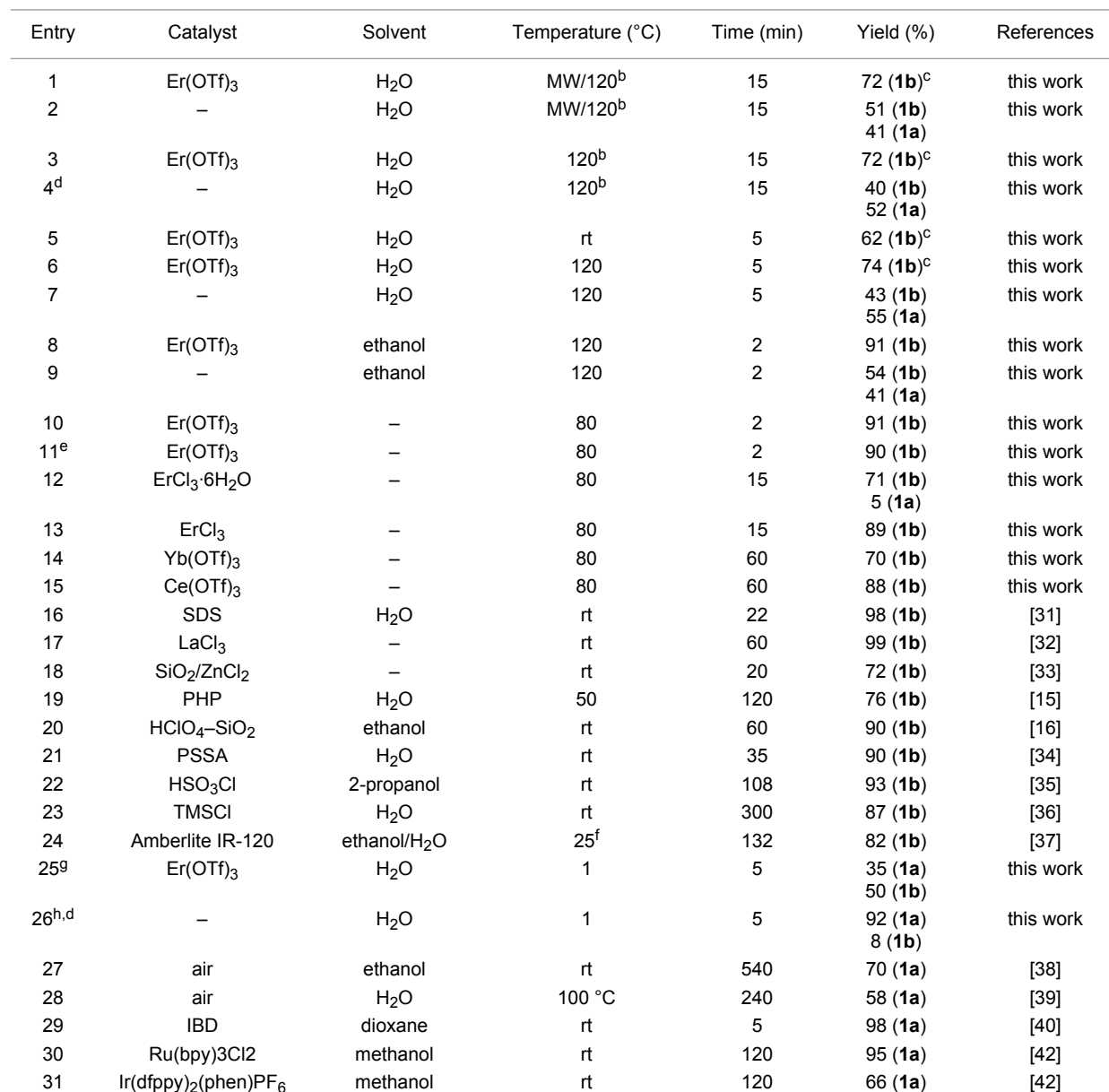
Results and Discussion

The benzimidazole core was obtained by air oxidative cyclocondensation of *o*-phenylenediamine with benzaldehyde under different conditions. In water and in the presence of Er(OTf)$_3$, the diamine and benzaldehyde (1:2 ratio) selectively afforded 1-benzyl-2-phenyl-1*H*-benzimidazole (**1b**) (72% yield), using both microwave irradiation and conventional heating for 15 minutes (Table 1, entries 1 and 3). In the absence of the catalyst, the same reaction afforded a mixture of products **1a** and **1b** using both conditions. Namely, under microwave irradiation, 41% of **1a** and 51% of **1b** were formed (Table 1, entry 2). While, using conventional heating, 52% of **1a** and 40% of **1b** were formed (Table 1, entry 4).

To shorten the reaction time, the catalyzed reaction was carried out during 5 minutes at room temperature. Using these last conditions, the reaction afforded selectively **1b** in 62% yield (Table 1, entry 5). On the other hand, when the reaction was

Scheme 1: Formation of the benzimidazole core.

Table 1: Comparison of the efficiency of various catalysts, solvents and temperatures in the reaction of *o*-phenylenediamine with benzaldehyde.[a]

Entry	Catalyst	Solvent	Temperature (°C)	Time (min)	Yield (%)	References
1	Er(OTf)$_3$	H$_2$O	MW/120[b]	15	72 (**1b**)[c]	this work
2	–	H$_2$O	MW/120[b]	15	51 (**1b**) 41 (**1a**)	this work
3	Er(OTf)$_3$	H$_2$O	120[b]	15	72 (**1b**)[c]	this work
4[d]	–	H$_2$O	120[b]	15	40 (**1b**) 52 (**1a**)	this work
5	Er(OTf)$_3$	H$_2$O	rt	5	62 (**1b**)[c]	this work
6	Er(OTf)$_3$	H$_2$O	120	5	74 (**1b**)[c]	this work
7	–	H$_2$O	120	5	43 (**1b**) 55 (**1a**)	this work
8	Er(OTf)$_3$	ethanol	120	2	91 (**1b**)	this work
9	–	ethanol	120	2	54 (**1b**) 41 (**1a**)	this work
10	Er(OTf)$_3$	–	80	2	91 (**1b**)	this work
11[e]	Er(OTf)$_3$	–	80	2	90 (**1b**)	this work
12	ErCl$_3$·6H$_2$O	–	80	15	71 (**1b**) 5 (**1a**)	this work
13	ErCl$_3$	–	80	15	89 (**1b**)	this work
14	Yb(OTf)$_3$	–	80	60	70 (**1b**)	this work
15	Ce(OTf)$_3$	–	80	60	88 (**1b**)	this work
16	SDS	H$_2$O	rt	22	98 (**1b**)	[31]
17	LaCl$_3$	–	rt	60	99 (**1b**)	[32]
18	SiO$_2$/ZnCl$_2$	–	rt	20	72 (**1b**)	[33]
19	PHP	H$_2$O	50	120	76 (**1b**)	[15]
20	HClO$_4$–SiO$_2$	ethanol	rt	60	90 (**1b**)	[16]
21	PSSA	H$_2$O	rt	35	90 (**1b**)	[34]
22	HSO$_3$Cl	2-propanol	rt	108	93 (**1b**)	[35]
23	TMSCl	H$_2$O	rt	300	87 (**1b**)	[36]
24	Amberlite IR-120	ethanol/H$_2$O	25[f]	132	82 (**1b**)	[37]
25[g]	Er(OTf)$_3$	H$_2$O	1	5	35 (**1a**) 50 (**1b**)	this work
26[h,d]	–	H$_2$O	1	5	92 (**1a**) 8 (**1b**)	this work
27	air	ethanol	rt	540	70 (**1a**)	[38]
28	air	H$_2$O	100 °C	240	58 (**1a**)	[39]
29	IBD	dioxane	rt	5	98 (**1a**)	[40]
30	Ru(bpy)3Cl2	methanol	rt	120	95 (**1a**)	[42]
31	Ir(dfppy)$_2$(phen)PF$_6$	methanol	rt	120	66 (**1a**)	[42]

[a]General reaction conditions: 2 mmol of benzaldehyde and 1 mmol of *o*-phenylenediamine, 10 mol % of Er(OTf)$_3$ under conventional heating. [b]The reaction mixture was heated in a bath at 120 °C using a closed vessel. [c]Only remaining reactants were observed. [d]At 40 min the yield of **1b** was 54%. [e]Under N$_2$ atmosphere. [f]Under sonication. [g]The amine/aldehyde molar ratio was 1:1.1. [h]The amine/aldehyde molar ratio was 4:1.

carried out at 120 °C during 5 minutes, with and without cata-lyst, product **1b** was also formed, with yields of 74% and 43% yield, respectively (Table 1, entries 6 and 7).

Next, different solvents were evaluated aiming at increasing the product yield. When ethanol/water was used as solvent, **1b** was formed together with a small amount of product **1a**. However,

changing to ethanol as the solvent, the reaction of diamine with benzaldehyde at 120 °C selectively afforded 91% of **1b** (Table 1, entry 8). Conversely, the reaction without catalyst in ethanol afforded a mixture of products **1a** (41%) and **1b** (54%) (Table 1, entry 9). The highest selectivity towards the double-condensation product **1b** was obtained in the reaction without any solvent at 80 °C. Under these conditions, product **1b** could be isolated in 91% yield after 2 min reaction time (Table 1, entry 10). The use of Er(OTf)$_3$ under a N$_2$ atmosphere did not change the yield nor the reaction times (Table 1, entry 11). Changing the catalyst to ErCl$_3$·6H$_2$O, the reaction afforded 71% **1b** with a small amount (5%) of **1a**, after 15 min (Table 1, entry 12). The reaction was more selective using ErCl$_3$ during 15 minutes (Table 1, entry 13). The reaction was also carried out with other lanthanides such as Yb(OTf)$_3$ and Ce(OTf)$_3$, both requiring longer times (60 min) to achieve comparable product yields (Table 1, entries 14 and 15).

Table 1 summarizes these results, comparing our current results with other catalysts previously used in the synthesis of benzimidazole derivatives. For instance, the reaction of *o*-phenylenediamine with aromatic aldehydes using sodium dodecyl sulfate (SDS) as the catalyst gave **1b** in 98% yield. However, the yields were low using aliphatic aldehydes together with SDS as catalyst (Table 1, entry 16) [31]. Conversely, good to moderate yields were observed in reactions between benzaldehyde and *o*-phenylenediamine catalyzed by lanthanum (LaCl$_3$) [32], SiO$_2$/ZnCl$_2$ [33], polymeric resin-bound hexafluorophosphate ion (PHP) [15], perchloric acid adsorbed on silica gel (HClO$_4$–SiO$_2$) [16], polystyrene sulfonic acid [34], HSO$_3$Cl in 2-propanol [35], trimethylsilyl chloride (TMSCl) [36], or Amberlite (IR-120) [37]. It is worth mentioning that these previously reported catalysts required longer reaction times than those used in our current protocol (Table 1, entries 17–24). Moreover, although other methods are quite satisfactory with regards to reaction yield, many of them were carried out at high temperatures, or require expensive catalysts. Furthermore, several previously reported reactions employed organic solvents, which are not environmentally friendly. Thereby, we propose the use of Er(OTf)$_3$ as catalyst to provide an eco-friendly, economical and easy to work-up procedure for the synthesis of 1,2-disubstituted benzimidazoles, which can be afforded in only two minutes.

In order to selectively obtain 2-phenyl-1*H*-benzimidazole (**1a**), the reaction was carried out using *o*-phenylenediamine and benzaldehyde (1:1.1 ratio) in water, at 1 °C, adding 10 mol % Er(OTf)$_3$. Under these conditions, 35% of 2-phenyl-1*H*-benzimidazole (**1a**) and 50% of 1-benzyl-2-phenyl-1*H*-benzimidazole (**1b**) were obtained after 5 min reaction (Table 1, entry 25). When this reaction was performed without catalyst,

92% of **1a** and 8% of **1b** were observed using a 4:1 amine/aldehyde ratio (Table 1, entry 26). This ratio favored the fast cyclization, affording excellent yields of mono-condensation product **1a**.

Several reactions between benzaldehyde and *o*-phenylenediamine to obtain 2-phenyl-1*H*-benzimidazole (**1a**) are known. However, they afforded moderate yields requiring longer reaction times in the presence of air (Table 1, entries 27 and 28) [38,39]. Product **1a** was also obtained in a shorter reaction time using hypervalent iodine as oxidant and dioxane as solvent [40,41] or in the presence of [Ru(bpy)$_3$Cl$_2$] or Ir(dfppy)$_2$(phen)PF$_6$ as catalysts [42] (Table 1, entries 29–31). The major disadvantage of these methods, however, is the cost of these catalysts.

Thus, comparing previous reports with our current method, it is concluded that the use of Er(OTf)$_3$ as catalyst provides many advantages over previous ones such as it makes use of an economical, eco-friendly and recyclable catalyst, excellent yields in short reaction times, a simple procedure, short reaction times, and an easy work-up.

In addition to the above mentioned advantages we observed that erbium is not involved in the formation of **1a**, but it catalyzes the formation of **1b**. The mechanism for the formation of **1b** using lanthanum catalysts (LaCl$_3$) was reported by Zhang et al. [32]. Considering all the evidences, and the essential role of Er(OTf)$_3$ on the selectivity between **1a** and **1b** observed in this work, two reaction pathways are proposed and shown in Scheme 2: (i) through bisimine rearrangement (path i) and (ii) through a monoamine cyclocondensation–aminal/immonium rearrangement (path ii).

In path i, when the aldehyde approaches Er(OTf)$_3$, the carbonyl carbon of the aldehyde becomes highly reactive toward the nucleophilic attack of *o*-phenylenediamine, generating dibenzylidenediamine **I**. Consequently, the 1,2-disubstituted benzimidazole (**b**) will be formed through bisimine **II**, under catalytic action of the Lewis acid Er(OTf)$_3$. Thus, the catalyst acts as an effective electrophilic activating agent for the formation of the bisimine and promotes the subsequent steps (intramolecular nucleophilic attack and the following 1,3-hydride shift), finally affording the 1,2-disubstituted imidazoles (**b**).

In contrast, path ii is a non-catalyzed reaction. In path ii, when the diamine reacts with the aldehyde, a monoimine **III** is formed. The latter intermediate undergoes an intramolecular nucleophilic attack on the C=N, leading to the formation of the imidazoline intermediate **IV**. This intermediate finally affords 2-substituted benzimidazole **1a**. Thus, the presence of erbium

Scheme 2: Proposed mechanism for the formation of 1,2-disubstituted benzimidazoles **b** and 2-substituted benzimidazoles **a**.
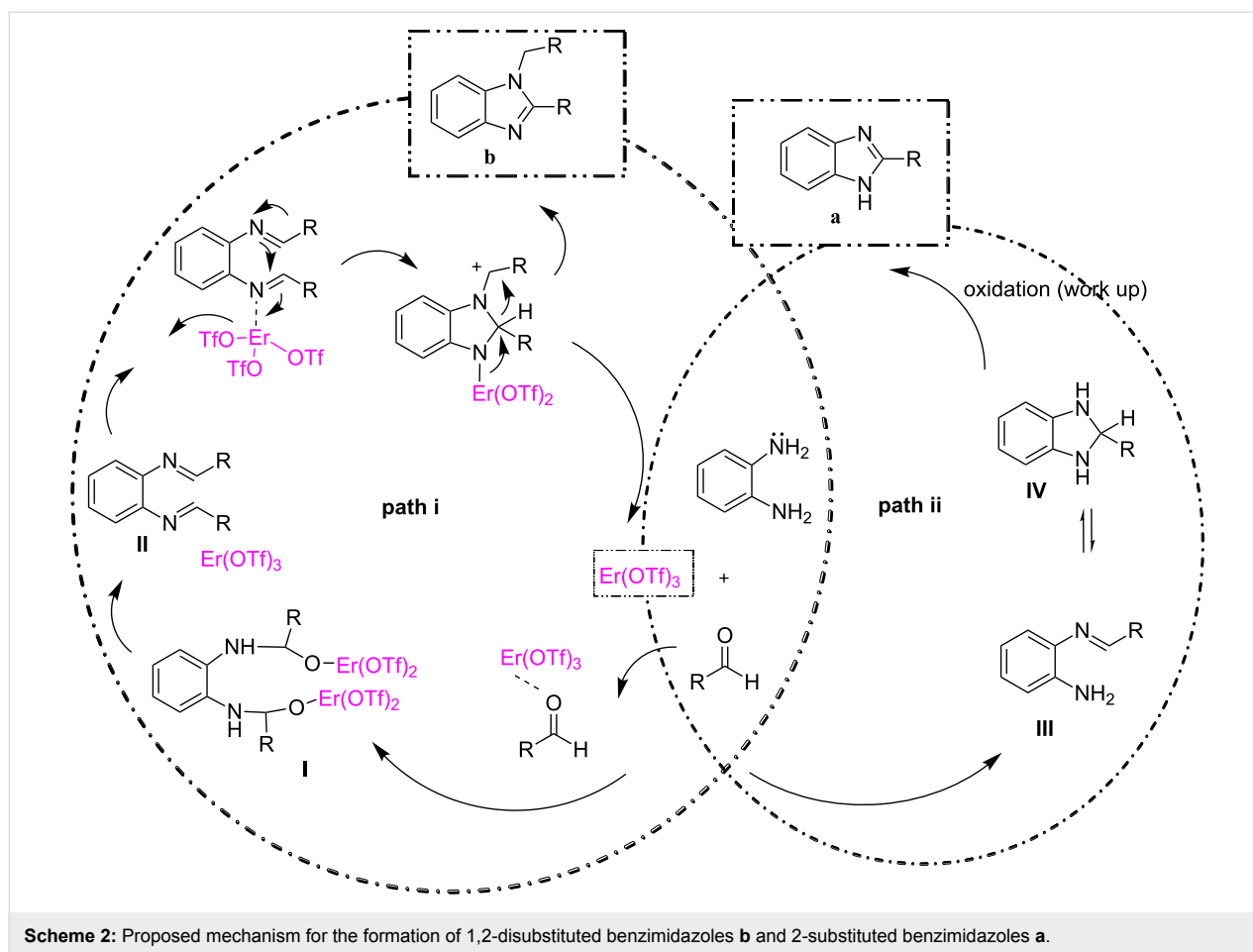
determines the reaction pathway (either i or ii), controlling the selective formation of 1,2-disubstituted vs 2-substituted benzimidazole. It is worth to remark that the presence of the carbonyl hydrogen in the aldehyde is necessary for the formation of the benzimidazole core. On the contrary, the reaction of the diamine with ketones affords benzodiazepine as products [29,30].

Next, we investigated the general applicability of our method in the reaction of *o*-phenylenediamine with several substituted aldehydes using the optimized conditions towards products **1a** or **1b**, respectively. For this, the best conditions to selectively obtain the double-condensation product **1b** (Table 1, entry 10) were chosen and a family of 1,2-disubstituted benzimidazoles was successfully synthesized. The results are listed in Table 2.

The reactions of *o*-phenylenediamine with electron-rich aldehydes, such as $4-CH_3OC_6H_4CHO$, $4-CH_3C_6H_4CHO$, CH_3CH_2CHO, CH_3CHO and $4-C_6H_5-CH_2CHO$ (Table 2, entries 2–6) afforded the corresponding 1,2-disubstituted benzimidazoles **2b–7b** in good yields (over 83%) under the optimized conditions. However when aldehydes containing electron-withdrawing groups, such as $4-ClC_6H_4CHO$,

$4-NO_2C_6H_4CHO$ and $4-CNC_6H_4CHO$ were used, unexpected products were observed (Table 2, entries 7–9). Instead of double-condensation products **b**, the corresponding mono-condensation products **7a–9a** were formed in excellent yields. The same products were obtained in comparable yields without the use of catalyst.
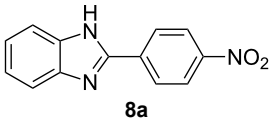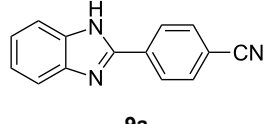
These results clearly show that the electronic effects of the substituents present in the aldehydes play a significant role in the reaction pathway. The 1,2-disubstituted benzimidazoles were obtained when electron-rich aldehydes were used, while 2-monosubstituted benzimidazoles were obtained from the reaction with electron-deficient aldehydes under the same conditions.

To shed light on this observation, we decided to carry out theoretical calculations, using the BPW91 functional at 6-31+G* level, as implemented in Gaussian 09 [43]. In order to evaluate the effect of the substituent on the reactivity of aldehydes, we used a molecular descriptor based on the electronic properties of the carbonyl group. These properties could determinate the affinity between the aldehyde and the catalyst.

Table 2: Synthesis of 1,2-disubstituted benzimidazoles.[a]

Entry	R	Time (min)	Product	Yield (%)
1[b]	Ph	2	**1b**	91
2[c]	4-H$_3$COC$_6$H$_4$	2	**2b**	85
3[d]	4-CH$_3$C$_6$H$_4$	2	**3b**	83
4[e]	CH$_3$CH$_2$	2	**4b**	96
5[f]	H$_3$C	2	**5b**	98
6	C$_6$H$_5$-CH$_2$	2	**6b**	97
7[g]	4-ClC$_6$H$_4$	2–5	**7a**	78

Table 2: Synthesis of 1,2-disubstituted benzimidazoles.[a] (continued)

8[g]	4-NO$_2$C$_6$H$_4$	2–5	**8a**	79
9[g]	4-CNC$_6$H$_4$	2–5	**9a**	82

[a]General reaction conditions: 1 mmol of benzaldehyde and 0.5 mmol of *o*-phenylenediamine, 10 mol % of Er(OTf)$_3$ under conventional heating at 80 °C for the indicated time. [b]With 9% of **1a**. [c]With 15% of **2a**. [d]With 17% of **3a**. [e]With 4% of **4a**. [f]With 2% of **5a**. [g]Product **b** was not detected. Similar yields were obtained without catalyst.

Geometries were optimized for all aldehydes and electrostatic potential (ESP) population analyses were done to obtain the charge density on the carbonyl group. The calculated charge density on the oxygen of carbonyl group could indicate the re-activity of these aldehydes. The greater the charge density on the oxygen, the greater the affinity of it to erbium, enabling the formation of 1,2-disubstituted benzimidazoles (Scheme 2, path i). As it can be seen from Figure 1, the charge density at

Figure 1: ESP maps and charge density on carbonylic oxygen atoms for the studied aldehydes obtained at the BPW91/6-31+G* level. All maps used consistent surface potential ranges (−0.05237 (red) to 0.05237 (blue)) and an isovalue of electron density of 0.0004. All values are expressed in atomic units.
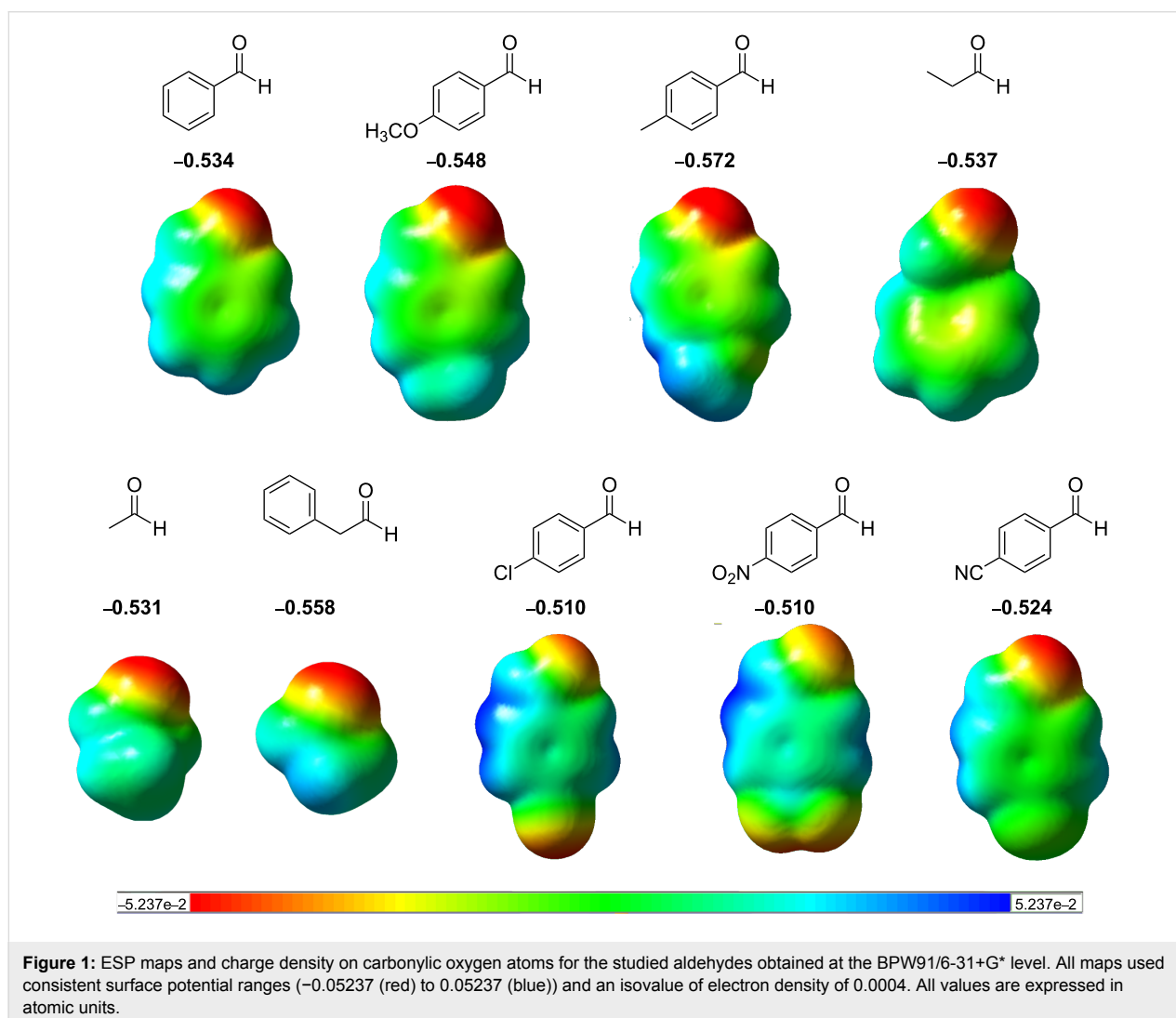
the oxygen of the carbonyl group is a well-suited molecular descriptor for the behavior of the aldehyde.

Our current results show that the charge density for aldehydes containing electron-donating or aliphatic groups varies from −0.57 to −0.53, while the corresponding densities for aldehydes containing electron-withdrawing groups were found to be in a range from −0.52 to −0.51. The aldehydes containing electron-donating or aliphatic groups show a higher density of negative charge on the oxygen atom than aldehydes containing electron-withdrawing groups (Figure 1). As a consequence, electron-rich aldehydes coordinate better with the catalyst, promoting the addition of the amine group to the carbonyl group, and affording double-substitution products (Scheme 2, path i). Conversely, aldehydes substituted with electron-withdrawing groups do not coordinate well due to their lower density of negative charge on the oxygen atom (Figure 1). In the latter case, the formation of mono-condensation products is favored without the intervention of the catalyst (Scheme 2, path ii). These results are consistent with our experimental results.

Next the selectivity towards the mono-condensation products **a** was investigated (Table 3) using the best conditions identified for the synthesis of 2-phenylbenzimidazole (**1a**, Table 1, entry 21). As it can be seen from Table 3, good reaction yields (>80%) were obtained with aldehydes containing both, electron-donating groups (Table 3, entries 2–6) and electron-withdrawing groups (Table 3, entries 7-8) at low temperature using short reactions times. Thus, the new procedure is highly versatile for the selective synthesis of 2-substituted benzimidazoles of general type **a**.

Conclusion

We reported a practical and environmentally friendly one-pot method for the simple and selective synthesis of 1,2-disubstituted or 2-substituted benzimidazoles, starting from *o*-phenylenediamine in the presence of aromatic or aliphatic aldehydes. The use of Er(OTf)$_3$ as commercially available and easily recyclable catalyst promoted the synthesis of 1,2-disubstituted benzimidazoles. Other lanthanides also catalyzed this reaction but required longer reaction times. On the other hand, 2-substituted benzimidazoles were selec-

Table 3: Synthesis of 2-substituted benzimidazoles **a**.[a]
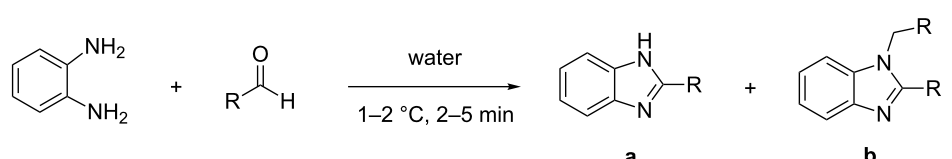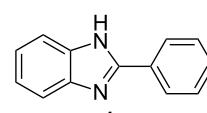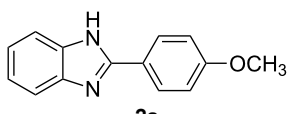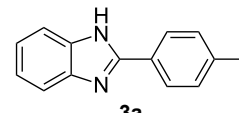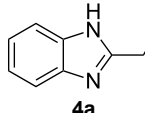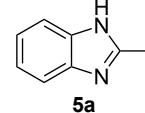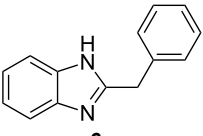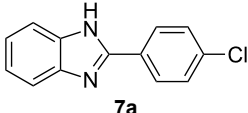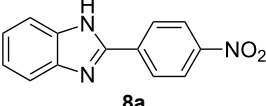
Entry	R	Time (min)	Product	Yield (%)
1[b]	Ph	2	**1a**	92
2[c]	4-H$_3$COC$_6$H$_4$	2	**2a**	99
3[d]	4-CH$_3$C$_6$H$_4$	2	**3a**	94
4[e]	CH$_3$CH$_2$	1	**4a**	96
5[f]	H$_3$C	1	**5a**	97

Table 3: Synthesis of 2-substituted benzimidazoles **a**.[a] (continued)

6[g]	C_6H_5-CH_2	2	**6a**	91
7[h]	4-ClC$_6$H$_4$	5	**7a**	81
8[h]	4-NO$_2$C$_6$H$_4$	5	**8a**	85

[a]General reaction conditions: 0.5 mmol of benzaldehyde and 2 mmol of *o*-phenylenediamine at 1–2 °C in 2–5 minutes without catalyst. [b]With 8% of **1b**. [c]Product **b** was not detected. [d]With 5% of **3b**. [e]With 4% of **4b**. [f]With 3% of **5b** and **7b**, respectively. [g]With 9% of **6b**. [h]Product **b** was not detected.

tively obtained in high yield and short reaction times by the reaction of phenylenediamine with various aldehydes at low temperature (1–2 °C) or at 80 °C in case of electron-deficient aldehydes.

The observed different reactivity, leading to the formation of either mono- or double-condensation products, was explained on the basis of calculated charge densities located on the carbonyl group that is necessary for the coordination of the catalyst. We suggest that the calculated charge densities on the oxygen could indicate the reactivity of these aldehydes. Moreover, the theoretical results predict that a charge density on the oxygen higher than −0.52 favors the coordination to the catalyst, therefore affording double-condensation products, which is in full agreement with the experimental results of this work.

The proposed methodology possesses numerous advantages over previously reported methods, such as high product yields (83–98%), environmentally friendly and mild reaction conditions, short reaction times (2–5 min), high selectivity and broad application. This method could help to produce bioactive compounds using an environmentally friendly procedure.

Supporting Information

Supporting Information File 1
Experimental section, spectroscopical data and XYZ coordinates for all compounds.
[http://www.beilstein-journals.org/bjoc/content/supplementary/1860-5397-12-235-S1.pdf]

Acknowledgements

References

1. Li, J. J., Ed. *Heterocyclic Chemistry in Drug Discovery;* John Wiley &Sons: Hoboken, 2013.
2. Klingensmith, M. J.; Norman, A. G. *Science* **1960,** *131,* 354–355. doi:10.1126/science.131.3397.354
3. Denny, W. A.; Rewcastle, G. W.; Baguley, B. C. *J. Med. Chem.* **1990,** *33,* 814–819. doi:10.1021/jm00164a054
4. Tebbe, M. J.; Spitzer, W. A.; Victor, F.; Miller, S. C.; Lee, C. C.; Sattelberg, T. R., Sr.; McKinney, E.; Tang, J. C. *J. Med. Chem.* **1997,** *40,* 3937–3946. doi:10.1021/jm970423k
5. Porcari, A. R.; Devivar, R. V.; Kucera, L. S.; Drach, J. C.; Townsend, L. B. *J. Med. Chem.* **1998,** *41,* 1252–1262. doi:10.1021/jm970559i
6. White, A. W.; Almassy, R.; Calvert, A. H.; Curtin, N. J.; Griffin, R. J.; Hostomsky, Z.; Maegley, K.; Newell, D. R.; Srinivasan, S.; Golding, B. T. *J. Med. Chem.* **2000,** *43,* 4084–4097. doi:10.1021/jm000950v
7. Boiani, M.; Gonzalez, M. *Mini-Rev. Med. Chem.* **2005,** *5,* 409–424. doi:10.2174/1389557053544047
8. Azam, M. A.; Suresh, B. *Sci. Pharm.* **2012,** *80,* 789–823. doi:10.3797/scipharm.1204-27
9. Herrera Cano, N.; Ballari, M. S.; López, A. G.; Santiago, A. N. *J. Agric. Food Chem.* **2015,** *63,* 3681–3686. doi:10.1021/acs.jafc.5b00150
10. Davey, D.; Erhadt, P. W.; Lumma, W. C., Jr.; Wiggins, J.; Sullivan, M.; Pang, D.; Cantor, E. *J. Med. Chem.* **1987,** *30,* 1337–1342. doi:10.1021/jm00391a012

11. Tomczuk, B. E.; Taylor, C. R., Jr.; Moses, L. M.; Sutherland, D. B.; Lo, Y. S.; Johnson, D. N.; Kinnier, W. B.; Kilpatrick, B. F. *J. Med. Chem.* **1991,** *34,* 2993–3006. doi:10.1021/jm00114a007

12. Spasov, A. A.; Yozhitsa, I. N.; Bugaeva, L. I.; Anisimova, V. A. *Pharm. Chem. J.* **1999,** *33,* 232–243. doi:10.1007/BF02510042

13. Mariappan, G.; Hazarika, R.; Alam, F.; Karki, R.; Patangia, U.; Nath, S. *Arabian J. Chem.* **2015,** *8,* 715–719. doi:10.1016/j.arabjc.2011.11.008

14. Salahuddin; Shaharyar, M.; Mazumder, A.; Ahsan, M. J. *Arabian J. Chem.* **2014,** *7,* 418–424. doi:10.1016/j.arabjc.2013.02.001

15. Ghosh, P.; Mandal, A. *Tetrahedron Lett.* **2012,** *53,* 6483–6488. doi:10.1016/j.tetlet.2012.09.045

16. Kumar, D.; Kommi, D. N.; Chebolu, R.; Garg, S. K.; Kumar, R.; Chakraborti, A. K. *RSC Adv.* **2013,** *3,* 91–98. doi:10.1039/C2RA21994H

17. Girish, Y. R.; Sharath Kumar, K. S.; Thimmaiah, K. N.; Rangappa, K. S.; Shashikanth, S. *RSC Adv.* **2015,** *5,* 75533–75546. doi:10.1039/C5RA13891D

18. Chebolu, R.; Kommi, D. N.; Kumar, D.; Bollineni, N.; Chakraborti, A. K. *J. Org. Chem.* **2012,** *77,* 10158–10167. doi:10.1021/jo301793z

19. Senthilkumar, S.; Kumarraja, M. *Tetrahedron Lett.* **2014,** *55,* 1971–1974. doi:10.1016/j.tetlet.2014.01.140

20. Kumar, A.; Kapoor, K. K. *J. Chem. Pharm. Res.* **2011,** *3,* 369–374.

21. Fan, L.; Kong, L.; Chen, W. *Heterocycles* **2015,** *91,* 2306–2314. doi:10.3987/COM-15-13326

22. Zhang, H.; Zhou, Z.; Yao, Z.; Xu, F.; Shen, Q. *Tetrahedron Lett.* **2009,** *50,* 1622–1624. doi:10.1016/j.tetlet.2009.01.103

23. Procopio, A.; Costanzo, P.; Curini, M.; Nardi, M.; Oliverio, M.; Sindona, G. *ACS Sustainable Chem. Eng.* **2013,** *1,* 541–544. doi:10.1021/sc4000219

24. Nardi, M.; Herrera Cano, N.; Costanzo, P.; Oliverio, M.; Sindona, G.; Procopio, A. *RSC Adv.* **2015,** *5,* 18751–18760. doi:10.1039/C4RA16683C

25. Nardi, M.; Sindona, G.; Costanzo, P.; Oliverio, M.; Procopio, A. *Tetrahedron* **2015,** *71,* 1132–1135. doi:10.1016/j.tet.2014.12.005

26. Procopio, A.; Alcaro, S.; Nardi, M.; Oliverio, M.; Ortuso, F.; Sacchetta, P.; Pieragostino, D.; Sindona, G. *J. Agric. Food Chem.* **2009,** *57,* 11161–11167. doi:10.1021/jf9033305

27. Procopio, A.; Celia, C.; Nardi, M.; Oliverio, M.; Paolino, D.; Sindona, G. *J. Nat. Prod.* **2011,** *74,* 2377–2381. doi:10.1021/np200405s

28. Nardi, M.; Bonacci, S.; De Luca, G.; Maiuolo, J.; Oliverio, M.; Sindona, G.; Procopio, A. *Food Chem.* **2014,** *162,* 89–93. doi:10.1016/j.foodchem.2014.04.015

29. Nardi, M.; Cozza, A.; Maiuolo, L.; Oliverio, M.; Procopio, A. *Tetrahedron Lett.* **2011,** *52,* 4827–4834. doi:10.1016/j.tetlet.2011.06.029

30. Nardi, M.; Cozza, A.; De Nino, A.; Oliverio, M.; Procopio, A. *Synthesis* **2012,** 800–804. doi:10.1055/s-0031-1289691

31. Bahrami, K.; Khodaei, M. M.; Nejati, K. *Green Chem.* **2010,** *12,* 1237–1241. doi:10.1039/c000047g

32. Zhang, L.-J.; Xia, J.; Zhou, Y.-Q.; Wang, H.; Wang, S.-W. *Synth. Commun.* **2012,** *42,* 328–336. doi:10.1080/00397911.2010.524337

33. Jacob, R. G.; Dutra, L. G.; Radatz, C. S.; Mendes, S. R.; Perin, G.; Lenardão, E. J. *Tetrahedron Lett.* **2009,** *50,* 1495–1497. doi:10.1016/j.tetlet.2009.01.076

34. Patil, P. P.; Deshmukh, M. B.; Mulik, A. G.; Chandam, D. R.; Patil, D. R.; Jagdale, S. D.; Anbhule, P. V.; Salunkhe, D. K.; Sankpal, S. A. *Pharma Chem.* **2011,** *3,* 599–605.

35. Shitole, N. V.; Niralwad, K.; Shingate, B. B.; Shingare, M. S. *Arabian J. Chem.* **2012,** *10,* 225–229.

36. Wan, J.-P.; Gan, S.-F.; Wu, J.-M.; Pan, Y. *Green Chem.* **2009,** *11,* 1633–1637. doi:10.1039/b914286j

37. Nile, S. H.; Kumar, B.; Park, S. W. *Arabian J. Chem.* **2015,** *8,* 685–691. doi:10.1016/j.arabjc.2012.12.006

38. Chen, G.-F.; Shen, H.-D.; Jia, H.-M.; Zhang, L.-Y.; Kang, H.-Y.; Qi, Q.-Q.; Chen, B.-H.; Cao, J.-L.; Li, J.-T. *Aust. J. Chem.* **2013,** *66,* 262–266. doi:10.1071/CH12458

39. Lin, S.; Yang, L. *Tetrahedron Lett.* **2005,** *46,* 4315–4319. doi:10.1016/j.tetlet.2005.04.101

40. Du, L.-H.; Wang, Y.-G. *Synthesis* **2007,** 675–678. doi:10.1055/s-2007-965922

41. Chen, C.; Chen, C.; Li, B.; Tao, J.; Peng, J. *Molecules* **2012,** *17,* 12506–12520. doi:10.3390/molecules171112506

42. Park, S.; Jung, J.; Cho, E. J. *Eur. J. Org. Chem.* **2014,** 4148–4154. doi:10.1002/ejoc.201402141

43. *Gaussian 09, Revision B.01;* Gaussian, Inc.: Wallingford, CT, 2010.

A new paradigm for designing ring construction strategies for green organic synthesis: implications for the discovery of multicomponent reactions to build molecules containing a single ring

John Andraos

Abstract

A new way of developing novel synthesis strategies for the construction of monocyclic rings found in organic molecules is presented. The method is based on the visual application of integer partitioning to chemical structures. Two problems are addressed: (1) the determination of the total number of possible ways to construct a given ring by 2-, 3-, and 4-component couplings; and (2) the systematic enumeration of those possibilities. The results of the method are illustrated using cyclohexanone, pyrazole, and the Biginelli adduct as target ring systems with a view to discover new and greener strategies for their construction using multicomponent reactions. The application of the method is also extended to various heterocycles found in many natural products and pharmaceuticals.

Introduction

The ring motif is a key feature in chemical structures that has long attracted the attention of synthetic organic chemists in their quest to implement novel synthesis strategies. Since ring construction poses significant challenges, it brings forth chemists' ingenuity and creativity in posing efficient synthetic routes to important target molecules. This is particularly true for complex ring systems found in natural products, such as the celebrated strychnine scaffold, and in pharmaceuticals that typically contain one of several kinds of nitrogen-containing hetero-cyclic rings. Synthetic organic chemists engaged both in methodology development for the discovery of new transformations and in natural product synthesis to new complex target molecules are now adopting principles of green chemistry. Such principles combine the goals of optimizing reactions to desired products and inventing novel reactions [1-6]. Central to these objectives is the design of highly atom-economical reactions [7,8] that maximize the transfer of atoms found in reactant starting materials to the final desired products. Recently, a

measure of the associated probability of achieving reaction intrinsic "greenness" based on simple reaction yield (RY) and atom economy (AE) threshold constraints was advanced [9]. That work demonstrated that both of these metrics, which define "intrinsic greenness", were critical in influencing whether or not chemical reactions could achieve a minimum standard of overall greenness, regardless of how much auxiliary material (solvents, etc.) was used. Optimization toward overall greenness was best achieved by first maximizing atom economy and reaction yield as far as possible before minimization of auxiliary material consumption. Two points need to be made clear in this discussion. It needs to be emphasized that the design and invention of "intrinsically green" reactions based on high atom economies requires significant chemical ingenuity compared with the simpler task of reducing, replacing, or eliminating solvent usage while maintaining the same chemistry. Furthermore, the bulk of waste from reactions originates from solvents used in work-up extraction and chromatographic purification stages, and not from solvents used in actually carrying out a reaction. Reduction of waste originating from the former group of solvents, however, can present challenges in process chemistry with respect to thermal control, solubility, mixing, and product separation issues when reactions are carried out in very large scale. The idea of "intrinsic greenness" as a core principle based on reaction design was applied to a database of named organic reactions [10] and multicomponent reactions (MCRs) [11-90], written out in a general structural format using Markush structures, to ascertain the fraction of reactions in an organic chemist's toolbox that meet modest conditions of achieving reaction greenness; namely, reactions having minimum atom economies (AE(min)) above 60%. Once these privileged reactions were selected, probabilities of achieving intrinsic reaction greenness were determined based on satisfying simultaneously the criteria that AE(min) > 60% and RY > 80%. Additionally, since the experimental reaction yield quantity is fractional, the analysis interpreted it as a probability of reaction occurrence to a given product given a set of reaction conditions and starting materials. Reaction outcomes with high yields mean that the probability that they occur is high; conversely those with low yields mean that the probability that they occur is low. Probability versus AE(min) distribution curves were generated for reactions producing various ring containing products according to ring size and types of ring systems. It was found that 5- and 6-membered monocyclic rings are most commonly made by [2 + 2 + 1] and [3 + 2 + 1] cycloadditions where 57% and 76% of them, respectively, have a 100% chance of being intrinsically green from a design perspective. A survey of over 2000 MCRs used to synthesize specific types of heterocyclic rings showed that benzimidazoles, Biginelli adducts, dihydropyridines, furans, pyrans, pyridinones, and thiophenes had a high representation of intrinsic greenness;

whereas, a high proportion of MCRs producing chromene-4-ones, coumarins, indoles, and pyrazoles had low probabilities of achieving intrinsic greenness.

In research practice, synthetic organic chemists rely on a combination of retrosynthetic analysis [91-97], similarity and analogy patterning to known reactions, bond dissociation energy and bond polarity analysis (forward and umpolung), chemical intuition, and random occurrences of serendipity to design novel ways to assemble given ring target structures. A favourite example of a serendipitous discovery is when the solvent of a reaction unexpectedly participates as a bone fide reactant rather than behaving as an innocent bystander. Often researchers will tap into their vast library of reactions that they are familiar with from personal experience or through their readings of the literature. Extending known reaction strategy and bond forming-bond breaking themes by analogy is a very useful method. Though retrosynthetic analysis is a powerful tool in the arsenal, its implementation relies entirely on knowledge of known transformations. Similarity and analogy patterning is limited to known reactions as starting points. Serendipity is purely based on accidental occurrences, which are rare, but can be capitalized to advantage by astute researchers. Reliance on all of these strategies to discover new ways to assemble rings is therefore somewhat limiting. There is also the widely held belief in the synthetic organic community that the magnitude of the chemical space of possible transformations that are possible in the forward sense from a finite set of starting building blocks is essentially infinite [98-102] and that despite amassing a database of 1000 or more named reactions and functional group transformations over a period of almost three centuries, synthetic organic chemists have barely scratched the surface in exploring and eventually discovering what transformations are possible in that vast chemical space. In addition, graph theoretical methods have been used to quantify various aspects of synthesis planning and efficiency including codification of construction reactions [103-105], connectivity analysis [106], complexity analysis [107-116], and the creation of encoded synthesis databases that purportedly assist chemists in proposing optimum syntheses to known target molecules subject to constraints, notably number of steps, and cost and availability of commercially available starting materials [117-122]. Despite these advances, these computer-assisted techniques are not routinely adopted by practicing synthetic organic chemists in their everyday work. Instead, they rely on the familiar and tractable methods described earlier.

Given this scenario we sought to address the question of ring construction strategy from a very different perspective that is rooted in an entirely different scientific field which also has enjoyed an even longer track record of research, namely combi-

natorics and enumeration. Specifically, we exploit the subject of integer partitioning [123-125], which is based on the idea of decomposing a given positive integer into smaller positive integers that add up to it. This topic was first investigated by Leonhard Euler in his book *Introductio in Analysin Infinitorum* published in 1748. This problem is akin to the analogous one considered by ancient Greek mathematicians, namely Eratosthenes, of prime factorization, which is based on decomposing a given positive integer into smaller (prime) numbers in a multiplicative sense. Integers already play prominent roles in chemistry. For example, they appear in molecular formulas of compounds, as stoichiometric coefficients in balanced chemical equations, as oxidation states of elements, as Miller indices and space groups in X-ray crystallography, as quantum numbers in atomic orbitals, as exponents in concentration terms in rate laws, as topological indices in knot theory applied to polymers, and as peak ratios and multiplicities in the characterization of functional groups in NMR peaks. They are also the basis of graph theoretical methods including deducing the expected minimum number of rings and unsaturations for a given molecular formula [126], counting and enumerating all possible structural isomers for a given molecular formula of a hydrocarbon [127,128], and parameterizing chemical properties with topological indices [129-131]. However, none of these integer applications involves partitioning of those integers. In this work we apply the concept of integer partitioning to retrosynthetic analysis of ring structures to systematically decompose given ring frameworks via 2-, 3-, and 4-component couplings akin to decomposing an integer into 2-, 3-, and 4-partitions. In this way we may explore the full spectrum of possible ring fragmentations and assess each possibility with respect to our previously published analysis on determining the likelihood of intrinsic greenness. This work is the first time that integer partitioning has been applied in a chemistry context. In fact, as we will demonstrate later, the ring construction problem posed by a synthetic chemist turns out to be an ideal visual representation of the algebraic, more abstract, problem of integer partitioning. There are two central questions that are considered in integer partitioning. The first is the determination of the total number of 2-, 3-, and 4-partitions of a ring system. In this presentation, we focus exclusively on monocyclic rings. This will lead directly to the total number of possible multicomponent coupling assemblages or fragmentations of a given ring skeleton. The second is the enumeration of those partitions in a systematic manner so that a list of unique combinations for each type of ring partition can be obtained. Simple formulas are used to answer the first question; however, they are unable to enumerate each pathway or possibility pictorially as would be needed to solve the chemical problem of finding assemblages using smaller fragment starting materials to build up a complex ring system, which would be of obvious practical significance to a synthetic

chemist. Nevertheless, the tedious task of enumeration can be automated by a simple counting procedure that also eliminates any redundancies. The essential trajectory of tasks presented in this paper is as follows. For a given ring framework, we first obtain the total number of possible 2-, 3-, and 4-partitions. These correspond to all possible 2-, 3-, and 4-component coupling assemblages. The 3- and 4-component couplings are commonly referred to as multicomponent reactions (MCRs). Next, we list and draw out each of these partitions in the form of target bond dissection maps, which highlight the target bonds made in the ring as bolded lines. Then, we permute these maps onto a specific type of ring to list all possible fragmentations of that ring according to a given partition type. This is done simply by overlaying the maps onto the target structure and rotating the fragment framework around the ring, either in a clockwise or anti-clockwise sense. The number and list of permutations of these dissection maps defines the chemical space of possibilities for building up a specified ring framework and is the precise visual representation of the integer partitioning exercise. For example, for a generalized 6-membered ring we find that there are only three possible 3-partitions; namely, [4 + 1 + 1], [3 + 2 + 1], and [2 + 2 + 2]. If we choose a pyridine ring as a target we permute each of these partitions to determine all possible unique [4 + 1 + 1], [3 + 2 + 1], and [2 + 2 + 2] partitions given the symmetry elements of the pyridine ring depending on its substitution pattern. Hence, for 2- or 3-substituted pyridines we have six [4 + 1 + 1], twelve [3 + 2 + 1], and two [2 + 2 + 2] target bond dissection maps; whereas, for 4-substituted pyridines the corresponding numbers are three, six, and one, where the number of each type of fragmentation is reduced by half. In general, rings that contain internal planes of symmetry have significantly fewer possible ring fragmentation patterns for a given partition type. This observation will figure prominently when we extend our present analysis to heterocycles considered in the last section of this paper. Having in hand the list of permutations for a given kind of partition applied to a given kind of ring allows a chemist to sift which ones have been documented in the literature and which ones have not. Of the possibilities that have not been documented a chemist is then forced to ask why this is the case: is it because that assemblage was never considered, or is it a non-viable option due to incompatible mechanistic, kinetic, or thermodynamic considerations. Clearly, if a possibility has not been considered before and is chemically viable, then it would be worth pursuing as a novel synthesis strategy to build up that ring. The integer partitioning method applied to rings therefore is a direct way to identify gaps in synthesis strategies and hence is a valuable aid for the discovery of new reaction assemblages. Since it does not pre-suppose knowledge of existing reactions it is an unbiased procedure. The privileged list of viable possible partitions of a given type on a given ring may be further

assessed according to the probability of intrinsic greenness once particular reactant structures are considered as precursors to the desired ring product structure. This allows the attainment of an elite list of "green" options for synthesizing a given target ring structure that satisfies the criteria of "intrinsic" greenness as defined by the inequality conditions imposed on the key metrics atom economy and reaction yield discussed earlier. The final arbiter of whether such options are indeed realizable is, of course, experimental verification.

The structure of the paper is as follows. We first elaborate on the integer partitioning analysis and apply it directly to the construction of monocyclic rings. As a proof of principle exercise, we use the consequences of that analysis to develop novel syntheses of cyclohexanone based on 2-partitions ([5 + 1], [4 + 2], and [3 + 3]) and 3-partitions ([4 + 1 + 1], [3 + 2 + 1], and [2 + 2 + 2]). Next, we apply all possible 3-partitions to the 5-membered pyrazole ring and compare them to what has been done in the literature. Finally, we apply all possible 3-partitions to the 6-membered Biginelli adduct to identify new assemblages for this structure that have potentially high probabilities of intrinsic greenness that exceed the material performance of the traditional way this heterocycle is synthesized from urea, aldehydes, and 1,3-diketones. The method described in this work is quite general and can be applied to any monocyclic structure. The Supporting Information contains an atlas of target bond dissection maps applied to 27 kinds of heterocyclic structures found in natural and pharmaceutical products.

Results and Discussion
Multicomponent motifs to build single rings

In this section we consider the partitioning of 3- to 12-membered monocyclic rings according to two-, three-, and four-component couplings since these ring sizes and partitions have immediate applications in synthetic organic chemistry. The formulas for these described partitions can of course be applied to any ring size in a mathematical sense. An interesting observation is that the total number of unique n-partitions is given by a polynomial of order $n - 1$. Hence, 2-, 3-, and 4-partitions lead to linear, quadratic, and cubic expressions, respectively. An important point in this analysis is that even- and odd-membered

rings are treated separately since no one set of formulas applies to all ring sizes. Tables S1–S4 in Supporting Information File 1 give key ladder patterns and generating sequences of digits that facilitate the determination of the total number of partitions. Also, simple algorithms for enumerating the individual 3- and 4-partitions are given along with worked examples.

(i) two-component couplings

Equation 1 gives the relationships for the number of unique two-partitions of monocyclic rings.

$$N_{2cr} = \begin{cases} \dfrac{r}{2}, & r = 4, 6, 8, \dots \\ \dfrac{r-1}{2}, & r = 3, 5, 7, \dots \end{cases} \tag{1}$$

where r is the ring size. Table 1 and Table 2 enumerate the possible 2-partitions for even- and odd-membered rings, respectively. Figure 1 shows the corresponding target bond dissection maps for three to eight-membered rings.

(ii) three-component couplings

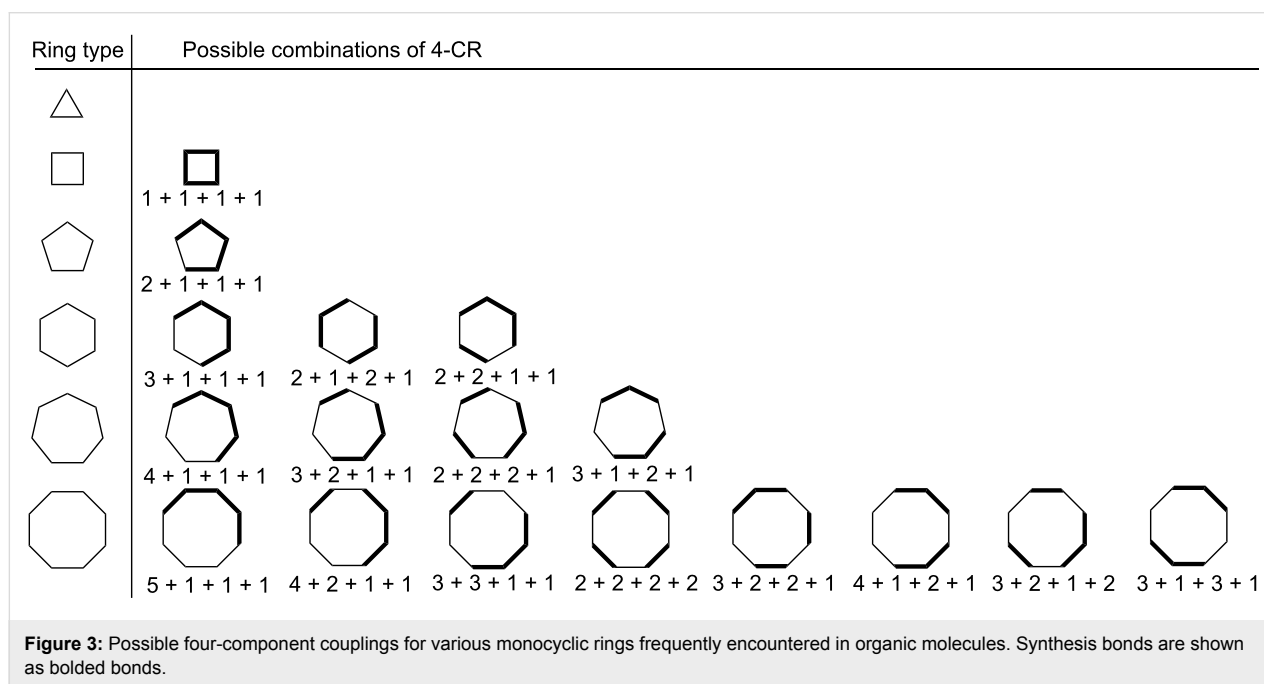Equation 2 and Equation 3 give the relationships for the number of unique three-partitions of even and odd monocyclic rings, respectively. Table 3 and Table 4 enumerate the possible 3-partitions for even- and odd-membered rings, respectively. Figure 2 shows the corresponding target bond dissection maps for three to eight-membered rings. A key observation about 3-partitions of a ring is that the order of the partition numbers is invariant. For example, a (3,2,1) partition of a six-membered ring framework results in an identical dissection map as a (2,3,1), (2,1,3), (1,2,3), (1,3,2), or (3,1,2) partition. Hence, for any 3-partition arranged in a circle, its algebraic representation is indistinguishable from its ring dissection map representation.

$$N_{3cr,even} = \begin{cases} \dfrac{r^2}{12}, & r \text{ is even and divisible by 3} \\ \dfrac{r^2}{12} - \dfrac{1}{3}, & r \text{ is even and not divisible by 3} \end{cases} \tag{2}$$

Table 1: Possible combinations of two-component couplings for various common even-membered monocyclic rings.

Ring size	Possible combinations						Number of combinations
4	3,1	2,2					2
6	5,1	4,2	3,3				3
8	7,1	6,2	5,3	4,4			4
10	9,1	8,2	7,3	6,4	5,5		5
12	11,1	10,2	9,3	8,4	7,5	6,6	6

Table 2: Possible combinations of two-component couplings for various common odd-membered monocyclic rings.

Ring size	Possible combinations					Number of combinations
3	2,1					1
5	4,1	3,2				2
7	6,1	5,2	4,3			3
9	8,1	7,2	6,3	5,4		4
11	10,1	9,2	8,3	7,4	6,5	5

Figure 1: Possible two-component couplings for various monocyclic rings frequently encountered in organic molecules. Synthesis bonds are shown as bolded bonds.

Figure 2: Possible three-component couplings for various monocyclic rings frequently encountered in organic molecules. Synthesis bonds are shown as bolded bonds.
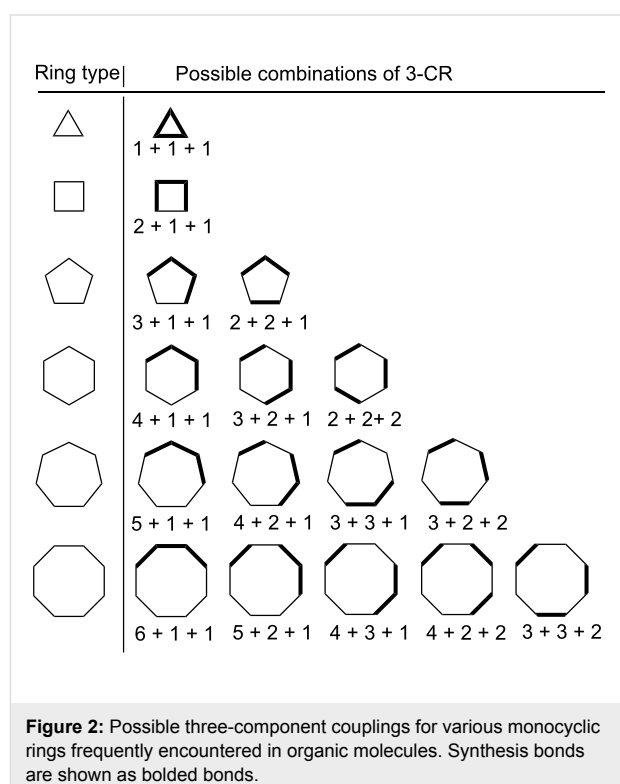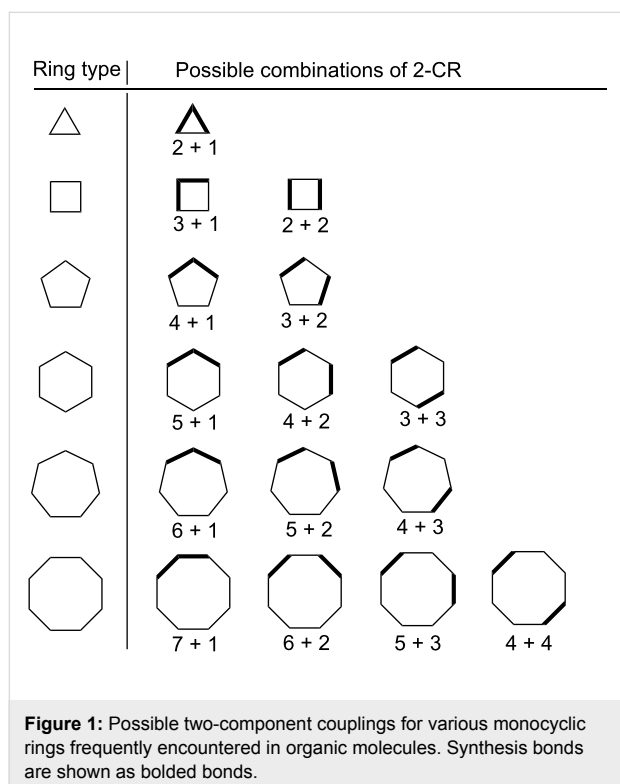
Table 3: Possible combinations of three-component couplings for various common even-membered monocyclic rings.

Ring size	Possible combinations					Number of combinations
4	2,1,1					1
6	4,1,1	3,2,1 2,2,2				3
8	6,1,1	5,2,1 4,2,2	4,3,1 3,3,2			5
10	8,1,1	7,2,1 6,2,2	6,3,1 5,3,2 4,3,3	5,4,1 4,4,2		8
12	10,1,1	9,2,1 8,2,2	8,3,1 7,3,2 6,3,3	7,4,1 6,4,2 5,4,3 4,4,4	6,5,1 5,5,2	12

Table 4: Possible combinations of three-component couplings for various common odd-membered monocyclic rings.

Ring size	Possible combinations					Number of combinations
3	1,1,1					1
5	3,1,1	2,2,1				2
		4,2,1				
7	5,1,1	3,2,2	3,3,1			4
			5,3,1			
		6,2,1	4,3,2			
9	7,1,1	5,2,2	3,3,3	4,4,1		7
			7,3,1	6,4,1		
		8,2,1	6,3,2	5,4,2		
11	9,1,1	7,2,2	5,3,3	4,4,3	5,5,1	10

where *r* is the ring size (4, 6, 8, …).

$$N_{3cr,odd} = \begin{cases} \dfrac{r^2}{12} + \dfrac{1}{4}, & r \text{ is odd and divisible by 3} \\[2mm] \dfrac{r^2}{12} - \dfrac{1}{12}, & r \text{ is odd and not divisible by 3} \end{cases} \qquad (3)$$

where *r* is the ring size (3, 5, 7, …).

(iii) four-component couplings

Equation 4 and Equation 5 give the relationships for the number of unique four-partitions of even and odd monocyclic rings, respectively. Table 5 and Table 6 enumerate the possible 4-partitions for even- and odd-membered rings, respectively. Figure 3 shows the corresponding target bond dissection maps for three to eight-membered rings. Unlike 3-partitions, the order of partition elements does matter for any 4-partition. Hence, algebraic representations of 4-partitions are distinguishable from their ring dissection map representations. For example, a (2,2,1,1) partition results in a different dissection map when drawn out in a ring format than a (2,1,2,1) partition though both partitions consist algebraically of the same kinds of fragment elements; namely, two 2s and two 1s. The fourth entry in Figure 3 shows the visual distinction between partitioning a 6-membered ring via [2 + 2 + 1 + 1] and [2 + 1 + 2 + 1] cycloaddi-

Table 5: Possible combinations of four-component couplings for various common even-membered monocyclic rings.

Ring size	Possible combinations					Number of combinations
4	1,1,1,1					1
	3,1,1,1					
6	2,2,1,1	2,1,2,1				3
	5,1,1,1					
	4,2,1,1	4,1,2,1				
8	3,3,1,1	3,2,2,1	3,2,1,2	3,1,3,1	2,2,2,2	8
		6,1,2,1				
	7,1,1,1	5,2,2,1				
	6,2,1,1	4,3,2,1			4,2,2,2	
	5,3,1,1	4,3,1,2	4,2,3,1	5,1,3,1	3,3,2,2	16
10	4,4,1,1	5,2,1,2	3,3,3,1	4,1,4,1	3,2,3,2	
					6,1,4,1	
					5,2,4,1	
					4,3,4,1	
					5,2,3,2	
		8,1,2,1			4,3,2,3	
	9,1,1,1	7,2,2,1	7,1,3,1		5,2,1,4	
	8,2,1,1	6,3,2,1	6,2,3,1		5,1,5,1	
	7,3,1,1	5,4,2,1	5,3,3,1	6,2,2,2	4,2,4,2	
	6,4,1,1	7,2,1,2	4,4,3,1	5,3,2,2	4,2,3,3	
12	5,5,1,1	6,3,1,2	5,3,1,3	4,4,2,2	3,3,3,3	29

Table 6: Possible combinations of four-component couplings for various common odd-membered monocyclic rings.

Ring size	Possible combinations					Number of combinations
3						0
5	2,1,1,1					1
7	4,1,1,1	3,1,2,1				4
	3,2,1,1	2,2,2,1				
9		5,1,2,1				10
	6,1,1,1	4,2,2,1				
	5,2,1,1	3,3,2,1	4,1,3,1			
	4,3,1,1	4,2,1,2	3,2,3,1	3,2,2,2		
11		7,1,2,1				20
		6,2,2,1				
	8,1,1,1	5,3,2,1	6,1,3,1		5,1,4,1	
	7,2,1,1	4,4,2,1	5,2,3,1		4,2,4,1	
	6,3,1,1	6,2,1,2	4,3,3,1	5,2,2,2	4,2,3,2	
	5,4,1,1	5,3,1,2	4,3,1,3	4,3,2,2	3,3,3,2	

Figure 3: Possible four-component couplings for various monocyclic rings frequently encountered in organic molecules. Synthesis bonds are shown as bolded bonds.

tions. Similarly, [3 + 2 + 1 + 1] and [3 + 1 + 2 + 1] partitions for a 7-membered ring are distinguishable; and for an 8-membered ring [4 + 2 + 1 + 1] and [4 + 1 + 2 + 1] are distinguishable as are [3 + 2 + 2 + 1] and [3 + 2 + 1 + 2], and [3 + 3 + 1 + 1] and [3 + 1 + 3 + 1].

$$N_{4cr,even} = \begin{cases} \dfrac{4}{3}\left(\dfrac{r}{4}\right)^3 - \left(\dfrac{r}{4}\right)^2 + \dfrac{2}{3}\left(\dfrac{r}{4}\right), & \dfrac{r}{2} \text{ is even} \\ \dfrac{(r-2)^3}{48} + \dfrac{(r-2)^2}{12} + \dfrac{r-2}{6}, & \dfrac{r}{2} \text{ is odd} \end{cases} \quad (4)$$

$$N_{4cr,odd} = \begin{cases} \left(\dfrac{r-1}{12}\right)\left(\dfrac{(r-1)^2}{3} - 1\right), & \dfrac{r-1}{2} \text{ is even} \\ \dfrac{(r-3)^3}{48} + \dfrac{(r-3)^2}{8} + \dfrac{r-3}{6}, & \dfrac{r-1}{2} \text{ is odd} \end{cases} \quad (5)$$

where r is the ring size.

Case studies
Cyclohexanone
Cyclohexanone is a 6-membered ring containing one asymmetric feature, namely the electrophilic carbonyl group. This

molecule is made industrially from precursors that already have the 6-membered ring preformed [132]. Example routes include dehydrogenation of cyclohexanol, which in turn is made either by catalytic hydrogenation of phenol, catalytic hydration of cyclohexene, or catalytic air oxidation of cyclohexane. However, as an intellectual exercise and proof of principle, we may be able to use the results described for integer partitioning to devise creative syntheses for cyclohexanone which involve actual ring construction via 2-component ([5 + 1], [4 + 2], and [3 + 3]) couplings not considered before. Figure 4 shows all permutations of the respective 2-partition target bond dissection maps onto the cyclohexanone ring framework. From these diagrams it is possible to conjecture syntheses according to these partition patterns. These are shown in Schemes 1 to 3. Also included in these schemes are atom economy values for each synthetic sequence. From these suggestions, we find that the [5 + 1] strategies produce the lowest atom economies and give rise to significant side product issues as evidenced by the number of additional unwanted possible side reaction pathways suggested by the analysis. The introduction of a single carbon atom in a ring in a nucleophilic sense may be achieved using dilithiomethane [133-135], tris(phenylthio)methyllithium [136], other reagents using established organolithium chemistry [137-139], or malonate diesters via Claisen condensations followed by hydrolysis and decarboxylation. The greenest routes appear in the [4 + 2] strategy. The three-step route beginning with photochemical ring opening of cyclobutenone to give vinylketene, followed by Diels–Alder addition to ethylene leading to cyclohexenone, followed by hydrogenation is 100% atom economical yielding no byproducts. The next best route with an 86% atom economy is the Diels–Alder addition of ketene, generated
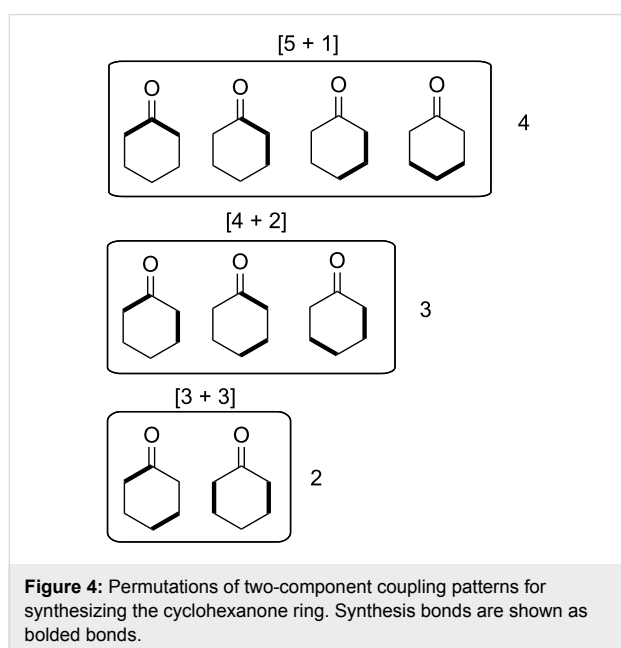
by pyrolysis of acetone, to 1,3-butadiene to give cyclohex-3-enone, which upon hydrogenation yields cyclohexanone. The only byproduct of that route is methane, which is produced in the fragmentation of acetone [140].

It should be emphasized that the given conjectured routes are a subset of a full spectrum of possible solutions to the problem of making bond connections between nucleophilic and electrophilic centres in the partition fragments. However, since cyclohexanone has only one atom in the ring that is electrophilic, this dictates certain restrictions in the overall possible patterns of how various 2-partition fragments come together to form bonds via ionic connections. Based on [5 + 1], [4 + 2], and [3 + 3] partitions shown in Figure 4, Figure 5 shows the overlay of nucleophilic and electrophilic labels on termini of partition fragments. The combinations considered to create the routes shown in Schemes 1 to 3 are shown in red. Other routes to cyclo-

Figure 5: Permutations of two-component coupling patterns for synthesizing the cyclohexanone ring overlayed with nucleophilic (*n*) and electrophilic (*e*) labels at the termini of partition fragments. Synthesis bonds are shown as bolded bonds. Red structures correspond to target templates that form the basis of conjectured syntheses shown in Schemes 1 to 3.

Figure 4: Permutations of two-component coupling patterns for synthesizing the cyclohexanone ring. Synthesis bonds are shown as bolded bonds.

Scheme 1: Conjectured syntheses of cyclohexanone via [5 + 1] strategies.

hexanone may be conjectured based on the remaining combinations. A thorough literature search using Reaxys indicates that cyclohexanone has been made by [5 + 1] and [4 + 2] cycloaddition strategies thus validating the patterns of assembly shown in the third and fourth entries of Scheme 1 and the fourth entry of Scheme 2. The [5 + 1] literature examples involved insertion either of carbon monoxide [141-143], carbon dioxide [144], dichloromethoxymethane [145,146], or methyl methylthiomethyl sulfoxide [147-149] as one-carbon fragments. The only literature example of a [4 + 2] strategy applied to cyclohexanone derivatives involved reaction of but-3-en-2-one with a cyclic enamine followed by reductive elimination of the amine moiety using lithium in liquid ammonia [150].

We may be able to repeat the exercise now using all possible 3-partition target bond dissection maps shown in Figure 6. For brevity the results are given in Supporting Information File 1 in Schemes S1 to S3. Among these options the [2 + 2 + 2] strategy of coupling ketene and two equivalents of ethylene is by far the most efficient with an atom economy of 86%. This route matches the closely related second-best performing [4 + 2] route shown in the third entry of Scheme 2. Again, we can superimpose nucleophilic and electrophilic labels on the termini of 3-partition fragments as before to scope out a complete list of possible connection combinations via ionic bond forming processes. These combinations are shown in Supporting Information File 1, Figure S1. Unlike the two-component assemblies,
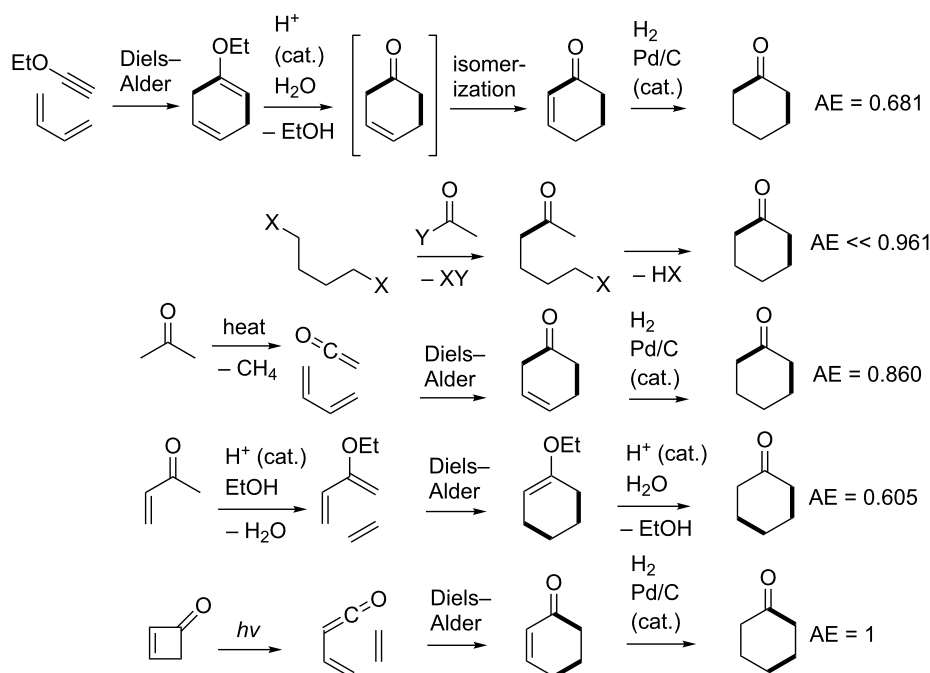
Scheme 2: Conjectured syntheses of cyclohexanone via [4 + 2] strategies.
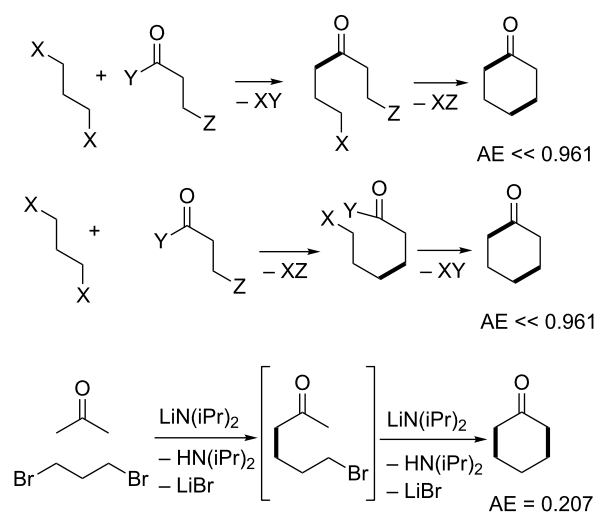
Scheme 3: Conjectured syntheses of cyclohexanone via [3 + 3] strategies.

there are no documented literature examples of constructing cyclohexanone by assembly of three fragments. For comparison we also show a similar nucleophilic–electrophilic centre analysis for the synthesis of piperidine by 2- and 3-partitions in Figures S2 and S3, whose structure is also made up of a six-membered ring but contains a pivoting nucleophilic centre instead of an electrophilic one. These results may be contrasted with the analogous five-membered ring compounds cyclopentanone and pyrrolidine in Figures S4 to S7 in Supporting Infor-

mation File 1. The nucleophilic–electrophilic connectivity patterns for cyclohexanone are the inverse of those for piperidine. The same observation is made when the patterns for cyclopentanone and pyrrolidine are compared. We may conclude that the fewer nucleophilic or electrophilic centres exist in a ring, the more bonding possibilities there are to consider for each partition type. Hence, the construction of hydrocarbon skeletons, containing no pivoting nucleophilic or electrophilic atoms, yields the highest range of possible assemblies and hence the greatest opportunities for creativity and novelty in synthesis design. This explains why such target compounds have attracted the greatest attention among leading synthetic organic chemists [94]. Another feature of key importance that dictates both the partition types and the range of possible assemblies for each partition type is whether the target ring is even- or odd-membered. Even-membered rings often lead to alternating nucleophilic-electrophilic connectivities and hence more direct synthesis routes; whereas, odd-membered rings often lead to connectivities between pairs of nucleophilic termini or pairs of electrophilic termini. This latter situation indicates that an extra redox reaction is a required operation on one of the like centres in order to ligate them. Hence, in order to link two nucleophilic centres, one of them must be oxidized to an electrophilic centre so that it can bond with its nucleophilic partner. Similarly, linking two electrophilic centres requires one of them to be reduced to a nucleophilic centre before bonding can take place. Such additional corrective operations reduce the overall material efficiencies of syntheses of odd-membered

rings compared to even-membered rings. This point will be made more evident when we examine literature multicomponent syntheses of pyrazole, a five-membered heterocycle containing two adjacent nitrogen atoms.
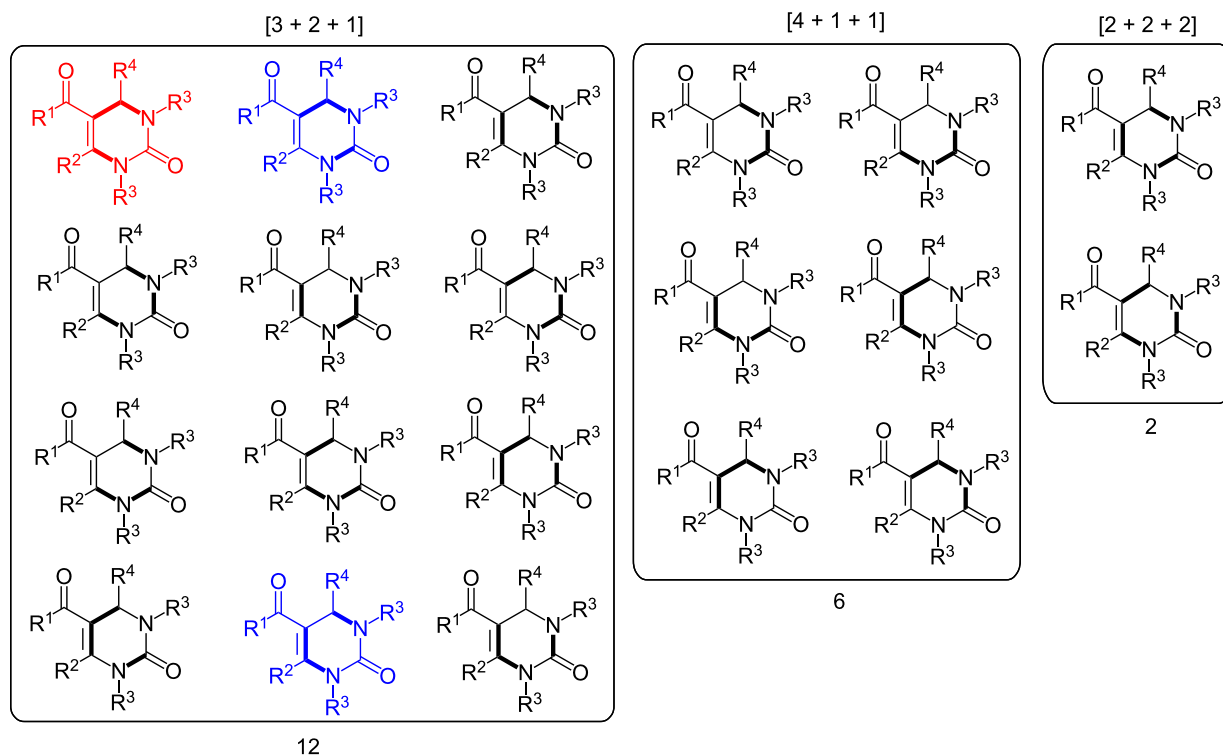

**Figure 6:** Permutations of three-component coupling patterns for synthesizing the cyclohexanone ring. Synthesis bonds are shown as bolded bonds.
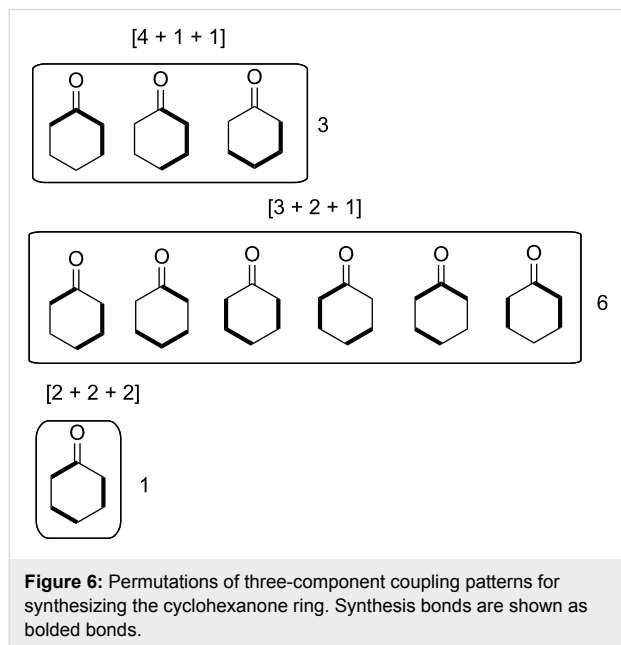
## Pyrazole

Pyrazole is a well-studied 5-membered heterocycle that has been traditionally synthesized either via the Knorr [151] (1,3-diketone and hydrazine) or von Pechmann [152] (olefin and diazomethane followed by oxidation) strategies. Figure 7 shows the five possible [2 + 2 + 1] (designated as "A" strategies) and five possible [3 + 1 + 1] (designated as "B" strategies) target bond dissection maps for constructing this ring via three-component coupling strategies. Schemes 4 to 6 show literature examples of how this ring was made according to the A4, A5, and A1 [2 + 2 + 1] strategies. Glorius [153] followed the A4 strategy; Shen [154,155], Müller [156], Odom [157], Heller [158], and Stonehouse [159] followed the A5 strategy; and Adib [160] and Raw [161] followed the A1 strategy. Scheme 7 shows a literature example of how this ring was made according to the B4 [3 + 1 + 1] strategy, which was followed by Mohanan [162]. The green performances of these syntheses and others are sum-

Figure 7: Permutations of three-component coupling patterns for synthesizing the pyrazole ring via [2 + 2 + 1] (A strategies) and [3 + 1 + 1] (B strategies). Synthesis bonds are shown as bolded bonds.
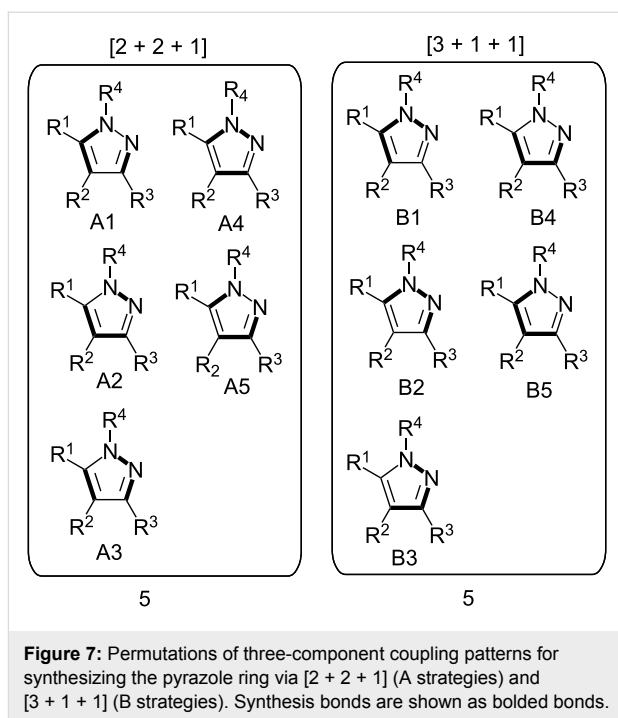
marized in Figure 8. About 40% of the documented examples have a better than 90% probability of meeting a moderate level of greenness; however, 40% of them have less than 60% probability of meeting the same criteria. The winning plans are the Adib and Raw strategies since they have high AE(min) thresholds of 71 and 67%, respectively. These performances are closely followed by the Shen and Odom strategies each with AE(min) values of 64%. The Glorius strategy deserves particular comment since it was claimed to have been discovered fortuitously as a result of solvent incorporation into the product structure when the reaction of amines and ketones with α-hydrogens was carried out in acetonitrile. The present partitioning method advanced in this work clearly shows that such a combination of fragments is entirely predictable on the basis of a simple combinatorial analysis that does not violate mechanistic requirements when these fragments come together in an electrophilic and nucleophilic sense. The discovery of reaction conditions that experimentally verify the prediction is therefore gratifying and demonstrates that the method is indeed a useful tool in discovering new ways to assemble known rings.
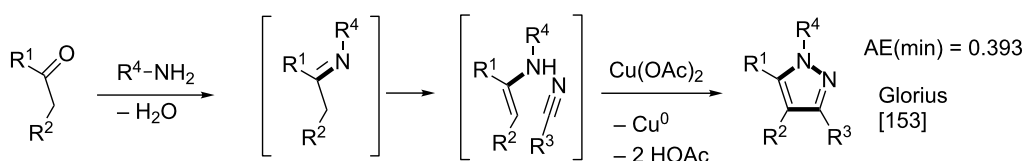
Scheme 4: Literature method for constructing the pyrazole ring via the A4 [2 + 2 + 1] strategy.
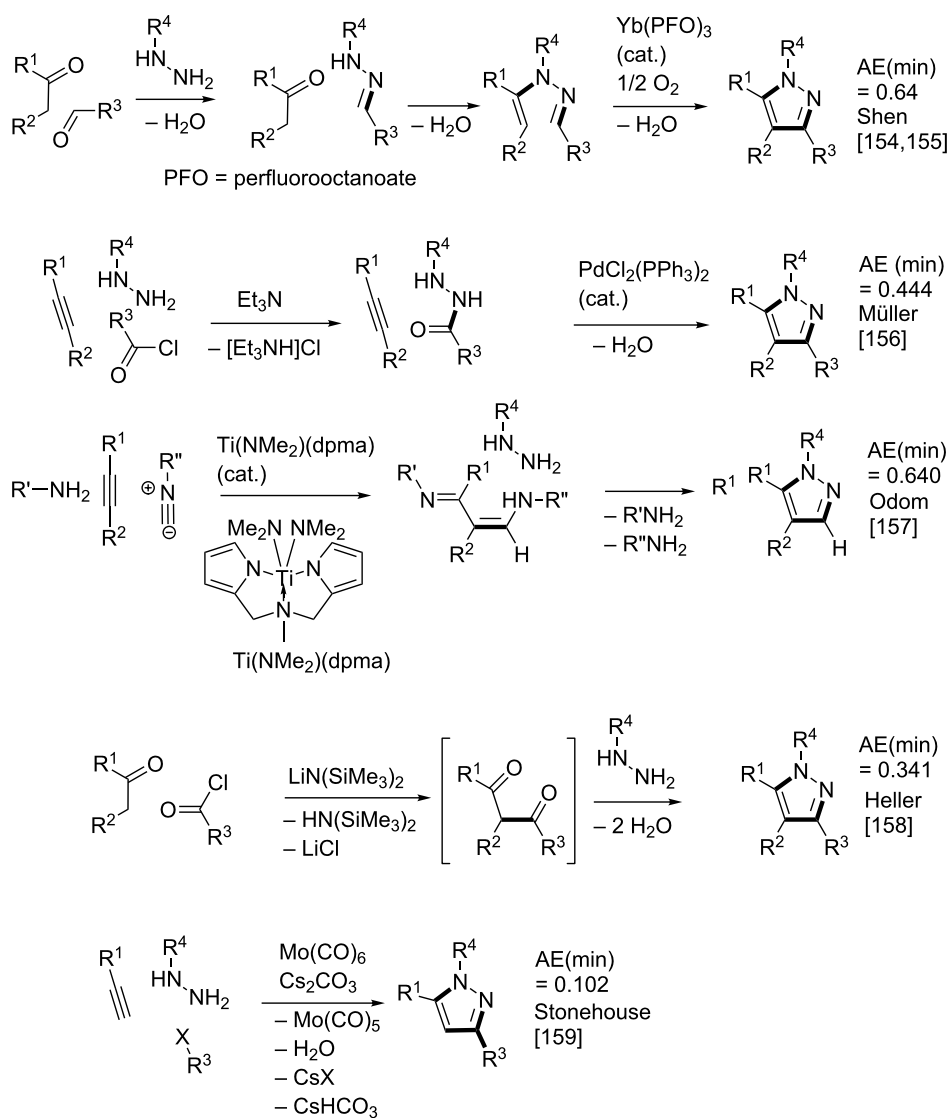
Scheme 5: Literature methods for constructing the pyrazole ring via the A5 [2 + 2 + 1] strategy.

Following from the preceding discussion about synthesizing odd-membered rings, the Glorius, Shen, and Stonehouse examples involve redox chemistries in order to complete the ligation to the five-membered pyrazole ring. A literature search revealed that there were no documented examples of the A2, A3, B1, B2, B3, and B5 strategies, which indicates that the chemical space for three-component coupling reactions to pyrazole has not yet been fully explored experimentally. Scheme 8 shows conjectured [2 + 2 + 1] A2 and A3 multicomponent options that appear to be chemically viable. The second entry in Scheme 8 potentially has the highest minimum atom economy among these conjectured couplings. Scheme 9 shows similarly conjectured [3 + 1 + 1] B1, B2, B3, and B5 strategies.
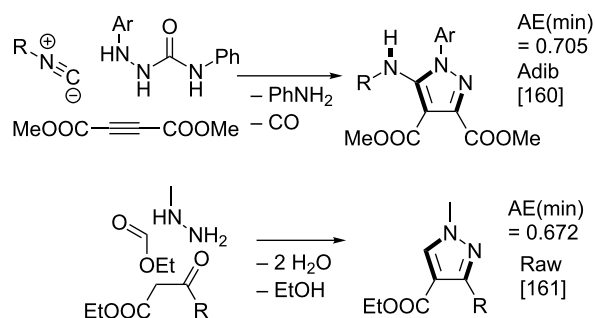
Scheme 6: Literature methods for constructing the pyrazole ring via the A1 [2 + 2 + 1] strategy.
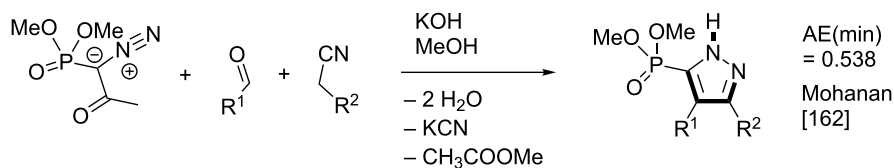
Scheme 7: Literature methods for constructing the pyrazole ring via the B4 [3 + 1 + 1] strategy.
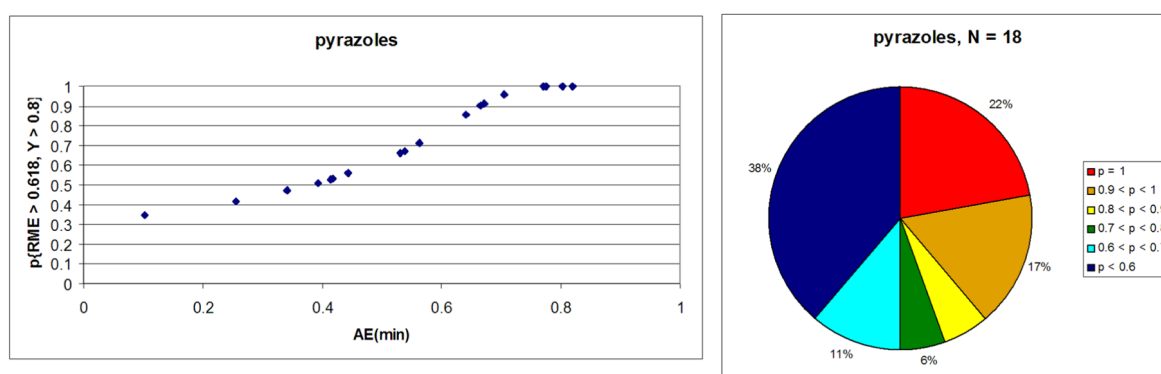
Figure 8: Intrinsic green performance of documented pyrazole syntheses according to [2 + 2 + 1] and [3 + 1 + 1] three-component couplings.
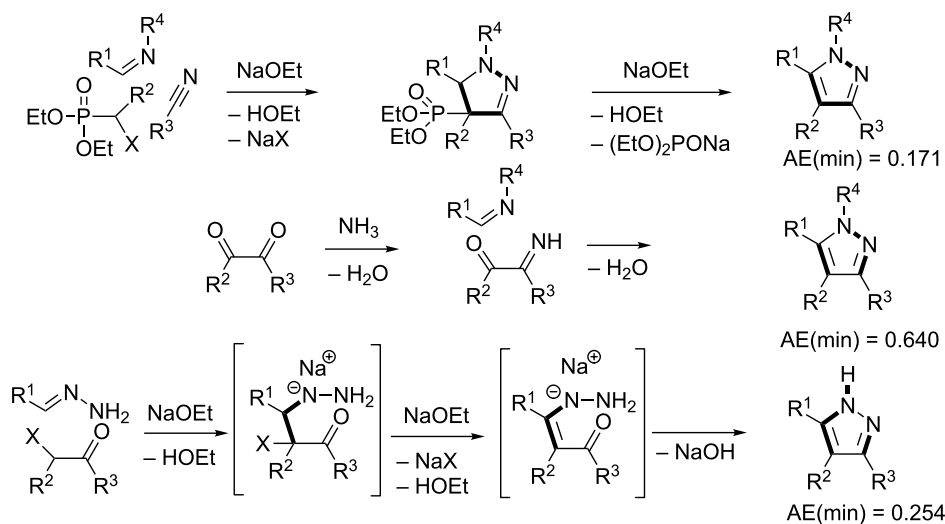
Scheme 8: Conjectured reactions for constructing the pyrazole ring via the A2 and A3 [2 + 2 + 1] strategies.

Biginelli adduct

The Biginelli reaction [163-165] is by far the most studied multicomponent reaction since its discovery in 1891 with nearly 2000 citations in the literature. The 3,4-dihydro-1*H*-pyrimidin-2-one adduct has been made essentially by one [3 + 2 + 1] strategy via condensation of 1,3-diketones, urea, and aldehydes. A full integer partitioning and target bond dissection mapping analysis for three-component couplings of this heterocycle, as

shown in Figure 9, indicates that the chemical space consists of twelve [3 + 2 + 1], six [4 + 1 + 1], and two [2 + 2 + 2] possible strategies. The traditional mapping is shown in red and only 2 out of 18 novel mappings shown in blue have been reported recently. Scheme 10 shows the following literature examples of [3 + 2 + 1] cycloadditions following the traditional mapping (red structure shown in Figure 9): Biginelli [163-165], Shaabani [166], Martins [167], Khodaei [168], Saxena [169], Zhu
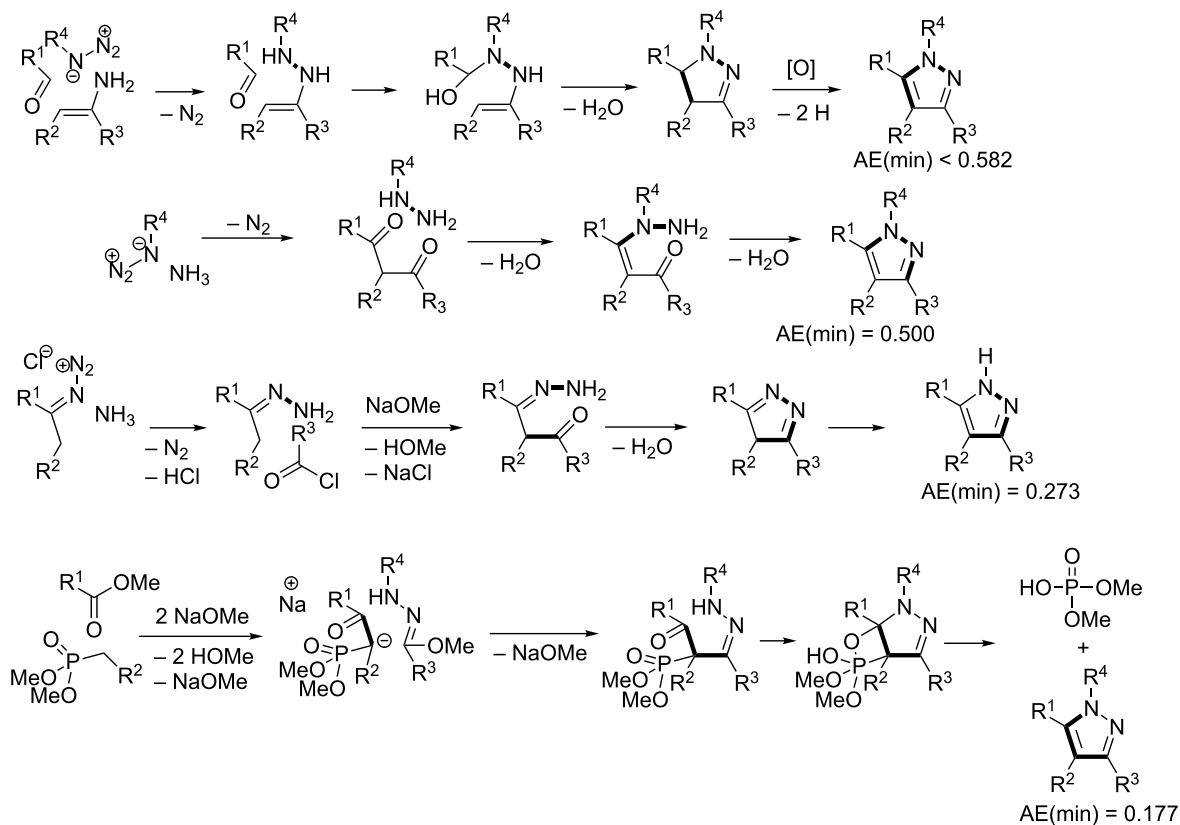
Scheme 9: Conjectured reactions for constructing the pyrazole ring via the B1, B2, B3, and B4 [3 + 1 + 1] strategies.

Figure 9: Permutations of three-component coupling patterns for synthesizing the Biginelli ring adduct. Synthesis bonds are shown as bolded bonds.
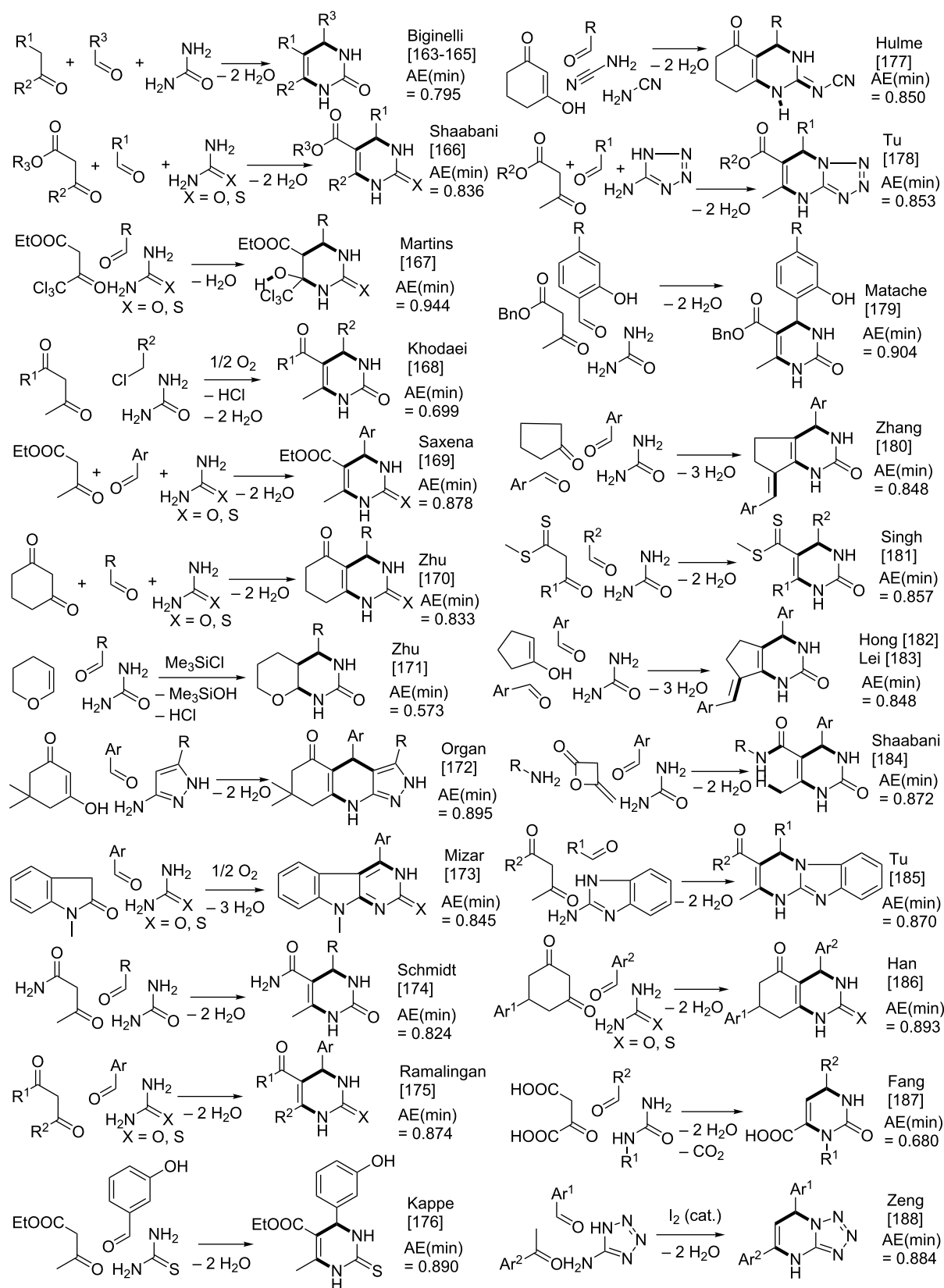
Scheme 10: Reported syntheses of the Biginelli adduct via the traditional [3 + 2 + 1] mapping strategy.

[170], Zhu [171], Organ [172], Mizar [173], Schmidt [174], Ramalingan [175], Kappe [176], Hulme [177], Tu [178], Matache [179], Zhang [180], Singh [181], Hong [182], Lei [183], Shaabani [184], Tu [185], Han [186], Fang [187], and Zeng [188]. Scheme 11 shows the following literature examples of [3 + 2 + 1] cycloadditions following novel mappings (blue structures shown in Figure 9): Dabiri [189,190], and Singh [191]. The Yi [192] example follows the traditional coupling using a nitrile instead of a urea precursor, which ultimately leads to a heterocyclic ring that contains only one nitrogen atom instead of two. Scheme 12 shows a novel [2 + 2 + 1 + 1] four-component strategy by Orru [193,194]. Since the Biginelli adduct is an even-membered ring with alternating nucleophilic and electrophilic centres, all but two of the cited examples do not involve redox chemistry and are simply characterized as condensation or coupling reactions. The exceptions, Khodaei and Mizar plans, involve substrates which require a corrective oxidation state change that fortunately do not require additional oxidizing agents beyond oxygen from the air. A full exploration of the remaining target bond dissection maps shown in Figure 9 reveals that there exist potentially new highly atom economical reactions that can lead to the Biginelli adduct. Scheme 13 and Scheme 14 list the most promising candidate reactions employing [2 + 2 + 2] and [3 + 2 + 1] cycloadditions, respectively along with their associated AE(min) estimates and probabilities of intrinsic greenness. In Supporting Information File 1, Schemes S4 and S5 list lesser performing
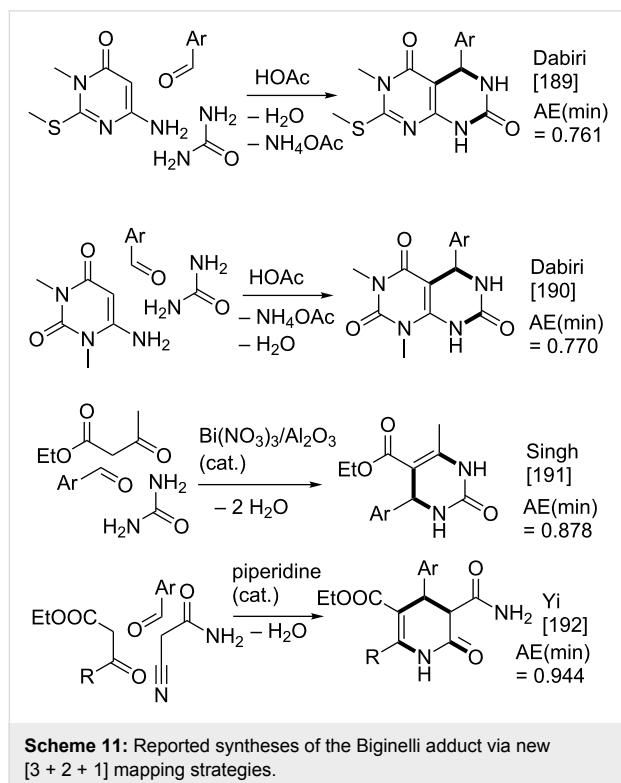
candidates following [3 + 2 + 1] and [4 + 1 + 1] strategies. As was found for the cyclohexanone example, the new [2 + 2 + 2] strategies outperform all others. Figure 10 and Figure 11 show the intrinsic green performances of the literature and newly conjectured syntheses of the Biginelli adduct, respectively. About 90% of literature Biginelli-type syntheses based on one strategy have a better than 90% chance of meeting the intrinsic greenness criterion compared to half of the newly conjectured reactions, based on a much broader range of strategies, found by a thorough partitioning analysis. These findings indicate that there are far more opportunities to pursue novel ways to assemble this product that have not yet been explored.

Scheme 12: Reported syntheses of the Biginelli adduct via a new [2 + 2 + 1 + 1] mapping strategy.
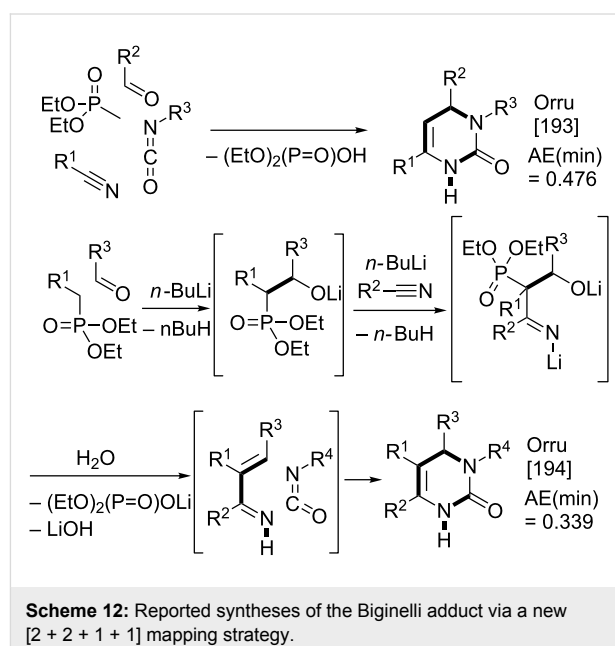
Extension to other monocyclic heterocycles

The methodology presented in this work can in principle be extended to any monocyclic heterocyclic ring system without restriction. In order to motivate synthetic chemists to further explore opportunities to discover new 3-component coupling reactions, an atlas of template target bond 3-partition dissection maps for 27 commonly found heterocyclic rings is given in the Supporting Information File 1 (see Schemes S6 to S32). These include benzimidazole, 2,3-dihydro-1*H*-benzo[*b*][1,4]diazepine, benzofuran, benzopyran, chromen-4-one, coumarin, cyclopent-2-enone, furan, Hantzsch dihydropyridine, hydantoin, imidazole, indole, isoquinoline, isoxazole, oxazole, 4*H*-pyran, pyrazine, pyridazine, pyridine, pyridinone, pyrimidine, pyrimidone, pyrrole, 3*H*-quinazolin-4-one, quinoline, 1*H*-quinolin-4-one, and thiophene. For heterocycles that are composed of a fused aromatic ring, such as benzimidazole, the 3-partitions that do not include the fused junction bond in the set of target synthesis bonds are the ones that have greatest potential for explo-

Scheme 11: Reported syntheses of the Biginelli adduct via new [3 + 2 + 1] mapping strategies.
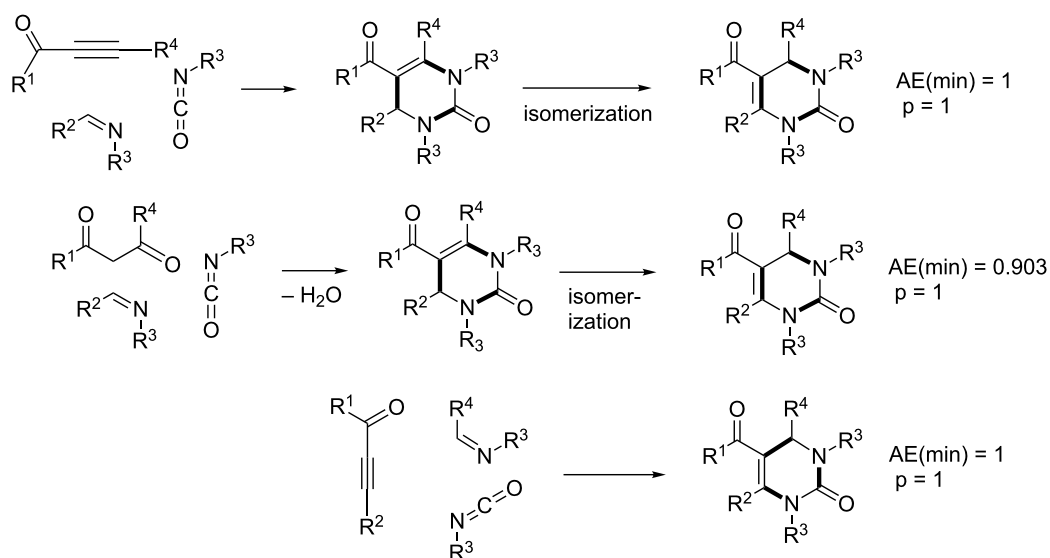
Scheme 13: Conjectured syntheses of the Biginelli adduct via new [2 + 2 + 2] mapping strategies.
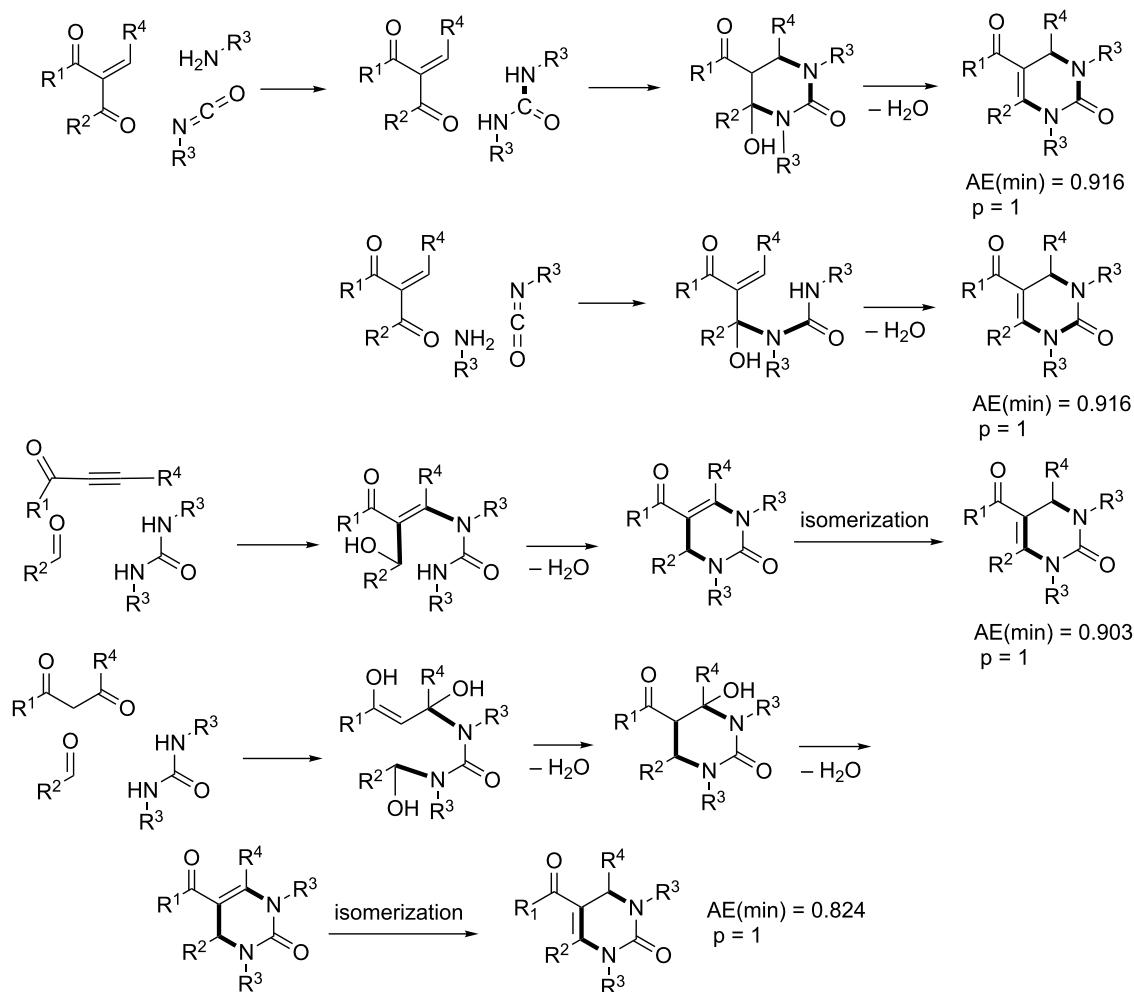
Scheme 14: Conjectured syntheses of the Biginelli adduct via new [3 + 2 + 1] mapping strategies.
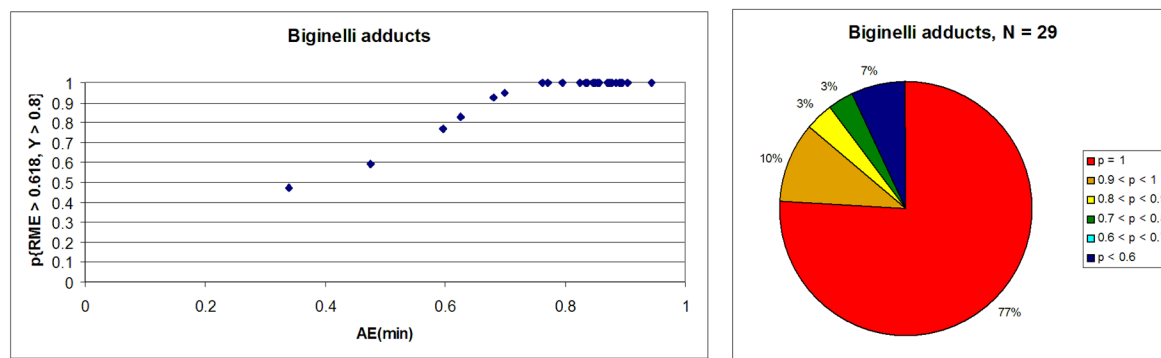
Figure 10: Intrinsic green performance of documented Biginelli adduct syntheses according to [3 + 2 + 1] three-component couplings.
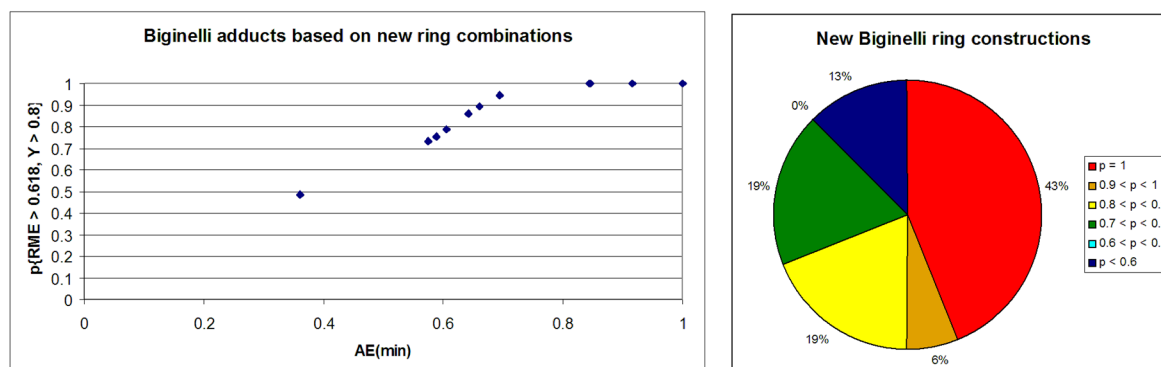
Figure 11: Intrinsic green performance of newly conjectured Biginelli adduct syntheses according to [4 + 1 + 1], [3 + 2 + 1], and [2 + 2 + 2] three-component couplings.

ration. Essentially choosing starting materials that already contain the aromatic moieties will lead to more efficient and green syntheses. These special structural cases are highlighted in red in the atlas wherever they appear. The Supporting Information File 2 and Supporting Information File 3 also contain an extensive listing in Excel format of literature MCRs for the 27 heterocyclic ring types catalogued along with their AE(min) and intrinsic probability performances. As discussed in the introduction, each of these 3-partition maps needs to be vetted by a thorough literature search to identify those that have not been documented. This set of maps will therefore form the basis of any new avenues of research in synthesis methodology that may be pursued in a meaningful, targeted, and systematic fashion. However, the current structure of literature databases such as SciFinder or Reaxys do not allow for facilitated structure searches based on synthesis strategy maps. What would be needed is for a user to input a target heterocyclic structure highlighting a particular 3- or other partition, rather than just inputting the structure itself. A similarity search would be conducted based on inputted target bond dissection maps already encoded in the database. Essentially each literature citation currently in any search engine, which reports syntheses of ring containing compounds, needs to have their associated target bond maps for products synthesized already included as part of the database in order for the map-to-map similarity search to be implemented. Hence, the present investigation also suggests the creation of a new kind of literature database based on synthesis strategy. The existence of such a powerful tool would have far reaching implications for researchers in synthetic chemistry. Since these scientists are always engaged in inventing novel new assemblages of either new or well-known structures, such a tool can easily sift what strategies have already been documented and allow a chemist to focus his or her efforts on new assemblages of rings not considered before. This will guarantee an answer to the oft-asked question of novelty of a planned synthesis. Furthermore, when coupled with the goals of optimizing syntheses that satisfy atom economical and intrinsic greenness probability thresholds, it can also satisfy the aim of inventing both novel and green syntheses of ring containing compounds.

Conclusion

The present study advances a new methodology of synthesis planning for ring containing compounds that combines the concept of retrosynthesis with integer partitioning. The determination of the total number of possible 2-, 3-, and 4-partitions of monocyclic rings of any ring size has been worked out. Simple algorithms for their precise enumeration have also been reported for ring sizes commonly encountered in natural products and pharmaceuticals (three to twelve-membered). Target bond dissection maps based on 3-partitions have been applied to syntheses of cyclohexanone, pyrazole, and the Biginelli adduct to identify potentially new three-component coupling reactions for their synthesis. These conjectured reactions were examined for their intrinsic greenness potential based on threshold atom economy and reaction yield values. The application of this methodology was extended to several kinds of monocyclic and fused aromatic heterocyclic rings. We will report on the application of the integer partition algorithm to fused bicyclic and bridged bicyclic ring frameworks elsewhere.

Supporting Information

Tables S1 to S4 (ladder patterns and generating sequences for determining the total number of unique 3- and 4-partitions of monocyclic rings); simple algorithms for enumerating the sets of unique 3- and 4-partitions of monocyclic rings; Schemes S1 to S3 showing [4 + 1 + 1], [3 + 2 + 1], and [2 + 2 + 2] coupling strategies to synthesize cyclohexanone; Figure S1 to S7 showing nucleophilic-electrophilic centre labels on 3-partition fragment possibilities for cyclohexanone, 2- and 3-partition fragment possibilities for piperidine, 2- and 3- partition fragment possibilities for cyclopentanone, and 2- and 3-partition fragment possibilities for pyrrolidine; Schemes S4 and S5 showing new [3 + 2 + 1] and [4 + 1 + 1] strategies to synthesize the Biginelli adduct; Schemes S6 to S32 showing superposition of 3-partition templates for various heterocycles.

Supporting Information File 1

Application of integer partitioning algorithm to monocyclic rings.

[http://www.beilstein-journals.org/bjoc/content/supplementary/1860-5397-12-236-S1.pdf]

Supporting Information File 2

Excel file of an MCR database of literature routes to various heterocycles.

[http://www.beilstein-journals.org/bjoc/content/supplementary/1860-5397-12-236-S2.xls]

Supporting Information File 3

Excel file of statistics AE(min) and probability of intrinsic greenness for heterocyclic MCRs.

[http://www.beilstein-journals.org/bjoc/content/supplementary/1860-5397-12-236-S3.xls]

References

1. Seebach, D. *Angew. Chem., Int. Ed. Engl.* **1990,** *29,* 1320–1367. doi:10.1002/anie.199013201
2. Wender, P. A.; Miller, B. L. In *Organic Synthesis: Theory and Applications;* Hudlicky, T., Ed.; JAI Press: Connecticut, 1993; Vol. 2.
3. Wender, P. A.; Handy, S. T.; Wright, D. L. *Chem. Ind. (London)* **1997,** *76,* 767–769.
4. Snieckus, V. *Med. Res. Rev.* **1999,** *19,* 342–347. doi:10.1002/(SICI)1098-1128(199909)19:5<342::AID-MED2>3.0.CO;2-E
5. Nicolaou, K. C.; Vourloumis, D.; Winssinger, N.; Baran, P. S. *Angew. Chem., Int. Ed.* **2000,** *39,* 44–122. doi:10.1002/(SICI)1521-3773(20000103)39:1<44::AID-ANIE44>3.0.CO;2-L
6. Nicolaou, K. C.; Snyder, S. A. *Proc. Natl. Acad. Sci. U. S. A.* **2004,** *101,* 11929–11936. doi:10.1073/pnas.0403799101
7. Trost, B. M. *Science* **1991,** *254,* 1471–1477. doi:10.1126/science.1962206
8. Trost, B. M. *Angew. Chem., Int. Ed. Engl.* **1995,** *34,* 259–281. doi:10.1002/anie.199502591
9. Andraos, J. *ACS Sustainable Chem. Eng.* **2013,** *1,* 496–512. doi:10.1021/sc3001614
10. Andraos, J. *Pure Appl. Chem.* **2011,** *83,* 1361–1378. doi:10.1351/PAC-CON-10-10-07
11. Posner, G. H. *Chem. Rev.* **1986,** *86,* 831–844. doi:10.1021/cr00075a007
12. Ugi, I.; Dömling, A.; Hörl, W. *Endeavour* **1994,** *18,* 115–122.
13. Armstrong, R. W.; Combs, A. P.; Tempest, P. A.; Brown, S. D.; Keating, T. A. *Acc. Chem. Res.* **1996,** *29,* 123–131. doi:10.1021/ar9502083
14. Ugi, I. *Proc. Est. Acad. Sci., Chem.* **1998,** *47,* 107–127.
15. Lombardo, M.; Trombini, C. *Seminars in Organic Synthesis XXIII Summer School 'A. Corbella;* Società Chimica Italiana: Milan, 1998; pp 7–32.
16. Dömling, A.; Herdtweck, E.; Ugi, I. *Acta Chem. Scand.* **1998,** *52,* 107–113. doi:10.3891/acta.chem.scand.52-0107
17. Ugi, I.; Almstetter, M.; Bock, M. *Croat. Chem. Acta* **1998,** *71,* 527–547.
18. Weber, L.; Illgen, K.; Almstetter, M. *Synlett* **1999,** 366–374. doi:10.1055/s-1999-2612
19. Tietze, L. F.; Modi, A. *Med. Res. Rev.* **2000,** *20,* 304–322. doi:10.1002/1098-1128(200007)20:4<304::AID-MED3>3.0.CO;2-8

20. Ugi, I.; Dömling, A.; Werner, B. *J. Heterocycl. Chem.* **2000,** *37,* 647–658. doi:10.1002/jhet.5570370322

21. Kappe, C. O. *Acc. Chem. Res.* **2000,** *33,* 879–888. doi:10.1021/ar000048h

22. Dömling, A. *Curr. Opin. Chem. Biol.* **2000,** *4,* 318–323. doi:10.1016/S1367-5931(00)00095-8

23. Ugi, I. *Pure Appl. Chem.* **2001,** *73,* 187–191. doi:10.1351/pac200173010187

24. Dömling, A. *Curr. Opin. Chem. Biol.* **2002,** *6,* 306–313. doi:10.1016/S1367-5931(02)00328-9

25. Weber, L. *Drug Discovery Today* **2002,** *7,* 143–147. doi:10.1016/S1359-6446(01)02090-6

26. Weber, L. *Curr. Med. Chem.* **2002,** *9,* 2085–2093. doi:10.2174/0929867023368719

27. Orru, R. V. A.; de Greef, M. *Synthesis* **2003,** 1471–1499. doi:10.1055/s-2003-40507

28. Jacobi von Wangelin, A.; Neumann, H.; Gördes, D.; Klaus, S.; Strübing, D.; Beller, M. *Chem. – Eur. J.* **2003,** *9,* 4286–4294. doi:10.1002/chem.200305048

29. Ugi, I.; Werner, B.; Dömling, A. *Molecules* **2003,** *8,* 53–66. doi:10.3390/80100053

30. Kappe, C. O. *QSAR Comb. Sci.* **2003,** *22,* 630–645. doi:10.1002/qsar.200320001

31. Simon, C.; Constantieux, T.; Rodriguez, J. *Eur. J. Org. Chem.* **2004,** 4957–4980. doi:10.1002/ejoc.200400511

32. Sapi, J.; Laronze, J.-Y. *ARKIVOC* **2004,** *xii,* 208–222. doi:10.3998/ark.5550190.0005.717

33. Ramachary, D. B.; Barbas, C. F., III. *Chem. – Eur. J.* **2004,** *10,* 5323–5331. doi:10.1002/chem.200400597

34. Zhu, J.; Bienyamé, H. *Multicomponent Reactions;* Wiley-VCH: Weinheim, 2005.

35. Nair, V.; Menon, R. S.; Sreekumar, V. *Pure Appl. Chem.* **2005,** *77,* 1191–1198. doi:10.1351/pac200577071191

36. Ramón, D. J.; Yus, M. *Angew. Chem., Int. Ed.* **2005,** *44,* 1602–1634. doi:10.1002/anie.200460548

37. Tejedor, D.; González-Cruz, D.; Santos-Expósito, A.; Marrero-Tellado, J. J.; de Armas, P.; Garciá-Tellado, F. *Chem. – Eur. J.* **2005,** *11,* 3502–3510. doi:10.1002/chem.200401267

38. Dondoni, A.; Massi, A. *Acc. Chem. Res.* **2006,** *39,* 451–463. doi:10.1021/ar068023r

39. Dömling, A. *Chem. Rev.* **2006,** *106,* 17–89. doi:10.1021/cr0505728

40. Chapman, C. J.; Frost, C. G. *Synthesis* **2007,** 1–21. doi:10.1055/s-2006-950379

41. Guillena, G.; Ramon, D. J.; Yus, M. *Tetrahedron: Asymmetry* **2007,** *18,* 693–700. doi:10.1016/j.tetasy.2007.03.002

42. Tejedor, D.; Garcia-Tellado, F. *Chem. Soc. Rev.* **2007,** *36,* 484–491. doi:10.1039/B608164A

43. Smith, A. B., III; Wuest, W. M. *Chem. Commun.* **2008,** 5883–5895. doi:10.1039/b810394a

44. Shestopalov, A. M.; Shestopalov, A. A.; Rodinovskaya, L. A. *Synthesis* **2008,** 1–25. doi:10.1055/s-2007-990942

45. Akritopoulou-Zanze, I. *Curr. Opin. Chem. Biol.* **2008,** *12,* 324–331. doi:10.1016/j.cbpa.2008.02.004

46. Isambert, N.; Lavilla, R. *Chem. – Eur. J.* **2008,** *14,* 8444–8454. doi:10.1002/chem.200800473

47. Touré, B. B.; Hall, D. G. *Chem. Rev.* **2009,** *109,* 4439–4486. doi:10.1021/cr800296p

48. González-López, M.; Shaw, J. T. *Chem. Rev.* **2009,** *109,* 164–189. doi:10.1021/cr8002714

49. Sunderhaus, J. D.; Martin, F. S. *Chem. – Eur. J.* **2009,** *15,* 1300–1308. doi:10.1002/chem.200802140

50. Wessjohann, L. A.; Rivera, D. G.; Vercillo, O. E. *Chem. Rev.* **2009,** *109,* 796–814. doi:10.1021/cr8003407

51. Ganem, B. *Acc. Chem. Res.* **2009,** *42,* 463–472. doi:10.1021/ar800214s

52. Godineau, E.; Landais, Y. *Chem. – Eur. J.* **2009,** *15,* 3044–3055. doi:10.1002/chem.200802415

53. Kouznetsov, V. V. *Tetrahedron* **2009,** *65,* 2721–2750. doi:10.1016/j.tet.2008.12.059

54. Wan, J.-P.; Liu, Y. *Synthesis* **2010,** 3943–3953. doi:10.1055/s-0030-1258290

55. Dömling, A.; Huang, Y. *Synthesis* **2010,** 2859–2883. doi:10.1055/s-0030-1257906

56. Basso, A.; Banfi, L.; Riva, R. *Eur. J. Org. Chem.* **2010,** 1831–1841. doi:10.1002/ejoc.200901438

57. Fernández-Rodríguez, M. A.; García-García, P.; Aguilar, E. *Chem. Commun.* **2010,** *46,* 7670–7687. doi:10.1039/c0cc02337j

58. Lu, P.; Wang, Y. *Synlett* **2010,** 165–173. doi:10.1055/s-0029-1218558

59. Bonne, D.; Coquerel, Y.; Constantieux, T.; Rodriguez, J. *Tetrahedron: Asymmetry* **2010,** *21,* 1085–1109. doi:10.1016/j.tetasy.2010.04.045

60. Mironov, M. A. *Russ. J. Gen. Chem.* **2010,** *80,* 2628–2646. doi:10.1134/S1070363210120297

61. Lygin, A. V.; de Meijere, A. *Angew. Chem., Int. Ed.* **2010,** *49,* 9094–9124. doi:10.1002/anie.201000723

62. Biggs-Houck, J. E.; Younai, A.; Shaw, J. T. *Curr. Opin. Chem. Biol.* **2010,** *14,* 371–382. doi:10.1016/j.cbpa.2010.03.003

63. Jiang, B.; Shi, F.; Tu, S.-J. *Curr. Org. Chem.* **2010,** *14,* 357–378. doi:10.2174/138527210790231892

64. Estévez, V.; Villacampa, M.; Menéndez, J. C. *Chem. Soc. Rev.* **2010,** *39,* 4402–4421. doi:10.1039/B917644F

65. Choudhury, L. H.; Parvin, T. *Tetrahedron* **2011,** *67,* 8213–8228. doi:10.1016/j.tet.2011.07.020

66. Shaabani, A.; Maleki, A.; Rezayan, A. H.; Sarvary, A. *Mol. Diversity* **2011,** *15,* 41–68. doi:10.1007/s11030-010-9258-1

67. Huang, Y.; Dömling, A. *Mol. Diversity* **2011,** *15,* 3–33. doi:10.1007/s11030-010-9229-6

68. Kruithof, A.; Ruijter, E.; Orru, R. V. A. *Curr. Org. Chem.* **2011,** *15,* 204–236. doi:10.2174/138527211793979817

69. Isambert, N.; del Mar Sanchez Duque, M.; Plaquevent, J.-C.; Génisson, Y.; Rodriguez, J.; Constantieux, T. *Chem. Soc. Rev.* **2011,** *40,* 1347–1357. doi:10.1039/C0CS00013B

70. Ramachary, D. B.; Jain, S. *Org. Biomol. Chem.* **2011,** *9,* 1277–1300. doi:10.1039/c0ob00611d

71. Ruijter, E.; Scheffelaar, R.; Orru, R. V. A. *Angew. Chem., Int. Ed.* **2011,** *50,* 6234–6246. doi:10.1002/anie.201006515

72. Bhojgude, S. S.; Biju, A. T. *Angew. Chem., Int. Ed.* **2012,** *51,* 1520–1522. doi:10.1002/anie.201106984

73. Nair, V.; Menon, R. S.; Biju, A. T.; Abhilash, K. G. *Chem. Soc. Rev.* **2012,** *41,* 1050–1059. doi:10.1039/c1cs15186j

74. De Graaf, C.; Ruijter, E.; Orru, R. V. A. *Chem. Soc. Rev.* **2012,** *41,* 3969–4009. doi:10.1039/c2cs15361k

75. Marson, C. M. *Chem. Soc. Rev.* **2012,** *41,* 7712–7722. doi:10.1039/c2cs35183h

76. van Berkel, S. S.; Bögels, B. G. M.; Wijdeven, M. A.; Westermann, B.; Rutjes, F. P. J. T. *Eur. J. Org. Chem.* **2012,** 3543–3559. doi:10.1002/ejoc.201200030

77. Dömling, A.; Wang, W.; Wang, K. *Chem. Rev.* **2012,** *112,* 3083–3135. doi:10.1021/cr100233r

78. Shiri, M. *Chem. Rev.* **2012,** *112,* 3508–3549. doi:10.1021/cr2003954

79. Gu, Y. *Green Chem.* **2012,** *14,* 2091–2128. doi:10.1039/c2gc35635j

80. Guo, X.; Hu, W. *Acc. Chem. Res.* **2013,** *46,* 2427–2440. doi:10.1021/ar300340k

81. Brauch, S.; van Berkel, S. S.; Westermann, B. *Chem. Soc. Rev.* **2013,** *42,* 4948–4962. doi:10.1039/c3cs35505e

82. van der Heijden, G.; Ruijter, E.; Orru, R. V. A. *Synlett* **2013,** *24,* 666–685. doi:10.1055/s-0032-1318222

83. Alvim, H. G. O.; da Silva Júnior, E. N.; Neto, B. A. D. *RSC Adv.* **2014,** *4,* 54282–54299. doi:10.1039/C4RA10651B

84. Rotstein, B. H.; Zaretsky, S.; Rai, V.; Yudin, A. K. *Chem. Rev.* **2014,** *114,* 8323–8359. doi:10.1021/cr400615v

85. Liu, Y. *ARKIVOC* **2014,** *i,* 1–20. doi:10.3998/ark.5550190.p008.183

86. Cior, R. C.; Ruijter, E.; Orru, R. V. A. *Green Chem.* **2014,** *16,* 2958–2975. doi:10.1039/C4GC00013G

87. Khan, M. M.; Yousuf, R.; Khan, S.; Shafiullah. *RSC Adv.* **2015,** *5,* 57883–57905. doi:10.1039/c5ra08059b

88. Malinakova, H. C. *Rep. Org. Chem.* **2015,** *5,* 75–90. doi:10.2147/ROC.S65115

89. Váradi, A.; Palmer, T. C.; Dardashti, R. N.; Majumdar, S. *Molecules* **2016,** *21,* No. 19. doi:10.3390/molecules21010019

90. Ziarani, G. M.; Moradi, R.; Lashgari, N. *ARKIVOC* **2016,** *i,* 1–81. doi:10.3998/ark.5550190.p009.385

91. Sheehan, J. C.; Buhle, E. L.; Corey, E. J.; Laubach, G. D.; Ryan, J. J. *J. Am. Chem. Soc.* **1950,** *72,* 3828–3829. doi:10.1021/ja01164a534

92. Corey, E. J.; Ohno, M.; Mitra, R. B.; Vatakencherry, P. A. *J. Am. Chem. Soc.* **1964,** *86,* 478–485. doi:10.1021/ja01057a039

93. Corey, E. J.; Mitra, R. B.; Uda, H. *J. Am. Chem. Soc.* **1964,** *86,* 485–492. doi:10.1021/ja01057a040

94. Corey, E. J.; Cheng, X. M. *The Logic of Chemical Synthesis;* Wiley: New York, 1989.

95. Corey, E. J.; Anderson, N. H.; Carlson, R. M.; Paust, J.; Vedejs, E.; Vlattas, I.; Winter, R. E. K. *J. Am. Chem. Soc.* **1968,** *90,* 3245–3247. doi:10.1021/ja01014a053

96. Corey, E. J.; Wipke, W. T. *Science* **1969,** *166,* 178–192. doi:10.1126/science.166.3902.178

97. Corey, E. J.; Long, A. K.; Rubenstein, S. D. *Science* **1985,** *228,* 408–418. doi:10.1126/science.3838594

98. Ertl, P. *J. Chem. Inf. Comput. Sci.* **2003,** *43,* 374–380. doi:10.1021/ci0255782

99. Oprea, T. I.; Gottfries, J. *J. Comb. Chem.* **2001,** *3,* 157–166. doi:10.1021/cc0000388

100. Fink, T.; Reymond, J.-L. *J. Chem. Inf. Model.* **2007,** *47,* 342–353. doi:10.1021/ci600423u

101. Cramer, R. D.; Soltanshahi, F.; Jilek, R.; Campbell, B. *J. Comput.-Aided Mol. Des.* **2007,** *21,* 341–350. doi:10.1007/s10822-006-9093-8

102. Ertl, P.; Jelfs, S.; Mühlbacher, J.; Schuffenhauer, A.; Selzer, P. *J. Med. Chem.* **2006,** *49,* 4568–4573. doi:10.1021/jm060217p

103. Hendrickson, J. B. *J. Am. Chem. Soc.* **1977,** *99,* 5439–5450. doi:10.1021/ja00458a035

104. Hendrickson, J. B. *J. Am. Chem. Soc.* **1975,** *97,* 5763–5784. doi:10.1021/ja00853a022

105. Hendrickson, J. B. *J. Am. Chem. Soc.* **1975,** *97,* 5784–5800. doi:10.1021/ja00853a023

106. Wender, P. A.; Miller, B. L. Toward the Ideal Synthesis: Connectivity Analysis and Multibond-Forming Processes. In *Organic Synthesis: Theory and Application;* Hudlicky, T., Ed.; JAI Press: Connecticut, 1993; Vol. 2, pp 27–65.

107. Bertz, S. H.; Sommer, T. J. Applications of Graph Theory to Synthesis Planning: Complexity, Reflexivity, and Vulnerability. In *Organic Synthesis: Theory and Application;* Hudlicky, T., Ed.; JAI Press: Connecticut, 1993; Vol. 2, pp 67–92.

108. Whitlock, H. W. *J. Org. Chem.* **1998,** *63,* 7982–7989. doi:10.1021/jo9814546

109. Bertz, S. H. *New J. Chem.* **2003,** *27,* 860–869. doi:10.1039/B210843G

110. Bertz, S. H. *New J. Chem.* **2003,** *27,* 870–879. doi:10.1039/B210844P

111. Bertz, S. H. *J. Am. Chem. Soc.* **1981,** *103,* 3599–3601. doi:10.1021/ja00402a071

112. Bertz, S. H. *J. Am. Chem. Soc.* **1982,** *104,* 5801–5803. doi:10.1021/ja00385a049

113. Bertz, S. H. *Bull. Math. Biol.* **1983,** *45,* 849–855. doi:10.1007/BF02460054

114. Hendrickson, J. B.; Huang, P.; Toczko, A. G. *J. Chem. Inf. Comput. Sci.* **1987,** *27,* 63–67. doi:10.1021/ci00054a004

115. Rücker, G.; Rücker, C. *J. Chem. Inf. Comput. Sci.* **2000,** *40,* 99–106. doi:10.1021/ci9900579

116. Rücker, G.; Rücker, C. *J. Chem. Inf. Comput. Sci.* **1993,** *33,* 683–695. doi:10.1021/ci00015a005

117. Hendrickson, J. B.; Miller, T. M. *J. Am. Chem. Soc.* **1991,** *113,* 902–910. doi:10.1021/ja00003a025

118. Long, A. K.; Kappos, J. C. *J. Chem. Inf. Comput. Sci.* **1994,** *34,* 915–921. doi:10.1021/ci00020a028

119. Bersohn, M.; Esack, A. *Chem. Rev.* **1976,** *76,* 269–282. doi:10.1021/cr60300a005

120. Ugi, I.; Bauer, J.; Bley, K.; Dengler, A.; Dietz, A.; Fontain, E.; Gruber, B.; Herges, R.; Knauer, M.; Reitsam, K.; Stein, N. *Angew. Chem., Int. Ed. Engl.* **1993,** *32,* 201–227. doi:10.1002/anie.199302011

121. Bauer, J.; Fontain, E.; Ugi, I. *Anal. Chim. Acta* **1988,** *210,* 123–134. doi:10.1016/S0003-2670(00)83884-2

122. Ugi, I.; Bauer, J.; Brandt, J.; Freidrich, J.; Gasteiger, J.; Jochum, C.; Schubert, W. *Angew. Chem., Int. Ed. Engl.* **1979,** *18,* 111–123. doi:10.1002/anie.197901111

123. Andrews, G. E.; Eriksson, K. *Integer Partitioning;* Cambridge University Press: Cambridge, 2004.

124. Andrews, G. E. *Bull. Am. Math. Soc.* **2007,** *44,* 561–573. doi:10.1090/S0273-0979-07-01180-9

125. Ahlgren, S.; Ono, K. *Not. Am. Math. Soc.* **2001,** *48,* 978–984.

126. Lodge, O. J. *Philos. Mag.* **1875,** *50,* 367–376.

127. Rouvray, D. H. *Endeavour* **1975,** *34,* 28–33.

128. Balaban, A. T.; Kennedy, J. W.; Quintas, L. V. *J. Chem. Educ.* **1988,** *65,* 304–313. doi:10.1021/ed065p304

129. Rouvray, D. H. *Am. Sci.* **1973,** *61,* 729–735.

130. Rouvray, D. H. *CHEMTECH* **1973,** 379–384.

131. Rouvray, D. H. *J. Chem. Educ.* **1975,** *52,* 768–773. doi:10.1021/ed052p768

132. Musser, M. T. Cyclohexanol and Cyclohexanone. *Ullmann's Encyclopedia of Industrial Chemistry;* Wiley-VCH: Weinheim, 2012; Vol. 11, pp 49–60.

133. Ziegler, K.; Nagel, K.; Patheiger, M. *Z. Anorg. Chem.* **1955,** *282,* 345–351. doi:10.1002/zaac.19552820136

134. van Eikema Hommes, N. J. R.; Bickelhaupt, F.; Klumpp, G. W. *Recl. Trav. Chim. Pays-Bas* **1987,** *106,* 514–515. doi:10.1002/recl.19871060909

135. West, R.; Rochow, E. G. *J. Org. Chem.* **1953,** *18,* 1739–1742. doi:10.1021/jo50018a018

136. Cohen, T.; McNamara, K.; Kuzemko, M. A.; Ramig, K.; Landi, J. J., Jr.; Dong, Y. *Tetrahedron* **1993,** *49,* 7931–7942. doi:10.1016/S0040-4020(01)88017-0

137. Marek, I.; Normant, J.-F. *Chem. Rev.* **1996,** *96,* 3241–3268. doi:10.1021/cr9600161

138. Clayden, J. *Organolithiums: Selectivity for Synthesis;* Pergamon Press: New York, 2002.

139. Xi, Z., Ed. *Organo-di-Metallic Compounds (or Reagents): Synergistic Effects and Synthetic Applications;* Springer: Heidelberg, 2014.

140. Hurd, C. D. *Org. Synth.* **1925,** *4,* 39. doi:10.15227/orgsyn.004.0039

141. Devasagayaraj, A.; Periasamy, M. *Tetrahedron Lett.* **1992,** *33,* 1227–1228. doi:10.1016/S0040-4039(00)91903-8

142. Lindner, E.; Leibfritz, T.; Fawzi, R.; Steimann, M. *Chem. Ber.* **1997,** *130,* 347–356. doi:10.1002/cber.19971300308

143. Yamashita, M.; Uchida, M.; Tashika, H.; Suemitsu, R. *Bull. Chem. Soc. Jpn.* **1989,** *62,* 2728–2729. doi:10.1246/bcsj.62.2728

144. Grignard, V.; Vignon, L. *C. R. Hebd. Seances Acad. Sci.* **1907,** *144,* 1359.

145. Brown, H. C.; Phadke, A. S.; Rangaishenvi, M. V. *J. Am. Chem. Soc.* **1988,** *110,* 6263–6264. doi:10.1021/ja00226a061

146. Carlson, B. A.; Brown, H. C. *J. Am. Chem. Soc.* **1973,** *95,* 6876–6877. doi:10.1021/ja00801a081

147. Ogura, K.; Yamashita, M.; Furukawa, S.; Suzuki, M.; Tsuchihashi, G. *Tetrahedron Lett.* **1975,** *16,* 2767–2770. doi:10.1016/S0040-4039(00)75235-X

148. Ogura, K.; Yamashita, M.; Suzuki, M.; Furukawa, S.; Tsuchinashi, G. *Bull. Chem. Soc. Jpn.* **1984,** *57,* 1637–1642. doi:10.1246/bcsj.57.1637

149. Ogura, K.; Suzuki, M.; Watanabe, J.; Yamashita, M.; Iida, H.; Tsuchihashi, G. *Chem. Lett.* **1982,** *11,* 813–814. doi:10.1246/cl.1982.813

150. Ogawa, S.; Kawara, T.; Takehara, S.; Ohnishi, H.; Takeuchi, K.; Takatsu, H.; Grahe, G.; Frings, R. B.; Fugger, C.; Pithart, C. Fused ring compound. Eur. Pat. Appl. EP1201632 A1, May 2, 2002.

151. Knorr, L. *Chem. Ber.* **1883,** *16,* 2597–2599. doi:10.1002/cber.188301602194

152. von Pechmann, H. *Chem. Ber.* **1895,** *28,* 855–861. doi:10.1002/cber.189502801189

153. Neumann, J. J.; Suri, M.; Glorius, F. *Angew. Chem., Int. Ed.* **2010,** *49,* 7790–7794. doi:10.1002/anie.201002389

154. Shen, L.; Cao, S.; Liu, N.; Wu, J.; Zhu, L.; Qian, X. *Synlett* **2008,** 1341–1344. doi:10.1055/s-2008-1072766

155. Shen, L.; Zhang, J.; Cao, S.; Yu, J.; Liu, N.; Wu, J.; Qian, X. *Synlett* **2008,** 3058–3062. doi:10.1055/s-0028-1087348

156. Willy, B.; Müller, T. T. J. *Eur. J. Org. Chem.* **2008,** 4157–4168. doi:10.1002/ejoc.200800444

157. Majumder, S.; Gipson, K. R.; Staples, R. J.; Odom, A. L. *Adv. Synth. Catal.* **2009,** *351,* 2013–2023. doi:10.1002/adsc.200900293

158. Heller, S. T.; Natarajan, S. R. *Org. Lett.* **2006,** *8,* 2675–2678. doi:10.1021/ol060570p

159. Stonehouse, J. P.; Chekmarev, D. S.; Ivanova, N. V.; Lang, S.; Pairaudeau, G.; Smith, N.; Stocks, M. J.; Sviridov, S. I.; Utkina, L. M. *Synlett* **2008,** 100–104. doi:10.1055/s-2007-1000839

160. Adib, M.; Mohammadi, B.; Bijanzadeh, H. R. *Synlett* **2008,** 3180–3182. doi:10.1055/s-0028-1087365

161. Raw, S. A.; Turner, A. T. *Tetrahedron Lett.* **2009,** *50,* 696–699. doi:10.1016/j.tetlet.2008.11.099

162. Mohanan, K.; Martin, A. R.; Toupet, L.; Smietana, M.; Vasseur, J.-J. *Angew. Chem., Int. Ed.* **2010,** *49,* 3196–3199. doi:10.1002/anie.200906781

163. Biginelli, P. *Gazz. Chim. Ital.* **1893,** *23,* 360–413.

164. Biginelli, P. *Chem. Ber.* **1891,** *24,* 1317–1319. doi:10.1002/cber.189102401228

165. Biginelli, P. *Chem. Ber.* **1891,** *24,* 2962–2967. doi:10.1002/cber.189102402126

166. Shaabani, A.; Bazgir, A.; Teimouri, F. *Tetrahedron Lett.* **2003,** *44,* 857–859. doi:10.1016/S0040-4039(02)02612-6

167. Martins, M. A. P.; Teixeira, V. M.; Cunico, W.; Scapin, E.; Mayer, R.; Pereira, C. M. P.; Zanatta, N.; Bonacorso, H. G.; Peppe, C.; Yuan, Y.-F. *Tetrahedron Lett.* **2004,** *45,* 8991–8994. doi:10.1016/j.tetlet.2004.10.048

168. Khodaei, M. M.; Khosropour, A. R.; Jowkar, M. *Synthesis* **2005,** 1301–1304. doi:10.1055/s-2005-861876

169. Saxena, I.; Borah, D. C.; Sarma, J. C. *Tetrahedron Lett.* **2005,** *46,* 1159–1160. doi:10.1016/j.tetlet.2004.12.081

170. Zhu, Y.; Pan, Y.; Huang, S. *Heterocycles* **2005,** *65,* 133–142. doi:10.3987/COM-04-10112

171. Zhu, Y.; Huang, S.; Wan, J.; Yan, L.; Pan, Y.; Wu, A. *Org. Lett.* **2010,** *8,* 2599–2602. doi:10.1021/ol060874b

172. Bremner, W. S.; Organ, M. G. *J. Comb. Chem.* **2007,** *9,* 14–16. doi:10.1021/cc060130p

173. Mizar, P.; Myrboh, B. *Tetrahedron Lett.* **2008,** *49,* 5283–5285. doi:10.1016/j.tetlet.2008.06.087

174. Schmidt, R. J.; Lombardo, L. J.; Traeger, S. C.; Williams, D. K. *Tetrahedron Lett.* **2008,** *49,* 3009–3010. doi:10.1016/j.tetlet.2008.02.162

175. Ramalingan, C.; Kwak, Y.-W. *Tetrahedron* **2008,** *64,* 5023–5031. doi:10.1016/j.tet.2008.03.078

176. Glasnov, T. N.; Tye, H.; Kappe, C. O. *Tetrahedron* **2008,** *64,* 2035–2041. doi:10.1016/j.tet.2007.12.056

177. Hulme, R.; Zamora, O. D. P.; Mota, E. J.; Pastén, M. A.; Contreras-Rojas, R.; Miranda, R.; Valencia-Hernández, I.; Correa-Basurto, J.; Trujillo-Ferrara, J.; Delgado, F. *Tetrahedron* **2008,** *64,* 3372–3380. doi:10.1016/j.tet.2008.01.087

178. Yao, C.; Lei, S.; Wang, C.; Yu, C.; Tu, S. *J. Heterocycl. Chem.* **2008,** *45,* 1609–1613. doi:10.1002/jhet.5570450609

179. Matache, M.; Dobrota, C.; Bogdan, N. D.; Dumitru, I.; Ruta, L. L.; Paraschivescu, C. C.; Farcasanu, I. C.; Baciu, I.; Funeriu, D. P. *Tetrahedron* **2009,** *65,* 5949–5957. doi:10.1016/j.tet.2009.05.088

180. Zhang, H.; Zhou, Z.; Yao, Z.; Xu, F.; Shen, Q. *Tetrahedron Lett.* **2009,** *50,* 1622–1624. doi:10.1016/j.tetlet.2009.01.103

181. Singh, O. M.; Devi, N. S. *J. Org. Chem.* **2009,** *74,* 3141–3144. doi:10.1021/jo802585b

182. Hong, M.; Cai, C. *J. Heterocycl. Chem.* **2009,** *46,* 1430–1432. doi:10.1002/jhet.241

183. Lei, M.; Ma, L.; Hu, L. *Monatsh. Chem.* **2010,** *141,* 1005–1008. doi:10.1007/s00706-010-0357-6

184. Shaabani, A.; Seyyedhamzeh, M.; Maleki, A.; Hajishaabanha, F. *Tetrahedron* **2010,** *66,* 4040–4042. doi:10.1016/j.tet.2010.04.028

185. Yao, C.; Lei, S.; Wang, C.; Li, T.; Yu, C.; Wang, X.; Tu, S. *J. Heterocycl. Chem.* **2010,** *47,* 26–32. doi:10.1002/jhet.215

186. Han, G.-F.; Cui, B.; Chen, L.-Z.; Wang, R.-H.; Jin, Y. *J. Heterocycl. Chem.* **2011,** *48,* 312–316. doi:10.1002/jhet.541

187. Fang, Z.; Lam, Y. *Tetrahedron* **2011,** *67,* 1294–1297. doi:10.1016/j.tet.2010.11.075

188. Zeng, L.-Y.; Cai, C. *J. Comb. Chem.* **2010,** *12,* 35–40. doi:10.1021/cc9000983

189. Dabiri, M.; Arvin-Nezhad, H.; Khavasi, H. R.; Bazgir, A. *J. Heterocycl. Chem.* **2007,** *44,* 1009–1011. doi:10.1002/jhet.5570440505

190. Dabiri, M.; Arvin-Nezhad, H.; Khavasi, H. R.; Bazgir, A. *Tetrahedron* **2007,** *63,* 1770–1774. doi:10.1016/j.tet.2006.12.043
191. Yi, H.; Song, L.; Wang, W.; Liu, J.; Zhu, S.; Deng, H.; Shao, M. *Chem. Commun.* **2010,** 6941–6943. doi:10.1039/C0CC01815E
192. Singh, J.; Mahajan, N.; Sharma, R. L.; Razdan, T. K. *J. Heterocycl. Chem.* **2011,** *48,* 1398–1403. doi:10.1002/jhet.768
193. Vugts, D. J.; Jansen, H.; Schmitz, R. F.; de Kanter, F. J. J.; Orru, R. V. A. *Chem. Commun.* **2003,** 2594–2595. doi:10.1039/B308243A
194. Vugts, D. J.; Koningstein, M. M.; Schmitz, R. F.; de Kanter, F. J. J.; Groen, M. B.; Orru, R. V. A. *Chem. – Eur. J.* **2006,** *12,* 7178–7189. doi:10.1002/chem.200600168

A new protocol for the synthesis of 4,7,12,15-tetrachloro[2.2]paracyclophane

Donghui Pan, Yanbin Wang and Guomin Xiao[*]

Abstract

We report a green and convenient protocol to prepare 4,7,12,15-tetrachloro[2.2]paracyclophane, the precursor of parylene D, from 2,5-dichloro-_p_-xylene. In the first bromination step, with H_2O_2–HBr as a bromide source, this procedure becomes organic-waste-free and organic-solvent-free and can appropriately replace the existing bromination methods. The Winberg elimination–dimerization step, using aqueous sodium hydroxide solution instead of silver oxide for anion exchange, results in a significant improvement in product yield. Furthermore, four substituted [2.2]paracyclophanes were also prepared in this convenient way.

Introduction

Parylene films (Figure 1) are desired uniform coating materials that are widely used in microelectronic engineering, automotive and medical industries, owing to their low dielectricity, high thermal and oxidative stability, and chemical inertness [1-4]. Parylene N was firstly commercialized, and its precursor [2.2]paracyclophane (Figure 2) was typically produced by Hofmann elimination [5,6]. As reported, the uniform coating properties of parylene films were improved by introducing halogen atoms to the structure of the parent [2.2]paracyclophane [7]. Therefore, the two chloride atoms on the benzene ring make parylene D superior to parylene N and parylene C. There are some creative strategies for the synthesis of 4,7,12,15-tetrachloro[2.2]paracyclophane (Figure 2), the precur-

sor of parylene D [8]. Theoretically, direct chlorination of [2.2]paracyclophane is an ideal route to prepare tetrachloroparacyclophane, but a pure polysubstituted product is difficult to obtain by electrophilic substitution without repeated crystallization or chromatographic purification [9]. Thus, we report an improved synthesis method using the Winberg dimerization of 2,5-dichloro-(4-methylbenzyl)trimethylammonium hydroxide without tedious purification.

The important chemical 1-(bromomethyl)-2,5-dichloro-4-methylbenzene is an intermediate in the preparation of 2,5-dichloro-(4-methylbenzyl)trimethylammonium hydroxide. During our investigation of the synthesis of 4,7,12,15-tetra-

Figure 1: Chemical structures of parylene N, parylene C, and parylene D.

Figure 2: Chemical structures of [2.2]paracyclophane and 4,7,12,15-tetrachloro[2.2]paracyclophane.
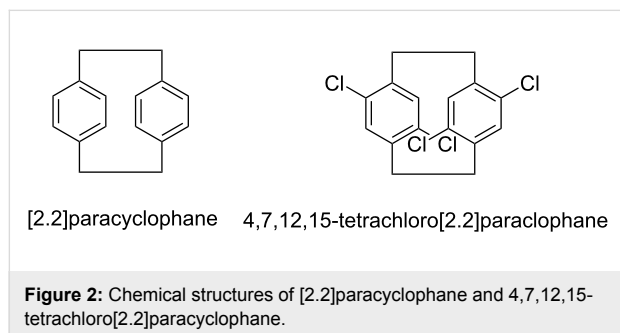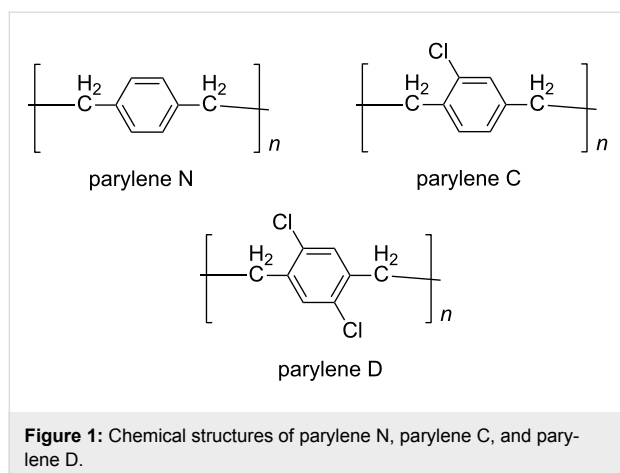
chloro[2.2]paracyclophane, we also adopted an improved bromination process to prepare 1-(bromomethyl)-2,5-dichloro-4-methylbenzene. Traditionally, there are several disadvantages when molecular bromine is used as a brominating reagent, such as toxicity, inconvenient handling and high reactivity, which lead to unsatisfactory results in the bromination process [10-12]. In addition, the release of corrosive HBr as a byproduct and the use of organic solvents make this protocol less environmentally friendly [13]. The use of other brominating agents, such as *N*-bromosuccinimide (NBS) and pyridinium tribromides, also has the drawbacks such as low atom efficiency and the requirement of reagent residue elimination [14]. In contrast to traditional brominating reagents, the H_2O_2–HBr system, which generates active bromine in situ, is a convenient and green brominating agent [15]. Furthermore, the use of the H_2O_2–HBr couple improves the selectivity and allows for the complete utilization of bromine atoms, thus increasing the atom economy [16]. These advantages prompted us to develop a novel method to prepare 1-(bromomethyl)-2,5-dichloro-4-methylbenzene and 4,7,12,15-tetrachloro[2.2]paracyclophane in a convenient and green way.

Results and Discussion

We initially planned to optimize the reaction conditions for the bromination of the benzylic position of 2,5-dichloro-*p*-xylene
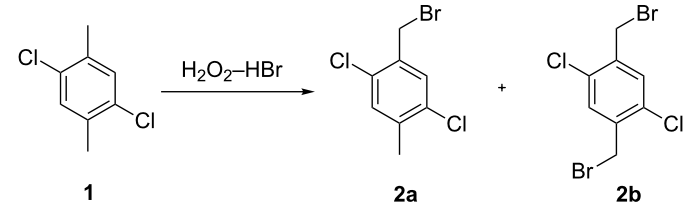
(**1**) by using the H_2O_2–HBr system, and investigated various factors, including the activation mode, the reagent stoichiometry, the solvent, and the reaction temperature (Table 1).

The bromination reaction activated by heating in the dark produced a 62.9% yield of the monobrominated product 1-(bromomethyl)-2,5-dichloro-4-methylbenzene (**2a**) accompanied by a small amount of 1,4-bis(bromomethyl)-2,5-dichlorobenzene (**2b**) (Table 1, entry 2). Next, a radical reaction was induced by adding 3 mol % of radical initiator (DBP or AMPA) and proceeded at 75 °C for 4 h (Table 1, entries 3 and 4). Though the yields in both processes increased, the selectivity of **2a** decreased due to the formation of some excessive brominated byproducts. Then, we tried visible light as activator of the racial process. Interestingly, the yield and the selectivity of **2a** increased when a 40 W incandescent light bulb was used at 25 °C for 6 h (Table 1, entry 5) compared to other activation modes.

To make the chemical process green, we designed a bromination process with water as the reaction medium rather than organic solvents. Despite the low solubility of the organic substrates, the yields of **2a** were improved without significant formation of byproducts (Table 1, entries 5 and 6). Furthermore, it was convenient to separate the organic product from the reaction mixtures. In small-scale experiments, a simple extraction with an appropriate organic solvent was efficient to obtain the product. However, in large-scale bromination processes, a clear phase separation occurred, so the product could be obtained by drying the organic phase after separation from the aqueous phase.

Considering the H_2O_2 decomposition in the presence of HBr and Br_2 in the reaction, the effect of the amount of H_2O_2 was investigated. Actually, the yields of **2a** increased to 73.1% and 80.4% when 1.5 and 2.0 equiv of H_2O_2 were used (Table 1, entries 7 and 8), respectively, in the bromination process. Similarly, when the amount of HBr increased to 1.1 equiv, the yield of **2a** was maximized (Table 1, entry 9). However, a large amount of **2b** was found when excessive HBr (1.5 equiv) was used, which decreased the selectivity of this bromination protocol (Table 1, entry 10).

The effect of reagent addition modes on the bromination yields was also studied. The results showed that gradual addition of H_2O_2 (method B) improved the yield of the main product **2a** in contrast to a one-time addition of H_2O_2 (method A). This may be due to a significant decrease of H_2O_2 decomposition during the slow addition process. In addition, the Br_2 generated in situ was reduced by stepwise addition of H_2O_2, which would improve the selectivity of **2a** by preventing the side reactions.

Table 1: Bromination of 2,5-dichloro-*p*-xylene (**1**) with H_2O_2–HBr.
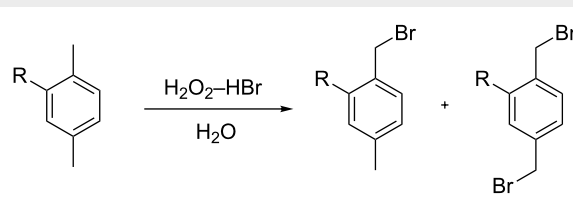
Entry	**1**/H_2O_2/HBr	Mode of initiation[a]	Solvent	Method[b]	Temp. (°C)	Yield[c] (%)	
						2a	**2b**
1	1:1:1	dark	CCl_4	A	25	22.8	–
2	1:1:1	dark	CCl_4	A	75	62.9	4.2
3	1:1:1	3% DBP	CCl_4	A	75	65.8	8.1
4	1:1:1	3% AMPA	CCl_4	A	75	62.3	7.8
5	1:1:1	incandescent light	CCl_4	A	25	70.2	3.5
6	1:1:1	incandescent light	H_2O	A	25	68.8	2.5
7	1:1.5:1	incandescent light	H_2O	A	25	73.1	4.6
8	1:2:1	incandescent light	H_2O	A	25	80.4	4.2
9	1:2:1.1	incandescent light	H_2O	A	25	85.1	3.5
10	1:2:1.5	incandescent light	H_2O	A	25	82.7	10.1
11	1:2:1.1	incandescent light	H_2O	B	25	89.9	1.2
12	1:2:1.1	incandescent light	H_2O	B	80	65.1	28.2

[a]Radical initiators: DBP (dibenzoyl peroxide), AMPA (2,2'-azobis(2-methylpropionamidine) dihydrochloride), 40 W incandescent light bulb. [b]Method A: H_2O_2 and HBr were added in one portion; Method B: H_2O_2 was added gradually (1 equiv per 2.5 h). [c]Yields were determined by ^{1}H NMR spectroscopy and were based on starting compound **1**.

Next, the bromination of other *para*-xylene derivatives under optimized conditions (see Table 1, entry 11) were investigated to examine the versatility of the protocol. As can be seen in Table 2, *para*-xylene (**3**), 2-chloro-1,4-dimethylbenzene (**5**) and 2-bromo-1,4-dimethylbenzene (**7**) were converted to the corresponding benzyl bromides in high yields with a small amount of dibrominated byproducts. However, in the case of 1-nitro-2,5-dimethylbenzene (**9**), a lower yield of benzyl brominated product was obtained. This could be explained by the deactivating effect of the nitro group [16]. Therefore, a 100 W high pressure mercury lamp ('solar' light) was used to increase the formation of bromide radical in the repeated bromination experiment of **9**. On this occasion the yield of the monobrominated product **10a** was high, and this was in agreement with the literature [16].

Five brominated products were obtained through the above bromination protocol, and were used to synthesize substituted (4-methylbenzyl)trimethylammonium bromides in diethyl ether at 0 °C with quantitative yields [17] (Scheme 1).

Then, we used 2,5-dichloro-(4-methylbenzyl)trimethyl-ammonium bromide (**11**) as starting material to prepare tetra-chloro[2.2]paracyclophane in an aqueous sodium hydroxide solution according to Winberg's method [18,19]. The interme-

Table 2: Visible-light induced free-radical bromination of substituted *p*-xylenes with H_2O_2–HBr.

Substrate	Time(h)	Yield[a] (%)
3: R = H	16	**4a**: 89.2, **4b**: 3.2
5: R = Cl	22	**6a**: 85.3, **6b**: 2.5
7: R = Br	25	**8a**: 82.7, **8b**: 4.2
9: R = NO$_2$[b]	60	**10a**: 78.5, **10b**: 2.3

[a]Yields were determined by ^{1}H NMR spectroscopy and were based on starting compounds. [b]The reaction mixture was irradiated with a 100 W high pressure mercury lamp.

diate 2,5-dichloro-(4-methylbenzyl)trimethylammonium hydroxide was formed and then decomposed in boiling toluene, resulting in a small amount of a dimer product **16** and a quantity of polymer byproduct (Table 3, entry 1). After the reaction, the polymer byproduct was removed by filtration, and the dimer product was obtained by concentrating the filtrate under

Scheme 1: Synthesis of substituted (4-methylbenzyl)trimethyl-ammonium bromides from substituted (4-methylbenzyl)bromides.
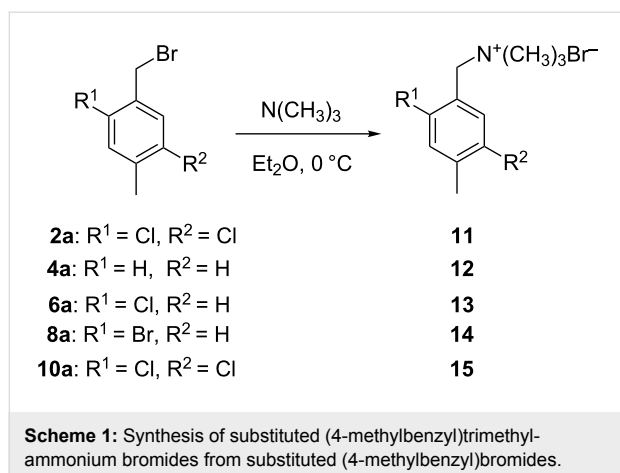
reduced pressure. Thus, a chromatographic purification was not necessary in the improved dimerization protocol.

To suppress the polymerization and to improve the yield of the dimer product, we attempted the addition of a polymerization inhibitor. As expected, the addition of 3 mol % phenothiazine significantly improved the yield of **16** to 25% (Table 3, entry 2). The addition of 2-chlorophenothiazine increased the yield to 35% (Table 3, entry 3), which was about three times than that without any inhibitor. In addition, the 35% yield of dimer product was about two times the yield (20%) when the protocol with silver oxide for anion exchange was used [17], and it was comparable to the commercial synthetic protocol with 36.5% yield [20]. Although two isomers from the dimerization reaction could be formed, only the 4,7,12,15-tetrachloro isomer was obtained. The structure of the product was confirmed by ^{1}H and ^{13}C NMR spectral analysis, and the data matched well with the reported results [17]. Furthermore, the ^{1}H NMR spectra of the CH_2CH_2 bridge in the paracyclophane structure was consistent with the data reported in the literature, which also identified the 4,7,12,15-tetrachloro isomer [21].

Then, four substituted [2.2]paracyclophanes were synthesized from substituted (4-methylbenzyl)trimethylammonium bromides in aqueous sodium hydroxide solution in the presence of a polymerization inhibitor (Table 4). It was found that the yields of dimer products were improved dramatically compared to the results obtained with silver oxide used for anion exchange reported by Chow [17]. We speculated that the replacement of silver oxide by aqueous sodium hydroxide solution might promote the formation of substituted (4-methylbenzyl)trimethylammonium hydroxide, but we are unable to provide any conclusive evidence at presence. For the dimerization of **12**, the [2.2]paracyclophane (**17**) was obtained in 33% yield, and its structure was confirmed by NMR spectroscopy and elemental analysis. Similarly, dimerization of **13**, **14**, and **15** resulted in regiospecific 4,16-disubstituted [2.2]paracyclophanes **18**, **19**, and **20**, respectively, in about 35% yield (Table 4, entries 2, 3 and 4). The structures of the synthesized 4,16-disubstituted [2.2]paracyclophanes were also consistent with their NMR spectral data.

Conclusion
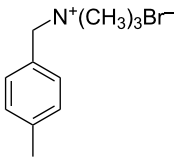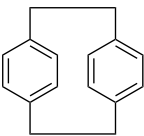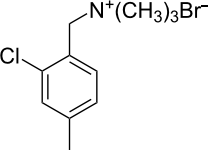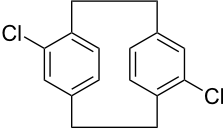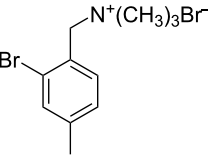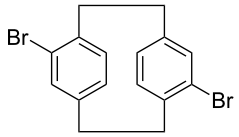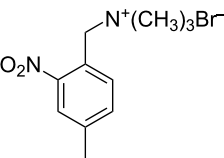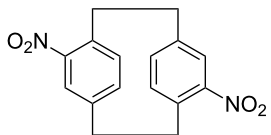
A convenient protocol was reported to synthesize 4,7,12,15-tetrachloro[2.2]paracyclophane. In the first bromination step, 1-(bromomethyl)-2,5-dichloro-4-methylbenzene was synthesized with high yield and selectivity from 2,5-dichloro-*p*-xylene by using a H_2O_2–HBr couple in water. The use of H_2O_2–HBr as a bromide source made this procedure organic-waste-free, organic-solvent-free and an appropriate replacement of the existing bromination methods. In the Winberg elimination–dimerization step, 35% yield of 4,7,12,15-tetrachloro[2.2]paracyclophane was obtained from 2,5-dichloro-(4-methylbenzyl)trimethylammonium bromide and aqueous sodium hydroxide solution in the presence of a polymerization inhibitor, which was about two folds than that used silver oxide as anion exchange. Moreover, four substituted [2.2]paracyclophanes were prepared in this convenient way.

Table 3: Synthesis of 4,7,12,15-tetrachloro[2.2]paracyclophane **16** from **11**.

Entry	Polymerization inhibitor	Yield[a] (%)
1	–	12
2	phenothiazine	25
3	2-chlorophenothiazine	35

[a]Yields of products were based on compound **11**.

Table 4: Synthesis of substituted [2.2]paracyclophanes from substituted (4-methylbenzyl)trimethylammonium bromides.

Entry	Starting material	Product	Yield[a] (%)
1	**12**	**17**	33 (23)
2	**13**	**18**	36 (24)
3	**14**	**19**	33 (19)
4	**15**	**20**	32 (18)

[a]In the presence of 2-chlorophenothiazine. The numbers in parenthesis are the yields in the presence of phenothiazine.

Experimental

General

2,5-Dichloro-*p*-xylene, *para*-xylene, 2-chloro-1,4-dimethylben-zene, 2-bromo-1,4-dimethylbenzene and 1-nitro-2,5-dimethyl-benzene were purchased from commercial suppliers. All chemi-cals were used as received without further purification. ^{1}H NMR spectra were recorded in $CDCl_3$ using an AVANCE III 400WB spectrometer. IR spectra were recorded on a Nicolet AVATAR 5700 FTIR spectrophotometer in the range of 4000–400 cm^{−1} using KBr pellets. Melting points were deter-mined using a Beijing TaiKe X-4 melting point apparatus and were uncorrected. Mass spectra were obtained using an Agilent 1260-6224 spectrometer with electron impact ionization (EI, 70 eV). Elemental analyses were recorded on an Elementar vario MICRO cube.

Typical reaction procedure for visible-light induced bromination with the H_2O_2–HBr system

Analogous as described in [16], substituted *p*-xylene (1.0 mmol) was added to 2.0 mL solution (CCl_4 or water) of 2.0 mmol of H_2O_2 (0.23 g, 30% H_2O_2 aqueous) and 1.1 mmol of HBr (0.22 g, 30% HBr aqueous). The mixture was stirred at 300 rpm at appropriate temperature under irradiation from a 40 W incan-descent light bulb. At the end of the bromination reaction (6–20 h), the mixture was transferred into a separating funnel and 4 mL of 0.005 M $NaHSO_3$ was added. The crude product was extracted using 3 × 5 mL CH_2Cl_2 and the combined organic phase was dried over $MgSO_4$. Then the solvent was evaporated under reduced pressure and the crude mixture was analyzed by ^{1}H NMR spectroscopy. Lastly the products were separated by column chromatography (SiO_2, hexane/EtOAc) and identified by comparison with literature data.

2a: colorless oil. ^{1}H NMR ($CDCl_3$) δ 2.24 (s, 3H, ArCH$_3$), 5.12 (s, 2H, ArCH$_2$), 7.29 (s, 1H, ArH), 7.33 (s, 1H, ArH); EIMS *m/z*: 254, 175, 173, 102.

4a: colorless oil. ^{1}H NMR ($CDCl_3$) δ 2.19 (s, 3H, ArCH$_3$), 4.66 (s, 2H, ArCH$_2$), 7.07–7.11 (m, 2H, ArH), 7.25–7.31 (m, 1H, ArH); anal. calcd for C_8H_9Br (185.06): C, 51.92; H, 4.90; found: C, 51.81; H, 4.96.

6a: colorless oil. ^{1}H NMR (CDCl$_3$) δ 2.31 (s, 3H, ArCH$_3$), 4.95 (s, 2H, ArCH$_2$), 6.96–6.98 (m, 1H, ArH), 6.99–7.24 (m, 1H, ArH), 7.26–7.37 (m, 1H, ArH); anal. calcd for C$_8$H$_8$BrCl (219.51): C, 43.77; H, 3.67; Cl, 16.15; found: C, 43.68; H, 3.72; Cl, 16.06.

8a: mp 53–55 °C; ^{1}H NMR (CDCl$_3$) δ 2.31 (s, 3H, ArCH$_3$), 4.93 (s, 2H, ArCH$_2$), 7.02–7.54 (m, 3H, ArH); anal. calcd for C$_8$H$_8$BrCl (219.51): C, 43.77; H, 3.67; Cl, 16.15; found: C, 43.68; H, 3.72; Cl, 16.06.

10a: mp 72–74 °C; ^{1}H NMR (CDCl$_3$) δ 2.41 (s, 3H, ArCH$_3$), 4.95 (s, 2H, ArCH$_2$), 6.96–7.37 (m, 3H, ArH); anal. calcd for C$_8$H$_8$BrNO$_2$ (230.06): C, 41.77; H, 3.51; N, 6.09; found: C, 41.68; H, 3.57; N, 6.12.

Typical reaction procedure for the preparation of substituted (4-methylbenzyl)trimethylammonium bromides

Substituted 4-methylbenzyl bromide (5.0 mmol) was added to 50.0 mL Et$_2$O solution in a 100 mL three-necked flask. The mixture was cooled at 0 °C and was stirred at 300 rpm. Me$_3$N was generated by heating an aqueous Me$_3$N solution (40% w/w, 15 mL) and passed into the flask for 4 h. The product was precipitated as a white solid. Then the mixture was stirred at room temperature overnight and the quaternary ammonium salt was obtained on a Büchner funnel and dried in a vacuum oven at 80 °C for 24 h.

11: highly hygroscopic solid. IR (KBr) v/cm^{-1}: 3004, 1635, 1617, 1477, 1375, 1190, 980.

12: highly hygroscopic solid. IR (KBr) v/cm^{-1}: 2989, 1521, 1483, 1382, 1125, 910, 805, 722.

13: highly hygroscopic solid. IR (KBr) v/cm^{-1}: 2968, 2935, 1632, 1452, 1371, 1154, 725, 672.

14: highly hygroscopic solid. IR (KBr) v/cm^{-1}: 3009, 2946, 1642, 1458, 1381, 1205, 653.

15: highly hygroscopic solid. IR (KBr) v/cm^{-1}: 2979, 1621, 1550, 1508, 1472, 1376, 1345, 1135, 663.

Typical reaction procedure for the synthesis of substituted tetrachloro[2.2]paracyclophanes

In a 100 mL three-necked flask equipped with a stirrer and a Dean–Stark water separator attached to a reflux condenser was placed 15 mL aqueous sodium hydroxide solution (40% w/w) and 45 mL toluene. With vigorous stirring, a solution of benzyltrimethylammonium bromides (50 mmol), dissolved in 5 mL water, was added dropwise in 30 min. The inhibitor (0.15 mmol) was then added to the solution and the mixture was heated under reflux for 4 h. After all water had been separated, a pale yellow solid polymer began to precipitate. When the evolution of Me$_3$N was finished, the reaction system was heated and stirred for another 1 h. The mixture was cooled and the solid was filtrated and washed with toluene (5 mL × 3). The filtrates were combined and evaporated under vacuum to give a solid product which was further washed with hexane (5 mL × 3).

16: white solid, mp >280 °C (dec); ^{1}H NMR (CDCl$_3$) δ 2.91 (m, 2H, ArCH$_2$), 3.26 (m, 2H, ArCH$_2$), 6.95 (s, 2H, ArH); ^{13}C NMR (CDCl$_3$) δ 30.8, 77.0, 131.8, 133.9, 138.6; anal. calcd for C$_{16}$H$_{12}$Cl$_4$ (346.07): C, 55.53; H, 3.50; Cl, 40.97; found: C, 55.47; H, 3.62; Cl, 40.89.

17: white solid, mp 281–283 °C; ^{1}H NMR (CDCl$_3$) δ 3.09 (s, 8H, ArCH$_2$), 6.50 (s, 8H, ArH); anal. calcd for C$_{16}$H$_{16}$ (208.30): C, 92.26; H, 7.74; found: C, 92.15; H, 7.82.

18: white solid, mp 163–165 °C; ^{1}H NMR (CDCl$_3$) δ 2.85–2.97 (m, 4H, ArCH$_2$), 3.03–3.37 (m, 4H, ArCH$_2$), 6.92–7.54 (m, 6H, ArH). anal. calcd for C$_{16}$H$_{14}$Cl$_2$ (277.19): C, 69.33; H, 5.09; Cl, 25.58; found: C, 69.27; H, 5.05; Cl, 25.65.

19: white solid, mp 238–240 °C; ^{1}H NMR (CDCl$_3$) δ 2.86–3.12 (m, 4H, ArCH$_2$), 3.15–3.34 (4H, m, ArCH$_2$), 6.43–7.15 (m, 6H, ArH); anal. calcd for C$_{16}$H$_{14}$Br$_2$ (366.10): C, 52.49; H, 3.85; found: C, 52.38; H, 3.82.

20: ^{1}H NMR (CDCl$_3$) δ 2.81–3.07 (m, 4H, ArCH$_2$), 3.27–3.35 (m, 4H, ArCH$_2$), 7.25–8.23 (m, 6H, ArH); anal. calcd for C$_{16}$H$_{14}$N$_2$O$_4$ (298.30): C, 64.42; H, 4.73; N, 9.39; found: C, 64.32; H, 4.75; N, 9.45.

Supporting Information

Supporting Information File 1
Copies of MS, ^{1}H and ^{13}C NMR spectra of the synthesized compounds.
[http://www.beilstein-journals.org/bjoc/content/supplementary/1860-5397-12-237-S1.pdf]

Acknowledgements

References

1. Dolbier, W. R., Jr.; Duan, J.-X.; Roche, A. J. *Org. Lett.* **2000,** *2,* 1867–1869. doi:10.1021/ol005943f
2. Dolbier, W. R., Jr.; Xie, P.; Zhang, L.; Xu, W.; Chang, Y.; Abboud, K. A. *J. Org. Chem.* **2008,** *73,* 2469–2472. doi:10.1021/jo7026849
3. Rossen, K.; Pye, P. J.; Maliakal, A.; Volante, R. P. *J. Org. Chem.* **1997,** *62,* 6462–6463. doi:10.1021/jo971300a
4. Hicks, C.; Duffy, B.; Hargaden, G. C. *Org. Chem. Front.* **2014,** *1,* 716–725. doi:10.1039/c4qo00110a
5. Morphy, J. R.; Rankovic, Z.; Rees, D. C. *Tetrahedron Lett.* **1996,** *37,* 3209–3212. doi:10.1016/0040-4039(96)00497-2
6. Seuron, P.; Solladie, G. *J. Org. Chem.* **1980,** *45,* 715–719. doi:10.1021/jo01292a033
7. Amii, H.; Hayashi, R.; Seo, M.; Katahira, Y.; Kobayashi, A.; Uneyama, K. *J. Fluorine Chem.* **2013,** *152,* 90–93. doi:10.1016/j.jfluchem.2013.04.001
8. Paradies, J. *Synthesis* **2011,** 3749–3766. doi:10.1055/s-0031-1289296
9. Bartholomew, G. P.; Bazan, G. C. *J. Am. Chem. Soc.* **2002,** *124,* 5183–5196. doi:10.1021/ja0121383
10. Pravst, I.; Zupan, M.; Stavber, S. *Green Chem.* **2006,** *8,* 1001–1005. doi:10.1039/B608446J
11. Heropoulos, G. A.; Cravotto, G.; Screttas, C. G.; Steele, B. R. *Tetrahedron Lett.* **2007,** *48,* 3247–3250. doi:10.1016/j.tetlet.2007.03.023
12. Pravst, I.; Zupan, M.; Stavber, S. *Tetrahedron* **2008,** *64,* 5191–5199. doi:10.1016/j.tet.2008.03.048
13. Podgoršek, A.; Stavber, S.; Zupan, M.; Iskra, J. *Green Chem.* **2007,** *9,* 1212–1218. doi:10.1039/b707065a
14. Guha, S. K.; Wu, B.; Kim, B. S.; Baik, W.; Koo, S. *Tetrahedron Lett.* **2006,** *47,* 291–293. doi:10.1016/j.tetlet.2005.11.023
15. Podgoršek, A.; Stavber, S.; Zupan, M. *Tetrahedron* **2009,** *65,* 4429–4439. doi:10.1016/j.tet.2009.03.034
16. Podgoršek, A.; Stavber, S.; Zupan, M.; Iskra, J. *Tetrahedron Lett.* **2006,** *47,* 7245–7247. doi:10.1016/j.tetlet.2006.07.109
17. Chow, H.-F.; Low, K.-H.; Wong, K. Y. *Synlett* **2005,** 2130–2134. doi:10.1055/s-2005-872270
18. Winberg, H. E.; Fawcett, F. S.; Mochel, W. E.; Theobald, C. W. *J. Am. Chem. Soc.* **1960,** *82,* 1428–1435. doi:10.1021/ja01491a037
19. Winberg, H. E.; Fawcett, F. S. *Org. Synth., Coll. Vol. V;* John Wiley and Sons, Ltd.: New York, 1973; pp 883–886.
20. Galley, R. A.; Landon, R. S.; Senior, K. C. [2.2]paracyclophane and derivatives thereof. U.S. Patent 5302767, April 12, 1994.
21. Dix, I.; Hopf, H.; Satyanarayana, T. B. N.; Ernst, L. *Beilstein J. Org. Chem.* **2010,** *6,* 932–937. doi:10.3762/bjoc.6.104

Catalytic Wittig and aza-Wittig reactions

Zhiqi Lao and Patrick H. Toy[*]

Abstract

This review surveys the literature regarding the development of catalytic versions of the Wittig and aza-Wittig reactions. The first section summarizes how arsenic and tellurium-based catalytic Wittig-type reaction systems were developed first due to the relatively easy reduction of the oxides involved. This is followed by a presentation of the current state of the art regarding phosphine-catalyzed Wittig reactions. The second section covers the field of related catalytic aza-Wittig reactions that are catalyzed by both phosphine oxides and phosphines.

Introduction

The Wittig reaction is a venerable transformation for converting the carbon–oxygen double bond of an aldehyde or a ketone into a carbon–carbon double bond of an alkene group (Scheme 1). Since its introduction over half a century ago [1,2], it has been widely employed in organic synthesis due to its versatility and reliability. The requirement of simple and inexpensive reagents to generate the necessary phosphonium ylide (phosphorane) reactant (a phosphine, typically Ph_3P (**1**), an alkyl halide and a base), also adds to its appeal [3,4]. However, despite its proven utility, the Wittig reaction suffers from limitations that may deter from its use, especially on a large scale, in the context of green sustainable chemistry. For example, it has low atom economy due to its requirement of one molar equivalent of a phosphine reagent, and the formation of a corresponding amount of a phosphine oxide, usually $Ph_3P=O$ (**2**). There is also the associated problem of separating a by-product from the desired product when they are formed in equal molar amounts. These major deficiencies of the Wittig reaction have led to numerous efforts towards developing variations of it which are catalytic in the required phosphine, or a surrogate for it, and this research is the major focus of this review [5-8]. Additionally, analogous catalytic aza-Wittig reactions, in which carbon–nitrogen double bonds of imine groups are formed, will also be discussed in the second section of this review.
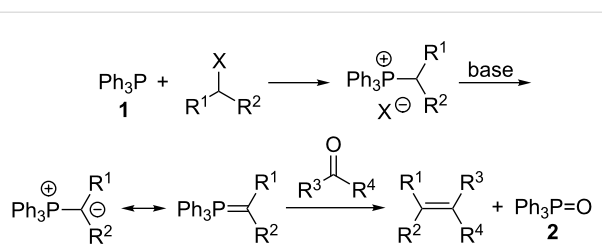
Scheme 1: Prototypical Wittig reaction involving in situ phosphonium salt and phosphonium ylide formation.

Review
Catalytic Wittig reactions

A key requirement for versions of the Wittig reaction that are catalytic in phosphine is the selective in situ reduction of the P(V) phosphine oxide byproduct back to the P(III) phosphine in the presence of a reducible aldehyde or ketone substrate, an alkyl halide and a base. Thus, it seems that the challenge in developing catalytic versions of the Wittig reaction distils down to identifying and implementing selective reducing conditions that enables the necessary catalyst redox cycling, yet does not reduce either the starting materials or the desired alkene-containing product.

Arsine and telluride-catalyzed reactions

As phosphine oxides are generally very stable and relatively difficult to reduce, the group of Yao-Zeng Huang used their prior findings that arsonium ylides can participate in Wittig-type reactions. Further they found that arsine oxides can be reduced using much milder reaction conditions compared to phosphine oxides. They developed the first reported catalytic Wittig-type reactions in which Bu$_3$As (**3**, 0.2 equivalents) was used as the catalyst (Scheme 2) [9,10]. The reaction of **3** with an alkyl halide **4** followed by deprotonation using potassium carbonate generated the corresponding arsonium ylide (**5**) which, in turn, reacted with an aldehyde substrate **6** to produce the alkene-containing product **7** together with Bu$_3$As=O (**8**). The byproduct **8** was then reduced in situ using triphenylphos-

phite to regenerate catalyst **3** for participation in another reaction cycle. Overall, the reaction conditions were quite mild, with the reactions being performed at room temperature with only slight excesses of base and reducing reagent being required. It should be noted that the use of only electron-withdrawing groups activated alkyl halides **4**, and that aromatic and aliphatic aldehydes **6** worked well in these reactions to produce products **7** in high yields with predominantly *E*-configuration.

Quite a few years later Yong Tang and co-workers, also of the Shanghai Institute of Organic Chemistry, carried on with this research and extended it by using a combination of Ph$_3$As (**9**, 0.2 equivalents), Fe(TCP)Cl (**10**, TCP = tetra(*p*-chlorophenyl)porphyrinate), and ethyl diazoacetate (**11**) to generate arsonium ylide **12** for use in biphasic catalytic Wittig-type reactions (Scheme 3) [11]. In these reactions sodium hydrosulfite replaced triphenylphosphite as the reducing reagent to convert the byproduct Ph$_3$As=O (**13**) back into **9** in the aqueous phase of the reaction mixture in order to make the reactions more environmentally friendly. As was the case in the previous work described above, both aromatic and aliphatic aldehydes **6** were suitable substrates in this reaction system to form products **7**.
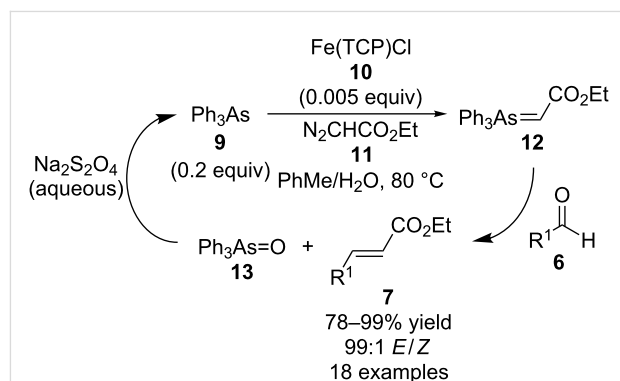
Scheme 3: Ph$_3$As-catalyzed Wittig-type reactions using Fe(TCP)Cl and ethyl diazoacetate for arsonium ylide generation.
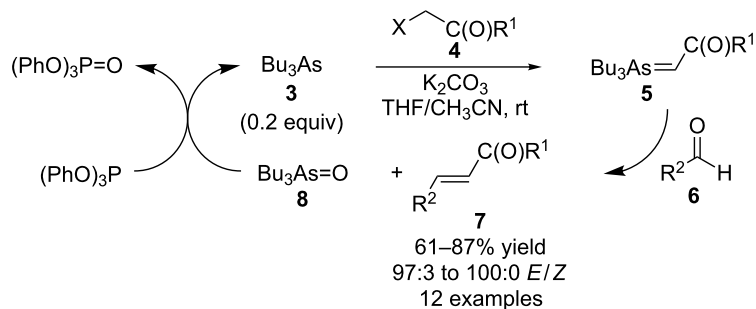
Scheme 2: Bu$_3$As-catalyzed Wittig-type reactions.

Most recently the Tang research group has reported the use of polymer-supported arsine **14** (0.008–0.04 equivalents) as the catalyst in related reactions (Figure 1) [12]. In this work, **14** was found to be the only arsine examined that was able to effectively catalyze Wittig-type reactions of ketone substrates to produce tri- and tetrasubstituted alkene products in very high yields. For these reactions, which required a higher operating temperature than before (110 °C compared to 80 °C), polymethylhydrosiloxane was used as the reductant, and **14** could be recovered and reused efficiently in numerous reaction cycles without loss of catalytic activity.
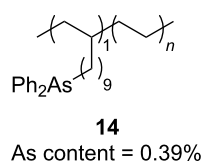
Figure 1: Recyclable polymer-supported arsine for catalytic Wittig-type reactions.

At about the time that Huang and co-workers reported their catalytic reactions using **3** (Scheme 2), they also disclosed that Bu_2Te (**15**) could function similarly as a catalyst in such Wittig-type reactions due to the relatively weak tellurium–oxygen bond of dialkyl telluroxides, such as $Bu_2Te=O$ (**16**) (Scheme 4) [13]. Aldehydes **6** were again used as substrates in reactions to form products **7**. No comments were made regarding the relative advantages or disadvantages of using either **3** or **15** as the catalyst for such reactions, and in fact similar alkyl halides **4** were used to generate ylides **16** as were used in the reactions catalyzed by **3**. The only notable differences regarding performing the reactions were that reactions with **15** required a higher temperature (50 °C compared to room temperature) and acetonitrile as a co-solvent. However, product yields and stereoselectivities were slightly improved when **15** was used at the same loading level (0.2 equivalents) and with a similar set of aldehyde **6** substrates.

Tang's research group also followed up this tellurium-based research many years later and published several papers describing the use of polymer-supported tellurides, such as **18**, as catalysts (Scheme 5) [14-16]. The major advantage reported for using **18** instead of **15** is that a much lower catalyst loading could be used in similar reactions (0.02 equivalents compared to 0.2 equivalents). Unfortunately, despite the fact that **19** could be easily reduced to **18** using triphenylphosphite or sodium bisulfite, and simply removed from the desired alkene products, recovered **18** had a much lower activity when attempts to reuse it were made. Nevertheless, the use of **18** with sodium bisulfite as the reducing reagent allowed for very simple product isolation, and reaction yields and stereoselectivities were similar to when **15** was used as the catalyst.
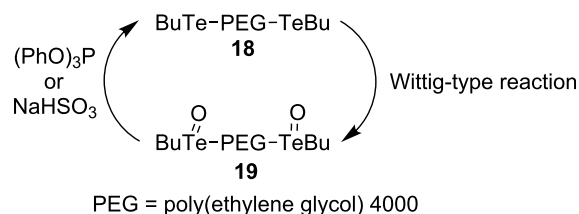
Scheme 5: Polymer-supported telluride catalyst cycling.

In the course of performing the research mentioned above, Tang and co-workers made the fortuitous observation that telluronium salt **20** (prepared from **15**) decomposed in the presence of water to form **21**. This compound could be used as a pre-catalyst in Wittig-type reactions because it is reduced to **15** by triphenylphosphite in the presence of potassium carbonate (Scheme 6) [17]. Since **21** was observed to be stable and odourless, its use has some practical advantages, and when it was used as a surrogate for **15**, very similar results were obtained.

While these arsenic and tellurium-based reactions are conceptually interesting and show the way in which phosphorous-based catalytic Wittig reactions might be performed, it appears that
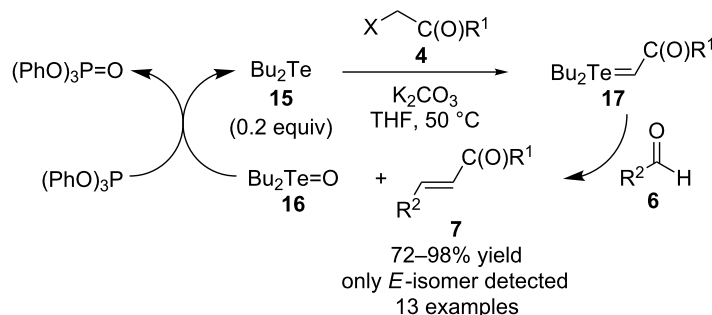
Scheme 4: Bu_2Te-catalyzed Wittig-type reactions.
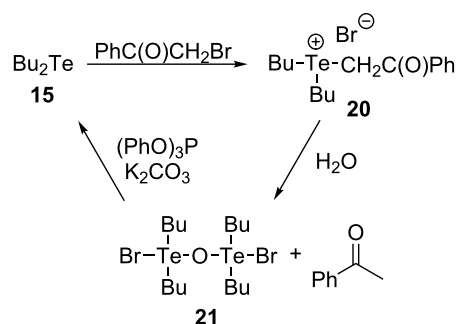
Scheme 6: Stable and odourless telluronium salt pre-catalyst for Wittig-type reactions.

they have not been used by anyone other than the original reporters.

Phosphine-catalyzed reactions

As alluded to above, it seems that the major impediment to the development of phosphine-catalyzed Wittig reactions was the stability of phosphine oxides and the harsh reaction conditions generally required to reduce them to the corresponding phosphines were thought to be incompatible with various necessary reactants and reagents, and the desired reaction products to be formed.

Christopher J. O'Brien and co-workers recently reported a breakthrough of identifying the necessary selective conditions for phosphine oxide reduction that allowed phosphorous-based catalytic Wittig reactions to become realized. In their initial publication they described the use of readily available phosphine oxide **22** as a pre-catalyst (0.1 equivalents), which was reduced in situ with diphenylsilane (Ph₂SiH₂) to phosphine **23**, which served as the actual catalyst in their Wittig reactions (Scheme 7) [18]. Once **23** was generated, it reacted with electron-withdrawing group activated alkyl halides **4** and sodium carbonate to form the corresponding phosphonium ylides that

reacted with aldehydes **6** to produce alkene products **7** and **22** as a byproduct.

Subsequently they reported that the soluble organic base *N,N*-diisopropylethylamine was a good replacement for sodium carbonate in such reactions [19], and that the addition of 4-nitrobenzoic acid facilitated the phosphine oxide reduction step using phenylsilane (PhSiH₃) instead of diphenylsilane [20]. Using this combination of 4-nitrobenzoic acid and phenylsilane for phosphine oxide reduction allowed reactions starting with phosphine oxide **24** (Figure 2) to be conducted at room temperature and for acyclic phosphine oxides **2** and **25** to be used as well, albeit at elevated operating temperature. Most recently they have found that the use of **26** as the pre-catalyst in conjunction with sodium *tert*-butoxycarbonate (NaOCO₂*t*-Bu, a slow release form of sodium *tert*-butoxide) as a precursor for the required base, catalytic Wittig reactions could be performed using semi or non-stabilized ylides [21].
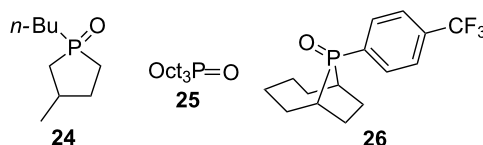
Figure 2: Various phosphine oxides used as pre-catalysts.

Thomas Werner's research group has also been active in this area of research, and reported the first example of a catalytic enantioselective Wittig reaction (Scheme 8) [22]. This reaction involved the intramolecular cyclization of **27** to form **28**. A variety of phosphines were examined as the catalyst, and (*S,S*)-**29** ((*S,S*)-Me-DuPhos, 0.1 equivalent) was found to provide the best combination of reactivity and stereoselectivity (39% yield, 62% ee). In these reactions butylene oxide was used as a base precursor, phenylsilane was the reducing reagent, and the reactions were performed using microwave irradiation (MWI). Subsequently, Werner et al. reported the scope and lim-
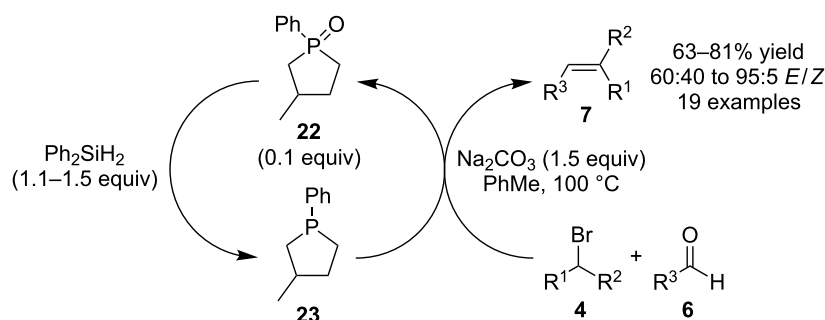
Scheme 7: Phosphine-catalyzed Wittig reactions.

itations of such microwave-assisted catalytic Wittig reactions using tributylphosphine, phenylsilane and butylene oxide [23,24], and reactions with the combination of achiral **30**, trimethoxysilane ((MeO)$_3$SiH) and sodium carbonate using conventional heating [25].

Scheme 8: Enantioselective catalytic Wittig reaction reported by Werner.
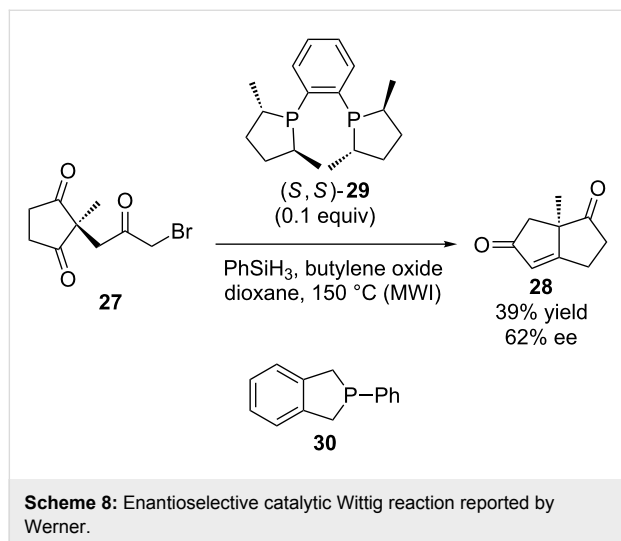
Additionally, the same authors have reported base-free Wittig reactions using diethyl maleate (**31**) as the starting material to form products **32** catalyzed by tributylphosphine (**33**, 0.05 equivalents) (Scheme 9) [26]. In these transformations the initial reaction between **31** and **33** generated zwitterion **34**, that underwent internal proton transfer to generate ylide **35**. This in turn reacted with aldehyde **6** to form **32** and phenylsilane was used as the reducing reagent to regenerate **33**. Most recently they refined such reactions using **22** as the pre-catalyst, trimethoxysilane as the reducing reagent, and catalytic benzoic acid to facilitate phosphine oxide reduction [27].

Scheme 9: Base-free catalytic Wittig reactions reported by Werner.
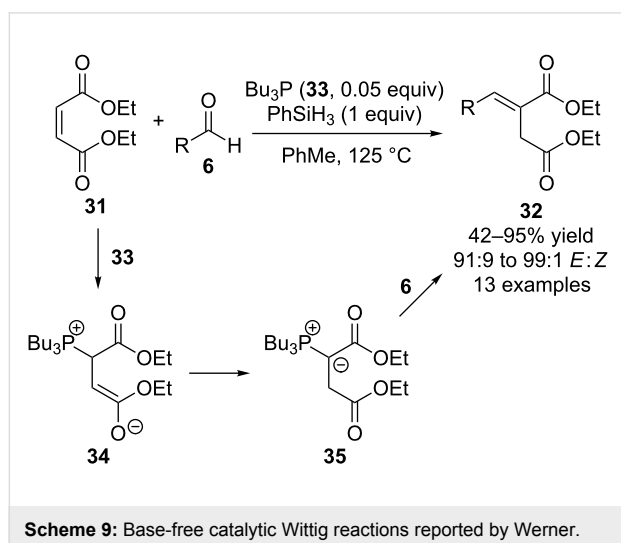
At about the same time as the penultimate report by Werner and co-workers appeared, Wenwei Lin and a co-worker published conceptually similar catalytic Wittig reactions that were based on their previous research regarding related non-catalytic phosphine-mediated base-free Wittig reactions (Scheme 10) [28]. They started with Michael acceptors **36** to generate products **37** using **22** as the pre-catalyst with triethylamine as the base, phenylsilane as the reducing reagent, and 4-nitrobenzoic acid as an acidic additive. It should be noted that the role of the base in these reactions is unclear and not directly commented on. According to the proposed mechanism for the formation of the required ylide intermediate, a base is not necessary, but the authors reported that when it was omitted from a control reaction, no reaction occurred.

Scheme 10: Catalytic Wittig reactions reported by Lin.
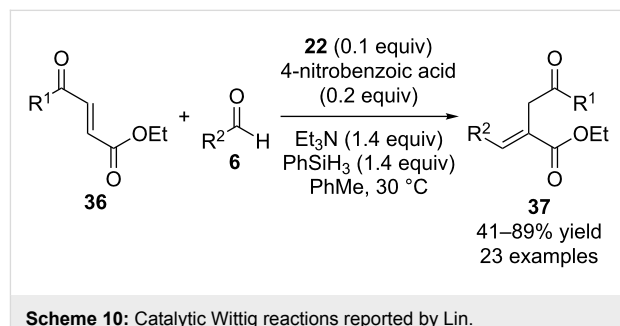
Finally, Bernd Plietker and co-workers have very recently reported the use of iron complex **38** as a catalyst for phosphine oxide reduction and have incorporated it into Wittig reactions catalyzed by **1** (Scheme 11) [29]. These reactions are similar to those mentioned previously by O'Brien's group [20] that involve the cycling between **1** and **2** using a silane reducing reagent.

As can be seen above, the issue of selective phosphine oxide reduction has been solved using various silane reagents and much progress has been made in phosphine-catalyzed Wittig reactions. Initial results were reported using phosphine oxides that were prepared from commercially available phosphine oxide starting materials that were relatively easy to reduce, such as **22**. However, relatively mild cycling between **1** and **2** can now be achieved, and this may make such catalytic Wittig reactions more popular, practical, and scalable due to the stability, wide availability and low cost of **1**.

Catalytic aza-Wittig reactions

Aza-Wittig reactions are similar to Wittig reactions in that they also involve the reaction of a phosphonium ylide, in this case an iminophosphorane (or phosphinimide) such as **39**, with a carbonyl group containing compound to form the carbon–nitrogen double bond of an imine along with a byproduct phosphine
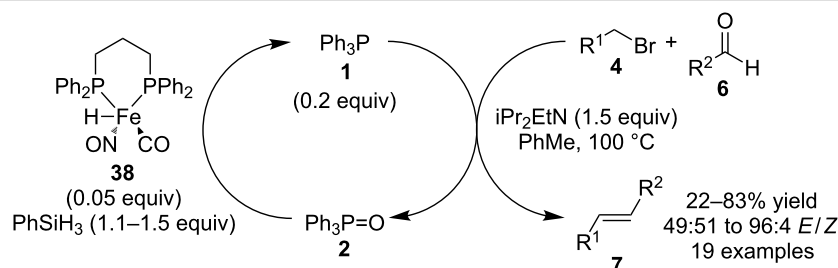
Scheme 11: Catalytic Wittig reactions reported by Plietker.

oxide such as **2** (Scheme 12). The difference is that the iminophosphorane reagents can be generated either from a phosphine such as **1** or from a phosphine oxide such as **2**, by reaction with either an azide or isocyanate reagent, respectively. Thus, two possible strategies for catalytic aza-Wittig reactions exist, one using a phosphorous(V) catalyst, and the other using a phosphorous(III) catalyst that is regenerated in the catalytic cycle. These strategies are the topic of this section of the review.

Phosphine oxide-catalyzed reactions

It is clear from Scheme 12 that when a phosphine oxide is used to generate the iminophosphorane **39** for an aza-Wittig reaction,

it is regenerated as a byproduct, and thus can participate directly in another reaction cycle. More than 25 years before Huang's research group made their first report regarding arsine catalysis [10], Tod W. Campbell and colleagues took advantage of this fact and reported a single example of a catalytic aza-Wittig reaction as part of their research on phosphine oxide-catalyzed carbodiimide synthesis (Scheme 13) [30]. In their reaction they used phosphine oxide **40** as the catalyst in the reaction between diisocyanate **41** and benzaldehyde (**42**, 2 equivalents) to form diimine **43** and carbon dioxide (2 equivalents). While this reaction was described as being catalytic, the mass of the catalyst used was not explicitly reported, so it is impossible to determine the number of catalyst turnovers that were involved in
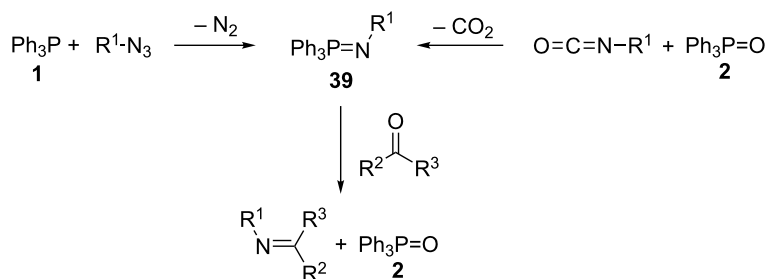
Scheme 12: Prototypical aza-Wittig reaction involving in situ iminophosphorane formation.
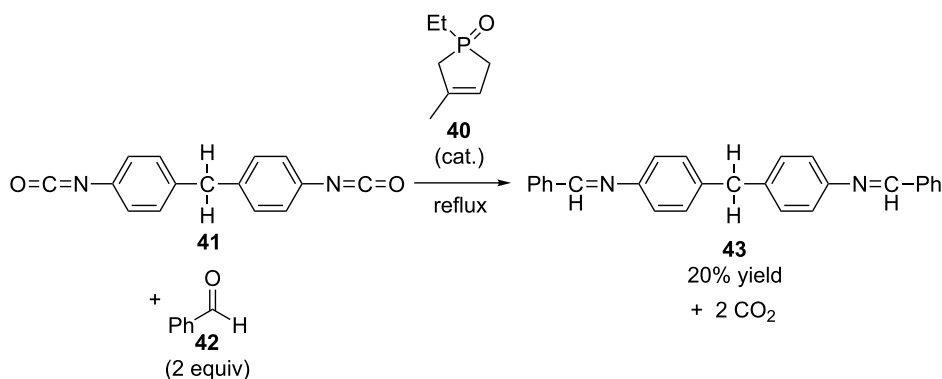
Scheme 13: First catalytic aza-Wittig reaction reported by Campbell.

generating the 20% isolated yield of **43**. The authors only reported that "one drop" of **40** was used in a reaction starting with 7 grams of **41**.

Subsequently, Stephen P. Marsden and co-workers reported intramolecular versions of catalytic aza-Wittig reactions for heteroaromatic compound synthesis using commercially available phosphine oxide **44** as the catalyst (Scheme 14) [31]. In this work, biaryl isocyanates **45** could be converted into phenanthridines **46**, and aryl isocyanates **47** could be transformed into benzoxazoles **48** directly in refluxing toluene together with the simultaneous release of carbon dioxide. Presumably these reactions proceeded via iminophosphorane intermediates that reacted intramolecularly with the carbonyl groups to form the obtained cyclic products. It is noteworthy that the loading of catalyst **44** could be as low as 0.01 equivalent.

More recently the research group of Ming-Wu Ding has extended this concept of phosphine oxide-catalyzed aza-Wittig reactions to the conversion of carboxylic acid derivatives **49** into 1,4-benzodiazepin-5-ones **50** using catalyst **44** (Scheme 15) [32]. The overall transformations were reported to occur via acyl azide intermediates **51** that were not purified, but instead used directly in thermal Curtius rearrangement reactions that afforded isocyanates **52**. These were in turn treated in situ with catalyst **44** to afford the final products **50** via presumed iminophosphorane intermediates **53**.

Scheme 14: Intramolecular catalytic aza-Wittig reactions reported by Marsden.
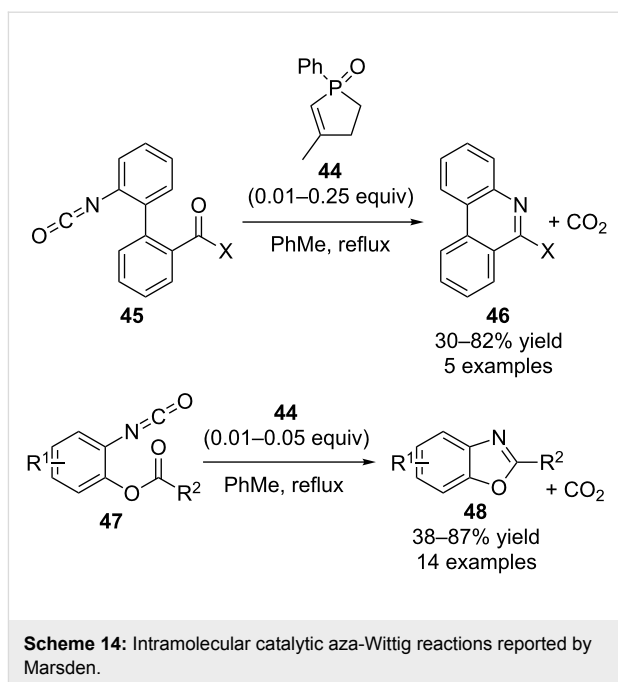
Subsequently this research group used a very similar strategy for the synthesis of polysubstituted benzimidazoles **54** via sequential Ugi and catalytic aza-Wittig reactions (Scheme 16) [33]. It was reported that mixing 2-aminobenzoyl azides **55**, carboxylic acids **56**, isocyanides **57** with aldehydes **6** in methanol generated intermediates **58**, which underwent rearrangement to isocyanates **59** in refluxing toluene. Finally, catalytic

Scheme 15: Catalytic aza-Wittig reactions in 1,4-benzodiazepin-5-one synthesis.
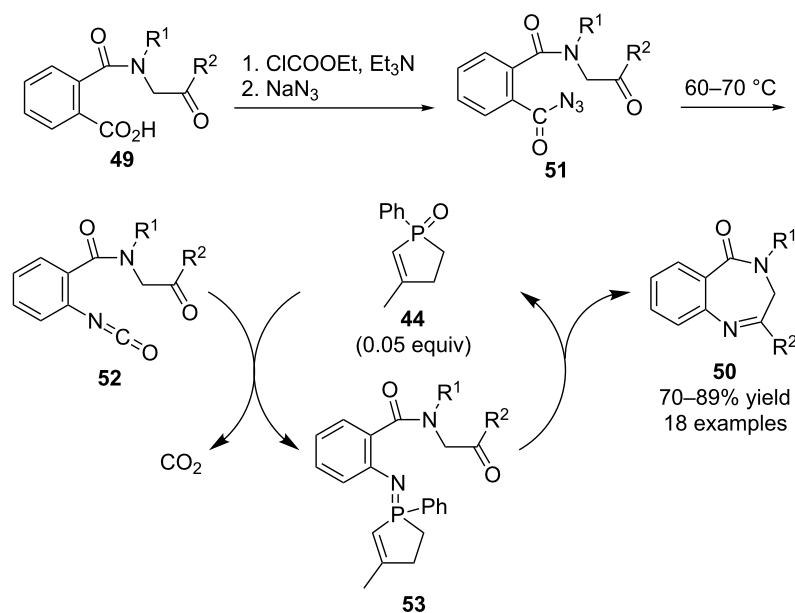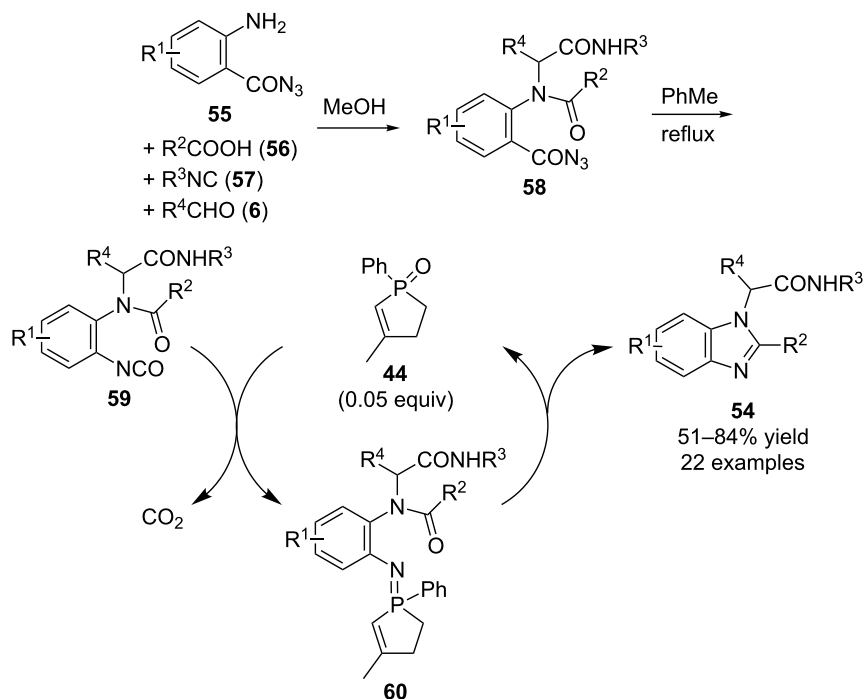
Scheme 16: Catalytic aza-Wittig reactions in benzimidazole synthesis.

aza-Wittig reactions with **44** produced cyclized final products **54** via iminophosphoranes **60**.

Phosphine-catalyzed reactions

The initial research in this area was performed by Floris L. van Delft and co-workers who reported the synthesis of **61** and its use in catalytic Staudinger reactions for the reduction of azides **62** to amines **63** (Scheme 17) [34]. Subsequently they extended such reactions to include aza-Wittig reactions using diphenylsilane as the reducing reagent [35]. For example, starting materials **64** could be converted into benzoxazoles **48** in overall net transformations that were similar as to those discussed above by Marsden (Scheme 14). In their report they also described the synthesis of various other classes of heterocyclic compounds such as 3*H*-1,4-benzodiazepin-2(1*H*)-ones **65**, 3*H*-1,4-benzodiazepin-5(4*H*)-ones **66**, and pyrrole **67** from the corresponding starting materials using similar reaction conditions.

In addition to phosphine oxide-catalyzed aza-Wittig reactions, Ding's research group has also explored the use of phosphine catalysis in such reactions. In their initial report regarding this strategy, they used **1** to catalyze intramolecular reactions that converted aryl azides **68** into 4(3*H*)-quinazolinones **69** via intermediate iminophosphoranes **70**, using the combination of titanium tetraisopropoxide and tetramethyldisiloxane (TMDS) for the in situ reduction of byproduct **2** (Scheme 18) [36].
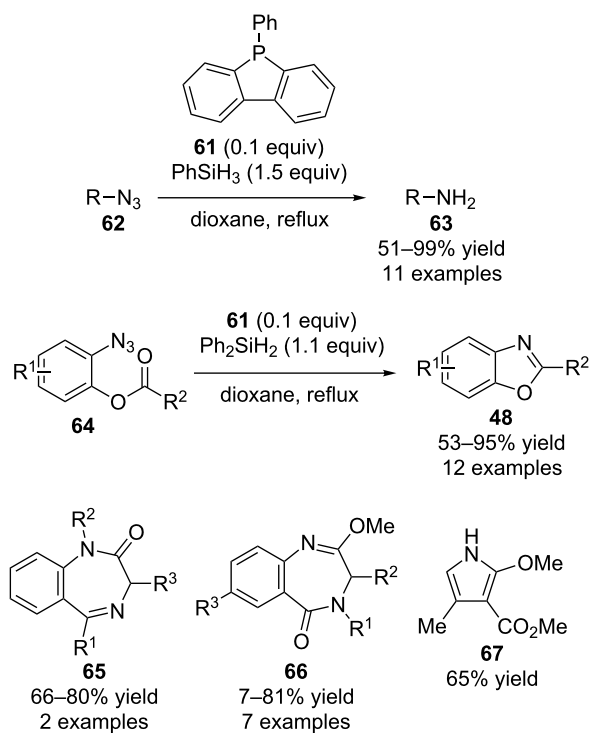
Scheme 17: Phosphine-catalyzed Staudinger and aza-Wittig reactions.
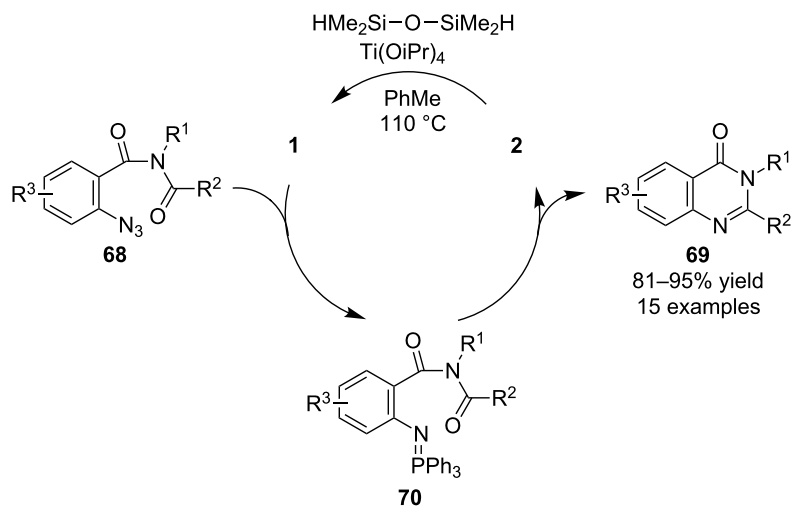
Scheme 18: Catalytic aza-Wittig reactions in 4(3*H*)-quinazolinone synthesis.

This group has more recently studied catalytic aza-Wittig reactions using carboxylic acid anhydrides as the starting materials (Scheme 19) [37]. For example, reactions of carboxylic acids **71** with acid chlorides **72** to generate the corresponding carboxylic acid anhydride in situ afforded 4*H*-benzo[*d*][1,3]-oxazin-4-ones **73**. In these reactions, **1** was used as the catalyst for the aza-Wittig reaction and copper triflate was used as the catalyst for phosphine oxide reduction. Using similar conditions the corresponding reactions of carboxylic acids **74** with aromatic acid chlorides **72** produced 4-benzylidene-2-aryloxazol-5(4*H*)-ones **75**.

Lastly, the research group of Piet Herdewijn extended this general concept and reported catalytic diaza-Wittig reactions (Scheme 20) [38]. In these reactions **76** (from the reduction of **44**) was the catalyst that transformed diazo group containing

starting materials **77** into pyridazine derivatives **78**. In these reactions **44** was actually added to the reaction mixtures as the pre-catalyst that was reduced using diphenylsilane.

It is readily evident from the above examples that regardless of whether phosphine or phosphine oxides were used as the catalyst, catalytic aza-Wittig reactions have emerged to become powerful tools in the synthesis of collections of various heterocyclic compounds since it seems that the required isocyanate or azide group containing precursors are readily synthesized from simple starting materials.

Conclusion

While great advances have been reported regarding the development of catalytic Wittig and aza-Wittig reactions, it remains to be seen how widely these methods will be adopted. Evidence
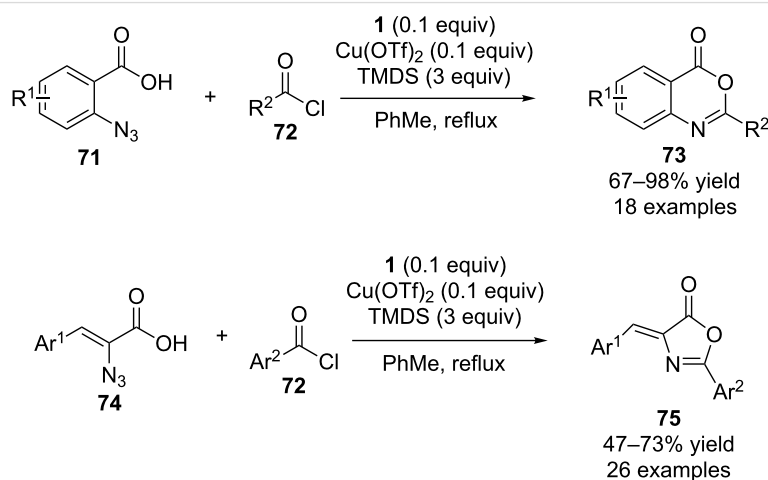
Scheme 19: Catalytic aza-Wittig reactions of in situ generated carboxylic acid anhydrides.
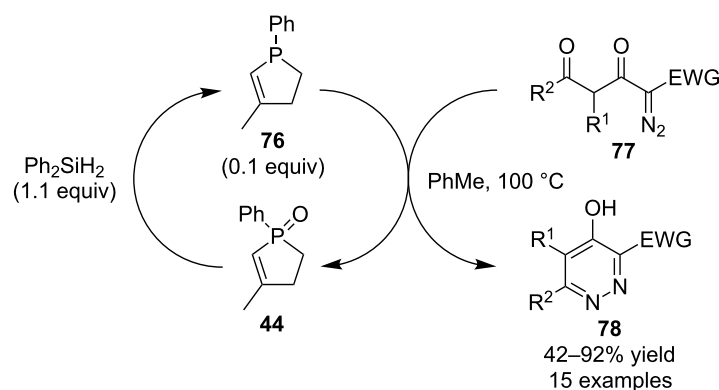
Scheme 20: Phosphine-catalyzed diaza-Wittig reactions.

that the former reactions are being described in the literature with increasing frequency are the very recent reports by Saleh and Voituriez [39], and Wenwei Lin and co-workers [40] regarding intramolecular reactions to form heterocycles that appeared as this review was being completed. However, will the research results summarized herein remain merely intellectual achievements or will they become commonly used synthetic methods in the future? Perhaps the answer to this question is how these new reaction systems are viewed from an environmental/green chemistry perspective. In this regard it is encouraging that a life cycle assessment indicates that the use of stoichiometric quantities of silanes as replacements for phosphines in catalytic Wittig reactions can offer environmental improvements [41]. Thus it seems somewhat reasonable to expect that as even more efficient methods for phosphine oxide reduction are discovered [42-47], catalytic reactions involving cycling between phosphines and phosphine oxides will become more environmentally friendly and more popular too. With regards to the phosphine oxide-catalyzed aza-Wittig reactions discussed, while no life cycle assessments have been performed, they do seem to be rather "green" since no redox cycling is necessary, and there appear to be few constraints to their potential application.

Acknowledgements

References

1. Wittig, G.; Geissler, G. *Justus Liebigs Ann. Chem.* **1953**, *580,* 44–57. doi:10.1002/jlac.19535800107
2. Byrne, P. A.; Gilheany, D. G. *Chem. Soc. Rev.* **2013**, *42,* 6670–6696. doi:10.1039/C3CS60105F
3. Xu, S.; He, Z. *RSC Adv.* **2013**, *3,* 16885–16904. doi:10.1039/C3RA42088D
4. McNulty, J.; McLeod, D.; Das, P.; Zepeda-Velázquez, C. *Phosphorus, Sulfur Silicon Relat. Elem.* **2015**, *190,* 619–632. doi:10.1080/10426507.2014.980907
5. Fairlamb, I. J. S. *ChemSusChem* **2009**, *2,* 1021–1024. doi:10.1002/cssc.200900208
6. van Kalkeren, H. A.; van Delft, F. L.; Rutjes, F. P. J. T. *ChemSusChem* **2013**, *6,* 1615–1624. doi:10.1002/cssc.201300368
7. Xu, S.; Tang, Y. *Lett. Org. Chem.* **2014**, *11,* 524–533. doi:10.2174/1570178611666140401223253
8. Voituriez, A.; Saleh, N. *Tetrahedron Lett.* **2016**, *57,* 4443–4451. doi:10.1016/j.tetlet.2016.08.036
9. He, H. S.; Chung, C. W. Y.; But, T. Y. S.; Toy, P. H. *Tetrahedron* **2005**, *61,* 1385–1405. doi:10.1016/j.tet.2004.11.031
10. Shi, L.; Wang, W.; Wang, Y.; Huang, Y. *J. Org. Chem.* **1989**, *54,* 2027–2028. doi:10.1021/jo00270a001
11. Cao, P.; Li, C.-Y.; Kang, Y.-B.; Xie, Z.; Sun, X.-L.; Tang, Y. *J. Org. Chem.* **2007**, *72,* 6628–6630. doi:10.1021/jo0709899
12. Wang, P.; Liu, C.-R.; Sun, X.-L.; Chen, S.-S.; Li, J.-F.; Xie, Z.; Tang, Y. *Chem. Commun.* **2012**, *48,* 290–292. doi:10.1039/C1CC16747B
13. Huang, Y.-Z.; Shi, L.-L.; Li, S.-W.; Wen, X.-Q. *J. Chem. Soc., Perkin Trans. 1* **1989,** 2397–2399. doi:10.1039/P19890002397
14. Huang, Z.-Z.; Ye, S.; Xia, W.; Tang, Y. *Chem. Commun.* **2001,** 1384–1385. doi:10.1039/B104100M
15. Huang, Z.-Z.; Ye, S.; Xia, W.; Yu, Y.-H.; Tang, Y. *J. Org. Chem.* **2002**, *67,* 3096–3103. doi:10.1021/jo025586h
16. Li, K.; Ran, L.; Yu, Y.-H.; Tang, Y. *J. Org. Chem.* **2004**, *69,* 3986–3989. doi:10.1021/jo049701v
17. Huang, Z.-Z.; Tang, Y. *J. Org. Chem.* **2002**, *67,* 5320–5326. doi:10.1021/jo025693b
18. O'Brien, C. J.; Tellez, J. L.; Nixon, Z. S.; Kang, L. J.; Carter, A. L.; Kunkel, S. R.; Przeworski, K. C.; Chass, G. A. *Angew. Chem., Int. Ed.* **2009**, *48,* 6836–6839. doi:10.1002/anie.200902525
19. O'Brien, C. J.; Nixon, Z. S.; Holohan, A. J.; Kunkel, S. R.; Tellez, J. L.; Doonan, B. J.; Coyle, E. J.; Lavigne, F.; Kang, L. J.; Przeworski, K. C. *Chem. – Eur. J.* **2013**, *19,* 15281–15289. doi:10.1002/chem.201301444
20. O'Brien, C. J.; Lavigne, F.; Coyle, E. E.; Holohan, A. J.; Doonan, B. J. *Chem. – Eur. J.* **2013**, *19,* 5854–5858. doi:10.1002/chem.201300546
21. Coyle, E. E.; Doonan, B. J.; Holohan, A. J.; Walsh, K. A.; Lavigne, F.; Krenske, E. H.; O'Brien, C. J. *Angew. Chem., Int. Ed.* **2014**, *53,* 12907–12911. doi:10.1002/anie.201406103

22. Werner, T.; Hoffmann, M.; Deshmukh, S. *Eur. J. Org. Chem.* **2014,** 6630–6633. doi:10.1002/ejoc.201402941

23. Werner, T.; Hoffmann, M.; Deshmukh, S. *Eur. J. Org. Chem.* **2014,** 6873–6876. doi:10.1002/ejoc.201403113

24. Hoffmann, M.; Deshmukh, S.; Werner, T. *Eur. J. Org. Chem.* **2015,** 4532–4543. doi:10.1002/ejoc.201500310

25. Werner, T.; Hoffmann, M.; Deshmukh, S. *Eur. J. Org. Chem.* **2015,** 3286–3295. doi:10.1002/ejoc.201500243

26. Schirmer, M.-L.; Adomeit, S.; Werner, T. *Org. Lett.* **2015,** *17,* 3078–3081. doi:10.1021/acs.orglett.5b01352

27. Schirmer, M.-L.; Adomelt, S.; Spannenberg, A.; Werner, T. *Chem. – Eur. J.* **2016,** *22,* 2458–2465. doi:10.1002/chem.201503744

28. Tsai, Y.-L.; Lin, W. *Asian J. Org. Chem.* **2015,** *4,* 1040–1043. doi:10.1002/ajoc.201500251

29. Rommel, S.; Belger, C.; Begouin, J.-M.; Plietker, B. *ChemCatChem* **2015,** *7,* 1292–1301. doi:10.1002/cctc.201500053

30. Campbell, T. W.; Monagle, J. J.; Foldi, V. S. *J. Am. Chem. Soc.* **1962,** *84,* 3673–3677. doi:10.1021/ja00878a015

31. Marsden, S. P.; McGonagle, A. E.; McKeever-Abbas, B. *Org. Lett.* **2008,** *10,* 2589–2591. doi:10.1021/ol800921n

32. Wang, L.; Qin, R.-Q.; Yan, H.-Y.; Ding, M.-W. *Synthesis* **2015,** *47,* 3522–3528. doi:10.1055/s-0034-1378874

33. Yan, Y.-M.; Rao, Y.; Ding, M.-W. *J. Org. Chem.* **2016,** *81,* 1263–1268. doi:10.1021/acs.joc.5b02575

34. van Kalkeren, H. A.; Bruins, J. J.; Rutjes, F. P. J. T.; van Delft, F. L. *Adv. Synth. Catal.* **2012,** *354,* 1417–1421. doi:10.1002/adsc.201100967

35. van Kalkeren, H. A.; te Grotenhuis, C.; Haasjes, F. S.; Hommerson, C. R. A.; Rutjes, F. P. J. T.; van Delft, F. L. *Eur. J. Org. Chem.* **2013,** 7059–7066. doi:10.1002/ejoc.201300585

36. Wang, L.; Wang, Y.; Chen, M.; Ding, M.-W. *Adv. Synth. Catal.* **2014,** *356,* 1098–1104. doi:10.1002/adsc.201300950

37. Wang, L.; Xie, Y.-B.; Huang, N.-Y.; Yan, J.-Y.; Hu, W.-M.; Liu, M.-G.; Ding, M.-W. *ACS Catal.* **2016,** *6,* 4010–4016. doi:10.1021/acscatal.6b00165

38. Bel Abed, H.; Mammoliti, O.; Bande, O.; Van Lommen, G.; Herdewijn, P. *Org. Biomol. Chem.* **2014,** *12,* 7159–7166. doi:10.1039/C4OB01201A

39. Saleh, N.; Voituriez, A. *J. Org. Chem.* **2016,** *81,* 4371–4377. doi:10.1021/acs.joc.6b00473

40. Lee, C.-J.; Chang, T.-H.; Yu, J.-K.; Reddy, G. M.; Hsiao, M.-Y.; Lin, W. *Org. Lett.* **2016,** *18,* 3758–3761. doi:10.1021/acs.orglett.6b01781

41. van Kalkeren, H. A.; Blom, A. L.; Rutjes, F. P. J. T.; Huijbregts, M. A. J. *Green Chem.* **2013,** *15,* 1255–1263. doi:10.1039/C3GC00053B

42. Kuroboshi, M.; Yano, T.; Kamenoue, S.; Kawakubo, H.; Tanaka, H. *Tetrahedron* **2011,** *67,* 5825–5831. doi:10.1016/j.tet.2011.05.044

43. Li, Y.; Lu, L.-Q.; Das, S.; Pisiewicz, S.; Junge, K.; Beller, M. *J. Am. Chem. Soc.* **2012,** *134,* 18325–18329. doi:10.1021/ja3069165

44. Keglevich, G.; Kovács, T.; Csatlós, F. *Heteroat. Chem.* **2015,** *26,* 199–205. doi:10.1002/hc.21249

45. Demchuk, O. M.; Jasiński, R.; Pietrusiewicz, K. M. *Heteroat. Chem.* **2015,** *26,* 441–448. doi:10.1002/hc.21279

46. Schirmer, M.-L.; Jopp, S.; Holz, J.; Spannenberg, A.; Werner, T. *Adv. Synth. Catal.* **2016,** *358,* 26–29. doi:10.1002/adsc.201500762

47. Hérault, D.; Nguyen, D. H.; Nuel, D.; Buono, G. *Chem. Soc. Rev.* **2015,** *44,* 2508–2528. doi:10.1039/C4CS00311J

Continuous-flow synthesis of primary amines: Metal-free reduction of aliphatic and aromatic nitro derivatives with trichlorosilane

Riccardo Porta, Alessandra Puglisi[*], Giacomo Colombo, Sergio Rossi and Maurizio Benaglia[*]

Abstract

The metal-free reduction of nitro compounds to amines mediated by trichlorosilane was successfully performed for the first time under continuous-flow conditions. Aromatic as well as aliphatic nitro derivatives were converted to the corresponding primary amines in high yields and very short reaction times with no need for purification. The methodology was also extended to the synthesis of two synthetically relevant intermediates (precursors of baclofen and boscalid).

Introduction

The reduction of nitro compounds to amines is a fundamental transformation in organic synthesis. The nitration of aromatic rings followed by reduction is the most classical entry for the preparation of anilines [1,2]. Lately, also aliphatic nitro derivatives have become more and more popular: a wide variety of highly functionalized and chiral aliphatic nitro compounds, precursors of the corresponding chiral amines, are accessible via several synthetic routes. In the last years nitro compounds have been the subject of numerous studies since they served as reactants in many, highly efficient, organocatalytic transformations [3-7]. Furthermore, the introduction of an amino group offers a well-known plethora of further synthetic elaborations.

Among the different available methodologies for the reduction of nitro compounds [8], we have recently reported a very convenient, mild, metal-free and inexpensive procedure, of wide applicability [9,10]. The simple combination of trichlorosilane (HSiCl$_3$) and a tertiary amine generates in situ a dichlorosilylene species which is the actual reducing species [11].

Even though nitro derivatives are fundamental building blocks in organic synthesis, their application on a large scale is still quite limited because they are dangerous and potentially explosive chemicals. Flow chemistry has recently emerged as a powerful technology in synthetic chemistry [12] as it can reduce

risks associated to the use of hazardous chemicals and favors reaction scale-up [13-17]. The possibility to efficiently perform nitro reduction in continuo would make the transformation safer and more appealing in view of an industrial application and a possible scale-up of the process [18-20].

Herein we report a very convenient, metal-free reduction of both aromatic and aliphatic nitro derivatives, including chiral compounds, to amines with $HSiCl_3$ under continuous-flow conditions.

Typically, the transformation of nitro compounds to amines under continuous-flow conditions is performed through the metal-catalyzed hydrogenation [21-23] with ThalesNano H-Cube®, which exploits H_2 generated in situ by water electrolysis [24]. The procedure involves relatively mild reaction conditions, but the presence of noble metal catalysts, packed into disposable cartridges, suffers from functional group compatibility and catalyst poisoning during time.

In 2012 Kappe's research group reported the microwave-assisted continuous-flow synthesis of anilines from nitroarenes using hydrazine as reducing agent and iron oxide nanocrystals as the catalyst [25]. This methodology ensured fast transformations (2 to 8 minutes) of a wide number of substrates and was extended to large scale preparation of pharmaceutically relevant anilines [26]. However, this procedure required harsh reaction conditions ($T = 150$ °C), is limited to aromatic substrates and could not be applied to compounds bearing ketones or aldehydes as functional groups.

In the present work we provide an alternative continuous-flow metal-free methodology for the synthesis of both aliphatic and aromatic amines, which requires inexpensive reagents, mild and fast reaction conditions (25 °C, 5 minutes), and a very simple and user-friendly reaction set-up.

Results and Discussion

In our methodology, a nitro derivative is reacted with commercially available $HSiCl_3$ in the presence of a tertiary base (typically Hünig's base) in an organic solvent (typically CH_2Cl_2, although CH_3CN affords comparable results). The continuous-flow reduction of 4-nitrobenzophenone (**1a**) was chosen as model reaction. A syringe pump equipped with two gas-tight 2.5 mL syringes was used to feed the reagents into a 0.5 mL PTFE reactor (i.d. = 0.58 mm, l = 189 cm) through a T-junction (syringe A: 0.8 M solution of $HSiCl_3$ in CH_2Cl_2; syringe B: 0.2 M solution of **1a** in CH_2Cl_2, Hünig's base 6 equiv, Scheme 1).

The outcome of the reactor was collected into a flask containing 10% NaOH solution in order to quench the reaction. After phase separation the crude reaction mixture was analyzed by ^{1}H NMR to determine the conversion. When the reaction reached a full conversion (>98%) no further purification step was required and the aniline was recovered as clean product after simple concentration of the organic phase and extraction with ethyl acetate. A screening of flow rates was initially performed and the results are reported in Table 1.

As data show, the reaction is very fast and a complete conversion of nitroarene **1a** to aniline **2a** was achieved with very short residence times (10, 5 and 2.5 min, Table 1, entries 1–3). With a 1.2 minutes residence time, 91% conversion was reached. The faster reaction in the flow process compared to the batch one (5 minute vs 18 hours [8]) can be partially attributed to the higher reaction temperature: the flow reaction can be performed at 25 °C while the batch reaction required a cooling to 0 °C, at least at the beginning of the reaction (the first few hours).

Having demonstrated that the flow transformation is very fast we next explored reaction scale-up employing a bigger flow
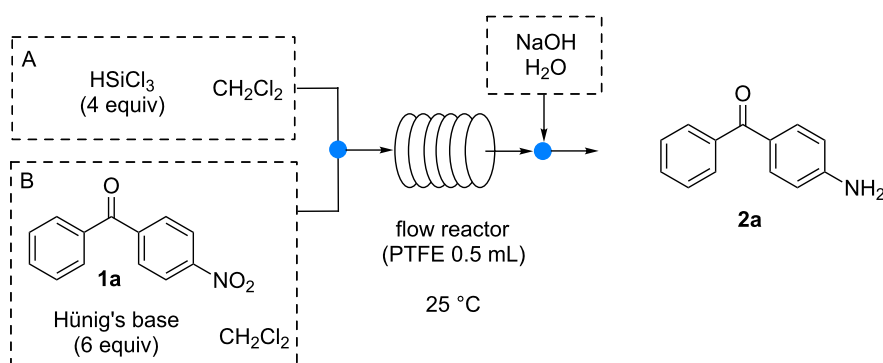
Scheme 1: Continuous flow reduction of 4-nitrobenzophenone using a 0.5 mL PTFE flow reactor.

Table 1: Screening of reaction conditions.

Entry[a]	Flow rate (mL/min)	Residence time (min)	Conversion (%)[b]
1	0.05	10	98 (96)
2	0.1	5	98 (96)
3	0.2	2.5	98 (93)
4	0.4	1.2	91 (85)
5[c]	0.1	50	97
6[c,d]	0.1	50	87
7[c]	0.2	25	82

[a]Reaction performed using a 0.2 M solution of Ar-NO$_2$ (0.6 mmol) in CH$_2$Cl$_2$, HSiCl$_3$ (4 equiv), Hünig's base (6 equiv) at room temperature; [b]reaction conversion determined by NMR of the crude; isolated yields in parentheses; [c]reaction performed in a 5 mL PTFE reactor; [d]reaction performed using TEA as a base.

reactor (5 mL PTFE reactor, i.d. = 2.54 mm, *l* = 100 cm), in order to increase the productivity of the process.

Using the same reaction set-up illustrated in Scheme 1, a residence time of 50 minutes was necessary to reach a full conversion of the starting material (Table 1, entry 5). This is mainly

due to the bigger internal diameter of the reactor (2.54 mm vs 0.58 mm) which affects the mixing of the reagents [27,28]. Lowering the residence time resulted in minor conversions (Table 1, entry 7, 25 min residence time, 82% conversion). A cheaper base than Hünig's base as TEA (triethylamine) could also effectively promote the reduction with only marginally lower conversion (Table 1, entry 6 vs entry 5) [9-11]. The possibility to use commercially available HSiCl$_3$, in combination with an inexpensive base as TEA, and the simple work-up make this very mild reduction methodology appealing for several future synthetic applications, also of industrial interest.

We next focused on expanding the scope of the reaction and proof the general applicability. Using both 0.5 mL and 5 mL reactors, under the best reaction conditions, the continuous-flow reduction of different nitroarenes was studied (Scheme 2).

As already demonstrated for the batch procedure [8], the reaction in continuo tolerates a large variety of functional groups: aromatic nitro groups are selectively reduced with quantitative conversions in the presence of ketones (Table 2, entry 1), halogens (Table 2, entries 3–5) and esters (Table 2, entry 6).
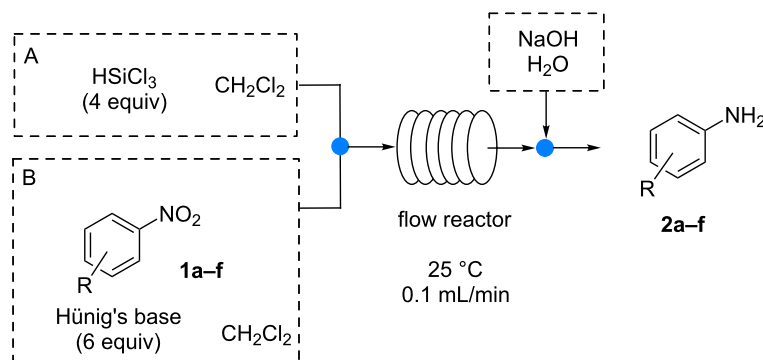
Scheme 2: Continuous flow reduction of aromatic nitro compounds.

Table 2: Scope of the reaction (see Scheme 2).

Entry[a]	R	0.5 mL Reactor[b] Conversion (%)[c]	5 mL Reactor[d] Conversion (%)[e]
1	4-nitrobenzoyl, **1a**	98 (96)	97
2	4-Me, **1b**	98 (96)	98
3	4-Br, **1c**	98 (92)	98
4	2,4-Cl$_2$, **1d**	98 (92)	92
5	4-F, **1e**	98 (90)	91
6	4-COOMe, **1f**	98 (95)	98

[a]Reaction performed using a 0.2 M solution of Ar-NO$_2$ in CH$_2$Cl$_2$, HSiCl$_3$ (4 equiv), Hünig's base (6 equiv) at room temperature; [b]Residence time = 5 min; [c]Reaction conversion determined by NMR of the crude; isolated yield in parenthesis; [d]Residence time = 50 min; [e]Determined by NMR of the crude.

The methodology was also extended to aliphatic nitro compounds (Scheme 3). These substrates are less reactive than aromatic ones and they typically require higher hydrogen pressures or reaction temperatures to be completely reduced to the corresponding aliphatic amines.

By employing our metal-free methodology, at 25 °C in a 0.5 mL reactor, aliphatic amines **2g** and **2h** were obtained with a full conversion of the starting material and isolated yields of 91% and 93%, respectively, by using a residence time of 10 minutes only (when a residence time of 5 minutes was used a slightly lower yield was obtained – 81% for amine **2g**).

We then applied the trichlorosilane-mediated continuous-flow nitro reduction to the synthesis of advanced precursors of molecules of pharmaceutical interest. The reduction of nitro compound **3** afforded 2-(4'-chlorophenyl)aniline (**4**), the direct precursor of the fungicide boscalid (Scheme 4). Under the best

reaction conditions in a 5 mL PTFE reactor (flow rate 0.1 mL/min, 50 min residence time), the desired amine **4** was obtained in quantitative yield as a clean product with no need for purification.

We also investigated the continuous-flow reduction of nitro ester **5**, which can be conveniently prepared in one step through the organocatalyzed addition of diethyl malonate to *trans*-β-nitrostyrene promoted by a chiral thiourea [29]. The corresponding amide **6** is a direct precursor of the GABA receptor agonist Baclofen (Scheme 5).

Nitro compound **5** was continuously reduced in a 5 mL reactor and, after work-up under neutral conditions, chiral lactam **6** was isolated in 48% yield.

Finally we explored the possibility of performing a reaction scale-up, followed by an in-line extraction in order to obtain a

Scheme 3: Continuous-flow reduction of aliphatic nitro compounds.

Scheme 4: Synthesis of 2-(4'-chlrophenyl)aniline (**4**) with a 5 mL flow reactor.

Scheme 5: Synthesis of intermediate **6**, a direct precursor of the drug baclofen.
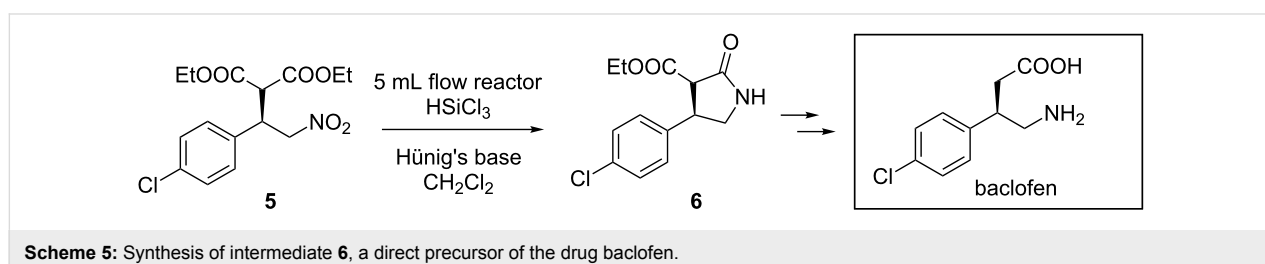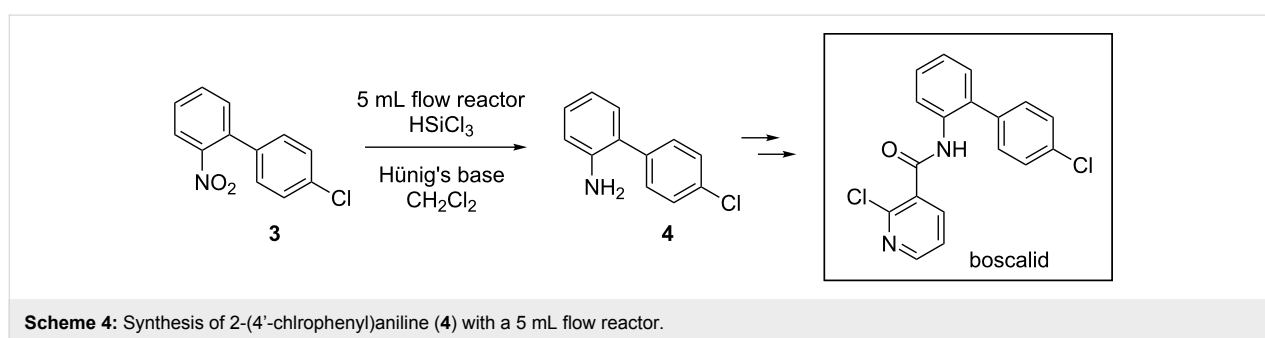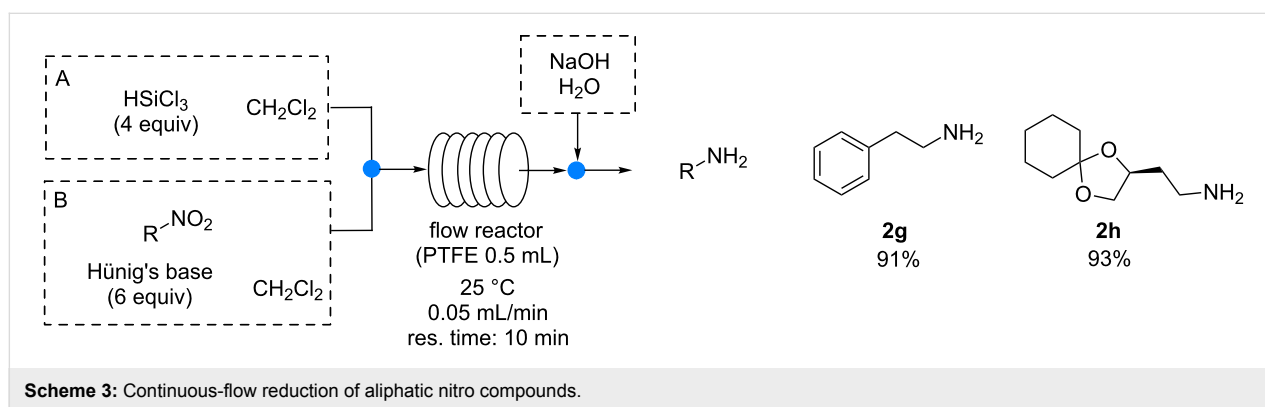
full continuous process with no need for intermediate operations (Scheme 6).

A syringe pump equipped with two SGE gas tight 25 mL syringes was used to feed the reagents into a 5 mL PTFE reactor through a T-junction (syringe A: $HSiCl_3$ (24 mmol) in 15 mL CH_2Cl_2.; syringe B: substrate **1a** (6 mmol), Hünig's base (36 mmol in 15 mL CH_2Cl_2)) with a flow rate of 0.1 mL/min (residence time 50 min). The outcome of the reactor was collected into a separatory funnel containing NaOH 10% solution (10 mL) and CH_2Cl_2 (10 mL). The biphasic system was kept under stirring and the organic layer was continuously collected into a flask. Removal of CH_2Cl_2 gave pure amino compound **2a** in 94% yield. This system allowed to easily obtaining almost 1 g of pure **2a** in about 4 hours (see Supporting Information File 1 for further details).

Conclusion

In conclusion, a very convenient, mild, metal-free reduction of aliphatic and aromatic nitro derivatives under continuous flow-conditions has been successfully developed. The general applicability to differently substituted compounds and the possibility to scale-up the process have been demonstrated. The use of extremely inexpensive and non-hazardous chemicals, the very high chemoselectivity and the possibility to realize a completely automated reduction/work-up/isolation process are distinctive features that make the protocol suitable for the reduction of a large variety of products and attractive also for future industrial applications.

Experimental

General procedure for the continuous-flow reaction using a 0.5 mL PTFE reactor: Syringe A was filled with a solution of $HSiCl_3$ (2.4 mmol) in dry CH_2Cl_2 (1.5 mL). Syringe B was loaded with a solution of the nitro compound (0.6 mmol) and Hünig's base (3.6 mmol) in dry CH_2Cl_2 (1.5 mL). Syringes A and B were connected to a syringe pump and the reagents were pumped into the microreactor at the indicated flow rate

(mL/min) at room temperature. The outcome of the reactor was collected in a flask containing a 10% NaOH solution. Five reactor volumes were collected. CH_2Cl_2 was removed in vacuo and the aqueous layer was extracted three times with ethyl acetate. The combined organic layers were washed with brine, dried with Na_2SO_4 and concentrated in vacuo. ^{1}H NMR spectroscopy of the crude was used to calculate the reaction conversion; in case of a full conversion of the starting material no further purification was required.

Supporting Information

Supporting Information File 1
General procedure for continuous-flow reactions, products characterization and NMR spectra of the compounds.
[http://www.beilstein-journals.org/bjoc/content/supplementary/1860-5397-12-257-S1.pdf]

References

1. Blaser, H. U.; Siegrist, U.; Steiner, H.; Studer, M. In *Fine chemicals through Heterogeneous Catalysis;* Sheldon, R. A.; van Bekkum, H., Eds.; Wiley-VCH: Weinheim, 2001; pp 389–471.
   See for an overview on synthetic aspects of the catalytic reduction of nitroarenes.
2. Blaser, H.-U.; Steiner, H.; Studer, M. *ChemCatChem* **2009,** *1,* 210–221. doi:10.1002/cctc.200900129
3. Ballini, R.; Bosica, G.; Fiorini, D.; Palmieri, A.; Petrini, M. *Chem. Rev.* **2005,** *105,* 933–972. doi:10.1021/cr040602r
4. Noble, A.; Anderson, J. C. *Chem. Rev.* **2013,** *113,* 2887–2939. doi:10.1021/cr300272t

Scheme 6: Continuous-flow reduction of **1a** and in-line extraction.
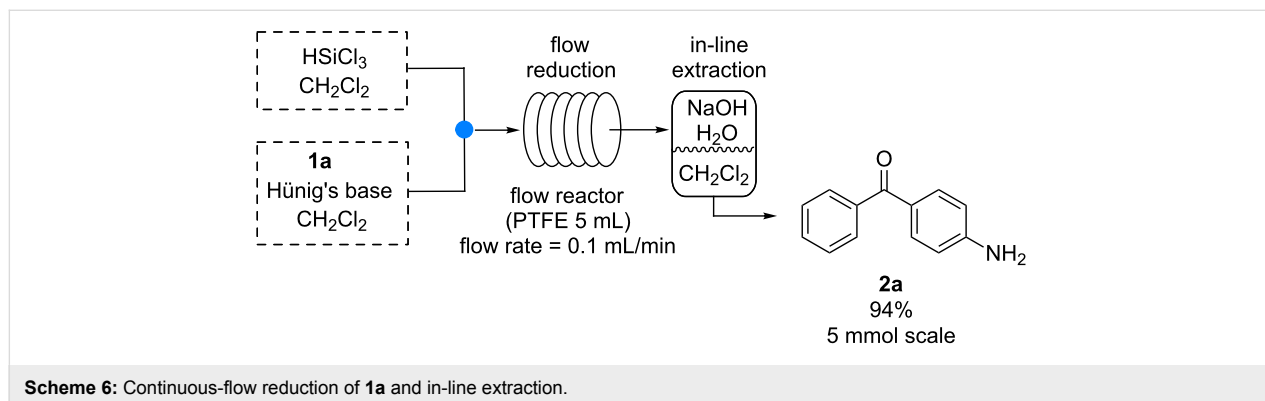
5. Roca-Lopez, D.; Sabada, D.; Delso, I.; Herrera, R. P.; Tejero, P.; Merino, P. *Tetrahedron: Asymmetry* **2010,** *21,* 2561–2601. doi:10.1016/j.tetasy.2010.11.001

6. Mukherjee, S.; Yang, J. W.; Hoffmann, S.; List, B. *Chem. Rev.* **2007,** *107,* 5471–5569. doi:10.1021/cr0684016

7. Enders, D.; Wang, C.; Liebich, J. X. *Chem. – Eur. J.* **2009,** *15,* 11058–11076. doi:10.1002/chem.200902236
See for a review on organocatalytic asymmetric conjugate additions.

8. Orlandi, M.; Brenna, D.; Harms, R.; Jost, S.; Benaglia, M. *Org. Process Res. Dev.* **2016**. doi:10.1021/acs.oprd.6b00205
See for a recent review.

9. Orlandi, M.; Tosi, F.; Bonsignore, M.; Benaglia, M. *Org. Lett.* **2015,** *17,* 3941–3943. doi:10.1021/acs.orglett.5b01698

10. The methodology is also described in a patent: International Patent Application: Bonsignore, M.; Benaglia, M. PCT/EP/2013/06837 (05.09.2013) (Università degli Studi di Milano, Milano, Italy), now owned by DexLeChem GmbH (Berlin, Germany).

11. Orlandi, M.; Benaglia, M.; Tosi, F.; Annunziata, R.; Cozzi, F. *J. Org. Chem.* **2016,** *81,* 3037–3041. doi:10.1021/acs.joc.6b00191

12. Gutmann, B.; Cantillo, D.; Kappe, C. O. *Angew. Chem., Int. Ed.* **2015,** *54,* 6688–6728. doi:10.1002/anie.201409318

13. Atodiresei, I.; Vila, C.; Rueping, M. *ACS Catal.* **2015,** *5,* 1972–1985. doi:10.1021/acscatal.5b00002

14. Puglisi, A.; Benaglia, M.; Porta, R.; Coccia, F. *Curr. Organocatal.* **2015,** *2,* 79–101. doi:10.2174/2213337202666150513002701

15. Munirathinam, R.; Huskens, J.; Verboom, W. *Adv. Synth. Catal.* **2015,** *357,* 1093–1123. doi:10.1002/adsc.201401081

16. Rodríguez-Escrich, C.; Pericàs, M. A. *Eur. J. Org. Chem.* **2015,** 1173–1188. doi:10.1002/ejoc.201403042

17. Porta, R.; Benaglia, M.; Puglisi, A. *Org. Process Res. Dev.* **2016,** *20,* 2–25. doi:10.1021/acs.oprd.5b00325

18. Poh, J.-S.; Tran, D. N.; Battilocchio, C.; Hawkins, J. M.; Ley, S. V. *Angew. Chem., Int. Ed.* **2015,** *54,* 7920–7923. doi:10.1002/anie.201501538

19. Fabry, D. C.; Ronge, M. A.; Rueping, M. *Chem. – Eur. J.* **2015,** *21,* 5350–5354. doi:10.1002/chem.201406653

20. Tran, D. N.; Battilocchio, C.; Lou, S.-B.; Hawkins, J. M.; Ley, S. V. *Chem. Sci.* **2015,** *6,* 1120–1125. doi:10.1039/C4SC03072A

21. Cossar, P. J.; Hizartzidis, L.; Simone, M. I.; McCluskey, A.; Gordon, C. P. *Org. Biomol. Chem.* **2015,** *13,* 7119–7130. doi:10.1039/C5OB01067E

22. Hartwig, J.; Ceylan, S.; Kupracz, L.; Coutable, L.; Kirschning, A. *Angew. Chem., Int. Ed.* **2013,** *52,* 9813–9817. doi:10.1002/anie.201302239

23. Tsubogo, T.; Oyamada, H.; Kobayashi, S. *Nature* **2015,** *520,* 329–332. doi:10.1038/nature14343

24. Jones, R. V.; Godorhazy, L.; Varga, N.; Szalay, D.; Urge, L.; Darvas, F. *J. Comb. Chem.* **2006,** *8,* 110–116. doi:10.1021/cc050107o

25. Cantillo, D.; Baghbanzadeh, M.; Kappe, C. O. *Angew. Chem., Int. Ed.* **2012,** *51,* 10190–10193. doi:10.1002/anie.201205792

26. Cantillo, D.; Moghaddam, M. M.; Kappe, C. O. *J. Org. Chem.* **2013,** *78,* 4530–4542. doi:10.1021/jo400556g

27. Hartman, R. L.; McMullen, J. P.; Jensen, K. F. *Angew. Chem., Int. Ed.* **2011,** *50,* 7502–7519. doi:10.1002/anie.201004637

28. Elvira, K. S.; Casadevall i Solvas, X.; Wootton, R. C. R.; deMello, A. J. *Nat. Chem.* **2013,** *5,* 905–915. doi:10.1038/nchem.1753

29. Okino, T.; Hoashi, Y.; Furukawa, T.; Xu, X.; Takemoto, Y. *J. Am. Chem. Soc.* **2005,** *127,* 119–125. doi:10.1021/ja044370p

Towards the development of continuous, organocatalytic, and stereoselective reactions in deep eutectic solvents

Davide Brenna[1], Elisabetta Massolo[1], Alessandra Puglisi[1], Sergio Rossi[1], Giuseppe Celentano[2], Maurizio Benaglia[*1] and Vito Capriati[3]

Abstract

Different deep eutectic solvent (DES) mixtures were studied as reaction media for the continuous synthesis of enantiomerically enriched products by testing different experimental set-ups. L-Proline-catalysed cross-aldol reactions were efficiently performed in continuo, with high yield (99%), *anti*-stereoselectivity, and enantioselectivity (up to 97% ee). Moreover, using two different DES mixtures, the diastereoselectivity of the process could be tuned, thereby leading to the formation, under different experimental conditions, to both the *syn*- and the *anti*-isomer with very high enantioselectivity. The excess of cyclohexanone was recovered and reused, and the reaction could be run and the product isolated without the use of any organic solvent by a proper choice of DES components. The dramatic influence of the reaction media on the reaction rate and stereoselectivity of the process suggests that the intimate architecture of DESs deeply influences the reactivity of different species involved in the catalytic cycle.

Introduction

The aldol reaction is a powerful synthetic tool to create new C–C bonds [1]. It offers several possibilities to control the stereochemical outcome of the process and to afford stereo-chemically defined chiral products [2]. Among all the possible options, the L-proline-catalysed stereoselective cross-aldol reaction remains the greener choice. After the pioneering works by List and Barbas [3], a huge effort was made by the scientific community to improve both the yield and the stereoselectivity of the reaction. The most explored strategies involve the development of a new class of catalysts (mainly prolinamide deriva-tives) [4-6], the study of additives in combination with proline itself [7-13], and the use of unusual reaction media [14-19].

In this context, it was recently reported that L-proline-catalysed direct aldol reactions may be successfully carried out also in deep eutectic solvents (DESs) [20-22]. Recently, our group reported on the possibility of running organocatalyzed, stereoselective reactions in DESs, promoted by an enantiopure primary amine, with advantages in terms of reaction sustainability. In particular, the possibility to strongly reduce the amounts of organic solvent and the recyclability of the catalyst were demonstrated [23]. Moreover, in this approach, no structural modification of the precious chiral catalyst was necessary.

A well-explored strategy aimed at positively realizing the recovery and the reuse of the catalyst is represented by the immobilization of the catalytic species [24-27]. Synthetic modifications of the original catalyst, however, are required in order to attach the catalyst to the material of choice. The aim of the present study was to develop a catalytic system working in continuo, whereas DES acts at the same time as catalyst trap and as reaction medium, immiscible with the organic reactants. The main advantage of this approach is that the catalyst (i.e., L-proline) would be kept in an environmentally benign reaction medium, without the need of any synthetic modification. Of note, in the herein proposed system, readily assembled using standard glassware, the use of the organic solvent, both for the reaction and for the isolation process, would be strongly reduced or even, ideally, eliminated.

Results and Discussion

Among the plethora of possible DES mixtures [28-33], based on our previous experience [34-39] and preliminary studies on the physicochemical properties of DES combinations, we decided to focus our attention on the use of a few choline chloride (ChCl)-based eutectic mixtures as reaction media (Table 1) [40].

The behaviour of DES mixtures A–E in the proline-catalysed model aldol reaction between cyclohexanone and 4-nitrobenzaldehyde was preliminarily investigated under standard batch conditions (Scheme 1).

In our hands, the reaction proceeded completely in 20 hours and with high conversion (≥95%) in all tested DESs (A–E, Table 2,

Table 1: ChCl-based eutectic mixtures used in the present work.

DES	Components	Molar ratio
DES A	ChCl/urea	1:2
DES B	ChCl/urea/H_2O	1:2:1.5
DES C	ChCl/urea/H_2O	1:2:4
DES D	ChCl/fructose/H_2O	1:1:1
DES E	ChCl/glycerol	1:2

entries 1–5). While low diastereoselectivity was observed in DES A (Table 2, entry 1), *anti*-stereoselectivity (up to 85:15) and high enantiomeric excess in favour of the *anti* isomer (up to 92% ee) were instead detected running the reaction in DESs B–E (Table 2, entries 2–5).

Table 2: DES screening for the proline-catalyzed in batch aldol reaction.

Entry	DES	Conv. (%)[a]	dr (*anti:syn*)[a]	ee % (*anti/syn*)[b]
1	A	99	57:43	81/80
2	B	98	82:18	89/69
3	C	96	85:15	92/54
4	D	95	75:25	84/67
5	E	96	70:30	82/67

[a]Conversion and dr were evaluated by NMR technique on the crude reaction mixture; [b]ee was evaluated by using an HPLC with a chiral stationary phase.

Based on these results, we turned our attention to design and realize a home-made system, to be easily assembled with common glassware, for the continuous synthesis of the aldol product, using a DES mixture as reaction media able to hold back the proline.

In these very explorative studies, different experimental set-ups were investigated, focusing especially on some points, such as (a) the phase contact between the organic phase, composed by cyclohexanone and the aldehyde, and the DES phase, (b) the ratio between DES and L-proline, and, finally, (c) the possible interaction between the aldol product and the DES network (Figure 1). Due to its favourable physical and mechanical prop-

(20 equiv)   L-proline 35 %   DES , rt, 20 h   1a   1b
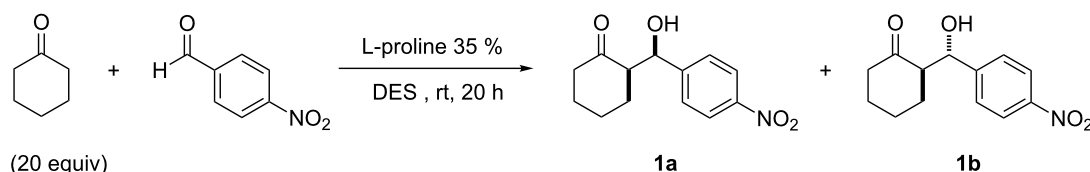
Scheme 1: L-Proline-promoted stereoselective aldol reaction in DES.

Set-ups

Figure 1: Experimental set-up I: test tube (*d* = 0.5 cm); flow 1 mL/min; DES (1.5 mL); L-proline/DES = 130 mg/mL. Experimental set-up II: test tube (*d* = 2.5 cm); flow 1 mL/min; DES (1.5 mL); L-proline/DES = 130 mg/mL. Experimental set-up III: test tube (*d* = 2.5 cm); flow 1 mL/min; DES (1.5 mL); L-proline/DES = 130 mg/mL.
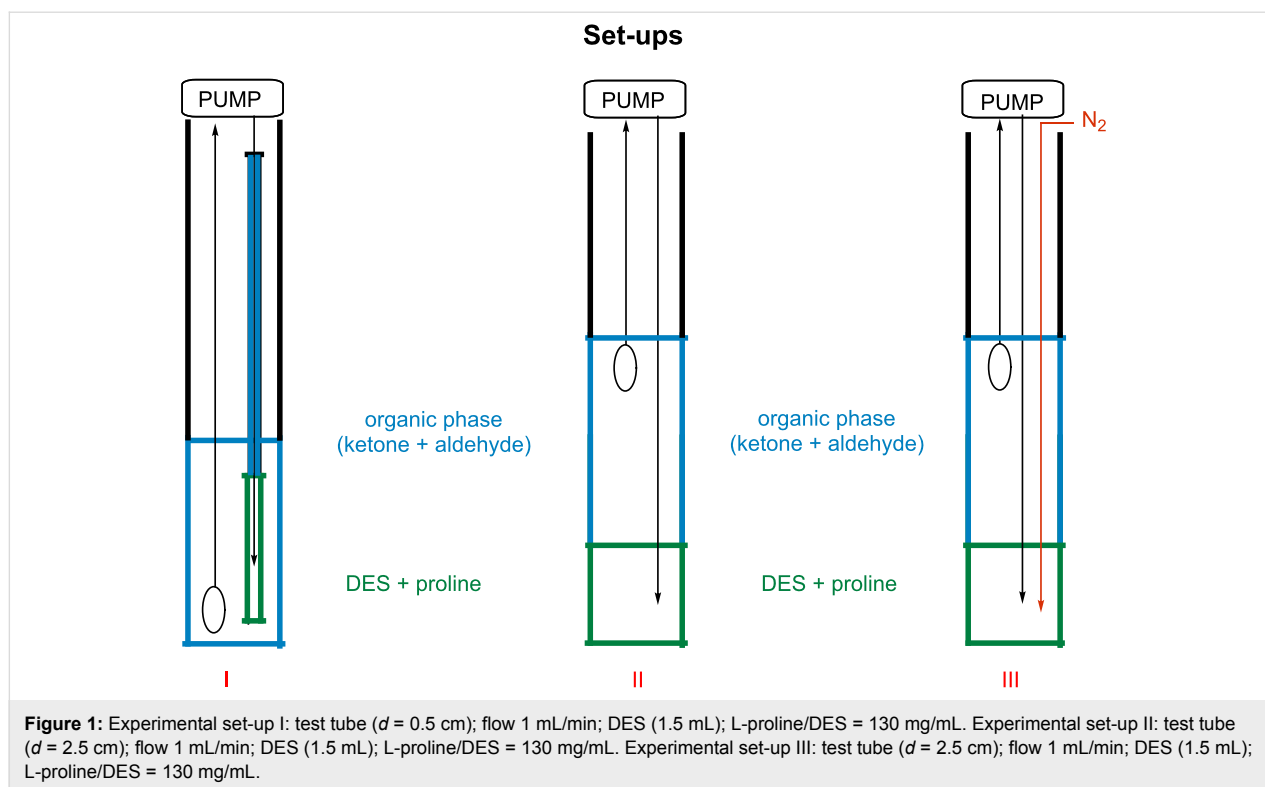
erties, DES A was selected for the initial screening of the different experimental conditions in continuo.

The first experimental set-up that was studied (Figure 1, I) was built using a test tube of reduced diameter (green color in the picture) containing the DES and L-proline, surrounded by an external, larger cylinder filled with a solution of cyclohexanone and 4-nitrobenzaldehyde. The organic solution, fluxed by a HPLC pump onto the bottom of the internal smaller tube, went back through DES due to the difference in the viscosity of the two phases, thereby generating a upper organic phase (blue in the picture) which finally ended into the organic phase of the larger tube, that was continuously pumped into the DES phase to realize a closed cycle.

In set-up II, the mixture of DES and L-proline was covered with the solution of ketone and aldehyde in a 10 mL graduated cylinder. The organic phase was continuously pumped on the bottom of the DES phase and recirculated (Figure 1, II). In order to improve the contact surface between the two phases and favour the phases interaction, nitrogen was used as a diffusor, thus realizing in set-up III a better mixing of the two phases (Figure 1, III).

By monitoring the transformations performed with the above-described different set-ups, it was observed that both the diastereoselection and the enantioselectivity were constant during the reaction time (Table 3). With set up I (Table 3, entries 1–5), after 20 h, a 39% conversion was reached, while full conversion was obtained after 48 h of reaction. Remarkably, high ee values for the *syn* adduct were observed (up to 94% ee), unfortunately, with a low diastereoisomeric ratio (dr). Using set-up II (Table 3, entries 6 and 7), after 24 h, the conversion was still very low (35%) and the ee for the *syn* aldol was up to 90%, the complete conversion was achieved after 48 h. Interestingly, the analysis of the mass of the crude mixture showed that a part of the product was trapped into the DES phase. In order to quantitatively collect the aldol adduct, the DES was diluted with 1 mL of water and extracted five times with 2 mL of ethyl acetate. Using this procedure, all the aldol adduct was completely recovered.

In the set-up III (Table 3, entries 8–11) the presence of a more efficient phase mixing led to a faster conversion. After only 5 h (Table 3, entry 8), 26% conversion was observed, with interesting diastereoselection and high enantioselection (up to 92% for the *syn* adduct). After 48 h, the aldehyde was almost quantitatively converted into the desired aldol product, with high enantioselectivity for both the *syn (*up to 92%) and the *anti* (up to 90%) isomers.

Having identified the system III as the best experimental set-up, the general scope was briefly investigated by running the reaction with a few different aldehydes and comparing the activities

Table 3: Three different set-ups for the aldol reaction in continuo.

Entry	Set-up	Time (h)	Conv. (%)[a]	*anti:syn*[a]	ee% (*anti/syn*)[b]
1	I	20	39	59:41	70/94
2	I	24	47	58:42	68/92
3	I	40	87	55:45	79/92
4	I	48	99	53:47	76/88
5	I	wash[c]	99	52:48	70/84
6	II	24	35	49:51	78/90
7	II	48	96	64:36	84/83
8	III	5	26	62:38	86/92
9	III	24	48	63:37	90/91
10	III	48	90	64:36	84/85
11	III	wash[c]	91	67:33	84/85

[a]Conversion and dr were evaluated after removing cyclohexanone from samples taken at indicated reaction times; [b]ee was evaluated by HPLC on chiral stationary phase. [c]in order to wash the pump 2 mL of cyclohexanone were used.

of DES mixtures A and B in the reactions performed in continuo (Scheme 2).

In the case of 4-nitrobenzaldeyde, the use of DES B (a ternary mixture of ChCl, urea and water, 1:2:1.5 ratio) led to impressive results, both in reaction rate and stereoselectivity, compared to the reaction run in DES A (Table 4, entries 1–4). The reaction proceeded completely in only 15 h, and afforded a clean product (aldol **1**, Scheme 2) that was easily isolated by evaporation of excess cyclohexanone, with high *anti*-diastereoselectivity (up to 90:10), and enantioselectivity (up to 92%) for the major *anti* isomer.

By performing the reaction with 4-chlorobenzaldehyde in DES A (entries 5 and 6, Table 4), the desired aldol product **2** was obtained in 99% yield after only 24 h, with up to 73% enantioselectivity for the *anti* isomer. Notably, using DES B (Table 4, entries 7 and 8) a high *anti* diastereoselectivity (up to 88:12) jointly with a very high ee for the major isomer (up to 88% ee) was detected. It is worth mentioning that when working in DES A, the aldol adduct **2** was partially retained in the DES phase and an extraction with ethyl acetate was necessary to quantita-

tively recover the product. However, as for the reaction in DES B, the whole aldol product was recovered simply by evaporating the organic phase (distilling off the excess of cyclohexanone; for experimental details see Supporting Information File 1).

Analogous results were obtained in the reaction with 4-bromobenzaldehyde. In DES B, the aldol product **3** was isolated in higher yield and stereoselectivity than in DES A (Table 4, entries 9–12; 93% ee for the major *anti* isomer). While the reaction with benzaldehyde led to poor results, the conversion of 2-nitrobenzaldehyde in the expected aldol adduct **5** proceeded in moderate yield (51% after 24 h), but with a remarkable *anti*-diastereoselectivity (93:7) and enantioselectivity (up to 97%).

The different stereoselectivities of the reaction observed in different DES phases could be related to the creation of different tridimensional networks between DES and L-proline, and thus of different chiral reaction environments possibly affecting the stereochemistry of the intermediate species involved in the catalytic cycle [41]. The equilibrating nature of the aldol reaction
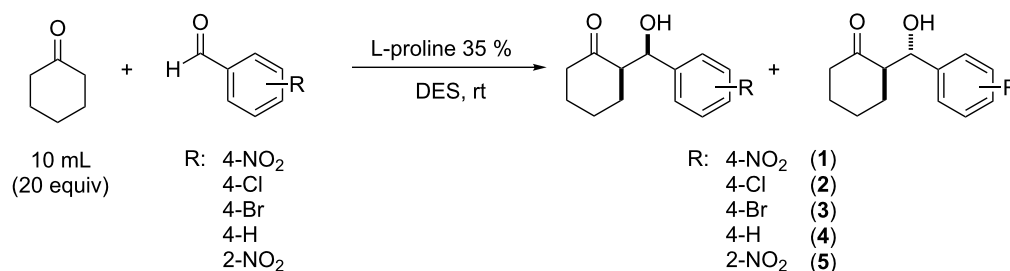
Scheme 2: Aldol reaction under continuous flow conditions in DESs.

Table 4: In continuo aldol reactions of different aldehydes in DES A and DES B.

Entry	DES	Aldol	R	Time (h)	Conv. (%)[a]	*anti:syn*[a]	ee % (*anti/syn*)[b]
1	A	**1**	4-NO$_2$	5	26	62:38	86/92
2	A	**1**	4-NO$_2$	20	48	63:37	90/91
3	B	**1**	4-NO$_2$	5	73	85:15	92/70
4	B	**1**	4-NO$_2$	15	99	90:10	90/70
5	A	**2**	4-Cl	3	13	71:29	73/78
6[c]	A	**2**	4-Cl	24	99	57:43	73/78
7	B	**2**	4-Cl	3	50	88:12	88/73
8	B	**2**	4-Cl	24	91	80:20	88/77
9	A	**3**	4-Br	24	67	65:35	81/70
10	A	**3**	4-Br	42	99	65:35	80/70
11	B	**3**	4-Br	3	10	70:30	91/85
12	B	**3**	4-Br	24	75	70:30	93/86
13	B	**4**	H	42	20	90:10	87/64
14	B	**5**	2-NO$_2$	3	9	90:10	95/50
15	B	**5**	2-NO$_2$	24	51	93:7	97/52

[a]Conversion and dr were evaluated after removing cyclohexanone from samples taken at indicated reaction times; [b]ee was evaluated using an HPLC with a chiral stationary phase; [c]in this case, it was necessary to use 10 mL of EtOAc to quantitatively recover the aldol adduct (Supporting Information File 1).

and the influence of such reversibility on its stereochemical outcome has recently been studied [42]. It has also been reported that the use of additives may have a dramatic influence on the diastereoselectivity and the enantioselectivity in proline-catalyzed aldol transformations [43].

Typically, reactions run in DES mixtures lead to a very clean crude mixture. The recovery of the final aldol adduct can be, indeed, achieved using a reduced quantity of cyclohexanone (12 mL for 1.3 grams of crude aldol), that could be recovered by distillation and reused in new reactions (for experimental details on the product recovery, mass balance and ^{1}H NMR spectra of the crude mixture see Supporting Information File 1).

Finally, we also performed preliminary recycling experiments using two different DESs and set-up III. DES mixtures A or B (1.5 mL), containing L-proline (0.35 equiv, 195 mg), previously used for 48 h in the aldol reaction of cyclohexanone with 4-nitrobenzaldehyde, were recycled in the same transformation. At the end of the reaction, the pump was washed with 3 mL of cyclohexanone, in order to recover the product present in the pump system, then the supernatant (cyclohexanone and aldol product) was separated from the DES phase, containing the catalyst, and analyzed. To the DES phase, new reagents (cyclohexanone and aldehyde) were added and the reaction was started again. While the catalytic system in DES A showed a lower activity, thus affording the product in a significant lower yield, the L-proline/DES B system afforded results comparable to the first run, both in terms of chemical yield and stereoselec-

tivity (93% yield, 92% ee for the major *anti* isomer; see Table S2 in Supporting Information File 1).

Conclusion

In conclusion, the possibility of a continuous, organocatalyzed, stereoselective process in DES was, for the first time, studied and successfully developed. Using different experimental setups, it was possible to realize efficient proline-catalysed cross-aldol reactions in continuo with high yield (99%), *anti*-stereoselectivity, and enantioselectivity (up to 97% ee). Moreover, using two different DES mixtures, the diastereoselection of the process could be tuned, to obtain both the *syn-* and the *anti*-isomer with very high ee values working under different experimental conditions.

DESs were successfully employed as reaction media for continuous production of enantioenriched aldol products, and the excess of cyclohexanone could be recovered and reused. It is worth noting that the reaction can be run and the product isolated without the use of any organic solvent by a proper choice of DES components. The dramatic influence of the reaction media, both on the reaction rate and the stereoselectivity of the process, is consistent with an unprecedented influence of 3D DES architecture on the reactivity of the different species involved in the catalytic cycle, even when using an apparently simple organocatalyst such as L-proline. These observations have important implications in the future design of chiral catalysts, thereby opening the floodgates to new intriguing opportunities for organocatalysis in unconventional reaction media.

Supporting Information

Supporting Information File 1
Experimental set-up and general procedures for the continuous reactions and in batch reactions; product characterization.
[http://www.beilstein-journals.org/bjoc/content/supplementary/1860-5397-12-258-S1.pdf]

Acknowledgements

References

1. Mahrwald, R. *Modern Aldol Reactions;* Wiley-VCH: Weinheim, Germany, 2004; Vol. 1 and 2. doi:10.1002/9783527619566
2. Berkessel, A.; Gröger, H. *Asymmetric Organocatalysis;* Wiley-VCH: Weinheim, Germany, 2005. doi:10.1002/3527604677
3. List, B.; Lerner, R. A.; Barbas, C. F., III. *J. Am. Chem. Soc.* **2000,** *122,* 2395–2396. doi:10.1021/ja994280y
4. Liu, X.; Lin, L.; Feng, X. *Chem. Commun.* **2009,** 6145–6158. doi:10.1039/b913411e
5. Orlandi, M.; Benaglia, M.; Raimondi, L.; Celentano, G. *Eur. J. Org. Chem.* **2013,** 2346–2354. doi:10.1002/ejoc.201201643
6. Guizzetti, S.; Benaglia, M.; Pignataro, L.; Puglisi, A. *Tetrahedron: Asymmetry* **2006,** *17,* 2754–2760. doi:10.1016/j.tetasy.2006.10.018
7. Cho, E.; Kim, T. H. *Tetrahedron Lett.* **2014,** *55,* 6470–6473. doi:10.1016/j.tetlet.2014.10.009
8. Karmakar, A.; Maji, T.; Wittmann, S.; Reiser, O. *Chem. – Eur. J.* **2011,** *17,* 11024–11029. doi:10.1002/chem.201101299
9. Opalka, S. M.; Steinbacher, J. L.; Lambiris, B. A.; McQuade, D. T. *J. Org. Chem.* **2011,** *76,* 6503–6517. doi:10.1021/jo200838v
10. El-Hamdouni, N.; Companyó, X.; Rios, R.; Moyano, A. *Chem. – Eur. J.* **2010,** *16,* 1142–1148. doi:10.1002/chem.200902678
11. Reis, O.; Eymur, S.; Reis, B.; Demir, A. S. *Chem. Commun.* **2009,** 1088–1090. doi:10.1039/b817474a
12. Mandal, T.; Zhao, C.-G. *Angew. Chem., Int. Ed.* **2008,** *47,* 7714–7717. doi:10.1002/anie.200803236
13. Clarke, M. L.; Fuentes, J. A. *Angew. Chem., Int. Ed.* **2007,** *46,* 930–933. doi:10.1002/anie.200602912
14. Rodriguez, B.; Bruckmann, A.; Bolm, C. *Chem. – Eur. J.* **2007,** *13,* 4710–4722. doi:10.1002/chem.200700188
    See for ball mill approach.
15. Clegg, W.; Harrington, R. W.; North, M.; Pizzato, F.; Villuendas, P. *Tetrahedron: Asymmetry* **2010,** *21,* 1262–1271. doi:10.1016/j.tetasy.2010.03.051
    See for the use of carbamates.
16. Mase, N.; Nakai, Y.; Ohara, N.; Yoda, H.; Takabe, K.; Tanaka, F.; Barbas, C. F., III. *J. Am. Chem. Soc.* **2006,** *128,* 734–735. doi:10.1021/ja0573312
    See for aldol reaction on water.
17. Hayashi, Y.; Sumiya, T.; Takahashi, J.; Gotoh, H.; Urushima, T.; Shoji, M. *Angew. Chem., Int. Ed.* **2006,** *45,* 958–961. doi:10.1002/anie.200502488
18. Guizzetti, S.; Benaglia, M.; Raimondi, L.; Celentano, G. *Org. Lett.* **2007,** *9,* 1247–1250. doi:10.1021/ol070002p
19. Mlynarski, J.; Bas, S. *Chem. Soc. Rev.* **2014,** *43,* 577–587. doi:10.1039/C3CS60202H
    See for a recent review on organocatalyzed reactions in/on water.
20. Ilgen, F.; König, B. *Green Chem.* **2009,** *11,* 848–854. doi:10.1039/B816551C
    See for pioneer studies of L-proline in DESs as catalysts of Diels-Alder reactions.
21. Müller, C. R.; Meiners, I.; Domínguez de María, P. *RSC Adv.* **2014,** *4,* 46097–46101. doi:10.1039/C4RA09307K
    See for proline-promoted aldol reaction.
22. Martínez, R.; Berbegal, L.; Guillena, G.; Ramón, D. J. *Green Chem.* **2016,** *18,* 1724–1730. doi:10.1039/C5GC02526E
23. Massolo, E.; Palmieri, S.; Benaglia, M.; Capriati, V.; Perna, F. M. *Green Chem.* **2016,** *18,* 792–797. doi:10.1039/C5GC01855B
    See for primary amine-catalysed transformations in DESs.
24. Kondo, K.; Yamano, T.; Takemoto, K. *Makromol. Chem.* **1985,** *186,* 1781–1785. doi:10.1002/macp.1985.021860906
    See for selected studies on proline immobilization, on polystyrene.
25. Sakthivel, K.; Notz, W.; Bui, T.; Barbas, C. F., III. *J. Am. Chem. Soc.* **2001,** *123,* 5260–5267. doi:10.1021/ja010037z
    See for selected studies on proline immobilization, on silica.
26. Benaglia, M.; Celentano, G.; Cozzi, F. *Adv. Synth. Catal.* **2001,** *343,* 171–173. doi:10.1002/1615-4169(20010226)343:2<171::AID-ADSC171>3.3.CO;2-V
    See for PEG-supported proline.
27. Calderón, F.; Fernández, R.; Sánchez, F.; Fernández-Mayoralas, A. *Adv. Synth. Catal.* **2005,** *347,* 1395–1403. doi:10.1002/adsc.200505058
    See for mesoporous silica.
28. Smith, E. L.; Abbott, A. P.; Ryder, K. S. *Chem. Rev.* **2014,** *114,* 11060–11082. doi:10.1021/cr300162p
29. Liu, P.; Hao, J.-W.; Mo, L.-P.; Zhang, Z.-H. *RSC Adv.* **2015,** *5,* 48675–48704. doi:10.1039/C5RA05746A
30. Ruß, C.; König, B. *Green Chem.* **2012,** *14,* 2969–2982. doi:10.1039/c2gc36005e
31. Gu, Y.; Jérôme, F. *Chem. Soc. Rev.* **2013,** *42,* 9550–9570. doi:10.1039/c3cs60241a
32. Francisco, M.; van den Bruinhorst, A.; Kroon, M. C. *Angew. Chem., Int. Ed.* **2013,** *52,* 3074–3085. doi:10.1002/anie.201207548
33. Alonso, D. A.; Baeza, A.; Chinchilla, R.; Guillena, G.; Pastor, I. M.; Ramón, D. J. *Eur. J. Org. Chem.* **2016,** 612–632. doi:10.1002/ejoc.201501197
34. Mallardo, V.; Rizzi, R.; Sassone, F. C.; Mansueto, R.; Perna, F. M.; Salomone, A.; Capriati, V. *Chem. Commun.* **2014,** *50,* 8655–8658. doi:10.1039/C4CC03149K
35. Sassone, F. C.; Perna, F. M.; Salomone, M.; Florio, S.; Capriati, V. *Chem. Commun.* **2015,** *51,* 9459–9462. doi:10.1039/C5CC02884A
36. García-Álvarez, J.; Hevia, E.; Capriati, V. *Eur. J. Org. Chem.* **2015,** 6779–6799. doi:10.1002/ejoc.201500757

37. Cicco, L.; Sblendorio, S.; Mansueto, R.; Perna, F. M.; Salomone, M.; Florio, S.; Capriati, V. *Chem. Sci.* **2016,** *7,* 1192–1199. doi:10.1039/C5SC03436A

38. Mancuso, R.; Maner, A.; Cicco, L.; Perna, F. M.; Capriati, V.; Gabriele, B. *Tetrahedron* **2016,** *72,* 4239–4244. doi:10.1016/j.tet.2016.05.062

39. Capua, M.; Perrone, S.; Perna, F. M.; Vitale, P.; Troisi, L.; Salomone, A.; Capriati, V. *Molecules* **2016,** *21,* 924. doi:10.3390/molecules21070924

40. García-Álvarez, J. *Deep Eutectic Solvents and Their Applications as New Green and Biorenewable Reaction Media*. In *Use, Health, and Environment,* 2nd ed.; Wypych, G., Ed.; Handbook of Solvents, Vol. 2; ChemTec Publishing: Toronto, 2014.

41. Hammond, O. S.; Bowron, D. T.; Edler, K. J. *Green Chem.* **2016,** *18,* 2736–2744. doi:10.1039/C5GC02914G
See for the first 3D liquid-phase structure of a ChCl-based DES.

42. Orlandi, M.; Ceotto, M.; Benaglia, M. *Chem. Sci.* **2016,** *7,* 5421–5427. doi:10.1039/C6SC01328G

43. Martínez-Castañeda, A.; Rodríguez-Solla, H.; Concellón, C.; del Amo, V. *J. Org. Chem.* **2012,** *77,* 10375–10381. doi:10.1021/jo3020352

Selective synthesis of thioethers in the presence of a transition-metal-free solid Lewis acid

Federica Santoro, Matteo Mariani, Federica Zaccheria, Rinaldo Psaro
and Nicoletta Ravasio[*]

Abstract

The synthesis of thioethers starting from alcohols and thiols in the presence of amorphous solid acid catalysts is reported. A silica alumina catalyst with a very low content in alumina gave excellent results in terms of both activity and selectivity also under solvent-free conditions. The reaction rate follows the electron density of the carbinol atom in the substrate alcohol and yields up to 99% and can be obtained for a wide range of substrates under mild reaction conditions.

Introduction

The need for more sustainable processes in the fine chemical industry is growing continuously. An optimal use of resources, both energy and starting materials, and a consequent waste reduction can be recognized as important factors for environmental protection. In this context organic synthesis over heterogeneous catalysts instead of homogeneous ones or without employing any organic solvents is of paramount interest [1,2]. In particular, metal-free coupling reactions are a very important field of research as traditional coupling methods, although they proved effective in industrial applications, generate harmful metal waste and many byproducts [3].

Thioethers are important building blocks for the synthesis of antibacterial and antifungal agents [4,5] and as antioxidants in polymers [6]. They are typically synthesized through the condensation of a thiol with organic halides under strong basic conditions [7-9], but due to the high toxicity of alkyl halides the introduction of new methods of access to this kind of materials is desirable. The ideal reaction from the green chemistry point of view would be the direct substitution of alcohols (that are also available at low cost) with thiols. In this case the only byproduct will be water. However, due to the lack of a good leaving group the use of an acid catalyst is mandatory. Both

Brønsted and Lewis acids can be used. The former ones, such as free or polymer bound *p*-toluenesulfonic acid, promote the formation of significant amounts of by-products and can give yields in the range of 80% only for propargylic, allylic or benzylic alcohols [10-14]. As far as Lewis acids are concerned $ZrCl_4$ [15] dispersed on silica is active in promoting the substitution of adamantanol, cinnamyl and benzyl alcohols with thiols whereupon significative amounts of Zr salt are required; whereas Wu and Han have shown that $Ga(OTf)_3$ is an effective catalyst for the substitution of a wide range of benzylic and allylic alcohols with phosphorothioic acid and with a wide range of alcohols with various sulfur nucleophiles in an effective way [16]. On the contrary $SmCl_3$ promotes the formation of thioethers only from 2-cyclohexen-1-ol and geraniol with thiophenol [17] while the use of cationic diruthenium complexes is limited to the displacement of propargyl alcohols with thiols [18].

Heterogeneous systems are very rare. Corma and Sabater used a heterogeneous system based on palladium on magnesium oxide under borrowing hydrogen conditions [19]. The reaction has to be carried out at 180 °C under N_2 in trifluorotoluene with a maximum yield of 83% and it can be used only for primary benzylic alcohols. On the contrary Ni nanoparticles act as chemoselective catalysts at room temperature [20]. 1,3,5-Triazo-2,4,6-triphosphorine-2,2,4,4,6,6-hexachloride (TAPC) allows the efficient preparation of thioethers from different thiols and benzylic alcohols under solvent-free conditions in excellent yields [21].

We already reported on the use of amorphous solid acid catalysts in organic synthesis. These solids are formed by dispersing a small amount of an inorganic oxide with Lewis acid nature onto the surface of silica [22]. In particular we found that 1-(4-methoxyphenyl)ethanol promptly reacts with 2-PrOH at 80 °C to give the asymmetric ether in 92% yield in the presence of a silica alumina mixed oxide [23]. This prompted us to investigate the reactivity of aromatic alcohols with thiols under the same conditions. Here we wish to report that excellent yields can be obtained in the presence of an amorphous solid catalyst under solvent-free conditions.

Results and Discussion

In order to test our hypothesis we carried out the reaction of 1-(4-methoxyphenyl)ethanol (**1a**) and benzyl mercaptan (**2a**) in the presence of different solid acids, namely 13% Al_2O_3 on silica (SiAl 13), 4.7% ZrO_2 on silica (SiZr 4.7), 2.3% TiO_2 on silica (SiTi 2.3) and 0.6% Al_2O_3 on silica (SiAl 0.6) whose textural properties are summed up in Supporting Information File 1, Table S1. Results are reported in Table 1.

It is worth underlining that under these experimental conditions the reaction does not proceed in the absence of a catalyst (Table 1, entry 1). Only a very low conversion was obtained

Table 1: Thioethers synthesis in solvent with different catalysts[a].

Entry	Catalyst	N_{OH}/nm^2	*t* (h)	Conv. (%)	**3a** (%)[b]	**4a** (%)[b]	**5a** (%)[b]	Dehydr. (%)[b,c]
1	No cat.	–	2	6.3	25.0	34.4	18.7	21.9
2	SiAl 13	11.5	0.5	15.8	66.9	–	25.7	7.4
			2	67.6	94.3	–	3.0	2.7
3	SiZr 4.7	7.35	0.5	47.4	93.5	–	6.5	–
			2	86.1	98.7	–	0.8	0.5
4	SiTi 2.3	4.85	0.5	71.2	92.2	0.1	3.0	4.7
			2	93.4	95.5	0.1	0.1	4.3
5	SiAl 0.6	3.55	0.5	93.4	98.8	–	1.0	0.2
			2	>99	99.9	–	–	0.1

[a]Reaction conditions: cat. = 100 mg, cat./ROH = 1:1 (w/w), ROH/RSH = 1:1 (mol/mol), toluene (8 mL), N_2 (1 atm), 80 °C (oil bath temp.), stirring (1000 rpm); reaction mixtures were analyzed by GC–MS (5% phenylmethyl polysiloxane capillary column, length 30 m, injection *T* = 60 °C), and by ^{1}H NMR and ^{13}C NMR spectroscopy; conversion was calculated with respect to the thiol. [b]percentage composition of reaction products. [c]Corresponding substituted styrene derived from alcohol dehydration.

with statistical product distribution. On the contrary all the four solid catalysts were found to be active in this reaction (Table 1, entries 2–5). This is in agreement with the acidic character of these materials, often shown by our group. In particular we reported on the relevant activity and robustness of SiZr 4.7 in the esterification of fatty acids with methanol [24] or with polyols [25,26].

However, significant differences were found among the four solids. Both activity and selectivity depend on the hydrophilic character of the solid, here represented by the number of hydroxy groups per surface area unit (N_{OH}/nm^2). The lower this parameter the higher are both reaction rate and selectivity.

This is particularly evident from the results obtained after 0.5 h reaction. When the surface hydroxy group number is higher as in SiAl 13, not only the activity but also the selectivity is very low (Table 1, entry 2). This may well be due to the hydrophilic surface preferentially attracting the alcohol molecules. Thus, at the beginning we can observe the formation of the symmetrical ether formed through reaction of two alcohol molecules, beside the desired product. For longer reaction times the selectivity increases due to conversion of the ether initially formed as it is suggested from data summed up in Table 1.

In particular a catalyst with a very low loading of alumina on silica and a very low number of surface hydroxy groups gave quantitatively the desired product in 2 hours (Table 1, entry 5).

The activity of this solid has to be ascribed to the presence of well dispersed Lewis acid sites on the surface, as put in evidence from the FTIR spectrum of adsorbed pyridine where the band due to Lewis acid sites is detectable (1456 cm^{-1}). This excellent performance prompted us to investigate the substrate scope of this reaction in the presence of SiAl 0.6. Figure 1 and Figure 2 report alcohols and thiols used as reagents while Figure 3 lists the products obtained.

A preliminary study on the substrate scope of this reaction summed up in Supporting Information File 1, Table S2 showed that only benzylic alcohols can be transformed under these conditions, particularly secondary ones, whereas secondary cyclic and acyclic aliphatic alcohols were found to be totally unreactive. As far as the thiol is concerned both aromatic and cyclic thiols gave excellent results.

The attempt to carry out the reaction in a solvent-free mode gave surprising results. The reaction was slower but selectivity was still very high. Results are reported in Table 2. Aromatic and aliphatic thiols gave excellent results in the reaction with **1a** whereas the structure of the alcohol had a more significant impact on the reactivity (Table 2, entries 1–7). Thus, **1b** was much less reactive than **1a** and to reach a 94% yield the temperature had to be raised to 110 °C. Moreover the reaction at the beginning gave almost equimolecular amounts of the thioether and the ether, although during time the ether converted into the desired product (Table 2, entry 9).

Figure 1: Overview of the structures of the alcohols **1a–i** used in the present work.

Figure 2: Structures of thiols **2a–f** used in the present work.
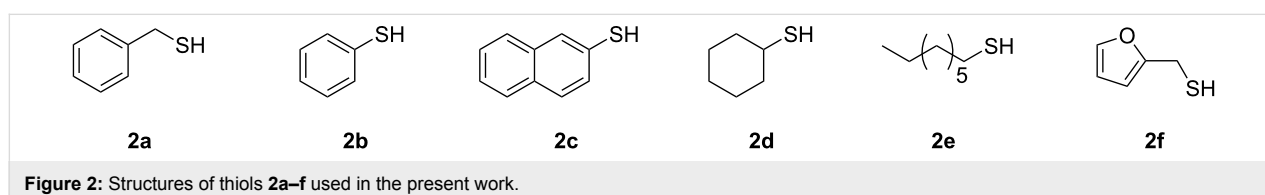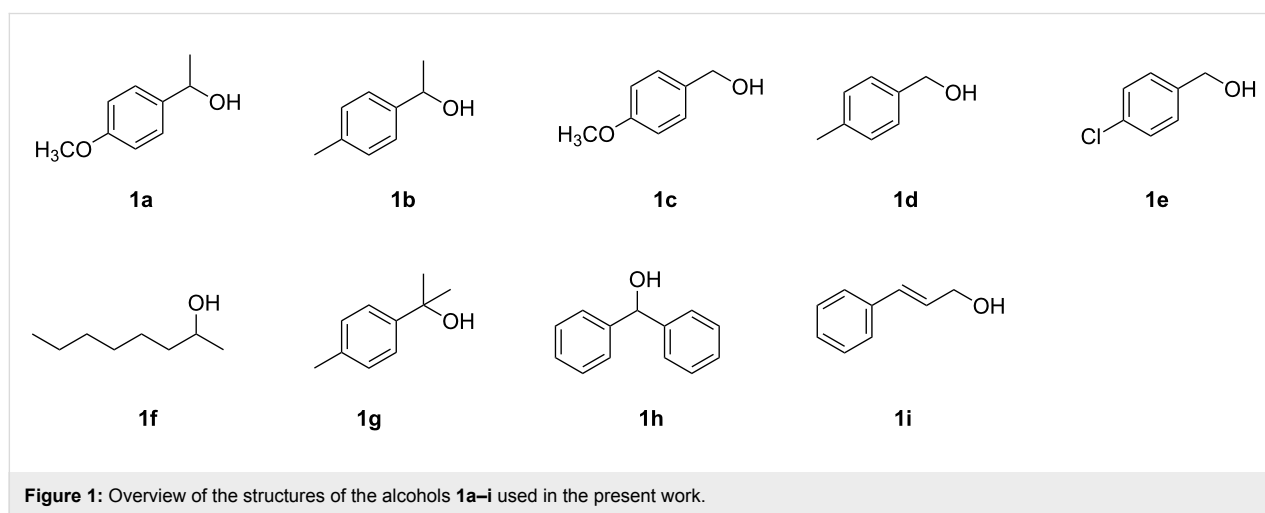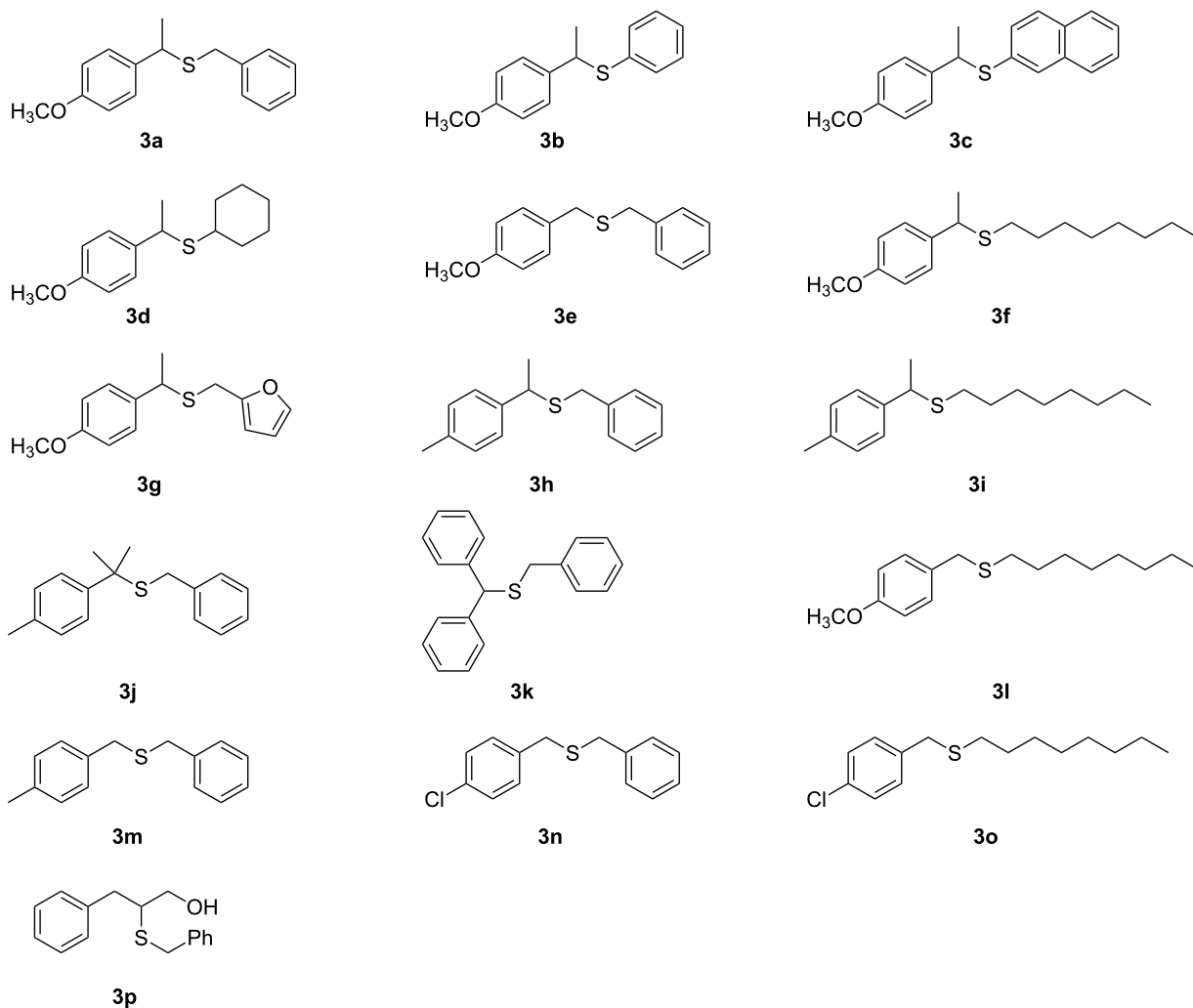
Figure 3: Structures of thioethers **3a–p** synthesized.

The higher reactivity of the substrate bearing the more electron donating group suggests that the reaction takes place through a nucleophilic substitution mechanism: the higher the electronic density on the carbinol C atom, the higher the reaction rate. When the electronic density is somewhat lower, competitive formation of the ether occurs but subsequent nucleophilic addition of the thiol to the ether restores a very high selectivity. A test carried out by reacting presynthetized ether 4,4'-(oxybis(ethane-1,1-diyl))bis(methylbenzene) (**5b**) with benzyl mercaptan (**2a**) showed indeed that the thioether is formed easily starting from these two molecules under the reaction conditions reported (Figure 4).

The dependence of the reaction rate on the stability of the intermediate carbocation is even more evident in the series of primary benzylic alcohols. Among them only the *p*-methoxy-substituted compound **1c** shows high activity. In particular, with thiol

2e some ether was formed that during time is converted into the product (Table 2, entry 15 and Figure 5).

On the other hand highly hindered alcohol **1g** with a tertiary carbinol atom gave a very fast and selective reaction (Table 2, entry 11).

Thus we can conclude that the reaction rate follows the carbocation stability according to an SN1 mechanism. To confirm this hypothesis the reaction of optically active (*R*)-1-phenylethanol gave a completely racemic compound (Scheme 1).

Unfortunately allylic alcohols gave unreproducible results. However, in the case of cinnamyl alcohol (**1i**) we could obtain a fairly good selectivity to the product of the thiol–ene reaction **3p** (Scheme 2).

Table 2: Synthesis of thioethers from different alcohols and thiols promoted by SiAl 0.6 without solvent[a].

Entry	1a–h	2a–f	T (°C)[b]	t (h)	Conv. (%)	3a–o[c] (%)	4a–f[c] (%)	5a–h[c] (%)
1	**1a**	**2a**				**3a**	**4a**	**5a**
			60	0.5	60	75.0	5.5	12.3
				1	97	94.8	1.4	3.8
				2	>99	99.0	0.6	0.4
2	**1a**	**2b**				**3b**	**4b**	**5a**
			60	0.5	74	80.2	3.5	12.8
				1	90	88.3	1.7	9.9
				2	98	98.9	1.1	–
3	**1a**	**2c**				**3c**	**4c**	**5a**
			60	0.5	57	63.5	20.7	13.9
				2	82	76.3	4.8	15.5
				5	>99	99.4	0.6	–
4	**1a**	**2c**				**3c**	**4c**	**5a**
			90	0.5	>99	98.7	1.3	–
5	**1a**	**2d**				**3d**	**4d**	**5a**
			60	0.5	56	56.6	1.4	32.1
				3	99	99.6	0.4	–
6	**1a**	**2e**				**3f**	**4e**	**5a**
			60	2	82	85.1	1.7	13.2
				4.5	>99	98.9	1.1	–
7	**1a**	**2f**				**3g**	**4f**	**5a**
			60	1	85	68.4	–	31.6
				3	99	86.9	–	1.5
8	**1b**	**2a**				**3h**	**4a**	**5b**
			60	2	3	29.4	32.9	37.8
				20	16	46.1	48.3	5.6
9	**1b**	**2a**				**3h**	**4a**	**5b**
			110	0.5	74	55.0	–	45.0
				6	99	74.4	1.0	24.6
				12	>99	86.8	1.4	12.1
				20	>99	95.2	1.5	3.3
10	**1b**	**2e**				**3i**	**4e**	**5b**
			110	0.5	89	72.2	2.1	25.7
				2	>99	93.1	2.2	4.7
11	**1g**	**2a**				**3j**	**4a**	**5g**
			90	0.5	>99	94.4	–	0.9

Table 2: Synthesis of thioethers from different alcohols and thiols promoted by SiAl 0.6 without solvent[a]. (continued)

Entry	1	2	T	t	conv.	3	4	5
12	**1h**	**2a**				**3k**	**4a**	**5h**
			60	0.5	14	89.5	10.5	–
				2	40	87.2	3.5	9.3
				20	95	91.3	0.7	8.0
13	**1c**	**2a**				**3e**	**4a**	**5c**
			90	6	98	92.8	1.0	6.2
14	**1c**	**2a**				**3e**	**4a**	**5c**
			110	0.5	99	93.8	1.2	5.0
				1	>99	97.7	1.1	1.2
15	**1c**	**2e**				**3l**	**4e**	**5c**
			90	0.5	57	41.9	1.8	52.8
				4	96	86.7	1.5	8.5
16	**1c**	**2e**				**3l**	**4e**	**5c**
			110	0.5	87	78	1	20
				1	97	91.9	1.2	5.6
17	**1d**	**2a**				**3m**	**4a**	**5d**
			90	6	2	–	>99	–
18	**1d**	**2a**				**3m**	**4a**	**5d**
			110	6	9	20.2	18.0	46.1
19	**1e**	**2a**				**3n**	**4a**	**5e**
			110	20	15	3.6	–	61.8
20	**1e**	**2e**				**3o**	**4e**	**5e**
			110	12	52	4.8	50.2	–
21	**1f**	**2e**				**3w**	**4e**	**5f**
			110	20	8	79.9	20.1	–

[a]Reaction conditions: cat. = 10 mg cat./ROH = 1:10 (w/w), ROH/RSH = 1:1 (mol/mol), no solvent, air, magnetic stirring (1000 rpm); reaction mixtures were analysed by GC–MS (5% phenylmethyl polysiloxane capillary column length 30 m, injection T = 60 °C), and by ^{1}H NMR and ^{13}C NMR spectroscopy; conversion was calculated with respect to the thiol. [b]Oil bath temperature. [c]Percentage composition of reaction products.

The protocol here described is very advantageous from the point of view of Green Chemistry. The direct substitution of hydroxy groups in alcohols is very difficult and generally they have to be converted into better leaving groups, typically halides, before reaction with nucleophiles. This process generates salt waste limiting industrial application. Moreover these compounds are generally toxic. The development of catalytic alternative methods for this reaction is highly sought after. However, the catalytic transformation of thiols is much less developed than that of amines and alcohols. This is due to the fact that transition metal ions are strongly thiophilics, therefore most of metallic catalysts are poisoned by the presence of sulfur compounds. Lanthanide complexes such as Yb(OTf)$_3$ are an excep-

tion [27] but only allylic and propargylic alcohols react under the reported conditions. The alkylation of thiols has also been carried out under flow conditions in the presence of a heterogeneous base in a packed bed reactor but also in this case alkyl halides were used as electrophiles [28].

The reaction we are presenting here takes place in the presence of a solid catalyst starting from the alcohol itself in stoichiometric ratio with the thiol; therefore the only byproduct is water. In some cases conversion and selectivity are so high under solvent-free conditions that at the end the product can be separated from the catalyst and purified without any other work up with an E factor = 0.07 for the reaction of **1a** and **2a**. This is
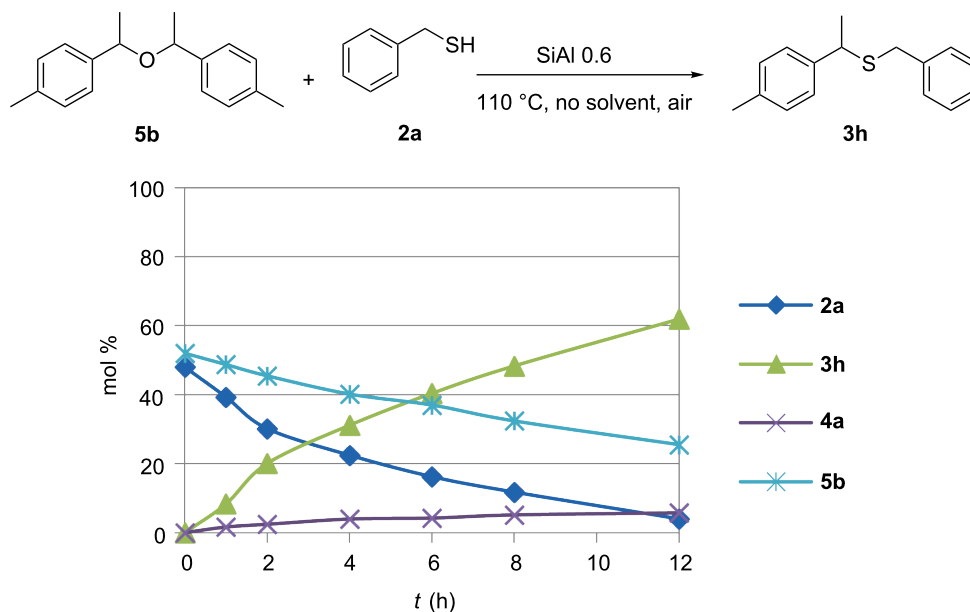
Figure 4: Product distribution during reaction of **5b** and **2a** over a solid acid catalyst.
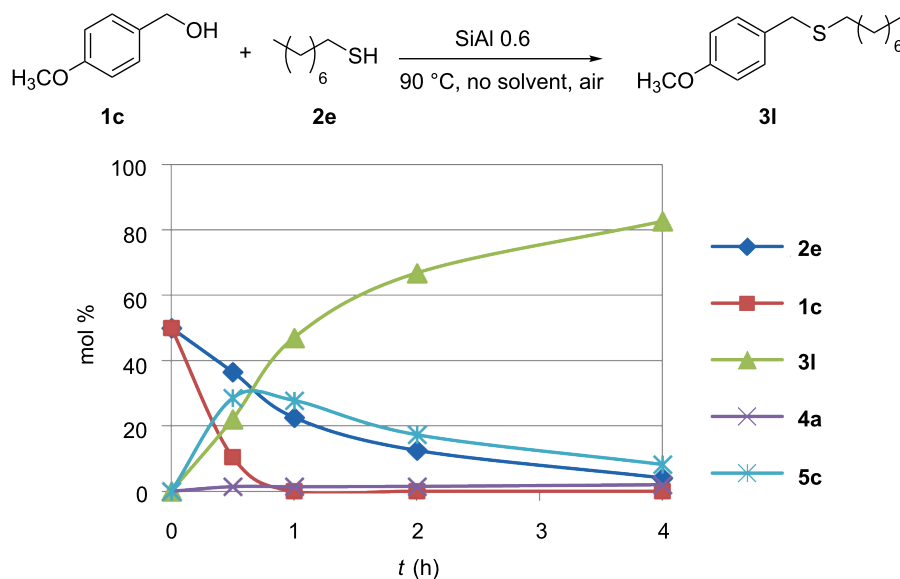
Figure 5: Product distribution during reaction of **1c** and **2e**.

quite different from the case of ZnI$_2$-catalyzed reaction that requires an excess of thiophenol, use of anhydrous CH$_2$Cl$_2$ as solvent, quenching of the catalyst with water, double extraction with dichloromethane, washing with brine, drying over sodium sulfate and evaporation of the solvent before chromatographic purification [29]. The reaction does not need to be carried out under inert atmosphere and moreover, the catalyst can be reused

several times without significant decrease in selectivity and only a little bit in activity (Figure 6).

The substrate scope is also quite wide as other systems only convert propargylic alcohols [30] or benzhydrol and electron-deficient thiols [31] in agreement with the high electrophilicity of these substrates.

Scheme 1: Racemization of (*R*)-1-phenylethanol during the reaction with benzylmercaptan (**2a**) in the presence of SiAl 0.6.

Scheme 2: Reaction of cinnamyl alcohol **1i** and benzylmercaptan (**2a**).

Figure 6: Recyclability test of SiAl 0.6 catalyst in the reaction of **1a** and **2a**.
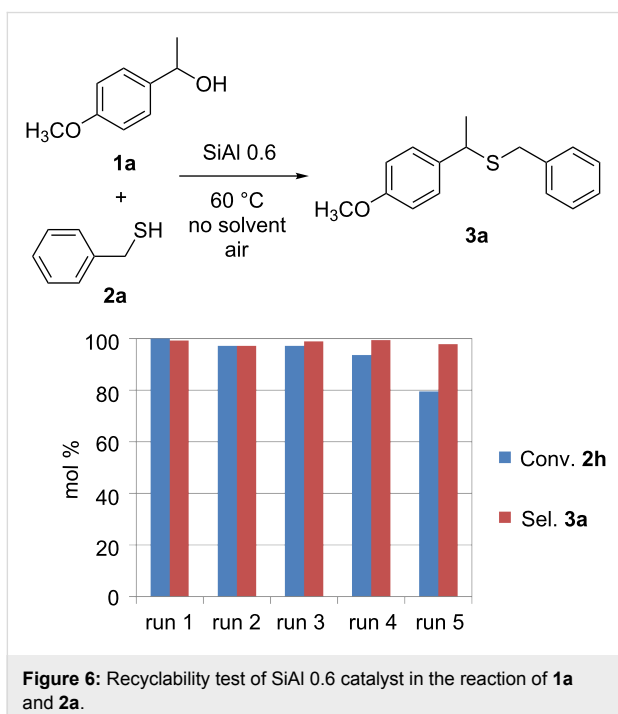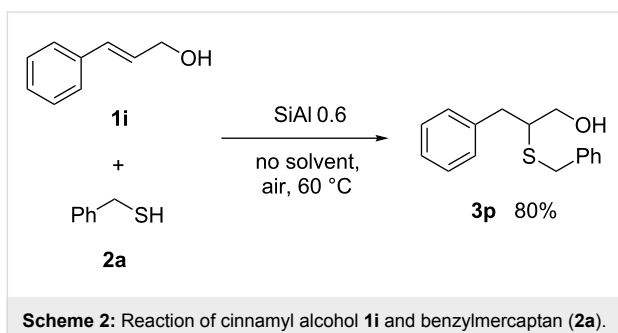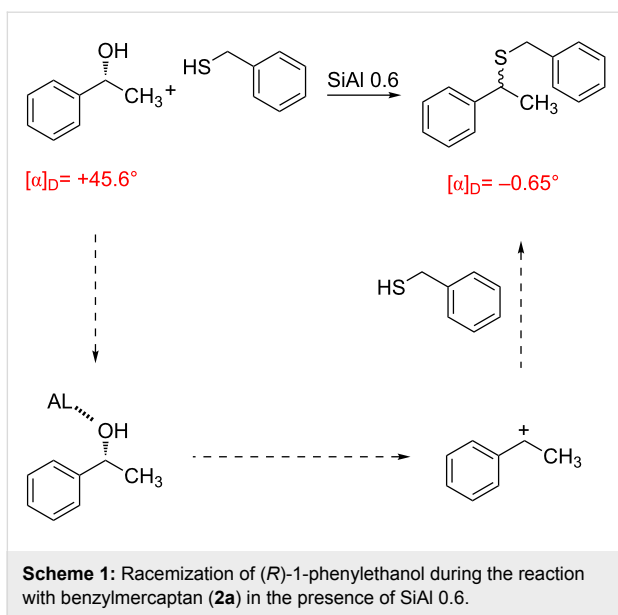
Conclusion

Amorphous solid acid catalysts are very promising materials in the roadmap to green and sustainable organic synthesis. They allow us to set up very selective processes without producing any waste and avoiding the use of toxic substrates or metals. In particular a 0.6% Al_2O_3 on silica, can be conveniently used for the green synthesis of thioethers starting from aromatic alcohols and aromatic or aliphatic thiols. The reaction can be carried out under solvent-free conditions with stoichiometric amounts of the reagents with excellent yield and the catalyst can be reused several times.

Supporting Information

Supporting Information File 1

Experimental, NMR analysis and copies of spectra.
[http://www.beilstein-journals.org/bjoc/content/supplementary/1860-5397-12-259-S1.pdf]

Acknowledgements

References

1. Luque, R.; Colmenares, J. C., Eds. *An Introduction to Green Chemistry Methods;* Future Science Ltd, 2013.
2. Sharma, S. K.; Mudhoo, A., Eds. *Green Chemistry for Environmental Sustainability;* CRC Press, 2010.
3. Arancon, R. A. D.; Lin, C. S. K.; Vargas, C.; Luque, R. *Org. Biomol. Chem.* **2014,** *12,* 10–35. doi:10.1039/C3OB41768A
4. Cremlyn, R. J. *An Introduction to Organosulfur Chemistry;* Wiley and Sons: New York, 1996.
5. McReynolds, M. D.; Doughtery, J. M.; Hanson, P. R. *Chem. Rev.* **2004,** *104,* 2239–2258. doi:10.1021/cr020109k
6. Coran, A. Y. *J. Appl. Polym. Sci.* **2003,** *87,* 24–30. doi:10.1002/app.11659
7. Patai, S. *The Chemistry of the Functional Groups-The Chemistry of the Thiol Group;* Wiley: London, 1974; p. 669.
8. Smith, M. B.; March, J. *March's Advanced Organic Chemistry,* 6th ed.; Wiley: Hoboken, New Jersey, 2007.
9. Greene, T. W.; Wuts, P. G. M. *Protective Groups in Organic Synthesis,* 3rd ed.; John Wiley & Son: New York, 1999.
10. Sanz, R.; Martínez, A.; Miguel, D.; Álvarez-Gutiérrez, J. M.; Rodríguez, F. *Adv. Synth. Catal.* **2006,** *348,* 1841–1845. doi:10.1002/adsc.200606183
11. Zhang, X.; Rao, W.; Chan, P. W. H. *Synlett* **2008,** 2204–2208. doi:10.1055/s-2008-1078254
12. Haynes, R. K.; Katsifis, A. G.; Vonwiller, S. C.; Hambley, T. W. *J. Am. Chem. Soc.* **1988,** *110,* 5423–5433. doi:10.1021/ja00224a030
13. Parker, K. A.; Johnson, W. S. *J. Am. Chem. Soc.* **1974,** *96,* 2556–2563. doi:10.1021/ja00815a039
14. Sneen, R. A.; Kay, P. S. *J. Am. Chem. Soc.* **1972,** *94,* 6983–6989. doi:10.1021/ja00775a020

15. Firouzabadi, H.; Iranpoor, N.; Jafarpour, M. *Tetrahedron Lett.* **2006,** *47,* 93–97. doi:10.1016/j.tetlet.2005.10.137

16. Han, X.; Wu, J. *Org. Lett.* **2010,** *12,* 5780–5782. doi:10.1021/ol102565b

17. Ouertani, M.; Collin, J.; Kagan, H. B. *Tetrahedron* **1985,** *41,* 3689–3693. doi:10.1016/S0040-4020(01)91389-4

18. Inada, Y.; Nishibayashi, Y.; Hidai, M.; Uemura, S. *J. Am. Chem. Soc.* **2002,** *124,* 15172–15173. doi:10.1021/ja027754t

19. Corma, A.; Navas, J.; Ródenas, T.; Sabater, M. J. *Chem. – Eur. J.* **2013,** *19,* 17464–17471. doi:10.1002/chem.201302226

20. Saxena, A.; Kumar, A.; Mozumdar, S. *Appl. Catal., A: Gen.* **2007,** *317,* 210–215. doi:10.1016/j.apcata.2006.10.027

21. Bahrami, K.; Khodaei, M. M.; Khodadoustan, N. *Synlett* **2011,** 2206–2210. doi:10.1055/s-0030-1261206

22. Santoro, F.; Zaccheria, F.; Shaik, N. I.; Ravasio, N. *Top. Catal.* **2012,** *55,* 606–611. doi:10.1007/s11244-012-9838-7

23. Zaccheria, F.; Psaro, R.; Ravasio, N. *Tetrahedron Lett.* **2009,** *50,* 5221–5224. doi:10.1016/j.tetlet.2009.06.123

24. Zaccheria, F.; Brini, S.; Psaro, R.; Scotti, N.; Ravasio, N. *ChemSusChem* **2009,** *2,* 535–537. doi:10.1002/cssc.200900047

25. Zaccheria, F.; Mariani, M.; Psaro, R.; Bondioli, P.; Ravasio, N. *Appl. Catal., B* **2016,** *181,* 581–586. doi:10.1016/j.apcatb.2015.08.032

26. Mariani, M.; Zaccheria, F.; Scotti, N.; Psaro, R.; Ravasio, N. *ChemistrySelect* **2016,** *1,* 2999–3004. doi:10.1002/slct.201600782

27. Huang, W.; Shen, Q.-S.; Wang, J.-L.; Zhou, X.-G. *Chin. J. Chem.* **2008,** *26,* 729–735. doi:10.1002/cjoc.200890136

28. Baker, A.; Graz, M.; Saunders, R.; Evans, G. J. S.; Pitotti, I.; Wirth, T. *J. Flow Chem.* **2015,** *5,* 65–68. doi:10.1556/1846.2015.00009

29. Guindon, Y.; Frenette, R.; Fortin, R.; Rokach, J. *J. Org. Chem.* **1983,** *48,* 1357–1359. doi:10.1021/jo00156a043

30. Zhan, Z.-p.; Yu, J.-l.; Liu, H.-j.; Cui, Y.-y.; Yang, R.-f.; Yang, W.-z.; Li, J.-p. *J. Org. Chem.* **2006,** *71,* 8298–8301. doi:10.1021/jo061234p

31. Hikawa, H.; Toyomoto, M.; Kikkawa, S.; Azumaya, I. *Org. Biomol. Chem.* **2015,** *13,* 11459–11465. doi:10.1039/C5OB01717C

Electron-transfer-initiated benzoin- and Stetter-like reactions in packed-bed reactors for process intensification

Anna Zaghi, Daniele Ragno, Graziano Di Carmine, Carmela De Risi, Olga Bortolini,
Pier Paolo Giovannini, Giancarlo Fantin and Alessandro Massi[*]

Abstract

A convenient heterogeneous continuous-flow procedure for the polarity reversal of aromatic α-diketones is presented. Propaedeutic batch experiments have been initially performed to select the optimal supported base capable to initiate the two electron-transfer process from the carbamoyl anion of the *N,N*-dimethylformamide (DMF) solvent to the α-diketone and generate the corresponding enediolate active species. After having identified the 2-*tert*-butylimino-2-diethylamino-1,3-dimethylperhydro-1,3,2-diazaphosphorine on polystyrene (PS-BEMP) as the suitable base, packed-bed microreactors (pressure-resistant stainless-steel columns) have been fabricated and operated to accomplish the chemoselective synthesis of aroylated α-hydroxy ketones and 2-benzoyl-1,4-diones (benzoin- and Stetter-like products, respectively) with a good level of efficiency and with a long-term stability of the packing material (up to five days).

Introduction

The polarity reversal (umpolung) of carbonyl compounds by N-heterocyclic carbene (NHC) or cyanide catalysis represents a straightforward strategy for the synthesis of valuable molecules such as, among the many examples, α-hydroxy ketones (benzoin reaction) and 1,4-diketones (Stetter reaction) [1-4]. The synthetic utility of the umpolung methodology has therefore spurred intensive research on process intensification through the heterogeneization of NHC catalysts [5-9] for facilitating the post-reaction phase and improving NHCs' stability towards air and moisture [10,11]. Quite surprisingly, however, implementation of continuos-flow techniques with micro- and meso-reactors is rare in this field [12-17]. Indeed, microreactor technology is today a powerful tool for the fine chemical and pharmaceutical industries facilitating the automation of the production processes with reduced costs and improved safety and sustainability [18-21]. Very recently, Monbaliu and co-workers

described a convenient continuous-flow setup for the generation of common free NHCs under homogeneous conditions and their subsequent utilization in transesterification and amidation processes by the reaction telescoping approach [12]. Similarly, the group of Brown reported on the oxidative esterification and amidation of aldehydes in undivided microfluidic electrolysis cells mediated by homogeneous NHCs [13,14]. On the other hand, heterogeneous catalysis in microstructured flow reactors represents a robust synthetic platform, with benefits over the corresponding batch processes such as catalyst stability, lower degradation of supports, and ease of scale-up with minimal changes to the reaction setup [22-24]. An integrated flow system for the synthesis of biodiesel employing an uninterrupted sequence of two fixed-bed reactors packed with a supported acid for esterification of free fatty acids and with an immobilized imidazolidene catalyst for transesterification has been recently described by Lupton and co-workers [15]. Our group also contributed to this area of research fabricating polystyrene monolithic columns functionalized with thiazolium salt pre-catalysts to perform umpolung racemic processes (benzoin, acyloin, and Stetter reactions) with a good level of efficiency [16]. The asymmetric version of acyloin-type reactions was also investigated in our laboratory operating packed-bed bioreactors functionalized with a suitable thiamine diphosphate (ThDP)-dependent enzyme supported on mesoporous silica [17]. Overall, the so far reported umpolung flow processes [12-17] required quite sophisticated procedures, eventually complicated by the separation of homogeneous azolium salt pre-catalysts [25]. In this contribution, we describe a convenient and straightforward continuos-flow protocol for the effective production of benzoin and Stetter-like products that relies on the use of a readily and commercially available supported base as packing material of

fixed-bed microreactors. The present study originated from our recent findings on a novel strategy for the umpolung of aromatic α-diketone donors [26] and their peculiar reactivity with aromatic aldehydes or α,β-unsaturated acceptors [27-29]. Indeed, activation of aromatic α-diketones may occur through a double electron-transfer (ET) process triggered by the carbamoyl anion derived from *N,N*-dimethylformamide (DMF) solvent with catalytic base, which generates an enediolate anion as key reactive species of umpolung catalysis (Figure 1). Significantly, the current investigation on the heterogeneous continuous-flow version of the α-diketone activation process resulted in the fabrication of fixed-bed reactors with elevated stability, allowing their operation for about five days with maintenance of productivity. Moreover, the disclosed flow procedure constituted an equally effective (complete chemoselectivity) and environmentally benign alternative to the analogous batch process towards benzoin- and Stetter-type products mediated by toxic cyanide anions [29,30].

Results and Discussion

The possibility of transposing the ET-mediated activation process of aromatic α-diketones (benzils) from a homogeneous batch protocol to a heterogeneous flow procedure was initially investigated by testing the efficacy of the commercially available supported bases **4**–**8** under batch conditions; the benzoin-type reaction of benzil **1a** with 2-chlorobenzaldehyde **2a** furnishing the benzoylated benzoin **3aa** (double aroylation product) was selected as the benchmark (Table 1). Quite surprisingly, the polystyrene-supported 1,8-diazabicyclo [5.4.0]undec-7-ene **4** (PS-DBU) was completely inefficient (DMF, 35 °C, Ar atmosphere) in both catalytic and equimolar amounts despite the detected activity of its homogeneous coun-
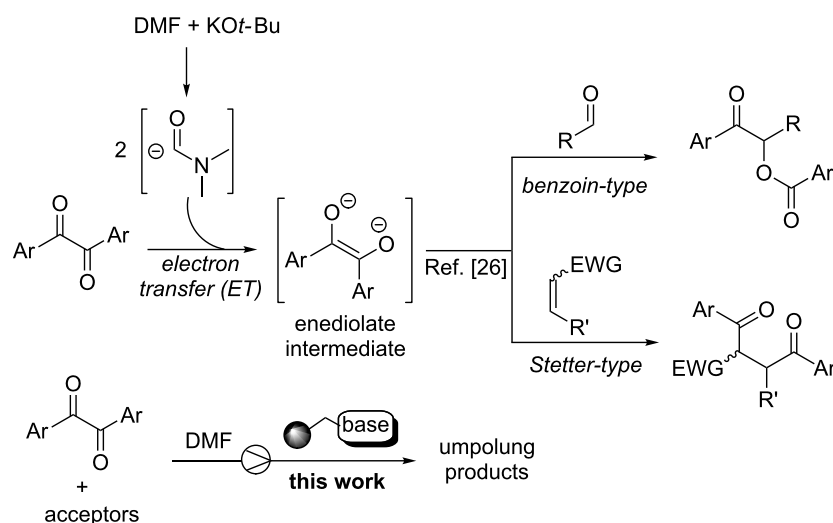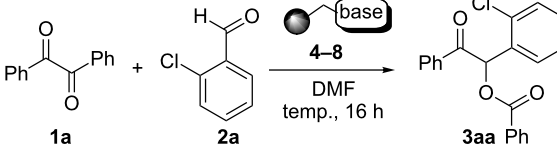
Figure 1: Electron-transfer initiated activation of α-diketones (background) and present study.

Table 1: Optimization of the cross-benzoin-type reaction of benzil **1a** with 2-chlorobenzaldehyde **2a** promoted by the supported bases **4–8** under batch conditions.[a]

Entry	Base [mol %]	Temp. [°C]	Yield [%][b]
1[c]	**4** (25)	35	<5
2[c]	**4** (100)	35	<5
3[c]	**5** (100)	35	95
4	**5** (100)	35	92
5	**5** (25)	35	78
6	**5** (25)	50	91
7	**5** (10)	50	28
8	**6** (100)	50	<5
9	**7** (100)	50	<5
10	**8** (100)	50	<5
11[d]	**5** (25)	50	89

[a]Reaction Conditions: benzil **1a** (0.50 mmol), 2-chlorobenzaldehyde **2a** (0.60 mmol), DMF (1.0 mL; water content 0.23% w/w), and the stated amount of base.
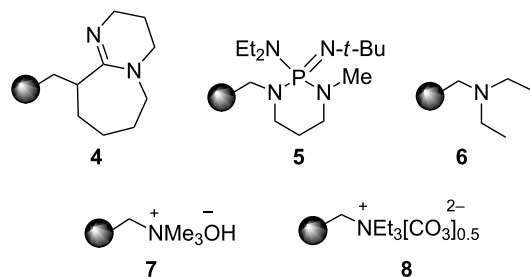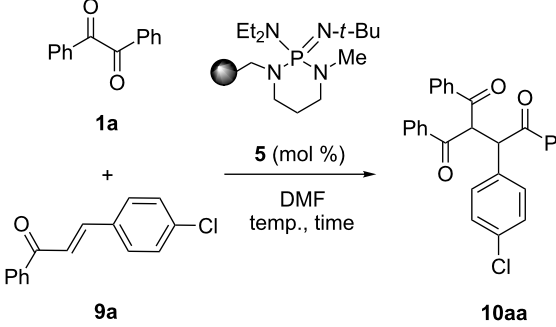
[b]Isolated yield. [c]Reaction conducted under Ar. [d]5th recycle.

terpart [26] (Table 1, entries 1 and 2). Gratifyingly, the highly basic, non-nucleophilic polymer-supported BEMP **5** (PS-BEMP: 2-*tert*-butylimino-2-diethylamino-1,3-dimethyl-perhydro-1,3,2-diazaphosphorine on polystyrene) afforded the target adduct **3aa** in almost quantitative yield (95%) when used in equimolar amounts under an argon atmosphere (Table 1, entry 3). Actually, we previously established the importance of operating under deaerated conditions with homogeneous bases to avoid a marked decrease of the reaction rate (vide infra). By contrast, as demonstrated by the experiment of Table 1, entry 4, the **1a/2a** coupling promoted by PS-BEMP **5** was found to be insensitive to the presence of air, thus further improving the practicality of the heterogeneous procedure for the umpolung of benzils. While the utilization of catalytic PS-BEMP **5** (25 mol %) at 35 °C slightly diminished the reaction yield (78%, Table 1, entry 5), the increase of temperature to 50 °C restored the reaction efficiency (91% yield, entry 6). A lower

amount of **5** (10 mol %) produced an unsatisfactory yield of **3aa** (28%, Table 1, entry 7), whereas the weaker bases diethylamine resin **6**, Ambersep 900 OH **7**, and the polymer-bound tetraalkylammonium carbonate **8** were completely inefficient (Table 1, entries 8–10). Finally, the conversion efficiency was maintained almost unaltered for recycled PS-BEMP **5** after five runs (Table 1, entry 11). The success of the recycle experiment paved the way for the application of **5** in continuous-flow processes with long-term stability.

Next, the heterogeneous procedure for the activation of aromatic α-diketones was applied to the model Stetter-like reaction of benzil **1a** with chalcone **9a** serving as activated α,β-unsaturated acceptor (Table 2). The optimal conditions disclosed for the benzoin-like reaction (25 mol % **5**, 50 °C) were not applicable to the **1a/9a** coupling (Table 2, entry 1). Also, the use of equimolar **5** gave the target 1,4-dione **10aa** in poor yield (26%, Table 2, entry 2) after filtration of **5** and its resuspension in a 10:1 CH₂Cl₂–AcOH mixture (30 min, rt). This work-up procedure was made necessary because of the sequestering by the basic resin **5** of compounds of type **10** displaying acidic protons at the α-position of carbonyl groups. A higher product yield (45%) was obtained at 70 °C (Table 2, entry 3), while a further

Table 2: Optimization of the Stetter-type reaction of benzil (**1a**) with chalcone **9a** promoted by PS-BEMP **5** under batch conditions.[a]

Entry	**5** [mol %]	Temp. [°C]	Time [h]	Yield [%][b]
1	25	50	16	<5
2	100	50	16	26
3	100	70	8	45
4	100	100	8	24
5[c]	100	120	1	31
6[d]	100	70	8	68
7[e]	100	70	8	41

[a]Reaction conditions: benzil (**1a**, 0.50 mmol), chalcone (**9a**, 0.50 mmol), DMF (1.0 mL; water 0.23% w/w), and the stated amount of **5**. [b]Isolated yield. [c]Reaction warmed by microwave irradiation (Biotage Initiator; temperature was measured externally by an IR sensor). [d]Reaction performed with 1.00 mmol of **1a**. [e]Reaction performed with 1.00 mmol of **9a**.

increase of temperature (100 °C) and the use of microwave irradiation at 120 °C (1 h) were not beneficial for the reaction outcome (Table 2, entries 4 and 5). The model Stetter-like reaction was finally optimized by varying the **1a/9a** ratio (Table 2, entries 6 and 7) and the best yield of **10aa** (68%) was achieved at 70 °C with an excess of benzil (**1a**, 2 equiv; Table 2, entry 6).

On the basis of our previous mechanistic investigation in solution phase [26], the above results may be interpreted as follows. The carbamoyl anion **A**, which is generated by deprotonation of DMF solvent with PS-BEMP **5**, is responsible for two sequential ET to the α-diketone **1** leading to the carbamoyl radical **B** (non-productive pathway) [26] and the key enediolate intermediate **I** bound to the polymer as ion pair (Scheme 1). In the case of benzoin-like reactions, the supported species **I** intercepts the aldehyde acceptor **2** to form the cyclic intermediate **III** through the first adduct **II**. Then, the final two ET from **III** to the α-diketone **1** affords the product **3** regenerating the dianion **I** ready for a chain process. It is important to underline the beneficial effect on the reaction outcome and practicability of the polymer support, which stabilizes the enediolate functionality through ionic interactions, thus preventing the fast oxidation by oxygen

of **I** to the α-diketone **1** and the consequent slowing down of the reaction as observed under homogeneous conditions. [26]

In analogy with the study under homogeneous conditions, a trapping experiment was also performed to confirm the crucial role in the catalytic cycle of the enediolate intermediate **I**. Accordingly, the suspension of benzil (**1a**) and equimolar PS-BEMP **5** in DMF was treated at 50 °C with an excess (10 equiv) of acetic anhydride recovering the expected *O,O'*-diacetyl-1,2-diphenylethen-1,2 diol (**11**) in 6% isolated yield (Scheme 2).

Scheme 2: Trapping experiment.
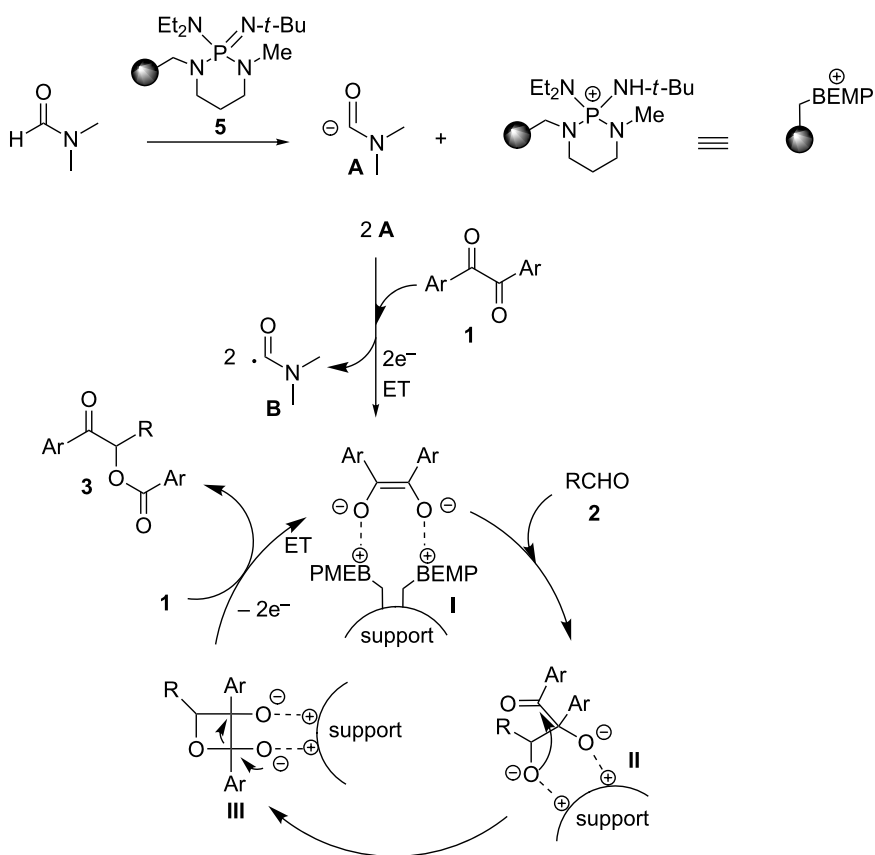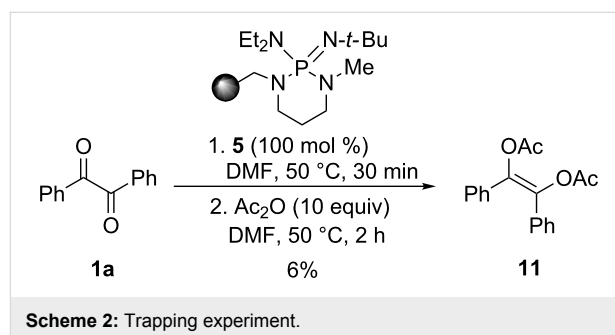
Scheme 1: Proposed dianionic pathway for the cross-benzoin-like reaction of benzils **1** with aldehydes **2** under heterogeneous conditions.

At this stage of our investigation, PS-BEMP **5** was tested as the packing material of fixed-bed reactors with potential long-term stability. A micro-HPLC with minimized extra-column volumes was used as the pumping system. The fixed-bed microreactor **R5** was then fabricated by packing a stainless steel column (10 cm length, 4.6 mm internal diameter) with PS-BEMP **5**. Pycnometer measurements provided the hold-up volume V_o and the total porosity ε_{tot} of **R5** [31], whereas the loaded amount of **5** was determined by weighing the filled and empty column. The main features of **R5** including the residence time and the observed backpressure are summarized in Table 3.

Continuous-flow experiments were performed by first considering the benzoin-like reaction of benzil (**1a**) with 2-chlorobenzaldehyde (**2a**) (Table 4). Different flow rates and substrate concentrations were initially evaluated to optimize the conversion efficiency and productivity (*P*) of the process. Hence, portions of the outlet stream were taken at regular intervals (60 min) and analyzed by NMR spectroscopy. While the highest productivity was obtained at 50 °C with a 0.1 M solution of the substrates and a flow rate of 10 µL min^{-1} (81% conversion; Table 4, entry 1), operating the microreactor **R5** at a lower flow rate (5 µL min^{-1}; residence time: 276 min) guaranteed the complete consumption of the reactants (Table 4, entry 2). Under these conditions, the benzoylated benzoin product **3aa** could be isolated in pure form by simple evaporation of the solvent. The long-term stability of **R5** was next examined to establish the effect of the flow regime on the deactivation rate of the PS-BEMP **5**. The analysis of the conversion versus process time plot showed that the steady-state conversion was reached after ca. 3 h at 50 °C and maintained unaltered for about 120 h on stream (Figure 2).

The scope and applicability of the flow cross-benzoin-type reaction were investigated by coupling various α-diketones **1** with aromatic aldehydes **2**. Higher efficiencies were detected with α-diketones **1a–c** displaying electron-neutral and withdrawing groups with expected lower values of reduction potentials (Table 4, entries 3–13), in agreement with the proposed reaction mechanism. The unreactivity of 4,4'-dimethylbenzil (**1d**) seemed to confirm our mechanistic hypothesis (Table 4, entry 14).

Following the thread of the previous study on the benzoin condensation, the Stetter-like reaction of benzil (**1a**, 0.1 M) with chalcone **9a** (0.05 M) was optimized at 70 °C with a flow rate of 5 µL min^{-1} (Table 5, entry 1). Because of the partial adsorption of the target 1,4-diketone **10aa** onto the basic packing material **5**, the reactor **R5** was flushed with pure DMF at the end of the coupling experiment, thus permitting the recovery of the whole amount of generated product (see the Experimental section). In general, a lower level of coupling efficiency was detected for the Stetter-like reaction compared to the benzoin condensation as confirmed by the higher residence time (276 min) required to reach satisfactory conversions. Again, benzil **1d** proved to be completely ineffective in the addition to α,β-unsaturated acceptors as well (Table 5, entry 7).

Conclusion

In summary, we have disclosed a practical continuous-flow procedure for the umpolung of aromatic α-diketones and demonstrated its efficacy in the chemoselective synthesis of benzoin- and Stetter-like products (aroylated α-hydroxy ketones and 2-benzoyl-1,4-diones, respectively) through the operation of fixed-bed reactors packed with a readily and commercially available polymer-supported base. Together with the ease of product/promoter separation, an important benefit of the flow regime has been the significant long-term stability of the packing bed (ca. 5 five days on streams). Small-scale reactors have been described in this work; nevertheless, an easy scale-up of the disclosed processes may be envisaged by the numbering up approach.

Experimental

Liquid aldehydes were freshly distilled before their utilization. Reactions were monitored by TLC on silica gel 60 F$_{254}$ with detection by charring with phosphomolybdic acid. Flash column chromatography was performed on silica gel 60 (230–400 mesh). ^{1}H (300 MHz), ^{13}C (101 MHz) and ^{19}F (376 MHz) NMR spectra were recorded for CDCl$_3$ solutions at room temperature unless otherwise specified. Peaks assignments were aided by ^{1}H,^{1}H COSY and gradient-HMQC experiments. For accurate mass measurements, the compounds were analyzed in positive ion mode by Agilent 6520 HPLC-Chip Q/TOF-MS (nanospray) using a quadrupole, a hexapole,

Table 3: Main features of microreactor **R5**.[a]

Packed **5** [g]	**5** Loading [mmol/g][b]	V_0 [mL][c]	Total porosity[d]	Time [min][e]	Pressure [bar][f]
0.99	2.20	1.38	0.83	138	4

[a]Geometric volume (V_G) of the stainless-steel column: 1.66 mL. [b]Value given by the supplier. [c]Determined by pycnometry (see the Experimental section). [d]Total porosity $\varepsilon_{tot} = V_0/V_G$. [e]Residence time calculated at 10 µL min^{-1}. [f]Backpressure measured at 10 µL min^{-1} (DMF, 50 °C).

Table 4: Scope of the continuous-flow benzoin-like reaction.[a]
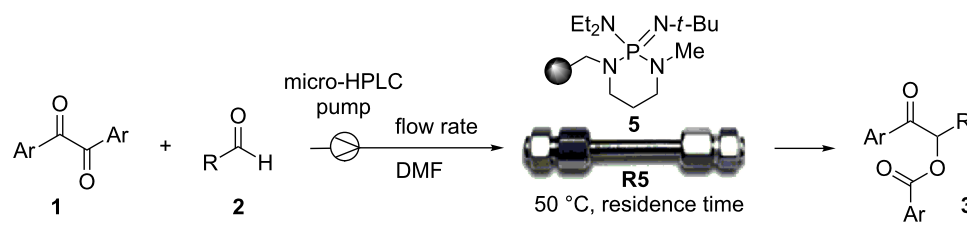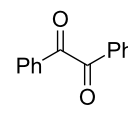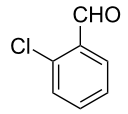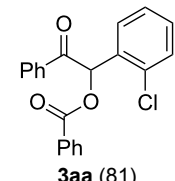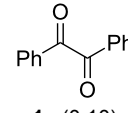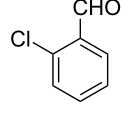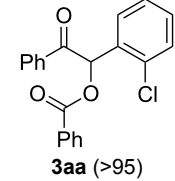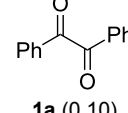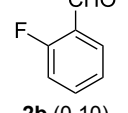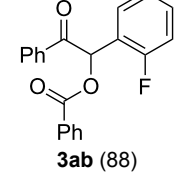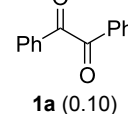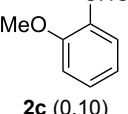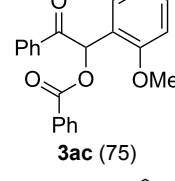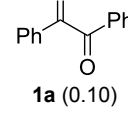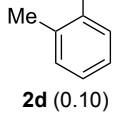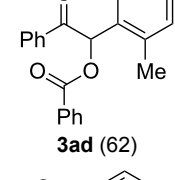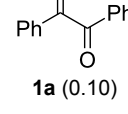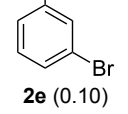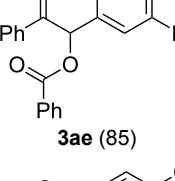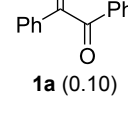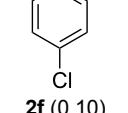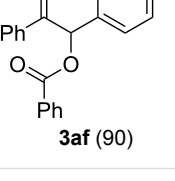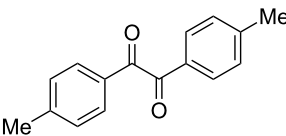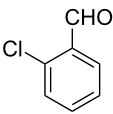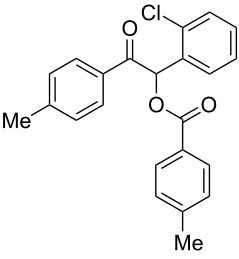
Entry	Donor (*c* [M])	Acceptor (*c* [M])	Flow rate [µL/min]	Time [min][b]	Product (Conv. [%])[c]	*P*[d]
1	**1a** (0.10)	**2a** (0.10)	10	138	**3aa** (81)	22
2	**1a** (0.10)	**2a** (0.10)	5	276	**3aa** (>95)	13
3	**1a** (0.10)	**2b** (0.10)	10	138	**3ab** (88)	24
4	**1a** (0.10)	**2c** (0.10)	10	138	**3ac** (75)	20
5	**1a** (0.10)	**2d** (0.10)	5	276	**3ad** (62)	8
6	**1a** (0.10)	**2e** (0.10)	10	138	**3ae** (85)	23
7	**1a** (0.10)	**2f** (0.10)	10	138	**3af** (90)	25

Table 4: Scope of the continuous-flow benzoin-like reaction.[a] (continued)

8	**1a** (0.10)	**2g** (0.10)	5	276	**3ag** (61)	8
9	**1a** (0.10)	**2h** (0.10)	5	276	**3ah** (66)	9
10	**1b** (0.10)	**2a** (0.10)	10	138	**3ba** (77)	19
11	**1c** (0.10)	**2b** (0.10)	15	207	**3cb** (82)	34
12	**1c** (0.10)	**2i** (0.10)	10	138	**3ci** (85)	23
13	**1c** (0.10)	**2c** (0.10)	10	138	**3cc** (69)	19

Table 4: Scope of the continuous-flow benzoin-like reaction.[a] (continued)

| 14 | **1d** (0.10) | **2a** (0.10) | 5 | 276 | **3da** (<5) | – |

[a]See the Experimental section for a description of the experimental setup. Experiments performed for 5 h in steady-state regime. Temperature was measured by a thermometer placed inside the thermostated unit containing the reactor. [b]Calculated residence time. [c]Instant conversion in steady-state regime as established by ^{1}H NMR analysis. [d]Productivities are measured in mmol(product) h^{-1} mmol(catalyst)$^{-1}$ × 10^3.

Figure 2: Conversion of the **1a/2a** coupling in microreactor **R5** operated for 150 h at 50 °C.
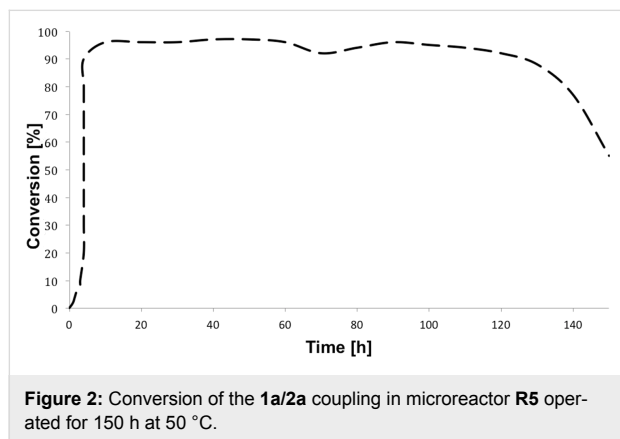
and a time-of-flight unit to produce spectra. The capillary source voltage was set at 1700 V; the gas temperature and drying gas were kept at 350 °C and 5 L/min, respectively. The MS analyzer was externally calibrated with ESI-L low concentration tuning mix from m/z 118 to 2700 to yield an accuracy below 5 ppm. Accurate mass data were collected by directly infusing samples in 40/60 H$_2$O/ACN 0.1% TFA into the system at a flow-rate of 0.4 mL/min. Microwave-assisted reactions were carried out using a single-mode cavity dedicated reactor (Biotage InitiatorTM). Reactions were performed with temperature-controlled programs in glass vials (0.5–2 mL) sealed with a Teflon septum. Temperatures were measured externally by an IR sensor. As described in [32], the system used for continuous-flow reactions was composed of an HPLC pump (Agilent 1100 micro series), an in-line pressure transducer, a thermostated microreactor holder (Peltier unit), a system to collect fractions and a data acquisition system (Agilent ChemStation). The units were connected by peek tubing (internal diameter 0.01 inch from Upchurch Scientific). The system hold-up volume was smaller than 80 µL. The temperature was controlled by inserting a thermometer inside the Peltier unit (temperature measurement error: ±0.5 °C). The supported bases **4–8**

were purchased from Sigma-Aldrich. All adducts **3** and **10** are known compounds [27-29] apart from compounds **3ab**, **3ag**, **3cb**, **3ci**, and **3cc**.

Procedure for the model cross-benzoin-like reaction under batch conditions (Table 1)

A mixture of benzil (**1a**, 105 mg, 0.50 mmol), 2-chlorobenzaldehyde (**2a**, 56 µL, 0.50 mmol), the stated base (see Table 1 for molar ratio) and DMF (1.0 mL) was stirred at the stated temperature for the stated time, then filtered and concentrated. The resulting residue was analyzed by ^{1}H NMR to determine the conversion. Subsequently, the residue was eluted from a column of silica gel with 20:1 cyclohexane–AcOEt to give isolated **3aa**.

Procedure for the model Stetter-like reaction under batch conditions (Table 2)

A mixture of benzil (**1a**, 105 mg, 0.50 mmol), (*E*)-3-(4-chlorophenyl)-1-phenylprop-2-en-1-one (**9a**, 121 mg, 0.50 mmol), PS-BEMP **5** (see Table 2 for molar ratio) and DMF (1.0 mL) was stirred at the stated temperature for the stated time, then filtered and concentrated. The resulting residue was analyzed by ^{1}H NMR to determine the conversion. Subsequently, the residue was eluted from a column of silica gel with 13:1 cyclohexane–AcOEt to give isolated **10aa**.

Trapping experiment (Scheme 2)

A mixture of benzil (**1a**, 210 mg, 1.00 mmol), PS-BEMP **5** (454 mg, 1.00 mmol) and DMF (2 mL) was stirred at 50 °C for 30 min then acetic anhydride (0.94 mL, 10.0 mmol) was added in one portion. The reaction mixture was stirred at 50 °C for 2 h, then cooled to room temperature, filtered, concentrated, and eluted from a column of silica gel with 7:1 cyclohexane–AcOEt to give (*Z*)-1,2-diphenylethene-1,2-diyl diacetate **11** as a white amorphous solid (17 mg, 6%). ^{1}H NMR (300 MHz, CDCl$_3$) δ 7.30–7.16 (m, 10H, Ar), 2.21 (s, 6H, CH$_3$); ^{13}C{^{1}H} NMR

Table 5: Scope of the continuous-flow Stetter-like reaction.[a]
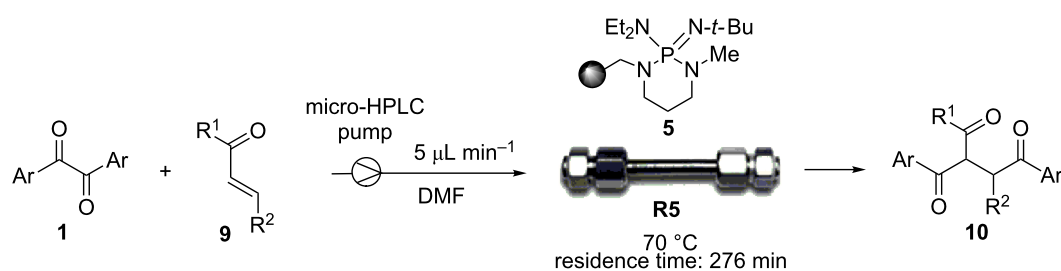
Entry	Donor (*c* [M])	Acceptor (*c* [M])	Product (conv. [%])[b]	*P*[c]
1	**1a** (0.10)	**9a** (0.05)	**10aa** (72)	5
2	**1a** (0.10)	**9b** (0.05)	**10ab** (68)	5
3	**1a** (0.10)	**9c** (0.05)	**10ac** (61)	4
4	**1a** (0.10)	**9d** (0.05)	**10ad** (55)[d]	4
5	**1a** (0.10)	**9e** (0.05)	**10ae** (47)[d]	4
6	**1a** (0.10)	**9f** (0.05)	**10af** (42)[d]	3

Table 5: Scope of the continuous-flow Stetter-like reaction.[a] (continued)
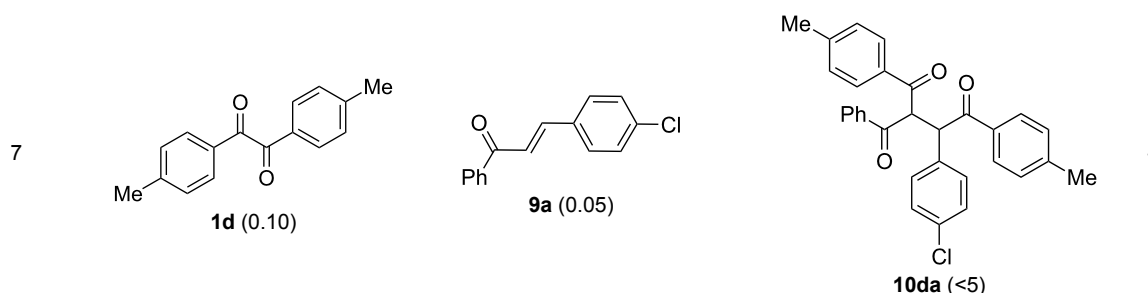
7	**1d** (0.10)	**9a** (0.05)	**10da** (<5)	–

[a]See the Experimental section for a description of the experimental setup. Experiments performed for 5 h in steady-state regime. [b]Instant conversion in steady-state regime as established by ^{1}H NMR analysis. [c]Productivities are measured in mmol(product) h[−1] mmol(catalyst)[−1]× 10[3]. [d]Diastereomeric mixture.

(101 MHz, CDCl$_3$) δ 168.1, 138.5, 133.0, 128.8, 128.8, 128.2, 20.7; HRMS–ESI/Q-TOF (*m/z*): [M]$^+$ calcd for C$_{18}$H$_{16}$O$_4$: 296.1049; found: 296.1105.

Determination of microreactor void-volume

Microreactor void volume (V_0) was determined by pycnometry [31]. This method consists in filling the microreactor successively with two distinct solvents (solvent 1: water; solvent 2: *n*-hexane) and weighing the filled microreactors accurately. Simple math shows that [33]: $V_0 = (\omega_1 - \omega_2) / (\delta_1 - \delta_2)$, where ω_1 and ω_2 are the weights of the microreactor filled with solvents 1 and 2 and δ_1 and δ_2 the densities of the solvents.

Continuous-flow cross-benzoin-like reactions (Table 4)

Microreactor **R5** was fed with a DMF solution of α-diketone **1** and aldehyde **2** (see Table 4 for molarity concentrations), and operated at the stated temperature and the stated flow rate for 5 h under steady-state conditions. Instant conversion was determined (^{1}H NMR analysis) every hour by taking a sample of the eluate. The collected solution was finally concentrated and eluted from a column of silica gel with the suitable elution system to give the corresponding aroylated α-hydroxy ketone **3**.

The long-term stability experiment was performed using benzil (**1a**, 0.10 M) and 2-chlorobenzaldehyde (**2a**, 0. 10 M) as the substrates; microreactor **R5** was operated at 50 °C with a flow rate of 5 μL min^{-1} for 150 h. After the achievement of the steady-state regime (ca. 3 h), an almost full conversion of **1a** (>95%) was maintained for ca. 120 h, while a progressive loss of catalytic activity was observed after that time.

Continuous-flow Stetter-like reactions (Table 5)

Microreactor **R5** was fed with a DMF solution of α-diketone **1** (0.10 M) and chalcone **9** (0.05 M), and operated at 70 °C with a

flow rate of 5 μL min^{-1} for 5 h under steady-state conditions. After that time, the reactor was flushed at room temperature with pure DMF for an additional 5 h. The collected solution was finally concentrated and eluted from a column of silica gel with the suitable elution system to give the corresponding 2-benzoyl-1,4-dione **10**.

1-(2-Fluorophenyl)-2-oxo-2-phenylethyl benzoate (3ab). ^{1}H NMR (300 MHz, CDCl$_3$) δ 8.15–8.06 (m, 2H, Ar), 8.06–7.97 (m, 2H, Ar), 7.61–7.50 (m, 3 H, Ar), 7.50–7.40 (m, 5H, Ar, H-1), 7.40–7.31 (m, 1H, Ar), 7.21–7.05 (m, 2H, Ar); ^{13}C{^{1}H} NMR (101 MHz, CDCl$_3$) δ 192.9, 165.9, 160.2 (d, *J* = 250 Hz), 134.4, 133.9, 133.5, 131.5 (d, *J* = 8.4 Hz), 130.1 (d, *J* = 2.5 Hz), 129.3, 129.0, 128.9, 128.7, 128.5, 125.0 (d, *J* = 3.3 Hz), 121.4 (d, *J* = 14 Hz), 116.3 (d, *J* = 22 Hz), 70.7; ^{19}F NMR (376 MHz, CDCl$_3$) δ −116.7 to −116.8 (m); HRMS–ESI/Q-TOF (*m/z*): [M + Na]$^+$ calcd for C$_{21}$H$_{15}$FNaO$_3$: 357.0903; found: 357.0988.

1-(2,6-Dichlorophenyl)-2-oxo-2-phenylethyl benzoate (3ag). ^{1}H NMR (300 MHz, CDCl$_3$) δ 8.19–8.11 (m, 2H, Ar), 7.85–7.78 (m, 3H, Ar, H-1), 7.62–7.51 (m, 1H, Ar), 7.51–7.41 (m, 3H, Ar), 7.41–7.31 (m, 4H, Ar), 7.27–7.18 (m, 1H, Ar); ^{13}C{^{1}H} NMR (101 MHz, CDCl$_3$) δ 192.8, 165.2, 136.7, 134.9, 133.4, 133.2, 132.0, 131.0, 130.2, 129.3, 129.3, 128.5, 128.4, 128.08, 75.1; HRMS–ESI/Q-TOF (*m/z*): [M + Na]$^+$ calcd for C$_{21}$H$_{14}$Cl$_2$NaO$_3$: 407.0218; found: 407.0301.

1-(2-Fluorophenyl)-2-oxo-2-(pyridin-2-yl)ethyl picolinate (3cb). ^{1}H NMR (300 MHz, CDCl$_3$) δ 8.81–8.72 (m, 1H, Ar), 8.59 (m, 1H, Ar), 8.21–8.13 (m, 1H, Ar), 8.08–8.00 (m, 1H, Ar), 7.97 (s, 1H, H-1), 7.86–7.73 (m, 2H, Ar), 7.57–7.36 (m, 3H, Ar), 7.36–7.26 (m, 1H, Ar), 7.16–7.01 (m, 2H, Ar); ^{13}C{^{1}H} NMR (101 MHz, CDCl$_3$) δ 193.3, 164.4, 161.0 (d, *J* = 250 Hz), 159.7, 151.2, 150.1, 149.1, 147.6, 137.0, 136.9, 131.2 (d, *J* = 8.4 Hz), 130.7 (d, *J* = 2.3 Hz), 127.7, 127.1, 125.70,

124.4 (d, *J* = 3.7 Hz), 122.9, 121.4 (d, *J* = 14 Hz), 116.2 (d, *J* = 22 Hz), 72.4; ^{19}F NMR (376 MHz, CDCl$_3$) δ −115.2 to −115.3 (m); HRMS–ESI/Q-TOF (*m/z*): [M + H]$^+$ calcd for C$_{19}$H$_{14}$FN$_2$O$_3$: 337.0988; found: 337.0908.

1-(2-Bromophenyl)-2-oxo-2-(pyridin-2-yl)ethyl picolinate (3ci). ^{1}H NMR (300 MHz, CDCl$_3$) δ 8.81–8.73 (m, 1H, Ar), 8.63–8.55 (m, 1H, Ar), 8.20–8.13 (m, 1H, Ar), 8.09–8.02 (m, 2H, Ar, H-1), 7.86–7.74 (m, 2H, Ar), 7.64 (m, 1H, Ar), 7.50–7.36 (m, 3H, Ar), 7.28–7.13 (m, 2H, Ar); ^{13}C{^{1}H} NMR (101 MHz, CDCl$_3$) δ 194.0, 164.3, 151.3, 150.2, 149.2, 147.6, 137.0, 136.9, 133.8, 133.7, 130.6, 130.5, 127.8, 127.7, 127.1, 125.8, 122.8, 78.0; HRMS–ESI/Q-TOF (*m/z*): [M + H]$^+$ calcd for C$_{19}$H$_{14}$BrN$_2$O$_3$: 397.0188; found: 397.0225.

1-(2-Methoxyphenyl)-2-oxo-2-(pyridin-2-yl)ethyl picolinate (3cc). ^{1}H NMR (300 MHz, CDCl$_3$) δ 8.79–8.68 (m, 1H, Ar), 8.59–8.46 (m, 1H, Ar), 8.17–8.07 (m, 1H, Ar), 8.06–7.99 (m, 2H, Ar, H-1), 7.82–7.70 (m, 2H, Ar), 7.46–7.39 (m, 1H, Ar), 7.39–7.29 (m, 2H, Ar), 7.29–7.23 (m, 1H, Ar), 6.93–6.83 (m, 2H, Ar), 3.83 (s, 3H, CH$_3$); ^{13}C{^{1}H} NMR (101 MHz, CDCl$_3$) δ 194.7, 164.6, 157.8, 151.9, 150.1, 149.0, 147.9, 137.0, 136.8, 130.7, 130.2, 127.4, 127.0, 125.6, 122.7, 122.6, 120.8, 111.7, 73.4, 55.9; HRMS–ESI/Q-TOF (*m/z*): [M + H]$^+$ calcd for C$_{20}$H$_{17}$N$_2$O$_4$: 349.1188; found: 349.1105.

Supporting Information

Supporting Information File 1

NMR spectra of new compounds.
[http://www.beilstein-journals.org/bjoc/content/supplementary/1860-5397-12-268-S1.pdf]

Acknowledgements

References

1. Menon, R. S.; Biju, A. T.; Nair, V. *Beilstein J. Org. Chem.* **2016,** *12,* 444–461. doi:10.3762/bjoc.12.47

2. Flanigan, D. M.; Romanov-Michailidis, F.; White, N. A.; Rovis, T. *Chem. Rev.* **2015,** *115,* 9307–9387. doi:10.1021/acs.chemrev.5b00060

3. Bugaut, X.; Glorius, F. *Chem. Soc. Rev.* **2012,** *41,* 3511–3522. doi:10.1039/c2cs15333e

4. Phillips, E. P.; Chan, A.; Scheidt, K. A. *Aldrichimica Acta* **2009,** *42,* 55–65.

5. Wang, L.; Chen, E. Y.-X. *ACS Catal.* **2015,** *5,* 6907–6917. doi:10.1021/acscatal.5b01410

6. Molina de la Torre, J. A.; Albéniz, A. C. *ChemCatChem* **2014,** *6,* 3547–3552. doi:10.1002/cctc.201402767

7. Powell, A. B.; Suzuki, Y.; Ueda, M.; Bielawski, C. W.; Cowley, A. H. *J. Am. Chem. Soc.* **2011,** *133,* 5218–5220. doi:10.1021/ja200602e

8. Zeitler, K.; Mager, I. *Adv. Synth. Catal.* **2007,** *349,* 1851–1857. doi:10.1002/adsc.200700174

9. Zhao, H.; Foss, F. W., Jr.; Breslow, R. *J. Am. Chem. Soc.* **2008,** *130,* 12590–12591. doi:10.1021/ja804577q

10. Ueno, A.; Kayaki, Y.; Ikariya, T. *Green Chem.* **2013,** *15,* 425–430. doi:10.1039/C2GC36414J

11. Zeng, T.; Song, G.; Li, C.-J. *Chem. Commun.* **2009,** 6249–6251. doi:10.1039/b910162d

12. Di Marco, L.; Hans, M.; Delaude, L.; Monbaliu, J.-C. M. *Chem. – Eur. J.* **2016,** *22,* 4508–4514. doi:10.1002/chem.201505135

13. Green, R. A.; Pletcher, D.; Leach, S. G.; Brown, R. C. D. *Org. Lett.* **2015,** *17,* 3290–3293. doi:10.1021/acs.orglett.5b01459

14. Green, R. A.; Pletcher, D.; Leach, S. G.; Brown, R. C. D. *Org. Lett.* **2016,** *18,* 1198–1201. doi:10.1021/acs.orglett.6b00339

15. Asadi, M.; Hooper, J. F.; Lupton, D. W. *Tetrahedron* **2016,** *72,* 3729–3733. doi:10.1016/j.tet.2016.03.075

16. Bortolini, O.; Cavazzini, A.; Dambruoso, P.; Giovannini, P. P.; Caciolli, L.; Massi, A.; Pacifico, S.; Ragno, D. *Green Chem.* **2013,** *15,* 2981–2992. doi:10.1039/c3gc41284a

17. Giovannini, P. P.; Bortolini, O.; Cavazzini, A.; Greco, R.; Fantin, G.; Massi, A. *Green Chem.* **2014,** *16,* 3904–3915. doi:10.1039/C4GC00838C

18. Pastre, J. C.; Browne, D. L.; Ley, S. V. *Chem. Soc. Rev.* **2013,** *42,* 8849–8869. doi:10.1039/c3cs60246j

19. Hessel, V.; Kralisch, D.; Kockmann, N.; Noël, T.; Wang, Q. *ChemSusChem* **2013,** *6,* 746–789. doi:10.1002/cssc.201200766

20. Roberge, D. M.; Zimmermann, B.; Rainone, F.; Gottsponer, M.; Eyholzer, M.; Kockmann, N. *Org. Process Res. Dev.* **2008,** *12,* 905–910. doi:10.1021/op8001273

21. Roberge, D. M.; Ducry, L.; Bieler, N.; Cretton, P.; Zimmermann, B. *Chem. Eng. Technol.* **2005,** *28,* 318–323. doi:10.1002/ceat.200407128

22. Finelli, F. G.; Miranda, L. S. M.; de Souza, R. O. M. A. *Chem. Commun.* **2015,** *51,* 3708–3722. doi:10.1039/C4CC08748H

23. Atodiresei, I.; Vila, C.; Rueping, M. *ACS Catal.* **2015,** *5,* 1972–1985. doi:10.1021/acscatal.5b00002

24. Puglisi, A.; Benaglia, M.; Chiroli, V. *Green Chem.* **2013,** *15,* 1790–1813. doi:10.1039/c3gc40195b

25. Sano, T.; Mizota, I.; Shimizu, M. *Chem. Lett.* **2013,** *42,* 995–997. doi:10.1246/cl.130396

26. Ragno, D.; Zaghi, A.; Di Carmine, G.; Giovannini, P. P.; Bortolini, O.; Fontagnolo, M.; Molinari, A.; Venturini, A.; Massi, A. *Org. Biomol. Chem.* **2016,** *14,* 9823–9835. doi:10.1039/C6OB01868H

27. Bortolini, O.; Fantin, G.; Ferretti, V.; Fogagnolo, M.; Giovannini, P. P.; Massi, A.; Pacifico, S.; Ragno, D. *Adv. Synth. Catal.* **2013,** *355,* 3244–3252. doi:10.1002/adsc.201300652

28. Ragno, D.; Bortolini, O.; Giovannini, P. P.; Massi, A.; Pacifico, S.; Zaghi, A. *Org. Biomol. Chem.* **2014,** *12,* 5733–5744. doi:10.1039/C4OB00759J

29. Ragno, D.; Bortolini, O.; Fantin, G.; Fogagnolo, M.; Giovannini, P. P.; Massi, A. *J. Org. Chem.* **2015,** *80,* 1937–1945. doi:10.1021/jo502582e

30. Demir, A. S.; Reis, Ö. *Tetrahedron* **2004,** *60,* 3803–3811. doi:10.1016/j.tet.2004.03.016

31. McCormick, R. M.; Karger, B. L. *Anal. Chem.* **1980,** *52,* 2249–2257. doi:10.1021/ac50064a005

32. Bortolini, O.; Caciolli, L.; Cavazzini, A.; Costa, V.; Greco, R.; Massi, A.; Pasti, L. *Green Chem.* **2012,** *14,* 992–1000. doi:10.1039/c2gc16673a

33. Gritti, F.; Kazakevich, Y.; Guiochon, G. *J. Chromatogr. A* **2007,** *1161,* 157–169. doi:10.1016/j.chroma.2007.05.102

Poly(ethylene glycol)s as grinding additives in the mechanochemical preparation of highly functionalized 3,5-disubstituted hydantoins

Andrea Mascitti[‡1,2], Massimiliano Lupacchini[‡1,2], Ruben Guerra[2], Ilya Taydakov[3,4], Lucia Tonucci[5], Nicola d'Alessandro[1], Frederic Lamaty[2], Jean Martinez[2] and Evelina Colacino[*2]

Abstract

The mechanochemical preparation of highly functionalized 3,5-disubstituted hydantoins was investigated in the presence of various poly(ethylene) glycols (PEGs), as safe grinding assisting agents (liquid-assisted grinding, LAG). A comparative study under dry-grinding conditions was also performed. The results showed that the cyclization reaction was influenced by the amount of the PEG grinding agents. In general, cleaner reaction profiles were observed in the presence of PEGs, compared to dry-grinding procedures.

Introduction

Poly(ethylene) glycols (PEGs) are eco-friendly solvents [1,2], finding applications in the biomedical field and for pharmaceutical formulations [3] and catalysis [4]. PEG-based reaction media [1] are safe reaction environments, efficiently heated by microwaves [5], but their use in organic transformations activated by other alternative energy inputs is still scarce. Only

three examples highlight their peculiar role for metal-catalysed processes in a ball mill (Mirozoki–Heck reaction) [6], by ultrasound (copper-catalysed cyanation reaction) [7], and for co-crystal formation in the polymer-assisted grinding process (POLAG) [8]. However, to the best of our knowledge, the systematic investigation of the influence of PEG polymers has not been reported yet for organic syntheses promoted by mechanical energy.

We firstly reported the positive influence of PEG solvents as grinding agents for the mechanochemical preparation of an active pharmaceutical ingredient (API), the anticonvulsant drug ethotoin **7** [9] (marketed as Peganone®, Scheme 1). We describe herein the impact of the addition of variable amounts of PEG, PEG chain length and end terminal groups, for the preparation of diverse 3,5-disubstituted hydantoins from α-amino methyl esters **1**, via an in situ intramolecular cyclization reaction of the ureido derivative **B**, which was obtained from *N*-carbamoylimidazole activated amino ester derivative **A** by reaction with various amines [9-11] (Scheme 1). Hanusa's formalism was used to represent the reaction activated by mechanochemical energy [12].

The yields, reaction rates and chemoselectivity obtained in the presence of melted PEGs were compared with the results obtained in dry-grinding conditions.

Results and Discussion

H-Leu-OMe was used as benchmark for the mechanochemical preparation of 3-ethyl-5-isobutylhydantoin (**2a**) ($R^1 = CH_2CH(CH_3)_2$ and $R^2 = CH_2CH_3$, Scheme 1) [9]. The reaction was screened in the presence of various PEG additives (Table 1), by adding variable amounts of PEGs, with different molecular weights ($600 < M_w < 5000$ Dalton) or chain end groups (dihydroxy, mono- or dimethyl ether substituents) in the second step (Table 1). The first set of experiments was aimed to determine if the addition of variable amounts of solid MeO-PEG-2000-OMe (Table 1, entries 2–5) or HO-PEG-3400-OH (Table 1, entries 7–10) could impact both the reaction yield and rate, compared to dry-grinding conditions previously reported [9] (Table 1, entry 1). Yields were generally improved in the presence of variable amounts of PEGs (Table 1, entries 2, 3 and 7, 8), starting to decrease when reaching a critical value at 675 mg (Table 1, entries 5 and 10). The substrate conversion remained moderate, the cyclization reaction of the corresponding ureido derivative B-Leu was slowed down and the methyl ester moiety was partially hydrolysed. Indeed, the base activity was increased due to the presence of water in PEG as well as by the PEG crown-ether-like effect [1], chelating the potassium cations.

It is worth noticing here that the crude mixture was cleaner in comparison with dry-grinding conditions. Indeed, the symmetri-

Scheme 1: PEG-assisted grinding strategy for the preparation of 3,5-disubstituted hydantoins.
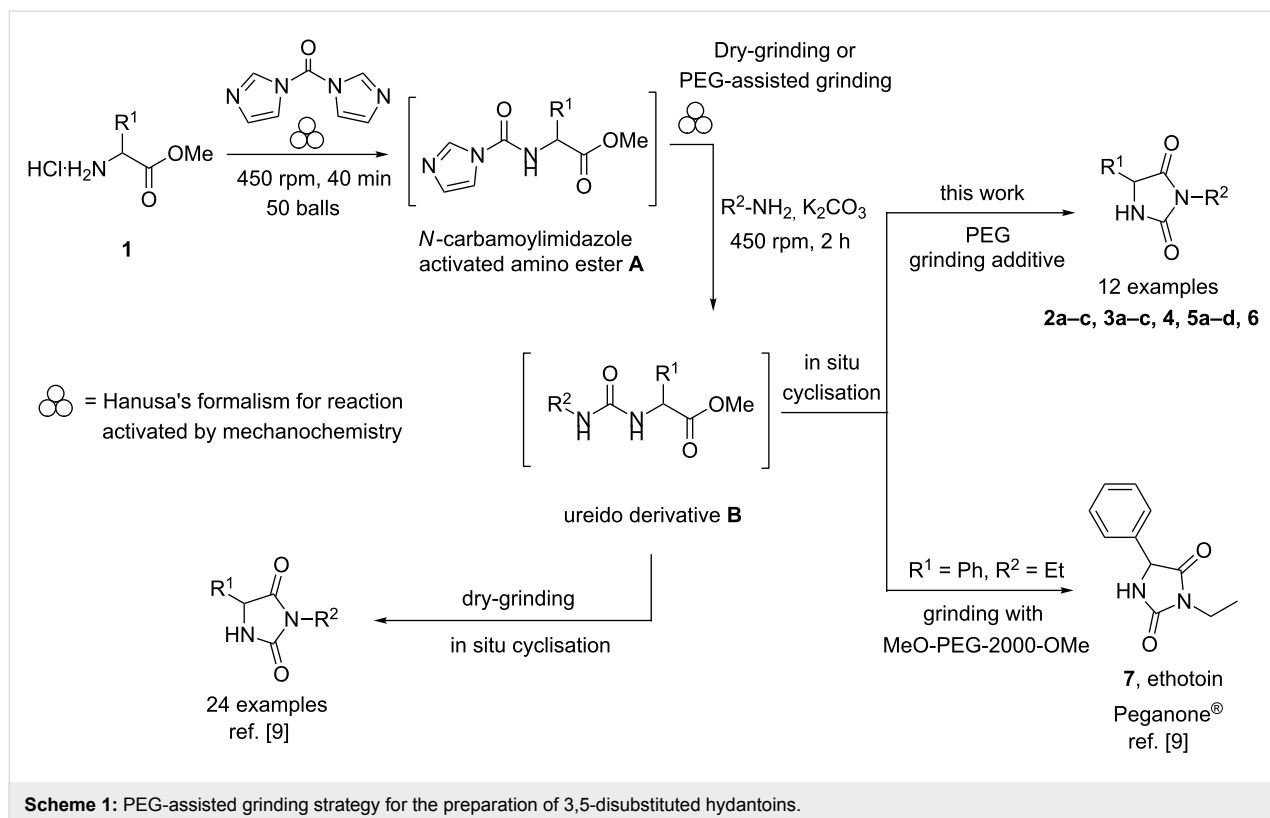
Table 1: Screening of grinding additives using (*L*)-H-Leu-OMe·HCl as benchmark for the preparation of compound **2a**.[a]

Entry	Grinding additive	Amount (mg)	Yield (%)[b]
1 [9]	–	–	61
2	MeO-PEG-2000-OMe	225	70
3 [9]		450	70
4[c,d]		450[c,d]	71[c,d]
5		675	29[e]
6	MeO-PEG-2000-OH	450	68
7	HO-PEG-3400-OH	225	77
8		450	73
9[c,d]		450[c,d]	73[c,d]
10		675	66[e]
11	HO-PEG-5000-OH	450	57
12	HO-PEG-1000-OH	450	66
13	HO-PEG-600-OH	450	56
14	Glycerol	450	58

[a]Conditions: (step 1) (*L*)-H-Leu-OMe·HCl (1 mmol) and CDI (1.3 equiv.) at 450 rpm, in a planetary ball mill (PBM) using a 12 mL SS jar with 50 balls (SS = stainless steel, 5 mm Ø) for 40 min; (step 2) EtNH$_2$·HCl (1.6 equiv), K$_2$CO$_3$ (3.6 equiv) and the grinding additive RO-PEG$_n$-OR (R = H, Me, *n* = 14, 23, 46, 77, 114) or glycerol (450 mg mmol^{-1}) (see Supporting Information File 1 for experimental details); [b]Isolated yields; [c]The reaction time in the second step was 3 h; [d]PEG was precipitated in diethyl ether, then filtered and dried in the air before use [16]; [e]^{1}H NMR yield.

cal urea of the starting amino ester – obtained from the corresponding *N*-carbamoyl imidazole amino ester **A** – was not observed, as shown by the LC–MS analyses of the crude mixture. An approach complementing similar strategies was already described to avoid the formation of symmetrical ureas in solution [13].

The preparation of the hydantoin **2a** was also investigated using batches of solid PEGs (M_w = 2000 and 3400) in which PEGs with lower molecular weight (M_w = 200–400) were eliminated before use by a precipitation/filtration procedure (Table 1, entries 4 and 9), according to a well-established protocol [14-16]. Even when the PEG polymers were supposed to be homogeneously liquids (melting point around 55 °C) at the operational temperature, comparable yields could be obtained only by extending the reaction time (3 h instead of 2 h), when 'pretreated' PEGs were used instead of 'unfiltered' PEGs (Table 1, entries 3 and 8).

This observation suggested that changes in the 'physical state of the system could be induced by specific interactions with PEG polymers and influenced both by the viscosity and the polymer

chain length. After selecting the optimal polymer amount (450 mg mmol^{-1}), the study was carried on by increasing (Table 1, entry 11) or reducing (Table 1, entries 12 and 13) the polymer chain length, changing the end terminal substituents (Table 1, entries 6 vs 3), and adding glycerol instead of PEGs as additive (Table 1, entry 14). As a result, the effect of using different end terminal groups was not markedly significant, the yield was a function of the average molecular weight of the PEG used: HO-PEG-5000-OH (Table 1, entry 11) was probably too viscous to allow the diffusion of reactants. Decreased and comparable yields were also observed by reducing the PEG chain length (Table 1, entry 13) and by using glycerol. It is also worth noting here that not only viscosity, but any modification of the physical state of the system impacted the outcome of the reaction. Indeed, HO-PEG-600-OH (0.119 cSt) led to comparable yields when replaced by a more viscous liquid like glycerol (1.12 cSt) (Table 1, entry 14), an eco-friendly solvent still not investigated for liquid-assisted grinding procedures. In fact such a compound is becoming a green source of several building blocks since glycerol is actually produced in very large amount as byproduct from biodiesel synthesis [17].

With this background, 3-ethyl-5-benzylhydantoin (**3a**) [9] (R^1 = CH$_2$Ph and R^2 = CH$_2$CH$_3$) was also prepared using solid MeO-PEG-2000-OMe and HO-PEG-3400-OH as additives (Table 2). Using (L)-H-Phe-OMe·HCl as substrate, as a general trend and in comparison with the dry-grinding procedure previously reported [9] (Table 2, entry 1), yields were generally lower with PEG additives, independently on their size and amounts (Table 2). This trend, apparently in contrast with the results illustrated so far for 3-ethyl-5-isobutylhydantoin (**2a**) [9] suggested that the reactivity of the system might be also a function of the nature of the amino ester side chain, influencing the solubility of the reactants, reaction intermediates and final products. However, no differences in yields were observed when (D)-H-Phe-OMe was used, instead of its enantiomer (Table 2, entry 3).

Therefore, the one-pot two-steps cyclization reaction was investigated with different amino ester/amine combinations (H-AA-OMe/R^2-NH$_2$) and comparative experiments using dry- or wet-grinding with PEGs (M_w = 2000 and 3400, 450 mg mmol^{-1}) were also performed (Table 3).

Indeed, compounds with the same *N*-R^2 substituent led to variable yields for different amino esters (R^1, Scheme 1 and Table 3), as shown for experiments performed in both dry-grinding conditions in the series **3b** and **5b** (R^2 = 1-[4-(4-methyl-1*H*-pyrazol-1-yl)phenyl]methyl, Table 3, entries 5 and 9), **3c** and **5c** (R^2 = furan-1-ylmethyl, Table 3, entries 6 and 10), and wet-grinding experiments with PEGs, for the series **2a, 3a**,

4 (Table 3, entries 1, 4, and 7, respectively) and **5a** (R^2 = ethyl, Table 3, entry 8) or **2b** and **6** (R^2 = allyl, Table 3, entries 2 and 12). However, the PEG influence on the reaction yield could not be excluded. The mechanochemical productivity was slightly improved when PEG polymers were used compared to dry-grinding conditions, as demonstrated for the synthesis of hydantoins **2a–c** (Table 3, entries 1–3), **5a** (Table 3, entry 8) and **6** (Table 3, entry 12), with the exception of hydantoins **3a** (Table 3, entry 4) and **5b** (Table 3, entry 9). Moreover, the preparation of hydantoins **3b** and **3c** (Table 3, entries 5 and 6) in the presence of PEG led to incomplete conversion of starting materials, together with the formation of various unknown byproducts. A possible explanation can be related to the solubility of reactants, reaction intermediates and final products in PEG polymers, although the existence of specific interactions with PEG polymers cannot be excluded. Indeed, especially under mechanical stress, PEGs are known to induce changes in the physical state of the system [8].

These results confirmed the role played by polymers in mechanochemical transformations, also leading to cleaner reaction profiles. However, the choice of the suitable polymer for a specific transformation was not trivial: the 'fine tuning' of the physical state of the system was also related to specific physical aspects also connected to the intrinsic properties of the polymer. In addition, PEG polymers were demonstrated as a valid eco-friendly and safe alternative to classic solvents used in liquid-assisted-grinding procedures (LAG) [18-22] due to their low melting point (45–60 °C), enabling their use as melt during

Table 2: Optimization of liquid-assisted grinding conditions using (*L*)-H-Phe-OMe·HCl as benchmark for the preparation of compound **3a**.[a]

Entry	Grinding additive	Amount (mg)	Yield (%)[b] [9]
1 [9]	–	–	84
2	MeO-PEG-2000-OMe	225	59
3[c]		450	70 (68)[c]
4	HO-PEG-3400-OH	225	58
5		450	60
6		675	62

[a]Conditions: (step 1) (L)-H-Phe-OMe·HCl (1 mmol) and CDI (1.3 equiv) at 450 rpm, in a planetary ball-mill (PBM) using a 12 mL SS jar with 50 balls (SS = stainless steel, 5 mm Ø) for 40 min; (step 2) EtNH$_2$·HCl (1.6 equiv), K$_2$CO$_3$ (3.6 equiv) and RO-PEG$_n$-OR (R = H, Me, *n* = 46, 77) (see Supporting Information File 1 for experimental details); [b]isolated yields; [c]*D*-H-Phe-OMe was used.

Table 3: Syntheses of 3,5-disubstituted hydantoins under dry-grinding (conditions A)[a] or PEG-assisted grinding (conditions B and C).[b]
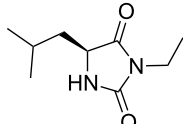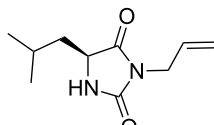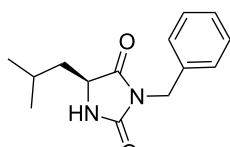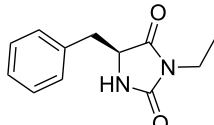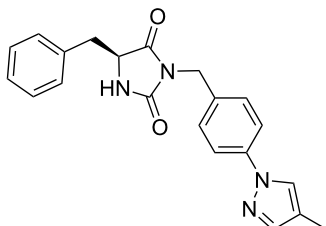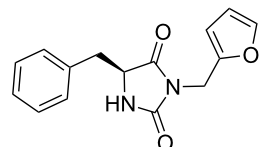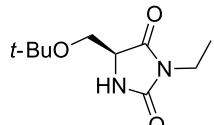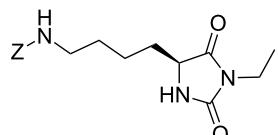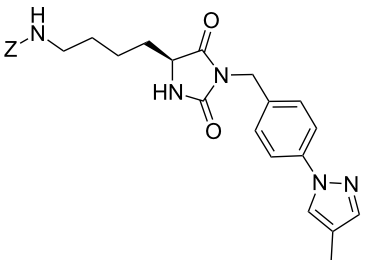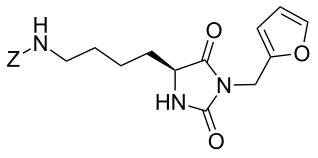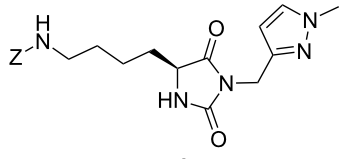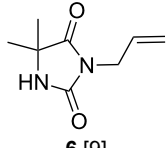
Entry	H-AA-OMe	Yields (%)[b] vs conditions[a]			Product
		A	B	C	
1	H-Leu-OMe	61 [9]	70	73	**2a** [9]
2		57 [9]	69	66[c]	**2b** [9]
3		38 [9]	n.p.[d]	48[c]	**2c** [9]
4	H-Phe-OMe	84 [9]	70	60	**3a** [9]
5		30	n.d.[e]	n.d.[e]	**3b**
6		70	n.d.[e]	n.d.[e]	**3c**
7	H-Ser(O*t*-Bu)-OMe	51 [9]	70	70	**4**
8	H-Lys(*Z*)-OMe	31 [9]	47[c]	50[c]	**5a** [9]

Table 3: Syntheses of 3,5-disubstituted hydantoins under dry-grinding (conditions A)[a] or PEG-assisted grinding (conditions B and C).[b] (continued)

9		62	n.p.[d]	37[c]

5b

10		37	n.p.[d]	n.p.[d]

5c

11		47	n.p.[d]	n.p.[d]

5d

12	H-Aib-OMe	46 [9]	62	62

6 [9]

[a]Conditions: (step 1) *(L)*-α-amino ester hydrochloride (1 equiv) and CDI (1.3 equiv) at 450 rpm, in a 12 mL inox jar with 50 balls (stainless steel, 5 mm Ø) for 40 min; (step 2) R^2NH_2 (1.6 equiv) and K_2CO_3 (3.6 equiv) at 450 rpm for 2 hours. A: the reaction was performed with no additive (dry-grinding); B: MeO-PEG-2000-OMe (450 mg mmol^{-1}); C: HO-PEG-3400-OH (450 mg mmol^{-1}) were added in the second step (wet-grinding conditions with a PEG additive; [b]isolated yields; [c]^{1}H NMR yield on the crude reaction mixture; [d]the reaction was not performed (n.p.); [e]the reaction yield was not determined (n.d.).

grinding, low toxicity and low vapour pressure, reducing the risk of explosions or overpressure that might be encountered on large scale LAG-procedures.

Supporting Information

Supporting Information File 1
Experimental procedures, characterization of new compounds and copies of ^{1}H and ^{13}C NMR spectra.
[http://www.beilstein-journals.org/bjoc/content/supplementary/1860-5397-13-3-S1.pdf]

Acknowledgements

References

1. Chen, J.; Spear, S. K.; Huddleston, J. G.; Rogers, R. D. *Green Chem.* **2005,** *7,* 64–82. doi:10.1039/b413546f
2. Prat, D.; Wells, A.; Hayler, J.; Sneddon, H.; McElroy, C. R.; Abou-Shehada, S.; Dunn, P. J. *Green Chem.* **2016,** *18,* 288–296. doi:10.1039/C5GC01008J
3. Knop, K.; Hoogenboom, R.; Fischer, D.; Schubert, U. S. *Angew. Chem., Int. Ed.* **2010,** *49,* 6288–6308. doi:10.1002/anie.200902672
4. Colacino, E.; Martinez, J.; Lamaty, F.; Patrikeeva, L. S.; Khemchyan, L. L.; Ananikov, V. P.; Beletskaya, I. P. *Coord. Chem. Rev.* **2012,** *256,* 2893–2920. doi:10.1016/j.ccr.2012.05.027
5. Kappe, C. O. *Angew. Chem., Int. Ed.* **2004,** *43,* 6250–6284. doi:10.1002/anie.200400655
6. Declerck, V.; Colacino, E.; Bantreil, X.; Martinez, J.; Lamaty, F. *Chem. Commun.* **2012,** *48,* 11778–11780. doi:10.1039/c2cc36286d
7. Giachi, G.; Frediani, M.; Oberhauser, W.; Lamaty, F.; Martinez, J.; Colacino, E. *ChemSusChem* **2014,** *7,* 919–924. doi:10.1002/cssc.201300997

8. Hasa, D.; Schneider Rauber, G.; Voinovich, D.; Jones, W.
    Angew. Chem., Int. Ed. **2015,** *54,* 7371–7375.
    doi:10.1002/anie.201501638
9. Konnert, L.; Dimassi, M.; Gonnet, L.; Lamaty, F.; Martinez, J.;
    Colacino, E. *RSC Adv.* **2016,** *6,* 36978–36986.
    doi:10.1039/C6RA03222B
10. Konnert, L.; Gonnet, L.; Halasz, I.; Suppo, J.-S.;
    Marcia de Figueiredo, R.; Campagne, J.-M.; Lamaty, F.; Martinez, J.;
    Colacino, E. *J. Org. Chem.* **2016,** *81,* 9802–9809.
    doi:10.1021/acs.joc.6b01832
11. Konnert, L.; Gonnet, L.; Halasz, I.; Suppo, J. S.;
    Marcia de Figueiredo, R.; Campagne, J.-M.; Lamaty, F.; Martinez, J.;
    Colacino, E. *J. Org. Chem.* **2016,** *81,* 12071.
    doi:10.1021/acs.joc.6b02671
12. Rightmire, N. R.; Hanusa, T. P. *Dalton Trans.* **2016,** *45,* 2352–2362.
    doi:10.1039/C5DT03866A
    The formalism for mechanochemically activated reactions was recently
    proposed by this group.
13. Duspara, P. A.; Islam, M. S.; Lough, A. J.; Batey, R. A. *J. Org. Chem.*
    2012, *77,* 10362–10368. doi:10.1021/jo302084a
14. Colacino, E.; Daïch, L.; Martinez, J.; Lamaty, F. *Synlett* **2007,**
    1279–1283. doi:10.1055/s-2007-980337
15. Colacino, E.; Villebrun, L.; Martinez, J.; Lamaty, F. *Tetrahedron* **2010,**
    66, 3730–3735. doi:10.1016/j.tet.2010.03.065
16. Bailey, F. E. J.; Koleske, J. V. *Poly(Ethylene Oxide);* Academic Press:
    New York, 1976.
17. Canale, V.; Tonucci, L.; Bressan, M.; d'Alessandro, N.
    Catal. Sci. Technol. **2014,** *4,* 3697–3704. doi:10.1039/C4CY00631C
18. Friščić, T. *J. Mater. Chem.* **2010,** *20,* 7599–7605.
    doi:10.1039/c0jm00872a
19. Friščić, T. *Chem. Soc. Rev.* **2012,** *41,* 3493–3510.
    doi:10.1039/c2cs15332g
20. Shimono, K.; Kadota, K.; Tozuka, Y.; Shimosaka, A.; Shirakawa, Y.;
    Hidaka, J. *Eur. J. Pharm. Sci.* **2015,** *76,* 217–224.
    doi:10.1016/j.ejps.2015.05.017
21. Juribašić, M.; Halasz, I.; Babić, D.; Cinčić, D.; Plavec, J.; Ćurić, M.
    Organometallics **2014,** *33,* 1227–1234. doi:10.1021/om500008v
22. Chen, L.; Regan, M.; Mack, J. *ACS Catal.* **2016,** *6,* 868–872.
    doi:10.1021/acscatal.5b02001

Contribution of microreactor technology and flow chemistry to the development of green and sustainable synthesis

Flavio Fanelli, Giovanna Parisi, Leonardo Degennaro[*] and Renzo Luisi[*]

Abstract

Microreactor technology and flow chemistry could play an important role in the development of green and sustainable synthetic processes. In this review, some recent relevant examples in the field of flash chemistry, catalysis, hazardous chemistry and continuous flow processing are described. Selected examples highlight the role that flow chemistry could play in the near future for a sustainable development.

Introduction

Green chemistry's birth was driven by the necessity to consider and face the urgent question of sustainability. Chemical production concerns an extended range of fields such as textiles, construction, food, cosmetic components, pharmaceuticals and so forth. An innovative approach to the chemistry world requires new strategies and criteria for an intelligent chemistry. It is understood that all this matter has big implications in economy and politics. Recent studies predicted a growth of green chemical processing up to $100 billion in 2020 (Pike Research study) [1]. All this offers important and arduous challenges expressed in terms of new synthetic strategies using sustainable, safe, and less toxic materials. On green chemistry we can read Paul Anastas and John Warne's 12 principles, set up in 1998, which

illustrate the characteristics of a greener chemical process or product [2]. Microreactor technology and flow chemistry could play a pivotal role in the context of sustainable development. In fact, flow chemistry is becoming a new technique for fulfilling several of the twelve green chemistry principles. The microreactor approach, could provide protection, preserves atom economy, guarantees less hazardous chemical synthesis and allows the use of safer solvents and auxiliaries. Furthermore, it pushes towards designing of chemistry with a lower environmental and economic impact, enhance the importance of catalysis, allows real-time analysis for pollution prevention and provides inherently safer chemistry (Figure 1) [3]. Without claiming to be exhaustive, in this review we report recently

Figure 1: Microreactor technologies and flow chemistry for a sustainable chemistry.
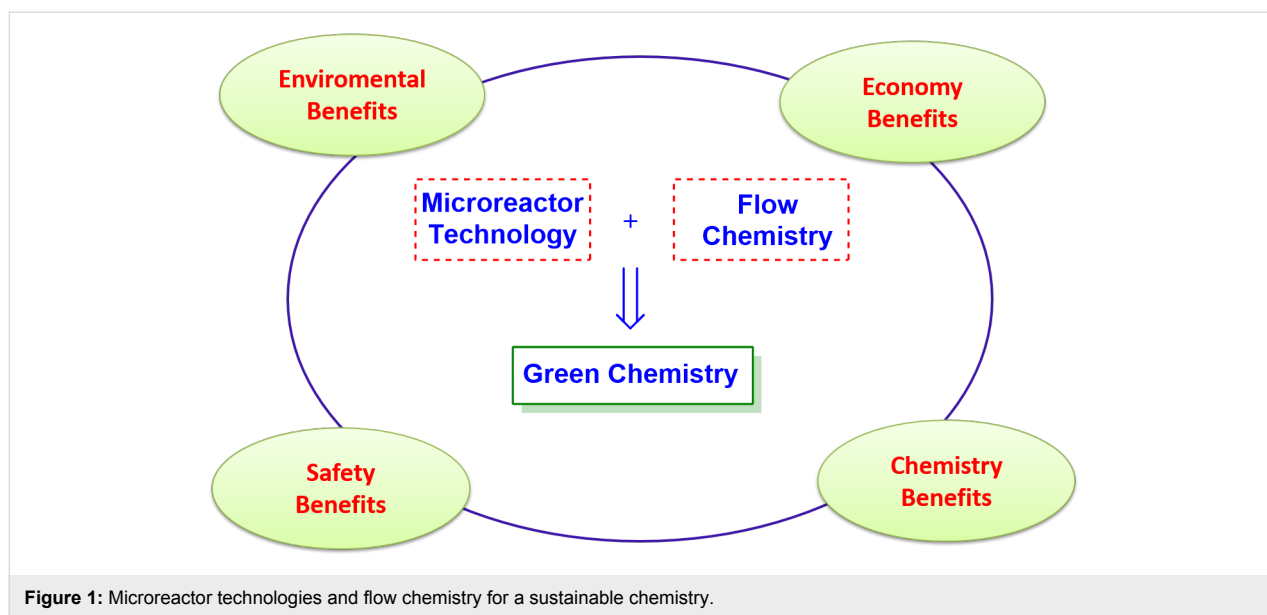
published representative synthetic applications that demonstrate the growing contribution of flow chemistry and microreactor technology in green and sustainable synthesis [4-7].

Review
Flow microreactors: main features

The peculiar properties of microreactors [8] derive from their small size and can be ascribed mainly to the following characteristics: a) fast mixing: in a flow microreactor, in striking contrast to batch conditions, mixing takes place by molecular diffusion so that a concentration gradient can be avoided; b) high surface-to-volume ratio: the microstructure of microreactors allows for a very rapid heat transfer enabling fast cooling, heating and, hence, precise temperature control; c) residence time: it is the period of time the solution of reactants spend inside the reactor, and it gives a measure of the reaction time. The residence time is strictly dependent on the characteristics of the reactor (i.e., length of the channels, volume), and on the flow rate. The residence time is one of the crucial factors to be considered in optimizing flow reactions, especially when unstable or short-lived reactive intermediates are concerned. Microreactor technology provides also several benefits. Safety benefits, because of the high efficiency in heat exchange, and avoided accumulation of unstable intermediates. Economy benefits, due to lower manufacturing and operating costs, reduced work-up procedures, use of less raw materials and solvents and reduced waste. Chemistry benefits associated to the use of microreactor technology are the improved yields and selectivities, the possibility to conduct reactions difficult or even impossible to perform in batch, and the use of reaction conditions that allow exploring new chemical windows [9].

Contribution of flash chemistry to green and sustainable synthesis

The concept of flash chemistry as a "*field of chemical synthesis using flow microreactors where extremely fast reactions are conducted in a highly controlled manner to produce desired compounds with high selectivity*" was firstly introduced by Yoshida [10]. Flash chemistry can be considered a new concept in both organic and sustainable synthesis involving chemical transformations that are very difficult or practically impossible to conduct using conventional batch conditions. With the aim to show how flow microreactor technology and flash chemistry could contribute to the development of a sustainable organic synthesis, very recent examples have been selected and will be discussed here. In the context of green chemistry [11], protecting-group free organic synthesis has received particular attention in the last years, because of atom economy [12-15] and reduction of synthetic steps [16]. It has been demonstrated by Yoshida that protecting-group-free synthesis could be feasible using flash chemistry and microreactor technology [17,18]. Recently, Yoshida and co-workers developed flash methods for the generation of highly unstable carbamoyl anions, such as carbamoyllithium, using a flow microreactor system [19]. In particular, they reported that starting from different substituted carbamoyl chloride **1** and lithium naphthalenide (LiNp) it was possible to generate the corresponding carbamoyllithium **2**, that upon trapping with different electrophiles provided several amides and ketoamide **3** (Scheme 1).

The use of an integrated microflow system allowed the preparation of functionalized α-ketoamides by a three-component reaction between carbamoyllithium, methyl chloroformate and

Scheme 1: A flow microreactor system for the generation and trapping of highly unstable carbamoyllithium species.
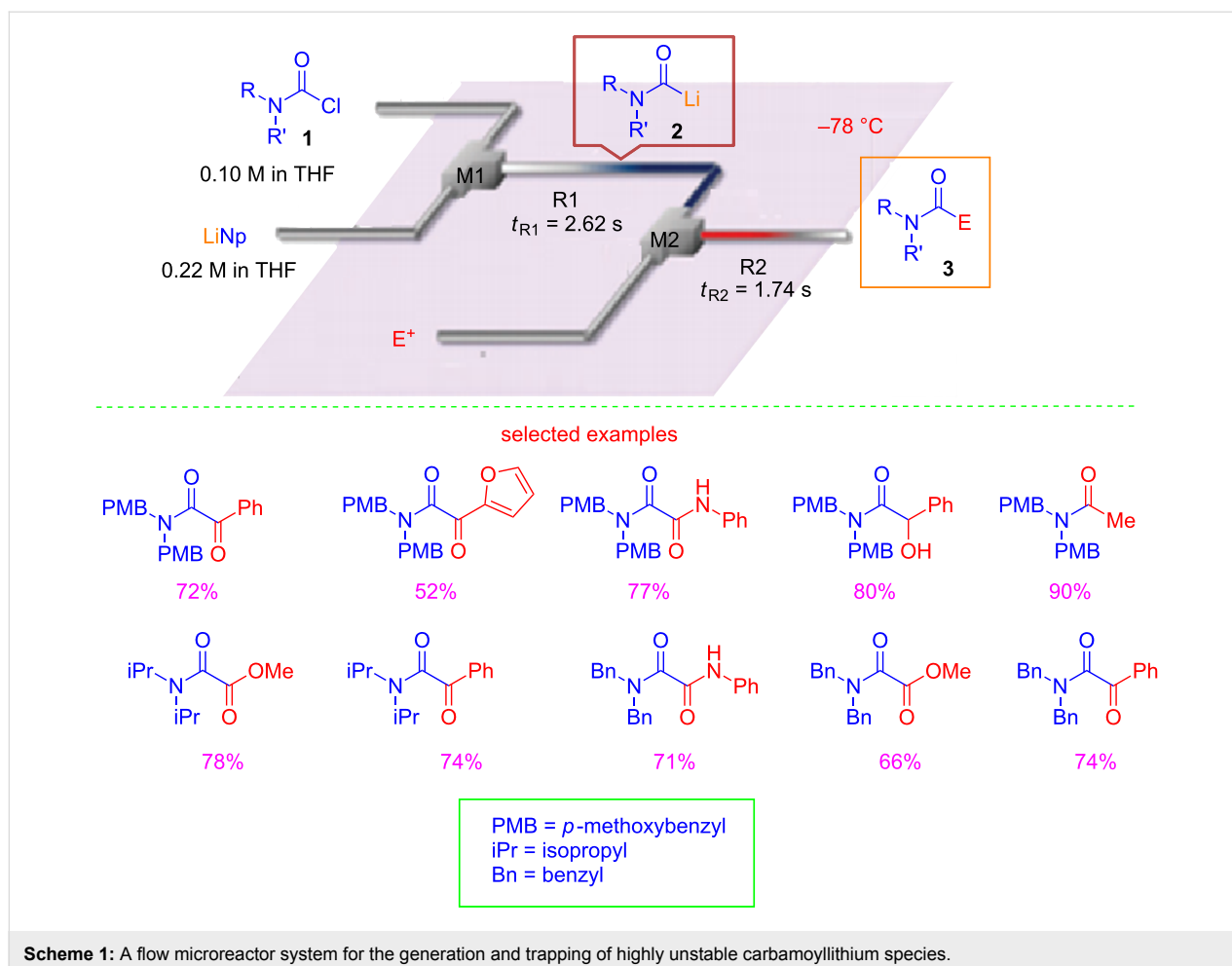
organolithium compounds bearing sensitive functional groups (i.e., NO$_2$, COOR, epoxide, carbonyl) (Scheme 2).
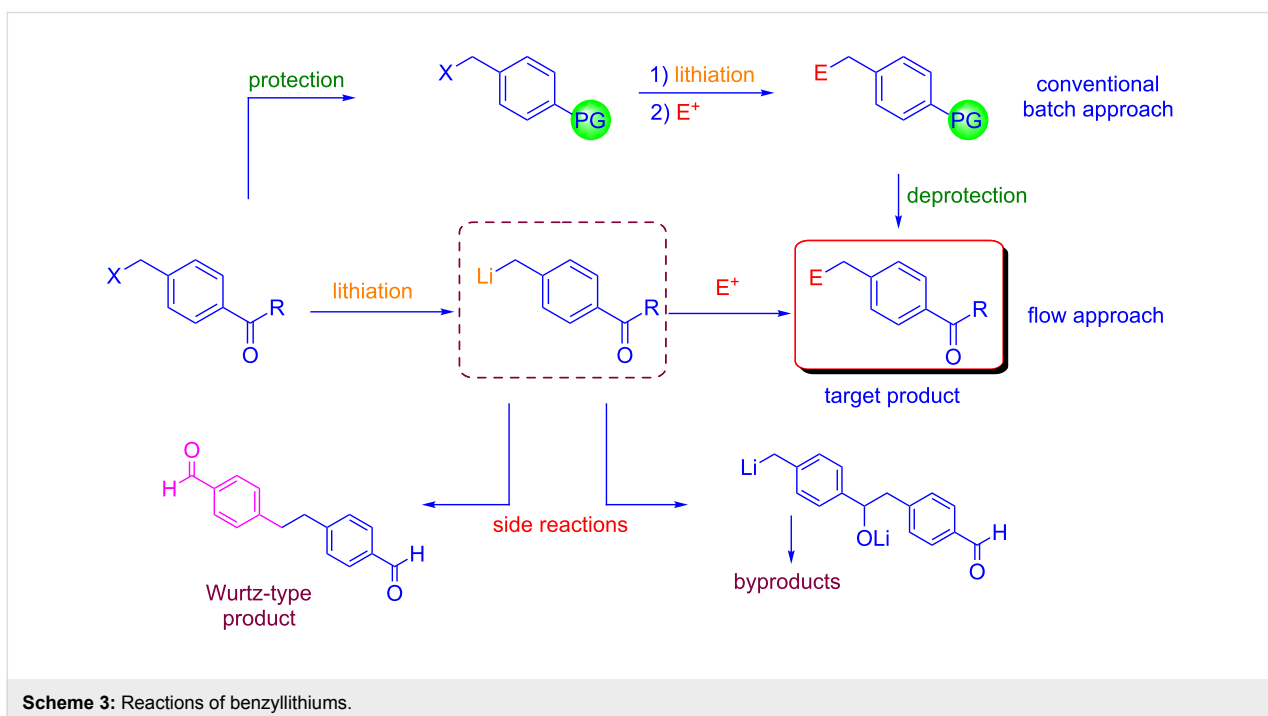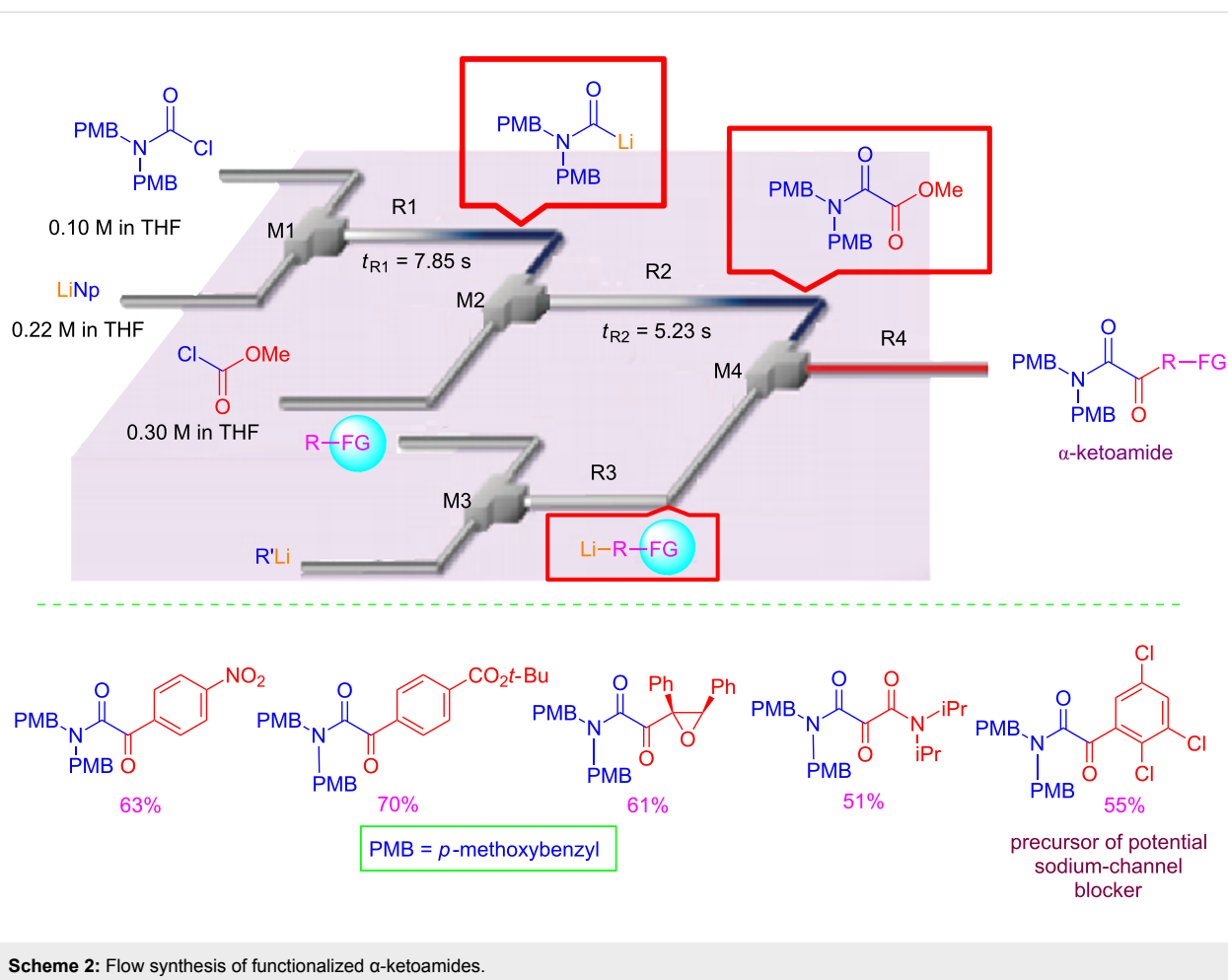
It should be stressed that this kind of sequential transformations are practically impossible to perform using conventional batch chemistry because of the incompatibility of sensitive functional groups with organolithiums, and because of the high chemical and thermal instability of the intermediates.

In 2015 Yoshida reported another remarkable finding on the use of protecting-group-free organolithium chemistry. In particular, the flash chemistry approach was exploited for generating benzyllithiums bearing aldehyde or ketone carbonyl groups [20]. This reaction could be problematic for two reasons: a) the competing Wurtz-type coupling, (i.e., the coupling of benzyllithiums with the starting benzyl halides); b) the nucleophilic attack of organolithium species to aldehyde or ketone carbonyl groups (Scheme 3).

The authors reported that the extremely fast micromixing avoided undesired Wurtz-type coupling [21,22]. It is well

known, that competitive reactions can be controlled or even avoided under fast micromixing [23-27]. Moreover, high-resolution residence time control was essential for survival of carbonyl groups. In fact, this transformation can be achieved only with a residence time of 1.3 ms at −78 °C. Under these flow conditions, the aldehyde or ketone carbonyl moiety can survive the nucleophilic organolithium attack. Remarkably, the flow microreactor system allowed also the generation of benzyllithiums at 20 °C, rather than under cryogenic (−95 °C) conditions adopted with a conventional batch protocol. In addition, THF could be used in place of mixed solvents (Et$_2$O/THF/light petroleum). Under the optimized conditions, the reactions of benzyllithiums with different electrophiles, gave adduct products in good yields (Scheme 4).

Another useful aspect of the flash chemistry relies on the possibility to generate highly reactive intermediates, such as halomethyllithium carbenoids, that need to be used under internal-quenching technique in batch mode. In 2014, the first example of effective external trapping of a reactive chloromethyllithium (CML) has been reported [28].

Scheme 2: Flow synthesis of functionalized α-ketoamides.

Scheme 3: Reactions of benzyllithiums.

Scheme 4: Trapping of benzyllithiums bearing carbonyl groups enabled by a flow microreactor. (Adapted with permission from [18], copyright 2015 The Royal Society of Chemistry).
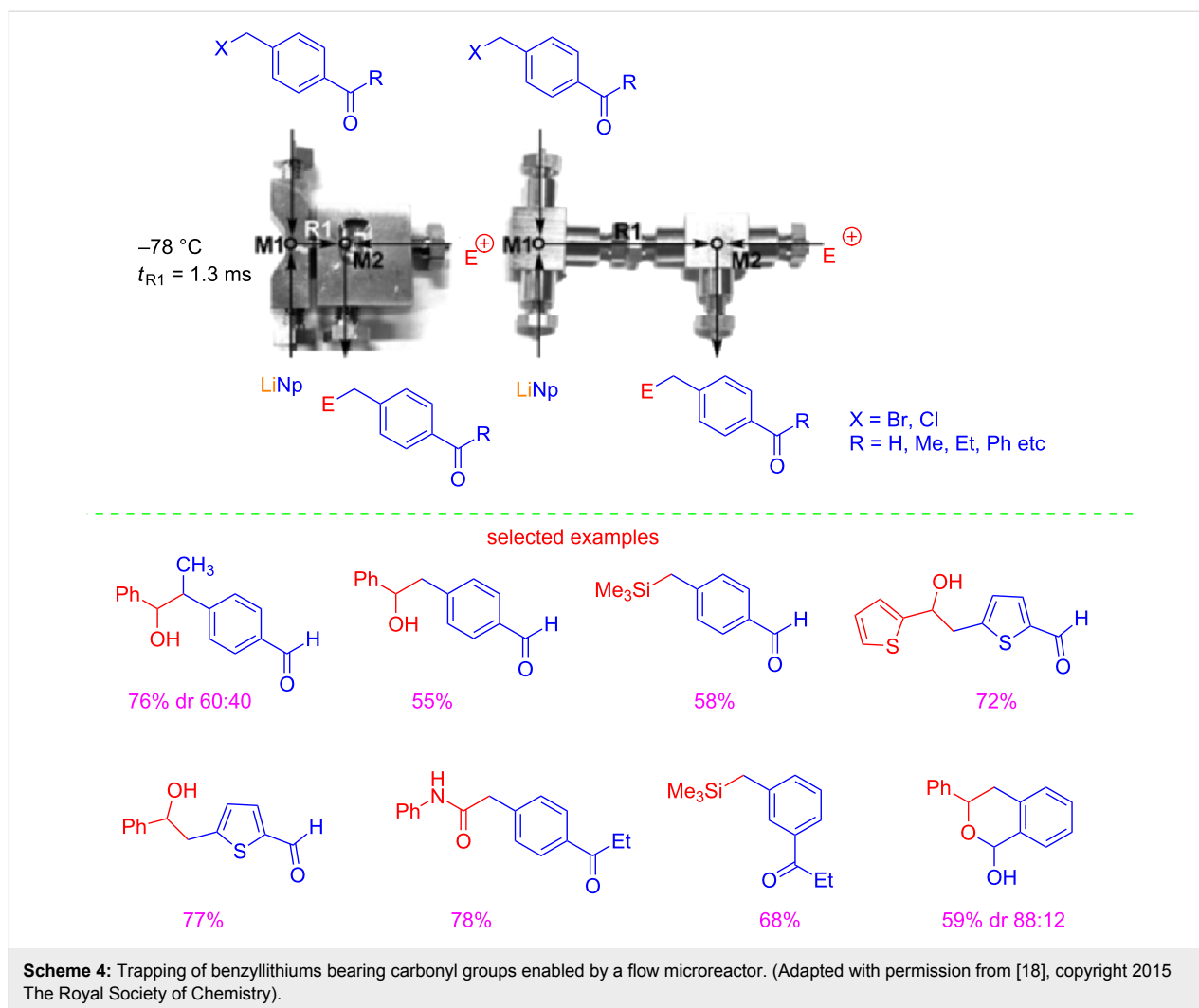
α-Haloalkyllithiums are a useful class of organometallic reagents widely employed in synthetic chemistry. In fact, they allow the direct homologation of carbonyl compounds and imines leading to β-halo-alcohols and amines that are useful building blocks [29-31]. This work represents a remarkable example of flash chemistry, and has elements of sustainability considering that in batch macroreactors, in order to avoid metal-assisted α-elimination, in situ quenching, an excess of reagents, and very low temperature are required [32,33].

Running the reaction in a flow system at −40 °C, by using residence times between 0.18–0.31 s high yields of homologated products have been obtained under external quenching conditions (Scheme 5).

The results described above nicely show the potential, as green technology, of flow microreactor systems for synthetic processes involving highly unstable intermediates. Another nice example on the use of microreactor technology for the development of sustainable chemical processes, is represented by the direct introduction of the *tert*-butoxycarbonyl group into organometallic reagents [34]. The reaction between organolithium reagents and di-*tert*-butyl dicarbonate run under flow conditions, allowed a straightforward preparation of several *tert*-butyl esters. The use of a flow process resulted more efficient, versatile and sustainable compared to batch. Moreover, this operationally simple procedure complements well with the already available strategies for the preparation of *tert*-butyl esters, avoiding the use of inflammable and explosive gaseous isobutylene [35], the use of harsh conditions [36], the use of peroxides [37], the use of toxic gas such as CO or transition metals [38-42]. The flow process, for the direct C-*tert*-butoxy-carbonylation of organolithiums, has been optimized in a green solvent such as 2-MeTHF by a precise control of the residence time, and without using cryogenic conditions (Scheme 6). In addition, many organolithiums were generated from the corresponding halo compounds by a halogen/lithium exchange reaction using hexyllithium as a more sustainable base [43,44].

Scheme 5: External trapping of chloromethyllithium in a flow microreactor system.
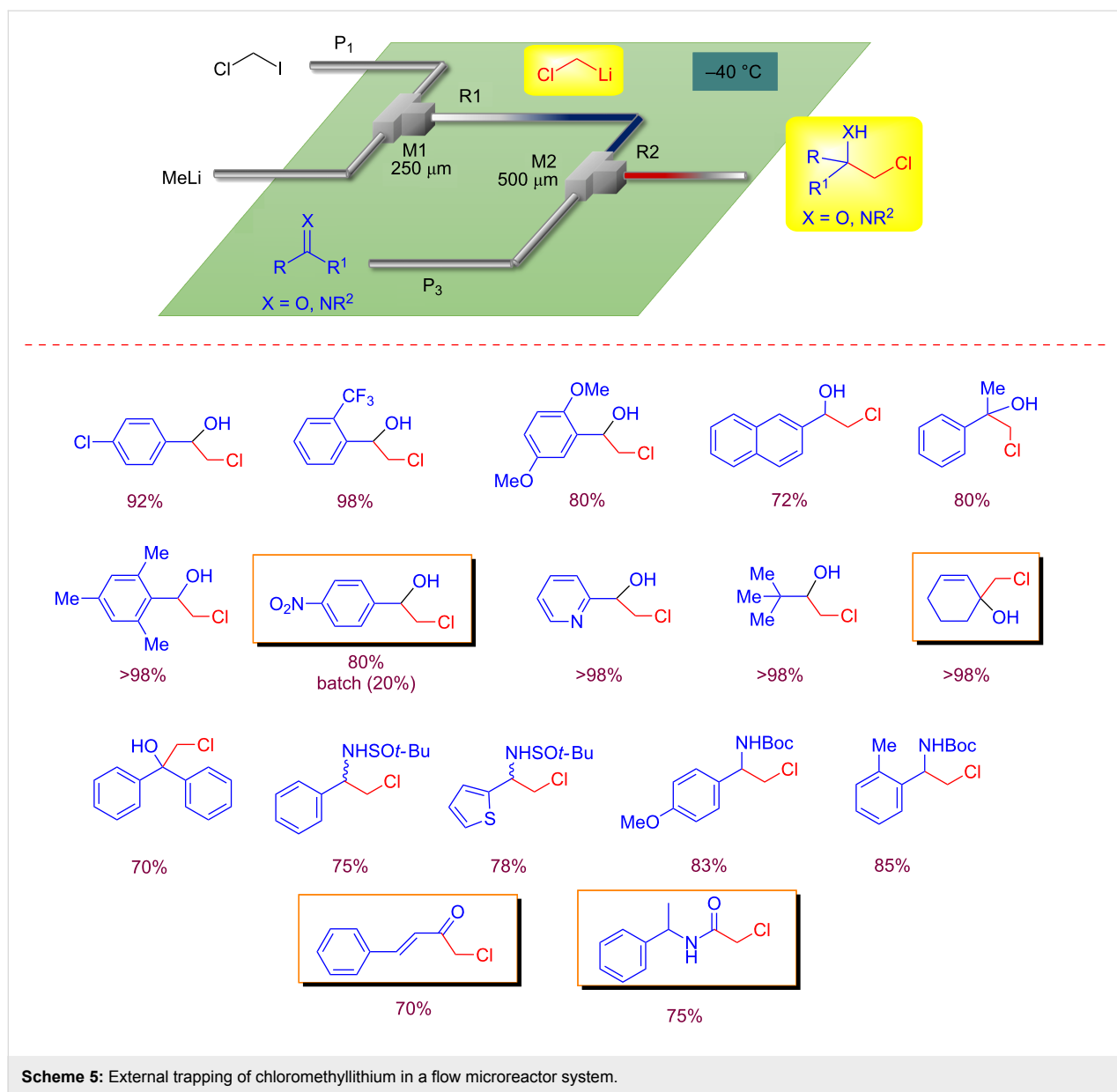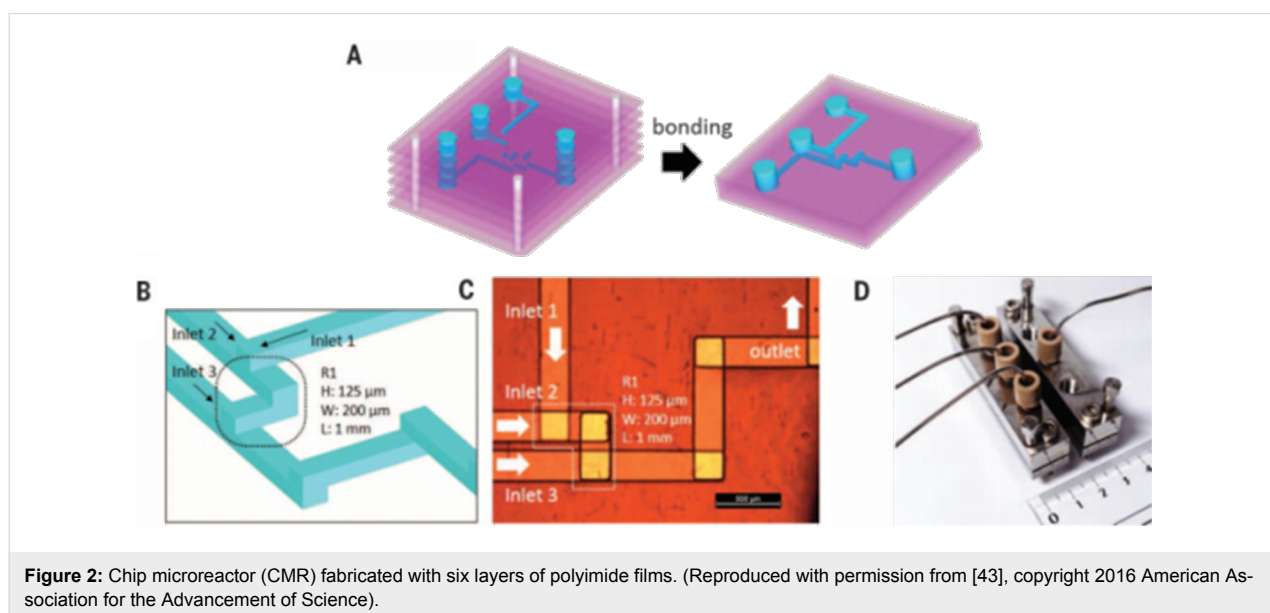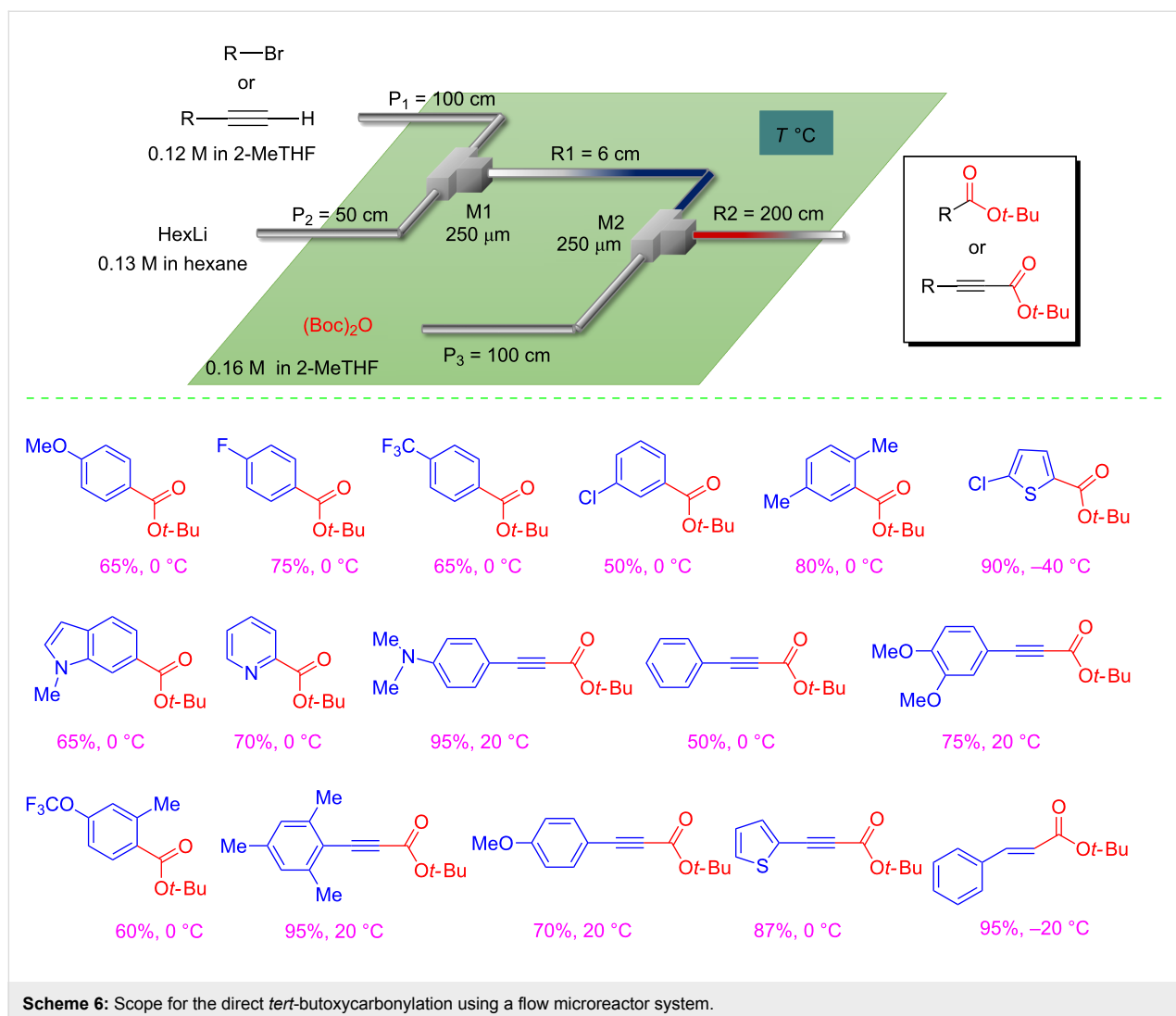
The concept of flash chemistry has been successfully employed for outpacing fast isomerization reactions. The accurate control of the residence time, realized in a microreactor, could suppress or avoid isomerization of unstable intermediates. This is often unavoidable when the same reactions are run in batch mode [45-47].
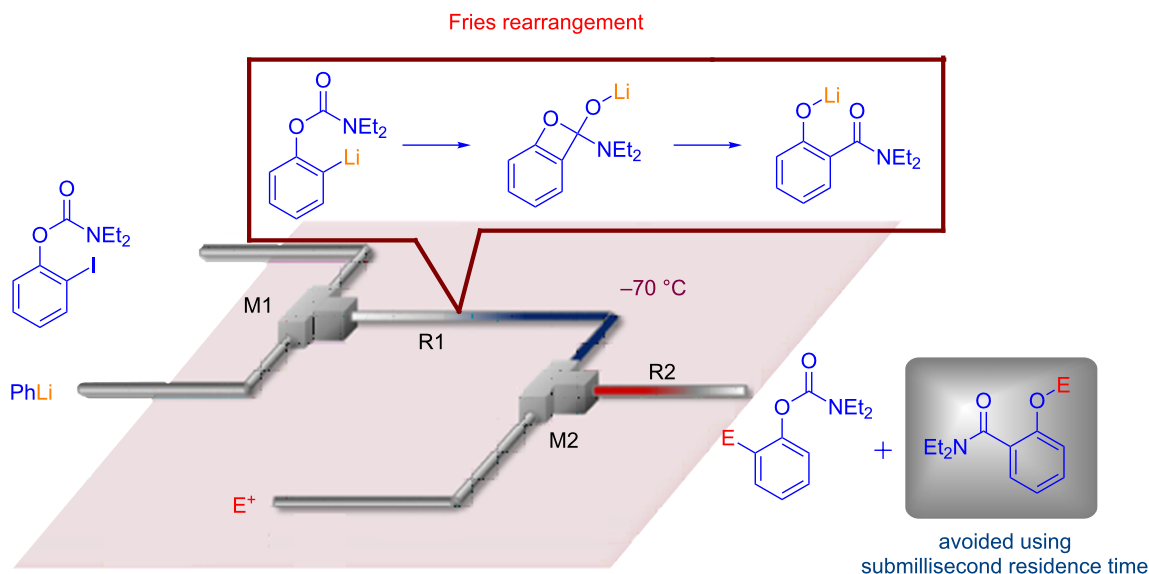
Yoshida and Kim recently provided an astonishing example on the potential of flash chemistry in controlling fast isomerization of organolithiums [48]. The authors designed a chip microreactor (CMR), able to deliver a reaction time in the range of submilliseconds (0.33 ms) under cryogenic conditions. By using such an incredible short residence time, it was possible to overtake the very rapid anionic Fries rearrangement, and chemose-

lectively functionalize *ortho*-lithiated aryl carbamates (Scheme 7).

This CMR has been developed choosing a fluoroethylene propylene–polymide film hybrid for fabrication because this material offers exceptional physical toughness at low temperature and high pressure as well as chemical inertness. The most relevant aspect of this microreactor, concerns the 3D design of the mixing zone (Figure 2). The mixing efficiency was evaluated on the basis of computational fluids dynamics (CFD). The simulation results showed that serpentine 3D-structured channels (Figure 2), possessing five turns after each mixing point in a total length of 1 mm, was able to deliver the highest mixing efficiency. The inner volume for the reactor was of 25 µL. This

Scheme 6: Scope for the direct *tert*-butoxycarbonylation using a flow microreactor system.

Figure 2: Chip microreactor (CMR) fabricated with six layers of polyimide films. (Reproduced with permission from [43], copyright 2016 American Association for the Advancement of Science).
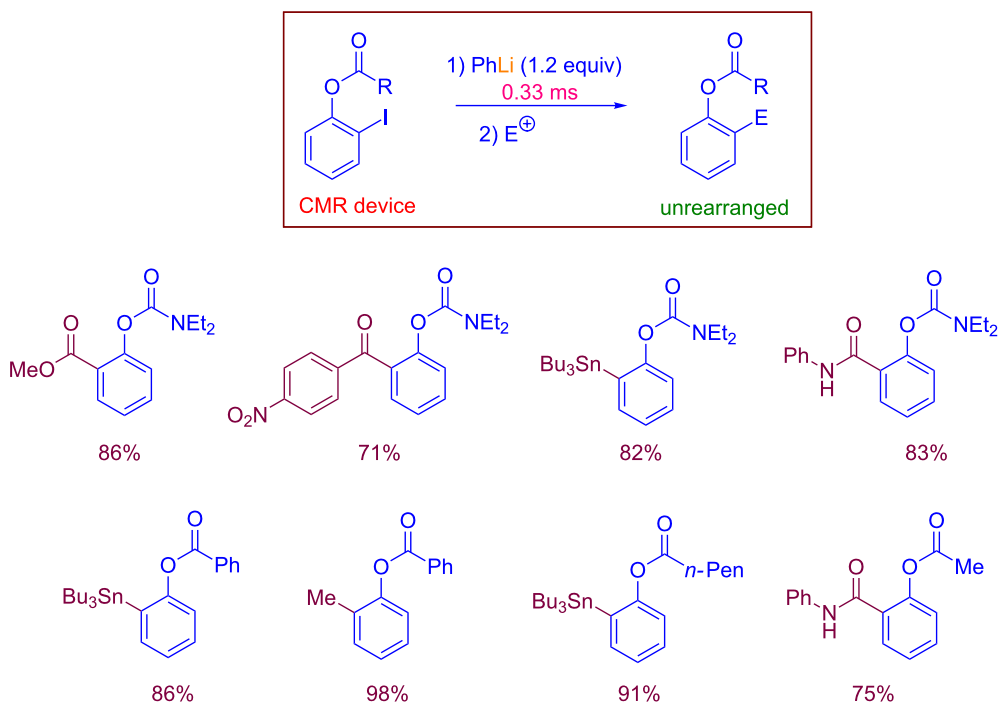
Scheme 7: Control of anionic Fries rearrangement reactions by using submillisecond residence time. (Adapted with permission [43], copyright 2016 American Association for the Advancement of Science).

CMR provides mixing efficiency levels of 95% with a total flow rates of 7.5 mL/min corresponding to a residence time of about 0.3 milliseconds.

To show the potential use of this microdevice in organic synthesis, the synthesis of Afesal [49], a biologically active compound having anthelmintic activity was reported as application.

This outstanding result by Yoshida and Kim, demonstrates how microdevices and flash chemistry could contribute to the development of new sustainable synthetic strategies, and how micro-

reactor technology could help in taming the reactivity of unstable species [50].

Contribution of continuous-flow metal-, organo-, and photocatalysis in green chemistry

The development of continuous-flow catalysis is appealing because it combines the advantages of a catalytic reaction with the benefits of flow microreactors. Under homogeneous conditions a soluble catalyst, which flows through the reactor together with the reactants, is employed. At the end of the process, a separation step would be required in order to remove the catalyst and byproducts. On the other hand, heterogeneous catalysis is widely used in the synthesis of bulk and fine chemicals. In a continuous-flow process, the catalyst can be fixed on a suitable hardware, and the reaction mixture allowed to flow

through the system. The use of recyclable catalysts in continuous-flow conditions represents an innovative strategy for the development of more environmentally friendly synthesis. In the last decade, organic photochemistry got a sort of renaissance, emerging as useful approach in modern sustainable and green synthesis.

Concerning the heterogeneous catalysis with palladium, practical procedures for recovering and reusing of the catalysts have been recently reported [51-53]. A versatile Pd-catalysed synthesis of polyfunctionalized biaryls, using a flow microreactor, has been recently reported by Yoshida [54]. Using the integrated microflow system reported in Scheme 8, arylboronic esters were prepared by a lithiation/borylation sequence, and used in a Suzuki–Miyaura coupling in a monolithic reactor. A remarkable aspect of the process was the use of an integrated sup-
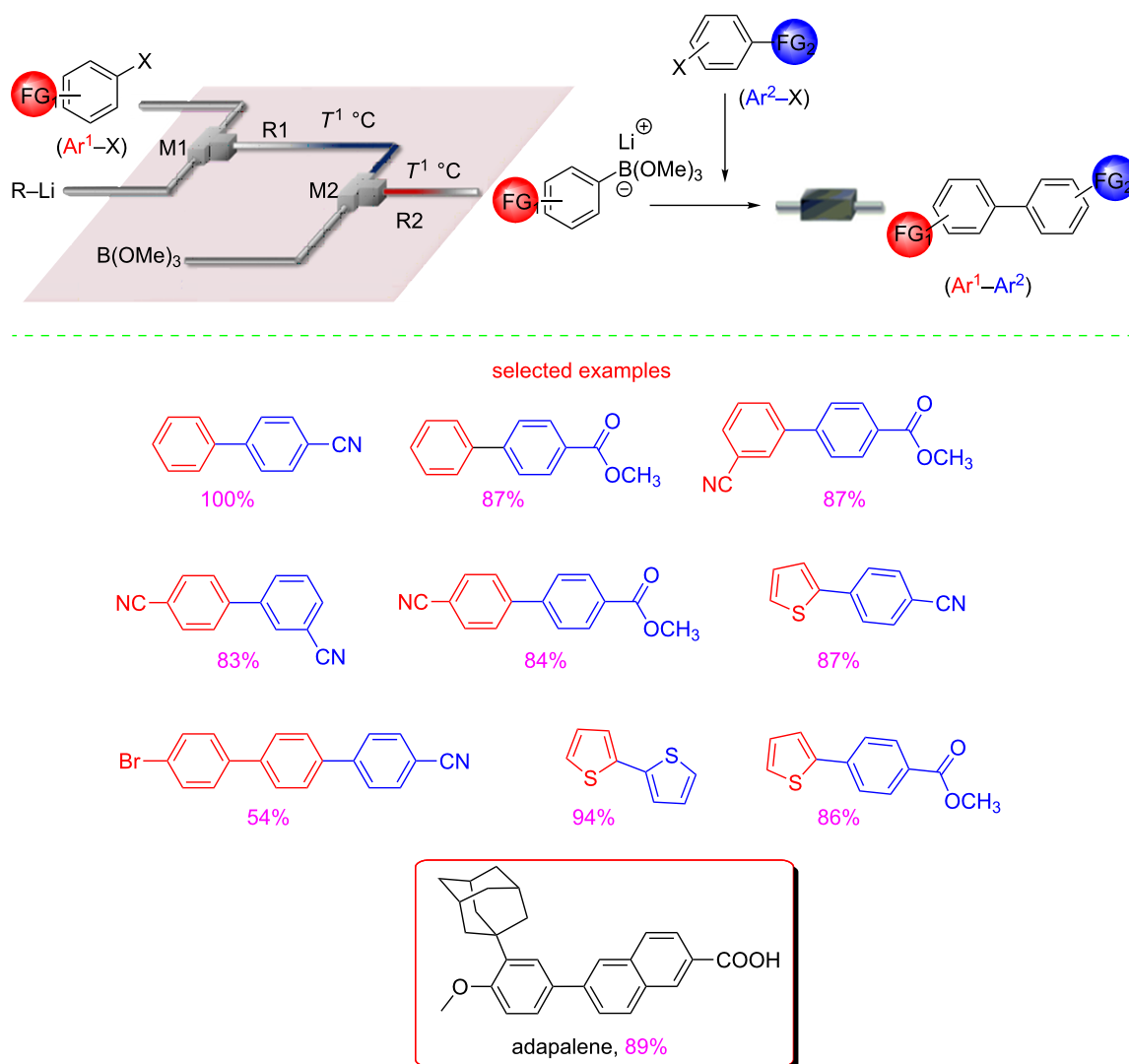
Scheme 8: Flow microreactor system for lithiation, borylation, Suzuki–Miyaura coupling and selected examples of products.

ported monolithic Pd(0) catalyst that allowed to perform cross-coupling reactions in continuous flow mode (Scheme 8).

This integrated microflow system allow to handle the borylation of aryl halides (Ar^{1}X), and the subsequent Suzuki–Miyaura coupling using different aryl halide (Ar^{2}X). Without requiring the protection of sensitive functionalities, running the flow system using a residence time (t_R) of about 4.7 min at a temperature above 100 °C, high yields of coupling products were obtained. Noteworthy, the Suzuki–Miyaura coupling did not require the use of a base. The authors applied the presented method to the synthesis of adapalene, used in the treatment of acne, psoriasis, and photoaging.

Fluorinated aromatic compounds are extremely important in agrochemical, pharmaceutical and medicinal fields [55-58]. Buchwald and co-workers suggested a telescoped homocatalysis procedure consisting of a three-step sequence (metalation,

zincation and Negishi cross-coupling) which furnishes an easy access to a variety of functionalized 2-fluorobiaryl and heteroaryl products (Scheme 9) [59]. This strategy is rightfully considered green because it guarantees the employment of readily available and cheap starting materials, the safe handling of highly thermally unstable or dangerous intermediates, and the use of higher temperature with respect to the batch mode in which the proposed reactions have to be carried out at −78 °C.

The use of 2-MeTHF as greener solvent, contributes to further validate the green procedure. The 2-MeTHF solutions of fluoroarenes **4** together with the hexane solution of *n*-BuLi were pumped into the flow system at −40 °C. The generated organozinc intermediate meets the solution of haloarenes and the catalyst, leading to the formation of the desired products **5a–j** (Scheme 9). Noteworthy, the homogeneous catalysis requires only 1% of the XPhos-based palladium catalyst. A

Scheme 9: Experimental setup for the flow synthesis of 2-fluorobi(hetero)aryls by directed lithiation, zincation, and Negishi cross-coupling. (Adapted with permission from [53], copyright 2016 Wiley-VCH Verlag GmbH & Co. KGaA, Weinheim).
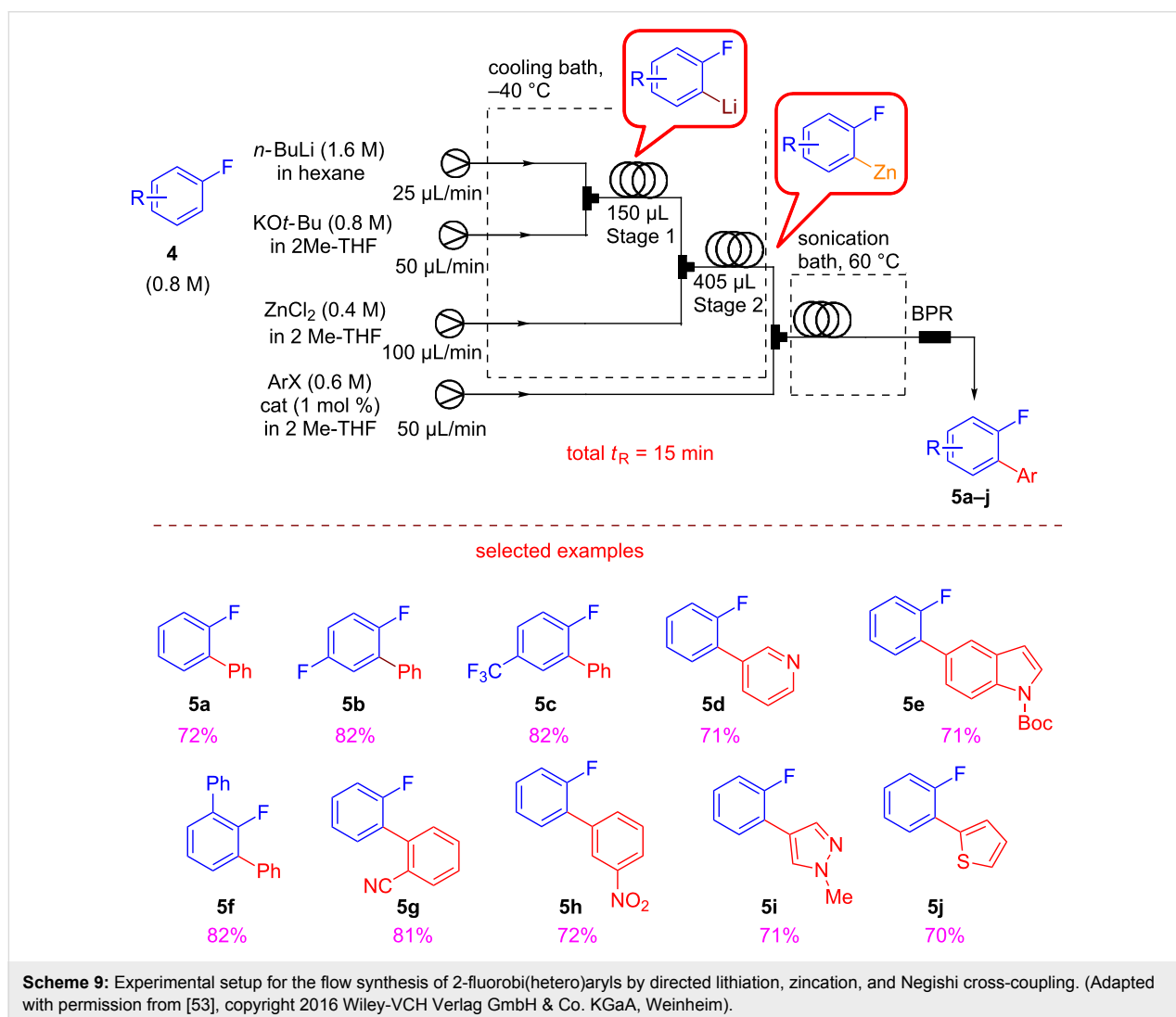
sonication bath was employed to prevent clogging and the reaction required a residence time of 15 min.
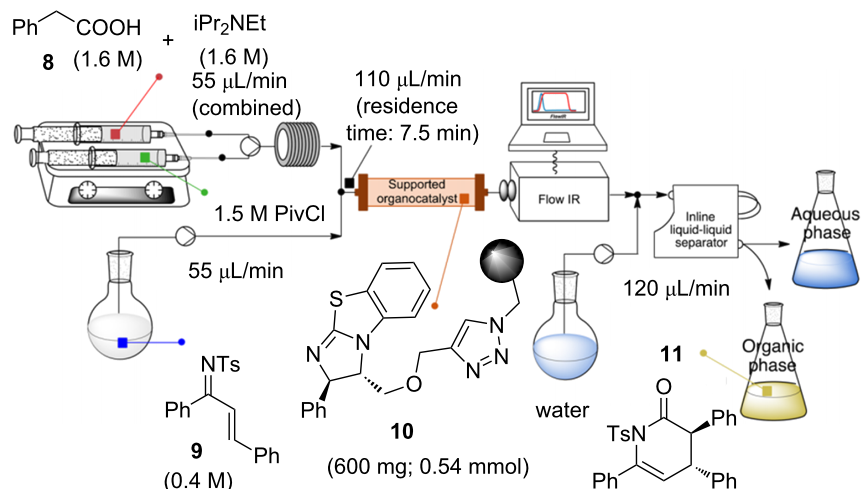
Next, they turned their attention to the arylation of fluoro-substituted pyridines. The regioselective lithiation of halo-pyridines with lithium diisopropylamide (LDA) was conducted under mild conditions on substrate **6** (Scheme 10). The addition of a little amount of THF was necessary in order to avoid clogging and the tendency of the lithiated intermediate to eliminate.

The optimized conditions were suitable for the functionalization of 2-fluoropyridine, 2,6- difluoropyridine and 4-(trifluoromethyl)pyridine leading to products **7a–g** reported in Scheme 10. Another promising field is the sustainable flow organocatalysis, and recently Pericàs reported an interesting synthesis and application of a recyclable immobilized analogue

of benzotetramisole (BMT) used in a catalytic enantioselective Michael addition/cyclization reactions under continuous-flow conditions (Scheme 11) [60].

Resin-bound catalyst **10** was swollen with dichloromethane in a medium-pressure chromatography column used as a reactor. Dichloromethane solutions of substrate **9** reacted with the mixed phenylacetic pivalic anhydride (deriving from phenylacetic acetic (**8**) and pivaloyl chloride) inside the catalytic reactor producing the expected products **11**. This ingenious system was equipped with an in-line FTIR probe, for monitoring the transformation, and an in line liquid–liquid separator to avoid tedious work-up procedures, thus saving solvents, resources and optimizing work times. This system was demonstrated to work for 11 h with higher conversion and enantioselectivity (er >99.9%) in comparison to the batch mode [61]. Pericàs and co-workers taking advantage of the high catalytic

Scheme 10: Experimental setup for the coupling of fluoro-substituted pyridines. (Adapted with permission from [53], copyright 2016 Wiley-VCH Verlag GmbH & Co. KGaA, Weinheim).
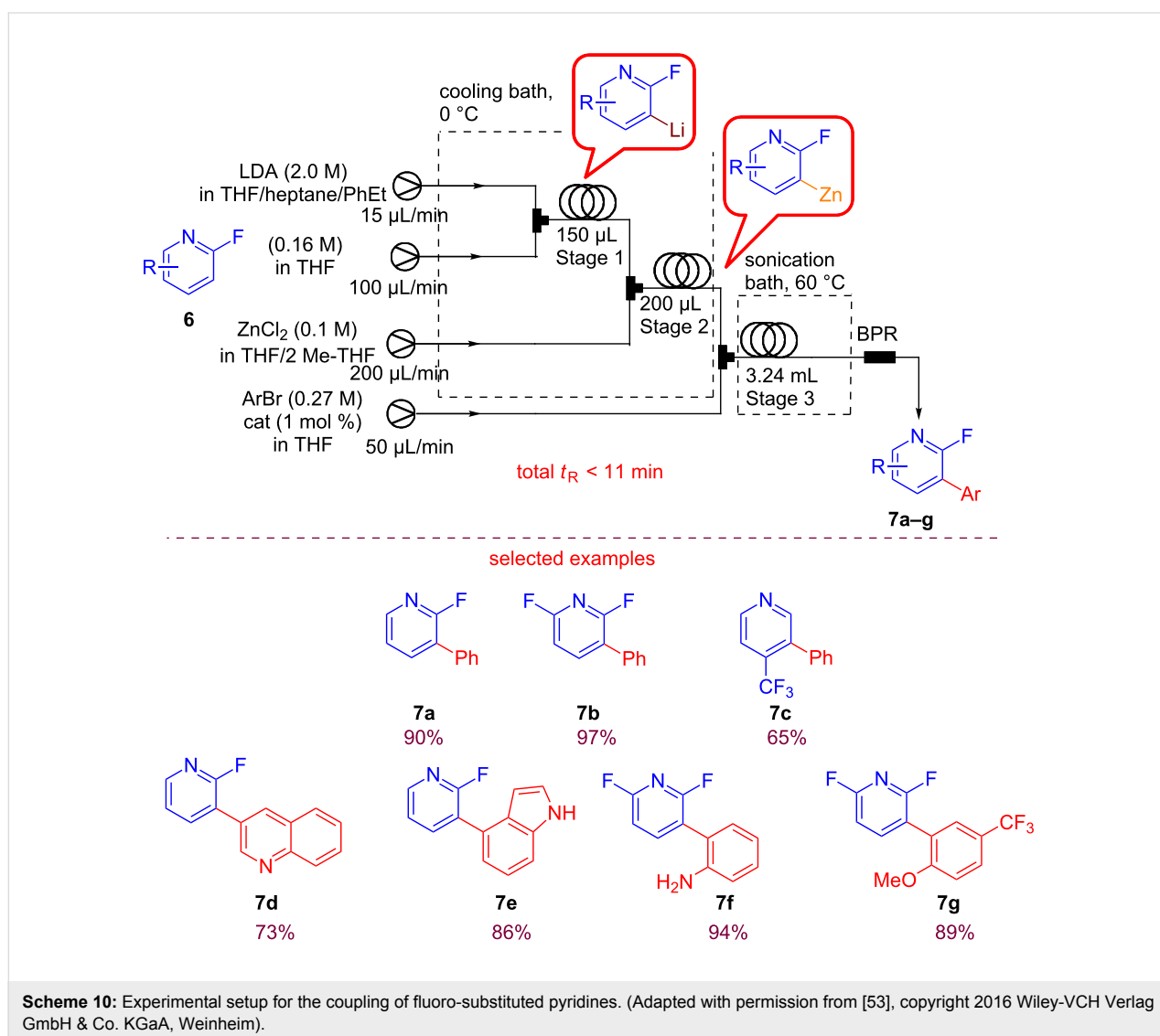
Scheme 11: Continuous flow process setup for the preparation of **11** (Reproduced with permission from [54], copyright 2015 American Chemical Society).

activity, robustness and recyclability of the supported catalyst, performed also straightforward gram synthesis of target compounds.

In the context of photocatalysis and oxidations using flow microreactors [62,63], Noël reported a metal-free photocatalytic aerobic oxidation of thiols to disulfides under continuous-flow conditions [64]. Disulfides are useful molecules employed as drugs, anti-oxidants or pesticides as well as rubber vulcanizing agents [65]. Symmetric disulfides are generally obtained by oxidative coupling of thiols [66]. Noël and co-workers set up a microflow system equipped with a mass flow controller (MFC) able to introduce pure oxygen as the oxidant to oxidize a solution of thiol containing 1% of Eosin Y. The flow stream was exposed to white LED light in order to activate the reaction, and a dilution with pure EtOH was needed at the output to avoid clogging (Scheme 12). The residence time of 20 min guaranteed a limited irradiation time and high purity of the products.

The disulfides were obtained with excellent yields, and the process was executed on challenging thiols as in the case of disulfide **12** (Scheme 12), used as food flavour additive [67]. To demonstrate the usefulness of the flow methodology, and its applicability, the photocatalytic aerobic oxidation of a peptide to obtain oxytocin in continuous flow was reported (Scheme 12). Full conversion was achieved in water with 200 s of residence time.

Noël optimized, for the first time, a trifluoromethylation of aromatic heterocycles by continuous-flow photoredox catalysis.

The process benefited from the use of microreactor technology and readily available photocatalysts. The process was also employable for perfluoroalkylation. The developed process occurred in less time with respect to batch mode, and under milder conditions. The set-up of the reactor allowed for the use of gaseous CF_3I by means of a mass flow controller. Selected examples of trifluoroalkylated products are reported in Scheme 13 [68].

Tranmer reported a "traceless reagents" chemistry with the continuous-flow photosynthesis of 6(5*H*)-phenanthridinones, poly(ADP-ribose) polymerase (PARP) inhibitors [69]. The relevance of the work resides in the use of green solvents, the absence of heavy metals, the use of convenient temperatures, and the increased safety by eliminating UV-exposure locating the UV lamp within the microreactor. Hazard of fires caused by the hot UV lamps approaching the auto-ignition temperature of flammable solvents, very often underestimated, is totally prevented thanks to a specific cooling system. 2-Halo-*N*-aryl-benzamides were converted into 6(5*H*)-phenanthridinones by a photocyclization reaction. In order to run this step, a flow system with a photochemical reactor equipped with a medium pressure Hg lamp and 10 mL reactor coil, was employed. Good yields were obtained from different 2-chlorobenzamides disclosing that either electron-donating or electron withdrawing *ortho*-substituents were tolerated (Scheme 14).

A metal- and catalyst-free arylation procedure carried out under continuous-flow conditions was recently reported by Fagnoni [70]. This photochemical process allowed for the preparation of a wide range of synthetic targets by Ar–Csp^3, Ar–Csp^2 and
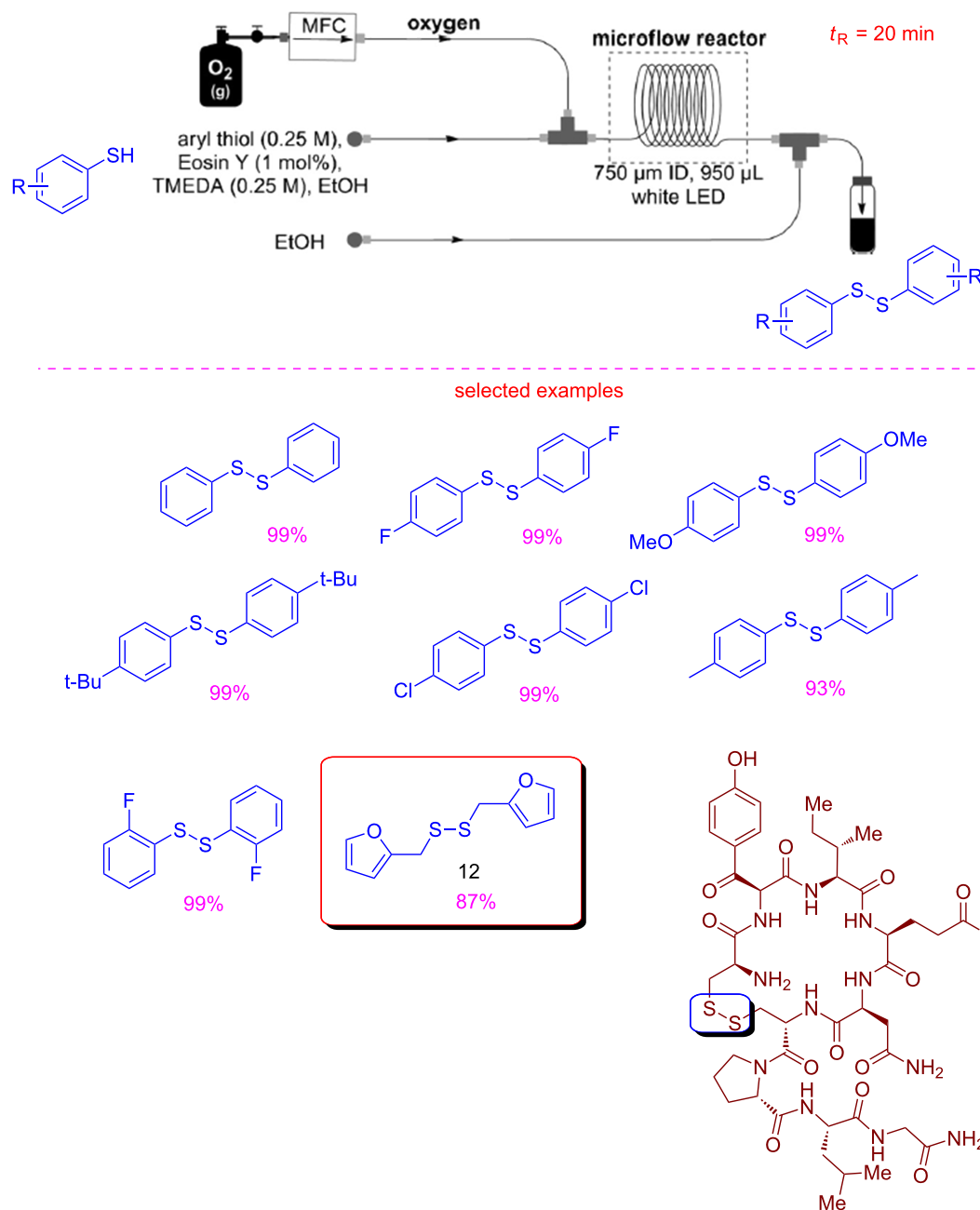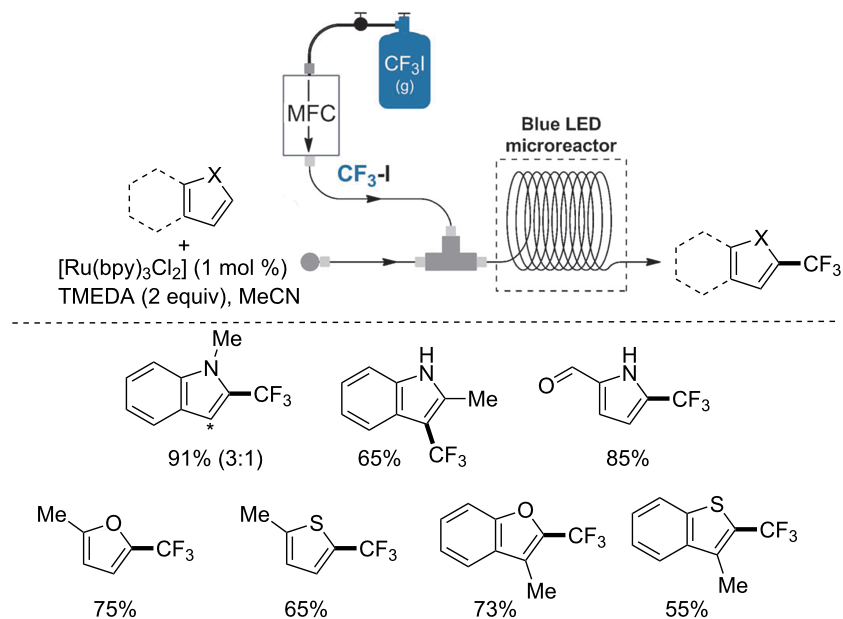
Scheme 12: Continuous-flow photocatalytic oxidation of thiols to disulfides.

Ar–Csp bond-forming reactions. The use of a photochemical flow reactor, consisting of a polyfluorinated tube reactor wrapped around a 500 W Hg lamp, allowed to overcome batch limitations paving the way for metal-free arylation reactions via phenyl cations. Derivatives **14a–g** were prepared with this greener flow approach (Scheme 15) starting from mesitylene **13**, and haloarenes using short irradiation times (<6 h), and a 5:1 MeCN/H$_2$O mixture.

The reported results show how photochemistry hold the potential to become a green tool for the development of sustainable photochemical flow synthesis.

Hazardous chemistry by using green and sustainable continuous-flow microreactors

We have already shown how continuous-flow technology could play an important role in improving chemical processes [5,71],

Scheme 13: Trifluoromethylation by continuous-flow photoredox catalysis.
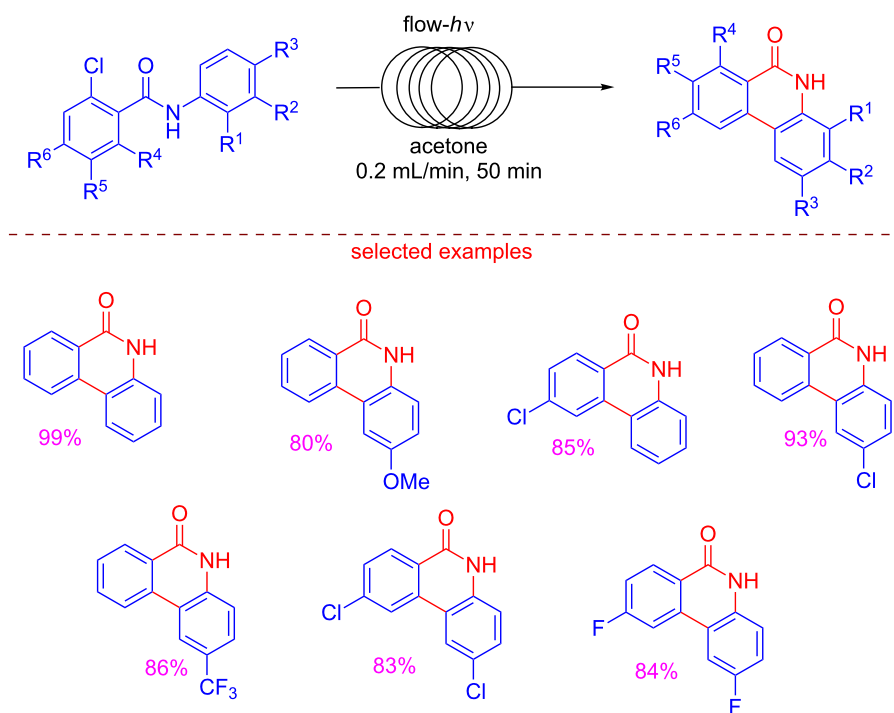
Scheme 14: Flow photochemical synthesis of 6(5*H*)-phenanthridiones from 2-chlorobenzamides.

providing different advantages over traditional batch mode. However, the hazardous nature of some chemicals makes handling at conventional lab or industrial scale difficult. The use of microreactors and continuous-flow chemistry offers the possibility to perform reactions using dangerous or hazardous materials that cannot be used in batch mode. In other word, syntheses previously "forbidden" for safety reasons, such as those involving diazo compounds, hydrazine, azides, phosgene,

Scheme 15: Synthesis of biaryls **14a–g** under photochemical flow conditions.
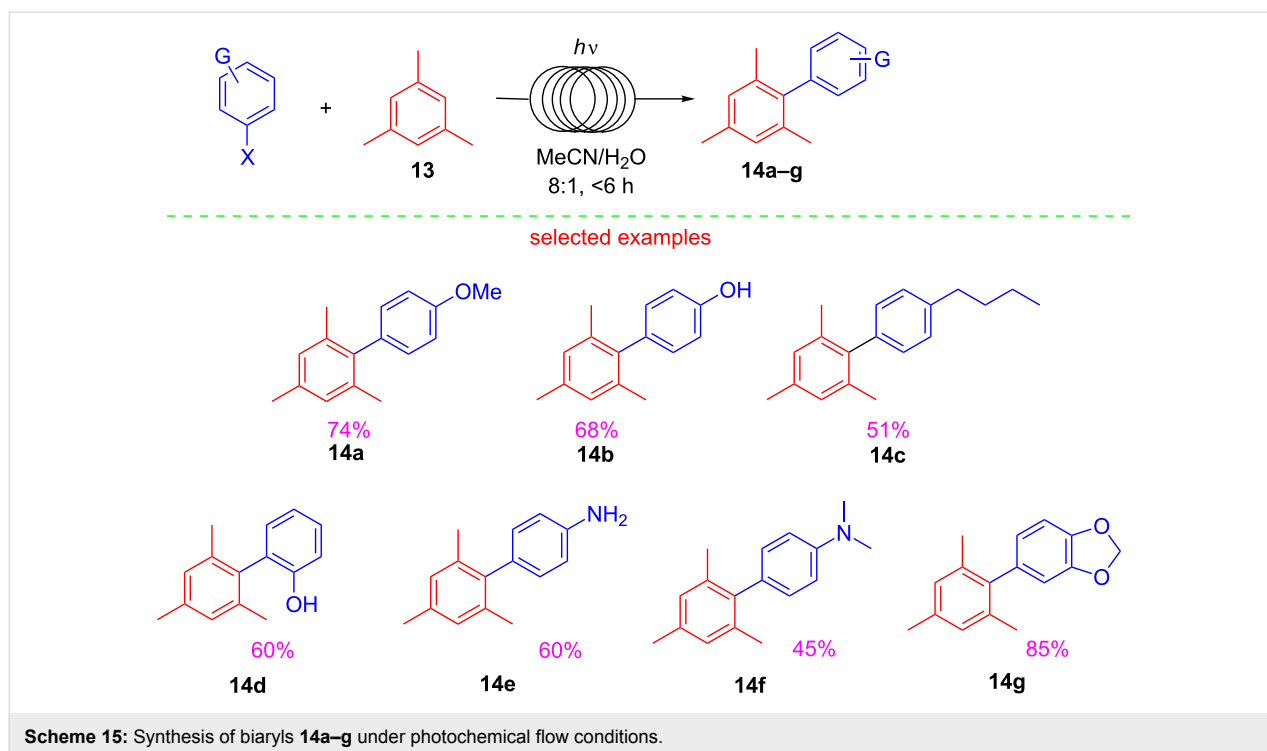
cyanides and other hazardous chemicals could be performed with relatively low risk using flow technology [72-76].

Several research groups investigated this aspect, as highlighted by several available reviews [77,78]. Here we describe very recent reports with the aim to highlight the potential of flow chemistry in the field of hazardous chemistry under a greener perspective.

Diazo compounds are recognized as versatile reagents in organic synthesis. Nevertheless, diazo compounds are also considered highly energetic reagents [79,80]. For this reason, the in situ generation of such reagents has been investigated under flow conditions. Moody and co-workers reported a new method for the in situ generation of diazo compounds as precursors of highly reactive metal carbenes (Scheme 16) [81].

As reported in Scheme 16, diazo species **18** could be generated from simple carbonyls **15** and hydrazine (**16**). Intermediate hydrazones **17** can be converted into the corresponding diazo compounds by oxidation using a recyclable oxidant based on *N*-iodo-*p*-toluenesulfonamide potassium salt. The possibility to regenerate a functionalized resin by simple washing with aqueous KI$_3$/KOH solution makes the process more sustainable. This method produces KI solution as waste, and it is an alternative way for the direct oxidation of hydrazones, that often requires the use of heavy metals such as HgO, Pb(OAc)$_4$ and AgO [82,83].

The diazo compounds could be collected as solution in dichloromethane at the output of the flow system, and obtained sufficiently pure for further use without requiring handling or isolation. Further mixing of solutions containing diazo deriva-

Scheme 16: Flow oxidation of hydrazones to diazo compounds.
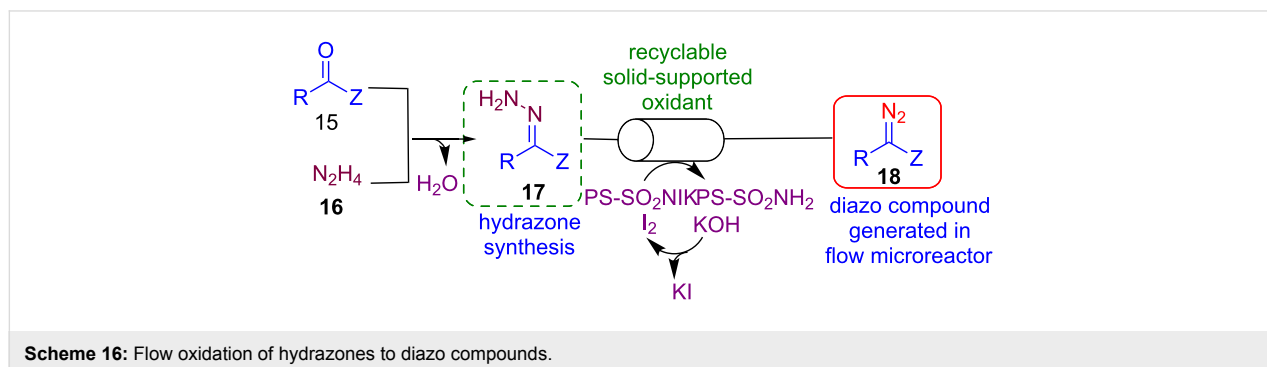
tives to a solution containing a Rh(II) catalyst, and reactants such as amines, alcohols or aldehydes led to a wide range of products as reported in Scheme 17.

Ley's group developed several continuous-flow approaches for generating diazo species from hydrazones [84,85]. Under flow conditions, diazo compounds were reacted with boronic acids in order to generate reactive allylic and benzylic boronic acids further employed for iterative C–C bond forming reactions [86].

The generation of unstable diazo species was possible using a cheap, recyclable and less toxic oxidant, MnO_2. The flow stream was accurately monitored by in-line FTIR spectroscopy in order to maximize the formation of the diazo compound (Scheme 18) [87].

Starting from this initial investigation, Ley and co-workers developed an elegant application of this strategy for a sequential formation of up to three C–C bonds in sequence, by an iterative

Scheme 17: Synthetic use of flow-generated diazo compounds.

Scheme 18: Ley's flow approach for the generation of diazo compounds.
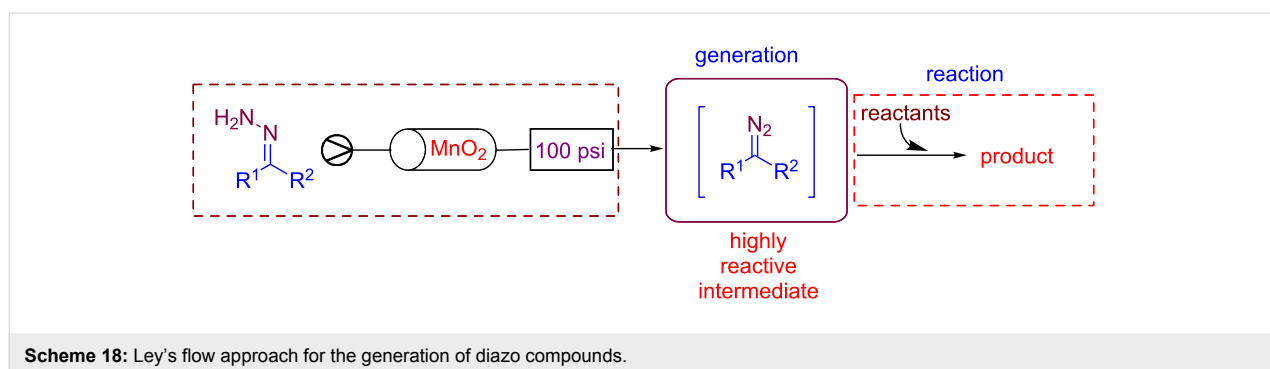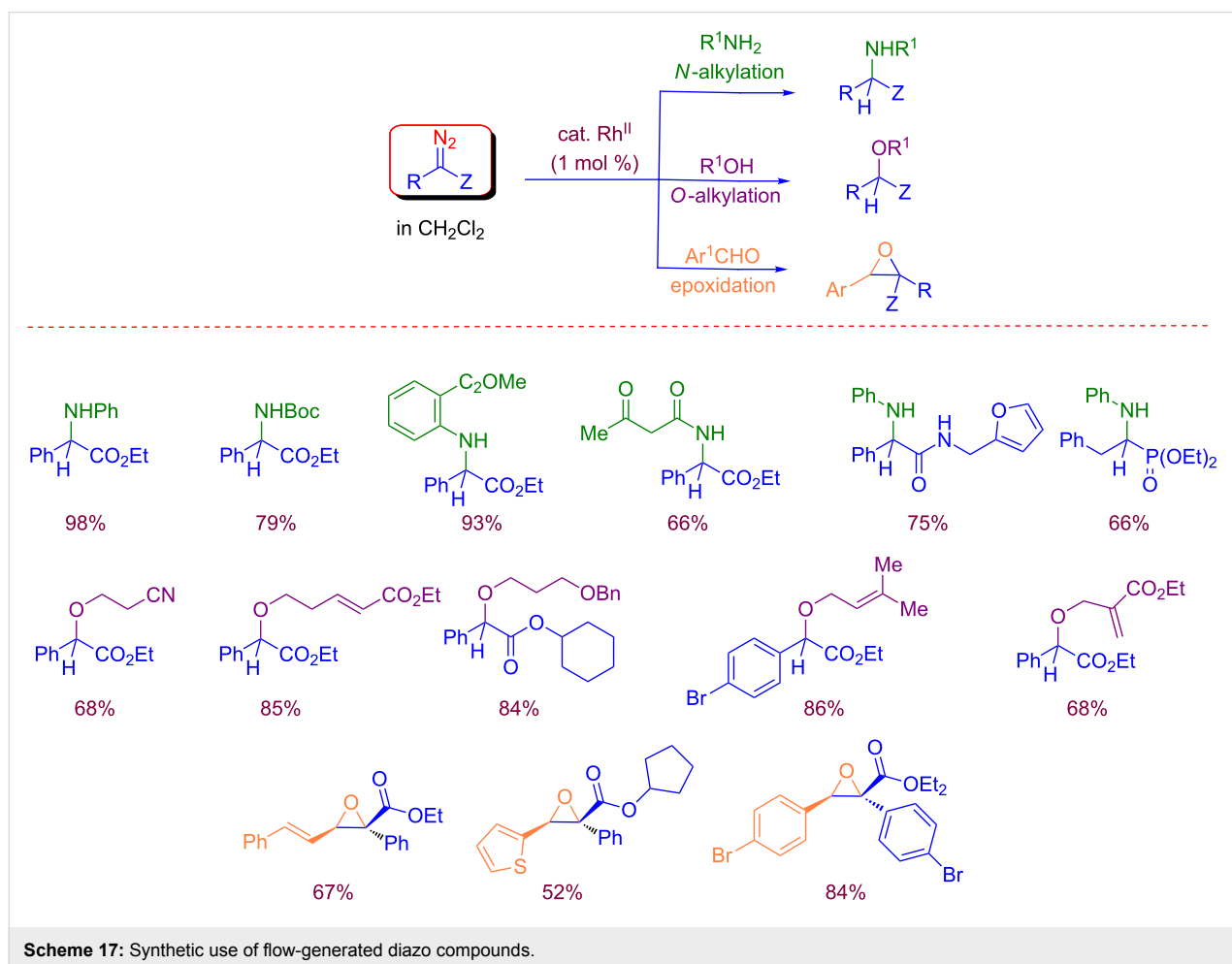
trapping of boronic acid species. The sequence starts with the reaction of diazo compound **20**, generated under flow conditions, and boronic acid **19** (Scheme 19). Further sequential coupling with diazo compounds **21** and **22** led to boronates **23** or protodeboronated products **24** at the end of the sequence (Scheme 19).
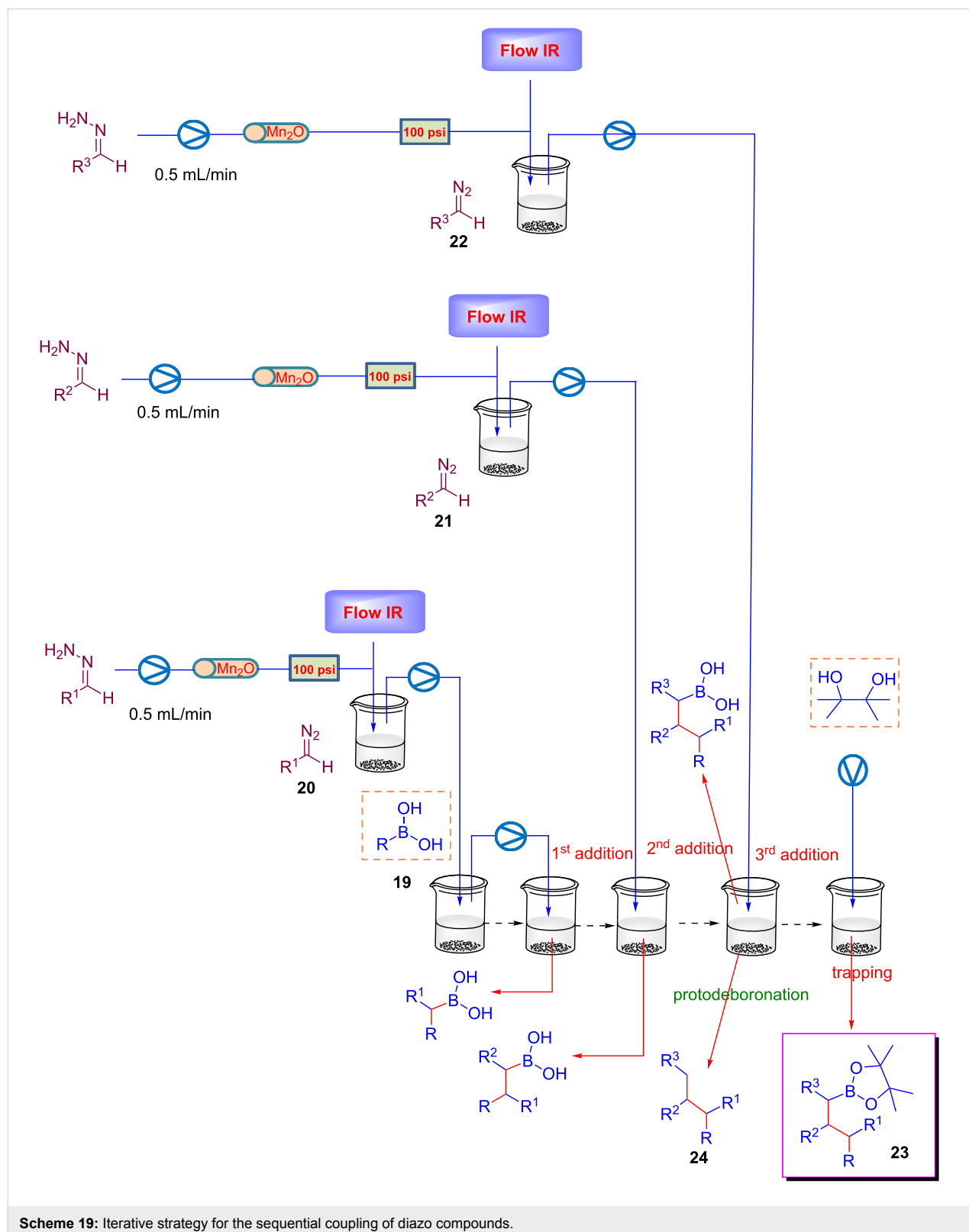
Scheme 19: Iterative strategy for the sequential coupling of diazo compounds.

With the aim to exploit the versatility of this approach, Ley and co-workers reported the allylations of carbonyl electrophiles such as aldehydes using the above reported strategy for the generation of allylboronic acids. The flow protocol considers the reaction of diazo compounds **25** (generated in flow) with boronic acid **26** and aldehyde **27** (Scheme 20). By this new iterative coupling it was possible to obtain alcohols as products. The usefulness of the method was demonstrated with the preparation in good yield (60%) of a precursor of the natural product bakuchiol **28** (Scheme 20) [88].

The microreactor technology offers the advantage to handle hazardous components such as hydrazine and molecular oxygen, which represent alternative reagents for selective reduction of C=C double bonds. In fact, combination of hydrazine hydrate ($N_2H_4 \cdot H_2O$) and O_2 provide diimide (HN=NH) as reducing agent. Nevertheless, this strategy is rarely used in traditional batch chemistry for safety reason.

Kappe and co-workers recently developed a reduction of the alkene to the corresponding alkane, by a catalyst-free generation of diimide by oxidation of hydrazine monohydrate ($N_2H_4 \cdot H_2O$) with molecular oxygen [89,90]. The flow system set-up is reported in Scheme 21, and consists in a HPLC pump for delivering the alkene and hydrazine monohydrate, while O_2 was delivered by a mass-flow controller (MFC) from a standard compressed-gas cylinder. After combination of the reagent streams, the resulting segmented flow was pumped through a heated residence unit (RTU) consisting in a fluorinated tube with low gas permeability (Scheme 21).

The flow system reported in Scheme 21 was able to reduce alkenes with high yields and selectivity by using residence times in the range of 10 to 30 min at 100 °C, and by employing a slight excess of hydrazine. Importantly, this strategy is compatible with sensitive functional groups such as silyl ether, halogenes, and benzyl groups. A very nice application of this ap-

Scheme 20: Integrated synthesis of Bakuchiol precursor via flow-generated diazo compounds.

Scheme 21: Kappe's continuous-flow reduction of olefines with diimide.
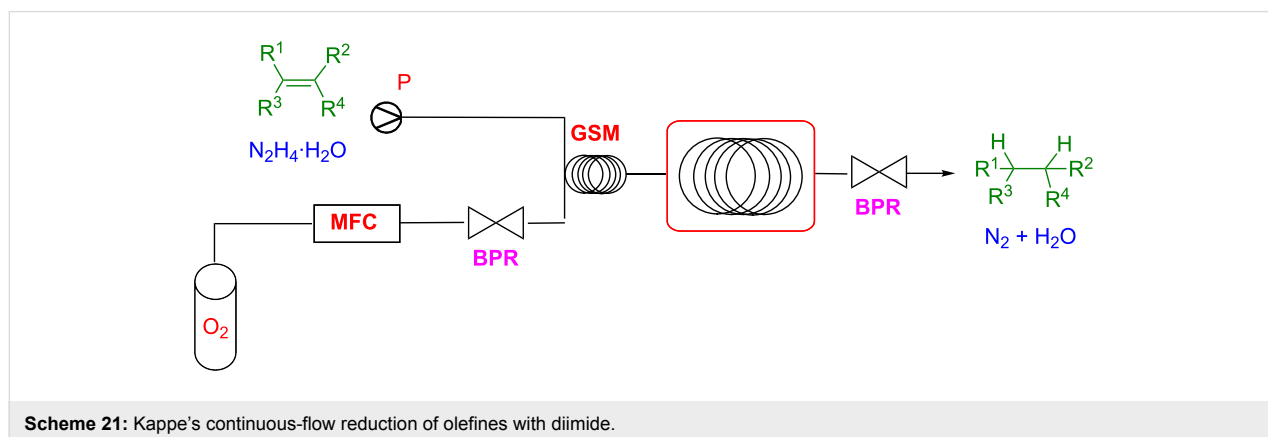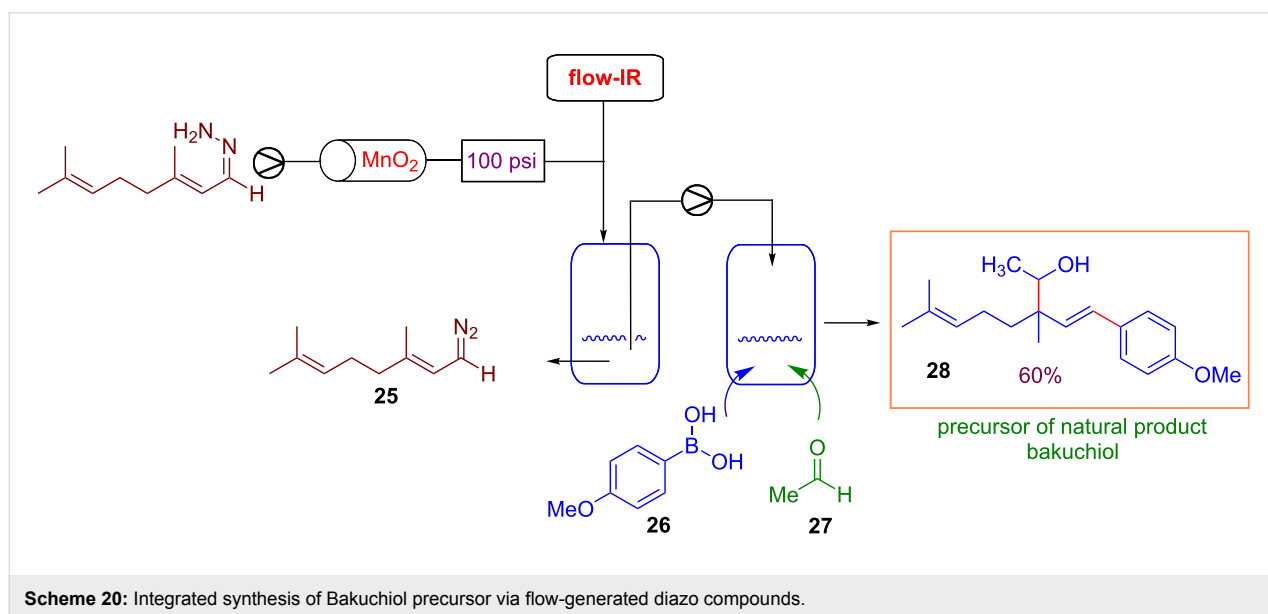
proach was the highly selective reduction of artemisinic acid to dihydroartemisinic acid, which are of interest in the synthesis of the antimalarial drug artemisinin. This industrially relevant reduction was executed by using O$_2$ at 20 bar, four residence units at 60 °C and consecutive feedings with N$_2$H$_4$·H$_2$O in order to obtain full conversion in dihydroartemisinic acid (**29**, DHAA, Scheme 22).

Continuous-flow sustainable production of APIs

With the aim to demonstrate the potential of microreactor technology and flow chemistry in sustainable synthesis, recent outstanding "proof of concepts" will be described. Kobayashi and co-workers reported a multistep continuous-flow synthesis of a drug target via heterogeneous catalysis. The developed process not requiring any isolation of intermediates, separation of the catalyst or other work-up procedures can be considered sustainable [91]. The syntheses of (*S*)-rolipram and a γ-aminobutyric acid (GABA) derivative were accomplished. Readily available starting materials and columns containing chiral heterogeneous catalysts to produce enantioenriched materials were employed. It is worth mentioning that this work represents a very nice example on the use of chiral catalysis in a multistep flow synthesis of a drug target on gram scale. The multistep synthesis of (*S*)-rolipram reported in Scheme 23 begins from a benzaldehyde derivative which undergoes a Henry-type reaction with nitromethane in the first flow step (Flow I). The resulting

nitroalkene undergoes an asymmetric addition catalyzed by a supported PS–(*S*)-pybox–calcium chloride catalyst at 0 °C using two columns (Flow II). This is the enantio-determining step of the process. The stereochemistry of the adduct can be simply switched to the opposite enantiomer, by using the enantiomeric supported catalyst PS–(*R*)-pybox–calcium chloride. The enantiomeric excess of the products was about 96%. Two more steps consisting in a Pd-catalyzed hydrogenation reaction and a decarboxylation (Flow III and Flow IV) led to the target (*S*)-rolipram in 50% overall yield. The systems was designed in order to keep the level of the palladium in solution as low as possible (<0.01 ppm).

Another outstanding proof of concept, which demonstrates the potential of flow chemistry for sustainable pharmaceutical manufacturing, has been recently reported by Jensen and his research team. The research team set up a compact and reconfigurable manufacturing platform for the continuous-flow synthesis and formulation of active pharmaceutical ingredients (APIs) [92]. The "mini" plant (reported in Figure 3) was very compact in size [1.0 m × 0.7 m × 1.8 m, (W × L × H)], and low-weighing (about 100 kg) and was able to perform complex multistep synthesis, work-up procedures as well as purification operations such as crystallization. This platform was also equipped with devices for real-time monitoring and final formulation of high purity APIs. For the preparation of target molecules, commercially available starting materials were employed.

Scheme 22: Multi-injection setup for the reduction of artemisinic acid.
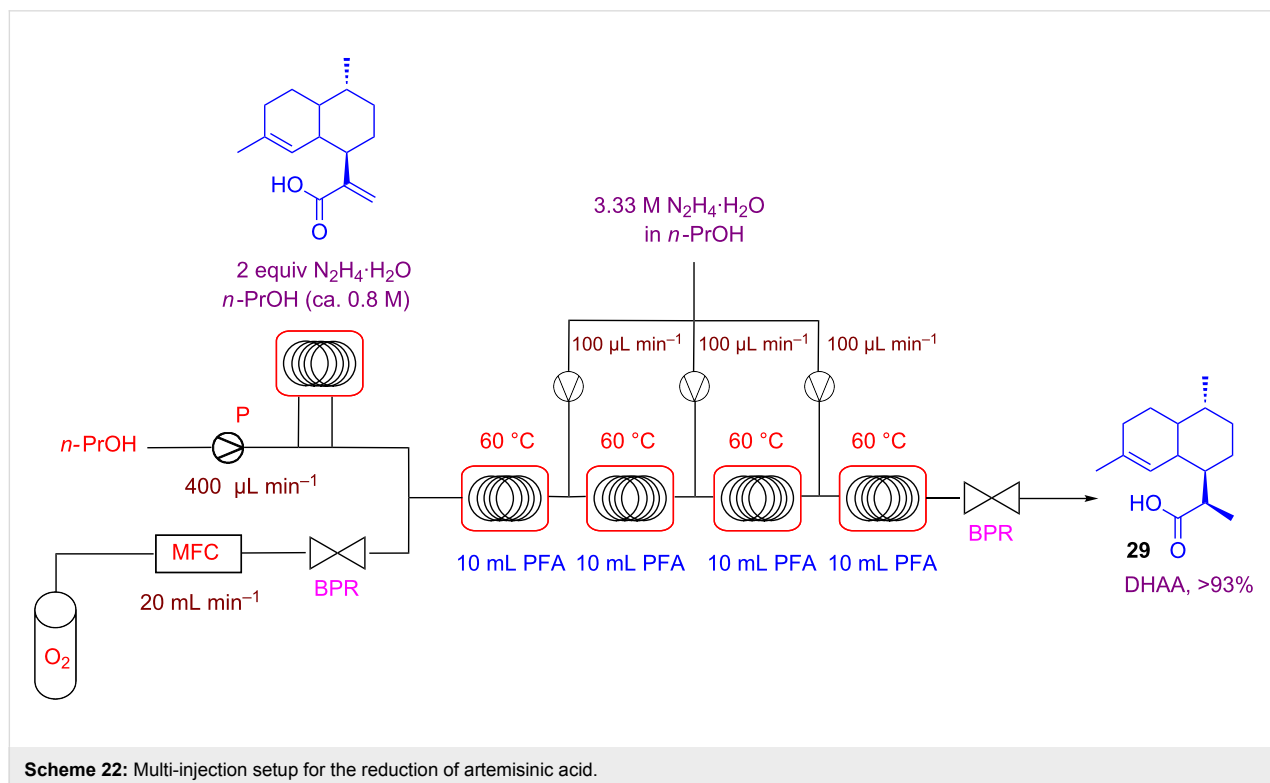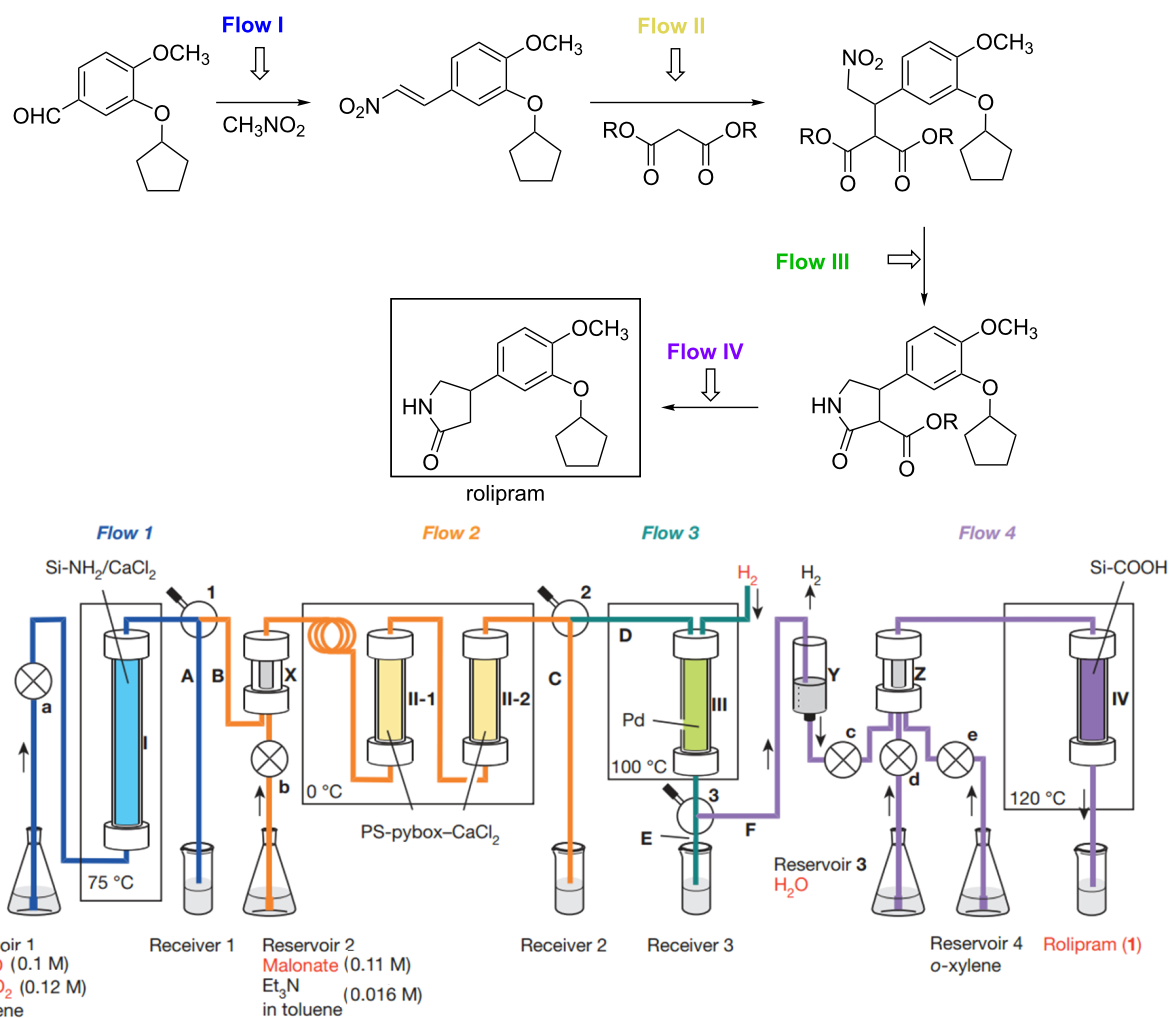
Scheme 23: Flow reactor system for multistep synthesis of (*S*)-rolipram. Pumps are labelled a, b, c, d and e; Labels A, B, C, D, E and F are flow lines. X are molecular sieves; Y is Amberlyst 15Dry; Z is Celite. (Reproduced with permission from [84], copyright 2015 Nature Publishing Group).

The platform was tested for the production and supply of hundreds to thousands doses per day of diphenhydramine hydrochloride, lidocaine hydrochloride, diazepam and fluoxetine hydrochloride.

Remarkably, for future applications of the platform, the produced medicines also met the U.S. Pharmacopeia standards.

The future use of this kind of platform would concern the "on-demand" production or the "instantaneous" production of short-lived pharmaceuticals (Figure 4). Other advantageous concerns of this reconfigurable platform are the lower production costs, the higher safety, the automation (computer controlled processes), the reduced waste (production could be done where is needed and in the right amount).

Conclusion

Flow chemistry and manufacturing engineering have become largely acknowledged as viable and very often superior alternative to batch processing. Continuous-flow techniques offer increased safety, scalability, reproducibility, automation, reduced waste and costs, and accessibility to a wide range of new chemical possibilities, seldom not accessible through classic batch chemistry. All those benefits are even more noteworthy and outstanding than what they might seem, because they widely fulfil most of the green chemistry principles. In this short overview, we tried to highlight progresses and potential of flow chemistry in the field of sustainable synthesis. Thus, it is expected that flow chemistry and microreactor technology could deeply change the way to perform sustainable chemical production in the near future [93].
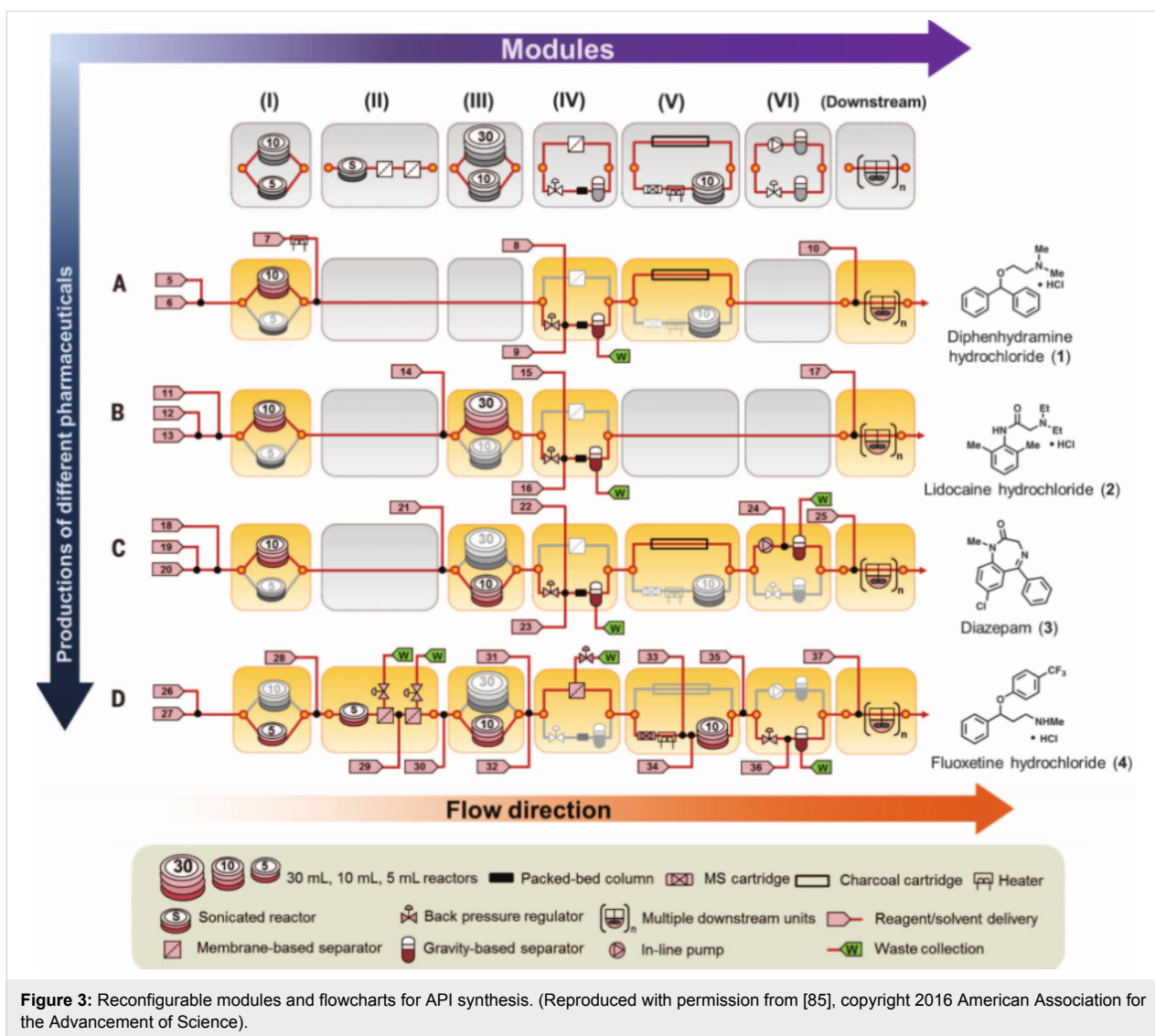
Figure 3: Reconfigurable modules and flowcharts for API synthesis. (Reproduced with permission from [85], copyright 2016 American Association for the Advancement of Science).
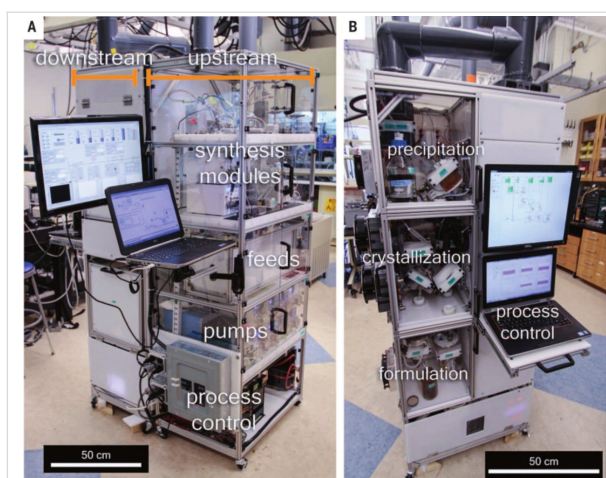

Figure 4: Reconfigurable system for continuous production and formulation of APIs. (Reproduced with permission from [85], copyright 2016 American Association for the Advancement of Science).

References

1. Navigant Pike Research Study.
   http://www.navigantresearch.com/research/green-chemistry (accessed May 13, 2014).
2. Anastas, P.; Eghbali, N. *Chem. Soc. Rev.* **2010,** *39,* 301–312. doi:10.1039/B918763B
3. Reschetilowski, W., Ed. *Microreactors in Preparative Chemistry;* Wiley-VCH: Weinheim, 2013.
4. Nagaki, A.; Yoshida, J.-I. *Top. Organomet. Chem.* **2015,** *57,* 137–175. doi:10.1007/3418_2015_154
5. Ley, S. V. *Chem. Rec.* **2012,** *12,* 378–390. doi:10.1002/tcr.201100041
6. Newman, S. G.; Jensen, K. F. *Green Chem.* **2013,** *15,* 1456–1472. doi:10.1039/c3gc40374b
7. Professor Jun-ichi Yoshida firstly introduced the concept of "micro + flow = green" during a plenary lecture at the 14th IMRET conference held in Beijing (China) in Septembeer 2016.
8. Yoshida, J.-i.; Kim, H.; Nagaki, A. *ChemSusChem* **2011,** *4,* 331–340. doi:10.1002/cssc.201000271

9. Hessel, V.; Schouten, J. C.; Renken, A.; Wang, Y.; Yoshida, J.-i., Eds. *Handbook of Micro Reactors;* Wiley-VCH: Weinheim, 2009.

10. Yoshida, J.-i. *Flash Chemistry: Fast Organic Synthesis in Microsystems;* Wiley-VCH: Weinheim, 2008. doi:10.1002/9780470723425

11. Poliakoff, M.; Fitzpatrick, J. M.; Ferren, T. R.; Anastas, P. T. *Science* **2002,** *297,* 807–810. doi:10.1126/science.297.5582.807

12. Trost, B. M. *Science* **1991,** *254,* 1471–1477. doi:10.1126/science.1962206

13. Trost, B. M. *Angew. Chem., Int. Ed. Engl.* **1995,** *34,* 259–281. doi:10.1002/anie.199502591

14. Sheldon, R. A. *Pure Appl. Chem.* **2000,** *72,* 1233–1246. doi:10.1351/pac200072071233

15. Trost, B. M. *Acc. Chem. Res.* **2002,** *35,* 695–705. doi:10.1021/ar010068z

16. Wender, P. A.; Verma, V. A.; Paxton, T. J.; Pillow, T. H. *Acc. Chem. Res.* **2008,** *41,* 40–49. doi:10.1021/ar700155p

17. Kim, H.; Nagaki, A.; Yoshida, J.-i. *Nat. Commun.* **2011,** *2,* No. 264. doi:10.1038/ncomms1264

18. Nagaki, A.; Yoshida, J.-i. *Microreactor Technology in Lithium Chemistry,* in: *Lithium Compounds in Organic Synthesis from Fundamentals to Applications.* Luisi, R.; Capriati, V., Eds.; Wiley-VCH: Weinheim, 2014; pp 491–512. doi:10.1002/9783527667512.ch17

19. Nagaki, A.; Takahashi, Y.; Yoshida, J.-i. *Angew. Chem., Int. Ed.* **2016,** *55,* 5327–5331. doi:10.1002/anie.201601386

20. Nagaki, A.; Tsuchihashi, Y.; Haraki, S.; Yoshida, J.-i. *Org. Biomol. Chem.* **2015,** *13,* 7140–7145. doi:10.1039/C5OB00958H

21. Rys, P. *Acc. Chem. Res.* **1976,** *10,* 345–351. doi:10.1021/ar50106a001

22. Rys, P. *Angew. Chem., Int. Ed. Engl.* **1977,** *16,* 807–817. doi:10.1002/anie.197708073

23. Nagaki, A.; Togai, M.; Suga, S.; Aoki, N.; Mae, K.; Yoshida, J.-i. *J. Am. Chem. Soc.* **2005,** *127,* 11666–11675. doi:10.1021/ja0527424

24. Yoshida, J.-i. *Basics of Flow Microreactor Synthesis;* SpringerBriefs in Molecular Science; Springer: Tokyo, 2015. doi:10.1007/978-4-431-55513-1

25. Yoshida, J.-i.; Nagaki, A.; Iwasaki, T.; Suga, S. *Chem. Eng. Technol.* **2005,** *28,* 259–266. doi:10.1002/ceat.200407127

26. Nagaki, A.; Takabayashi, N.; Tomida, Y.; Yoshida, J.-i. *Org. Lett.* **2008,** *18,* 3937–3940. doi:10.1021/ol8015572

27. Nagaki, A.; Ichinari, D.; Yoshida, J.-i. *Chem. Commun.* **2013,** *49,* 3242–3244. doi:10.1039/c3cc40392k

28. Degennaro, L.; Fanelli, F.; Giovine, A.; Luisi, R. *Adv. Synth. Catal.* **2015,** *357,* 21–27. doi:10.1002/adsc.201400747

29. Pace, V.; Holzer, W.; De Kimpe, R. *Chem. Rec.* **2016,** *16,* 2061–2076. doi:10.1002/tcr.201600011

30. Gessner, V. H. *Chem. Commun.* **2016,** *52,* 12011–12023. doi:10.1039/C6CC05524A

31. Pace, V. *Aust. J. Chem.* **2014,** *67,* 311–313. doi:10.1071/CH13416

32. Emerson, C. R.; Zakharov, L. N.; Blakemore, P. R. *Chem. – Eur. J.* **2013,** *19,* 16342–16356. doi:10.1002/chem.201302511
    See for a tactic to prolong the life-time of carbenoids consisting in the introduction of anion-stabilizing groups and see references cited therein.

33. Kupper, C.; Molitor, S.; Gessner, V. H. *Organometallics* **2014,** *33,* 347–353. doi:10.1021/om4010862
    See for examples of "stabilized" chloro carbenoids stable at room temperature and references cited therein.

34. Degennaro, L.; Maggiulli, D.; Carlucci, C.; Fanelli, F.; Romanazzi, G.; Luisi, R. *Chem. Commun.* **2016,** *52,* 9554–9557. doi:10.1039/C6CC04588J

35. Furniss, B. S.; Hannaford, A. J.; Smith, P. W. G.; Tatchell, A. R. *Vogel's Textbook of Practical Organic Chemistry,* 5th ed.; Wiley: New York, 1989; p 1266.

36. Dawar, P.; Raju, M. B.; Ramakrishna, R. A. *Tetrahedron Lett.* **2011,** *52,* 4262–4265. doi:10.1016/j.tetlet.2011.04.100

37. Zhu, Y.; Wei, Y. *RSC Adv.* **2013,** *3,* 13668–13670. doi:10.1039/c3ra40246k

38. Zhang, H.; Shi, R.; Ding, A.; Lu, L.; Chen, B.; Lei, A. *Angew. Chem., Int. Ed.* **2012,** *51,* 12542–12545. doi:10.1002/anie.201206518

39. Majek, M.; Jacobi von Wangelin, A. *Angew. Chem., Int. Ed.* **2015,** *54,* 2270–2274. doi:10.1002/anie.201408516

40. Magano, J.; Dunetz, J. R. *Chem. Rev.* **2011,** *111,* 2177–2250. doi:10.1021/cr100346g

41. Brennführer, A.; Neumann, H.; Beller, M. *Angew. Chem., Int. Ed.* **2009,** *48,* 4114–4133. doi:10.1002/anie.200900013

42. Xin, Z.; Gøgsig, T. M.; Lindhardt, A. T.; Skrydstrup, T. *Org. Lett.* **2012,** *14,* 284–287. doi:10.1021/ol203057w

43. Zenzola, M.; Degennaro, L.; Trinchera, P.; Carroccia, L.; Giovine, A.; Romanazzi, G.; Mastrorilli, P.; Rizzi, R.; Pisano, L.; Luisi, R. *Chem. – Eur. J.* **2014,** *20,* 12190–12200. doi:10.1002/chem.201403141

44. Parisi, G.; Capitanelli, E.; Pierro, A.; Romanazzi, G.; Clarkson, G. J.; Degennaro, L.; Luisi, R. *Chem. Commun.* **2015,** *51,* 15588–15591. doi:10.1039/C5CC06323J

45. Giovine, A.; Musio, B.; Degennaro, L.; Falcicchio, A.; Nagaki, A.; Yoshida, J.-i.; Luisi, R. *Chem. – Eur. J.* **2013,** *19,* 1872–1876. doi:10.1002/chem.201203533

46. Tomida, Y.; Nagaki, A.; Yoshida, J.-i. *J. Am. Chem. Soc.* **2011,** *133,* 3744–3747. doi:10.1021/ja110898s

47. Nagaki, A.; Matsuo, C.; Kim, S.; Saito, K.; Miyazaki, A.; Yoshida, J.-i. *Angew. Chem., Int. Ed.* **2012,** *51,* 3245–3248. doi:10.1002/anie.201108932

48. Kim, H.; Min, K.-I.; Inoue, K.; Im, D. J.; Kim, D.-P.; Yoshida, J.-i. *Science* **2016,** *352,* 691–694. doi:10.1126/science.aaf1389

49. Semple, J. E.; Rossignol, J.-F. Pharmaceutical compositions and methods of use of salicylanilides for treatment of hepatitis viruses. PCT Int. Appl. WO2012058378 A1, May 3, 2012.

50. Degennaro, L.; Carlucci, C.; De Angelis, S.; Luisi, R. *J. Flow Chem.* **2016,** *6,* 136–166. doi:10.1556/1846.2016.00014

51. Pavia, C.; Ballerini, E.; Bivona, L. A.; Giacalone, F.; Aprile, C.; Vaccaro, L.; Gruttadauria, M. *Adv. Synth. Catal.* **2013,** *355,* 2007–2018. doi:10.1002/adsc.201300215

52. de M. Muñoz, J.; Alcázar, J.; de la Hoz, A.; Díaz-Ortiz, A. *Adv. Synth. Catal.* **2012,** *354,* 3456–3460. doi:10.1002/adsc.201200678

53. Mennecke, K.; Sodolenko, W.; Kirschning, A. *Synthesis* **2008,** 1589–1599. doi:10.1055/s-2008-1072579

54. Nagaki, A.; Hirose, K.; Moriwaki, Y.; Mitamura, K.; Matsukawa, K.; Ishizuka, N.; Yoshida, J.-i. *Catal. Sci. Technol.* **2016,** *6,* 4690–4694. doi:10.1039/C5CY02098K

55. Kirsch, P. *Modern Fluoroorganic Chemistry: Synthesis, Reactivity, Applications,* 2nd ed.; Wiley-VCH: Weinheim, 2013. doi:10.1002/9783527651351

56. Wang, J.; Sànchez-Rosellò, M.; Aceña, J. L.; del Pozo, C.; Sorochinsky, A. E.; Fustero, S.; Soloshonok, V. A.; Liu, H. *Chem. Rev.* **2014,** *114,* 2432–2506. doi:10.1021/cr4002879

57. Gillis, E. P.; Eastman, K. J.; Hill, M. D.; Donnelly, D. J.; Meanwell, N. A. *J. Med. Chem.* **2015,** *58,* 8315–8359. doi:10.1021/acs.jmedchem.5b00258

58. Smart, B. E. *J. Fluorine Chem.* **2001,** *109,* 3–11.
doi:10.1016/S0022-1139(01)00375-X
59. Roesner, S.; Buchwald, S. L. *Angew. Chem., Int. Ed.* **2016,** *55,*
10463–10467. doi:10.1002/anie.201605584
60. Izquierdo, J.; Pericas, M. A. *ACS Catal.* **2016,** *6,* 348–356.
doi:10.1021/acscatal.5b02121
61. Izquierdo, J.; Ayats, C.; Henseler, A. H.; Pericàs, M. A.
Org. Biomol. Chem. **2015,** *13,* 4204–4209. doi:10.1039/C5OB00325C
62. Cambié, D.; Bottecchia, C.; Straathof, N. J. W.; Hessel, V.; Noël, T.
Chem. Rev. **2016,** *116,* 10276–10341.
doi:10.1021/acs.chemrev.5b00707
63. Gemoets, H. P. L.; Su, Y.; Shang, M.; Hessel, V.; Luque, R.; Noël, T.
Chem. Soc. Rev. **2016,** *45,* 83–117. doi:10.1039/C5CS00447K
64. Talla, A.; Driessen, B.; Straathof, N. J. W.; Milroy, L.-G.; Brunsveld, L.;
Hessel, V.; Noël, T. *Adv. Synth. Catal.* **2015,** *357,* 2180–2186.
doi:10.1002/adsc.201401010
65. Cremlyn, R. J. *An Introduction to Organosulfur Chemistry;* Wiley–VCH:
New York, 1996.
66. Witt, D. *Synthesis* **2008,** 2491–2509. doi:10.1055/s-2008-1067188
67. Blank, I.; Pascual, E. C.; Devaud, S.; Fay, L. B.; Stadler, R. H.;
Yeretzian, C.; Goodman, B. A. *J. Agric. Food Chem.* **2002,** *50,*
2356–2364. doi:10.1021/jf011329m
68. Straathof, N. J. W.; Gemoets, H. P. L.; Wang, X.; Schouten, J. C.;
Hessel, V.; Noël, T. *ChemSusChem* **2014,** *7,* 1612–1617.
doi:10.1002/cssc.201301282
69. Fang, Y.; Tranmer, G. K. *Med. Chem. Commun.* **2016,** *7,* 720–724.
doi:10.1039/C5MD00552C
70. Bergami, M.; Protti, S.; Ravelli, D.; Fagnoni, M. *Adv. Synth. Catal.*
2016, *358,* 1164–1172. doi:10.1002/adsc.201600019
71. Wiles, C.; Watts, P. *Green Chem.* **2012,** *14,* 38–54.
doi:10.1039/C1GC16022B
72. Yoshida, J.-i. *Flash Chemistry: Fast Organic Synthesis in
Microsystems;* John Wiley & Sons: Chichester, UK, 2008.
doi:10.1002/9780470723425
73. Yoshida, J.-i. *Chem. Commun.* **2005,** 4509–4516.
doi:10.1039/b508341a
74. Yoshida, J.-i.; Nagaki, A.; Yamada, T. *Chem. – Eur. J.* **2008,** *14,*
7450–7459. doi:10.1002/chem.200800582
75. Yoshida, J.-i. *Chem. Rec.* **2010,** *10,* 332–341.
doi:10.1002/tcr.201000020
76. Nieuwland, P. J.; Koch, K.; van Harskamp, N.; Wehrens, R.;
van Hest, J. C. M.; Rutjes, F. P. J. T. *Chem. – Asian J.* **2010,** *5,*
799–805. doi:10.1002/asia.200900705
77. Gutmann, B.; Cantillo, D.; Kappe, C. O. *Angew. Chem., Int. Ed.* **2015,**
54, 6688–6728. doi:10.1002/anie.201409318
78. Movsisyan, M.; Delbeke, E. I. P.; Berton, J. K. E. T.; Battilocchio, C.;
Ley, S. V.; Stevens, C. V. *Chem. Soc. Rev.* **2016,** *45,* 4892–4928.
doi:10.1039/C5CS00902B
79. Clark, J. D.; Shah, A. S.; Peterson, J. C.; Patelis, L.; Kersten, R. J. A.;
Heemskerk, A. H.; Grogan, M.; Camden, S. *Thermochim. Acta* **2002,**
386, 65–72. doi:10.1016/S0040-6031(01)00760-2
80. Hosmane, R. S.; Liebman, J. F. *Struct. Chem.* **2002,** *13,* 501–503.
doi:10.1023/A:1020573723147
81. Nicolle, S. M.; Hayes, C. J.; Moody, C. J. *Chem. – Eur. J.* **2015,** *21,*
4576–4579. doi:10.1002/chem.201500118
82. Regitz, M.; Maas, G. *Diazo Compounds Properties and Synthesis;*
Academic Press: Orlando, Florida, 1986.

83. Soldi, C.; Lamb, K. N.; Squitieri, R. A.; González-López, M.;
Di Maso, M. J.; Shaw, J. T. *J. Am. Chem. Soc.* **2014,** *136,*
15142–15145. doi:10.1021/ja508586t
See for a recent example of hydrazone oxidation using manganese
dioxide.
84. Roda, N. M.; Tran, D. N.; Battilocchio, C.; Labes, R.; Ingham, R. J.;
Hawkins, J. M.; Ley, S. V. *Org. Biomol. Chem.* **2015,** *13,* 2550–2554.
doi:10.1039/C5OB00019J
85. Poh, J.-S.; Tran, D. N.; Battilocchio, C.; Hawkins, J. M.; Ley, S. V.
Angew. Chem., Int. Ed. **2015,** *54,* 7920–7923.
doi:10.1002/anie.201501538
86. Battilocchio, C.; Feist, F.; Hafner, A.; Simon, M.; Tran, D. N.;
Allwood, D. M.; Blakemore, D. C.; Ley, S. V. *Nat. Chem.* **2016,** *8,*
360–367. doi:10.1038/nchem.2439
87. Tran, D. N.; Battilocchio, C.; Lou, S.-B.; Hawkins, J. M.; Ley, S. V.
Chem. Sci. **2015,** *6,* 1120–1125. doi:10.1039/C4SC03072A
88. Esumi, T.; Yamamoto, C.; Fukuyama, Y. *Synlett* **2013,** *24,* 1845–1847.
doi:10.1055/s-0033-1338968
89. Pieber, B.; Martinez, S. T.; Cantillo, D.; Kappe, C. O.
Angew. Chem., Int. Ed. **2013,** *125,* 10431–10434.
doi:10.1002/ange.201303528
90. Pieber, B.; Glasnov, T.; Kappe, C. O. *Chem. – Eur. J.* **2015,** *21,*
4368–4376. doi:10.1002/chem.201406439
91. Tsubogo, T.; Oyamada, H.; Kobayashi, S. *Nature* **2015,** *520,* 329–332.
doi:10.1038/nature14343
92. Adamo, A.; Beingessner, R. L.; Behnam, M.; Chen, J.; Jamison, T. F.;
Jensen, K. F.; Monbaliu, J.-C. M.; Myerson, A. S.; Revalor, E. M.;
Snead, D. R.; Stelzer, T.; Weeranoppanant, N.; Wong, S. Y.; Zhang, P.
Science **2016,** *352,* 61–67. doi:10.1126/science.aaf1337
93. Hessel, V.; Kralisch, D.; Kockmann, N., Eds. *Novel Process Windows:
Innovative Gates to Intensified and Sustainable Chemical Processes;*
Wiley-VCH: Weinheim, 2015.

Ultrasound-promoted organocatalytic enamine–azide [3 + 2] cycloaddition reactions for the synthesis of ((arylselanyl)phenyl-1*H*-1,2,3-triazol-4-yl)ketones

Gabriel P. Costa[1], Natália Seus[1], Juliano A. Roehrs[1], Raquel G. Jacob[1], Ricardo F. Schumacher[1], Thiago Barcellos[2], Rafael Luque[*3] and Diego Alves[*1]

Full Research Paper

Address:
[1]Laboratório de Síntese Orgânica Limpa - LASOL - CCQFA - Universidade Federal de Pelotas - UFPel - P.O. Box 354 - 96010-900, Pelotas, RS, Brazil, [2]Laboratory of Biotechnology of Natural and Synthetic Products, Universidade de Caxias do Sul, Caxias do Sul, RS, Brazil and [3]Departamento de Quimica Organica, Universidad de Cordoba, Campus de Rabanales, Cordoba, Spain

Email:
Rafael Luque[*] - q62alsor@uco.es; Diego Alves[*] - diego.alves@ufpel.edu.br

* Corresponding author

Abstract

The use of sonochemistry is described in the organocatalytic enamine–azide [3 + 2] cycloaddition between 1,3-diketones and aryl azidophenyl selenides. These sonochemically promoted reactions were found to be amenable to a range of 1,3-diketones or aryl azidophenyl selenides, providing an efficient access to new ((arylselanyl)phenyl-1*H*-1,2,3-triazol-4-yl)ketones in good to excellent yields and short reaction times. In addition, this protocol was extended to β-keto esters, β-keto amides and α-cyano ketones. Selanyltriazoyl carboxylates, carboxamides and carbonitriles were synthesized in high yields at short times of reaction under very mild reaction conditions.

Introduction

Substituted 1,2,3-triazoles are an interesting class of heterocyclic compounds distinguished by their biological activities [1-3] as well as in various fields of chemistry [4-15]. The most attractive way for their preparation is the thermal 1,3-dipolar cycloaddition of alkynes and azides, introduced by Huisgen which usually gives rise to a mixture of 1,4 and 1,5-isomers [16-19]. More recently, transition metal catalysts based on copper, ruthenium, silver and iridium salts have been used for this cycloaddition reaction [20-29].

Organocatalytic approaches based on β-enamine–azide or enolate–azide cycloadditions have been employed to synthesize

1,2,3-triazole scaffolds [30-32]. Depending on the organocatalyst employed, different carbonyl compounds could successfully generate an enamine or an enolate, and these species react as dipolarophiles with organic azides in organocatalyzed 1,3-dipolar cycloadditions. Our research group has demonstrated β-enamine–azide cycloaddition reactions for the synthesis of selenium-functionalized 1,2,3-triazoles [33-37]. Selanyltriazoyl carboxylates, carboxamides, carbonitriles or sulfones were synthesized in good to excellent yields using catalytic amounts of an organocatalyst.

Organoselenium compounds are attractive synthetic targets because of their selective reactions [38-43], photophysical properties [44-49] and interesting biological activities [50-52]. An interesting class of molecules are the selanyl-1,2,3-triazoles [53-61] which can present some biological applications. As example, 4-phenyl-1-(phenylselanylmethyl)-1,2,3-triazole **A** (Se-TZ) demonstrated an antidepressant-like effect (Figure 1) [60]. In another example, 5-phenyl-1-(2-(phenylselanyl)phenyl)-1*H*-1,2,3-triazole-4-carbonitrile **B** (Se-TZCN) was reported to exhibit antioxidant activities in different in vitro assays (Figure 1) [36]. Selenanyl-quinone-based 1,2,3-triazoles **C** and **D** were synthesized and evaluated against six types of cancer cell lines. The synthesized compounds emerge as promising molecules for the therapeutic use of cancers overexpressing NQO1 (Figure 1) [61].

Thus, the search for efficient methods using appropriate and environmentally sound substrates for the preparation of selenium-functionalized 1,2,3-triazoles still remains a challenge in organic synthesis.

Ultrasonic irradiation has emerged in the past decades as a versatile tool in industrial and academic applications [62-67]. The use of sonication in organic synthesis (sonochemistry) is well documented and is generally considered as an environmentally sound energy source, comparatively less energy intensive to conventional heating and microwave irradiation, also able to reduce the number and quantities of side reaction products [62-67].

There are only a few contributions describing the use of sonochemistry for the preparation of functionalized 1,2,3-triazoles [68-74]. As a recent example, our research group described the use of sonochemistry in the organocatalytic enamine–azide [3 + 2] cycloadditions of β-oxo-amides with a range of substituted aryl azides providing and efficient access to new *N*-aryl-1,2,3-triazoyl carboxamides in good to excellent yields and short reaction times of [75].

However, to the best of our knowledge, the use of sonochemistry to synthesize complex selenium-functionalized 1,2,3-triazoles via organocatalytic enamine–azide cycloaddition has not been explored to date. As a continuation of our ongoing studies towards the development of new 1,2,3-triazoles bearing organoselenium moieties, this contribution was aimed to disclose a sonochemical approach for the organocatalyzed synthesis of ((arylselanyl)phenyl-1*H*-1,2,3-triazol-4-yl)ketones by reacting a range of 1,3-diketones with substituted aryl azidophenyl selenides (Scheme 1).

Results and Discussion

Due to the fact that organocatalyzed β-enamine–azide cycloaddition reactions between azidophenyl aryl selenides and 1,3-diketones were not described, preliminary studies were attempted to react 2-azidophenyl phenyl selenide (**1a**) and 2,4-pentanedione (**2a**) as model reaction substrates. Based on our previous report on such reaction [33], a mixture of substrates **1a** (0.3 mmol) and **2a** (0.3 mmol) in DMSO (0.6 mL) was stirred at room temperature in the presence of 1 mol % of Et$_2$NH as organocatalyst, providing an excellent yield (98%) of the desired product **3a** after 2 h (conditions A, Scheme 2).

With the aim to compare the effect of different energy sources in this β-enamine–azide cycloaddition, the reaction between

Figure 1: Biologically relevant selanyl-1,2,3-triazoles.
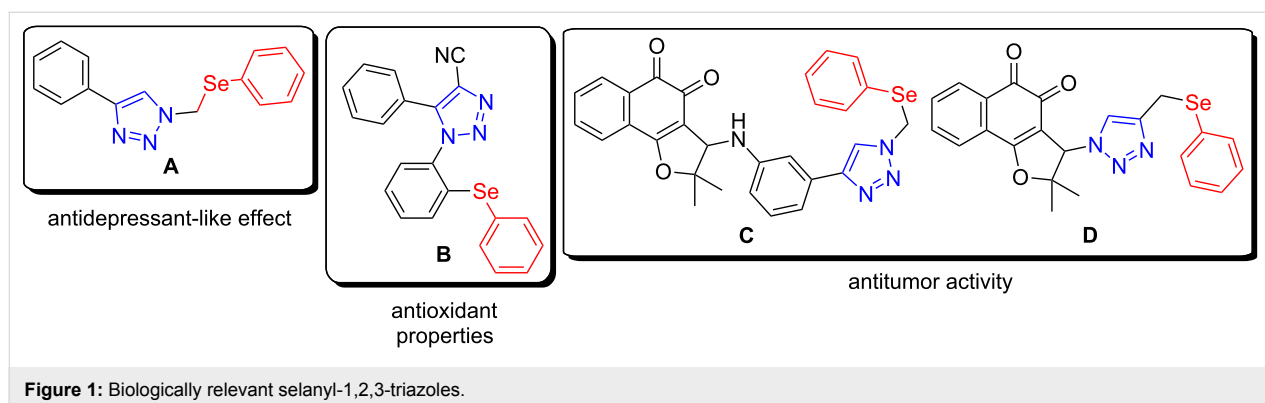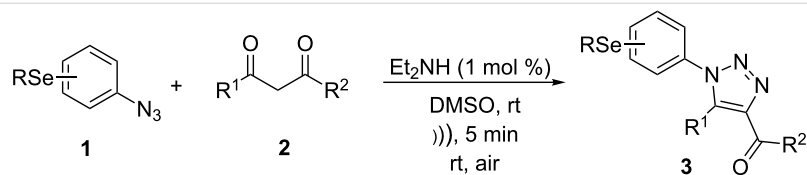
Scheme 1: General scheme of the reaction.
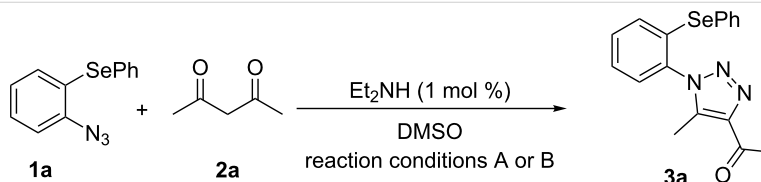
Scheme 2: Comparative study of the conventional conditions and ultrasound irradiation. Conditions A: Reaction at 25 °C for 2 h (**3a**, 98%); Conditions B: Reaction under ultrasound irradiation (20% of the amplitude) at 25 °C for 20 min (**3a**, 92%).

substrates **1a** and **2a** in DMSO using Et$_2$NH (1 mol %) was also performed under ultrasound irradiation.

The reaction performed under ultrasound irradiation with 20% of the amplitude for 20 minutes (followed by TLC until the total consumption of the starting materials) yielded product **3a** in 92% (conditions B, Scheme 2). Inspired by results described under conditions B, we performed additional experiments using ultrasound irradiation with Et$_2$NH as organocatalyst (Table 1).

Initially, substrates **1a** and **2a** were reacted in DMSO under ultrasound irradiation for 20 min using different amplitudes (Table 1, entries 1–4). We observed that the desired product **3a** was obtained in excellent yields in all reactions. However, product yield of **3a** decreased to 70% (Table 1, entry 5) in 10 minutes under 20% sonochemistry amplitude. To our delight, reactions performed using 40% of amplitude during 10 or 5 min gave excellent yields of selanyltriazole **3a** (Table 1, entries 6 and 7). We observed that the amplitude effect could be

Table 1: Optimization of reaction conditions.[a]

Entry	Amplitude	Et$_2$NH (mol %)	Time (min)	Yield **3a** (%)[b]
1	20	1	20	92
2	25	1	20	92
3	30	1	20	93
4	40	1	20	96
5	20	1	10	70
6	40	1	10	95
7	40	1	5	93
8	40	0.5	25	85
9	40	0.1	60	n.d.
10	40	–	60	n.d.
11[c]	40	1	5	27
12[d]	40	1	5	85

[a]Reactions were performed with 2-azidophenyl phenyl selenide (**1a**, 0.3 mmol) and 2,4-pentanedione (**2a**, 0.3 mmol) in DMSO (0.6 mL) as solvent under ultrasound irradiation at 25 °C. [b]Yields are given for isolated products. [c]Reaction was performed with L-proline as a catalyst. [d]Reaction was performed with pyrrolidine (1 mol %). n.d.: not detected.

correlated to the product formation time, since that in reaction carried out in 40% of amplitude the yield of compound **3a** was excellent (93%) after 5 min reaction time (Table 1, entry 5 vs 7). A slight decrease in reaction yields could be observed after decreasing the loading of organocatalyst to 0.5 mol % (Table 1, entry 8). Finally, in blank runs (in the absence of organocatalyst) or performed using 0.1 mol % of catalyst the reaction did not occur, even under sonication for 60 min using 40% of amplitude (Table 1, entries 9 and 10). Reactions performed with other catalysts (L-proline and pyrrolidine) gave lower yields of **3a** than those using 1 mol % of Et$_2$NH (Table 1, entry 7 vs entries 11 and 12).

From Table 1, optimum reaction conditions to obtain 1-(5-methyl-1-(2-(phenylselanyl)phenyl)-1*H*-1,2,3-triazol-4-yl)ethan-1-one (**3a**) were clearly present in entry 7, in which a mixture of azidophenyl phenyl selenide (**1a**, 0.3 mmol), 2,4-pentanedione (**2a**, 0.3 mmol) and Et$_2$NH (1 mol %) in DMSO (0.6 mL) was sonicated using 40% of amplitude at room temperature for 5 minutes. In order to extend the scope of the reaction, optimum reaction conditions were extended to other 1,3-diketones **2a–e** with different substitution patterns (Table 2). High yields of desired 1,2,3-triazoles were obtained using β-diketones **2a**, **2b** and **2c** bearing methyl, ethyl and phenyl substituents (Table 2, entries 1–3). However, we observed that the

steric hindrance effect in 2,2,6,6-tetramethyl-3,5-heptanedione **2d** displays an important role in the overall reaction and only traces of product **3d** was observed (Table 2, entries 1–3 vs 4). Unfortunately, no reaction occurred when cyclic β-diketone **2e** was employed as substrate (Table 2, entry 5). We next evaluated the reactivity of 2,4-pentanedione (**2a**) with different functionalized aryl azidophenyl selenides **1b–f** under identical reaction conditions. Aryl azidophenyl selenides containing either an EDG or an EWG on the aromatic ring delivered the expected selanyltriazoles **3f–i** in good isolated yields (Table 2, entries 6–9). However, a decrease in yield was observed when the reaction was performed with aryl azidophenyl selenide containing a –CF$_3$ group (Table 2, entry 9). In addition, 4-azidophenyl phenyl selenide (**1f**) was treated with 2,4-pentanedione (**2a**) to afford the desired product **3j** in 92% yield as a mixture of regioisomers (6:1) (Table 2, entry 10).

In addition, the possibility to perform the reaction of 2-azidophenyl phenyl selenide (**1a**) with β-keto-esters, β-keto-amides and α-cyano-ketones **2f–k** was also investigated. The reaction conditions optimized for 1,3-diketone **2a** were employed, but independently using as substrates ethyl acetoacetate (**2f**), ethyl benzoylacetate (**2g**), 3-oxo-*N*-phenylbutanamide (**2h**), 3-oxo-*N*-(*p*-tolyl)butanamide (**2i**), benzoylacetonitrile (**2j**) and 4-toluoylacetonitrile (**2k**). The corresponding esters **3k,l**

Table 2: Scope of substrates: Variation of the aryl azidophenyl selenides **1** and 1,3-diketones **2**.[a]
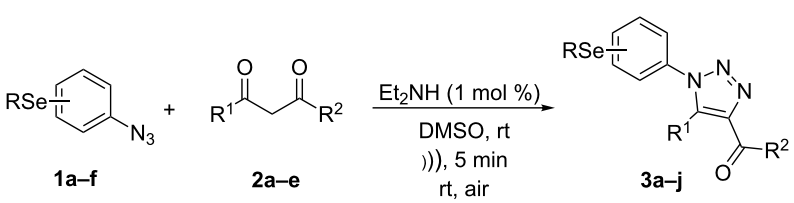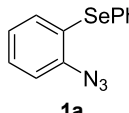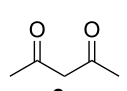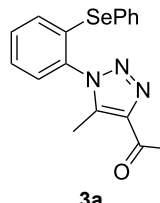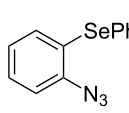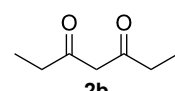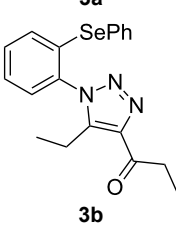

Entry	Aryl azidophenyl selenides **1**	1,3-Diketone **2**	Product **3**	Isolated Yield (%)[b]
1	**1a**	**2a**	**3a**	93
2	**1a**	**2b**	**3b**	91

Table 2: Scope of substrates: Variation of the aryl azidophenyl selenides **1** and 1,3-diketones **2**.[a] (continued)

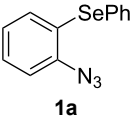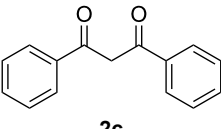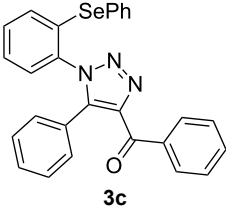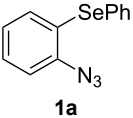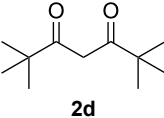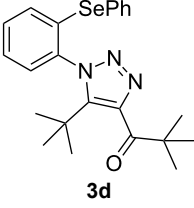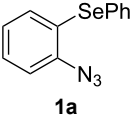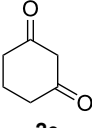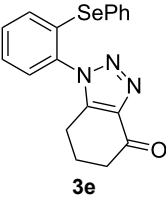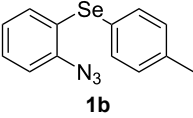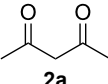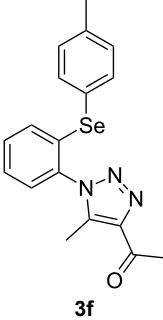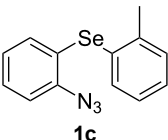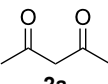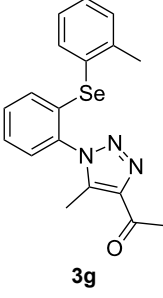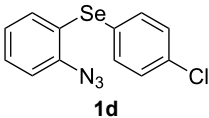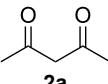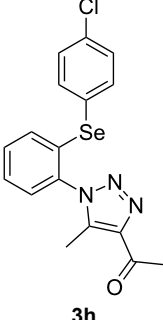|				
3	**1a**	**2c**	**3c**	85
4	**1a**	**2d**	**3d**	traces
5	**1a**	**2e**	**3e**	n.d.
6	**1b**	**2a**	**3f**	74
7	**1c**	**2a**	**3g**	84
8	**1d**	**2a**	**3h**	87

Table 2: Scope of substrates: Variation of the aryl azidophenyl selenides **1** and 1,3-diketones **2**.[a] (continued)

| 9 | 1e | 2a | 3i | 56 |
| 10 | 1f | 2a | 3j | 92 |
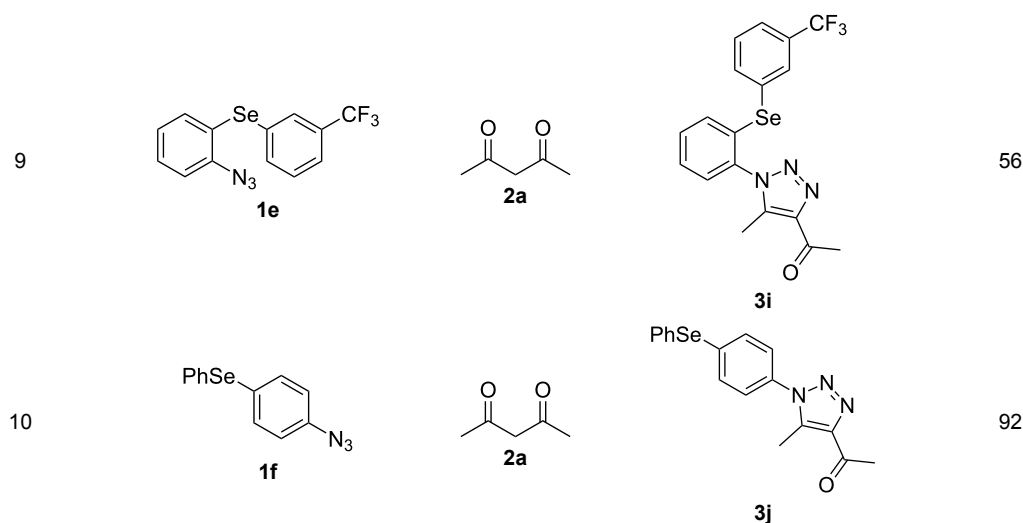
[a]Reactions were performed with aryl azidophenyl selenides **1a–f** (0.3 mmol) and 1,3-diketones **2a–e** (0.3 mmol), using Et$_2$NH (1 mol %) as catalyst in DMSO (0.6 mL) as solvent under ultrasound irradiation (40% of amplitude) at room temperature for 5 min. [b]Yields are given for isolated products. n.d.: not detected.

[33], amides **3m,n** [34] and nitriles **3o,p** [36] were obtained in good yields (Scheme 3) after 5 minutes reaction under ultrasound irradiation (40% of amplitude) at room temperature.

Comparing these results with already published ones under conventional conditions, our methodology using ultrasound irradiation affords the products in 5 minutes and in comparable

3k
89%

3m
88%

3o
90%

3l
64%

3n
86%

3p
87%
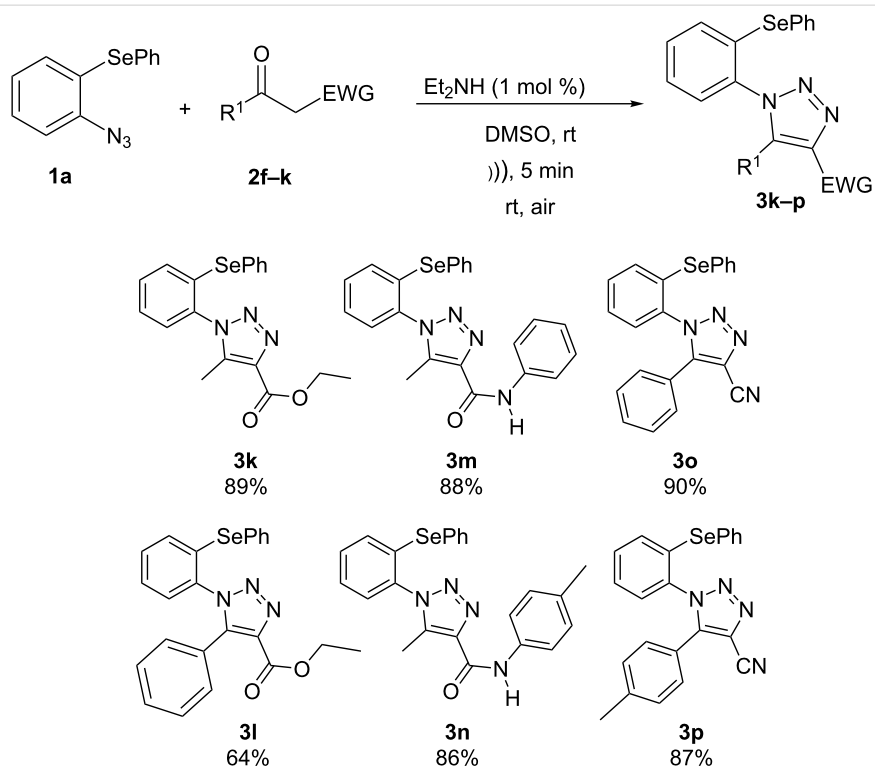
Scheme 3: Reaction of 2-azidophenyl phenyl selenide **1a** with activated ketones **2f–k**.

yields while the other methods mostly provide the products in times above 60 minutes [33,34,36].

Conclusion

In summary, we have described the use of sonochemistry in the organocatalytic enamine–azide [3 + 2] cycloaddition between 1,3-diketones and aryl azidophenyl selenides. These sonochemical promoted reactions were found to be amenable to a range of 1,3-diketones or aryl azidophenyl selenides, providing an efficient access to novel selenium-containing 1,2,3-triazole compounds in good to excellent yields, in a few minutes of reaction at room temperature. The protocol was extended to activated ketones and selanyltriazoyl carboxylates, with carboxamides and carbonitriles synthesized in high yields and short times of reaction.

Experimental
General information

The reactions were monitored by TLC carried out on Merck silica gel (60 F$_{254}$) by using UV light as visualizing agent and 5% vanillin in 10% H$_2$SO$_4$ and heat as developing agents. Baker silica gel (particle size 0.040–0.063 mm) was used for flash chromatography. A Cole Parmer-ultrasonic processor Model CPX 130, with a maximum power of 130 W, operating at an amplitude of 40% and a frequency of 20 kHz was used. The temperature of the reaction was monitored using an Incoterm digital infrared thermometer Model Infraterm (Brazil) (in most reactions the temperature was in the range between 60 and 65 °C). Proton nuclear magnetic resonance spectra (^{1}H NMR) were obtained at 400 MHz on Bruker DPX 400 spectrometer. Spectra were recorded in CDCl$_3$ solutions. Chemical shifts are reported in ppm, referenced to tetramethylsilane (TMS) as the external reference. Coupling constants (*J*) are reported in Hertz. Abbreviations to denote the multiplicity of a particular signal are s (singlet), d (doublet), t (triplet), q (quartet) and m (multiplet). Carbon-13 nuclear magnetic resonance spectra (^{13}C NMR) were obtained at 100 MHz on Bruker DPX 400 spectrometer. Chemical shifts are reported in ppm, referenced to the solvent peak of CDCl$_3$. Low-resolution mass spectra were obtained with a Shimadzu GC-MS-QP2010 mass spectrometer. High resolution mass spectra (HRMS) were recorded on a Bruker Micro TOF-QII spectrometer 10416.

General procedure for the synthesis of selanyltriazoles **3a–r** under ultrasound irradiation

Aryl azidophenyl selenides **1a–f** (0.3 mmol), activated ketones **2a–k** (0.3 mmol), Et$_2$NH (1 mol %) and DMSO (0.6 mL) were added to a glass tube. The ultrasound probe was placed in a glass vial containing the reaction mixture. The amplitude of the ultrasound waves was fixed in 40%. Then, the reaction mixture

was sonicated for 5 min. The crude product obtained was subsequently purified by column chromatography on silica gel using a mixture of hexane/ethyl acetate (5:1) as eluent to afford the desired products **3a–p**.

Supporting Information

Supporting Information File 1
Experimental and analytical data.
[http://www.beilstein-journals.org/bjoc/content/supplementary/1860-5397-13-68-S1.pdf]

References

1. Dehaen, W.; Bakulev, V. A. *Chemistry of 1,2,3-triazoles,* 1st ed.; Springer International Publishing: New York, 2014.
2. For a set of reviews in this area see the themed issue: Click chemistry: function follows form, in *Chem. Soc. Rev.* **2010,** *39,* 1221. doi:10.1039/C003926H
3. For a set of reviews in this area see the themed issue: Bioorthogonal Chemistry in Biology, in *Acc. Chem. Res.* **2011,** *44,* 651. doi:10.1021/ar200193f
4. Nandivada, H.; Jiang, X.; Lahann, J. *Adv. Mater.* **2007,** *19,* 2197. doi:10.1002/adma.200602739
5. Lee, B. S.; Lee, J. K.; Kim, W.-J.; Jung, Y. H.; Sim, S. J.; Lee, J.; Choi, I. S. *Biomacromolecules* **2007,** *8,* 744. doi:10.1021/bm060782+
6. Deobald, A. M.; Camargo, L. R. S.; Alves, D.; Zukerman-Schpector, J.; Corrêa, A. G.; Paixão, M. W. *Synthesis* **2011,** 4003. doi:10.1055/s-0031-1289606
7. Pérez-Labrada, K.; Brovard, I.; Morera, C.; Estévez, F.; Bermejo, J.; Rivera, D. G. *Tetrahedron* **2011,** *67,* 7713. doi:10.1016/j.tet.2011.08.003
8. Días, D. D.; Rajagopal, K.; Strable, E.; Schneider, J.; Finn, M. G. *J. Am. Chem. Soc.* **2006,** *128,* 6056. doi:10.1021/ja061251w
9. Astruc, D.; Liang, L.; Rapakousiou, A.; Ruiz, J. *Acc. Chem. Res.* **2012,** *45,* 630. doi:10.1021/ar200235m
10. Tasdelen, M. A.; Yilmaz, G.; Iskin, B.; Yagci, Y. *Macromolecules* **2012,** *45,* 56. doi:10.1021/ma202438w
11. Font, D.; Jimeno, C.; Pericàs, M. A. *Org. Lett.* **2006,** *8,* 4653. doi:10.1021/ol061964j
12. Font, D.; Bastero, A.; Sayalero, S.; Jimeno, C.; Pericàs, M. A. *Org. Lett.* **2007,** *9,* 1943. doi:10.1021/ol070526p
13. Font, D.; Sayalero, S.; Bastero, A.; Jimeno, C.; Pericàs, M. A. *Org. Lett.* **2008,** *10,* 337. doi:10.1021/ol702901z
14. Lallana, E.; Riguera, R.; Fernandez-Megia, E. *Angew. Chem., Int. Ed.* **2011,** *50,* 8794. doi:10.1002/anie.201101019
15. Hong, V.; Presolski, S. I.; Ma, C.; Finn, M. G. *Angew. Chem., Int. Ed.* **2009,** *48,* 9879. doi:10.1002/anie.200905087

16. Huisgen, R. *Angew. Chem.* **1963,** *75,* 604. doi:10.1002/ange.19630751304
17. Huisgen, R. *Proc. Chem. Soc., London* **1961,** 357. doi:10.1039/PS9610000357
18. Huisgen, R. In *1,3-Dipolar Cycloaddition Chemistry;* Padwa, A., Ed.; Wiley: New York, 1984; Vol. 1, 1.
19. Huisgen, R. *Pure Appl. Chem.* **1989,** *61,* 613. doi:10.1351/pac198961040613
20. Rostovtsev, V. V.; Green, L. G.; Fokin, V. V.; Sharpless, K. B. *Angew. Chem., Int. Ed.* **2002,** *41,* 2596. doi:10.1002/1521-3773(20020715)41:14<2596::AID-ANIE2596>3.0.CO;2-4
21. Tornøe, C. W.; Christensen, C.; Meldal, M. *J. Org. Chem.* **2002,** *67,* 3057. doi:10.1021/jo011148j
22. Krasiński, A.; Radić, Z.; Manetsch, R.; Raushel, J.; Taylor, P.; Sharpless, K. B.; Kolb, H. C. *J. Am. Chem. Soc.* **2005,** *127,* 6686. doi:10.1021/ja043031t
23. Lee, L. V.; Mitchell, M. L.; Huang, S.-J.; Fokin, V. V.; Sharpless, K. B.; Wong, C.-H. *J. Am. Chem. Soc.* **2003,** *125,* 9588. doi:10.1021/ja0302836
24. Hein, J. E.; Tripp, J. C.; Krasnova, L. B.; Sharpless, K. B.; Fokin, V. V. *Angew. Chem., Int. Ed.* **2009,** *48,* 8018–8021. doi:10.1002/anie.200903558
25. Zhang, L.; Chen, X.; Xue, P.; Sun, H. H. Y.; Williams, I. D.; Sharpless, K. B.; Fokin, V. V.; Jia, G. *J. Am. Chem. Soc.* **2005,** *127,* 15998. doi:10.1021/ja054114s
26. Boren, B. C.; Narayan, S.; Rasmussen, L. K.; Zhang, L.; Zhao, H.; Lin, Z.; Jia, G.; Fokin, V. V. *J. Am. Chem. Soc.* **2008,** *130,* 8923. doi:10.1021/ja0749993
27. McNulty, J.; Keskar, K.; Vemula, R. *Chem. – Eur. J.* **2011,** *17,* 14727. doi:10.1002/chem.201103244
28. McNulty, J.; Keskar, K. *Eur. J. Org. Chem.* **2012,** 5462. doi:10.1002/ejoc.201200930
29. Ding, S.; Jia, G.; Sun, J. *Angew. Chem., Int. Ed.* **2014,** *53,* 1877. doi:10.1002/anie.201309855
30. Lima, C. G. S.; Ali, A.; van Berkel, S. S.; Westermann, B.; Paixão, M. W. *Chem. Commun.* **2015,** *51,* 10784. doi:10.1039/C5CC04114G
31. Ramasastry, S. S. V. *Angew. Chem., Int. Ed.* **2014,** *53,* 14310–14312. doi:10.1002/anie.201409410
32. John, J.; Thomas, J.; Dehaen, W. *Chem. Commun.* **2015,** *51,* 10797. doi:10.1039/C5CC02319J
33. Seus, N.; Gonçalves, L. C.; Deobald, A. M.; Savegnago, L.; Alves, D.; Paixão, M. W. *Tetrahedron* **2012,** *68,* 10456. doi:10.1016/j.tet.2012.10.007
34. Seus, N.; Goldani, B.; Lenardão, E. J.; Savegnago, L.; Paixão, M. W.; Alves, D. *Eur. J. Org. Chem.* **2014,** 1059. doi:10.1002/ejoc.201301547
35. Saraiva, M. T.; Costa, G. P.; Seus, N.; Schumacher, R. F.; Perin, G.; Paixão, M. W.; Luque, R.; Alves, D. *Org. Lett.* **2015,** *17,* 6206. doi:10.1021/acs.orglett.5b03196
36. Savegnago, L.; do Sacramento, M.; Brod, L. M. P.; Fronza, M. G.; Seus, N.; Lenardão, E. J.; Paixão, M. W.; Alves, D. *RSC Adv.* **2016,** *6,* 8021. doi:10.1039/C5RA22445D
37. Saraiva, M. T.; Krüger, R.; Baldinotti, R. S. M.; Lenardão, E. J.; Luchese, C.; Savegnago, L.; Wilhelm, E. A.; Alves, D. *J. Braz. Chem. Soc.* **2016,** *27,* 41. doi:10.5935/0103-5053.20150239
38. Alberto, E. E.; Braga, A. L. In *Selenium and Tellurium Chemistry - From Small Molecules to Biomolecules and Materials;* Derek, W. J.; Risto, L., Eds.; Springer-Verlag: Berlin Heidelberg, 2011.
39. Wirth, T. *Organoselenium Chemistry: Synthesis and Reactions;* Wiley-VCH: Weinheim, 2011. doi:10.1002/9783527641949
40. Menezes, P. H.; Zeni, G. *Vinyl Selenides. Patai's Chemistry of Functional Groups;* John Wiley & Sons: Oxford, 2011. doi:10.1002/9780470682531.pat0568
41. Perin, G.; Lenardão, E. J.; Jacob, R. G.; Panatieri, R. B. *Chem. Rev.* **2009,** *109,* 1277. doi:10.1021/cr8004394
42. Perin, G.; Alves, D.; Jacob, R. G.; Barcellos, A. M.; Soares, L. K.; Lenardão, E. J. *ChemistrySelect* **2016,** *1,* 205. doi:10.1002/slct.201500031
43. Freudendahl, D. M.; Santoro, S.; Shahzad, S. A.; Santi, C.; Wirth, T. *Angew. Chem., Int. Ed.* **2009,** *48,* 8409. doi:10.1002/anie.200903893
44. Rampon, D. S.; Santos, F. S.; Descalzo, R. R.; Toldo, J. M.; Gonçalves, P. F. B.; Schneider, P. H.; Rodembusch, F. S. *J. Phys. Org. Chem.* **2014,** *27,* 336. doi:10.1002/poc.3229
45. Rampon, D. S.; Rodembusch, F. S.; Schneider, J. M. F. M.; Bechtold, I. H.; Gonçalves, P. F. B.; Merlo, A.; Schneider, P. H. *J. Mater. Chem.* **2010,** *20,* 715. doi:10.1039/B917366H
46. Samb, I.; Bell, J.; Toullec, P. Y.; Michelet, V.; Leray, I. *Org. Lett.* **2011,** *13,* 1182. doi:10.1021/ol200066p
47. Goswami, S.; Hazra, A.; Chakrabarty, R.; Fun, H.-K. *Org. Lett.* **2009,** *11,* 4350. doi:10.1021/ol901737s
48. Tang, B.; Xing, Y.; Li, P.; Zhang, N.; Yu, F.; Yang, G. *J. Am. Chem. Soc.* **2007,** *129,* 11666. doi:10.1021/ja072572q
49. Balaguez, R. A.; Ricordi, V. G.; Duarte, R. C.; Toldo, J. M.; Santos, C. M.; Schneider, P. H.; Gonçalves, P. F. B.; Rodembusch, F. S.; Alves, D. *RSC Adv.* **2016,** *6,* 49613. doi:10.1039/C6RA04157D
50. Nogueira, C. W.; Rocha, J. B. T. *Organoselenium and organotellurium compounds: Toxicology and pharmacology*. In *Patai's Chemistry of Functional Groups;* Rappoport, Z., (Org.), Ed.; Wiley: Chichester, 2011. doi:10.1002/9780470682531.pat0567
51. Santoro, S.; Azeredo, J. B.; Nascimento, V.; Sancineto, L.; Braga, A. L.; Santi, C. *RSC Adv.* **2014,** *4,* 31521. doi:10.1039/C4RA04493B
52. Nogueira, C. W.; Zeni, G.; Rocha, J. B. T. *Chem. Rev.* **2004,** *104,* 6255. doi:10.1021/cr0406559
53. Tiecco, M.; Testaferri, L.; Santi, C.; Tomassini, C.; Marini, F.; Bagnoli, L.; Temperini, A. *Angew. Chem., Int. Ed.* **2003,** *42,* 3131. doi:10.1002/anie.200351229
54. Back, T. G.; Bethell, R. J.; Parvez, M.; Taylor, J. A.; Wehrli, D. *J. Org. Chem.* **1999,** *64,* 7426. doi:10.1021/jo990730t
55. Stefani, H. A.; Silva, N. C. S.; Manarin, F.; Lüdtke, D. S.; Zukerman-Schpector, J.; Madureira, L. S.; Tiekink, E. R. T. *Tetrahedron Lett.* **2012,** *53,* 1742. doi:10.1016/j.tetlet.2012.01.102
56. Stefani, H. A.; Leal, D. M.; Manarin, F. *Tetrahedron Lett.* **2012,** *53,* 6495. doi:10.1016/j.tetlet.2012.09.062
57. Deobald, A. M.; Camargo, L. R. S.; Hörner, M.; Rodrigues, O. E. D.; Alves, D.; Braga, A. L. *Synthesis* **2011,** 2397. doi:10.1055/s-0030-1260083
58. Seus, N.; Saraiva, M. T.; Alberto, E. E.; Savegnago, L.; Alves, D. *Tetrahedron* **2012,** *68,* 10419. doi:10.1016/j.tet.2012.07.019
59. Saraiva, M. T.; Seus, N.; de Souza, D.; Rodrigues, O. E. D.; Paixão, M. W.; Jacob, R. G.; Lenardão, E. J.; Perin, G.; Alves, D. *Synthesis* **2012,** *44,* 1997. doi:10.1055/s-0031-1291135
60. Donato, F.; de Gomes, M. G.; Goes, A. T. R.; Seus, N.; Alves, D.; Jesse, C. R.; Savegnago, L. *Life Sci.* **2013,** *93,* 393. doi:10.1016/j.lfs.2013.07.024

61. da Cruz, E. H. G.; Silvers, M. A.; Jardim, G. A. M.; Resende, J. M.;
    Cavalcanti, B. C.; Bomfim, I. S.; Pessoa, C.; de Simone, C. A.;
    Botteselle, G. V.; Braga, A. L.; Nair, D. K.; Namboothiri, I. N. N.;
    Boothman, D. A.; da Silva Júnior, E. N. *Eur. J. Med. Chem.* **2016,** *122,*
    1. doi:10.1016/j.ejmech.2016.06.019
62. Mojtahedi, M. M.; Abaee, M. S. *Ultrasound applications in synthetic
    organic chemistry.* In *Handbook on Applications of Ultrasound
    Sonochemistry for Sustainability;* Chen, D.; Sharma, S. K.; Mudhoo, A.,
    Eds.; CRC Press: New York, 2012; pp 281 ff.
63. Li, Z.; Hong, J.; Zhou, X. *Tetrahedron* **2011,** *67,* 3690.
    doi:10.1016/j.tet.2011.03.067
64. Cravotto, G.; Cintas, P. *Chem. Soc. Rev.* **2006,** *35,* 180.
    doi:10.1039/B503848K
65. Mason, T. J. *Ultrason. Sonochem.* **2007,** *14,* 476.
    doi:10.1016/j.ultsonch.2006.10.008
66. Nüchter, M.; Ondruschka, B.; Jungnickel, A.; Müller, U.
    J. Phys. Org. Chem. **2000,** *13,* 579.
    doi:10.1002/1099-1395(200010)13:10<579::AID-POC272>3.0.CO;2-M
67. Mason, T. J. *Chem. Soc. Rev.* **1997,** *26,* 443.
    doi:10.1039/cs9972600443
68. Cravotto, G.; Fokin, V. V.; Garella, D.; Binello, A.; Boffa, L.; Barge, A.
    J. Comb. Chem. **2010,** *12,* 13. doi:10.1021/cc900150d
69. Mady, M. F.; Awad, G. E. A.; Jørgensen, K. B. *Eur. J. Med. Chem.*
    2014, *84,* 433. doi:10.1016/j.ejmech.2014.07.042
70. Marzag, H.; Alaoui, S.; Amdouni, H.; Martin, A. R.; Bougrin, K.;
    Benhida, R. *New J. Chem.* **2015,** *39,* 5437. doi:10.1039/C5NJ00624D
71. Nallapati, S. B.; Sreenivas, B. Y.; Bankala, R.; Parsa, K. V. L.;
    Sripelly, S.; Mukkanti, K.; Pal, M. *RSC Adv.* **2015,** *5,* 94623.
    doi:10.1039/C5RA20380E
72. Naeimi, H.; Dadashzadeh, S.; Moradian, M. *Res. Chem. Intermed.*
    2015, *41,* 2687. doi:10.1007/s11164-013-1379-6
73. Stefani, H. A.; Canduzini, H. A.; Manarin, F. *Tetrahedron Lett.* **2011,**
    52, 6086. doi:10.1016/j.tetlet.2011.09.004
74. Jiang, Y.; Chen, X.; Qu, L.; Wang, J.; Yuan, J.; Chen, S.; Li, X.; Qu, C.
    Ultrason. Sonochem. **2011,** *18,* 527.
    doi:10.1016/j.ultsonch.2010.09.009
75. Xavier, D. M.; Goldani, B. S.; Seus, N.; Jacob, R. G.; Barcellos, T.;
    Paixão, M. W.; Luque, R.; Alves, D. *Ultrason. Sonochem.* **2017,** *34,*
    107. doi:10.1016/j.ultsonch.2016.05.007

Cyclodextrins tethered with oligolactides – green synthesis and structural assessment

Cristian Peptu[*1,2], Mihaela Balan-Porcarasu[2], Alena Šišková[1], Ľudovít Škultéty[3] and Jaroslav Mosnáček[1]

Abstract

Biodegradable oligolactide derivatives based on α-, β- and γ-cyclodextrins (CDs) were synthesized by a green procedure in which CDs play the role of both the initiator and the catalyst. The synthetic procedure in which CDs and L-lactide (L-LA) are reacting in bulk at relatively high temperature of 110 °C was investigated considering the structural composition of the products. The obtained products were thoroughly characterized via mass spectrometry methods with soft ionization like matrix-assisted laser desorption ionization (MALDI) and electrospray ionization (ESI). Liquid chromatography (LC) separation with evaporative light scattering detection (ELSD) and NMR analysis were employed in order to elucidate the structural profiles of the obtained mixtures. The results clearly demonstrate that the cyclodextrins were tethered with more than one short oligolactate chain per CD molecule, predominantly at the methylene group, through ring opening of L-LA initiated by primary OH groups.

Introduction

Cyclodextrin derivatives are increasingly important and their variety is dictated by the wide range of applications in which these compounds are employed with preponderance in the pharmaceutical field [1,2]. The employed strategies for the modification with small molecular weight compounds are taking advantage of the different reactivity of the hydroxy groups in 2, 3 or 6 position, thus allowing selective modifications [3]. While modified CDs with low molecular weight substituents, such as methyl, (2-hydroxy)propyl, sulfobutyl, etc. are already available as commercial products, the modification with polymers is

still under development [4,5]. So far, several polymerization reactions were used for CD modification, including free radical polymerization, reversible-deactivation radical polymerizations [5] as well as ring opening polymerizations (ROP) of cyclic esters [6], oxiranes [7] and oxazolines [8]. However, the ROP of cyclic esters should also be considered as a method of producing polymer-modified CDs with some particular features, such as possibility of employing green polymerization procedures and availability of renewable monomers like cyclic esters. The methods published so far for polymerization of cyclic esters initiated by cyclodextrins employed catalysts commonly used in ROP, such as Sn-octoate [9-11] or amine-based organic catalysts [12], resulting in star polymers with a more or less well defined structure. CD functional polylactides have been prepared using different catalytic systems with good results in synthesis of star polymers with relatively high molecular weight and low polydispersity, by the "core first" method. Polymerization of L-lactide was performed by anionic ROP initiated by potassium alkoxides of α-CD partially modified with trimethylsilazane [13]. The L- or DL-lactide were polymerized in the presence of organocatalysts like 4-dimethylaminopyridine [12] using β-CD and modified CD (β-CD-(OBn)$_{19}$(OH)$_2$) as initiators. Normand et al. [14] applied a similar approach as Zinck and co-workers [12] in order to prepare CD-containing polymers while simplifying the complexity induced by multifunctional initiator through partial benzylation of the β-CD resulting in a CD-diol. Also, the ROP of D,L-LA catalyzed by 4-dimethylaminopyridine and initiated by all 21 OH groups of β-CD was employed by Xu et al. [15].

However, the above mentioned methods were using CDs only as a scaffold for growing star polymers with properties belonging more to the class of polymers and, in consequence, the CD core influenced the properties of the final product in a small proportion. Thus, these polymers do not differ significantly from other star polymers with different core and similar number of arms. The modification of CDs with a reduced amount of monomer units results in CD-oligomer materials which still keep an important property of the starting CDs, like their inclusion ability [16]. The CD-oligoester conjugate, compounds with a relatively low content of oligoester components were first prepared by a totally green procedure by Harada and co-workers [17]. They succeeded to polymerize a series of cyclic esters including β-butyrolactone (BL), δ-valerolactone (VL) and ε-caprolactone (CL). A recent work published by Galia et al. [18] brings new insights on the effect of pressure on bulk polymerization of CL initiated by β-CD. The lactides polymerization (L-LA, D-LA and DL-LA) was also attempted [19,20] but with less success, as compared with previously mentioned cyclic esters, possibly, due to the fact that the LA monomers (especially DL-LA) are solid in the range of temperature

applied during the reaction. Attempts to resolve the reactants mixing problem were made by using δ-valerolactone (VL) as dispersion environment for the lactides. A better overall conversion and increased molecular weights were observed but the authors did not asses their products whether these were CD-VL, CD-LA or CD-VL/LA covalent conjugates [19,20]. The results presented by the Harada group generally evaluated the CD-oligoester samples by matrix-assisted laser desorption ionization mass spectrometry (MALDI–MS) and nuclear magnetic resonance (NMR) spectroscopy, however, in case of CD-oligolactides no such structural proofs were presented. Later, the LA was polymerized in dimethylformamide (DMF) solution to result in well-defined and homogenous β-CD functionalized with oligolactides as demonstrated by electrospray mass spectrometry (ESI–MS) and NMR spectroscopy [16].

Herein we analyze the products resulted from a green synthetic approach and clarify the structure of the obtained products. Therefore, we present an alternative route of bulk polymerization of L-LA, in the presence of α-, β- and γ-cyclodextrins, in melt system and the obtained products are thoroughly evaluated by various analytical methods, such as mass spectrometry, NMR spectroscopy and reversed-phase liquid chromatography. Results for particular cyclodextrins (α-, β- and γ-) are compared in order to understand the influence of type of CD on the course of modification.

Results and Discussion

The properties of cyclodextrin-oligoester covalent conjugates, situated at the border of low and high molecular weight compounds can be influenced by both the carbohydrate and the oligoester components. The properties of such materials like solubility, miscibility with other materials, inclusion capacity or even degradability in different environments will depend on their structure which is therefore crucially important to be uncovered at the molecular level.

Nevertheless, to completely understand the related structural issues is a difficult task due to the level of complexity of such products. One particular problem is arising from the presence of multiple reactive points, i.e., OH groups, in the CD structure. On any given CD molecule there are three types of OH groups with their own specificities, like OH6 groups are the most accessible for bulky substituents, the OH2 are the most acidic and OH3 groups are the least reactive [3]. This heterogeneity may favor a specific attachment of cyclic esters to the CDs but also can lead to a certain non-uniformity or isomeric distribution (dispersity) of the modified CDs. Another source of sample dispersity is the molecular weight dispersity commonly encountered in synthetic polymers. Moreover, the presence of multiple initiating sites may favor the formation of star-like

oligomers. A particular issue, still under debate, is related to the possibility that in spite of multiple reactive points, namely the OH groups, which can be involved in ring opening of cyclic esters, one cyclodextrin molecule initiates a single polymer chain [17,20]. This fact was justified by the steric hindrance created by a first covalent attachment of a cyclic ester to the CD, which does not allow the growth of another chain from a single CD molecule. However, we already showed by MS in combination with NMR spectroscopy that, in case of β-BL bulk and solution polymerization in the presence of (−)-sparteine as organic catalyst, multiple chain attachment was possible in spite of possible steric hindrance [21,22]. Considering all that, a cautious and deep characterization should be performed in order to fully describe such systems. We showed that understanding of molecular level structural features of such complex mixtures (free CDs, homopolymers, CD-oligoesters) have to take into consideration the mass spectrometry methods in direct correlation with the NMR spectroscopy. Liquid chromatography and tandem MS fragmentation studies [21-23] are also important additions in deeper structural characterization of CD-oligoester conjugates.

The L-LA was reacted with α-, β- and γ-CD (Scheme 1) in bulk at 110 °C in order to ensure a good dispersion of reactants. The molar ratio between L-LA and OH groups of CDs was kept to a value of 5 for all types of CDs (Table 1) and the reaction was stopped after 72 hours. Although the cyclodextrins were only dispersed in the molten monomer the magnetic stirring insured a good dispersion of the reactants. In previous studies [19], the molar ratio between CD and the total monomer amounts introduced in the reaction was about 1/5 which even, in conditions of melted monomer, would not ensure a good mixture of reactants and therefore the reaction would be considered as a heterogeneous system with all disadvantages resulting from this.

The assessment of reaction products, obtained under the above mentioned conditions, was rather complicated because the products were not fully soluble either in water or in organic solvents
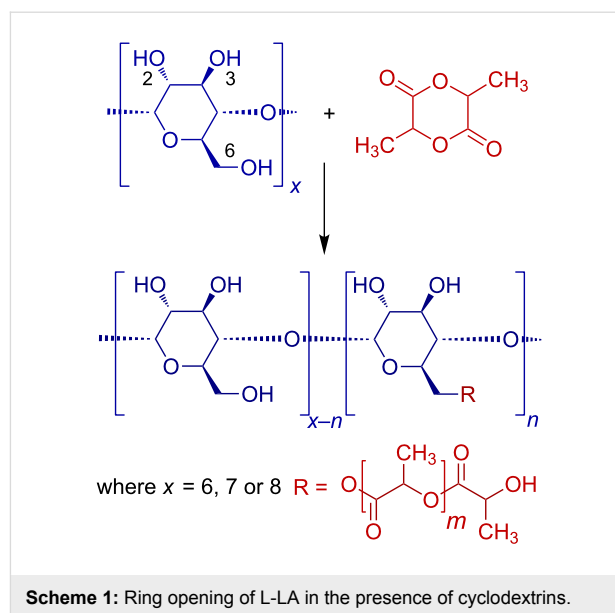
Scheme 1: Ring opening of L-LA in the presence of cyclodextrins.

like THF or ACN. In principle, the resulted mixture contained free CD, CD modified with polylactide units (CD-LA), polylactide (PLA) homopolymers and unreacted L-LA monomer. The ^{1}H NMR of crude reaction mixture showed that monomer conversion after 72 h was slightly over 5% for all CD initiators, which is in good correlation with conversion described by other authors for similar systems [18,19].

First we performed the reversed-phase liquid chromatography (LC) separation of the crude reaction mixture with evaporative light scattering detection (ELSD) for all CD-LA products. The chromatogram depicted in Figure 1a contains two distinct groups of chromatographic peaks of β-CD-LA reaction mixture. The first group appear at low elution time (from 2 to 4 min) and has increased water solubility, suggesting the presence of unmodified CD and CDs with low substitution degree. The second group, eluted from 9 to 18 minutes, contained modified CDs and PLA oligomers. The overlaid LC chromatograms for crude α-, β- and γ-CD-LA products are shown in Supporting

Table 1: Characterization of CD-LA products.

Sample	OH/LA molar ratio	CD/LA molar ratio	% of free CD[a]	Weight % of F1 fraction	$M_n/Đ$[b]	MS analysis of F1[c]	MS analysis of F2[c]
α-CD-LA	1/5	1/90	10	2	1600/1.75	1192/1.36	2798/12.52
β-CD-LA	1/5	1/105	10.2	5.5	2400/1.68	1296/0.96	3725/17.83
γ-CD-LA	1/5	1/120	30.5	9	1700/1.52	1878/3.87	3264/13.50

[a]Fraction determined by integration of peaks from ELSD after application of reversed-phase chromatography. Calculated as % free CD = total area peaks/area of free CD in LC ELSD chromatograms of raw reaction mixtures. [b]Determined by GPC of F2. [c]Average molecular weight and number of dilactate monomer units for one cyclodextrin (α-, β- or γ-CD) molecule determined by MALDI–MS [average mass = sum($m_i n_i$)/sum(n_i), where m_i = the *m/z* value of all peaks of CD derivatives from the MALDI–MS spectrum and n_i = the relative intensities of the corresponding MS peaks; average number of monomer units = (average mass–mass of corresponding CD–mass of Na cation)/mass of dilactate monomer unit]
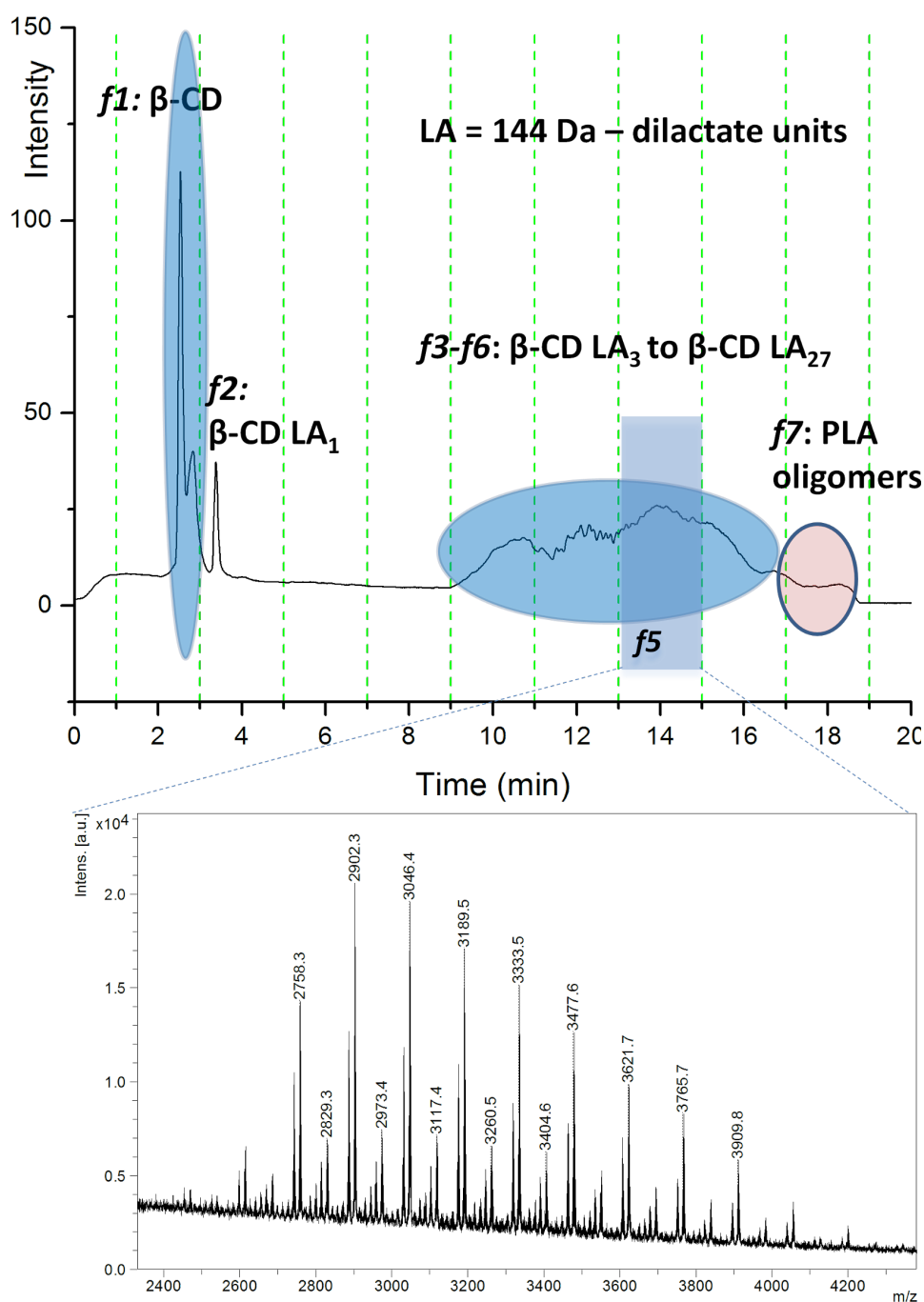
Figure 1: (a) ELSD chromatogram of crude β-CD-LA reaction mixture and (b) MALDI–MS spectrum of fraction *f*5.

Information File 1, Figure S1. The nature of the separated compounds was partially confirmed by "off line" MALDI–MS measurements of the eluted fractions. Full MALDI–MS identification of all collected LC fractions for α-, β- and γ-CD-LA and LC ELSD chromatograms are shown in Supporting Information File 1, Figures S3–S21.

Based on the MALDI–MS identification, the main chromatographic peak in Figure 1a has been assigned to free β-CD (fraction *f*1) while the other eluted species are β-CD-LA having from 1 to 27 monomer units (dilactate), fractions *f*2–*f*6 (elution times: *f*2 – 3–5 min, *f*3 – 9–11 min, *f*4 – 11–13 min, *f*5 – 13–15 min, *f*6 – 15–17 min and *f*7 – 17–19 min). In Figure 1b the

MALDI–MS identification of chromatographic peaks for the β-CD-LA sample, chromatographic fraction *f*5 eluted between 13 and 15 minutes, is exemplified. In the MS spectrum, the structural assignment was performed for the respective *m/z* values using the following equation: $m/z = 1134$ (β-CD) $+ n *$ 144 (LA) $+ 39$ (K). The main peaks of the considered series were adducts of K^+, but adducts with Na^+ were also identified ($\Delta m/z = -16$). Considering the lactate (72 Da) as a monomer unit, the oligomers with odd number of monomer units could be observed as well. These oligomer species with odd number of lactates resulted from intramolecular and/or intermolecular transesterification reactions and are in lower amount, when compared with the oligomers containing even number of monomers. This signifies that the predominance of transesterification is rather low in the employed reaction conditions. The presented spectrum was measured directly from the HPLC collected fraction with rather low concentration of products, thus resulting in a poor spectrum quality.

The *f*7 fraction (Figure 1 – LC–ELSD chromatogram and Figure S9 (Supporting Information File 1) – MALDI–MS spectrum) contained only PLA oligomers having from 16 to 28 lactate monomer units. However, all fractions from *f*3 to *f*7 may contain PLA homopolymers which are co-eluted with the CD-LA product (vide infra LC–ESI–MS characterization). The LC–MALDI–MS allowed estimating the maximum number of monomer units per CD molecule for each of the α-, β- and γ-CD systems. It may be observed that the highest number of L-LA monomer units were grafted on β-CD (27 dilactate units) while for α-CD and γ-CD were obtained maximum values of 18 and 19 dilactate units, respectively. Thus, β-CD seems to have the best activity in ring opening of L-LA.

The ELS detection allowed a quantitative evaluation of the reaction mixture content (Table 1). Thus, it may be observed that similar values of the relative content of free CD were obtained for α- and β-CD while, in case of γ-CD, the relative amount of free CD in the reaction mixture was three times higher. Therefore we may hypothesize that for similar reaction conditions the γ-CD is less active in the ring opening of L-LA. The calculation of the relative amount of free CD was performed by integration of chromatographic peaks corresponding to free CD and to modified CD in ELSD chromatograms. However, this estimation was made under the reserve that CD-LA mixtures eluted after 8 min may contain also PLA oligomer species initiated by the presence of residual water in the reaction system.

We chose "off line" confirmation of the eluted species by MALDI–MS over other available methods, as LC with "on line" ESI–MS detection has problems in the analysis of polymer species related to the formation of multicharged species, thus

creating difficulties in the spectra interpretation, especially in the case of polydisperse oligomer mixtures [24,25]. However, the presence of PLA oligomers was clearly confirmed by LC–ESI–MS, which has a better sensitivity for linear low-molecular-weight oligolactides. In the case of MALDI–MS identification, the presence of the substance used as matrix prevents accurate observation of the region below $m/z = 600$ and therefore only PLA oligomers with a mass higher than this threshold were observed (e.g., *f*7 for β-CD-LA). The LC separation with ESI–MS detection, performed only for β-CD-LA sample showed clearly that PLA oligomers are co-eluted with the β-CD-LA products. The presence of PLA oligomers can be justified by water initiation of L-lactide ring opening. The relative amount of homooligolactide species is highly exaggerated in the presented ESI chromatogram (Supporting Information File 1, Figure S22) due to mass discrimination of low-molecular-weight compounds (PLA) against co-eluting higher molecular-weight compounds (β-CD-LA) under electrospray conditions. This mass discrimination together with the formation of multiple charged species (example of ESI–MS spectrum of double and triple charged β-CD-LA is provided in Supporting Information File 1, Figure S23) is actually hindering a comprehensive evaluation of these CD-LA samples by LC with ESI–MS detection [26].

The presence of water in the reaction mixture may be debated, however, it was previously stated that, even with thorough procedures of water removal from cyclodextrin, water traces are still present [7]. Moreover, it was shown recently [18] that water is actually improving the overall process in case of bulk polymerization of ε-caprolactone (CL) under conditions of increased pressure. In the above mentioned study, β-CD modified with CL was characterized by MALDI–MS. Mixtures of PCL hompolymers and CD-caprolactone modified conjugates were evaluated in view of the products relative content only based on the MALDI–MS spectra. Generally, compounds with different ionization efficiency in MALDI–MS will give different MS response or intensity of the corresponding MS peaks [27] which does not allow a precise quantitative measurement. In our current study we do not attempt such comparison considering that the relative amount of modified CD and homopolyester obtained by such calculation would be highly biased.

Previously, we showed that LC–ESI–MS evaluation is possible for CD-(3-OH butyrate) conjugates taking into consideration only the MS peaks of structurally similar compounds with low molecular weight and molecular weight dispersity, i.e., CDs tethered with an average of 12 monomer units [21]. In the work of Shen et al. [16], where homogenous CD-LA conjugates were evaluated by ESI–MS with direct sample injection, the average number of dilactate monomer units per CD molecule was

around 3.5 which is clearly lower than in the case of CD-LA products described here.

The ESI–MS evaluation proved to be difficult and it was obvious that a different mass spectrometry evaluation of CD-LA products would be needed. In the previous papers [17] it was stated that CD-oligoester products may be separated from the reaction mixture by dissolution in DMF and precipitation into excess of dry THF in order to remove the unreacted CD. The procedure applied here resulted in two fractions for each sample, the THF insoluble (F1) and THF soluble (F2). This fractionation allowed analysis by MALDI–MS of the CD fraction with higher substitution degree.

The fractions separated (Experimental section – vide infra) in case of α-CD-LA (F1A and F2A) are both described using the MALDI–MS. The MS spectrum of the F1A fraction, in Figure 2a, revealed the presence of free α-CD and α-CD-LA oligomers having from 1 to 8 dilactate monomer units. The general formula used for the calculation of the m/z values corresponding to the assigned structures was $m/z = 972$ (α-CD) + n * 144 (LA) + 23 (Na). The most intense peaks corresponded to the species having from 0 to 2 monomer units. Thus, the fractionation procedure led to the loss of CD conjugates with a low

number of LA monomer units. The THF soluble fraction, F2A, (Figure 3a) was composed of α-CD-LA oligomers having from 5 to 22 dilactate units. The average M_n calculated from the relative intensities of the MS peaks was 2800 g/mol and corresponded to an average degree of polymerization of 13 dilactate monomer units. In the F2A spectrum a second series of peaks situated at 72 Da difference from the members of the main series may be also be observed, which correspond to α-CD-LA species with an odd number of lactate monomer units. These species could be formed as a result of transesterification reactions (intra- or intermolecular), which may occur in the melt reaction system. The presence of PLA homopolymers was also observed, their corresponding m/z being calculated by the following equation: $m/z = 18$ (H_2O) + n * 144 (LA) + 23 (Na)].

In a similar manner, the fractions collected in the case of β- and γ-CD-LA were analyzed by MALDI–MS (Figure 2b and Figure 3b). For β-CD-LA the formula used for the assignment of the MS peaks was $m/z = 1134$ (β-CD) + n * 144 (LA) + 23 (Na). Based on these calculations, we could remark that also in the case of the β-CD-LA fractionation some part of the species with lower polymerization degree were precipitated together with free CD (β-CD-LA F1B fraction had dilactate monomer units from $n = 0$ to $n = 10$ – Figure 2b). On the other hand, the
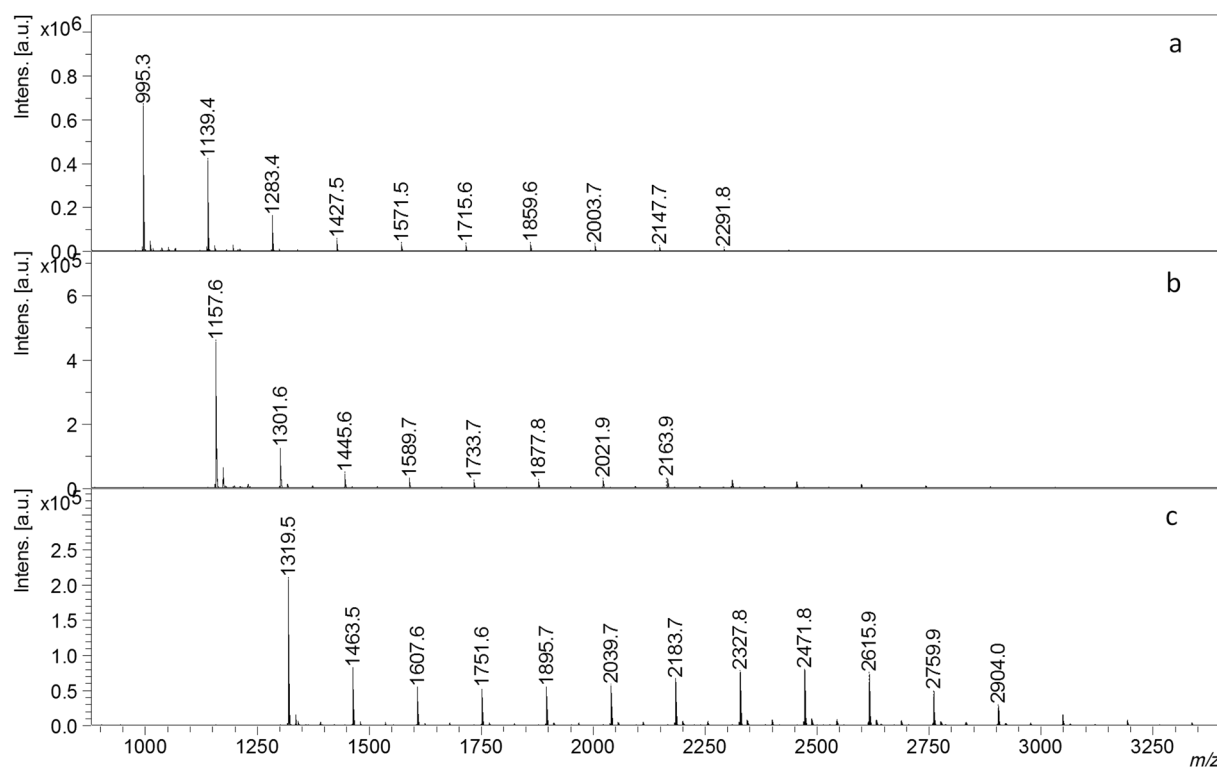

Figure 2: MALDI–MS spectra of the fractionated α-, β- and γ-CD-LA products – fractions precipitated in THF: (a) α-CD-LA fraction F1A, (b) β-CD-LA fraction F1B and (c) γ-CD-LA fraction F1C.

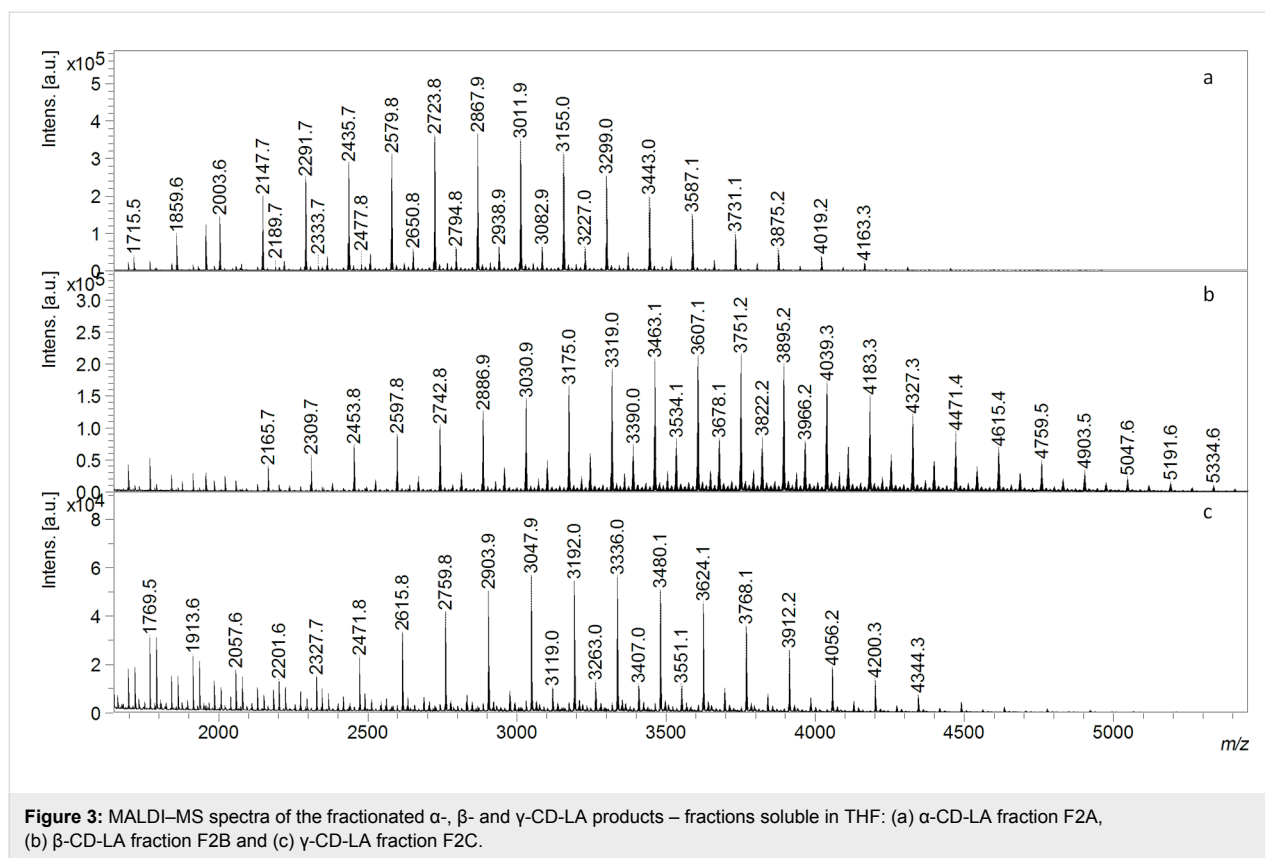**Figure 3:** MALDI–MS spectra of the fractionated α-, β- and γ-CD-LA products – fractions soluble in THF: (a) α-CD-LA fraction F2A, (b) β-CD-LA fraction F2B and (c) γ-CD-LA fraction F2C.

β-CD-LA fraction F2B (Figure 3b) had a number of monomer units ranging from 6 to 28 dilactate units. The M_n inferred from the MS spectrum had a value of 3800 g/mol corresponding to approximately 18 dilactate monomer units. The peaks from the species with an odd number of lactate monomer units formed by transesterification reactions ($\Delta m/z = 72$ Da from the main series) were also present in the spectra. In addition, in the lower region of the MALDI spectrum some peaks corresponding to PLA homopolymers in the lower mass region of the spectrum could also be observed.

The γ-CD-LA fractions, γ-CD-LA F1C (precipitated in THF) and γ-CD-LA F2C (soluble in THF), presented in Figure 2c and Figure 3c, could be described based on the MS spectra by using the following equation: $m/z = 1296$ (γ-CD) $+ n * 144$ (LA) $+23$ (Na). The F1C fraction (Figure 2c) was more abundant in CD-LA species having from $n = 0$ to $n = 13$ dilactate units. The F2C fraction (Figure 3c) contains γ-CD-LA species having from 7 to 21 dilactate monomer units with an average of 14 monomer units corresponding to an $M_n = 3300$ g/mol. Also, PLA homopolymers having up to 9 dilactate monomer units were present in this sample. The presence of PLA oligomer species in all the analyzed F2 fractions was also confirmed by GPC of all F2 fractions. It was observed that in each case the GPC curves were bimodal with dispersity of around 1.6 (Table 1).

Exact evaluation of the resulted products was prevented due to the complexity of the mixtures containing CD-LA, PLA and L-LA. The MALDI analysis of F1 fractions (Figure 2) showed that the number of lactate units attached to the CD is different according to the influence of the type of cyclodextrin. The F1C fraction had more lactate units as compared with F1A and F1B fractions. This could be explained by a more significant contribution of the γ-CD part, which is bigger than other CD homologues (8 glycoside units), to the lower solubility in THF resulting in precipitation of γ-CD-LA species with higher content of dilactate units. This fact is also reflected by the different weight percentage of F1 fractions. The α-CD-LA F1 was on 2%, β-CD-LA F1 was 5.5% and γ-CD-LA-F1 was 9% weight from total reaction mixture (Table 1).

Thus, the proposed fractionation of the CD-oligoester samples did not provide proper purification and a significant part of the sample can be lost by precipitation. The purification procedure applied in the work of Shen et al. [16] was based on a precipitation of CD-LA, synthesized in DMF, in excess of dry ether and subsequent washing of precipitate with acetone. However, this also can lead to the loss of fraction with high content of lactate units. Nevertheless, the reaction in DMF allowed the isolation of a homogenous product, with low polymerization degree, useful for preparation of inclusion complexes. However, for char-

acterization purposes this sample fractionation is useful as long as both fractions are analyzed. MALDI spectra of F2 fractions (Figure 3) are clearly showing that the average number of monomer units per CD (Table 1) is the highest for the β-CD initiated reaction while α- and γ-CD gave almost similar results. Thus, we may infer that β-CD is the best fit for this reaction system. Also, if LC with ELSD is taken into consideration (free CD vs CD-LA) we may state that free CD is in the highest amount for γ-CD while for α- and β-CD this ratio is similar. Therefore, the performance of different CDs in L-LA polymerization (in current reaction conditions) is decreasing in the order β-CD > α-CD > γ-CD.

The structural analysis aimed the following targets: to determine the substitution degrees for CD based products; the substitution site on the glycosidic rings (C2, C3 and/or C6) and the average length of the oligolactide sequences. So far, the MALDI–MS measurement of the fractionated reaction mixtures allowed the observation of the average number of monomer units per CD molecule for the respective fractions. In order to elucidate the other structural issues NMR spectroscopy has been employed.

First, the ^{1}H NMR spectroscopy analysis (Figure 4) was performed for the precipitated fractions (F1). These fractions had a lower content of L-lactide derived moieties, i.e., a high amount of free cyclodextrins and small amounts of functionalized CD-LA and L-lactide monomer. All samples showed peaks for the unreacted L-lactide and separated peaks for the protons of the substituted glucopyranose units. In the ^{1}H NMR spectra the substitution pattern of the glycoside rings of cyclodextrins can be followed by comparing the integral for the anomeric proton, H1, with the integrals for the OH groups which must have a 1:1:1:1 ratio for the unreacted cyclodextrin. Upon substitution of one or more OH groups the integration ratio becomes unbalanced. In the case of the F1 fractions of α-CD-LA, β-CD-LA and γ-CD-LA we observed that this ratio is slightly unbalanced as some of the OH6 groups were esterified (Supporting Information File 1, Figures S24–S26). However, in the case of the β-CD-LA F2 fraction (Supporting Information File 1, Figure S27), the substitution degree was increased. An exact quantitation is prevented due to NMR peaks overlapping.

Generally, in the ^{1}H NMR spectrum of the F2 fraction, the peaks corresponding to the cyclodextrin protons are broadened and the intensity of the signal corresponding to OH6 is flattened (almost not present) while those corresponding to OH2 and OH3 are still present but also broadened, with a ratio towards H1 proton close to 1:0.9, demonstrating that the CDs are substituted predominantly at C6. The analysis of the β-CD-LA F2 fraction was repeated at different time intervals in order

to prevent errors in integral ratio calculations caused by a slow H/D exchange between the OH groups and DMSO-d_6. Even though, these observations do not exclude some low degree of substitution of OH2 and OH3 groups, a certain tendency of selective substitution at C6 was confirmed, similar to the results obtained by Shen et al. [16], using DMF as solvent and possibly catalyst.

The covalent binding of the substituent induced a significant downfield shift for the peaks of the H6' protons bound to the esterified carbon and also to the neighboring H5' proton. These peaks, at about 4.2–4.3 ppm (H6') and 3.8 ppm (H5') were assigned by correlating the data obtained from ^{1}H NMR, ^{13}C NMR, DEPT135-NMR and 2D NMR spectroscopy (Supporting Information File 1, Figures S24–S31).

In the ^{13}C NMR spectra of β-CD-LA F1 and F2 (Figure 5), the peaks assigned to C5' (69.1 ppm) and C6' (64.4 ppm) of the substituted glucopyranose unit are clearly isolated. The rest of the peaks for the carbons of the substituted unit appear as a small broadening of the peaks for the unsubstituted units.

Similar compounds (CDs esterified with δ-valerolactone, β-butyrolactone and ε-caprolactone obtained by bulk polymerization) were reported by Harada et al. and were also analyzed by ^{13}C NMR [17]. The structural assignment of the esterified CDs was supported in Harada's work [17] by comparing the NMR spectra with those obtained for a monoesterified β-cyclodextrin at C2 position (mono-2-O-(6-benzyloxypentanoyl)-β-cyclodextrin). The peak at 63.4 ppm was assigned as C2' of the monosubstituted glucose ring belonging to mono-2-*O*-(6-benzyloxypentanoyl)-β-cyclodextrin. The peak at 64.4 ppm, observed in our experiment, was differently assigned using a DEPT135 experiment on β-CD-LA-F1 and F2 (Figure 6). In the DEPT135-NMR spectra the peaks at 60 and 64.4 ppm are in opposite phase compared to the CH and CH$_3$ peaks, indicating that they correspond to CH$_2$ units; therefore, we assigned the peak observed in the same region for our compounds as esterified C6'. Interestingly, our structural assignment is in good agreement with the study published by Shen et al. [16] for solution ring opening of DL-LA initiated by β-CD and catalyzed by DMF. While, in their case the presence of DMF can justify an activation mechanism of the OH groups by the amines (similar with the mechanism proposed by Zinck et al. [6]), in the present work the activation mechanism of OH groups is not applicable.

By comparing the ^{13}C NMR spectra of F1 and F2 fractions of β-CD-LA it may be observed that the intensity ratios of the C6 and C6' are reversing with increase of the lactate moieties amounts per CD (Figure 5 and Figure 6). This suggests that the degree of substitution at the C6 is also increasing, thus being
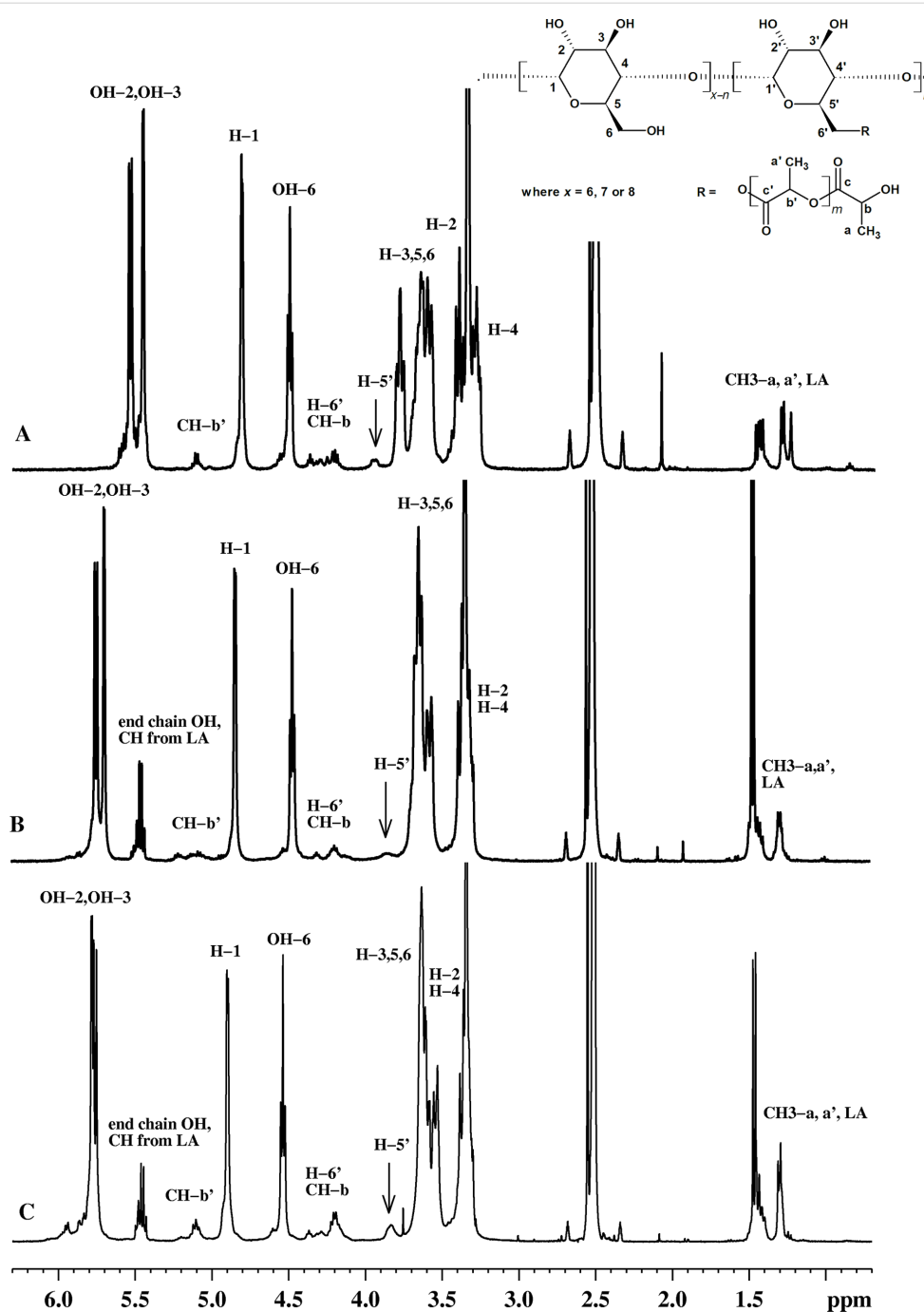
Figure 4: ¹H NMR spectrum of fractions precipitated in THF of (A) α-CD-LA, (B) β-CD-LA and (C) γ-CD-LA.

implied that for higher degrees of polymerization more glycoside rings are substituted predominantly at C6. This is also supported by the comparison between the ¹H NMR integral ratios of OH2 and OH3 versus OH6 as previously discussed (Supporting Information File 1, Figure S27).

Therefore, we may conclude that the lactide ring opening is performed mostly by the OH groups from C6. The DEPT135-NMR

experiment was also performed for α- and γ-CD-LA F1 samples (spectra given in Supporting Information File 1, Figures S28 and S29) confirming also the substitution at the C6.

The evaluation of the oligolactide chains attached to the CD may also include measuring of the average length. However, due to peak overlapping resulted from the presence of L-LA monomer and PLA homopolymer peaks this evaluation was not
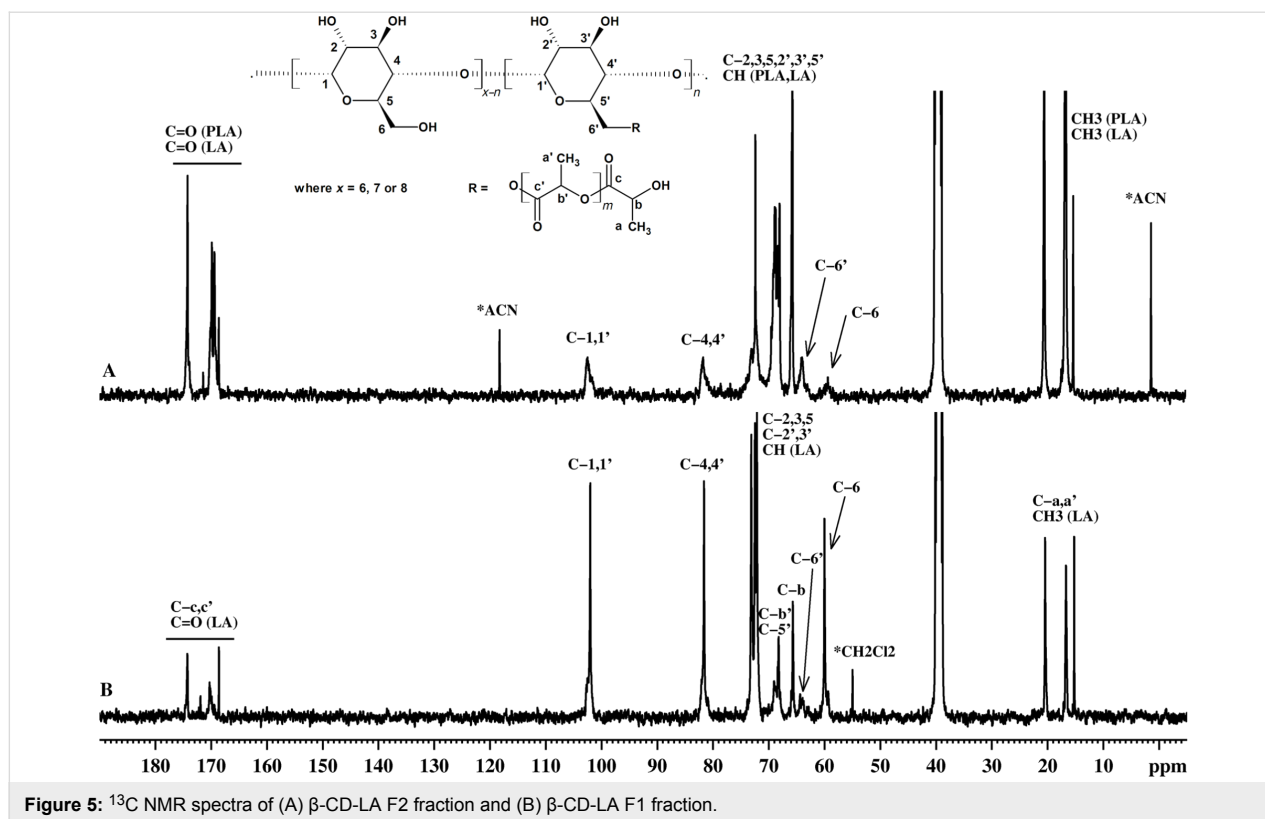
Figure 5: ^{13}C NMR spectra of (A) β-CD-LA F2 fraction and (B) β-CD-LA F1 fraction.

possible. However, the ratio between unsubstituted C6 and substituted C6' corresponding peaks (Figure 5 and Figure 6) is changing, thus implying that cyclodextrins are substituted with more than one chain of oligolactide. If we take into consideration the β-CD-LA F2 sample, with an almost full substitution at C6 (approximately 6 glycosidic units of a total 7) and compare with the MALDI–MS results which gave an average of 36 lactate (18 dilactate) units per CD molecule we may infer that CDs can be tethered with 6 chains having an average length of 6 lactate units.

Conclusion

Bulk polymerization of L-LA in the presence of α-, β- and γ-CD proceeds with the formation of oligolactides tethered cyclodextrins. In the conditions of monomer excess the initiator doesn't fully react, free CDs being also detected in characterization by LC–ELSD with "off line" MALDI–MS detection. During this process PLA homopolymers are also formed, as confirmed by LC–ESI–MS analysis, possibly because of water traces in the reaction. The reactivity of different cyclodextrins in the ring opening of L-lactide may be summarized as follows: β-CD > α-CD > γ-CD. This statement is supported by liquid chromatography with evaporative light scattering detection providing the relative amount of free CD versus CD-LA products and PLA homopolymers. In addition, MALDI–MS characterization of the fractionated samples showed that the average mo-

lecular weight of β-CD-LA was the highest, with an average of 36 lactate units per cyclodextrin molecule. The NMR spectroscopy showed that the obtained products are best described as random-(6-*O*-oligolactide)cyclodextrins thus demonstrating a certain selectivity in the cyclodextrin's modification. The presented combination of analytical methods can help in further studies to optimize the reaction conditions in order to achieve a modification of all CD molecules. Further characterization studies will aim for the quantitative measurement of cyclodextrin derivatives and PLA homopolymers in the reaction mixture.

Experimental
Materials

L-lactide (L-LA) (Sigma-Aldrich) was recrystallized twice from ethyl acetate, dried under vacuum and sublimated before use; α-, β- and γ-cyclodextrins (CDs) (Cyclolab, Hungary) were dried over P_2O_5 under vacuum at 80 °C for 72 hours and kept over P_2O_5 in the desiccator under Ar atmosphere. All used solvents were HPLC grade and were used as received.

Instruments

The HPLC system consisted of a gradient pump of the Agilent 1260 series (Agilent Technologies, USA) coupled with an evaporative light scattering detector (ELSD) model ELS-1000 from PL-Agilent Technologies, Stretton, UK. Mass spectra of poly-
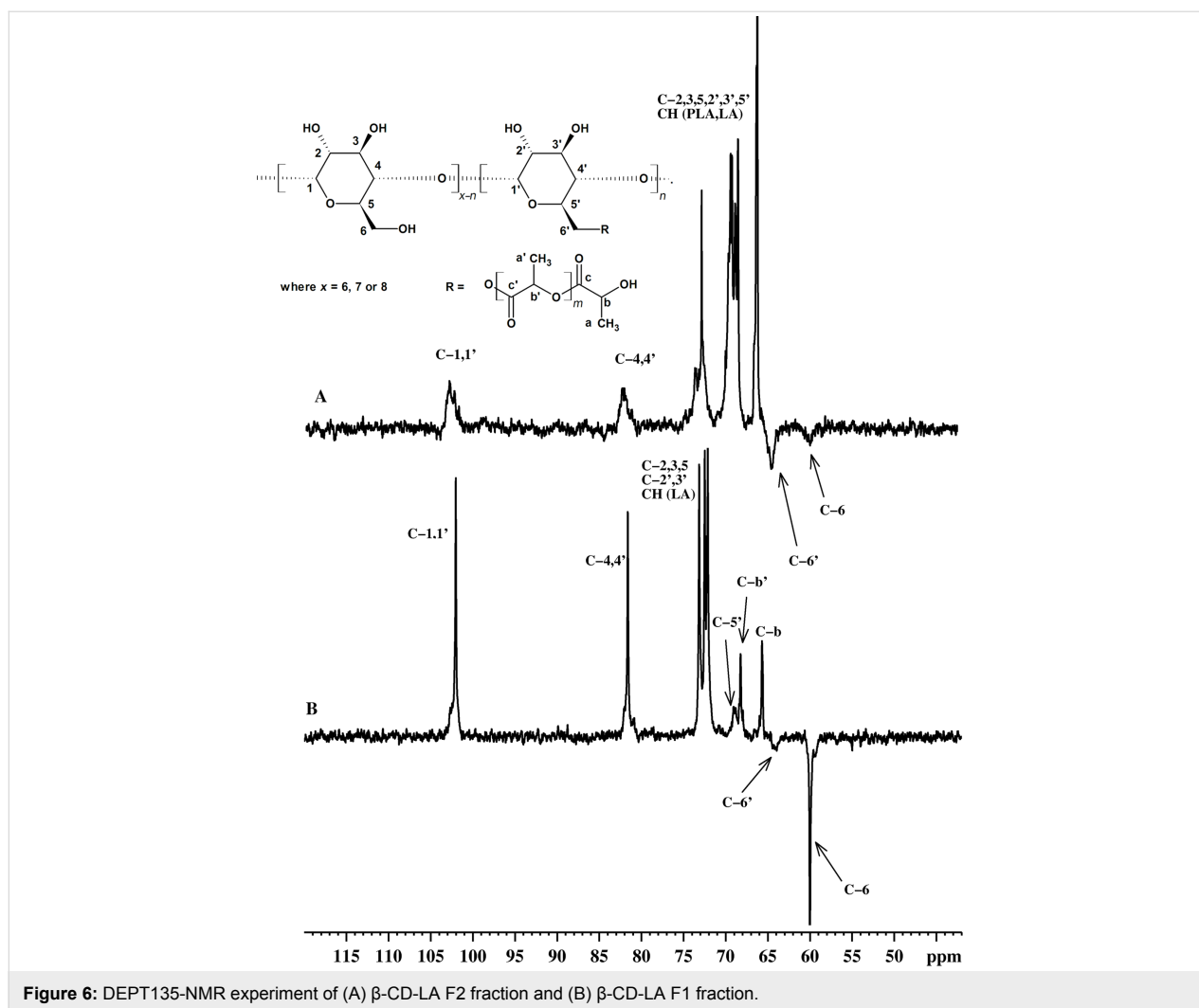
Figure 6: DEPT135-NMR experiment of (A) β-CD-LA F2 fraction and (B) β-CD-LA F1 fraction.

mers were measured on an UltrafleXtreme TOF instrument (Bruker), equipped with a 355 nm smartbeam-2 laser, capable of a pulsing frequency of 1 kHz. The mass spectrometer was operated by FlexControl 3.3 software (Bruker). The acquired spectra were processed by FlexAnalysis 3.3 software (Bruker). LC–ESI–MS experiments were conducted using the AGILENT 6520 LC QTOF MS equipped with a dual ESI source. The data were analyzed using the Mass Hunter software. The NMR spectra were recorded on a Bruker Avance DRX 400 MHz Spectrometer equipped with a 5 mm QNP direct detection probe and z-gradients. Spectra were recorded in DMSO-d_6, at room temperature. The chemical shifts are reported as δ values (ppm) and were referenced to the solvent residual peak (2.512 ppm for ^{1}H and 39.47 ppm for ^{13}C). The assignments of the peaks from the 1D NMR spectra were performed using 2D NMR experiments (H,H-COSY, H,C-HMQC, H,C-HMBC). The molecular parameters of the cyclodextrin–oligolactide covalent conjugates were also determined by GPC using a Shimadzu LC-20 isocratic pump and a Shimadzu refractive index detector in size

exclusion mode using a PSS PFG precolumn and three PPS PFG columns (d = 8 mm, l = 300 mm) filled with particles with a size of 7 μm and pore sizes of 100, 300 and 1000 Å, respectively. 2,2,2-Trifluoroethanol was used as an eluent. Poly(methyl methacrylate) standards were used for the internal calibration.

Methods
Bulk polymerization of L-LA

In a typical reaction 0.2 g of CD and 2.66 g of L-LA were weighted together under protection of Ar flow, in a dried flask containing a magnetic stirrer. The molar ratio between the L-LA and OH groups of CD was kept at a 5:1 value for all the polymerizations. All operations were conducted carefully under Ar atmosphere. The flask isolated with a rubber septum was completely immersed in an oil bath, over a heater with magnetic stirring and the temperature was brought to 110 °C. The L-LA monomer was quickly melted and the CDs were homogenously dispersed in the reaction mixture. The heating was maintained

for 72 h under continuous stirring. The reaction was stopped by simply removing the flask from the heating source. In order to analyze the products, the samples were fractionated by three times washing with THF. Thus, two fractions were obtained for each reaction system, a fraction precipitated in THF, rich in free CDs or CD molecules with low substitution degree, noted with F1, and a second fraction, fully soluble in THF (composed of three fractions resulted from combining the resulted solutions from three repeated washing procedures), containing CDs with high substitution degree and unreacted L-LA monomer, noted with F2. The F2 fraction was further purified by partial removal of unreacted monomer through sublimation under vacuum at 40 °C temperature, in order to facilitate the NMR characterization. The unfractionated samples were first assessed by liquid chromatography with evaporative light scattering detection (LC–ESLD) "on line" and also using "off line" MALDI–MS. The F1 and F2 fractions obtained for each type of CD (α-CD-LA F1 – 2%) and F2 (98%), β-CD-LA F1 (5.5%) and F2 (94.5%) and γ-CD-LA F1 (9%) and F2 (91%) were characterized by MALDI–MS, NMR spectroscopy while the F2 fraction was also characterized by gel permeation chromatography (Table 1).

α-CD-LA F1: ^{1}H NMR (400.13 MHz, DMSO-d_6, δ ppm) 5.60–5.45 (OH2, OH3, end chain OH), 5.11 (CH-b'), 4.81 (H1), 4.51 (OH6), 4.29–4.19 (H6', CH-b), 3.94 (H5'), 3.78 (H5), 3.68–3.58 (H3, H6), 3.40 (H4), 3.29 (H2), 1.47–1.43 (CH3-a'), 1.31–1.29 (CH3-a); ^{13}C NMR (100.6 MHz, DMSO-d_6, δ ppm) 174.01 (C-c), 170.11 (C-c'), 101.7 (C1), 81.8 (C4), 73.0 (C3), 71.8 (C2, C5), 68.2 (C5'), 67.9 (C-b'), 65.3 (C-b), 64.2 (C6'), 59.7 (C6), 20.1 (C-a), 16.5 (C-a').

β-CD-LA F1: ^{1}H NMR (400.13 MHz, DMSO-d_6, δ ppm) 5.92–5.69 (OH2, OH3), 5.47–5.42 (end chain OH, CH from L-LA), 5.10 (CH-b'), 4.84 (H1), 4.47 (OH6), 4.31–4.19 (H6', CH-b), 3.86 (H5'), 3.64–3.56 (H3, H5, H6), 3.38–3.10 (H2 and H4 overlapped with water from solvent), 1.47–1.42 (CH3 from L-LA, CH3-a'), 1.3–1.29 (CH3-a); ^{13}C NMR (100.6 MHz, DMSO-d_6, δ ppm) 174.2 (C-c), 170.3 (C-c'), 170.3 (C=O from L-LA), 102.0 (C1), 81.6 (C4), 73.1 (C3), 72.5 (C2), 72.1 (C5), 69.1 (C5'), 68.2 (C-b'), 65.7 (C-b), 64.4 (C6'), 60.0 (C6), 20.4 (C-a), 16.7 (C-a'), 15.2 (CH3 from L-LA).

γ-CD-LA F1: ^{1}H NMR (400.13 MHz, DMSO-d_6, δ ppm) 5.96–5.75 (OH2, OH3), 5.49–5.43 (end chain OH, CH from L-LA), 5.10 (CH-b'), 4.90 (H1), 4.55 (OH6), 4.28–4.2 (H6', CH-b), 3.83 (H5'), 3.63–3.53 (H3, H5, H6), 3.83–3.3 (H2 and H4 overlapped with water from solvent), 1.47–1.40 (CH3 from lactide, CH3-a'), 1.31–1.29 (end chain CH3-a); ^{13}C NMR (100.6 MHz, DMSO-d_6, δ ppm) 174.2 (C-c), 170.2 (C-c'), 101.7 (C1), 81.0 (C4), 73.0 (C3), 72.6 (C2), 72.2 (C5, CH from

L-LA), 68.8 (C5'), 68.2 (C-b'), 65.6 (C-b), 64.2 (C6'), 60.0 (C6), 20.4, 16.7 (CH3), 15.2 (CH3 from lactide).

β-CD-LA F2: ^{1}H NMR (400.13 MHz, DMSO-d_6, δ ppm) 5.94–5.70 (OH2, OH3), 5.5–5.42 (end chain OH, CH from L-LA), 5.20–5.12 (CH), 4.85 (H1), 4.65–4.18 (OH6, H6', CH-b), 3.90 (H5'), 3.64–3.37 (H3, H5, H6, H2, H4), 1.49–1.41 (CH3 from L-LA, CH3), 1.3–1.28 (CH3); ^{13}C NMR (100.6 MHz, DMSO-d_6, δ ppm) 174.2–168.6 (C=O), 102.4 (C1, C1'), 81.7 (C4, C4'), 73.0 (C3, C3'), 72.2–65.7 (C2, C2', C3, C3', C5, C5', CH), 63.9 (C6'), 59.3 (C6), 20.4–16.59 (CH3).

The peaks from the ^{1}H NMR spectra for the F2 fractions of α- and γ-CD-LA samples cannot be exactly assigned due to the large amount of free PLA homopolymer. The CH and OH protons from the PLA homopolymer give peaks in the 5.5–4 ppm region and they overlap with those from α- and γ-CD-LA so their separate integration is not possible. The ^{13}C NMR spectrum for the α-CD-LA-F2 sample shows peaks for C6 at 59.55 ppm, for C6' at 64.05 ppm, for C1 and C1' at 102.2–101.6 ppm and for C4 and C4' at 81.9 ppm. The ^{13}C NMR spectrum for the γ-CD-LA-F2 shows peaks for C6 at 60.03 ppm, for C6' at 63.59 ppm, C1 and C1' at 102–101 ppm and for C4, C4' at 80.9 ppm. The rest of the peaks from the ^{13}C NMR spectra for F2 fractions of α- and γ-CD-LA samples cannot be fully assigned due to the large amount of free PLA homopolymer: 174–168 ppm (-CO), 72–65 ppm (-CH-), 20–15 ppm (-CH3).

Liquid chromatography with evaporative light scattering detection (LC ELSD)

Temperature of evaporator was set at 80 °C and gas flow rate was 1.5 mL·min^{-1}. HPLC column was Purospher Star RP-18 end capped column (5 µm) 250 × 4.6 mm purchased from Merck, Germany. The mobile phase consisted of (A) water and (B) acetonitrile. Gradient elution was realized as follows: solvent (A) was maintained at 90% for 3 min, followed by linear gradient to 10% of (A) in 10 min. These conditions were held for 5 min. The initial conditions were obtained in 5 min and to recondition the column 3 min post-run with the initial mobile phase composition was performed. Injecting volume was 20 µL. The flow rate of mobile phase was set on 1 mL/min. The HPLC measurements were performed at ambient temperature. Data were collected and processed using the software Clarity from DataApex, Czech Republic.

Matrix-assisted laser desorption ionization (MALDI–MS)

The raw samples withdrawn directly from the polymerization mixture were dissolved in a 1:1 water/acetonitrile mixture to a concentration of 10 mg/mL. The liquid chromatography frac-

tions were used as such. Samples were mixed with a matrix solution (saturated solution of α-cyano-hydroxy-cinnamic acid in water/acetonitrile mixture) in a ratio of 1:100 (v/v). 1 µL of this mixture was deposited on polished steel MALDI target (Bruker). The ionization laser power was adjusted just above the threshold in order to produce charged species. The mass spectra were collected in amount of above 10000 spectra for each sample.

Liquid chromatography with electrospray ionization mass spectrometry detection (LC–ESI–MS)

The ESI–MS parameters were set as follows: Vcap = 4000 V, fragmentor voltage = 200 V, drying gas temperature = 325 °C, drying gas flow = 10 L/min and nebulizer pressure = 35 psig. Nitrogen was used as spraying gas. LC separations were performed by using a C18 column - Agilent ZORBAX 300SB-C18 4.6 × 150 mm, 5 µm. The samples were separated by gradient elution using water/acetonitrile solvent mixture at 26 °C constant temperature in column compartment. The used eluents were: A – 2 mM formic acid solution and B – acetonitrile. The samples were solved in a 1:1 (vol/vol) water/acetonitrile mixture and 10 µL were injected. For the LC–MS analysis of β-CD-LA, the mobile phase was delivered at 1 mL/min in linear gradient mode: 0–3 min, 20% B; 10 min, 100% B; 5 min, 100% B; 3 min, 20% B.

Supporting Information

Supporting Information File 1
Analytical data.
[http://www.beilstein-journals.org/bjoc/content/
supplementary/1860-5397-13-77-S1.pdf]

Acknowledgements

References

1. Loftsson, T.; Duchêne, D. *Int. J. Pharm.* **2007,** *329,* 1–11. doi:10.1016/j.ijpharm.2006.10.044
2. Szejtli, J. *Chem. Rev.* **1998,** *98,* 1743–1753. doi:10.1021/cr970022c
3. Wenz, G. *Angew. Chem., Int. Ed. Engl.* **1994,** *33,* 803–822. doi:10.1002/anie.199408031
4. van de Manakker, F.; Vermonden, T.; van Nostrum, C. F.; Hennink, W. E. *Biomacromolecules* **2009,** *10,* 3157–3175. doi:10.1021/bm901065f
5. Yhaya, F.; Gregory, A. M.; Stenzel, M. H. *Aust. J. Chem.* **2010,** *63,* 195–210. doi:10.1071/CH09516
6. Miao, Y.; Zinck, P. *Polym. Chem.* **2012,** *3,* 1119–1122. doi:10.1039/c2py00567k
7. Huin, C.; Eskandani, Z.; Badi, N.; Farcas, A.; Bennevault-Celton, V.; Guégan, P. *Carbohydr. Polym.* **2013,** *94,* 323–331. doi:10.1016/j.carbpol.2012.12.062
8. Adeli, M.; Kalantari, M.; Zarnega, Z.; Kabiri, R. *RSC Adv.* **2012,** *2,* 2756–2758. doi:10.1039/c2ra00813k
9. Gou, P.-F.; Zhu, W.-P.; Xu, N.; Shen, Z.-Q. *J. Polym. Sci., Part A: Polym. Chem.* **2008,** *46,* 6455–6465. doi:10.1002/pola.22955
10. Adeli, M.; Zarnegar, Z.; Kabiri, R. *Eur. Polym. J.* **2008,** *44,* 1921–1930. doi:10.1016/j.eurpolymj.2008.03.028
11. Mooguee, M.; Omidi, Y.; Davaran, S. *J. Pharm. Sci.* **2010,** *99,* 3389–3397. doi:10.1002/jps.22106
12. Miao, Y.; Rousseau, C.; Mortreux, A.; Martin, P.; Zinck, P. *Polymer* **2011,** *52,* 5018–5026. doi:10.1016/j.polymer.2011.08.040
13. Nagahama, K.; Shimizu, K.; Ouchi, T.; Ohya, Y. *React. Funct. Polym.* **2009,** *69,* 891–897. doi:10.1016/j.reactfunctpolym.2009.09.004
14. Normand, M.; Kirillov, E.; Carpentier, J.-F.; Guillaume, S. M. *Macromolecules* **2012,** *45,* 1122–1130. doi:10.1021/ma202400e
15. Xu, Z.; Liu, S.; Liu, H.; Yang, C.; Kang, Y.; Wang, M. *Chem. Commun.* **2015,** *51,* 15768–15771. doi:10.1039/C5CC02743H
16. Shen, J.; Hao, A.; Du, G.; Zhang, H.; Sun, H. *Carbohydr. Res.* **2008,** *343,* 2517–2522. doi:10.1016/j.carres.2008.06.010
17. Takashima, Y.; Osaki, M.; Harada, A. *J. Am. Chem. Soc.* **2004,** *126,* 13588–13589. doi:10.1021/ja047171e
18. Galia, A.; Scialdone, O.; Spanò, T.; Valenti, M. G.; Grignard, B.; Lecomte, P.; Monflier, E.; Tilloy, S.; Rousseau, C. *RSC Adv.* **2016,** *6,* 90290–90299. doi:10.1039/C6RA20211J
19. Osaki, M.; Takashima, Y.; Yamaguchi, H.; Harada, A. *Kobunshi Ronbunshu* **2007,** *64,* 607–616. doi:10.1295/koron.64.607
20. Harada, A.; Osaki, M.; Takashima, Y.; Yamaguchi, H. *Acc. Chem. Res.* **2008,** *41,* 1143–1152. doi:10.1021/ar800079v
21. Peptu, C.; Nicolescu, A.; Peptu, C. A.; Harabagiu, V.; Simionescu, B. C.; Kowalczuk, M. *J. Polym. Sci., Part A: Polym. Chem.* **2010,** *48,* 5581–5592. doi:10.1002/pola.24372
22. Peptu, C.; Kwiecień, I.; Harabagiu, V. *Cellul. Chem. Technol.* **2014,** *48,* 1–10.
23. Peptu, C.; Harabagiu, V. *Dig. J. Nanomater. Bios.* **2013,** *8,* 1551–1561.
24. Nielen, M. W. F.; Buijtenhuijs, F. A. *Anal. Chem.* **1999,** *71,* 1809–1814. doi:10.1021/ac981141a
25. Koster, S.; Mulder, B.; Duursma, M. C.; Boon, J. J.; Philipsen, H. J. A.; van Velde, J. W.; Nielen, M. W. F.; Koster, C. G.; Heeren, R. M. A. *Macromolecules* **2002,** *35,* 4919–4928. doi:10.1021/ma011234l
26. Hart-Smith, G.; Barner-Kowollik, C. *Macromol. Chem. Phys.* **2010,** *211,* 1507–1529. doi:10.1002/macp.201000107
27. Nielen, M. W. F. *Mass Spectrom. Rev.* **1999,** *18,* 309–344. doi:10.1002/(SICI)1098-2787(1999)18:5<309::AID-MAS2>3.0.CO;2-L

Mechanochemical synthesis of graphene oxide-supported transition metal catalysts for the oxidation of isoeugenol to vanillin

Ana Franco[1], Sudipta De[1,2], Alina M. Balu[1], Araceli Garcia[1] and Rafael Luque[*1]

Abstract

Vanillin is one of the most commonly used natural products, which can also be produced from lignin-derived feedstocks. The chemical synthesis of vanillin is well-established in large-scale production from petrochemical-based starting materials. To overcome this problem, lignin-derived monomers (such as eugenol, isoeugenol, ferulic acid etc.) have been effectively used in the past few years. However, selective and efficient production of vanillin from these feedstocks still remains an issue to replace the existing process. In this work, new transition metal-based catalysts were proposed to investigate their efficiency in vanillin production. Reduced graphene oxide supported Fe and Co catalysts showed high conversion of isoeugenol under mild reaction conditions using H_2O_2 as oxidizing agent. Fe catalysts were more selective as compared to Co catalysts, providing a 63% vanillin selectivity at 61% conversion in 2 h. The mechanochemical process was demonstrated as an effective approach to prepare supported metal catalysts that exhibited high activity for the production of vanillin from isoeugenol.

Introduction

Vanillin is the main flavor and aroma compound in vanilla. It is an aromatic compound (4-hydroxy-3-methoxybenzaldehyde) containing two reactive functional groups that are useful for the synthesis of thermoplastic polymers [1-4].

Vanillin is one of the most important chemicals in the aroma industry, because it is abundantly used in food, pharmaceutical, cosmetic, and fine chemical industries. Therefore much attention has been paid to research on the improvement of its production [5].

At the present time only 1% of total vanilla production is from extraction of natural material. This extraction is a very long and expensive process [6]. The remaining 99% is being produced

via chemical and biochemical routes. Biotechnology-based approaches, particularly enzymatic processes, have been well known for many years for vanillin production and are considerably less harmful to the environment. However, they have inherent disadvantages including comparatively high costs, slowness, difficult purification and the requirement of selected strains of microorganisms [7-9]. Major quantities (85%) of the world supply are still produced from petroleum-based intermediates, especially guaiacol and glyoxylic acid using the most employed Riedel process [10,11]. The classical synthetic routes are not "environment friendly" and the vanillin produced by these methods is considered to be of lower quality because it does not contain some trace components that contribute to the natural vanilla flavor.

Nowadays, 15% of the overall vanillin production comes from lignin, more precisely from lignosulfonates. Different products can be synthesized by lignin oxidation being vanillin the most well and valuable product. Recently, eugenol, isoeugenol and ferulic acid have been used as substrates for vanillin manufacturing due to their economic and commercial availability. These compounds are easily derived from lignin and have the common structural unit with that of vanillin, being potentially useful for vanillin production via simple oxidation pathways [12-14]. Photocatalytic oxidation has been reported for the production of vanillin where TiO_2-based materials have been used as effective catalysts in recent years [15-18]. Although the conversion was high in some cases, vanillin selectivity was never significant. Another problem related to the slow reaction rates, unsuitable for commercial production. As a result, chemical oxidation pathways were also followed. To achieve faster kinetics and better selectivity of vanillin, homogeneous catalysts based on different transition metal salts/complexes were employed [14,19-21]. However, the selectivity of vanillin still remains an important issue.

In this work, we report the mechanochemical design of transition-metal-based catalysts supported on reduced graphene oxide support for the oxidation of isoeugenol into vanillin using H_2O_2

as oxidant. The catalytic support, RGO, a graphene derived material are normally produced by chemical reduction of graphene oxide (GO) [22,23].

The materials were prepared using a simple and effective ball milling approach and were characterized by different techniques.

Results and Discussion

The supported RGO materials were characterized by using several techniques including BET, SEM, TEM, XRD, and IR spectroscopy. N_2 adsorption/desorption isotherms of the reduced graphene sample (Figure 1a) can be classified as type IV corresponding to the mesoporous materials. The RGO sample showed a BET surface area of 103 m^2 g^{-1} with a pore diameter of 39 nm and pore volume of 0.74 cm^3 g^{-1} (Table 1). After the ball milling with metal precursors, the mesoporous structure of RGO was found to be partially collapsed as observed from BET isotherms in Figure 1b and c. BET surface areas of metal supported RGO materials consequently decreased, with increased pore diameter and pore volume as a consequence of the structure deterioration observed after milling. Additional macroporosity (interparticular) was created upon milling, which increased both pore diameter and volume. SEM results also support the observation from BET analysis. The mesoporous nature of the RGO can be easily observed from SEM images (Figure 2a and b), whereas metal-supported RGO materials show a smooth surface with decreased crystallinity.

TEM images of RGO materials with different thickness show a sheet like morphology with different transparencies (Figure 3). Dark areas result from the superposition of several graphene oxide and/or graphene layers containing oxygen functional groups. Most transparent areas are from thinner films composed of a few layers of reduced graphene oxide from stacking nanostructure exfoliation. A significant collapse of the structure could be observed upon metal incorporation (see Figure 3, images c and d), although several domains remained to be almost unchanged as compared to those of RGO (see Figure 3f).

Table 1: Textural properties of RGO and NPs supported RGO materials.

Material	S_{BET}[a] (m^2 g^{-1})	D_{BJH}[b] (nm)	V_{BJH}[c] (cm^3 g^{-1})
RGO	103	39	0.74
1% Fe/RGO	<10	205	1.46
1% Co/RGO	<15	190	2.04

[a]S_{BET}: specific surface area was calculated by the Brunauer–Emmet–Teller (BET) equation. [b]D_{BJH}: mean pore size diameter was calculated by the Barret–Joyner–Halenda (BJH) equation. [c]V_{BJH}: pore volumes were calculated by the Barret–Joyner–Halenda (BJH) equation.
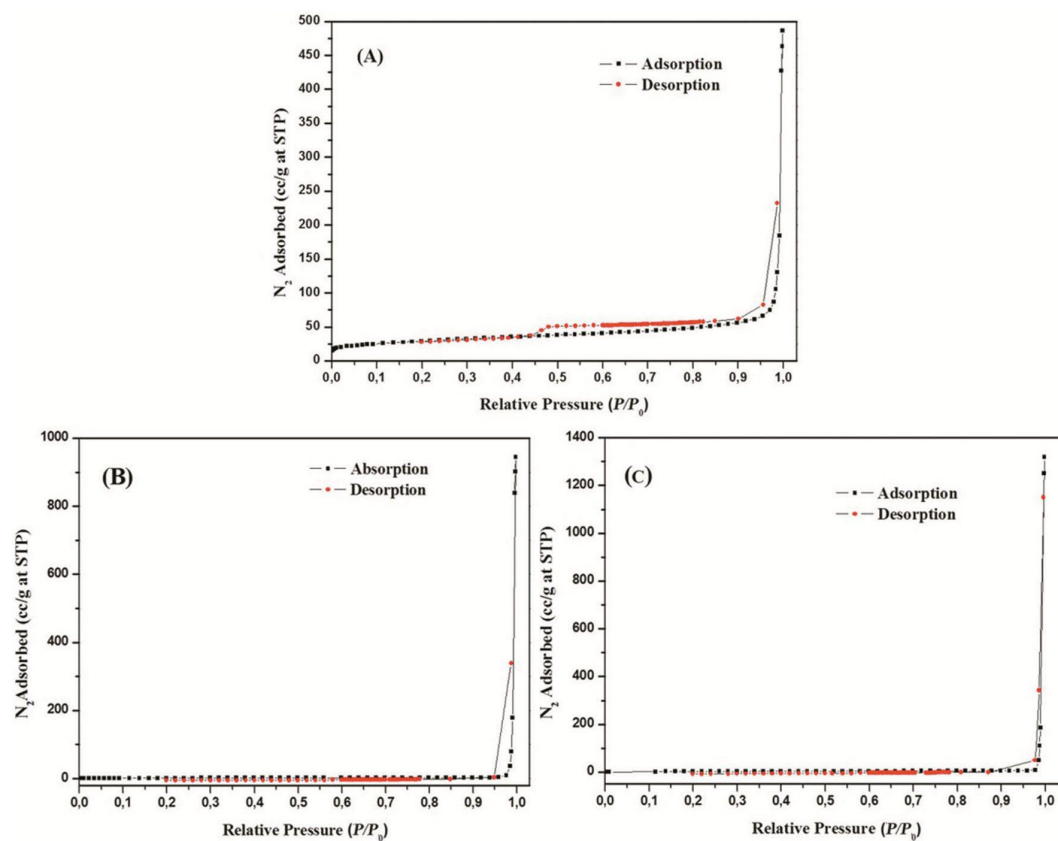
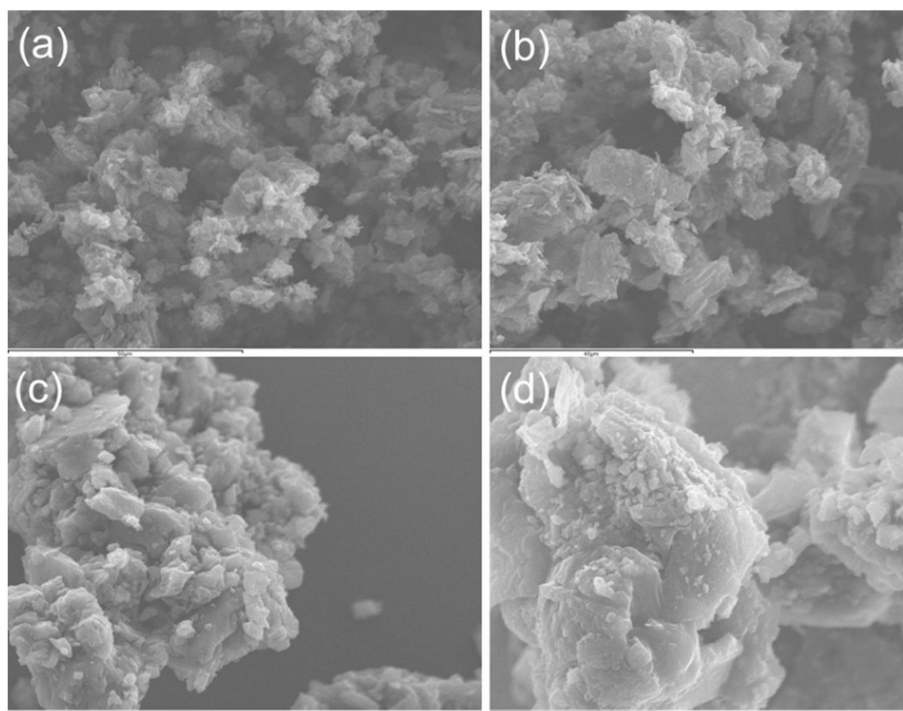**Figure 1:** N$_2$ isotherms of (a) RGO, (b) Fe/RGO, and (c) Co/RGO.

Figure 2: SEM images of (a and b) RGO, (c) 1% Fe/RGO, and (d) 1% Co/RGO.
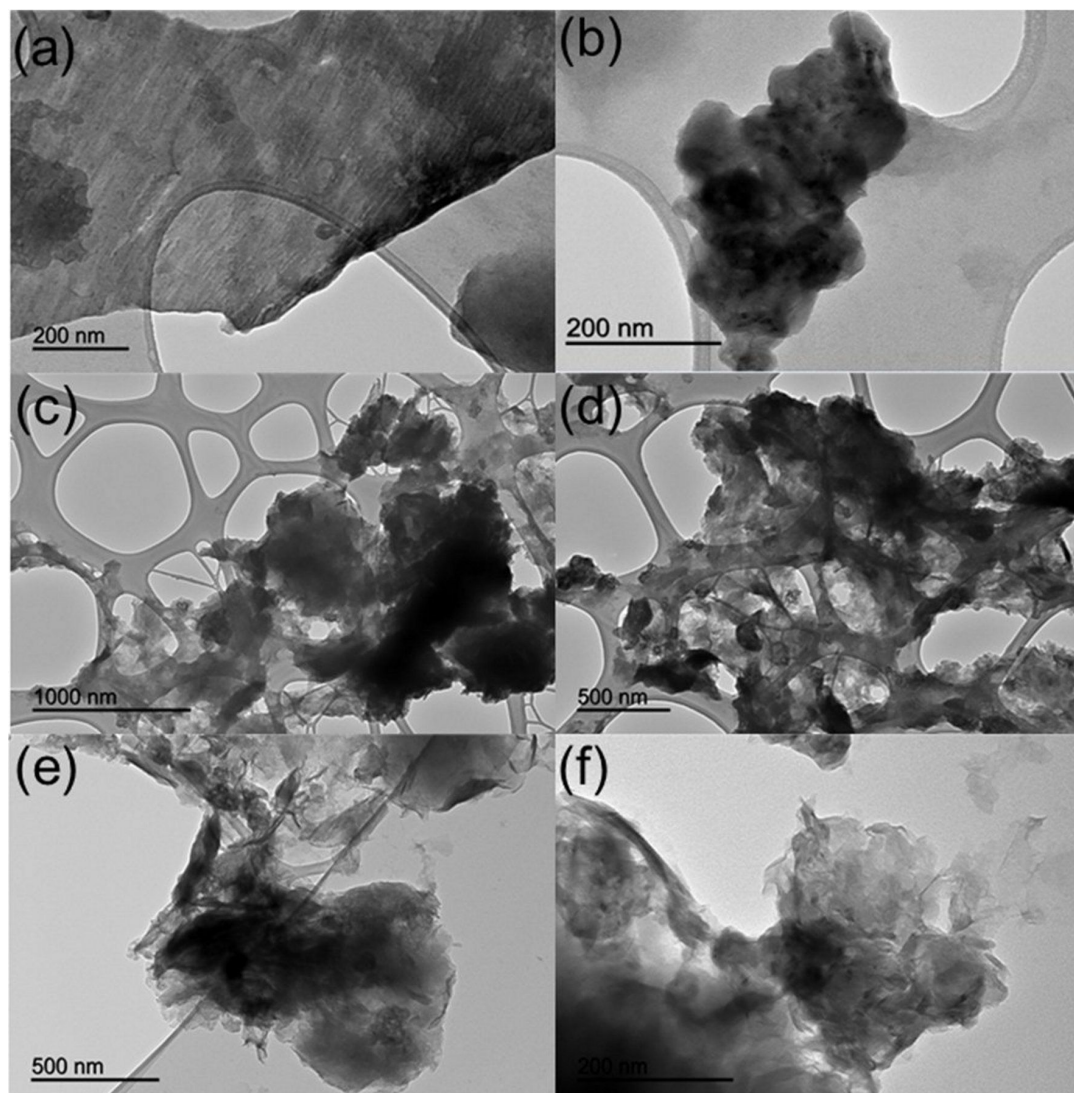
Figure 3: TEM micrographs at different magnifications of (a and b) RGO, (c and d) 1% Fe/RGO, and (e and f) 1% Co/RGO.

X-ray diffraction patterns of RGO-supported materials are shown in Figure 4. Two characteristic peaks at $2\theta = 26°$ and $2\theta = 43°$ correspond to the typical RGO material. The broad nature of the peak confirms the highly amorphous nature of the RGO support. A closer look at the figures pointed out the presence of iron in the form of a FeO/Fe_2O_3 mixture (mixed phases) as compared to a more pure CoO phase in the case of Co. Due to the amorphous nature of RGO and low metal loading, the corresponding metal oxide peaks could not be well resolved.

Additionally, IR spectra (Figure 5) showed that there is no such peak in the range of 1700–1740 cm^{-1}, indicating the absence of any oxidized groups such as carbonyl or carboxylic acid groups. One peak at around 1600 cm^{-1} could be observed that corresponds to C=C from aromatic groups.

Table 2 summarizes the experimental results for the oxidation of isoeugenol using supported RGO catalysts. Reaction conditions were optimized under various conditions. Blank runs (in absence of catalysts) were also performed, with a low conversion in the systems, which could be attributed to the effect of the strong oxidizing agent H_2O_2. However, the reaction produced a higher amount of ether compounds with a very low selectivity to vanillin. When RGO was used as catalyst, the conversion increased but the selectivity of vanillin was still lower than other side products. Importantly, metal incorporation on RGO support significantly increased both conversion and vanillin selectivity in the systems (Table 2, entries 3 and 4).

The optimum results were obtained after 2 h of reaction as seen in results from Table 2. The Fe-containing catalysts were found
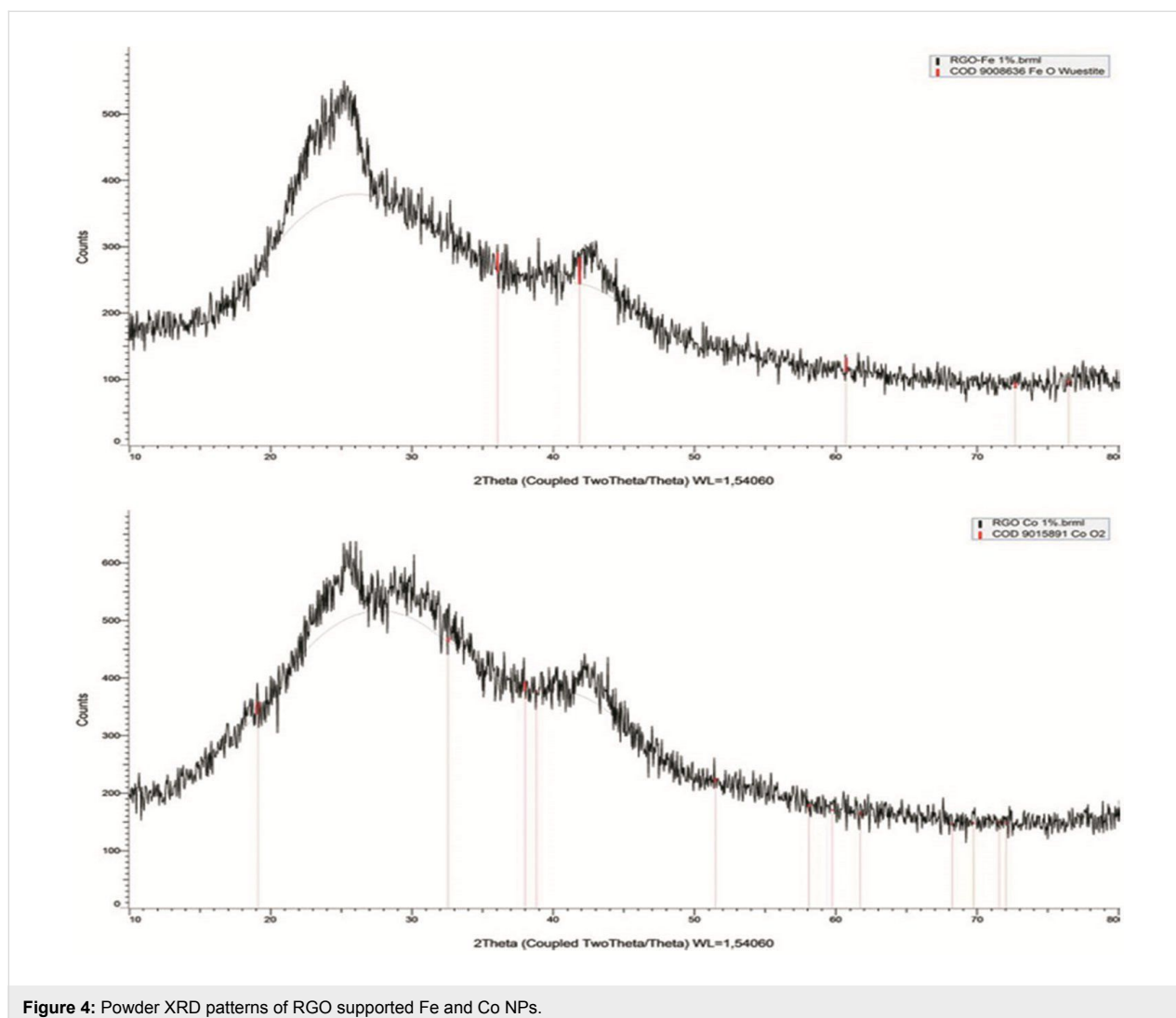
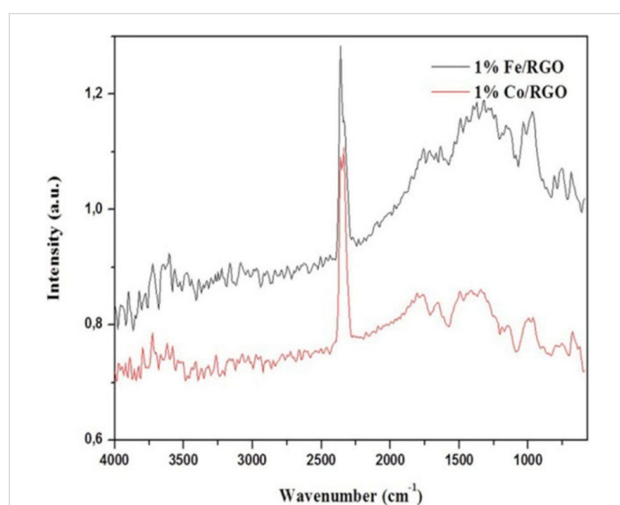**Figure 4:** Powder XRD patterns of RGO supported Fe and Co NPs.

Figure 5: IR spectra of 1% Fe/RGO and 1% Co/RGO catalysts collected by using diffuse reflectance infrared transform spectroscopy (DRIFT) at room temperature.

to be more selective than the Co-containing catalysts at similar conversions under otherwise identical reaction conditions. After prolonged reaction times, Fe/RGO remained selective towards vanillin, but Co/RGO experienced a significant drop in selectivity (although the conversion increased). This could be explained by the strong oxidizing nature of Co that might facilitate further reactions of vanillin to other compounds. To investigate the stability of the Fe/RGO and Co/RGO the materials were subjected to different reuses. The results showed a significantly decrease in the catalytic activity due to material deactivation.

Conclusion

A simple mechanochemical ball milling process was used to prepare highly active transition-metal-supported reduced graphene oxide catalysts. The catalysts were used to produce the highly useful aromatic compound vanillin, by oxidizing naturally abundant isoeugenol. The catalysts showed good ac-

Table 2: Results for the catalytic oxidation of isoeugenol.[a]

Entry	Catalyst	Time (h)	Conversion (mol %)	Selectivity (mol %)		
				Vanillin	Diphenyl ether	Others
1.	blank	2	18	7	84	9
2.	RGO	2	39	26	47	27
3.	1% Fe/RGO	2	61	63	8	29
4.	1% Co/RGO	2	60	32	9	59
5.	blank	3	19	8	79	13
6.	RGO	3	41	25	47	28
7.	1% Fe/RGO	3	64	58	13	29
8.	1% Co/RGO	3	70	27	6	67
9.	blank	5	20	11	73	16
10.	RGO	5	54	19	30	51
11.	1% Fe/RGO	5	64	54	13	33
12.	1% Co/RGO	5	75	21	4	75
13.	blank	7	22	16	70	14
14.	RGO	7	59	26	23	51
15.	1% Fe/RGO	7	62	52	14	34
16.	1% Co/RGO	7	81	19	2	79

[a]Reaction conditions: 5 mmol isoeugenol, 1.2 mL H_2O_2, 8 mL acetonitrile, 0.1 g catalyst, 90 °C.

tivity and vanillin selectivity at mild reaction conditions using H_2O_2 as oxidizing agent. A better selectivity was observed for the Fe-based catalyst.

Materials and Methods
Preparation of materials
In a typical synthesis of ball-milled materials, reduced graphene oxide (RGO) support, together with an appropriate amount of the iron precursor ($FeCl_2 \cdot 4H_2O$) to reach a theoretical 1% iron loading, was ground by using a Retsch-PM-100 planetary ball mill with a 25 mL reaction chamber and 8 mm stainless steel ball. Milling was conducted at 350 rpm for 10 min. The same protocol was used to design a 1% Co catalyst using the Co precursor $Co(NO_3)_2 \cdot 6H_2O$. Graphene oxide was kindly donated by Nano Innova Technologies SL (http://www.nanoinnova.com).

Characterization of materials
Materials were characterized by using N_2 physisorption, powder X-ray diffraction (XRD), transmission electron microscopy (TEM), scanning electron microscopy (SEM) and diffuse reflectance infrared Fourier transform spectroscopy (DRIFT). N_2 adsorption measurements were performed at 77 K by using a

Micromeritics ASAP 2000 volumetric adsorption analyzer. The samples were degassed for 24 h at 30 °C under vacuum ($P_0 < 10^{-2}$ Pa) and subsequently analyzed. Surface areas were calculated according to the BET (Brunauer–Emmet–Teller) equation. Mean pore size diameter and pore volumes were measured from porosimetry data by using the BJH (Barret–Joyner–Halenda) method. Wide-angle X-ray diffraction experiments were performed on a Pan-Analytic/Philips X`pert MRD diffractometer (40 kV, 30 mA) with Cu Kα (λ = 0.15418) radiation. Scans were performed over a 2θ range between 10–80° at step size of 0.0188 with a counting time per step of 5 s. TEM images of the samples were recorded on JEM 2010F (JEOL) and Phillips Analytical FEI Tecnai 30 microscopes. SEM micrographs were recorded on a JEOL-SEM JSM-6610 LV scanning electron microscope in backscattered electron model at 3/15 kV. DRIFT spectra were recorded on a PIKE Technologies MB 3000 ABB at room temperature.

Catalytic activity tests
In a typical experiment, isoeugenol (5 mmol) and 0.1 g catalyst, H_2O_2 (1.2 mL) and acetonitrile (8 mL) were heated at 90 °C under continuous stirring in a carrusel place reaction station.

Products were analyzed at different time interval by GC Aligent 7890 fitted with a capillary column Petrocol 100 m × 0.25 nm × 0.5 μm and a flame ionization detector (FID). The results were finally confirmed by GC–MS.

Acknowledgements

References

1. Stanzione, J. F., III; Sadler, J. M.; La Scala, J. J.; Reno, K. H.; Wool, R. P. *Green Chem.* **2012**, *14*, 2346–2352. doi:10.1039/c2gc35672d
2. Fache, M.; Boutevin, B.; Caillol, S. *Eur. Polym. J.* **2015**, *68*, 488–502. doi:10.1016/j.eurpolymj.2015.03.050
3. Harvey, B. G.; Guenthner, A. J.; Meylemans, H. A.; Haines, S. R. L.; Lamison, K. R.; Groshens, T. J.; Cambrea, L. R.; Davis, M. C.; Lai, W. W. *Green Chem.* **2015**, *17*, 1249–1258. doi:10.1039/C4GC01825G
4. Llevot, A.; Grau, E.; Carlotti, S.; Grelier, S.; Cramail, H. *Macromol. Rapid Commun.* **2016**, *37*, 9–28. doi:10.1002/marc.201500474
5. Fache, M.; Boutevin, B.; Caillol, S. *ACS Sustainable Chem. Eng.* **2016**, *4*, 35–46. doi:10.1021/acssuschemeng.5b01344
6. Dignum, M. J. W.; Kerler, J.; Verpoorte, R. *Food Rev. Int.* **2001**, *17*, 119–120. doi:10.1081/FRI-100000269
7. Serra, S.; Fuganti, C.; Brenna, E. *Trends Biotechnol.* **2005**, *23*, 193–198. doi:10.1016/j.tibtech.2005.02.003
8. Hua, D.; Ma, C.; Lin, S.; Song, L.; Deng, Z.; Maomy, Z.; Zhang, Z.; Yu, B.; Xu, P. *J. Biotechnol.* **2007**, *130*, 463–470. doi:10.1016/j.jbiotec.2007.05.003
9. Gallage, N. J.; Hansen, E. H.; Kannangara, R.; Olsen, C. E.; Motawia, M. S.; Jørgensen, K.; Holme, I.; Hebelstrup, K.; Grisoni, M.; Møller, B. L. *Nat. Commun.* **2014**, *5*, No. 4037. doi:10.1038/ncomms5037
10. Pinto, P. C. R.; da Silva, E. A. B.; Rodrigues, E. A. Lignin as Source of Fine Chemicals: Vanillin and Syringaldehyde. In *Biomass Conversion: The Interface of Biotechnology, Chemistry and Materials Science;* Baskar, C.; Baskar, S.; Dhillon, S. R., Eds.; Springer: Berlin, Heidelberg, 2012; pp 381–420.
11. Huang, W.-B.; Du, C.-Y.; Jiang, J.-A.; Ji, Y.-F. *Res. Chem. Intermed.* **2013**, *39*, 2849–2856. doi:10.1007/s11164-012-0804-6
12. Mishra, S.; Sachan, A.; Sachan, S. G. *J. Ind. Microbiol. Biotechnol.* **2013**, *40*, 545–550. doi:10.1007/s10295-013-1255-9
13. Luu, T. X. T.; Lam, T. T.; Le, T. N.; Duus, F. *Molecules* **2009**, *14*, 3411–3424. doi:10.3390/molecules14093411
14. Gusevskaya, E. V.; Menini, L.; Parreira, L. A.; Mesquita, R. A.; Kozlov, Y. N.; Shul'pin, G. B. *J. Mol. Catal. A: Chem.* **2012**, *363–364*, 140–147. doi:10.1016/j.molcata.2012.06.001
15. Augugliaro, V.; Camera-Roda, G.; Loddo, V.; Palmisano, G.; Palmisano, L.; Parrino, F.; Puma, M. A. *Appl. Catal., B: Environ.* **2012**, *111–112*, 555–561. doi:10.1016/j.apcatb.2011.11.007
16. Parrino, F.; Augugliaro, V.; Camera-Roda, G.; Loddo, V.; López-Muñoz, M.; Márquez-Álvarez, C.; Palmisano, G.; Palmisano, L.; Puma, M. A. *J. Catal.* **2012**, *295*, 254–260. doi:10.1016/j.jcat.2012.08.018
17. Camera-Roda, G.; Augugliaro, V.; Cardillo, A.; Loddo, V.; Palmisano, G.; Palmisano, L. *Chem. Eng. J.* **2013**, *224*, 136–143. doi:10.1016/j.cej.2012.10.037
18. Di Paola, A.; Bellardita, M.; Megna, B.; Parrino, F.; Palmisano, L. *Catal. Today* **2015**, *252*, 195–200. doi:10.1016/j.cattod.2014.09.012
19. Mao, H.; Wang, L.; Zhao, F.; Wu, J.; Huo, H.; Yu, J. *J. Chin. Chem. Soc.* **2016**, *63*, 261–266. doi:10.1002/jccs.201500357
20. Adilina, I. B.; Hara, T.; Ichikuni, N.; Shimazu, S. *J. Mol. Catal. A: Chem.* **2012**, *361–362*, 72–79. doi:10.1016/j.molcata.2012.05.005
21. Salanti, A.; Orlandi, M.; Tolppa, E.-L.; Zoia, L. *Int. J. Mol. Sci.* **2010**, *11*, 912–926. doi:10.3390/ijms11030912
22. Stankovich, S.; Dikin, D. A.; Dommett, G. H. B.; Kohlhaas, K. M.; Zimney, E. J.; Stach, E. A.; Piner, R. D.; Nguyen, S. T.; Ruoff, R. S. *Nature* **2006**, *442*, 282–286. doi:10.1038/nature04969
23. Park, S.; Ruoff, R. S. *Nat. Nanotechnol.* **2009**, *4*, 217–224. doi:10.1038/nnano.2009.58